Characterising response and resistance mechanisms to Faslodex in breast cancer

Hayley Elizabeth Francies

A thesis presented for the degree of Doctor of Philosophy at Cardiff University

September 2013

Breast Cancer Molecular and Pharmacology Group
School of Pharmacy and Pharmaceutical Sciences
Redwood Building
Cardiff University
King Edward VII Avenue
Cardiff, CF103NB

Abstract

In ER+ breast cancer initial responses to antihormones are variable, complete responses are rare and resistance is eventually acquired by many patients. It is important to model these events to discover predictive markers of antihormone outcome and so targeted strategies can be developed to maximise antihormone effectiveness. To date, most studies have employed the MCF-7 cell line which fails to represent the variability of ER+ disease. Focusing on Faslodex, the thesis objective was to use 4 cell lines *in vitro* encompassing ER+/HER2- (MCF-7/T47D) and ER+/HER2+ (BT474/MDA-MB-361) disease to (i) characterise the magnitude of initial antihormone response, (ii) monitor the onset of resistance by prolonged treatment and (iii) detail gene expression changes during Faslodex treatment.

All models were initially growth-inhibited by Faslodex, with superior responses in HER2- lines. Microarray analysis revealed gene cohorts affected by Faslodex treatment differed between HER2+ and HER2- models. While MCF-7, BT474 and MDA-MB-361 cells acquired Faslodex resistance, this failed to develop in the T47D line, providing a model of complete-response. A filtering process identified genes involved in the varying Faslodex responses and clinical relevance was determined using the NEWEST Faslodex clinical trial dataset.

Of interest was the Faslodex-induction of CXCR4, as a potential mediator of acquired resistance, while suppression of the RET signalling pathway related to improved initial response in the ER+/HER2- setting. Importantly up-regulation of DCN by Faslodex was associated with improved Faslodex response in T47D cells and also with proliferation (Ki67) fall in the NEWEST clinical trial. shRNA knockdown of DCN reduced the sensitivity of T47D cells to Faslodex and enabled development of resistance.

This thesis has successfully identified novel elements of Faslodex response and resistance and further work is now required to clarify the importance of these mediators and to determine if DCN could prove a useful clinical biomarker of Faslodex response.

Acknowledgements

DECLARATION

This work has not been submitted in substance for any other degree or award at this or any other university or place of learning, nor is being submitted concurrently in candidature for any degree or other award.

Signed ...H.E.Francies... (candidate)   Date 1/4/14

STATEMENT 1

This thesis is being submitted in partial fulfillment of the requirements for the degree of ...PhD...(insert MCh, MD, MPhil, PhD etc, as appropriate)

Signed ...H.E.Francies... (candidate)   Date 1/4/14

STATEMENT 2

This thesis is the result of my own independent work/investigation, except where otherwise stated.

Other sources are acknowledged by explicit references. The views expressed are my own.

Signed ...H.E.Francies... (candidate)   Date 1/4/14

STATEMENT 3

I hereby give consent for my thesis, if accepted, to be available for photocopying and for inter-library loan, and for the title and summary to be made available to outside organisations.

Signed ...H.E.Francies... (candidate)   Date 1/4/14

Table of Contents

Abbreviations

ADAM12	ADAM metallopeptidase domain 12
AF	activating function
AFFY	affymetrix
AI	aromatase inhibitor
AKT	v-*akt* murine thymoma viral oncogene homolog
ALOX5	arachidonate 5-lipoxygenase
ALOX5	arachidonate 5-lipoxygenase
ANK1	ankyrin 1
ANOVA	Analysis of variance
AP-1	activator protein 1
ARTN	artemin
ATAC	Anastrozole or Tamoxifen Alone in Combination
ATCC	American Type Cell Collections
ATLAS	Adjuvant Tamoxifen Longer Against Shorter
BCL2	B-cell lymphoma 2
BLAST	Basic Local Alignment Search Tool
bp	basepairs
BRCA1	breast cancer type 1 susceptibility protein
cAMP	cyclic adenosine monophosphate
CASP1	caspase 1
CBS	Cardiff University Central Biotechnology Services
CCL5	chemokine (C-C Motif) ligand 5
CDH2	cadherin 2
Chip-seq	ChIP-sequencing
CI	confidence interval
CNS	central nervous system
CO_2	Carbon Dioxide
Con	Control
CONFIRM	Comparison of Faslodex in Recurrent or Metastatic Breast Cancer
COUP	chicken ovalbumin upstream promoter
CR	complete response
CXCL12/SDF-1	C-X-C motif chemokine 12/stromal cell-derived factor 1
CXCR4	chemokine (C-X-C motif) receptor 4
CYP2B6	cytochrome P450, family 2, subfamily B, polypeptide 6
CYP2B7P1	cytochrome P450, family 2, subfamily B, polypeptide 7 pseudogene 1
CYP-P450	cytochrome P450
DAB	diaminobenzidine
DBD	DNA binding domain
DCN	decorin
DCN-KO	DCN-knockout
DDX3Y	DEAD (Asp-Glu-Ala-Asp) box polypeptide 3, Y-linked
DFS	disease free survival

DNTP	deoxynucleotide triphosphates
DPX	mixture of Distyrene, a plasticizer, and xylene
dsDNA	double stranded DNA
DTT	dithiothreitol
DUSP4	dual specificity protein phosphatase 4
E2	oestrogen/oestradiol
EBCTCG	Early Breast Cancer Clinical Trialist's Collaborative Group
EGF	epidermal growth factor
EGFR	epidermal growth factor receptor
ELOVL2	ELOVL fatty acid elongase 2
EMT	epithelial-mesenchymal transition
ER/ESR1	oestrogen receptor
ERE	oestrogen response element
ERK	extracellular-signal-regulated kinases
EtBr	ethidium bromide
EU	European Union
FAM155A	family with sequence similarity 155, member A
FAS	Faslodex
Faslodex-R	Faslodex resistance/resistant
FCS	foetal calf serum
FDA	Food and Drug Administration
FDR	false discovery rate
FGF	fibroblast growth factor
FGFR	fibroblast growth factor receptors
FIRST	Fulvestrant First-Line Study Comparing Endocrine Treatments
FLT4	fms-related tyrosine kinase 4
FOXA1	forkhead box protein A1
GABA	gamma-aminobutyric acid
GABBR2	gamma-aminobutyric acid (GABA) B receptor, 2
GAD1	glutamate decarboxylase 1
GAD2	glutamate decarboxylase 2
GDNF	glial cell-derived neurotrophic factor
GFP	green fluorescent protein
GFRA1	GDNF family receptor alpha 1
GFRA3	GDNF family receptor alpha 3
GOBO	Gene Expression-Based Outcome for Breast Cancer Online
GOLM1	golgi membrane protein 1
GPCR	G-Protein Coupled Receptor
GPR37	G protein-coupled receptor 37
GREB1	growth regulation by estrogen in breast cancer 1
HCA	hierarchical clustering analysis
HDAC	histone deacetylases
HER2	human epidermal growth factor receptor 2
HER3	human epidermal growth factor receptor 3
HER4	human epidermal growth factor receptor 4
HFE	hemochromatosis

HIF	hypoxia-inducible factors
HR	hazard ratio
HRT	hormone replacement therapy
HSPG	heparan sulfate proteoglycan
HSPG2	heparan sulfate proteoglycan 2.
ICC	immunocytochemistry
ICR	Institute of Cancer Research
ID4	inhibitor of DNA binding 4
IFNγ	interferon gamma
IGF	insulin growth factor
IGF1R	insulin-like growth factor 1 receptor
IGFBP5	insulin-like growth factor binding protein 5.
IHC	immunihistochemistry
IKZF1	ikaros family zinc finger protein 1
IL	interleukin
IL6ST/GP130	interleukin 6 signal transducer
IMPACT	Immediate Preoperative Anastrozole, Tamoxifen, or Combined With Tamoxifen
IRF1	interferon regulatory factor 1
ITIH1	inter-alpha-trypsin inhibitor heavy chain 1
IVT	in vitro transcription
JAK	janus kinase
KDR	kinase insert domain receptor
KITLG	kit ligand
KO	knockout
KRT4	keratin 4
LBD	ligand binding domain
LH-RH	luteinizing hormone-releasing hormone
MAPK	mitogen-activated protein kinases
MAS 5.0	Affymetrix Microarray Suite 5.
MgCl2	magnesium chloride
miR	micro RNA
MMP	matrix metallopeptidase
MNAR	proline, glutamate and leucine rich protein 1
mTOR	mammalian target of rapamycin
MYO5A	myosin VA
MYO7A	myosin VIIA
MYRIP	myosin VIIA and Rab interacting protein
NCAD	neural cadherin (CDH2)
NCOA	nuclear receptor coavtivator
NCOR	nuclear receptor co-repressor
NEWEST	Neoadjuvant Endocrine Therapy for Women with Estrogen-Sensitive Tumors
NF-κB	nuclear factor kappa-light-chain-enhancer of activated B cells
NPY5R	neuropeptide Y receptor Y5
NR	nuclear receptor
NR2F1	nuclear receptor subfamily 2, group F, member 1
NT	non-targeting

NTN	neurturin
PBS	phosphate-buffer solution
PCDH7	protcadherin 7
PCR	polymerase chain reaction
PD	progressive disease
PDCD10	programmed cell death gene 10
PDGFR	platelet-derived growth factor receptor
PGE2	prostaglandin E2
PGR	progesterone receptor
PI3K	phosphatidylinositide 3-kinases
PKA	protein Kinase A
PR	Partial response
PRKACB	protein kinase, cAMP-dependent, catalytic, beta
PTGER3	prostaglandin E receptor 3 (subtype EP3)
PTPRJ	protein tyrosine phosphatase, receptor type, J
PYY	peptide YY
QPCR	quantitative PCR
RAFTK	related adhesion focal tyrosine kinase
RET	REarranged during Transfection
RFS	relapse free survival
ROS	reactive oxygen species
RPM	revolutions per minute
RTK	receptor tyrosine kinase
RT-PCR	Reverse-Transcription PCR
S118	serine 118
S167	serine 167
SAM	significance analysis of microarrays
SCF	stem cell factor
SD	stable diseae
SDF-1	stromal-derived factor-1
SEPT6	septin 6
SEM	standard error of the mean
Ser	serine
SERD	selective estrogen receptor down-regulator
SERM	selective estrogen modulator
SERPINI1	serpin peptidase inhibitor, clade I (neuroserpin), member 1
SFK	Src family kinase
SH3TC2	SH3 domain and tetratricopeptide repeats 2
SH3TC2	SH3 domain and tetratricopeptide repeats 2
shRNA	short-hairpin RNA
SKAP2	src kinase associated phosphoprotein 2
SLC6A14	solute carrier family 6 (amino acid transporter), member 14
SMRT	silencing mediator of retinoic acid and thyroid hormone receptor
SNP	small nucleotide polymorphism
ssDNA	single stranded DNA
STAT	signal transducer and activator of transcription

SULF1	sulfatase 1
TAE	Tris base, acetic acid and EDTA
TAF1	TAF1 RNA Polymerase II, TATA Box Binding Protein (TBP)-Associated Factor,
TAZ	tafazzin.
TEA	transcription enahancer activator
TEF	TEA family of transcription factors
TGFB	transforming growth factor, beta 1
TGFB2	transforming growth factor, beta 2
TGFBR	transforming growth factor, beta receptor
Thr	threonine
TIMP3	TIMP metallopeptidase inhibitor 3
TRX	thioredoxin
TXNIP	thioredoxin interacting protein
Tyk2	tyrosine kinase 2
UPK3B	uroplakin 3B
UV	ultra violet
VECAD	vascular-endocthelial cadherin
VE-cad	vascular endothelial cadherin
VEGFC	vascular endothelial growth factor C
VGLL1	vestigial like 1
ZNF343	zinc finger protein 343

Chapter 1

Introduction

1.1 Incidence and Mortality

Breast cancer is the most common female cancer in the UK and 1 in 8 women will be diagnosed with breast cancer during their lifetime. The incidence of breast cancer has increased by 70% in the last 30 years but improved treatments, increased awareness and an established screening system has resulted in more than 8 out of 10 women surviving the disease beyond 5 years (Cancer Research UK Statistics, 2010 (latest statistics available). Unfortunately, however, 1000 women in the UK still die from breast cancer every month. In many patients the disease manages to progress despite treatment so further research and improved treatments are clearly required (Cancer Research UK Statistics, 2010 (latest statistics available).

1.2 Oestrogen and breast cancer risk

Although the majority of breast cancers are sporadic and result from an accumulation of uncorrected genetic changes in somatic genes over a patient's lifetime, exposure to the steroid hormone oestrogen is a major risk factor for the development of the disease (Clemons *et al.*, 2001). As such, breast cancer is primarily a female disease and increasing age, women who begin menarche at a young age or have a late menopause (factors which increase a woman's lifetime exposure to oestrogen) all increase breast cancer risk (Hunter *et al.*, 1997; Collaborative Group on Hormonal Factors in Breast Cancer, 1997). Similarly, women with increased levels of endogenous oestrogen and testosterone following the menopause are at a higher risk of developing breast cancer compared to those with the lowest levels (Endogenous Hormones and Breast Cancer Collaborative Group,

2002). Also, women who take hormone replacement therapy (HRT) for 5 years have a 66% increased risk of developing breast cancer (Nomura *et al.*, 1986).

Further evidence for a link with endocrine status came from the observation that women who have children have a decreased risk of developing breast cancer, even more so if they breast feed (MacMahon *et al.*, 1970; Siskind *et al.*, 1989). Significantly, the incidence of breast cancer in developing countries is much less than in the developed world and it is thought that this may, in part, be due to women in such countries having more children and breast feed for longer (Cancer Research UK, Risk Factors).

1.3 Molecular basis for oestrogen action

Oestrogen signalling in normal breast and in breast tumours is mediated through two oestrogen receptors, ERα and ERβ, which belong to the steroid nuclear receptor family of ligand-dependent transcription factors (Tsai *et al.*, 1994). Importantly, however, ERα is the dominant ER subtype in breast cancer, found by immunohistochemistry in many of these tumours, and it is thought that the inhibitory properties of antihormones in breast cancer treatment primarily result from the blocking of the actions of ERα (subsequently termed ER throughout this project) as both an oncogenic transcription factor and signal transducer (Nicholson *et al.*, 1995; Wakeling *et al.*, 2000). Several mechanisms have been determined that provide the molecular basis for ER signalling. With respect to genes impacted by ER signalling these include the induction of a number of pro-proliferative genes such as cyclin D1, myc and IGF1R (Frasor *et al.*, 2003; Dubik *et al.*, 1992; Kahlert *et al.*, 2000) and pro-survival elements such as bcl-2 (Teixeira *et al.*, 1995) that ultimately drive ER+ breast cancer. ER signalling also represses a number of other genes in order to further regulate cell growth including the suppression of adverse growth factor pathways such EGFR, HER2 and NF-κB (Yarden *et al.*, 2001; Russell *et al.*, 1992; Lobanova *et al.,* 2007).

1.3.1 Classical and Non-classical Genomic Functions of ER

1.3.1.1 Classical Genomic ER Functions

The transcription of ER-regulated genes is regulated by 2 activating function (AF) domains in the oestrogen receptor: AF-2 is found near the carboxy-terminus of ER and requires oestrogen (E2) binding to the ligand-binding domain (LBD) of the receptor, while AF-1 at the N-terminus of the receptor, is hormone-independent (Figure 1) (Kumar *et al.*, 1987; Metzger *et al.*, 1995). Both transactivation domains are required for maximal ER transcriptional activity, but in the presence of particular ER-regulated gene promoters they can function independently (Tzukerman *et al.*, 1994).

Figure 1: Structure of ER. Receptor consists of 6 functional domains (A-F), which include the AF-activating function domains 1 and 2, DBD-DNA binding domain and LBD-ligand binding domain.

In the absence of E2, chromatin is condensed and the transcription of ER-regulated genes is suppressed. In response to E2 binding into a hydrophobic "pocket" in the LBD (Figure 1), the ER becomes activated with a conformational change which allows helix 12 of ER to seal the pocket containing the E2 and the dissociation of chaperone proteins follows. The conformational change of the receptor allows it to dimerise with another ER. The ER dimer recruits nuclear coactivators which contribute to chromatin remodelling and enhance ER transcriptional activity (Metivier *et al.,* 2003). One such transcription factor is FOXA1 which has been shown to be required for global ER binding and when FOXA1 is silenced >90% of ER binding events are reduced. This correlates with a loss in the accessibility of chromatin and the suppression of ER-mediated transcription and proliferation (Hurtado *et al.,* 2011). Such factors have been named pioneer factors and, in the

absence of FOXA1, ER is unable to bind to DNA as it is incapable of physically associating with compacted chromatin (Carroll *et al.,* 2005).

The oestrogen-activated ER binds to target oestrogen response elements (ERE) in the promoter regions of oestrogen-responsive genes via the DBD (Figure 1) and forms a transcriptional complex via the recruitment and binding of oestrogen co-regulatory proteins such as AIB1 (McKenna *et al.*, 1999) and the general transcription machinery leading to transcription of such genes by synergistic activity of AF-2 and AF-1. However, ER is also able to inhibit the transcription of many other genes (Dobrzycka *et al.*, 2003). Its ability to suppress the expression of many genes is thought to be due to differences in gene promoter sequences resulting in the recruitment of corepressor proteins to these transcriptional complexes (McKenna *et al.,* 1999; Horwitz *et al.*, 1996). For example, such repressive actions of oestrogen have been postulated to be the cause of TGF-β signalling repression (Malek *et al.*, 2006).

1.3.1.2 Non-classical Genomic ER Functions

In addition to the classical ER functions described above, oestrogen is also capable of regulating gene transcription without direct DNA binding of ER. This occurs by protein-protein interactions of ER with other transcription factors. Such interactions were indicated when O'Lone *et al.,* reported that at least one third of ER-regulated genes do not possess EREs and thus the regulation of their expression by ER cannot be via a direct DNA interaction (O' Lone *et al.*, 2004). Instead ER modulates other transcription factors such as AP-1, Sp-1 or NF-κB, indirectly regulating these ER-responsive genes, known as transcriptional crosstalk (Gottlicher *et al.*, 1998).

Genes known to be positively or negatively regulated in this non-classical manner include cyclin D1 (Castro-Rivera *et al.,* 2001) Hsp27 (Porter *et al.*, 1997), VCAM-1 (Simoncini *et al.*, 2000) and EGFR (Salvatori *et al.*, 2009). Importantly, ER signalling not only suppresses EGFR but also other members of the erbB family (Russell *et al.*, 1992). The role of ER in this non-classical system can vary; in the case of some genes it will act to stabilise a transcription factor complex to aid transcription of a particular gene via alternative response elements (essentially acting as a

coactivator) (Teyssier *et al.*, 2001), while in other cases, such as repression of IL6 transcription, ER prevents the association of NF-κB and C/EBPβ with DNA (Ray *et al.*, 1997).

Interestingly, many ER-responsive/ ERE-lacking genes contain ERE half-sites, or binding sites for SF-1 (an orphan nuclear hormone receptor) where SF-1 can act as a alternate direct ER binding site (O'Lone *et al.*, 2004). To add further complexity to this, non-classical ER signalling can be cell (Cerillo *et al.*, 1998) and ligand specific (Webb *et al.,* 2003; Kushner *et al.*, 2000) which may partly explain the varied action of oestrogens in different tissues.

1.3.2 Ligand-independent genomic ER functions

Critically, in environments where oestrogen is not present other kinase signalling pathways, notably those downstream of EGFR and IGF1R, are capable of activating ER via phosphorylation of particular residues within the ligand-independent AF-1 domain (Driggers *et al.*, 2002). Phosphorylation of these ER residues, in particular serine 118 which is a MAPK target, can re-activate ER in the absence of ligand, allowing transcription of oestrogen-responsive genes and the promotion of cell growth (Kato *et al.*, 1995). Growth factor signalling has also been shown to activate ER coregulator proteins providing an alternative route for growth factors to influence the ER pathway (Schiff *et al.*, 2003). p42/44 MAPK, AKT, p38 MAPK and PKA (Kato *et al.*, 1995., Campbell *et al.*, 2001., Lazennec *et al.,* 2001) are some of the kinases that have been described to activate ER by direct phosphorylation and/or via phosphorylation of ER coregulators.

1.3.3 Non-Genomic ER Functions

Further to these nuclear transcriptional functions, rapid non-genomic actions have been ascribed to oestrogen. Such actions are believed to occur via oestrogen acting at membrane-associated ER and result in the phosphorylation of growth factor receptors such as IGF1R and HER2 (Fan *et al.*, 2007; Kahlert *et al.*, 2000), as well as downstream effectors such as the p85 subunit of phosphoinositide-3-kinase (PI3K) (Simoncini *et al.,* 2000) resulting in pro-survival signalling.

Although ER at the plasma membrane can initiate signalling via its ligand binding domain (Kousteni *et al.,* 2001), it is possible that other domains that make up the receptor structure may also be involved in the signalling cascades initiated. It is likely that a number of ER domains provide docking stations for various scaffold proteins which may alter the magnitude of signalling via various protein-protein interactions, or the presence of certain scaffold proteins may promote interactions with particular downstream proteins thus modulating ER signalling cascades. For example, the scaffold protein MNAR promotes the interaction of activated ER with Src kinase, leading to increased Src activity and thus MAPK activation (Wong *et al.,* 2002). Like genomic signalling, the effects of ER non-genomic signalling can vary depending on cell type. The effect elicited by plasma-membrane associated ER following activation by oestradiol may depend on the availability of signal transduction molecules within a particular cell type as well as the downstream targets. As such, the non-genomic responses may be varied (Bjornstrom *et al.,* 2005) and their contribution to malignant growth differs from patient to patient and can evolve over time.

1.3.4 Convergence of non-genomic and genomic ER actions

Signal transduction pathways are likely to connect non-genomic actions of oestrogens to genomic responses. The functions of many transcription factors are regulated via protein kinase phosphorylation and thus may be downstream targets of non-genomic actions of oestrogens. One such transcription factor is AP-1; oestradiol activation of the MAPK pathway enhances AP-1 DNA binding and thus increases its transcriptional activity (Dos Santos *et al.,* 2002; Bjornstrom *et al.,* 2004). However, oestradiol can also suppress AP-1 activity by inhibiting the c-Jun amino-terminal kinase signalling cascade (Kousteni *et al.,* 2003). Such a mechanism also provides another way for ER to regulate the transcription at alternative response elements. In addition, kinase signalling pathways downstream of membrane ER may trigger ligand-independent phosphorylation of ER AF-1 residues, with activity thus promoting ER-regulated gene expression (Pietras *et al.,* 1995).

Collectively, therefore, data suggests that ER is capable of modulating gene transcription by four mechanisms (Figure 2):

- Direct binding of E2-ER to EREs (classical signalling).

- E2-ER protein-protein interactions with other transcription factors within the nucleus, indirectly activating ER-responsive genes.

- Ligand-independent genomic activation of ER-responsive genes by protein kinase cascade phosphoryaltion of ER

- Membrane-associated ER activating signalling pathways from the plasma membrane that lead to activation or repression of their target transcription factors within the nucleus or their activation of ER (AF-1) to mediate transcription of ER-responsive
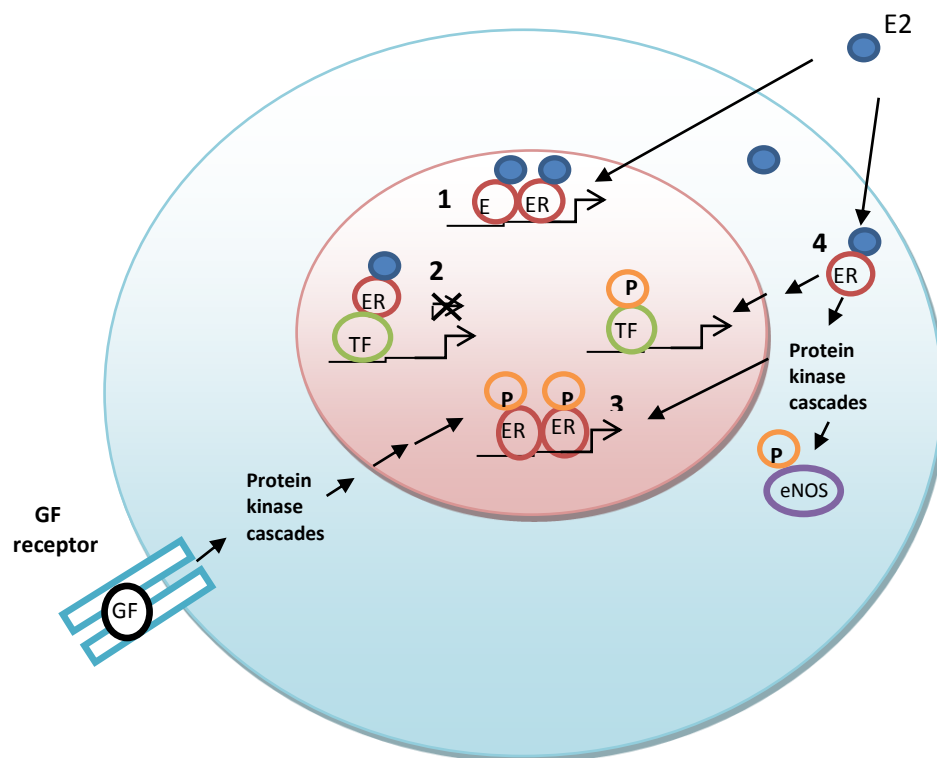
Figure 2: Schematic diagram of the various mechanisms utilised by ERα to regulate gene expression of ER-responsive genes. 1. Classical signalling; E2-ER binds to ERE promoter on target genes. 2. ERE-independent activation; E2-ER interacts with other transcription factors within the nucleus to indirectly regulate transcription. 3. Ligand-independent genomic activation; Activation of protein kinase domains by growth factors results in phosphorylation of ER in the absence of E2. 4. Non-genomic signalling; membrane-associated E2-ER activates protein kinase cascades which alter the function of cytoplasmic proteins e.g. eNOS as well as regulating gene expression.

1.4 Therapeutic options for ER+ breast cancer: Targeting ER signalling

Approximately 70% of all breast cancers are ER+; molecular studies have determined several subtypes of ER+ breast cancer (Cancer Genome Atlas Network., 2012). However, from a therapeutic perspective it is useful to sub-divide ER+ disease into 2 molecular subtypes according to status of HER2 (an erbB receptor); those that are ER+/HER2+ and those that ER+/HER2-. 80% of ER+ tumours are HER2- (Harvey *et al.*, 1999) while the remainder co-express HER2 (amplification or over-expression (Slamon *et al.*, 1987; Press *et al.*, 1997). It has been widely reported (Brufsky *et al.,* 2005) that reduced drug responses are observed in ER+/HER2+ tumours following endocrine treatment such as tamoxifen (while these tumours can be appropriate for the HER2-targeted therapy Herceptin (Spector and Blackwell, 2009).

In 1896 Dr George Thomas Beatson described how removal of the ovaries from women with advanced breast cancer could bring about an improvement in their condition. Although Beatson had yet to make the connection between oestrogen and breast cancer, from his observations of lactation in farm animals and women who had recently given birth he demonstrated that certain functions of the breast were under the control of the ovaries (Beatson, 1896).

Today the mainstay treatments for ER+ breast cancer are antihormonal drugs, of which there are several classes which have been designed to interfere with oestrogen/ER signalling and hence its regulation of genes involved in breast cancer growth. Predominately used in the clinic are tamoxifen and aromatase inhibitors, the latter having recently become the "gold standard" antihormonal approach in postmenopausal early breast cancer. Faslodex (fulvestrant) is also emerging as an antihormone of increasing importance for ER+ disease treatment. Figure 3 displays the actions of tamoxifen and Faslodex in inhibiting oestrogen signalling and how oestrogen drives gene transcription through the activation of ER and thus how the inhibition of oestrogen synthesis via the use of aromatase inhibitors would prevent such action and thus be of therapeutic use. Antihormones are invaluable adjuvant systemic treatments after surgery in ER+ early breast cancer patients to hinder relapse and extend survival or cure (Jordan *et al.*, 2011). They can also be beneficial

in limiting advanced (metastatic) ER+ breast cancer growth (Joensuu *et al.*, 2005), and furthermore in the neoadjuvant setting to reduce the size of large tumours allowing more conservative breast surgery (Olson *et al.,* 2009).
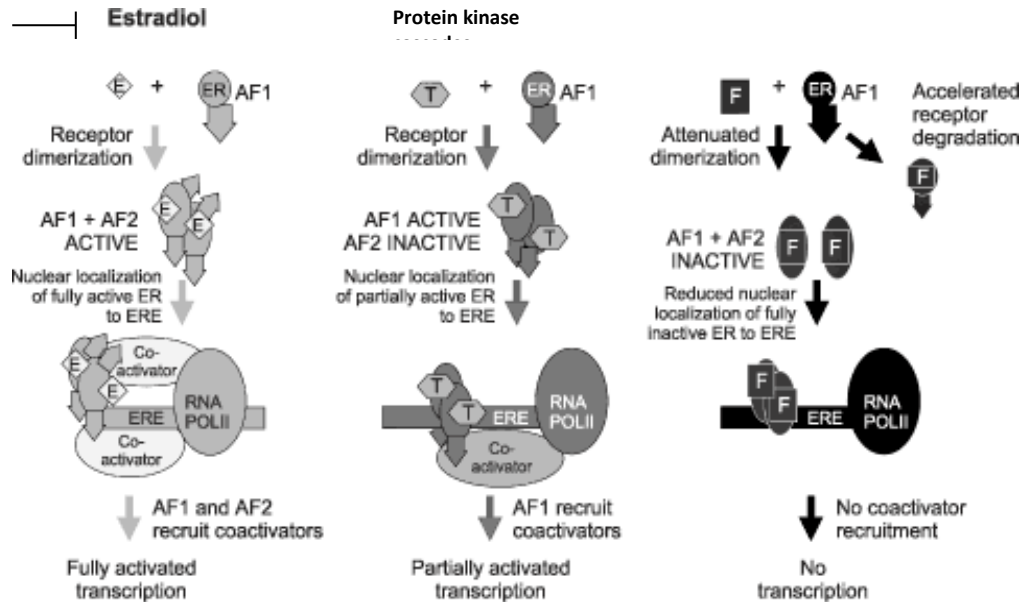
Figure 3: The mechanism of oestrogen-induced gene transcription and how this is affected by the use of tamoxifen and Faslodex. Further aromatase inhibitors prevent the synthesis of oestrogen thus inhibiting oestrogen-driven transcription (modified from Buzdar, 2004).

1.4.1 The Selective ER Modulator (SERM) Tamoxifen

Tamoxifen is a non-steroidal anti-oestrogen which acts as a competitive oestrogen antagonist of ER. As a consequence of its binding to the LBD, tamoxifen is able to prevent the action of oestrogen and thereby hinders transcription of oestrogen-induced genes. Significantly, however, the bulky side chain of tamoxifen causes an ER conformational change so that Helix 12 of the ER protein is displaced. This conformational change inactivates AF-2 driven transcription, but does not hinder AF-1 transcriptional activity (Metzger *et al.*, 1992). The agonist/antagonistic effects of tamoxifen, together with other SERMs, thus depend on the relative importance of AF-1 and AF-2 in driving ER-regulated transcription within a tissue. As ER activity in the hormone responsive breast is predominantly mediated by AF-2, an overall antagonistic effect of tamoxifen is observed, while in bone and the uterus where

tamoxifen has been shown to be agonistic, ER actions are driven primarily though AF-1 (MacGregor *et al.*, 1998). Significantly, in some instances the conformation change induced by tamoxifen binding to ER can result in the recruitment of nuclear co-repressors (NCORs) to the receptor instead of co-activators (NCOA's) thereby inhibiting transcription of oestrogen-regulated genes (Smith *et al.*, 1997; Lavinsky *et al.*, 1998). Ultimately however, alterations in the contributions of AF-1/AF-2 to transcription, as well as the availability of NCOA's and NCOR's and of growth factor/kinase signalling activity that can activate AF-1 phosphorylation can shift the balance of tamoxifen activity towards a more agonistic state (Jepsen *et al.*, 2000) and may contribute to resistance to this agent (Britton *et al.*, 2008).

Until relatively recently tamoxifen was the gold standard endocrine treatment for ER+ breast cancer, but with the emergence of superiority of aromatase inhibitors in postmenopausal disease, it is now most commonly used in ER+ premenopausal women. Tamoxifen has been approved for use in the adjuvant clinical setting for premenopausal, postmenopausal and also male patients with ER+ disease who have undergone surgery to remove the primary tumour mass. 5 years of adjuvant therapy in this setting has been shown to reduce relapse rates significantly and improve patient survival (EBCTCG, 2011). It may also be alternated with an aromatase inhibitor, again for a 5 year period (Rao *et al.*, 2012), and studies are now reporting benefits of more extended treatment timeframes (e.g. ATLAS trial: Davies *et al.*, 2013). Tamoxifen is similarly approved for initial treatment of metastatic ER+ breast cancer in both males (Giordano *et al.*, 2005) and females (pre- and post-menopausal women) (Michaud *et al.*, 2001) and has also been approved for use in females at high risk of developing ER+ breast cancer (Cuzick *et al.*, 2013).

1.4.2 Aromatase Inhibitors (AI)

With the menopause, although ovarian oestrogen production ceases, oestrogens can nevertheless still be detected in women. Such levels arise primarily from androgens found in peripheral tissues, such as adipose tissue, which can be converted to oestrone and oestradiol by the enzyme aromatase (CYP450; Bulun *et al.*, 1993). Oestrogens in breast cancers can also be derived from stromal

aromatase activity (Miki *et al.*, 2007). It has been reported that breast cancer growth can be promoted by these low levels of oestrogen (Masamura *et al.*, 1995) and aromatase inhibitors (AIs) have been developed to block the activity of aromatase and thus prevent the conversion of androgens to oestrogens. There are two classes of aromatase inhibitors available for the treatment hormone-dependent breast cancer, steroidal AIs (e.g. exemestane) and the third generation nonsteroidal AIs (e.g. anastrozole and letrozole), which all act to severely deprive breast cancer cells of oestrogen and it's signalling.

Non-steroidal (reversible) AIs behave as competitive antagonists by occupying the substrate binding site of aromatase preventing androgen binding (Cole *et al.,* 1990). However, as binding is competitive they can be displaced by the endogenous ligand. In contrast, steroidal AIs are analogues of the natural aromatase ligand androstenedione and thus are recognised as an alternative substrate by aromatase. Steroidal AIs are converted into a reactive intermediate which permanently bind to the enzyme resulting in irreversible inactivation (Hong *et al.*, 2007). AIs can achieve over 95% inhibition of aromatase enzymatic activity and suppress circulating oestrogens to almost undetectable levels in postmenopausal ER+ breast cancer patients (Geisler *et al.*, 1996).

AIs are only currently approved for use in ER+ postmenopausal breast cancer patients (with an alternative approach for oestrogen deprivaion, the luteinizing hormone-releasing hormone (LH-RH) agonist Zoladex, used in premenopausal women). Anastrozole was initially approved as a first-line treatment for locally advanced or metastatic ER+ disease in postmenopausal patients and is valuable where tamoxifen fails. However, it has now become the gold-standard treatment in the adjuvant setting of early disease for ER+ postmenopausal women (5 year treatment) based on results from the ATAC (Arimidex, Tamoxifen, Alone or in Combination) trial where anastrozole was found to be superior to tamoxifen in this setting (Howell *et al.*, 2005). Letrozole is approved for first-line treatment in the adjuvant setting for ERα+ postmenopausal women as well as subsequent to patients receiving 5 year adjuvant tamoxifen therapy and results in improved

disease free survival (DFS). Exemestane is the only steroidal aromastase inhibitor that is FDA approved for use in the adjuvant setting in ER+ postmenopausal patients who have already received 2-3 years of tamoxifen treatment in order to complete 5 years of endocrine treatment (Food and Drug Administration, 1999).

1.4.3 The Selective ER down-regulator (SERD) Faslodex (Fulvestrant)

The steroidal anti-oestrogen Faslodex, a 7-alpha derivative of oestradiol-17B with a long-unbranched 7-alpha alkylsufinyl sidechain (Wakeling *et al.*, 1992) has been termed a "selective ER down-regulator" (SERD). Faslodex can be administered intramuscular (as fulvestrant) to postmenopausal patients with ER+ metastatic disease who have progressed following alternative antihormone treatments (AI or tamoxifen). It is also being trialled in the first line advanced disease clinical setting. It is described as a "pure antioestrogen" as it lacks any agonistic activity. Like tamoxifen, Faslodex competitively binds to the ER preventing the binding of oestrogen, but in contrast to SERMs its long side-chain very severely disrupts ER conformation, resulting in down-regulation of ER in a dose-dependent manner. This occurs via Faslodex disrupting ER shuttling between the cytoplasm and nucleus, thus increasing ER cytoplasmic levels, leading to increased receptor ubiquitinisation and degradation and hence loss of nuclear ER (Dauvois *et al*., 1993; Linstedt *et al.*, 1986). Additionally, Faslodex binding to the receptor induces a distinct conformational change that no longer allows receptor dimerization (Wakeling, 2000). Faslodex also interferes with helix 12 of the ER, blocking all co-activator recruitment but favouring co-repressor recruitment. Through a combination of these actions, Faslodex hinders expression of classic oestrogen-induced genes and blocks ER transcriptional activity via inhibition of both AF-1 and AF-2 domains (Wakeling *et al.*, 1991; Kousteni *et al.*, 2001; Kousteni *et al.*, 2003; Dos Santos *et al.*, 2002).

Due to the capacity of Faslodex to down-regulate ER in a dose-dependent manner and its substantial growth-inhibitory activity in ER+ breast cancer cells both *in vitro* and in xenograft studies (Nicholson *et al.,* 1995; Wakeling *et al.*, 1991; Osborne *et al.,* 2004), early clinical studies were undertaken to establish whether this property related to clinical outcome. Data from 2 pre-operative studies upheld this

suggestion where patients received different doses of Faslodex for short-periods and the down-regulation of ER, the oestrogen regulated gene progesterone receptor (PGR) and Ki67 (a measure of tumour cell proliferation rate) were observed by immunohistochemistry to be dose-dependent (Robertson *et al.*, 2001; DeFriend *et al.*, 1994). A number of clinical trials were subsequently carried out to further investigate the efficacy of 250mg and also a high dose 500mg Faslodex treatment regime during the various phases of ER+ disease management. In total, based on such trials (and several additional ongoing studies), it is envisaged that the use of high dose Faslodex will be increasingly a viable therapeutic option at various stages during the management of ER+ postmenopausal disease in the clinic. Three of the recent pivotal Faslodex trials are summarised below:

1.4.3.1 CONFIRM (Comparison of Faslodex in Recurrent or Metastatic Breast Cancer)

Two phase III trials in tamoxifen pre-treated postmenopausal ER+ patients indicated that 250mg Faslodex was at least as effective as anastrozole when tamoxifen has failed (Howell *et al.*, 2002; Osborne *et al.*, 2002) resulting in FDA/EU approval of this dosage between 2002 and 2004. The phase III CONFIRM trail was subsequently initiated to compare 250mg Faslodex per month with 500mg Faslodex per month (with an additional loading dose of 500mg of Faslodex on day 14 of month 1) in the metastatic ER+ setting. The trial established the superiority of the 500mg regime and demonstrated a clinically relevant extended progression free survival, primarily by increasing the duration of disease stabilisation (Di Leo *et al.*, 2010), resulting in FDA approval of this higher dose in ER+ postmenopausal patients who had failed on tamoxifen in 2010. Further studies have also suggested value of Faslodex after AI failure in ER+ breast cancer (Ingle *et al.,* 2004; Perey *et al.*, 2004).

1.4.3.2 NEWEST (Neoadjuvant Endocrine Therapy for Women with Estrogen-Sensitive Tumours)

The NEWEST phase II study was undertaken to compare the biological and clinical (e.g. ER, Ki67, PGR and tumour size) activity of Faslodex 500 versus 250mg in the neoadjuvant ER+ breast cancer setting. Postmenopausal patients with newly diagnosed ER+, locally advanced breast cancer who had received no prior

treatments were selected. Patients were randomly assigned to receive 500mg Faslodex per month (plus 500mg loading dose on day 14 of month 1) or 250mg per month, for 16 weeks prior to surgery. Core biopsies were taken at week 0 (baseline), at week 4, and in some instances at surgery to assess biomarker changes. The primary biological endpoint was Ki67 proliferation marker expression from baseline to week 4 and secondary endpoints were ER and ER-regulated PGR protein expression, and tolerability (Kuter *et al.*, 2012). The immunohistochemical results from NEWEST showed that the 500mg Faslodex was superior to 250mg in terms of significantly greater decreases in Ki67 (-78.8% vs. -47.4% ; p <0.0001), ER (-50.3 vs. -13.7%; p < 0.0001) and PGR (-80.5 vs. -46.3%; p = 0.0018) protein expression (Kuter *et al.*, 2012).

1.4.3.3 FIRST (Fulvestrant First-Line Study Comparing Endocrine Treatments)

Following the superior results of a 500mg Faslodex regime in down-regulating ER and decreasing Ki67, and that 250mg Faslodex was found to be at least as effective as anastrozole in the second line setting for postmenopausal ER+ patients with advanced disease (Robertson *et al.,* 2003), the FIRST trial (phase II, open-label study) was designed in order to investigate the efficacy of 500mg Faslodex versus anastrozole in the first line setting for advanced disease (Robertson *et al.,* 2009). ER+ and/or PGR+ postmenopausal patients were randomly assigned to receive 1mg anastrozole per day or 500mg Faslodex per month (plus 500mg loading dose on day 14 of month 1), and continued treatment until progression (or due to any other reason that required discontinuation). The high clinical benefit rates for both Faslodex and anastrozole confirmed the high clinical efficacy of both agents; 72.5% and 62% respectively indicating 500mg Faslodex was at least as effective as anastrozole. Moreover, median time to progression was found to be significantly longer in patients receiving 500mg Faslodex versus anastrozole. Duration of response and duration of clinical benefit were also superior in the Faslodex trial arm, promisingly suggesting 500mg Faslodex may provide a longer-lasting effect than anastrozole if given first-line in the advanced disease setting (Robertson *et al.,* 2009).

1.5 Response and Resistance to endocrine therapies

The oestrogen receptor is arguably the biomarker that has had the most profound effect on clinical practice in medical oncology (McDermott *et al.,* 2009). The presence of ER in early-stage breast cancer identifies patients who may benefit from anti-hormone therapy where treatment has been shown to significantly reduce mortality and recurrence rates not only during the treatment period but for the following 15 years post treatment (Early Breast Cancer Trialists Collaborative Group, 2011). Unfortunately, ER is not an absolute predictor of endocrine response (in both the primary or metastatic setting) and it is believed that upwards of 40% of patients with ER+ disease are de novo resistant to antihormones, while a significant number of patients who initially respond will acquire resistance during therapy (Osborne *et al.,* 2011). Moreover, relapse during endocrine therapy has been suggested to be associated with accelerated growth, increased aggressive tumour behaviour and morphological changes characteristic of cells undergoing partial epithelial-to-mesenchymal transition (Gilles *et al.,* 1996; Hiscox *et al.,* 2006).The 'CONFIRM' clinical trial shows the spectrum of response/resistance achieved with Faslodex treatment: Table 1 displays the numerical data of the clinical responses observed in the 500mg arm of this trial. Only 45.6% of the patients within this trial obtained clinical benefit from Faslodex while over half of the patients demonstrated disease progression or stable disease for less than 24 weeks.

Table 1: Objective response and clinical benefit rates of patients within the Faslodex 500mg trial arm of the 'CONFIRM' clinical trial (Di Leo *et al.*, 2010).

Response	Number of Patients	% Number of Patients
Complete response (CR)	4	1.1
Partial response (PR)	29	8
Objective response (CR+PR)	33	9.1
Stable disease (SD) >24 weeks	132	36.5
Clinical benefit (CR+PR+SD >24 weeks)	165	45.6
Stable disease (SD) >24 weeks	47	13
Progressive disease (PD)	140	38.7
Not evaluable	10	2.8

Taken together, these clinical findings suggest that ER is not the only survival/growth-promoting pathway driving some ER+ tumours, and that escape pathways are invariably established when ER is inhibited which serve to limit response. Although in several studies HER2 positivity (HER2+) has also been found to be a biomarker of reduced endocrine sensitivity for a number of antihormones (AIs and tamoxifen), the relationship between Faslodex and HER2 is less established. Overall, the current consensus is that while ER+/HER2+ co-positive patients can exhibit a response to endocrine therapy (AI and tamoxifen), generally these responses are inferior in comparison to HER2- patients (Rasmussen *et al.,* 2008). As such expression of HER2 has become a marker of poorer endocrine response and tumours exhibiting this phenotype are often treated with trastuzumab (combined with chemotherapy; Piccart-Gebhart *et al.*, 2005). Significantly, the relationship between HER2 expression and endocrine response does not seem so clear for Faslodex where a number of researchers have demonstrated activity of Faslodex in the ER+/HER2+ setting (Robertson *et al.,* 2010; Mello *et al.,* 2011), possibly due to the unique action of Faslodex in down-regulating ER and thus inhibiting any ER-HER2 crosstalk.

1.5.1 Mechanisms of antihormone resistance

Faslodex resistance is poorly characterised pre-clinically and the potential molecular mechanisms of both response and resistance are poorly understood. Furthermore, the majority of research carried out has utilised a limited number of cell models which fail to reflect the clinical heterogeneity of ER+ breast cancer. However, several mechanisms have been proposed to contribute to antihormone resistance, generally reflecting work carried out on tamoxifen and AI resistance and can be broadly divided into mechanisms dependent on altered growth factor signalling and those that can be independent of such events. Preclinical and clinical observations suggest that some of these mechanisms may translate to the Faslodex-resistant setting.

1.5.2 Antihormone resistance mechanisms that can be independent of growth factor signalling

These mechanisms are generally associated with changes in expression level of ER or other factors that influence ER activity. For example, along with ~30% patients who are intrinsically ER negative, 15-20% of ER+ patients treated with endocrine therapy have been reported to lose ER expression thus rendering them insensitive to anti-oestrogen therapy (Kumar *et al.,* 1996; Gutierrez *et al.,* 2005). While hyperactivation of growth factor signalling pathways may be contributory to ER loss (Oh *et al.*, 2001; Stoica *et al.*, 2003), epigenetic modifications to the ER gene ESR1 have been implicated in the loss of ER expression. The majority of ER-negative tumours demonstrate ER promoter methylation (Wei *et al.,* 2008) while a proportion of ER+ breast cancer patients' also exhibit ER promoter methylation (Giacinti *et al.,* 2006). As an ER down-regulator, loss of ER at the protein level has also been reported *in vitro* following continued long-term Faslodex treatment (Liu *et al.,* 2004)

Further alterations in ER co-regulator levels can influence antihormone activity. ER drives transcription by associating with a group of regulatory proteins that form the transcription complex (McKenna *et al.*, 1999) and changes in the level of such proteins can influence the effectiveness of endocrine therapy. The equilibrium of ER

corepressors and coactivators can directly control the agonistic versus antagonistic properties of SERMs and the overexpression of the ER coactivator AIB1 has been associated with tamoxifen resistance (Shou *et al.*, 2004; Osborne *et al.,* 2003). Similarly, the increased activity of transcriptional factors associated with ER signalling, such as AP-1, Sp-1 and NF-κB, have been linked to endocrine resistance (Schiff *et al.*, 2000; Zhou *et al.*, 2007). The ER coactivator MED1 has been associated with development of Faslodex resistance and knockdown of this gene renders cells sensitive to Faslodex *in vitro* and *in vivo* (Zhang *et al.*, 2013). Differential ER binding of co-activators may also be contributory to resistance. Recently, the transcription factor FoxA1 has been shown to be essential for ER-mediated transcription where its distinct ER binding profiles promoted differential gene expression in a pattern unique to tamoxifen resistant cells and also associated with adverse clinical outcome in ER+ disease (Ross-Innes *et al.*, 2012).

There is also considerable preclinical and clinical data implicating the activity of several cell cycle regulators in determining tumour sensitivity to endocrine agents, with data again primarily available in relation to tamoxifen (Musgrove *et al.*, 2009). Overexpression of MYC and amplification and/or overexpression of cyclins E1 and D1 have been associated with the development of endocrine resistance by either activating drivers of the cell cycle, such as cyclin-dependent kinases which are critical for the transition of cells through the G1 phase, or relieving the inhibitory effects of the negative cell cycle regulators p21 and p27 (Butt *et al.*, 2005). Reduced expression or activity of the negative regulators p21 and p27 is similarly associated with endocrine resistance (Chu *et al.*, 2008; Perez-Tenorio *et al.*, 2006).

1.5.3 Growth factor signalling and endocrine resistance

1.5.3.1 Ligand independent ER activation

Most resistant tumours continue to express ER (Johnston *et al.*, 1995; Guiterrez *et al.,* 2001). Although this does not dictate continued dependence on ER signalling, nevertheless a cohort of resistant patients do respond to second-line endocrine treatment (Howell *et al.*, 1996; Buzdar *et al.*, 2001) indicating maintained reliance on ER signalling for resistant growth and disease progression.

It has been suggested that ligand-independent activation of ER (independent or downstream of any non-genomic ER input) is linked to endocrine resistance, with ER becoming activated despite E2 deprivation or presence of tamoxifen. Such events can promote hypersensitivity to any residual oestrogens (Chan *et al.*, 2002) or tamoxifen agonism (Shou *et al.*, 2004). Phosphorylation of 2 key AF-1 residues in ER have been associated with resistance, serine 118 (S118) and serine 167 (S167). Both are reported to be important for ER activity (Arnold *et al.*, 1994; Thrane *et al.*, 2013). Phosphorylation of S118 has been shown to be mediated by not only oestrogen but also by growth factor ligands such as EGF and IGF-1 (Joel *et al.*, 1998; Lannigan *et al.*, 2003) as well as downstream growth factor signalling molecules ERK1/2 and p38 MAPK (Kato *et al.*, 1998; Joel *et al.*, 1998; Gutierrez *et al.*, 2005; Britton *et al.*, 2006). Further the PI3K/AKT signalling pathway has also been implicated in phosphorylation of S167 (Campbell *et al.*, 2001). Subsequently, up-regulation of these signalling pathways has been associated with endocrine resistance (Shim *et al.*, 2000; Campbell *et al.*, 2001; Gutierrez *et al.*, 2005). There is also cell model evidence that some of the target growth factor receptors in such pathways (e.g. erbB family members HER2 and EGFR) are oestrogen-repressed and antihormone-induced elements, and so increases in such receptors have also been implicated in the development of resistance, cross-talking with ER through their downstream kinase signalling to drive acquired resistant cell growth (Gee *et al.*, 2003; Nicholson *et al.*, 2005; Britton *et al.*, 2006). HER2 induction in resistance is believed to be a consequence of loss of the transcription factor PAX2, which is involved in its oestrogen/ER-mediated repression (Hurtado *et al.*, 2008)

Most of the above research was carried out in relation to tamoxifen treatment and in light of the mechanism of action of Faslodex, ligand independent activation of ER should be reduced as the ER protein is degraded and activity of both AF-2 and AF-1 are blocked. Nevertheless, as explained previously 250mg Faslodex failed to sufficiently suppress ER level leading to the approval of 500mg Faslodex. While this dosage was found to be biologically and clinically superior, clinical trials also indicate that this higher dose fails to completely suppress ER expression and

function (Kuter *et al.*, 2012; Di Leo *et al.*, 2010; Robertson *et al.*, 2009) and thus it remains feasible that ligand independent ER activation may contribute to Faslodex resistance. Indeed, the responses observed to further endocrine agents following Faslodex failure at least in a proportion of patients implies some retained importance for this receptor (Vergote *et al.*, 2003), and trials are ongoing to determine if higher doses, or combination with alternative endocrine agents, can promote superior ER blockade (Robertson *et al.,* 2009; Di Leo *et al.,* 2010; Kuter *et al.,* 2012; Mehta *et al.*, 2012).

1.5.3.2 Loss of reliance on ER signalling

A proportion of resistant tumours appear to be ER independent: they are no longer reliant on ER signalling for resistant cell growth and survival and thus are not growth inhibited by further antihormone treatments. It seems that such tumours have acquired the ability to employ alternative signalling pathways which ultimately leads to the emergence of a resistant cancer cell population. This has been observed in a significant number of patients who fail to respond to second-line endocrine therapy (Buzdar *et al.*, 2001). The hyperactivation of growth factor signalling pathways specifically has again been heavily implicated in ER-independent tumour growth and survival (Normanno *et al.,* 2005).

In MCF-7-derived acquired tamoxifen-resistant and Faslodex-resistant cells, HER2 and/or EGFR expression is elevated in comparison to wild-type cells. These antioestrogen-resistant cells can also show increased EGFR/HER2 heterodimerisation and activity. Such partners activate MAPK and PI3K/AKT signalling pathways driving antioestrogen-resistant cell growth (McClelland *et al.*, 2001; Knowlden *et al.*, 2003; Jordan *et al.*, 2004). While in the tamoxifen resistant cells hyperactivated EGFR/HER2 signalling activates ER in a ligand independent manner (Britton *et al.,* 2006), such growth factor receptor signalling must function independently of ER where acquired Faslodex resistant cells lose this receptor. Faslodex has also been shown to differentially regulate EGFR ligands leading to an increase in EGFR signalling reducing Faslodex response in MCF-7 cells (Zhang *et al.,* 2013). Nf-κB may also be involved, as its p65 subunit has been shown to increase in Faslodex resistant MCF-7 cells (Gu *et al.*, 2002; Riggins *et al.*, 2005)

1.5.3.3 Impact of targeting growth factor pathways in resistance

The potential importance of growth factor signalling pathways in driving resistant cell growth, either through their cross-talk with ER or in an ER-independent manner, has been demonstrated by using agents that specifically target these growth factor receptor pathways. EGFR or HER2 blockade in either acquired tamoxifen-resistant or Faslodex-resistant MCF-7 cells using gefitinib or trastuzumab respectively results in potent growth inhibition, whereas in antihormonal untreated cells inhibition is small due to the low basal levels of such growth factor receptors in the presence of functional E2/ER signalling which represses these receptors (McClelland *et al.*, 2001; Knowlden *et al.*, 2003). Co-treatment with such targeted agents alongside antihormones such as tamoxifen can also subvert emergence of resistance in MCF-7 cells (Gee *et al.*, 2003; Leary *et al.*, 2010). Targeted therapy of the downstream kinases such as MAPK or PI3K/AKT has also been shown to inhibit growth of such antiestrogen-resistant cells (McClelland *et al*., 2001; Knowlden *et al.*, 2003; Jordan *et al.*, 2004). Immunohistochemical analysis of clinical breast cancer tissue has also shown increased expression and/or activity of EGFR, HER2 and MAPK members in samples from de novo ER+ (and ER-) tamoxifen resistant patients as well as in some patients who acquired resistance (Gutierrez *et al.*, 2005) including samples obtained from tamoxifen-treated ER+ primary elderly patients (Gee *et al.*, 2005).

In total, such findings have provided the rationale for the introduction of trials looking at EGFR/HER2 targeted therapies alongside antihormones to control resistance in the clinic (Christofanilli *et al.*, 2010; Osborne *et al.,* 2011; Carlson *et al.,* 2012). Emerging data indicates that some tamoxifen or AI treated breast cancer patients (notably those who are also HER2+) can respond to such targeted agents (Gutteridge *et al.,* 2010; Osborne *et al.,* 2011) but responses can be short-lived, indicating further contributory resistance mechanisms. The impact of growth factor–targeted treatments in Faslodex resistant disease remains to be established in the clinic. However, it is already clear that up-regulation of EGFR, HER2 along with MAPK activity is not observed in all Faslodex-resistant cell models where, for example, other members of the erbB family have been reported to contribute to

reduced efficacy of Faslodex (Sonne-Hansen *et al.*, 2010; Thrane *et al.*, 2013). Further, ER has been observed to be lost in some cell models of Faslodex resistance while retained in others (Liu *et al.,* 2004; Nicholson *et al.,* 2007). Importantly, the long-term biological effects of Faslodex in the clinic are not well reported and thus the prevalence of growth factor pathways and relation to any retained ER following the development of Faslodex resistance are unknown. Further studies are clearly required to understand both response and resistance mechanisms to Faslodex, within and beyond growth factor signalling, particularly given the limited success of antihormone (tamoxifen and AI's) alongside further targeted therapies in the clinic.

1.6 Gene expression profiling and breast cancer

Following the completion of the sequencing of the human genome which demonstrated the potential breadth of genes that could be expressed came the advent of gene expression microarray profiling. Such profiling allows analysis of gene transcription on a genome-wide scale rather than the traditional "one gene at a time" thus creating a global picture of potential cellular function and providing another level of detail to the functionality of the genes present in the human genome.

High throughput gene expression profiling using microarray-based methods has achieved many successes with relation to breast cancer research. Without such data, we would lack an understanding of the heterogeneity that exists in breast cancer which has challenged the concept that breast cancer is a single disease (Perou *et al.,* 2000; Sorlie *et al.,* 2001). Instead, it is now accepted that breast cancer is a collection of different diseases that affect the same organ site but have different transcriptional profiles, risk factors, clinical presentation, histopathological features, outcome and response to therapies (Reis-Filho *et al.,* 2010; Weigelt *et al.,* 2010). These studies have also shown that response to a given treatment is at least in part determined by inherent molecular characteristics of the tumours and such findings have been taken advantage of in order to discover genes over-expressed in breast cancer or to identify molecular gene signatures that can predict prognosis and response to therapies (Sotiriou *et al.,* 2009; Weigelt *et al.,* 2010). Some gene

signatures are available in commercial formats, e.g. the 21 gene OncotypeDX test, a genetic test used to determine if node negative early ER+ breast cancer patients are at risk of 10 year distant recurrence and would thus benefit from the addition of chemotherapy to their standard endocrine treatment (Paik *et al.*, 2004). Although there are further tests that may be able to predict risk of recurrence on tamoxifen therapy including measurement of the ratio of HOXB13 gene to interleukin 17B receptor (Ma *et al.,* 2004), such tests have not generally been independently validated for clinical use.

Critically, tests such as OncotypeDX only provide prognostic data and have failed to unveil new therapeutic targets that could possibly improve response. While immunohistochemical measurement of Ki67 remains the most widely used marker of drug response, it again is unable to accurately predict resistance and fails to provide information on the underlying mechanism of response, only that suppression of the protein indicates a tumour with reduced proliferative capability. Also, even with such prognostic information available a number of patients present with intrinsic resistance while others ultimately acquire endocrine resistance. The molecular mechanisms of response and acquired resistance, particularly to Faslodex, thus remain largely unknown. It is unlikely that sole investigation of the intrinsic cancer phenotype will provide a full explanation of how a patient will respond to endocrine therapy and eventually acquire resistance and relapse.

A number of predictive gene signatures have been reported which relate gene expression to clinical and pathological response to endocrine therapy in ER+ patients. However, very few have been validated for clinical use. Further no such studies have been carried out in relation to Faslodex.

Miller *et al* published a study in which they reported a signature that could discriminate between clinically-responsive and non-responsive tumours to aromatase inhibitors (Miller *et al.*, 2009). 205 genes were found to be differentially expressed between responding and non-responding tumours and hierarchical clustering of these genes successfully grouped responding and resistant tumours.

Unfortunately, the gene signature was not validated using an independent cohort of patients. However, as the case for predictive signatures, this research has failed to identify novel response and resistance pathways and thus the mechanisms of the various antihormone responses remain uncharacterised.

1.7 Aims and Objectives

As described, antihormone treatments are a mainstay for early and advanced ER positive breast cancer. Unfortunately response to treatment is variable with complete response being rare and resistance eventually will be acquired by many patients. To delay, or ultimately treat resistance, these varying responses need to be modelled and the underlying signalling mechanisms determined so strategies can be developed to maximise drug effectiveness. Cell lines can provide an amenable opportunity to monitor signalling changes in a dynamic manner during treatment, although it is important that such studies should also aim to consider aspects of ER+ breast cancer heterogeneity if clinically-relevant mechanisms are to be determined.

In this regard, the work in the thesis focuses on the pure-antioestrogen Faslodex. This is important because to date, the majority of experimental work regarding resistance has employed the ER+/HER2- MCF-7 cell line and the antioestrogen tamoxifen. It is particularly important that the responses and resistance mechanisms to Faslodex are explored as the increased dose of 500mg has been shown to more effective than the 250mg dose, thus allowing the drug to be of potential further use in the clinic which is currently being trialled in the first line setting. Four cell lines are to be used in this thesis *in vitro* to account for key genetic contexts present in clinical ER+ breast cancer i.e. ER+/HER2-: MCF-7 and T47D and ER+/HER2+: BT474 and MDA-MB-361. These will be used to elucidate the extent of initial Faslodex response in each cell model, to monitor the duration of response in continuous culture with Faslodex and to track any emergence of resistance. Such studies should provide further information on how HER2 status impacts on these events in ER+ breast cancer. With respect to tamoxifen it has been widely reported that HER2-amplification is associated with resistance to the drug

(Schiff *et al.*, 2005). However, it has been suggested that HER2-positive tumours may retain some initial responsiveness to Faslodex (Robertson *et al.,* 2009).

Gene expression changes following 10 day Faslodex treatment will also be analysed in the 4 models to further aid explanation of *in vitro* growth behaviour and to identify specific Faslodex response or failure signalling mechanisms. Assuming the ER+ cell models show varying responses to Faslodex (mirroring the spectrum of responses seen clinically in ER+ disease with this agent (Di Leo *et al.,* 2010), analysis of the gene microarray data will allow us to (i) identify potential biomarkers of Faslodex response or resistance that may ultimately be of relevance to clinical use of the drug, as well as (ii) identify possible new therapeutic targets that may promote an enhanced response when given in combination with Faslodex

1.7.1 Objectives

➢ To establish the duration of Faslodex response and determine if acquired resistance develops in cell models of ER+/HER2- and ER+/HER2+ breast cancer *in vitro* through growth studies.

➢ To identify genes most likely to associate with the Faslodex response profiles *in vitro* via Affymetrix gene expression profiling of the cell models prior and subsequent to Faslodex treatment. Subsequently a stringent filtering procedure, including detailed investigation of gene expression data across the models, ontology, expression in silica clinical datasets and PCR verification of profile, will be used to prioritise genes of interest.

➢ To explore clinical relevance of the genes of interest in relation to Faslodex treatment and its anti-proliferative impact by examining their profiles in the NEWEST (Neoadjuvant Endocrine Therapy for Women with Estrogen-Sensitive Tumours) clinical trial gene expression dataset (investigation of Faslodex in the neoadjuvant setting).

➢ Faslodex response genes identified of highest priority from the *in vitro* and NEWEST data will be further investigated, including verifying their profile at the protein level and examining impact of genetic manipulation on drug response.

Chapter 2

Materials and Methods

Unless otherwise stated, all tissue culture medium and their chemical constituents were purchased from Life Technologies (Paisley, UK). All tissue culture plastic wares were purchased from Nunc (Roskilde, Denmark), supplied by Fisher Scientific (Loughborough, UK). All general molecular grade chemicals, organic solvents and molecular biology reagents were obtained from Sigma-Aldrich (Poole, UK) unless otherwise stated.

2.1 Cell Culture

2.1.1 Routine maintenance

All 4 ER+ human breast cancer cell lines were obtained from American Type Cell Collections (ATCC) and routinely cultured as monolayer cultures *in vitro* in phenol red-containing RPMI medium (2mM glutamine) containing foetal calf serum (FCS), (optimal FCS concentration for culture depended on each cell line; MCF-7 and T47D 5%; BT474 and MDA-MB-361 10%). Further medium additives comprised penicillin-streptomycin (100U/ml-10µg/ml) and fungizone (2.5µg/ml). For all routine maintenance and experimental studies, cells were grown under sterile conditions in a $37^{o}C/5\%$ CO_2 incubator (Sanyo MCO-17AIC incubators, Sanyo Gallenkamp, Loughborough, UK).

Cell growth was visually assessed using a phase-contrast microscope (Nikon Eclipse TE200n phase contrast microscope, Nikon Ltd, Kingston-upon-Thames, UK) and passaged when confluency reached 70-80%. For passaging, medium was aspirated from the flask using a glass pipette and 0.05% trypsin with 0.02% EDTA was added to the flask. Trypsin, a proteolytic enzyme, acts to detach the cells from the flask wall and EDTA is used to chelate Mg^{2+} and Ca^{2+} present in the serum that can potentially act as trypsin inhibitors. The flasks were placed in the $37^{o}C/5\%$ CO_2

incubator for 3-5 minutes to allow the cells to fully detach. An equal volume of the routine maintenance media was subsequently added to the flask to neutralise the trypsin/EDTA solution. The cell suspension was then transferred to a universal tube and placed in a centrifuge (Mistral 3000i centrifuge, Sanyo Gallenkamp, Loughborough, UK) for 5 minutes at 1000rpm. The supernatant was discarded and the cell pellet resuspended in 1-10ml of routine maintenance medium and mixed gently using a pipette to avoid cell clumps. A proportion of the cell suspension was then dispensed into a clean flask and diluted with the appropriate medium; this dilution fluctuated depending on the cell line and its growth rate: BT474 and MDA-MB-361 underwent a 1:6 dilution, while the MCF-7 and T47D models underwent a 1:10 dilution for passaging. Cells were subsequently maintained with fresh medium changes every 3 days until required for experimentation or further passaging.

Table 2 displays the key features of each of the human breast cancer cell models used in this project.

Table 2: Key molecular features and characteristics of the ER+ cell models used in this project (adapted from Neve *et al.*, 2006).

Cell Line	Molecular Subtype	ER status	PGR status	Original source of cells	Tumour type
BT474	Luminal B	+	+	Primary breast tumour	Invasive ductal carcinoma
MDA-MB-361	Luminal B	+	-	Mammary breast: derived from metastatic site: brain	Adenocarcinoma
MCF-7	Luminal A	+	+	Pleural effusion	Invasive ductal carcinoma
T47D	Luminal A	+	+	Pleural effusion	Invasive ductal carcinoma

2.1.2 Short-term cell growth studies

Cells were trypsinised from flasks and re-suspended in phenol red-free RPMI containing 5% FCS with no further addition of oestradiol as the concentration of oestrogen is very low in FCS (<100pM) (Briand *et al*, 1984) as observed in

postmenopausal women (<35pg/ml/1000pM), 2mM glutamine, penicillin-streptomycin (100U/ml-10µg/ml) and fungizone (2.5µg/ml). Cells were then passed through a sterile 25G syringe needle in order to obtain a single cell suspension. 100µl of this suspension was added to 10ml of Isoton solution and cell number was determined using a CoulterTM Multisizer II (Beckman Coulter UK Ltd, High Wycombe, UK). Cells were seeded into 24 well plates at required cell densities according to growth rate (i.e. MCF-7 and T47D - 40,000 cells per well; BT474 and MDA-MB-361 – 120,000 cells per well) in 1 ml of media and left to adhere overnight. Various treatments (as described in the Results sections) were then added to the cells the next day and replenished every 3 days before cells were counted following 7-10 days of treatment. Cell were trypsinized and re-suspended in the appropriate medium. Cells were then passed through a sterile 25G syringe needle 3 times in order to obtain a single cell suspension. 3 x 1ml of Isoton solution was added to each well and transferred to the same syringe to make up 4ml cell suspension. The latter was mixed with 6ml Isoton solution in a counting cup to give a total of 10ml cell suspension and cell number was determined using a CoulterTM Multisizer II (Beckam Coulter UK, Ltd, High Wycombe, UK) according to manufacturer's instructions.

2.1.3 Treatments

Throughout this study, cells were subjected to treatments with various compounds. Details of these treatments (durations and compound concentrations) are indicated in the figure legends throughout the Results chapters (Chapters 3-10). Table 3 lists the compounds used in this study and where they were obtained. All experiments included appropriate controls which again are stated in the figure legends of the results chapters.

Table 3: List of treatments used in this project along with where they were compounds were obtained and the diluents used to store them

Treatment	Source	Diluent
Faslodex	AstraZeneca, UK	Ethanol
Tamoxifen	T5648, (Sigma-Aldrich, UK)	Ethanol
Herceptin	Roche Pharmaceuticals, Penzberg, Germany	Water
Decorin	D8422, Sigma UK	PBS
Charcoal stripped FCS	Carried out in-house. (see Appendix A)	

2.1.4 Statistical analysis of short-term cell growth

The statistical software package SPSS was used for all statistical analyses. An independent 2-tailed t-test was used for direct comparisons of cell growth between controls and treatments for each cell line utilising the data from the experimental replicates (at least n=3). If more than 3 treatment groups were to be examined a one-way ANOVA with post-hoc tests. Differences were deemed significant if $p < 0.05$

2.1.5 Long term growth experiments.

Cells were cultured in phenol red free RPMI medium containing 5% foetal calf serum (FCS), penicillin-streptomycin (100U/ml-10μg/ml), fungizone (2.5μg/ml) in T25 flasks until 60% confluent before the addition of 10^{-7}M Faslodex while untreated cells were also continually grown as a control arm of the experiment. The effect of continuous Faslodex treatment on cell growth was subsequently monitored until the acquisition of resistance was observed, tracking cell growth (including estimating percentage cell coverage of the flask) on a weekly basis using a phase-contrast microscope and also recording the number of passages each cell model underwent under control or Faslodex treated conditions during the culture time as indicators of growth behaviour during treatment. Respective media was regularly replenished by changing every 3 days. Culture was continued until

Faslodex resistant cell populations began to emerge (evidenced by recovery of regular passaging) or until treatment led to complete cell loss so that further culture was not possible.

2.2 Immunocytochemistry (ICC)

Cells were grown on sterile 3-aminopropyltriethoxysilane coated (see Appendix B.1) glass coverslips seeded at 1×10^4 cells/cm^2 in 35mm dishes in phenol red free RPMI supplemented with 5% FCS, 2mM glutamine (and antibiotics) for 10 days in the presence or absence of 100nM Faslodex prior to appropriate cell fixation and assayed for ER, Ki67, HER2 and DCN. Assays for all markers had already been previously optimised (Gee *et al.*, 2003) with the exception of DCN which was optimised during this project.

2.2.1 Ki67 (proliferation marker)

2.2.1.1 Formal saline fixation for Ki67

Cell medium was removed using a pipette before each coverslip was immersed in 3.7% formal saline (see Appendix B.2) at room temperature for 10 minutes. Coverslips were then immersed in 70% ethanol and left for 5 minutes before being washed twice with PBS for 10 minutes. Coverslips were then stored at -20°C in sucrose storage medium (see Appendix B.3).

2.2.1.2 Ki67 ICC assay

The storage medium was poured away from the dishes containing the fixed cells on coverslips and they were then washed several times using PBS (see Appendix B.4) followed by 30 seconds wash in PBS/Tween (P5927, Sigma) (0.02% see Appendix B.5) in a humidity chamber. Ki67 primary antibody (M7240 Dako Ltd Species: mouse anti human) was diluted at 1:150 in PBS. 50µl of primary antibody was then dispensed onto each coverslip, ensuring full coverage before being placed back into the humidity chamber for 60 minutes at room temperature. The coverslips were then briefly washed in PBS several times and PBS/Tween (0.02%) was added twice each for 5 minutes minutes before the solution was drained off. The secondary antibody (Dako Envision+ system-HRP labelled polymer antimouse, Dako, K4001)

was dispensed onto the coverslips, again ensuring full coverage of the coverslip before placing back into the humidity chamber to incubate for 75 minutes at room temperature. The 2 x 5 minute washes described above were then repeated and the slides drained. 50µl of Dako diaminobenzidine (DAB)/substrate chromagen system solution (Dako Ltd, K3468) was then dispensed onto the coverslips and left for 10 minutes at room temperature before being rinsed off several times with distilled water. Methyl green counterstain (M8884, Sigma) (0.05%) was then added to each coverslip for 4 minutes. Coverslips were washed with distilled water before being left to air dry and mounting onto glass microscope slides (FB58628, Fisher Scientific, UK) using DPX (a mixture of Distyrene, a plasticizer, and xylene, 06522, Sigma-Aldrich, UK). Positivity was indicated as brown staining against green counterstained negative cells. Ki67 positivity was scored as the % of cells with nuclear staining.

2.2.2 HER2

2.2.2.1 Formaldehyde/methanol/acetone fixation for HER2

Coverslips were immersed in 4% Formaldehyde solution in PBS at room temperature for 15 minutes before being placed in PBS for 5 minutes. Coverslips were then immersed in methanol (maintained at -10 to -30°C) for 5 minutes before being immersed in acetone (maintained at -10 to -30°C) for 3 minutes. Coverslips were then placed washed in PBS for 5 minutes at RT before being stored in a -20°C freezer in sucrose storage medium.

2.2.2.2 HER2 ICC assay

The storage medium was removed from coverslips and they were then briefly washed several times using PBS followed by 30 seconds in PBS/Tween (0.02%) in a humidity chamber. 80µl of 5% normal goat serum with 5% normal human serum in PBS was then added to each of the coverslips for 10 minutes as a blocking step to prevent non-specific binding of this primary antibody. HER2 primary antibody (Dako Ltd, c-ErbB-2 (A0485): species rabbit antihuman) was diluted 1:50 (for ER+/HER2- cells lines) and 1:100 (for ER+/HER2+ cell lines) in PBS supplemented with 5% normal goat serum (X0907, Dako) and 5% normal human serum. The block was

then removed before 50µl of diluted HER2 antibody was dispensed onto the coverslips and left to incubate for 2 hours at room temperature in a humidity chamber. The coverslips were then washed in PBS several times and PBS/Tween (0.02%) was added for 2x 5 minutes. A secondary antibody (Sigma Goat anti-Rabbit IgG peroxidase conjugate A4914) was also prepared in PBS supplemented with 5% normal goat serum and 5% normal human serum at a concentration of 1:50 and applied for 60 minutes at room temperature. The 10 minute washes were repeated before 50µl of Dako DAB/substrate chromagen system solution was then dispensed onto the coverslip and left for 10 minutes at room temperature before being rinsed several times with distilled water. Counterstaining and mounting was then performed as for Ki67 Brown HER2 plasma membrane immunostaining was then evaluated in each coverslip across at least 3 fields using a continuous HScore (also checking for any cytoplasmic staining). Hscore, on a 0-300 scale, is calculated using the following formula which considers both percentage positivity and staining intensity (where negative staining cells=0, weak staining cells= 1+, moderate staining cells=2+ and high staining cells =3+): H-Score = (% at 0) * 0 + (% at 1+) * 1 + (% at 2+) * 2 + (% at 3+) * 3).

For HER2 staining, it was also noted which of the models exhibited a strong complete membrane stain in 10% or more of the tumour cells i.e. defined as 3+ in the CAP/ASCO guidelines (Wolff *et al.,* 2007)

2.2.3 Oestrogen-receptor ICC Assay

For ER, cell coverslip fixation and storage was as described for the HER2 ICC assay. Coverslips were subsequently washed several times with PBS to remove storage medium followed by 10 minute incubation with 0.02% PBS/Tween to block non-specific binding. ER primary antibody (6F11, VP-E613, Vector Laboratories, mouse anti human antibody) was diluted 1:175 in PBS and dispensed onto the coverslips and incubated for 90 minutes at room temperature in a humidity chamber. Sections were then washed three times with PBS (3 minutes) and twice with 0.02% PBS/Tween (5 minutes) before the secondary antibody was dispensed on to the coverslips (Dako Mouse EnVision labelled polymer, K4001) for 75 minutes in a humidity chamber at room temperature. 5 minute washes with PBS and 0.02%

PBS/Tween was repeated before Dako DAB/substrate chromagen system solution was added for 10 minutes and washed off using distilled water. Coverslips were then counterstained and mounted as for Ki67. ER was again evaluated using HScoring, in this instance also encompassing an additional very weak (+/-) staining category which has been employed for previous evaluation of Faslodex treated material (Kuter *et al.*, 2012).

H-Score = (% at 0) * 0 + (% at +/-) *0.5 + (% at 1+) * 1 + (% at 2+) * 2 + (% at 3+) * 3).

2.2.4 Decorin

2.2.4.1 Decorin Optimisation of Fixation

Various fixatives and also ICC assay conditions were examined during staining optimisation for decorin. This optimisation was performed in relation to DCN mRNA profile established across the 4 ER+ models with/without Faslodex treatment (Table 4).

Table 4: Summary of DCN ICC assay optimisation procedure

Procedure	Reason for rejection
Fixation	
Phenol formal saline	Staining improved with removal of phenol.
Formal saline	Chosen for assay
Antibody	
LF-122 (a gift from Dr Larry Fisher, NIH)	Non-uniformed staining
AB60425 (Abcam)	Improved membrane staining
Antibody dilution	
1:50	Saturated staining
1:200	Too weak staining
1:100	Chosen for assay

Optimal staining profile across the models was achieved using formal/saline fixed cell coverslips (as for Ki67 assay) and the following ICC assay protocol:

2.2.4.2 Decorin ICC assay

The storage medium was poured away from the dishes containing the cell coverslips and washed several times with PBS followed by 5 minutes in PBS/Tween (0.02%) in a humidity chamber. The coverslips were then drained and 50µl of decorin primary antibody (AB60425, goat anti human polyclonal, Abcam, UK) diluted at 1:100 in PBS supplemented with 1% bovine serum albumin (A7030, Sigma), was dispensed onto the coverslip. Full coverage was ensured before placing back into the humidity chamber for 90 minutes at room temperature. The coverslips were then washed in PBS several times and PBS/Tween (0.02%) for 2 x 5 minutes before the solution was drained off. The secondary antibody (a polyclonal rabbit anti-goat horseradish- peroxidase secondary antibody; P0449, Dako Ltd., Ely, UK) at 1:100 in PBS was dispensed onto the coverslips and incubated in the humidity chamber for 1 hour at room temperature. The 10 minute washes described above were then repeated. Once completed 50µl of Dako DAB/ substrate chromagen system solution was dispensed onto the coverslip and left for 6 minutes at room temperature before being rinsed several times with distilled water. Counterstaining and mounting was as described for Ki67. Decorin expression was scored using the H-score method as used for HER2, evaluating both membrane and cytoplasmic staining.

2.3 Microarray Gene Expression Profiling

Prior to this project, mRNA samples from each of the ER+ models before and after short-term Faslodex treatment (grown in phenol-red-free RPMI and 5% FCS medium) were routinely prepared by the Breast Cancer Molecular Pharmacology group cell culture staff and the samples microarrayed using a Cardiff University commercial service, so that gene expression analysis using the resultant microarray data could be performed as a focus of this project. In addition, further microarray data was made available for this analysis from triplicate samples similarly prepared from oestradiol (10^{-9}M) treated control MCF-7 cells and an acquired Faslodex resistant MCF-7 cell line in logarithmic growth phase (grown in phenol-red-free

RPMI and 5% charcoal-stripped FCS medium, the Faslodex-resistant model also cultured in the presence of 10^{-7}M Faslodex as described in Hiscox *et al.*, 2006). The methodologies employed for this cell preparation and commercial arraying are as described below:

2.3.1 Cell Lysis

For each ER+ cell model, untreated control cells and Faslodex treated (10^{-7}M) cells were seeded at 3 million cells per dish in phenol-red-free RPMI and 5% FCS and grown in experimental triplicate for 10 days in 150mm diameter dishes to determine the effects of short term Faslodex exposure on gene expression. Similarly, the Faslodex-resistant cell line and oestrogen-treated control were also grown in 150mm dishes in phenol-red-free RPMI and 5% charcoal-stripped FCS.

Medium was poured from each dish and briefly drained, followed by the addition of 10ml of tissue culture grade PBS which was left for 10 seconds before being poured away. This was repeated three times, with a thorough drainage following the last PBS addition. 1.5ml of Tri-Reagent was then dispensed onto the dish surface and gently rocked for 1 minute to ensure complete coverage of the plate. If cells on treatment plates were growth inhibited at time of lysis, 1.5ml of Tri-Reagent was used to lyse cells on 2 combined dishes to ensure adequate RNA yield for further experimentation. Using a sterile disposable cell scraper, the lysate was collected to one area at the bottom of the dish and half transferred via pipette into each of the two 1.5ml micro-centrifuge tubes. The lids were closed and inverted twice before being placed on dry ice. Once the process was completed for all dishes the frozen tubes were transferred to a -80°C freezer for storage.

2.3.2 Total RNA Isolation for Tri-Reagent-Lysed Samples

Cell lysates were removed from -80°C storage and thawed on ice. Samples were adjusted to 1ml using extra Tri-Reagent tubes were closed and gently mixed by inversion. Samples were left to stand for 5 minutes at room temperature to equilibrate. 200µl of chloroform was then added to each sample and vortexed for 20 seconds allowing a thorough mix of the solution and then left to stand at RT for 10 minutes. The tubes were placed into a precooled centrifuge (4°C, Labofuge 400R

centrifuge, Heraeus, Germany) and spun for 10 minutes at 16000g. At this point, the samples separated into 3 phases; the upper aqueous phase contains the RNA, while the mid phase contains DNA and the lower phenolic phase contains protein. Using a 200µl pipette the upper phase was removed carefully avoiding genomic DNA contamination and dispensed into a clean micro-centrifuge tube. 500µl of isopropanol was added to the RNA to precipitate it and vortexed briefly and allowed to stand at room temperature for 10 minutes. Samples were spun again for 10 minutes in a pre-cooled (4^oC) centrifuge at 16000g. The supernatant was discarded and the RNA remained as a pellet at the bottom of the microfuge tube. 500µl of 70% ethanol was added to wash the RNA pellet before being spun again in the pre-cooled centrifuge for 10 minutes at 16000g. The ethanol was discarded and the tube inverted to drain away any remaining ethanol. The RNA pellet was left to air dry for 5 minutes before being resuspended in 50µl of RNase-free water. The RNA concentration and purity was determined by spectrophotometry (260/280nm) and integrity checked via gel electrophoresis for each sample. If the RNA was intact then gel electrophoresis would result in the formation of 2 strong bands identifying the 18s and 28s ribosomal RNA with a smear in between identifying mRNA of different sizes. The identification of 2 strong bands implies RNA is in intact, and this was apparent for all samples subsequently examined in this project. All RNA samples were subsequently stored at -80^oC.

2.3.3 DNase Treatment of isolated RNA

This protocol used the RNase-free DNase reagents supplied with the Qiagen RNeasy Micro Kit in order to remove any trace of contaminating genomic DNA. For each sample, 45µg of RNA was adjusted to 87.5µl of water and 10µl of kit buffer and 2.5µl of DNAse I mix was added before being thoroughly mixed and incubated at room temperature for 10 minutes. 350µl of RLT buffer from the kit (supplemented with β-mercaptoethonal according to manufacturer's directions) was then added to the solution and mixed thoroughly. The RLT kit buffer is a denaturing lysis buffer that inactivates RNases and other proteins to prevent degradation of RNA. Once mixed, 250µl of 100% ethanol was added to each tube and mixed well.

An RNeasy MiniElute spin column (provided in kit) was then inserted into a 2ml kit collection tube and the entire contents of each micro-centrifuge tube transferred into the spin column. Lids were closed and spun at 10000g for 15 seconds using a benchtop microfuge (Biofuge, Heraeus, Germany). The flow-through was discarded and 700µl of RW1 kit buffer added to the column and spun again for 15 seconds at 10000g to wash the spin column membrane. Again the flow-through was discarded along with the collection tube. The column was then placed into a clean collection tube and 500µl of RPE kit buffer added. The tube was spun again at 10000g for 15 seconds and flow-through discarded; this again washed the spin column membrane. 500µl of 80% ethanol was then added to the column and spun for 2 minutes at 10000g. Flow-through and the collection tube were subsequently discarded. The column was then placed into a clean collection tube and spun with the lids open for 5 minutes at 10000g to dry the column. Drying was essential to prevent residual ethanol interfering with subsequent experimentation. The column was placed into a sterile 1.5ml micro-centrifuge tube and 14µl of RNase-free sterile water was added into the centre of the column, lids were closed and spun at 13000g for one minute to elute the RNA. The column was then removed and discarded and the micro-centrifuge containing approximately 12µl of eluted RNA was closed and placed on ice. The RNA concentration and integrity (spectrophotometery and gel electrophoresis (detailed in 2.3.2) was then determined for each sample, and all RNA samples subsequently aliquoted (1µg/7µl H20) and stored at -80°C.

2.3.4 Affymetrix microarraying procedure

Triplicate preparations of control and Faslodex-treated RNA samples prepared from all four cell models (and from the E2-treated MCF-7 and derived Faslodex resistant line) were sent to the Cardiff University Central Biotechnology Services (CBS), where initial quality assessments of the RNA were carried out using a Agilent bioanalyser. All samples provided were deemed appropriate for arraying (i.e. no RNA degradation or contamination) and so were then ran by CBS on Affymetrix Human Genome UI33Aplus2 Array GeneChips (containing approximately 23,000 gene probes) using standard Affymetrix protocols. In brief, this included first and

second strand synthesis of the RNA to obtain cDNA (Certa *et al.*, 2001). This subsequently underwent an *in vitro* transcription (IVT) reaction which biotinylated the cDNA which was then hybridised to the genechip. A biotinylated anti-streptavidin stain was then used to allow scanning of the chip to determine relative expression levels for all genes (using Affymetrix GeneChip Software) and the transcript level of a gene was determined by a fluorescent probe following the subtraction of mismatch and negative control probe expression. Affymetrix Microarray Suite 5.0 (MAS 5.0) provides powerful algorithms that analyse the resultant intensity data and generates the appropriate analysis output files for analysis for upload into appropriate programs for further analysis.

2.3.5 Hierarchical Clustering Analysis (HCA) of microarray data

Using an in-house software program, the raw gene expression data were uploaded for all 4 ER+ cell lines untreated and 10 day Faslodex treated, a median normalisation was carried out across all the arrays and all data was log-transformed. Statistical tests within the software were then carried out to identify robust transcriptome changes, firstly a t-test for significance (p<0.05) and also a significance analysis of microarrays (SAM) (Larsson *et al.*, 2005) with the false discovery rate (FDR) for gene changes set at <0.05. This stringent approach allowed identification of genes displaying robust transcriptome changes following Faslodex treatment in each model, where these genes were subsequently used by the program to generate hierarchical clustering diagrams, performing clustering in samples before or after Faslodex treatment to examine patterns across the models (and also encompassing further clustering as a quality control check for the triplicate data from each model).

2.3.6 Genesifter analysis of microarray data

Triplicate raw data was also uploaded to the online bioinformatic software GeneSifter (available at: https://login.genesifter.net/) where a median normalisation across all datasets and log transformation was carried out. Initial examination of two genes known to be ER-regulated (pS2, GREB2) was performed to further ensure the preparations were appropriate to determine novel Faslodex-

deregulated genes. This was achieved using the heatmap function within the software to visualise the expression profile across the models before and after Fasldoex treatment. Log2 intensity plots were also generated by the software to visualise level of expression across the models. The Faslodex-altered genes previously identified as significant using the t-test and SAM analysis were subsequently further analysed using this program. The fold change of change in gene expression was calculated by the software for all gene probes of interest, and analyses carried out to identify gene probes that underwent a significant, greater than 1.5 fold change in one or more cell lines (depending on hypothesis being examined).

Following identification of genes of interest, any multiple gene probes for a given gene were also analysed. The Affymetrix UI33Aplus2 genechips in some instances contained more than one gene probe for each gene, so expression changes of interest can be assessed via the multiple probes to evaluate if a consistent direction of change is occurring, providing further confidence that any Faslodex-promoted change in expression is robust.

However, it must be noted that particular importance was placed on the "jetset" gene probe for each particular gene in this project. Jetset is an online tool generated by the Technical University of Denmark and gives each Affymetrix gene probe a score based on specificity, splice isoform coverage, and robustness against transcript degradation. Using these scores the Jetset tool has selected a best single probe set for a given gene as the representative probe (see Appendix C for further information) (Li *et al.*, 2011) which can subsequently be used to determine most reliable profile in the array project of interest. In this project, therefore, for each gene of interest, expression heatmaps and log2 intensity plots were visualised across the models before and after Faslodex treatment, together with reporting associated fold changes, primarily using the jetset probe. Such data were also provided for genes indentified of interest in the oestradiol-treated MCF-7 versus Faslodex-resistant MCF-7 cells following data upload, median normalisation and log transforming of triplicate data. Expression "call" was also retrieved by GeneSifter across the models for genes of interest before and after Faslodex treatment.

Affymetrix UI33Aplus2 genechips provide further information on the reliability of a given expression change via the 'detection call algorithm'. This is intended to gauge whether the expression of a transcript has been reliably detected. A detection call of 'absent' suggested unreliable detection of expression or no expression while a 'present' detection call indicated expression had been reliably detected. A 'marginal' detection call signified partial detection of expression.

2.4 Ontological investigation of genes of interest from microarray data

Along with expression profiling using HCA and Genesifter analysis, ontological investigations were carried out for the genes of interest identified by microarray analysis in order to help prioritise these for further study. Using the multiple acronyms and names for genes of interest derived from Genesifter and Genecards (http://www.genecards.org/), PubMed (http://pubmed.com/) and Scopus (http://www.scopus.com) were used to ascertain reported function and also to carry out searches using a number of key words to identify any literature associations with cancer and anti-hormone response. Examples of key words and phrases used for this search were:

"breast cancer " "cancer" "proliferation" "survival" "apoptosis" "growth inhibition" "resistance" "anti-hormone" "Faslodex" "response" "estrogen" "estrogen receptor" "HER2" "erbB signalling" "complete-response" "Ki-67" "growth factor".

Ontological analysis in some instances revealed elements potentially critical in any function of the gene of interest (e.g. ligand where identified gene was a receptor), and so additional heatmaps and log intensity plots were retrieved to examine profile of such elements in the models. Additional bioinformatic analysis for the high priority gene DCN was performed using UCSC (http://genome.ucsc.edu/) and Transcriptomine (http://www.nursa.org/nursaGrails/transcriptomine/) tools to further determine if this was ER-regulated.

2.5 Verification of genes of interest from microarray data using RT-PCR

Following determining genes of interest across the ER+ model panel before and after Faslodex treatment using microarray analysis and ontological studies, it was important to attempt to verify their expression profile to help determine high-priority genes. Further triplicate RNA samples from the ER+ cell models both before and after 10 days Faslodex treatment were thus prepared in this project using an equivalent approach for lysis and RNA isolation to that in Sections 2.3.1 AND 2.3.2 Profile verification was then achieved using these samples for Reverse Transcription followed by Polymerase Chain reaction (RT-PCR):

2.5.1 Reverse Transcription (RT)

This procedure converts isolated RNA molecules into their complementary DNA (cDNA), which is necessary for the performance of PCR experiments. A mastermix solution was generated using 5μl of dNTPs (2.5mM, Invitrogen, UK), 2μl PCR 10x buffer (10mM Tris-HCl, pH8.3, 50mM NH4, 0.001% w/v gelatin) and 0.5μl MgCl$_2$ (50mM) in order to stabilise the ATP molecules, while also aiding the transfer of the phosphate groups during DNA extension. 2μl of dithiothreitol (DTT) (0.1M) was then added to the solution, where DTT is a reducing agent that breaks disulfide bonds of proteins. Finally, 2μl of random hexamers (100μM, Pharmacia Biotechnologies, UK) were added, which comprised a mixture of single stranded random hexanucleotides that aid the replication process (11.5μl total volume). All amounts as described were for one RNA sample.

1μg of RNA (in a total of 7.0μl water) of sample RNA was then added to the 11.5μl mastermix solution. The solution was then put into the PTC-100 thermocycler (MJ Research Ltd, USA) and denatured at 95°C for 5 minutes and then cooled rapidly to ice for 5 minutes. It was then pulse spun in a microfuge (Biofuge, Heraeus, Germany) to collect the solution and placed back on ice. 1μl of MMLV a reverse transcriptase enzyme along with 0.5μl of a commercial RNAse inhibitor RNasin^{TM} was then added giving a final volume of 20μl. The solution was then placed back

into the PCR machine to be reverse transcribed using the following programme parameters:

10 minutes at 22°C for annealing

40 minutes at 42°C to allow for reverse transcriptase extension

5 minutes at 95°C for denaturing.

The cDNA was cooled to 4°C before being stored at -20°C until needed.

2.5.2 Polymerase Chain Reaction (PCR)

This technique is used to amplify a particular DNA region that lies between two regions of a known DNA sequence. Two short DNA fragments known as oligonucleotide primers are synthesised to be complementary to DNA sequences on both strands of DNA, flanking the region of interest. The reaction exploits the ability of DNA polymerases to make copies of genetic material. In the presence of deoxynucleotide triphosphates (dNTPs) consisting of all four bases, dATP, dTTP, dGTP, dCTP, the heat stable DNA polymerase, Taq, will copy a strand of DNA. During the PCR reaction there are repeated cycles of heat denaturation to separate the newly formed double strand DNA, followed by subsequent cooling to allow the DNA primers to attach to their complementary sequences and then extension of the annealed primers with the polymerase. Following the first cycle of the reaction the products formed can stand as DNA templates for subsequent cycles, thus after each cycle the amount of DNA produced doubles to that of the previous cycle, with exponential production of the PCR product.

2.5.3 Oligonucleotide Design

As the PCR was to be carried out in order to verify gene expression profiles identified as of interest from the microarray data, PCR primers were first designed which recognised similar mRNA regions to those used by the differentially-expressed gene probes on the Affymetrix Human Genome UI33Aplus2 GeneChips. To do this, the relevant Affymetrix selected gene probe sequence was input into the online program Primer3 (http://primer3.ut.ee/). From these sequences, Primer3 identified potential primer pairs whilst allowing the user to consider the product size and melting temperature as well as the likelihood of unwanted primer dimer

formation (ratio of guanine to cytosine bases) (Rozen *et al.,* 2000). Once primer pairs had been selected, they were input into another online program called the Basic Local Alignment Search Tool, BLAST (http://blast.ncbi.nlm.nih.gov/). BLAST primarily compares sequences across the genome and locates regions of similarity between DNA sequences and calculates the statistical significance of matches. Inputting the primer sequences ensured that the primer sequence was specific to the gene of interest (McGinnis and Madden, 2004).

Specific Oligonucleotide sequences employed in this study

Table 5: Primer sequences used in the PCR verification experiments with the predicted PCR product size (amplicon) and optimised cycle number.

Gene Name	Forward Primer	Reverse Primer	Product size (bp)	Cycle Number used
DCN	GAAGGGAGAAGACATTGGTTTG	GCAGAGGGGTAAATTGAAACA	193	33
CASP1	TTTCTTGGAGACATCCCACA	CTCTTTCAGTGGTGGGCATC	162	31
PCDH7	CTACTCCGAAACCTGCTGGA	CCGCCTCTTTAAGAATGGAA	215	30
PRKACB	AAGAGCCTTGGTGTCTGTCC	CCAATGGGCAGTTAACACAA	150	29
KITLG	GGATGGATGTTTTGCCAAGT	TCTTTCACGCACTCCACAAG	172	29
VEGFC	GGAAAGAAGTTCCACCACCA	TTTGTTAGCATGGACCCACA	249	29
CXCR4	TTCTACCCCAATGACTTGTG	ATGTAGTAAGGCAGCCAACA	206	28
GABBR2	TATGCCTACAAGGGACTTCTCATGTTG	ATGATGACCAGAGCCACGATGCAG	206	28
TXNIP	TGGTGATCATGAGACCTGGA	AGGGGTATTGACATCCACCA	200	30

TGFB2	CCCGAGACTGACACACTGAA	CCCTGACTTTGGCGAGTAAG	128	30
UPK3B	TTTCTCTCCCTCTCCAAGCA	AACAACCAGATCCCATGAGC	110	30
GFRA1	AACATCCCTAACGAGCATCC	AGCTCAGCATGCAGCGAT	420	28
VGLL1	CCAGCCTTCCAAATGAAACT	ATGCTGCAGGTATCGATGTG	101	28
ARTN	TTCATGGACGTCAACAGC	AGGCACTTTCAACCAAGC	478	27
CDH2	TTGGGGAGGGAGAAAAGTTC	GCTGGGTCAGAGGTGTATC	230	27
β-actin (big)	CTACGTCGCCCTGGACTTCGAGG	GATGGAGCCGCCGATCCACACACGG	385	24
β-actin (small)	GGAGCAATGATCTTGATCTT	CCTTCCTGGGCATGGAGTCCT	204	24
ERα	GGAGACATGAGAGCTGCCAAC	CCAGCAGCATGTCGAAGATC	432	26
HER2	CCTCTGACGTCCATCATCTC	ATCTTCTGCTGCCGTCGCTT	98	25

2.5.4 PCR procedure

Using a 0.5ml sterile eppendorf tube and keeping all solutions on ice, the PCR mastermix was generated using the following (amounts shown are per individual sample):

17.8μl sterile RNA/DNAse free water

2.5μl of PCR 10x buffer (10mM Tris-HCl, pH8.3, 50mM NH4, 0.001% w/v gelatin)

0.75μl MgCl$_2$ (50mM)

2μl dNTPs (2.5mM)

0.625μl of each primer for gene of interest (20μM)

0.2μl TAQ DNA polymerase (5units/μl)

The mastermix solution was mixed thoroughly and 0.5µl cDNA from each sample (equivalent to 0.05µg RNA) was added, giving a final volume of 25µl. 1 drop of sterile mineral oil was dispensed onto the top of each resultant sample to prevent evaporation during the reaction. Reaction mixtures were then placed into a PTC-100 thermocycler (MJ Research Ltd, Massachusetts, USA) using the following cycle parameters

First cycle:

2 minutes at 94°C to allow denaturation of the DNA. This was followed by temperature reduction to 55°C for 1 minute to allow the annealing of the primers and Taq polymerase to the cDNA. The temperature then increased to 72°C for 5-10 minutes to allow extension of the primers, thus generating the PCR product.

Subsequent cycles (20-40, optimised according to gene of interest):

The solution was heated to 94°C for 30 seconds, cooled to 55°C for 1 minute, and then reheated to 72°C for another minute.

Final cycle

The solution was heated to 94°C for 1 minute, cooled to 55°C for 1 minute and the reheated to 60°C for 10 minutes.

Once the reaction was finished, the PCR products were visualised on ethidium bromide (EtBr) stained agarose gels under ultra violet (UV) light illumination. For equivalence of loading on such gels and to subsequently gauge the expression of the gene of interest, the constantly expressed house-keeping gene β-actin was amplified in parallel, using the cycle sequence parameters as above for a total of 25 cycles.

2.5.5 PCR product visualisation via gel electrophoresis

A 2% agarose gel was prepared in 1X Tris acetate (TAE) buffer (pH8.3) and ethidium bromide added to a final concentration of 0.1µg/ml. Once set, the gel was placed into a Mini-Sub Cell GT electrophoretic tank (Bio-Rad Laboratories Ltd, Herts, UK) and filled with 1X TAE buffer. 5-10µl of each sample PCR product was mixed with

3µl of gel loading buffer (40% sucrose and bromophenol blue) and added to each well of the gel. For product size determination, a DNA marker ladder was routinely loaded alongside the samples on the gels (Hyperladder IV, Bioline Ltd, Herts, UK). Once loaded the gel was run at 100V for 30 minutes and visualised on a standard UV transilluminator using the AlphaDigiDoc imaging software (Genetic Technologies Inc, Miami, USA).

2.5.6 Real-Time quantitative PCR (qPCR)

Real-Time PCR was carried out to further confirm the efficient knockdown of DCN by shRNA.

RNA was extracted and reverse-transcribed as previously described in Sections 2.3.2, 2.3.3 and 2.5.1 using further triplicate preparations of each model before and after 10 days Faslodex treatment. The resulting cDNA was then analysed in triplicate using the MJ Research DNA Engine Opticon 2 system. SYBR green hot-start polymerase assays were used to determine the gene expression of the priority target gene DCN, along with β-actin which was used as an endogenous control and for normalisation of data. All PCR reactions were carried out in 96 well PCR plates (Bio-Rad Laboratories, Herts, UK) in a total of 25µl comprising 12.5µl of 1x DyNAmo PCR solution (Finnzymes, Finland) containing dNTPs, PCR buffer, Taq polymerase and SYBR green dye), 20µM forward and reverse primers (0.18µl), 5.14µl water and 0.05µg cDNA. Plates were briefly centrifuged (30 seconds, 2000rpm, Lbofuge 400R centrifuge, Heraeus, Germany) before undergoing the following qPCR cycling conditions:

Step 1: Initial denaturation - 95°C/15minutes
Step 2: Denaturation - 94°C/30seconds
Step 3: Annealing - 55°C/30 seconds
Step 4: Extension - 72°C/30 seconds
Step 5: Melting curve analysis – from 55°C to 95°C

PCR product homogeneity in standards and unknown samples was routinely checked by 'melt curve' analysis which was performed following every PCR run. A

melt curve allows a comparison of the melting temperatures of amplification products. To produce melt curves, the final PCR product was exposed to a temperature gradient from 55°C to 95°C while fluorescent read outs were continually detected. This causes denaturation of all double-stranded DNA (dsDNA) and at a given point dsDNA melts into single-stranded DNA (ssDNA) and a drop in fluorescence is observed. As products of different lengths and sequences will melt at different temperatures, distinct peaks would be observed if more than one PCR product is present. However, product amplification should be specific for a given product expected from the primer pair and thus only one peak should be observed. If multiple peaks are present this may indicate non-specific binding of the primers. A single peak was observed in this project for DCN as shown in Figure 4. Expression of genes of interest was subsequently normalised to β-actin and quantified using a standard curve generated from serial dilutions of cDNA from a pool of breast cancer cell lines for both the gene of interest and the housekeeping gene.
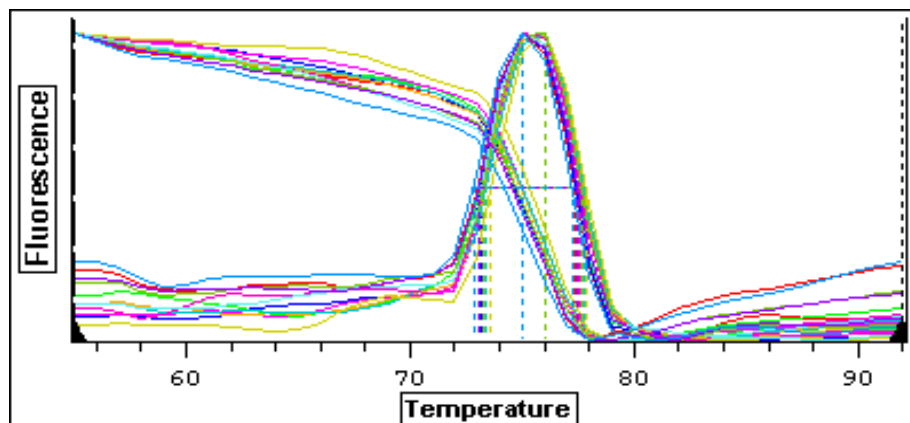
Figure 4: DCN melt curve demonstrating the single peak where ds-DNA becomes ss-RNA and the drop in fluorescence that occurs during this event.

2.5.7 PCR statistical tests

As stated in 2.1.4.

2.6 Analysis of genes of interest in Clinical Breast Cancer Expression Microarray Datasets

2.6.1 Analysis of genes of interest in patients with tamoxifen outcome data

To begin to gauge relation of the genes of interest with endocrine outcome in the clinic (and thus potential relevance to response or failure), virtual datasets comprising Affymetrix microarray expression data from ER+ tamoxifen-treated breast cancer patients were interrogated using publically-available KMPlotter and GOBO tools:

2.6.1.1 Kaplan-Meier Outcome Plotter (KMPlotter)

KMPlotter (http://kmplot.com/analysis/) is an online tool that can interrogate Affymetrix microarray chip-derived mRNA expression data accumulated in KMPlotter from breast cancer patients prior to therapy in relation to outcome measures including relapse free survival. The aim of the tool is to generate survival plots which can be used to assess how expression levels of a particular gene relate to clinical outcome (Györffy *et al.,* 2010). KMPlotter splits the patients into two groups based on best fit of expression of a particular gene (i.e. high and low expressers, obtained for example using median, lower quartile or upper quartile cut-points) and integrating this data simultaneously with clinical data so the two groups can be compared with respect to relapse free survival (Györffy *et al.*, 2010). In this project, KMPlotter was used to analyse clinical relevance of genes identified of interest from the models in an ER+ breast cancer patient cohort (n=657, with up to 20 year followup) who had been subsequently been treated with tamoxifen to determine the relationship with response duration to this antihormone (RFS). Equivalent analysis was also carried out on ER+ patients who were systemically untreated to investigate any inherent prognostic value of genes of interest (n=785 patients). All analyses were carried out using the jetset Affymetrix gene probe (Li *et al.,* 2011), with output presented as Kaplan-Meier survival curves with associated Hazard ratio (HR) and significance value (log rank p <0.05).

2.6.1.2 Gene expression-based Outcome for Breast cancer Online (GOBO)

The GOBO tool (http://co.bmc.lu.se/gobo) operates in similar manner to KMPlotter. This tool has diverse capabilities but again fundamentally aims to integrate Affymetrix gene expression data with patient outcome parameters in order to determine the relevance of a gene of interest clinically in breast cancer. Of note, GOBO allows splitting of the patient dataset into more than 2 groups based on increasing level of gene expression thus gauging whether the magnitude of gene expression is associated with an improved or poorer outcome (e.g. RFS). This analysis is again displayed as Kaplan-Meier plots with a significance value ($p < 0.05$). One further capability of the tool is that it can determine if the expression of a given gene is associated with a particular molecular subtype of breast cancer as well as with disease grade, where relationships are displayed as boxplots. In this project, GOBO was used to determine the clinical relevance of genes of interest in relation to tamoxifen outcome in the same manner as KMPlotter but patients were split into 3 groups to determine if gene expression level displayed a graded relationship with RFS GOBO was also used to determine if gene expression was associated with particular molecular subtype to gauge further if the gene associated with a more or less aggressive disease (for example, HER2+ vs. Luminal A). It should be noted that GOBO does not contain as many datasets as KMPlotter thus patient numbers are lower (n=326 for tamoxifen treated patients, with 10 year follow-up). Again, all analyses were carried out using jetset gene probe sets to represent each gene of interest (Li *et al.*, 2011)

2.6.2 Analysis of genes of interest using Faslodex-treated breast cancer clinical trial (NEWEST) data

Through collaboration with AstraZeneca, this project was able to access gene expression data accumulated from a clinical breast cancer trial treated with Faslodex to interrogate genes of interest from the cell models. The NEWEST (Neoadjuvant Endocrine Therapy for Women with Estrogen-Sensitive Tumors; 9238IL/0065) trial is a neoadjuvant clinical trial designed by AstraZeneca in order to compare 250mg Faslodex with 500mg Faslodex in ER+ postmenopausal patients. The trial design was based on previous immunohistochemical (IHC) marker data (i.e.

ER, PgR and Ki67) indicating that Faslodex acted in a dose-dependent manner in clinical breast cancers. Thus, by doubling the dose efficacy should be increased (including greater inhibition of ER signalling), potentially leading to an improved anti-tumour response (Kuter *et al.*, 2012). This trial collected core tumour biopsies at baseline, week 4 and at week 16 (surgery). Cores were formalin-fixed and paraffin-embedded before biomarker assessment was carried out using established IHC assays (Ki67, ER and PR) and assessed using percentage positivity and H-score as described in Kuter *et al*. In addition, a proportion of samples primarily at baseline and at 4 weeks treatment had been microarrayed for gene expression analysis. RNA was extracted from core biopsies from a subset of patients in both trial arms and underwent microarray gene expression profiling using the Illumina platform (carried out by the laboratory of Professor Mitch Dowsett, ICR, London). In the present project, the resultant microarray expression database (and parallel IHC marker data) was made available for n=24 matched samples to allow interrogation of whether 500mg Faslodex treatment altered expression of the genes of interest, and to examine if such gene changes associated with changes in proliferation (Ki67) during treatment. To interrogate genes of interest in this project, the Illumina expression data was first transformed using Illumina software (LumiExpresso) which performed background correction, variance stabilisation and log2 normalisation of the data and removed genes that are were not expressed above the background level (as defined by the negative control gene probes) ensuring that the remaining probes are detecting expression.

Normalised microarray data and the associated IHC data from the NEWEST trial were then uploaded into SPSS for statistical analysis. A paired t-test was initially carried out using the matched baseline and on-therapy (4 weeks) data to determine if gene expression for genes of interest was significantly altered by Faslodex treatment in the patient samples. Genes that neared significance or met significance were more closely analysed and fold change of expression was calculated.

A Mann-Whitney U test was then used to determine if the change in gene expression promoted by Faslodex (induction or suppression) was significantly

(p<0.05) associated with change in Ki67 and ER protein expression (IHC data) following 4 weeks of treatment. Change in Ki67 was calculated by subtracting the on-therapy % positivity value from the baseline % positivity value while for ER on therapy Hscore was subtracted from baseline Hscore.

2.6.3 Analysis of genes of interest using aromatase inhibitor-treated breast cancer clinical trial (Trial 223) data

Microarray data from Trial 223 were also available for interrogation of the genes of interest in this project. Trial 223 was a neoadjuvant study designed to determine if combination treatment of anastrozole and gefitinib (an EGFR inhibitor) may increase drug sensitivity in those tumours that are generally not sensitive to anti-hormonal measures (Smith *et al.*, 2007). In this study, breast cancer patients were postmenopausal, with non-metastatic disease and tumours were ER and/or PgR positive. All patients received 1mg anastrozole daily for 16 weeks before surgery took place. There were 3 arms to the trial and patients were split in 2:5:5 ratio to receive anastrozole and gefitinib 250mg daily for 16 week trial period (arm A); placebo daily for initial 2 weeks followed by 14 weeks of 250mg gefitinib daily (arm B); and finally patients received placebo tablet daily for the complete 16 week trial (arm C). Core biopsies were taken at baseline, 2 weeks and 16 weeks (surgery). The primary endpoint in the trial was KI67 IHC analysis and secondary endpoint was tumour response. However, microarray gene expression profiling was also again carried out by the laboratory of Professor Mitch Dowsett. ICR, London. RNA samples were taken from the core biopsies from a subset of patients in trial arms B and C. RNA was extracted in conjunction with Illumina protocols and gene expression profiling was carried using the Illumine platform and data transformed using the appropriate software as detailed previously. Again by collaboration with AstraZeneca, access to this normalised microarray data in the present project allowed analysis of anastrozole-induced gene changes focussing on the genes of interest from the models and utilising the matched expression data at baseline and at 2 weeks, which encompassed a patient cohort who had only received anastrozole treatment. The statistical approach was comparable to that taken for the NEWEST data using SPSS

2.7 Functional studies of high priority gene (decorin) using shRNA

2.7.1 Lentiviral DCN shRNA

Short-hairpin RNA (shRNA) is a sequence of RNA that can make a short turn hairpin, silencing expression of a target gene. This technology was utilised to permanently silence the decorin (DCN) gene in the T47D cell line, permitting growth studies to investigate if such knockdown influenced Faslodex response and parallel DCN expression analysis using PCR. The Dharmacon® SMARTvector 2.0 system was employed, which uses lentiviral vectors to stably deliver and express genetically engineered RNA to silence the target gene. The lentiviral shRNA particle binds to the cell and delivers the genetically engineered RNA into the cytoplasm where it is reverse-transcribed into DNA. The DNA is transported into the host cell nucleus where it is incorporated into the host genome. Subsequently, the silencing construct is stably and constitutively expressed as a pri-microRNA (pri-miRNA) and is processed by Drosha. Exportin 5 then transfers the pre-shRNA out of the nucleus for it to be processed by Dicer and subsequently enters the RNA-induced silencing complex (RISC) pathway. The antisense strand of the shRNA directs RISC to mRNA of a complementary sequence; when RNA of perfect complementation is found (target mRNA) RISC cleaves the target mRNA resulting in target/DCN silencing.

The SMARTvector 2.0 lentiviral constructs contain a turboGFP reporter gene allowing assessment of transduction. The constructs also contain a puromycin resistant gene (PuroR) to allow for selection of cells that have been successfully transduced.

2.7.2 Puromycin Selection Conditions

T47D cells were plated into a 24-well plate (40,000 cells per well) in RPMI medium + 5% FCS and left to adhere overnight. Growth medium was replaced with medium containing a range of puromycin concentrations (in triplicate); 0.1, 1, 2, 5, 7, 10μg/ml (as suggested by the manufacturer and diluted in cell medium). Medium was replenished every two days and the cells were assessed via a microscope daily to determine the minimal concentration of puromycin that killed all cells between days 4-6 (1μg/ml).

2.7.3 Lentiviral shRNA

The lentiviral shRNA experiments were carried out at Imperial College London under the supervision of Professor Simak Ali and Dr Laki Buluwela who have much experience in carrying out shRNA gene knockdown. The SMARTvector 2.0 system provides 3 constructs targeting various sequences of the target gene allowing evaluation of each of the constructs targeting the gene of interest (Table 6 for DCN), as well as a negative non-targeting (NT) control construct. Following the manufacturer's instructions, using a 96 well plate, T47D cells were plated in triplicate at seeding densities of 5000 or 10,000 cells per well. The shRNA lentiviral particles were then added at varying multiplicity of infections (MOI) i.e. the ratio of transducing units (TU) (viral particles) per cell set at 0.5, 1.8, 5 and 10. Some wells were left devoid of particles as a negative experimental control. To calculate the amount of virus required for a given MOI, the following formula was used as indicated by the manufacturer:

$$(MOI*CN)/VT$$

MOI-Multiplicities of infection

CN-Cell number

VT-stock viral titre (TU/µl)

Table 6: The gene target sequence for each of the shRNA constructs used to target DCN gene expression as well as the viral titer provided by the manufacturer (number of transducing units provided (TU/ml)

Gene symbol	Gene target sequence	Titer (TU/ml)
DCN (SH1)	CTGTCAATGCCATCTTCGA	1.82×10^5
DCN (SH2)	GTTGATGTTAACTGAGCTA	1.41×10^5

The plate was then placed back into the incubator for 24 hours before the medium containing lentiviral particles was removed and replaced with the usual medium (RPMI + 5% FCS). Within 48-72 hours the genetically engineered material should be

incorporated into the host genome and thus the turboGFP gene should be expressing detectable levels of GFP allowing the transduction efficiency to be assessed. Once detectable levels of turboGFP were detected using a fluorescence microscope (Leica Microsystems) and the cell confluency was greater than 70%, 1µg/ml of puromycin was added to the growth media in order to select for those cells that had been effectively transduced. The puromycin selection was subsequently maintained throughout the culture of each of the new cell lines. Other than puromycin addition, each model was cultured the same as the T47D wild-type cell line for growth and PCR studies to compare the DCN knockdown constructs versus the NT control using procedures as described in Sections 2.1, 2.2.4 and 2.5 (including cell growth experiments, ICC and PCR, further information provided in the figure legends of chapter 10).

Chapter 3

In vitro evaluation of the duration of initial Faslodex response and the development of acquired resistance in cell models of ER+/HER2- and ER+/HER2+ breast cancer

3.1 Introduction

Two important principles of targeted therapy have recently arisen: (1) that significant genomic heterogeneity exists among tumours of the same origin and such heterogeneity can have a profound impact on clinical response (Carey *et al.*, 2013; Higgins *et al.*, 2011) and (2) drug-induced transcriptome events can also affect the subsequent clinical response (Gee *et al.*, 2003; Nicholson *et al.*, 2005).

With regards to breast cancer heterogeneity, this is often not factored into research activities. In most instances, the field largely relies on single cancer cell lines and with respect to hormone-dependent breast cancer the MCF-7 cell line is primarily used due to its high ER expression and subsequent hormone-sensitivity (Levenson *et al.*, 1997). As such it is becoming increasingly clear that the use of the MCF-7 cell line to represent all ER+ breast cancer is not adequate. This issue has been summarised and discussed in the published report from Holliday and Speirs where they have concluded that even though significant advances have been made in cancer biology through the use of individual cancer cell lines, it is time to move from the "one marker, one cell line" approach (Holliday and Speirs, 2011). Certainly, breast cancer has been subdivided into at least 6 molecular subtypes all associated with different clinical prognoses and it is a fair assumption that these differing responses are in part due to inherent genetic differences between the sub-types.

Similarly, drug-induced genomic events have been poorly characterised (Gee *et al.*, 2011), particularly to Faslodex and it is self evident that a further understanding of

such events may aid in the identification of novel therapies to improve antihormone response or new biomarkers to help stratify patients who will undergo an improved clinical response. While absence of ER in a breast cancer is a robust marker of endocrine resistance (Gutierrez *et al.*, 2005; Kumar *et al.*, 1996), currently in ER+ disease we are unable to competently predict the magnitude/duration of patient response (if any) to anti-hormone treatment and our knowledge in this regard is again poorest for Faslodex.

The purpose of the work described in this thesis is to identify and characterise mechanisms of response and resistance to the antihormone Faslodex *in vitro*, encompassing drug-induced events and also taking into account an aspect of heterogeneity that exists in ER+ breast cancer; HER2 status. Four ER+ breast cancer cell lines were utilised; 2 where the HER2 gene is amplified (BT474 and MDA-MB-361) and 2 that have inherently low levels of HER2 and thus represent ER+ HER2- disease (MCF-7 and T47D) (Neve *et al.*, 2006). Approximately 15-20% of breast cancers over-express the oncogene HER2 (Baehner *et al.*, 2010) and this tumour subset has been deemed the HER2+ molecular subtype and is associated with a poorer prognosis and more aggressive disease. Approximately 10% of ER+ breast cancer patients express HER2 (Dowsett *et al.*, 2008) and it has been recognised for many years that inherent overexpression of HER2 predicts a reduced response to anti-hormone measures including tamoxifen (Pietras *et al.*, 1995; Sabnis *et al.*, 2009). However, the relationship between Faslodex response and HER2 has not been fully established.

In this chapter, the ER and HER2 status of each of the cell lines is confirmed and the effect of continuous Faslodex treatment on their growth is examined. By carrying out such investigations the aim was to determine the duration of initial Faslodex response in each of the cell models and to determine if and when a resistant phenotype emerged.

3.2 Results

3.2.1 ER and HER2 status of the 4 cell lines

PCR and ICC staining prior to Faslodex treatment was carried out to confirm the status of ER and HER2 in the four cell lines (as described by Neve *et al.*, 2006); Figures 4 and 5.
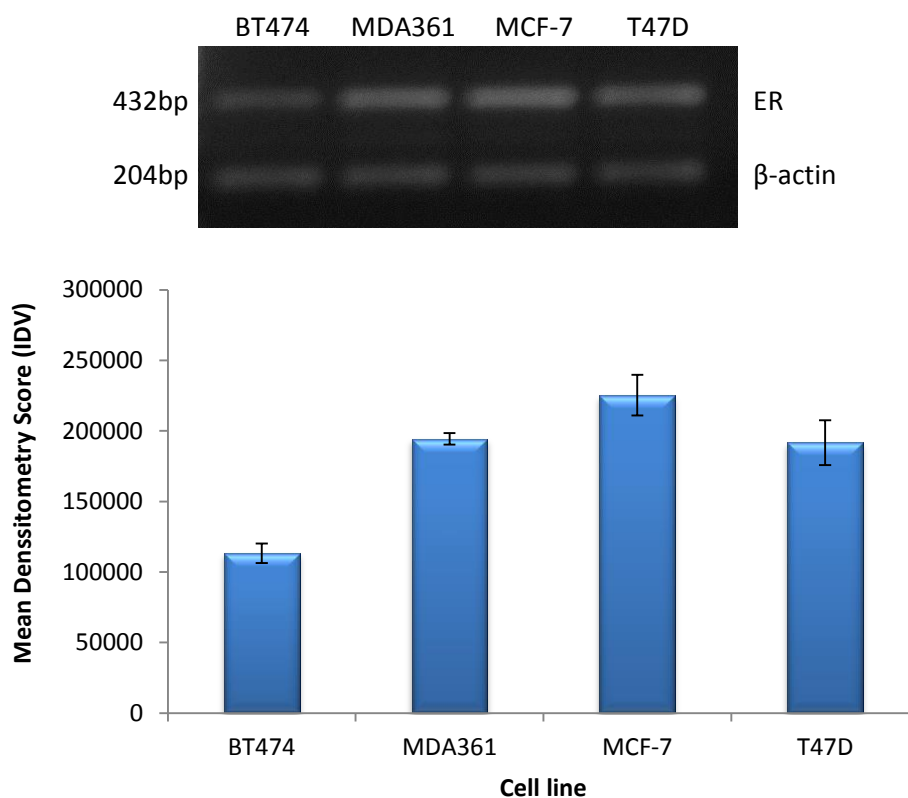
Figure 4: Representative PCR image in the 4 breast cancer cell lines, with the corresponding densitometry graph representing the mean data for ER expression normalised to β-actin (n=3).

MCF-7	**T47D**

H-Score: 179
95% positivity

H-Score: 76
85% positivity

BT474	**MDA-MB-361**

H-Score: 64
80% positivity

H-Score: 74
80% positivity

Figure 5: ICC analysis of ER in the 4 breast cancer cell lines utilised in this project, showing representative images (original magnification=x20) and associated average Hscores examined over replicate coverslips

All of the 4 cell lines used in the study expressed ER at the mRNA level (Figure 4) and displayed at least 80% ER positivity at the protein level (Figure 5). Staining, however, was highly heterogeneous with levels varying not only across the cell models but also within any one cell line. The strongest ER staining was observed in the MCF-7 cell line and lowest ER stain (and ER mRNA expression) in BT474.
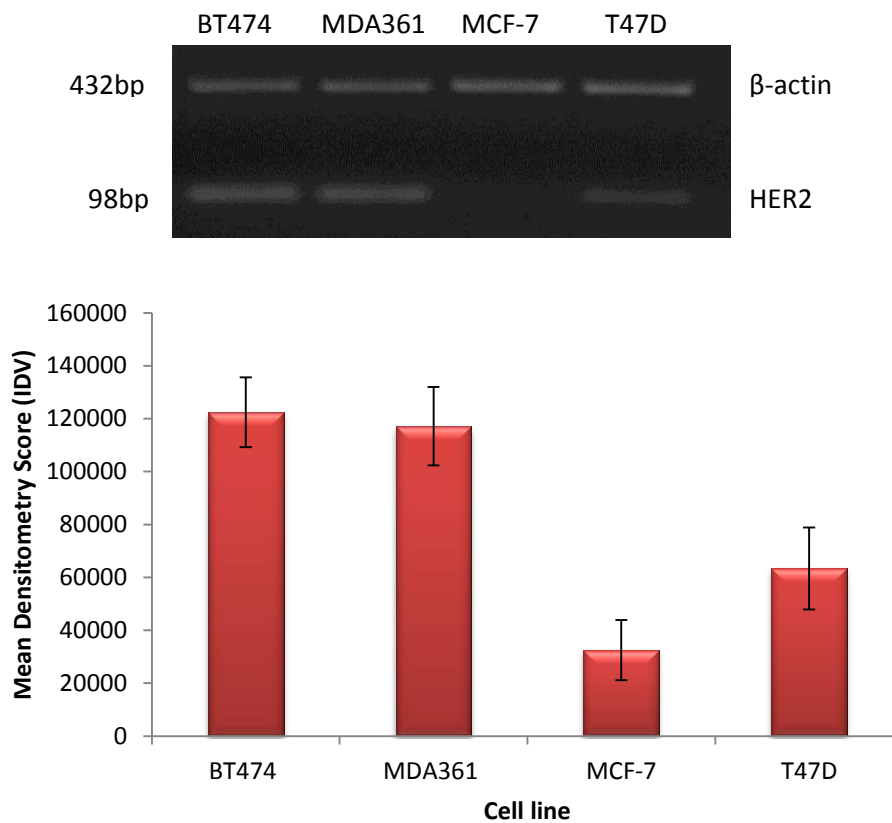
Figure 6: Representative PCR image in the 4 breast cancer cell lines, with the corresponding densitometry graph representing the mean data for HER2 expression normalised to β-actin (n=3).

The expression of the RTK HER2 gene in the 4 cell lines is shown in Figure 6. High levels of HER2 mRNA were recorded in BT474 and MDA-MB-361 cell lines, consistent with its reported amplification in these cells. Lowest levels of HER2 mRNA were seen in the MCF-7 cell model, with weak detection in T47D cells. Figure 4 displays intense immuno-staining of this RTK at the plasma membrane and to a lesser extent throughout the cytoplasm in the BT474 and MDA-MB-361 cell lines. Indeed, in each of these cell lines, it was necessary to dilute the HER2 primary antibody 2x further than recommended in the immunocytochemical test due to the extremely high levels of HER2 to allow HScore analysis. Clinically, patient biopsies undergo the Hercep Test to determine immunocytochemically if HER2 is expressed by a tumour and thus determine if Herceptin treatment is appropriate or not. In order to receive Herceptin, stained samples must meet the requirements for 3+ staining, described as "a strong complete membrane stain in 10% or more of the tumour cells". Both BT474 and MDA-MB-361 cell lines meet this requirement

indicating that they are a good representation of the clinical HER2+ phenotype. In contrast, only very low levels of HER2 staining was seen at the plasma membrane of the MCF-7 and T47D cell lines (Figure 7) and moreover in only a small proportion of cells. For the purpose of this study, these cell lines have been taken to represent ER+/HER2- disease.

MCF-7

H-Score: Membrane: 20
Cytoplasmic: 10

T47D

H-Score: Membrane: 30
Cytoplasmic: 15

BT474

H-Score: Membrane: 220
Cytoplasmic: 140

MDA-MB-361

H-Score: Membrane: 200
Cytoplasmic: 90

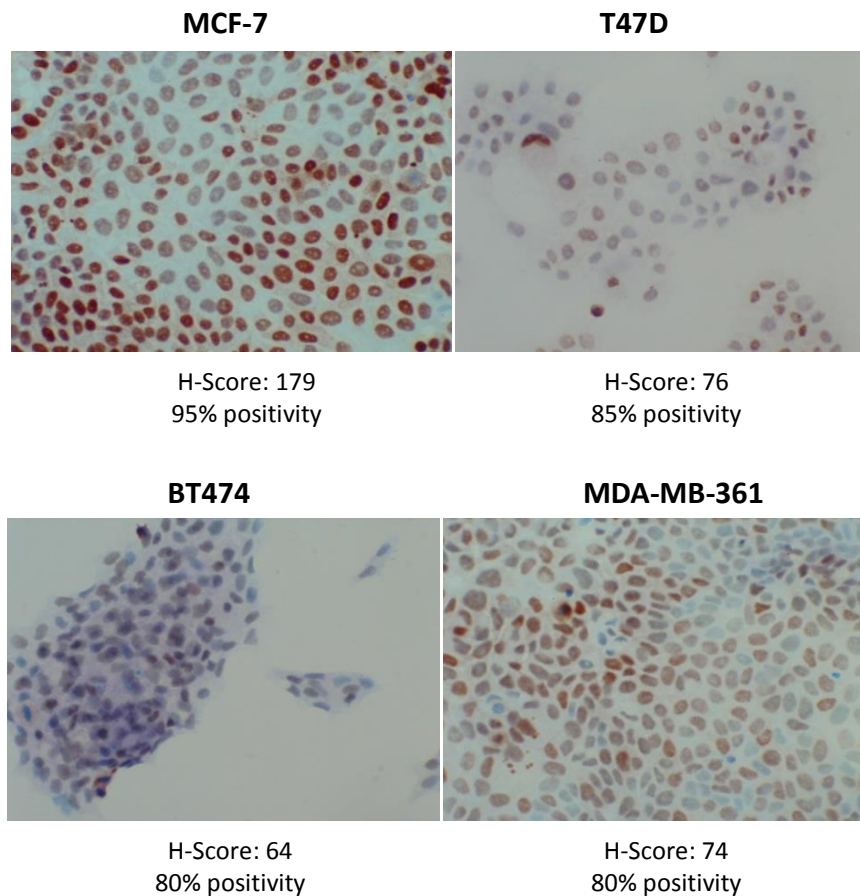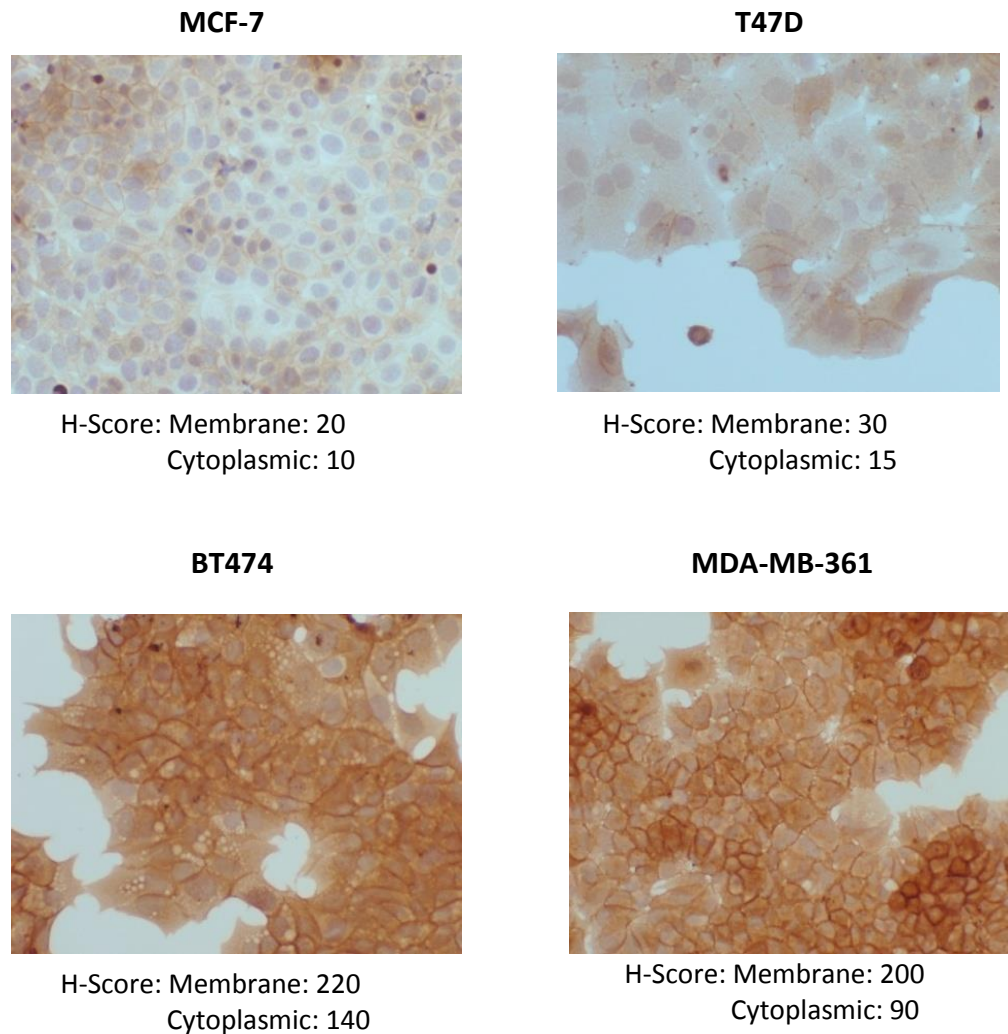Figure 7: ICC analysis of HER2 in the 4 breast cancer cell lines utilised in this project, showing representative images (original magnification=x20) and associated average H-scores examined over replicate coverslips

3.2.2 Faslodex dose-response and down-regulation of ER

An extensive Faslodex dose-response experiment was initially performed on the MCF-7 cell line to measure the degree of Faslodex promoted ER down-regulation. This was deemed maximal at 10^{-7}M (Appendix D). This concentration is in keeping

with that used by the majority of researchers who have also demonstrated effective ER down-regulation and growth inhibition in ER+ breast cancer cell lines as well as inhibition of oestrogen stimulated growth (Memminger *et al.*, 2012; Lupien *et al.*, 2010; Frogne *et al.*, 2009).

A narrower dose response study was subsequently examined in the 4 cell lines, which verified the maximal growth inhibitory properties of 10^{-7}M Faslodex. At this dose, Faslodex significantly reduced cell proliferation in the four cell lines, as monitored by cell growth data (Figure 8), and also decreased ER level (Figure 9). Of the 4 cell lines examined, MCF-7 cells showed an approximately 90% fall in cell number, while an 80%, 60% and 50% fall was seen in MDA-MB-361, T47D and BT474 cells respectively, declines broadly paralleling the maximum growth inhibition achieved in each line Substantial ER down-regulation (MCF-7 55%, T47D 88%, BT474 96%, MDA-MB-361 91%) was observed in all 4 models.
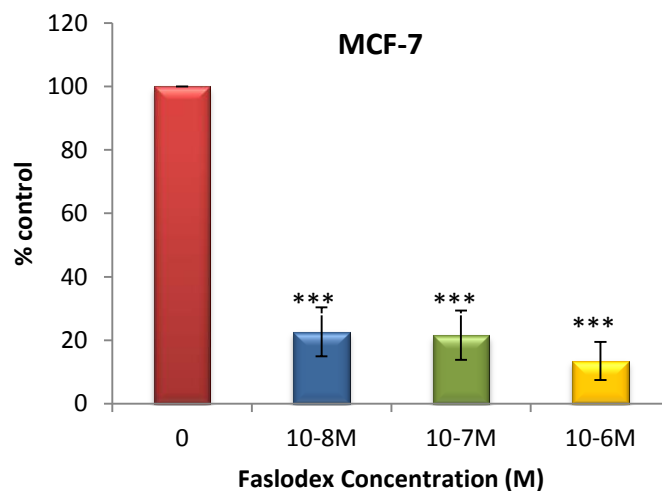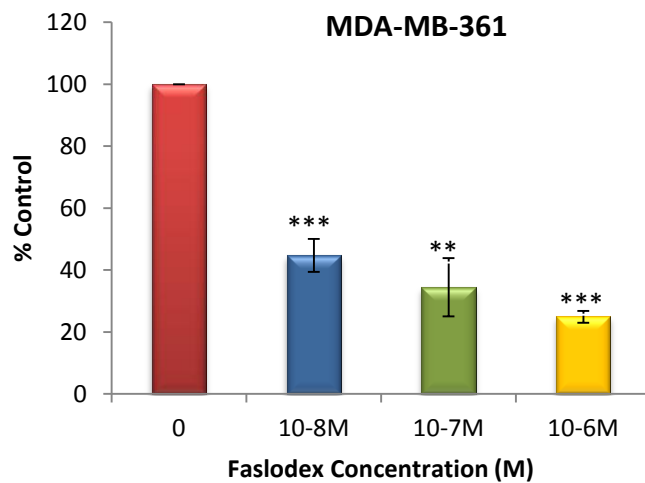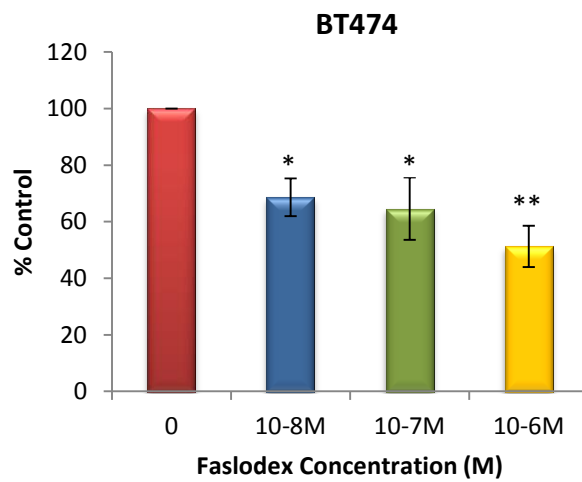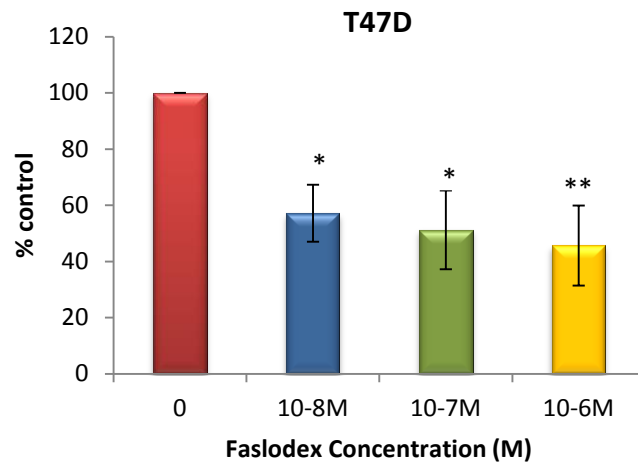
Figure 8: Effects of increasing concentrations of Faslodex (0.01 to 1 μM) on the basal growth of MCF-7, T47D, BT474 and MDAMB361 cells after 7 day treatment. The results are expressed as means ± SEM of triplicate experiments. *$P < 0.05$ versus untreated control, **$P < 0.01$ versus untreated control, ***$P < 0.001$ versus untreated control.

	Control	Faslodex 10^{-7}M
MCF-7	Hscore: 150	Hscore: 63
T47D	Hscore: 85	Hscore: 5
BT474	Hscore: 60	Hscore: 2.5
MDA-MB-361	Hscore: 80	H-Score: 7.5
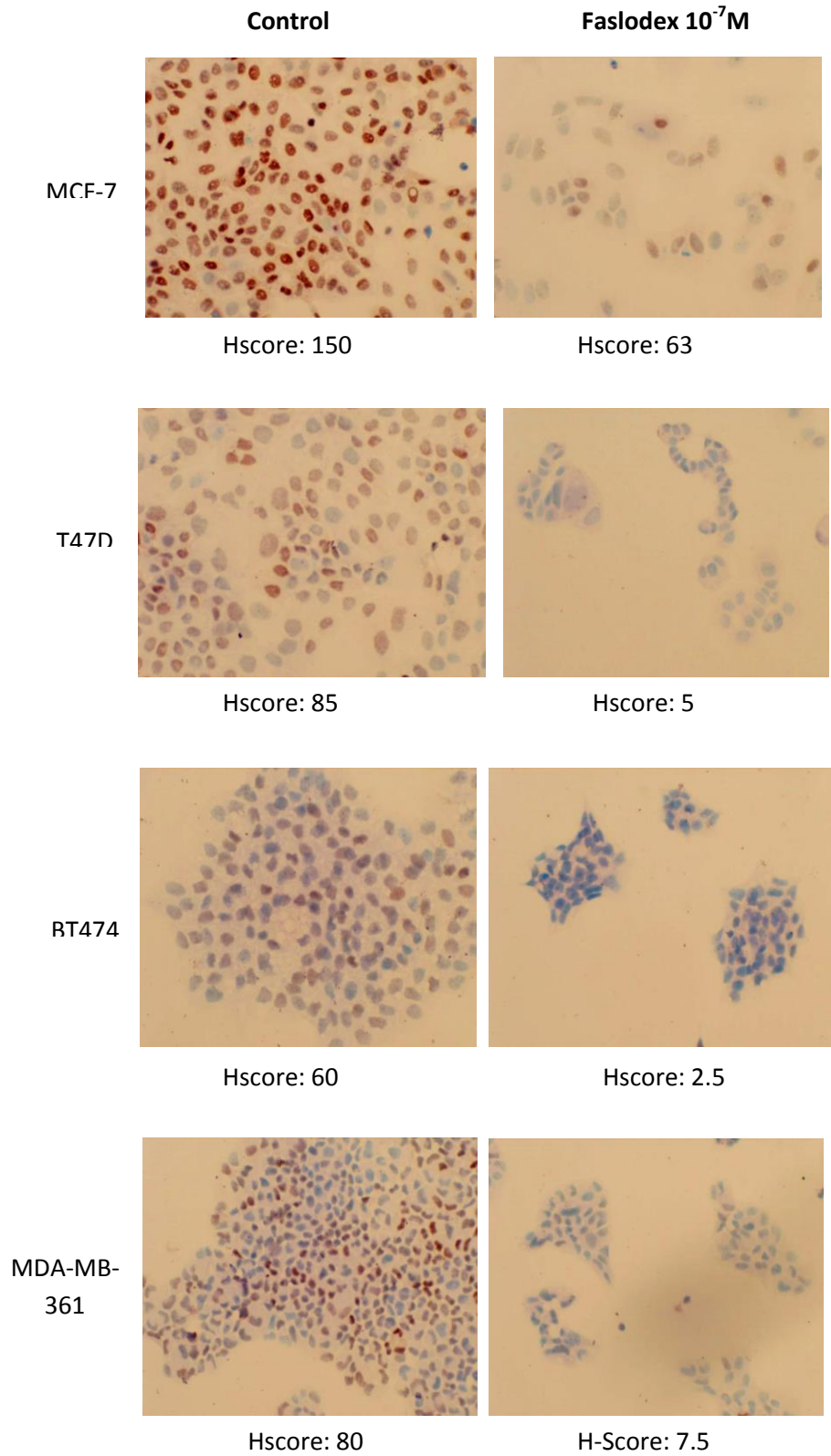
Figure 9: ICC analysis of ER down-regulation by 10^{-7}M Faslodex in 4 ER+ breast cancer cell lines, showing representative images (original magnification=x20) and associated average Hscore.

3.2.3 Effect of long term culture on the four ER+ breast cancer cell lines in the presence of Faslodex.

3.2.3.1 Duration of Faslodex response and establishment of Faslodex-resistance

Previously an acquired tamoxifen-resistant cell line was successfully established by culturing MCF-7 cells in the presence of 4-OH-tamoxifen for an extended period of time *in vitro* (Nicholson *et al.*, 2001; Knowlden *et al.*, 2003). In this project, long term culture was similarly carried out using the MCF-7, T47D, BT474 and MDA-MB-361 cell lines in the presence of 10^{-7}M Faslodex. By using ER+ cell lines with differing HER2 status it was hoped to relate HER2 and duration of Faslodex response *in vitro*.

Figures 10-13 comprise these long-term growth data. The graphs have been constructed using the number of days each cell line was in culture (x-axis) and the number of passages carried out during this culture period (y-axis). The absence of passaging indicates a period of Faslodex-induced growth inhibition while recovery of routine passaging indicates the establishment of a resistant phenotype. Table 7 summarises these data.
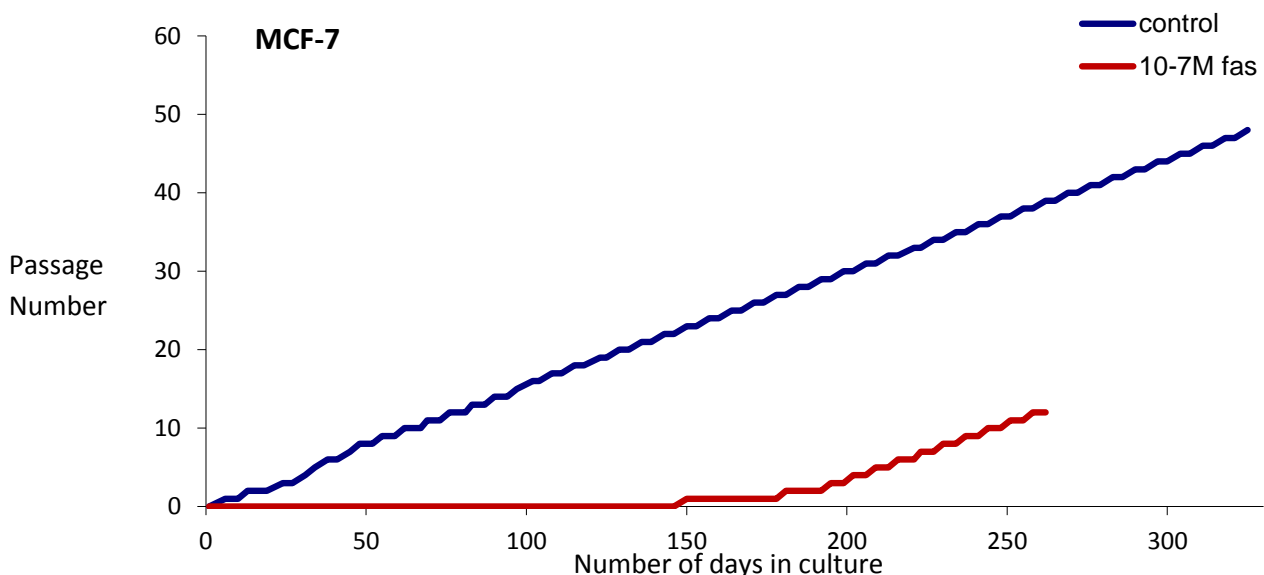
Figure 10: Growth inhibitory effect of continuous Faslodex (10^{-7}M) on the ER+/HER2- MCF-7 cell l ine *in vitro*. Growth inhibition is displayed by lack of cell passages compared to continuously increasing passage number for untreated control cells.
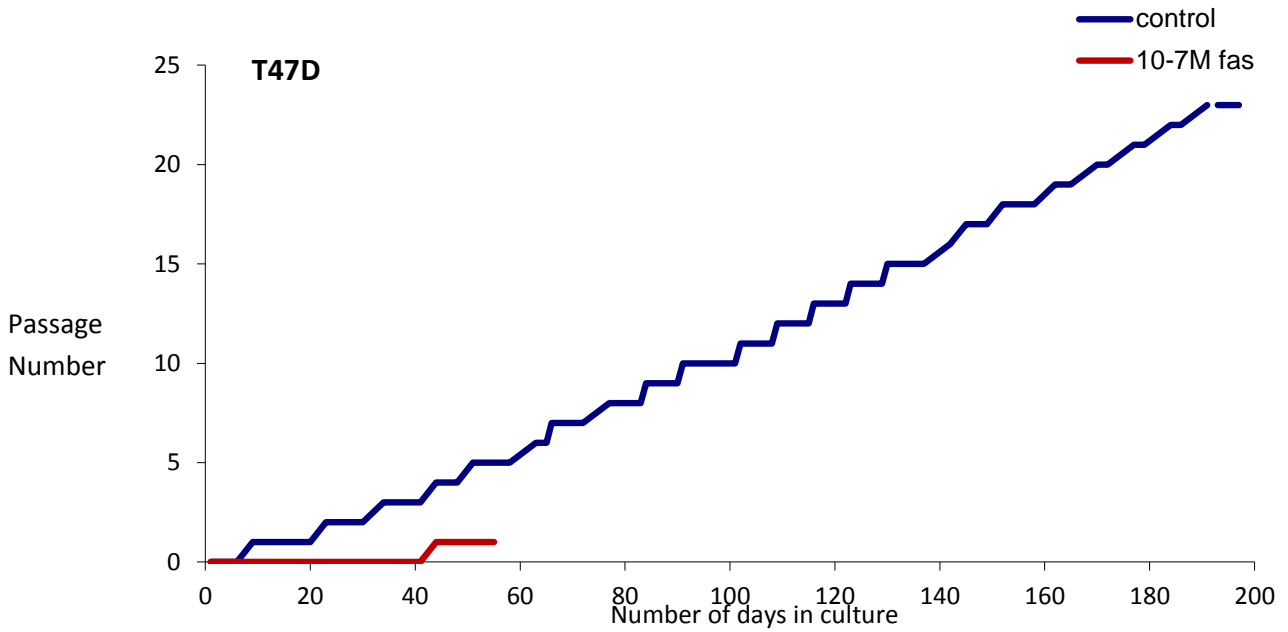
Figure 11: Growth inhibitory effect of continuous Faslodex (10^{-7}M) on the ER+/HER2- T47D cell line *in vitro*. Growth inhibition is displayed by lack of cell passages compared to continuously increasing passage number for untreated control cells.
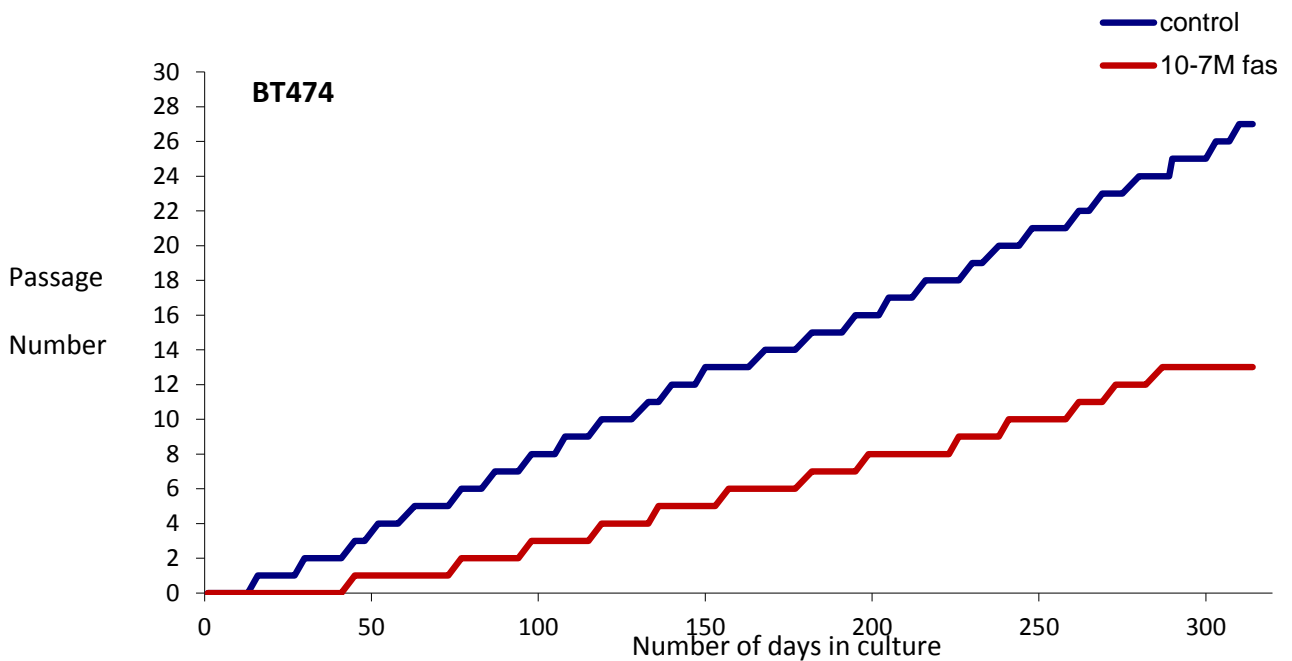
Figure 12: Growth inhibitory effect of continuous Faslodex (10^{-7}M) on the ER+/HER2+ BT474 cell line *in vitro*. Growth inhibition is displayed by lack of cell passages compared to continuously increasing passage number for untreated control cells.
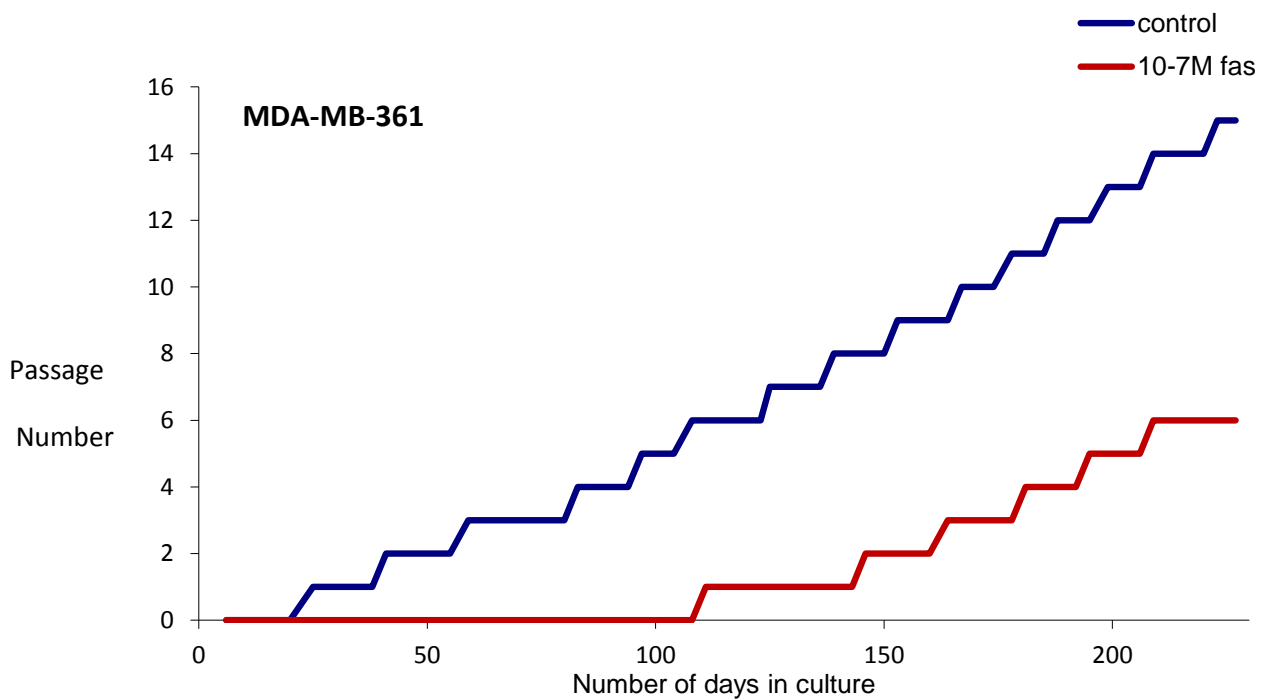
Figure 13: Growth inhibitory effect of continuous Faslodex (10^{-7}M) on the ER+/HER2+ MDA-MB-361 cell line *in vitro*. Growth inhibition is displayed by lack of cell passages compared to continuously increasing passage number for untreated control cells.

Table 7: Number of days taken for each cell line to develop resistance to Faslodex in continuous culture. The response duration *in vitro* was determined by the time taken until the first passage occurred and subsequent cell growth was maintained in the presence of Faslodex.

Cell line	Number of days until development of resistance during Faslodex treatment
MCF-7	~150 days
T47D	Complete cell loss by ~day 60.
BT474	~50 days
MDA-MB-361	~110 days

In total, all of the cell lines exhibited a period of Faslodex-induced growth inhibition, although this was highly variable. Of the 4 cell lines examined, T47D cells were most sensitive to Faslodex, while BT474 cells were least sensitive (Figures 10-13 and Table 7). Stratification of the inhibitory responses by the HER2 status of the

cells revealed that the ER+/HER2- cell lines underwent an enhanced Faslodex response compared to the HER2+ cell lines, evidenced by the superior duration of growth inhibition in the MCF-7 line and by the complete cell loss in the T47D cell line in the presence of this antihormone by ~60 days (Figures 10 and 11; Table 7). Although Faslodex resistance developed during treatment in MCF-7, MDA361 and BT474 cells, it occurred more rapidly in the HER2+ cells.

This experiment was repeated several times confirming the growth profiles observed, and where failure to develop Faslodex resistance by T47D cells (contrasting the 3 further models) was reproducibly observed (Figure 14) during the same time frame. The failure of T47D cells to develop Faslodex resistance resulted from a complete cell loss beginning after ~8.5 weeks of treatment (Figure 15), when the cell coverage of the culture flasks began to dramatically drop, indicative of a complete response. It is believed that this is the first reported Faslodex complete-response model.
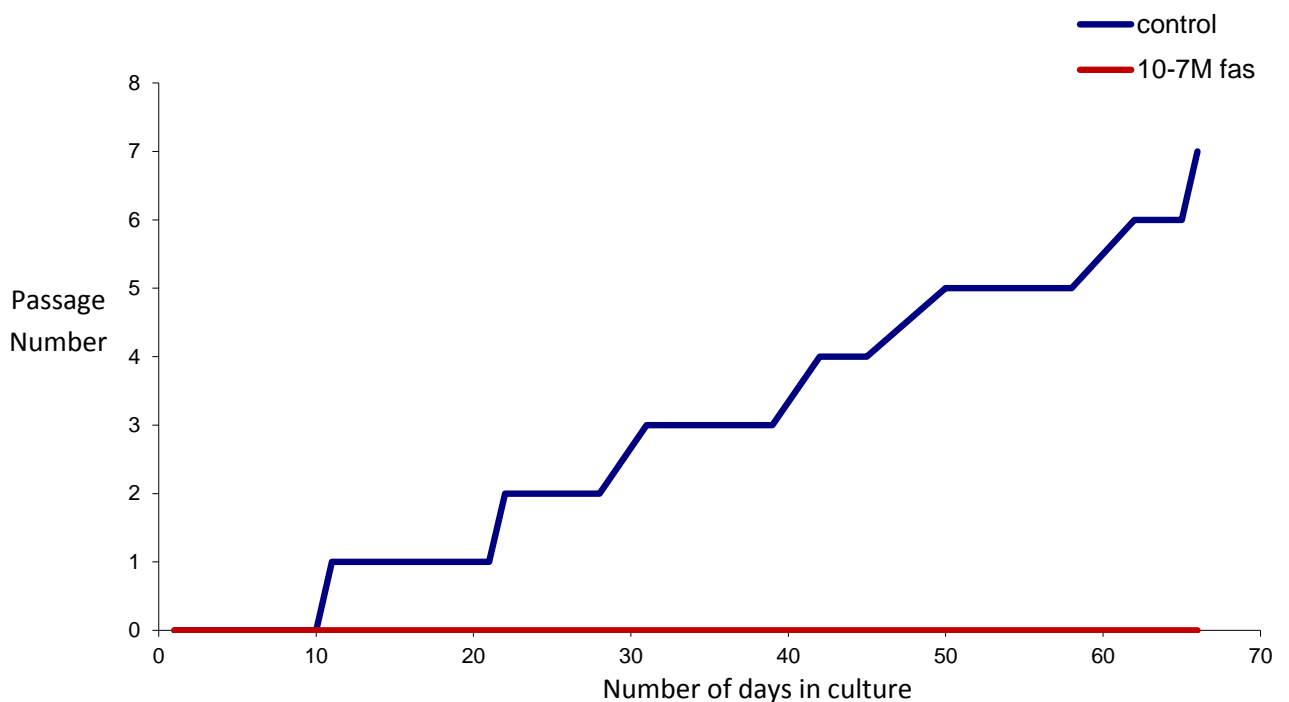
Figure 14: Growth inhibitory effect of continuous Faslodex on the ER+/HER2- T47D cell line *in vitro* (replicate experiment). Growth inhibition is again displayed by lack of cell passages compared to control.
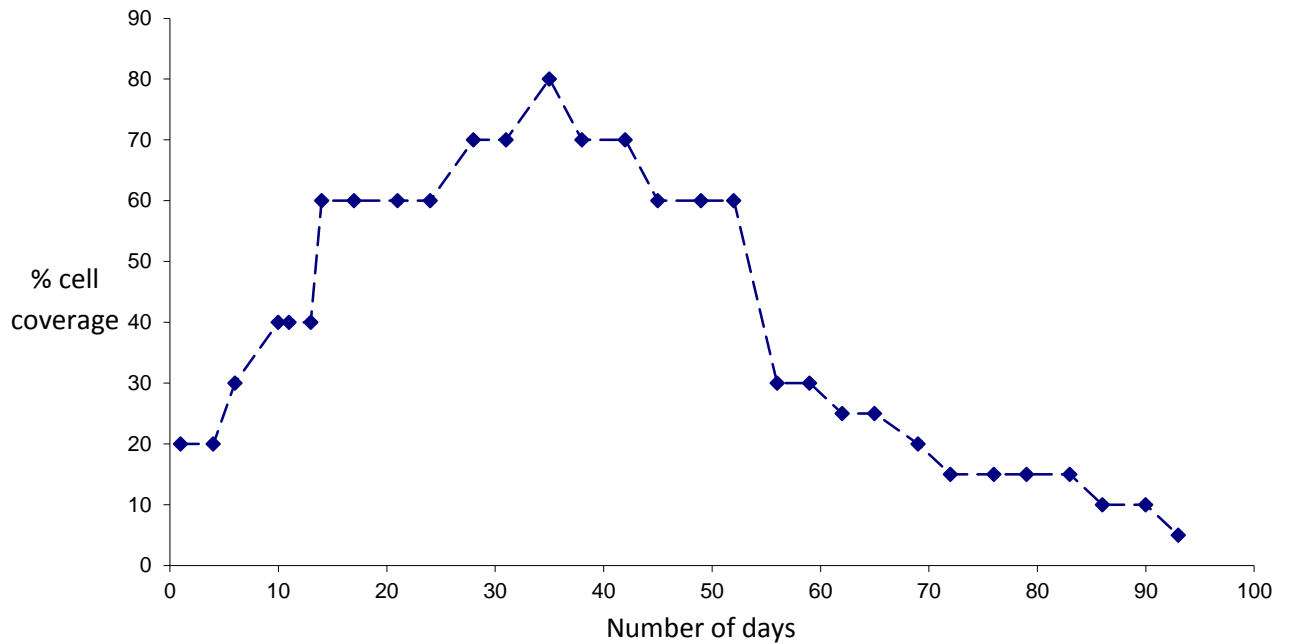
Figure 15: % cell coverage of T47D cells in a culture flask undergoing continuous Faslodex treatment (viewed under a microscope, magnification x10).

In summary, these cell models reflected several important phenomena observed with antihormones in the clinic (but in some instances as yet only poorly-described for Faslodex), most notably:

The ER+/HER2+ tumour cells exhibited a reduced duration of response to Faslodex compared to HER2- tumour cells.

Resistance is commonly acquired by the ER+ tumour cells during Faslodex treatment, but significantly, T47D cells underwent a complete response to Faslodex treatment.

3.3 Discussion

In this chapter the statuses of ER and HER2 in 4 breast cancer cell lines that were to be utilised for the remainder of this project were assessed. The results obtained established that all were ER+ and that MCF-7 and T47D cells and MDA-MB-361 and BT474 cells could be categorised as HER2- and HER2+ respectively. These data are

consistent with the published literature where MDA-MB-361 and BT474 cells show HER2 gene amplification (She *et al.*, 2008; Ithimakin *et al.*, 2013).

Subsequent studies showed that Faslodex efficiently down-regulates ER, independently of the HER2 status of the cells, and impacted on tumour cell number and cell proliferation rate, as determined by cell growth data. The responsiveness of the ER+ cells to the growth inhibitory effects of continuous Faslodex exposure was, however, highly variable, where the HER2+ cell lines showed the least favourable response to Faslodex, each developing resistance within a shorter period. Significantly, within the two HER2- cell lines, while acquired resistance to Faslodex was eventually observed in MCF-7 cells, T47D cells showed a complete response to Faslodex, a rarely described phenomenon with targeted treatments such as antihormones in breast tumour models. Heterogeneity of response, therefore, occurs both between HER2 positive and negative cell models and within HER2 negative cell types. The 4 cell model panel with its varied anti-tumour response provides a new research tool to delineate determinants of Faslodex response and failure, critical given use of this antihormone is increasing clinically.

Degree of ER positivity has been associated with an improved response to anti-hormone therapy (Goldhirsch *et al.*, 2009) and more recently there have been suggestions that patients with low levels of ER should receive chemotherapy in addition to endocrine therapy while high expressers would receive little benefit from the addition of chemotherapy (Pagani *et al.*, 2009). Thus the high inherent ER positivity in the MCF-7 cell line probably partially explains its sensitivity to oestrogens and short-term anti-hormone measures. Immunostaining of ER revealed that ER expression varied from cell line to cell line and also within cell lines (Figure 5). This is not unique to the cells used in this project but has also been described by other laboratories (Bock *et al.*, 2012). Variations within a given cell line are partly explained by cell-cycle related variations of ER expression (Caldon *et al.*, 2010). Such variations are also observed in ER positive tumours from different patients (Charpin *et al.*, 1988) and within individual ER+ tumours (Nassar *et al.*, 2010). However, there is little available clinical information regarding relationship between degree of initial ER positivity and response to Faslodex. The studies here indicated

that expression of ER failed to relate to initial degree of response to short-term Faslodex treatment or subsequent duration of response in all cell lines. The MCF-7 cell line displayed markedly higher ER protein expression than the MDA-MB-361 cell line but following short-term Faslodex treatment growth inhibition was largely equivalent (Figure 9). In addition, degree of ER expression also failed to relate to response to long-term Faslodex treatment.

The long-term growth studies revealed that the HER2- cell lines displayed a superior Faslodex response versus the HER2+ models (Figures 10 and 11) but the T47D cell line emerged as a model of Faslodex complete response even though expressing substantially less ER than the MCF-7 cell line (Figure 5) which subsequently developed resistance. Based on these observations that response is clearly independent of initial level of ER (including within MCF-7 and T47D cells), measuring ER prior to treatment may prove unhelpful in predicting response outcome within ER+ disease for the agent Faslodex. Significant ER down-regulation was observed with Faslodex in all models, and has also been reported in pre-surgical studies in primary breast cancer with this drug showing dose dependency (Kuter *et al.*, 2012; Robertson *et al.*, 2010). No clinical study has related magnitude of ER down-regulation to duration of response, but again the cell model findings here showing lack of relationship between the capacity of Faslodex to down-regulate the cellular levels of this protein and initial or long-term Faslodex growth response suggest such measurement may be uninformative.

The long term cell growth studies with Faslodex treatment agree with the varying responses observed with antihormones in the clinic. Clinically, many HER2- patients display a partial response before an antihormone resistant phenotype emerges, an event represented by the MCF-7 cell line (Figure 10). As previously stated the T47D cell line underwent a complete response following long-term Faslodex treatment despite short-term treatment failing to initiate the most robust growth inhibition, indicating that degree of inhibition induced by short-term treatment is not indicative of long-term outcome. The stark difference between the relatively-poor magnitude of response of the T47D cell line to Faslodex following short-term treatment compared to complete response achieved during long-term exposure

could be due to a drug-induced event(s). Faslodex treatment may result in a unique genomic event in the T47D cell line i.e. up or down-regulation of gene expression respectively modulating an important apoptotic or cell survival pathway in the T47D line that does not occur in the other cell models, so that over time an eventual complete-response is observed. With respect to the use of the T47D cell line as a model for ER+ breast cancer, this may be of particular relevance with respect to those patients who show a complete response following endocrine therapy. Complete-response to Faslodex is not a common phenomenon, Table 1 from the introduction states that 1.1% of patients demonstrated a clinical response in the CONFIRM study (Di Leo *et al.*, 2010). Complete response is described as the disappearance of all signs of cancer in response to treatment as indicated by the National Cancer Institute.

Very few trials have assessed the relationship between pathological complete response and endocrine therapy. It has been shown that pathological complete response is associated with an improved clinical outcome (Milla-Santos *et al.*, 2004), although it is also known that patients can relapse following complete response to therapy. Using the T47D cell line in comparison with the further ER+ models to determine the precise mechanism of such an effect in relation to Faslodex could be key to helping explain the varying responses to Faslodex treatments observed in patients and hopefully aid identification of patients who will elicit superior response and thus potentially benefit from Faslodex therapy.

Generally patients with HER2+ disease are associated with a more aggressive tumour and the period of initial response to anti-hormones such as tamoxifen is reduced (Osborne *et al.*, 2003). Experimental studies by other laboratories, primarily utilising stable HER2-transfected MCF-7 cells, indicate this may involve establishment of an "escape" growth survival pathway (i.e. HER2 as alternative to ER) (Schiff *et al.*, 2005; Wardley and Howell, 2006). There is also emerging evidence that HER2 blockade can temporarily improve tamoxifen or aromatase inhibitor outcome in some ER+/HER2+ patients (Johnston *et al.*, 2009). However, studies are only beginning in this area for Faslodex clinically and there are no substantial preclinical data with this agent in ER+/HER2+ cells, so the response relationship for

Faslodex with HER2 status is not fully established). In the HER2+ *in vitro* models in this project, a reduced initial response to Faslodex was observed compared to the MCF-7 cell line providing some evidence that HER2 overexpression de novo may also contribute to limiting maximal Faslodex response. Also of interest in this regard is the superior long-term Faslodex response observed in the HER2- cell lines compared to the HER2+ cell lines (Figures 10- 13). Even though the MCF-7 cell line eventually developed Faslodex-resistance the duration of initial drug response was superior compared to the HER2+ cell lines. Again, this is in keeping with current literature stating that endocrine response is reduced in the HER2+ disease setting (Schiff *et al.*, 2005; Wardley and Howell, 2006).

These data do suggest the presence of HER2 can contribute to limiting Faslodex response. However, the ER+/HER2+ as well as the ER+/HER2- cell lines exhibited initial Faslodex responses, and also the HER2+ phenotype does appear able to display some response to Faslodex in the clinic (Robertson *et al.*, 2010). Furthermore, Faslodex resistance was ultimately acquired in both the HER2- MCF-7 line and the HER2+ lines. These data in total suggest that additional factors alongside amplification of HER2 contribute to determining response or failure to this antihormone in ER+ disease. It is feasible that the varying growth inhibitory responses and subsequent acquisition of resistance (where observed) in the HER2- and HER2+ cell lines may be due to Faslodex induced genomic changes in addition to aspects of the intrinsic phenotype, particularly HER2 status.

In the following chapters, microarray gene expression profiling has been utilised in order to determine Faslodex-induced transcriptome alterations that may explain these varying drug responses in each of the cell lines *in vitro*. It is feasible that this approach could identify novel therapeutic strategies or biomarkers of these varying responses with the ultimate aim of maximising Faslodex impact.

Chapter 4

Microarray gene expression profiling to identify genes that may associate with Faslodex response profiles *in vitro*

4.1 Introduction

Following the completion of the sequencing of the human genome, which demonstrated the potential breadth of genes that could be expressed in any tissue, came the advent of gene expression microarray profiling. Such profiling allows the analysis of gene transcription on a genome-wide scale rather than the traditional "one gene at a time". This creates a global picture of potential cellular function and thus provides another level of detail to the functionality of the genes present in the human genome.

High throughput gene expression profiling using microarray-based methods has achieved many successes in relation to breast cancer research. Without such data, we would lack a fuller understanding of the heterogeneity that exists in breast cancer which has now challenged the concept that breast cancer is a single disease (Perou *et al.*, 2000; Sorlie *et al.*, 2001). Instead, it is currently accepted that breast cancer is a collection of different diseases that affect the same organ site but have widely different transcriptional profiles, risk factors, clinical presentation, histopathological features, outcome and response to therapies (Reis-Filho *et al.*, 2010; Weigelt *et al.*, 2010). These studies have shown that response to a given treatment is at least in part determined by inherent molecular characteristics of the tumours and such findings have been taken advantage of in order to discover genes over-expressed in breast cancer or to identify molecular gene signatures that can potentially predict prognosis and response to therapies (Sotiriou *et al.*, 2009; Weigelt *et al.*, 2010). Although there is as yet no accepted signature to distinguish

endocrine sensitive from resistant patients, some gene signatures are available in commercial formats, e.g. OncotypeDX, a genetic test that can be used to determine if ER+ patients are at risk of distant recurrence and would thus benefit from the addition of chemotherapy to their standard endocrine treatment (Paik *et al.*, 2004).

Significantly however, little data are available which correlate changes in gene expression profiles during therapy with either initial tumour response or the subsequent development of endocrine resistance, with data particularly lacking for Faslodex. Importantly, therefore this chapter builds on the data presented in chapter 3 to determine if meaningful information using gene expression analysis can be generated from the 4 ER+ cell lines with their differing HER2 status and Faslodex response/resistance data. Affymetrix U133Aplus2 arrays were used to chart the gene expression profiles in each model before and after treatment in order to identify de-regulation of genes by Faslodex (10^{-7}M, 10 day treatment) that may subsequently contribute to a given response. The approach in part mirrors a study by Frasor *et al.*, confined to MCF-7 cells, who demonstrated that antihormones can induce as well as suppress the expression of ER-regulated genes (Frasor *et al.*, 2004) and where some gene changes contributed to eventual tumour re-growth and resistance, essentially limiting the efficacy of the treatment.

4.2 Results

4.2.1 Hierarchical clustering analysis: Quality control of replicate data

Following the completion of the microarray gene expression profiling experiment, the resultant triplicate expression data were normalised prior to a number of statistical tests. Firstly, a simple t-test ($p<0.05$) was conducted to identify gene probes that were significantly altered by 10 day Faslodex treatment compared to untreated cells. This was followed by a further statistical test, SAM (Significant Analysis of Microarrays), with a false discovery rate (FDR) set also at 0.05. The stringent statistical testing was chosen to maximise chances of determining robust expression changes occurring in the cell models following Faslodex treatment. The total gene probe changes with Faslodex thus identified in each model are shown in Table 8 as well as the number of individual gene probes were de-regulated by

Faslodex in all models. It can be seen from Table 8 that of the 10517 genes probes de-regulated; approximately 50% are induced by 10 day treatment while approximately 50% were suppressed.

Table 8: Total number of gene probes induced or suppressed by 10 day Faslodex treatment (10^{-7}M) in each of the cell lines and number of individual gene probes analysed.

Experimental arm	Number of gene probes altered by Faslodex	
MCF-7	5559	
T47D	2240	
BT474	3319	
MDA-MB-361	2946	
Total number de-regulated (individual gene probes)	10517	
	Induced	5279
	Suppressed	5238

Cumulating these significant gene probes, hierarchical clustering analysis (HCA) was then carried out on these selected induced or suppressed gene probes pre- and post- Faslodex treatment using an in-house software program as a quality check to ensure the individual replicates for each control and experimental arm appropriately clustered for each model before further analysis (Figures 16-19). Areas in green indicate low gene expression, while red indicates high gene expression.
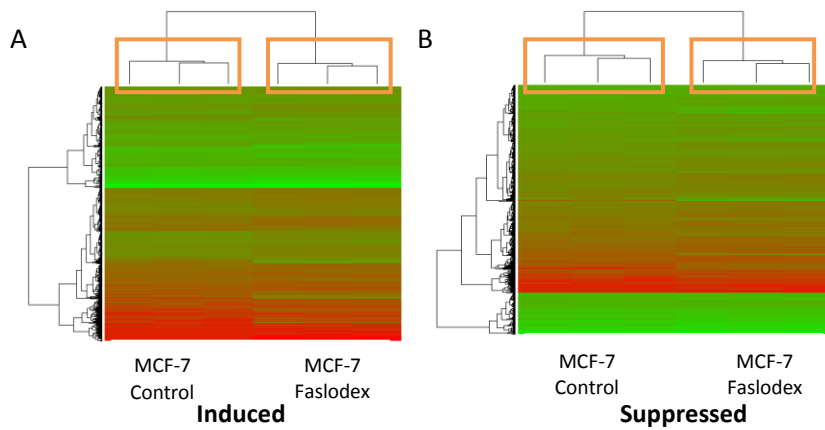
Figure 16: Hierarchical clustering analysis of the expression of genes that were (A) – induced by Faslodex or (B)- suppressed by Faslodex in one or more of the cell lines, examined in the MCF-7 cell line (untreated and Faslodex treated). Clustering of the triplicate data for each experimental arm is highlighted in orange boxes.
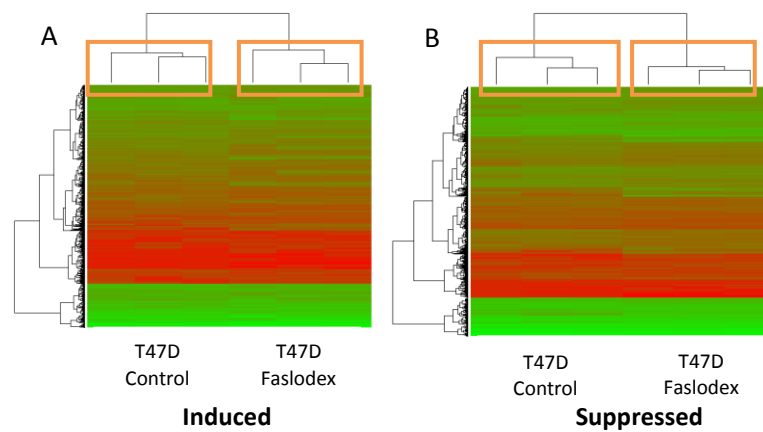
Figure 17: Hierarchical clustering analysis of the expression of genes that were (A) – induced by Faslodex or (B)- suppressed by Faslodex in one or more of the cell lines, examined in the T47D cell line (untreated and Faslodex treated). Clustering of the triplicate data for each experimental arm is highlighted in orange boxes.
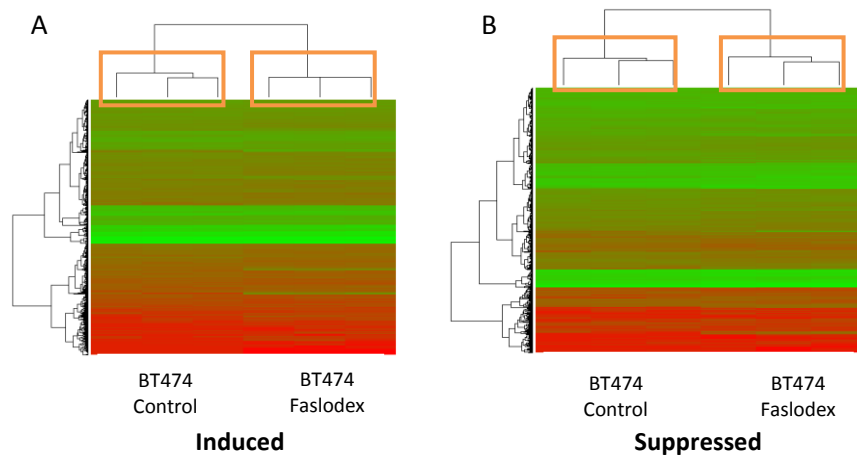
Figure 18: Hierarchical clustering analysis of the expression of genes that were (A) – induced by Faslodex or (B)- suppressed by Faslodex in one or more of the cell lines, examined in the BT474 cell line (untreated and Faslodex-treated). Clustering of the triplicate data in each experimental arm is highlighted in orange boxes.
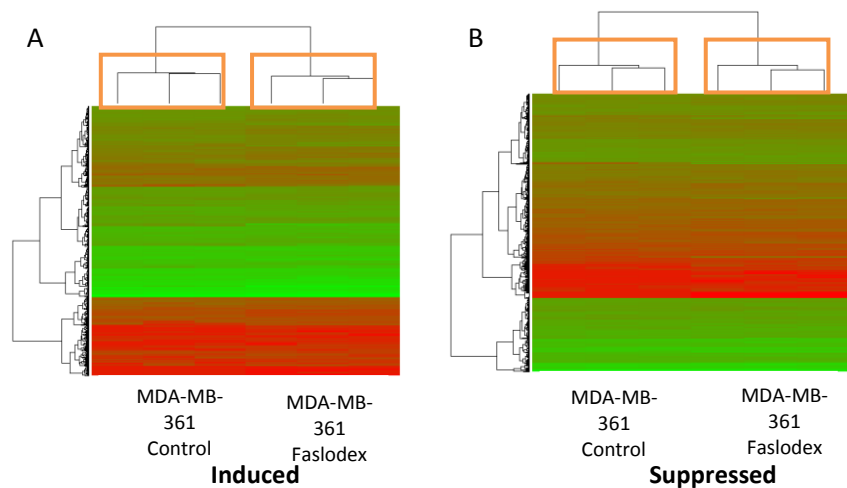
Figure 19: Hierarchical clustering analysis of the expression of genes that were (A) – induced by Faslodex or (B)- suppressed by Faslodex in one or more of the cell lines, examined in the MDA-MB-361 cell line (untreated and Faslodex treated). Clustering of the triplicate data in each experimental arm is highlighted in orange boxes.

Using gene probes that were significantly Faslodex-de-regulated in any of the cell lines, all the replicate microarray expression data clustered together for pre or post treatment (highlighted by orange), with pre-treatment clustering distinct from post-treatment, indicating good quality data (Figures 16-19) for the statistically-discriminated Faslodex-induced and suppressed genes.

4.2.2 Confirmation of suppression of two known ER-regulated genes following 10 day Faslodex using the gene expression datasets.

In parallel with the above, the raw gene expression data were also uploaded into an analysis software program called Genesifter. Genesifter is commercially available and carries out a median normalisation and log-transfromation on the data before profile analysis begins. Genesifter allows the user to use heatmaps, and log2-expression intensity plots in order to investigate individual gene expression changes. This program was used to further gauge the quality of the pre- and post-treatment array data by analysing the change in expression exerted by 10 days Faslodex treatment on two known ER-regulated genes PGR and GREB1 (growth regulation by oestrogen in breast cancer 1; an oestrogen-responsive gene that is an early response gene in the oestrogen receptor-regulated pathway).

The data presented in Figure 20 (heatmaps and intensity plots) shows that PGR and GREB1 were suppressed to varying degrees by Faslodex treatment evidencing its expected anti-oestrogenic impact in all models. Indeed, in some instances, gene expression levels below 0 were observed in the 10 day treatment samples, indicative of very low (if any) expression levels of these mRNAs after treatment.
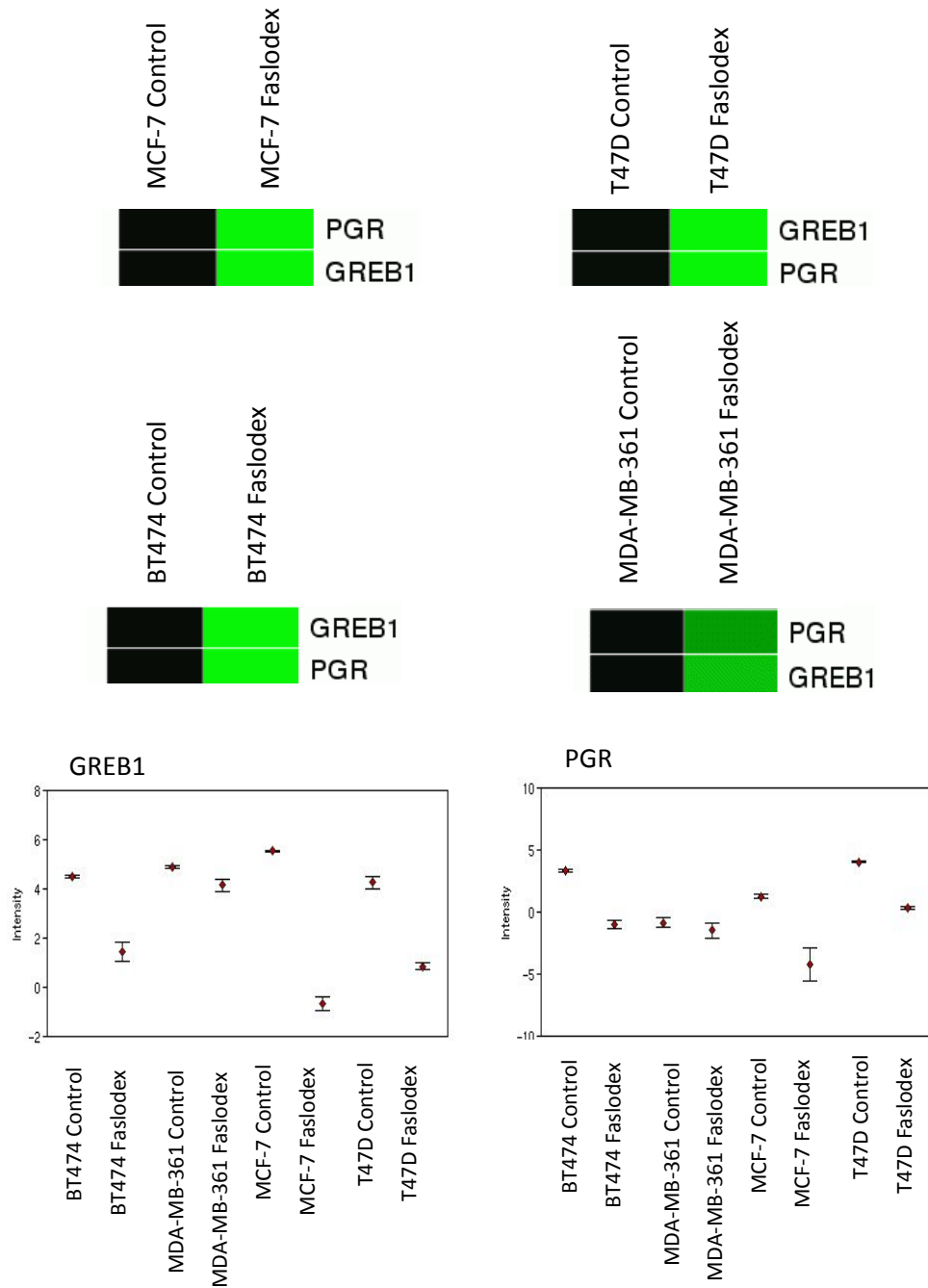
Figure 20: (A) Heatmaps of known ER-regulated genes (PGR and GREB1) to determine the effect of 10 day Faslodex treatment on expression of these genes (B) Gene expression intensity plots for each gene in all cell lines pre and post Faslodex treatment. Genesifter uses a log2 intensity scale for display of mean of triplicate normalised expression data +/- SEM for each experimental arm.

4.2.3 Interrogation of gene changes in each cell model following Faslodex treatment

Following the validation of the quality of the array expression data and confirmation that Faslodex was de-regulating known ER-regulated genes in all the models at the expression level, the expression data were further interrogated by analysing the number of genes that were induced or suppressed by Faslodex within each of the individual cell lines (Table 9).

Table 9: The number of gene probes induced or suppressed by 10 day Faslodex treatment in each of the cell lines investigated. Also displayed is the % of the genome that is Faslodex de-regulated (based on total Affymetrix HGU133A probe number of n=22215)

Experimental arm	Number of gene probes	% of gene probes Faslodex-regulated	
MCF-7 suppressed probes	2795	12.6	24.9
MCF-7 induced probes	2764	12.3	
BT474 suppressed probes	1674	7.5	14.9
BT474 induced probes	1645	7.4	
MDA-MB-361 suppressed probes	1468	6.6	13.2
MDA-MB-361 induced probes	1478	6.6	
T47D suppressed probes	1261	5.7	11
T47D induced probes	1179	5.3	

The greatest number of gene probe changes was observed in MCF-7 cells with over 5000 being recorded. This represented approximately one quarter of all the gene sets on the Affymetrix array. Although substantially fewer changes were seen in T47D, MDA-MB-361 and BT474 cells, as in MCF-7 cells these alterations were almost equally divided between Faslodex induced and suppressed events.

Interestingly, while the T47D cell line which exhibited the greatest response to Faslodex in vitro, the fewest Faslodex-induced gene changes were observed (11% of all gene probes), the number of changes were not too dissimilar to those observed in the HER2+ models (13-14% of all gene probes) which displayed the poorest Faslodex response. As such the overall frequency of gene changes promoted by Faslodex, together with the proportion of induced and suppressed events (approximately 50% in each cell line), failed to discriminate between the heterogeneity of Faslodex growth inhibitory response in the models or to relate to HER2 status.

4.2.4 Hierarchical clustering analysis in relation to HER2 status and Faslodex response

Investigation of the total number of gene probe changes occurring in each of the cell lines post Faslodex treatment failed to discriminate between the varying Faslodex growth inhibitory responses observed following long term Faslodex treatment *in vitro*. Subsequently, hierarchical clustering analysis was carried out in order to determine if such an analysis could provide detail into the varying Faslodex responses observed in the cell lines or could cluster cell lines based on HER2 status. Hierarchical clustering analysis was carried out before and after treatment, using the gene probe cohort that had been identified as Faslodex-deregulated (induced or suppressed by Faslodex in one or more of the cell lines). This analysis included all gene probes that were de-regulated in one cell line or more thus multiple gene probes for one gene may be included in the analysis as well as very good and poor performing probes.

Figure 21: HCA of expression data for the cell models before Faslodex treatment using all probes that were induced or suppressed following treatment in one or more of cell lines. The orange squares highlight the clustering of the HER2- and HER2+ cell lines, while the highlighted 1-3 along the right-hand side of the heatmap indicate the dominant gene clusters.

Figure 21 displays the clustering of all the Faslodex-deregulated genes prior to treatment. It can be seen that analysis of the intrinsic phenotype of the cells according to this gene cohort clustered the HER2- and HER2+ cell lines separately (highlighted by orange boxes).

With respect to the gene clustering across the four models, there were 2 major cohorts of approximately equivalent size, one cluster of gene probes at a higher expression level (cluster 1-yellow) in the majority of the models and another representing those genes expressed at low levels (comprising clusters 2+3-red and blue). The gene profiles in cluster 3 mainly consisted of genes expressed at low intensity levels. However, it can be clustered as separate from cluster 2 as there

appeared to be some variability and somewhat higher expression levels, evidenced by the increase in red in some cell models. Beyond these dominant clusters the clustering of various gene profiles became very complex which is probably due to the vast number of genes being analysed and the lack of shared gene expression profiles across all of the 4 cell models.

Figure 22: HCA of expression data for the cell models post Faslodex treatment using all probes that were induced or suppressed following treatment in one or more of cell lines. The orange squares highlight the clustering of the HER2+ cell lines with the MCF-7 cell line and also the separation of the T47D cell line from the MCF-7 line, while the highlighted areas 1-3 within the heatmap indicate the dominant gene clusters.

In contrast following Faslodex treatment, HCA of the Faslodex-deregulated genes failed to clearly discriminate between the HER2- and HER2+ cell lines (Figure 22). Interestingly, the HER2- T47D cell line no longer closely clustered with the HER2-MCF-7 cell line suggesting that the de-regulation of these genes in the T47D cell line is different both to the MCF-7 and the HER2+ cell lines (highlighted in orange). Both HER2+ models clustered suggesting that there are some Faslodex-deregulated

events shared by both models. However, although the HER2- MCF-7 cell line continued to cluster separately from both HER2+ cell lines, this clustering was closer (highlighted in orange) than seen pre-treatment. This suggests some similarity with regards to the genes that are Faslodex deregulated in these 3 models.

There were 3 dominant gene clusters after Faslodex treatment (Figure 22). Cluster 2 represents those gene probes that were expressed at a low intensity in the majority of the models while in cluster 1 the majority of gene profiles were expressed at a higher intensity. Cluster 3 represents those genes with a more variable expression profile and thus much of this cluster is a mix of red and green indicating elevated expression in some cell models and low expression in others suggesting varying de-regulation exerted by Faslodex treatment. Further analysis of the smaller gene clusters that make up the dominant gene clusters was very difficult as the clustering became very complex due both to the high variability of gene expression profiles across the 4 cell models and the number of gene probes being analysed in the HCA.

Following the interesting clustering of the gene expression data after Faslodex treatment, HCA was used to interrogate the induced and suppressed gene probes separately, determining that both gene cohorts again showed separation of the T47D cluster from the 3 remaining cell lines (Figures 23 and 24; highlighted in orange). While they also showed some clustering of the 2 HER2+ lines, there was again clustering overlap between these and the HER2- MCF-7 cells (highlighted in orange). Figure 23 which analyses the genes suppressed by Faslodex treatment in any of the cell lines identified a substantial cluster 2 (blue) which highlights genes expressed at a lower intensity level compared to cluster 1 (yellow), in keeping with Faslodex suppression. In contrast, Figure 24 which only represents those genes induced by Faslodex in any of the cell lines identified that cluster 1 is now larger than cluster 2 indicating more genes expressed at a higher intensity in keeping with induction by Faslodex for this gene cohort. Further analysis of the gene clustering to identify individual genes in relation to the varying *in vitro* drug responses was not possible via this HCA approach due to the sub-clustering complexity.
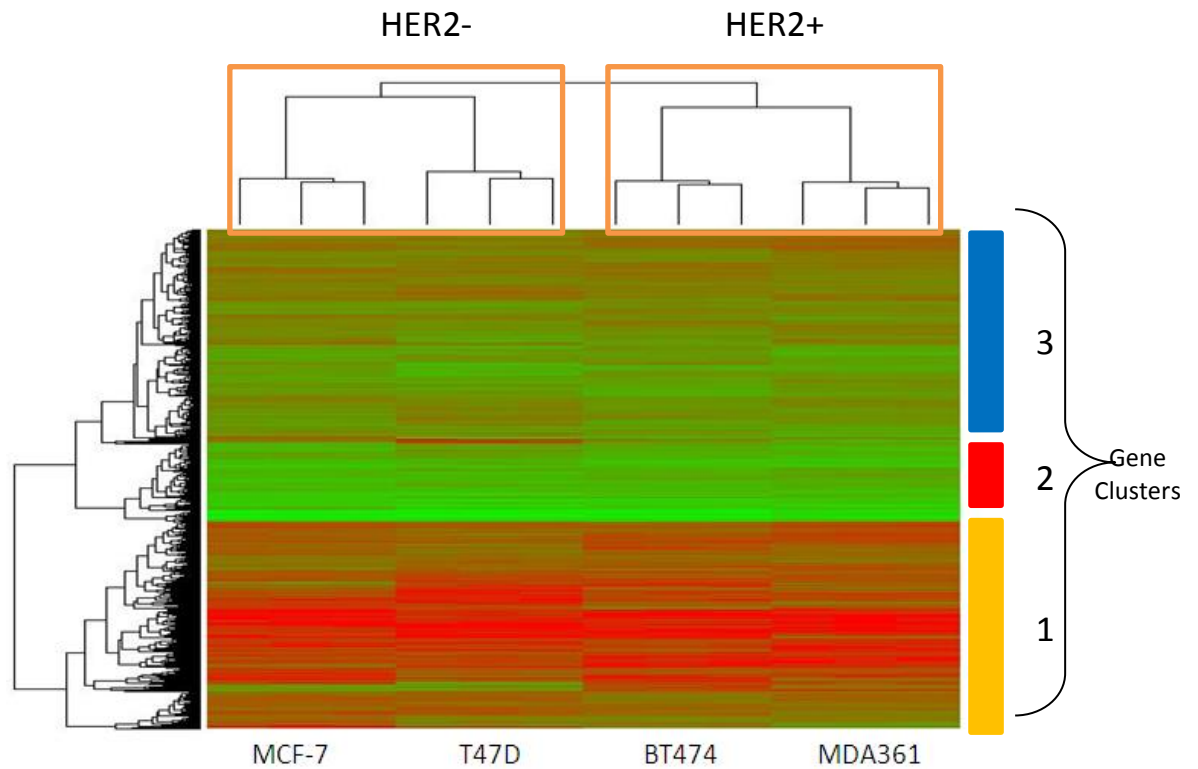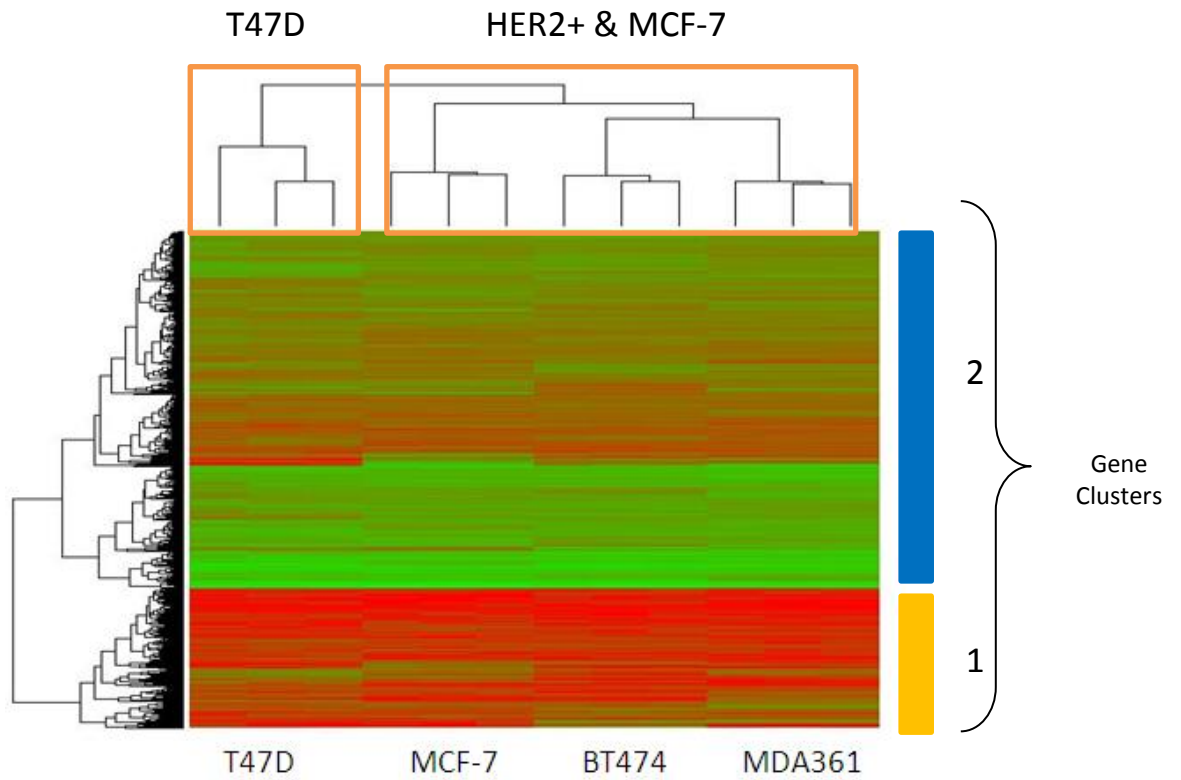
Figure 23: HCA of expression data for the cell models post Faslodex treatment using all probes that were suppressed following treatment in one or more of cell lines. The orange squares highlight the clustering of the HER2+ cell lines with the MCF-7 cell line and the separation of the T47D cell line from the MCF-7 line while the highlighted areas 1-2 within the heatmap indicate the main gene clusters
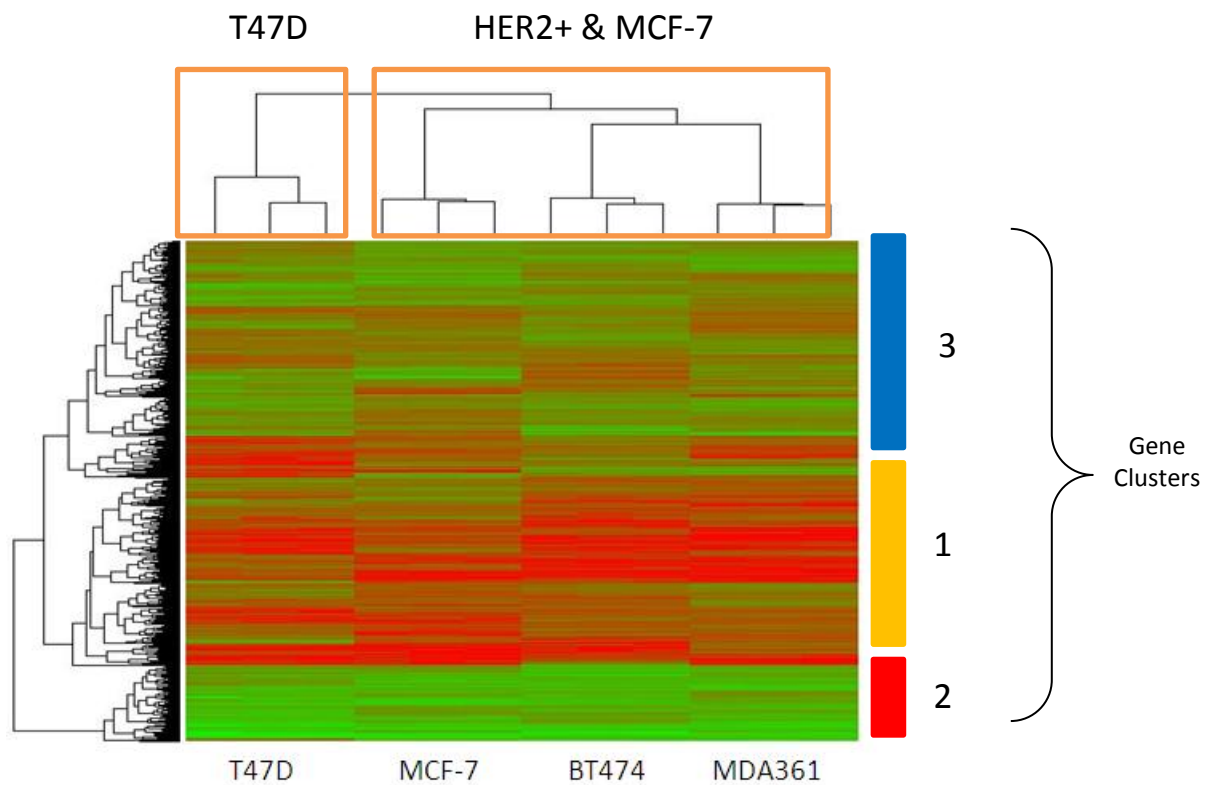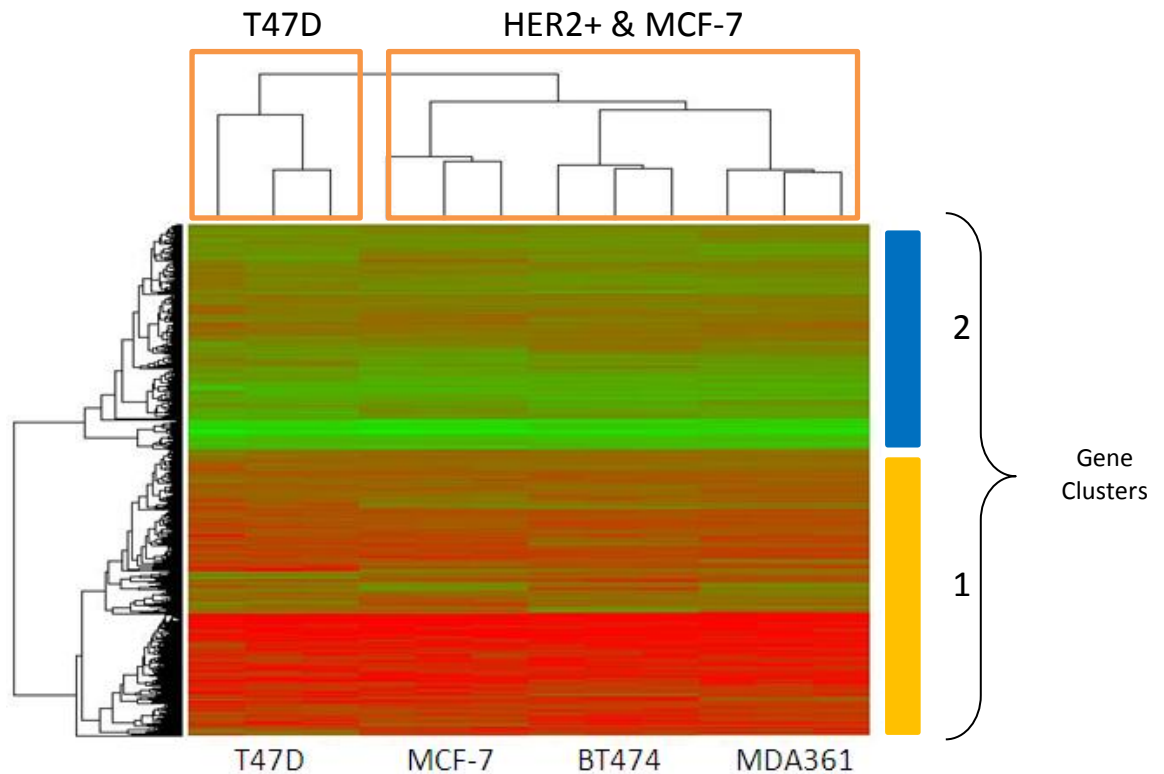
Figure 24: HCA of expression data for the cell models post Faslodex treatment using all probes that were induced following treatment in one or more of cell lines. The orange squares highlight the clustering of the HER2+ cell lines with the MCF-7 cell line and the separation of the T47D cell line from the MCF-7 line while the highlighted areas 1-2 within the heatmap indicate the main gene clusters

In an attempt to identify genes/pathways that were de-regulated by Faslodex in the varying models instigating a given response, genes were identified that were significantly de-regulated (according to SAM) and analysed using a pathway analyser (fold change not considered). Four gene lists were generated based on the following hypotheses:

- Genes Faslodex de-regulated in the T47D cell line only (complete response-associated)
- Genes Faslodex de-regulated in the BT474, MDA-MB-361 and MCF-7 cell lines (resistance-associated)
- Genes Faslodex de-regulated in the HER2-amplified lines; BT474 and MDA-MB-361 cell lines (reduced response genes).
- Genes Faslodex de-regulated in the HER2-not amplified lines; MCF-7 and T47D cell lines (extended response genes)

Some pathways of interest were identified (Appendix E) but there did not seem to be de-regulation of a whole pathway by Faslodex treatment. Instead there were instances of one component of a pathway being de-regulated. Subsequently a more stringent analysis which included fold change was carried out to identify individual genes associated with the differing responses and these are described in Chapters 5-8.

4.3 Discussion

In this chapter, analysis of the quality of microarray gene expression data was first assessed to justify the use of these data to robustly identify potential mediators of Faslodex response/resistance. The results in this chapter successfully show that all microarray data consisted of good replicate expression data both pre and post Faslodex, with clear separation of these data before and after treatment in each model (Figures 16-19); furthermore, the down-regulation of known oestrogen-induced genes (GREB1 and PGR (Kalyuga *et al.*, 2012), Figure 20) is in keeping with the anti-oestrogenic mechanism of action of Faslodex. Further analysis of the numbers of gene probes de-regulated by Faslodex in each of the cell models (Table 9), confirmed data from Frasor *et al* which showed that antihormone treatment can equally induce and suppress gene expression (Frasor *et al.*, 2004). The overall frequency of gene changes and the proportion of induced or suppressed genes failed to relate Faslodex response or HER2 status across the models. Hierarchical clustering analysis of genes de-regulated by Faslodex revealed that pre Faslodex treatment the cell lines clustered based on their HER2 status (Figure 21). This was less clear after treatment. Following Faslodex treatment, the T47D cell line was found to cluster as a distinctive phenotype indicating Faslodex treatment had some unique effects on the transcriptome of this cell line in keeping with its complete response. Furthermore, the HER2- MCF-7 cell line clustered separately from T47D and more closely to the HER2+ lines suggesting Faslodex treatment promoted common genomic events in those cell lines that eventually develop resistance (Figures 22-24). In summary therefore, following Faslodex treatment the cell lines clustered in relation to their varying growth responses following long term Faslodex treatment suggesting that continued interrogation of Faslodex-induced genomic changes may provide further detail to the mechanisms of Faslodex

response/resistance.

As stated above, analysing the Faslodex-induced gene changes in each of the cell models revealed that following treatment a similar number of genes were induced and suppressed in each of the cell lines (Table 9), in agreement with array studies showing that antiestrogen treatment has the ability to induce and suppress gene expression (Frasor *et al.*, 2004). Frasor *et al* also stated that approximately 70% of genes regulated by E2 are down-regulated by treatment, thus more gene inductions might have been expected with antihormones in each of the cell lines; however, it should be noted that Frasor *et al* (2003, 2004) only carried out treatment for 48 hours, while the gene expression data in this project was collected following 10 days of Faslodex treatment. It is thus feasible that the effects on genes indirectly regulated by E2 may not have been fully observed in the data from Frasor *et al.*, and moreover was MCF7-specific where the present project has utilised 4 ER+ models for analysis.

Oestrogen induces growth-promoting genes (e.g. cyclin D1, bcl2, c-myc) and these in turn can be decreased by antihormones (Musgrove *et al.*, 1994; Perillo *et al.*, 2000; Kalyuga *et al.*, 2013), events which may potentially contribute to response. Induction of oestrogen-suppressed growth inhibitory elements by antihormones may also feasibly contribute to response. However, several oestrogen-suppressed genes have also been described that are proliferative and cell survival elements (Frasor *et al.*, 2004). Anti-hormone treatment can lead to the re-expression of such genes which can provide a compensatory mechanism and limit anti-hormone response (Gee *et al.*, 2003, 2005; Shaw *et al.*, 2005). The Faslodex-promoted gene expression changes identified here are thus likely to include some genes contributory to features of drug response or failure exhibited by the model panel. However, considering the overall frequency of gene changes in each cell model cannot discriminate the cell lines based on their response to long-term Faslodex treatment. There were nearly double the number of gene changes with Faslodex observed in the MCF-7 cell line compared to the other 3 cell lines but despite these additional gene changes the establishment of resistance in a reduced

timeframe, as observed in the HER2+ cell models, was not observed (Figures 10-13; Chapter 3). It is possible that the reduced number of gene changes in the HER2+ cell lines may represent fewer tumour suppressive elements being induced and fewer growth promoting genes being suppressed by Faslodex compared with MCF-7, where such a profile could equate with the limited drug response and subsequent more rapid drug failure observed *in vitro*. However, the T47D complete response cell line underwent the very fewest gene changes. This could possibly encompass lack of induction of compensatory growth-promoting signalling which would equate with a markedly improved drug response. Alternatively Faslodex could promote unique genomic events in the T47D transcriptome subsequently resulting in a complete response (e.g. induction of T47D-specific growth suppressive elements). The frequency of Faslodex-altered genes across the models has some agreement with the Carroll laboratory data showing a higher number of ER binding events as mapped by Chip-seq in MCF-7, lower in BT474 and lowest in T47D (Ross-Innes *et al.*, 2012). Although the latter study did not encompass genes that are indirectly regulated by ER whereas the 10 day Faslodex treatment here would encompass both direct and indirect transcriptional impact of the drug.

Along with examining frequency of gene changes, hierarchical clustering analysis was carried out using the Faslodex-deregulated gene cohort to determine if clustering was able to better discriminate between the cell lines based on their response to long-term Faslodex treatment. Analysis of the intrinsic cell phenotype (control samples) saw the cell lines cluster clearly by HER2 status; the HER2- T47D and MCF-7 cell lines clustered together, while the HER2+ BT474 and MDA-MB-361 cell lines clustered (Figure 21). Tumour subclasses have been clustered by HER2 status using whole genome analysis (Sorlie *et al.*, 2001) but this is thought to be the first time that a Faslodex-regulated gene cohort has been used to successfully discriminate ER+ cell lines by HER2 status.

However, while a relationship with HER2 status has been identified, the data also showed that analysis of Faslodex de-regulated genes in the intrinsic cell phenotype was unable to predict response outcome to Faslodex across the 4 models (Figure 21). In contrast, HCA of the Faslodex-regulated gene cohort using the 10 day

Faslodex-treated datasets found the T47D cell line clustering separately to the other 3 cell lines (Figure 22) suggesting potential to identify some genes altered only in the complete responding model from this gene probe cohort (e.g. induction in T47D of individual genes with tumour suppressive function or alternatively suppression of growth-promoting elements). The MCF-7 cell line, while still clustering separately from the HER2+ cell lines clustered more closely to these cell lines. This suggested that Faslodex treatment is inducing common genomic changes in the 3 cell lines that may be associated with their development of resistance (e.g. induction of oncogenes or suppression of tumour suppressors). There may thus be potential to identify particular mediators of acquired Faslodex resistance involved in both the HER2+ and HER2- disease setting from within this gene probe cohort. The partial separation of clustering of the MCF-7 model from the HER2+ cell lines is likely to be due to the extra 1000 genes Faslodex-deregulated (Table 9) and could encompass increased induction of mediators of growth inhibition which may relate to the improved response in this model before the changes shared with the HER2+ cell lines provide a compensatory signalling pathway and ultimately drug resistance. While the two HER2+ models still clustered indicating there are some Faslodex-deregulated events shared by both models, post-Faslodex treatment HER2 status is no longer the clear mediator of cell line clustering suggesting Faslodex-induced transcriptional changes are responsible for the varying growth responses across the model panel.

The clustering patterns observed across the models, which extended to the induced and suppressed gene cohorts on examining the post-Faslodex expression data by HCA, provide confidence that more detailed analysis of gene expression changes exerted by Faslodex at this 10 day time point could provide insight into the varying long-term drug responses observed in these cell lines. Subsequently, the gene expression data has been used in this project to identify genes that are Faslodex-deregulated in one or more cell lines in the hope that further detail of the mechanisms of the various responses could be revealed and also to attempt to identify novel biomarkers of response. The following hypotheses have subsequently been considered in order to identify mediators of Faslodex response and/or

resistance:

1. **T47D versus MCF-7/MDA361/BT474**

   Further investigating the Faslodex-induced or suppressed gene expression profiles associated with complete response (T47D) versus those in the 3 models developing acquired resistance (MCF-7, BT474 and MDA-MB-361) should be valuable in determining (i) Faslodex-altered profiles promoting acquired resistance in the other cell lines (i.e. induction of oncogenes or suppression of tumour suppressors) (chapter 3) and (ii) Faslodex-altered elements promoting improved drug response in the T47D cell line (i.e. induction of tumour suppressors or suppression of oncogenes) (chapter 4).

2. **T47D/MCF-7 (HER2-) versus MDA-MB-361/BT474 (HER2+)**

   While Faslodex has been shown to be effective in ER+/HER2+ patients (Robertson *et al.*, 2010), the cell growth data in this project adds further detail in that it indicates responses are likely to be inferior vs. HER2- disease with resistance emerging earlier during treatment. The data in this chapter gives reason to investigate the genomic effects of Faslodex in each pair of cell lines in order to identify Faslodex-induced or suppressed gene expression profiles that are associated with (i) superior anti-tumour response in HER2- cells (genes altered by Faslodex in both MCF-7 and T47D only) (chapter 5) and (ii) limited drug responses and earlier failure in HER2+ cells (genes altered by Faslodex in both BT474 and MDA-MB-361 only) (chapter 6), since this may provide further experimental detail on the relationship of HER2 with Faslodex response in ER+ disease.

Chapter 5

Identification of Faslodex-regulated genes potentially involved in the promotion of Faslodex resistance in the BT474, MDA-MB-361 and MCF-7 cell lines.

5.1 Introduction

In this chapter the microarray data obtained from the 4 breast cancer cell lines has been used to identify genes that could potentially be involved in the emergence of Faslodex-resistance in both the HER2+ and MCF-7 cell lines. Following HCA of the gene expression data it was noted that the gene cohort identified as being Faslodex de-regulated in MCF-7 did not cluster well with the other ER+/HER2- cell line T47D, but instead clustered more closely to the HER2+ cell lines. This suggests that there are some comparable Faslodex-promoted gene changes occurring in the 3 cell lines that developed Faslodex resistance and that any shared drug-induced gene changes could provide further detail into the mechanisms of resistance emerging during treatment in ER+ cells regardless of HER2 status.

Only a few gene signatures have been developed that relate to targeted therapy in breast cancer. Generally the best signatures of response to date include the intrinsic mutation or overexpression of the drug target leading to potential pathway addiction (Garnett *et al.*, 2012). As discussed previously, ER is one such target, where its significant expression in breast cancer dictates treatment with ER targeted therapies (AIs, tamoxifen or Faslodex) which cumulatively have significantly reduced mortality and recurrence rates (Early Breast Cancer Trialists Collaborative Group, 2011). Another example of such a target is HER2 where a cohort of breast cancer patients display amplification of HER2 and treatment with

the HER2-targeted therapy trastuzumab (Herceptin) has a significant effect on the survival rates for this particular breast cancer subtype (Vogel *et al.*, 2002).

With regards to predicting acquired resistance following initial therapy, however, there are very few promising markers, especially for Faslodex resistance. Generally, such markers have been identified by comparing drug-resistant cell models with their wild-type counterparts (Konecny *et al.*, 2006; Lynch *et al.*, 2004). Even though valuable biological information has been gathered following such studies, in particular identifying alterations in signalling pathways utilised by resistant cell models, the genomic and phenotypic changes that occur during the acquisition of resistance have not been intensely investigated and their clinical relevance is largely unknown.

However, as a promising example relevant to aromatase inhibition, Weigel *et al.,* have recently carried out such a study to identify genomic changes involved in the acquisition of resistance of oestrogen-deprivation, where they identified significant elevations in the PDGF/Abl pathway as early as one week after the initiation of treatment (Weigel *et al.*, 2012). Importantly, by identifying early drug-induced promoters of resistance, it may be possible to stratify patients based on the likelihood of extended response to targeted treatments, as well as using the information to predict the optimum second line treatments based on the mechanisms utilised to establish the resistant phenotype. Indeed, Weigel and her colleagues (2012) demonstrated that the inhibition of PDGFRβ and Abl using nilotinib, while having little effect on wild-type MCF-7 cells, significantly added to the inhibitory response to oestrogen deprivation in the same cell line.

Similarly, the Clarke laboratory (Crawford *et al.*, 2010) have investigated differences between wild-type MCF-7 cells and Faslodex-resistant cells in an attempt to identify signalling pathways utilised by cells in the resistant state which if targeted re-sensitise them to Faslodex treatment. In their studies, they have shown that BCL2, a known survival factor for breast cancer cells (Martin and Dowsett, 2013), although lowered during the responsive phase of Faslodex action, is restored in resistance, enabling the cells to evade apoptosis. In the resistant setting, an increase in

Faslodex-regulated BCL-2 mRNA, protein and promoter activity was observed, and inhibition of BCL-W and BCL-2 was shown to restore Faslodex sensitivity (Crawford *et al.*, 2010). Critically, they also showed that the tumour suppressor IRF-1 is a key mediator of the initial pro-apoptotic response to Faslodex in MCF-7 cells and the emergence of resistance in this cell line is associated with a loss of IRF-1 (Bouker *et al.*, 2004). Finally, an elevation in the NF-κB pathway has also been associated with Faslodex resistance and pharmacological inhibition of this pathway *in vitro* similarly can restore Faslodex sensitivity (Riggins *et al.*, 2005).

However, few studies of Faslodex resistance have extended past profiling of MCF7-derived lines and it is important that such studies are extended more broadly to ER+ models given the emerging applicability of this agent in both the ER+ HER2- and ER+ HER2+ setting. In this chapter, by carrying out whole genome analysis, it was hoped that biomarkers and/or drivers of Faslodex-resistance promoted by short-term Faslodex treatment in the two HER2+ and the MCF-7 cell lines (or alternatively any potential growth inhibitory genes suppressed by this agent in these models) could be revealed which transcend the HER2 status of ER+ cells.

5.3 Results

5.3.1 Identification of genes that undergo comparable Faslodex-de-regulation in the HER2+ and MCF-7 cell lines

Using those gene probes that were identified in Chapter 4 as robustly Faslodex induced or suppressed, the data were further interrogated with the fold-change tool in Genesifter to identify gene probes with a greater than 1.5 fold change in expression of comparable direction in each of the 3 cell lines (MCF-7, MDA-MB-361 and BT474 cells) during Faslodex treatment versus control cells.

Identified gene probes were then analysed in the T47D cell line dataset to ensure that the Faslodex-promoted gene changes were not shared by this cell line which showed a complete response to Faslodex, maximising likelihood of association between the identified genes and emergence of Faslodex resistance.

As you can see from Figure 24, 43 genes were significantly altered in those models that develop resistance and further only 9 were identified to exhibit at least 1.5 fold change in all 3 models with limited change in the T47D line.
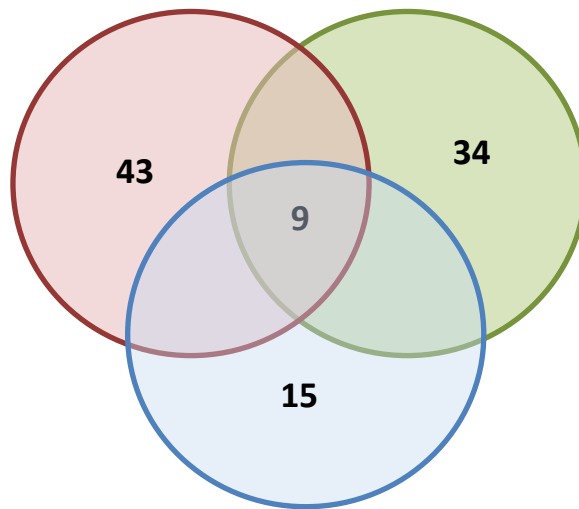
Figure 24: The Venn diagram illustrates the identification of the 9 genes taken forward as potential mediators/biomarkers of Faslodex resistance in the BT474, MDA-MB-361 and MCF-7 cell lines. The red circle represents all those genes significantly altered in the 3 cell lines that develop resistance. The green circle, shows the number of these genes that were not altered by at least 1.5 fold in these models and the blue circle are those that were found to be also altered to some extent in the T47D cell line. The 9 genes represented by the overlapping circles identify those genes that met the criteria to be taken forward.

Table 10: Genes with a greater than 1.5 fold change in gene expression following 10 days Faslodex treatment in all cell lines that eventually developed Faslodex-resistance (BT474, MDA-MB-361, MCF-7). Also listed is the total number of probes representing each gene on the UI33Aplus2 genechip, together with the number of those probes which exhibited a robust change in expression with Faslodex.

Potential resistance-promoting genes	Gene Name	Gene expression change following Faslodex treatment (in both HER2+ and MCF-7 cell lines)	Total number of probes per gene	Total number of probes exhibiting change in expression		
				BT474	MDA-MB-361	MCF-7
IKZF1	Ikaros family zinc finger protein 1	Induced	3	3	1	2
GPR37	G protein-coupled receptor 37	Induced	2	2	2	2
GABBR2	Gamma-aminobutyric acid (GABA) B receptor, 2	Induced	4	4	3	4
CXCR4	C-X-C chemokine receptor type 4	Induced	3	3	3	3
VEGFC	Vascular endothelial growth factor C	Induced	1	1	1	1
KITLG	KIT ligand	Induced	2	2	2	2
PRKACB	Protein kinase, cAMP-dependent, catalytic, beta	Induced	2	2	2	2
ZNF343	Zinc finger protein 343	Suppressed	1	1	1	1
GFRA1	GDNF family receptor alpha 1	Suppressed	1	1	1	1

The 9 genes found to be Faslodex-deregulated in only MCF-7, MDA-MB-361 and BT474 cells and their pattern of change are listed in Table 10. In instances where more than 1 probe set was present for a particular gene on the U133Aplus2

genechip, although some variability existed between the 3 cells lines with regards to the number of probe sets showing a significant alteration in level, generally the probe profile concordance was good (Table 10).

Heatmaps and gene expression intensity plots were subsequently generated to visualise the magnitude of change in expression for each of the genes listed in Table 10 for each of the cell models. The optimal jetset Affymetrix gene probe for each gene was used to generate these heatmaps and gene expression intensity plots (see section 2.3.6 of Materials and Methods for further details) and their respective gene probe ID's are listed in Table 11, along with the jetset score (where a score closer to 1 indicates a better predicted probe performance (has best sequence coverage for a given gene and accounts for splice variants thus provides a higher confidence of the de-regulation of a specific gene following Faslodex treatment). All jetset probes exhibited the directional change in expression initially observed following Faslodex treatment in heatmaps for MCF7, MDA-MB-361 and BT474 cells (Figure 25). However, Figures 5-13 further illustrate the basal and post Faslodex treatment expression for the each of the jetset probes along with the calculated fold change for each gene of interest and it is apparent that not all jetset gene probes exhibited a fold change greater than 1.5 in each of the 3 models. This was because in some instances the initial identification of the gene of interest arose from a non-jetset gene probe. In each instance, however, the directional change was identical.

Table 11: Genes of interest in relation to the promotion of resistance in MCF7, BT474 and MDA-MB-361 cells with their corresponding jetset gene probe Affymetrix ID's and jetset score (closer to 1 the better the predicted performance of the probe).

Gene Acronym	Jetset Affymetrix Probe ID	Jetset score
IKZF1	205039_s_at	0.42
GPR37	209631_s_at	0.57
GABBR2	209990_s_at	0.47
CXCR4	217028_at	0.54
VEGFC	209946_at	0.43
KITLG	207029_at	0.56
PRKACB	202741_at	0.49
ZNF343	207296_at	0.58
GFRA1	205696_s_at	0.39

The jetset profiles confirmed the majority of identified genes were substantially induced by Faslodex in each of the models, with the exception of ZNF343 and GFRA1 which were suppressed. These data are presented in Figure 25.
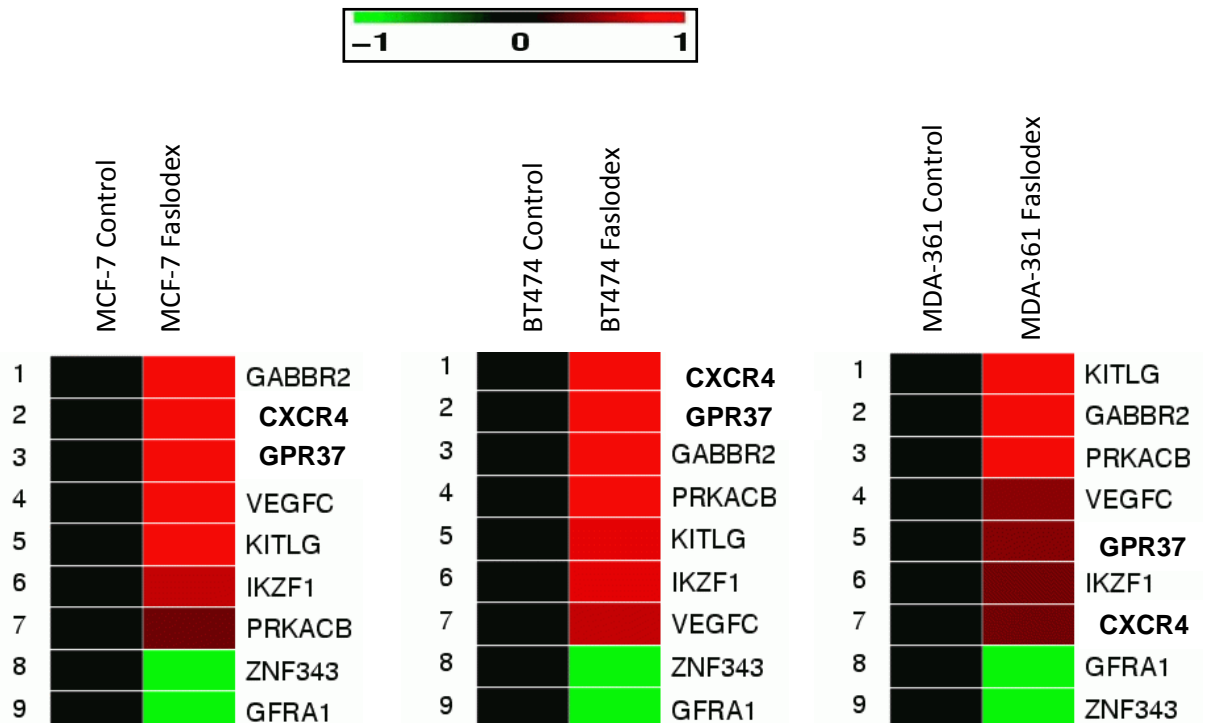
Figure 25: Heatmaps displaying change in expression of the genes of interest following 10 day Faslodex treatment in the 3 cell lines that eventually develop resistance to this antihormone. Red indicates expression is greater in the Faslodex-treated arm versus control while green indicates reduced expression versus control and black no change from control.

The 9 genes were also analysed across the 3 cell models and also comparing with the T47D cells using the gene expression intensity plots (log2 scale) generated in GeneSifter. The intensity plots displayed the average normalised expression data (+/-SEM) for each jetset probe from the triplicate data sets for each model both prior to and subsequent to 10 day Faslodex treatment.

5.3.1.1 Genes induced by Faslodex in BT474, MDA-MB-361 and MCF-7 cells:

5.3.1.1.1 IKZF1

Figure 26 shows the log2 intensity plot for the gene IKZF1. Although the error bars proved relatively large for all samples, IKZF1 was induced by Faslodex treatment in MCF-7, MDA361 and BT474 cells (Figure 26A, B), an effect not observed in T47D cells where a marginal suppression of this gene was observed. Importantly, however, all of the log2 expression values were below 0 and absent gene calls were recorded in each instance, indicative of extremely low/no gene expression in all models.

Gene Acronym	Fold change of expression following Faslodex treatment			
	BT474	**MDA-MB-361**	**MCF-7**	**T47D**
IKZF1	1.86	1.58	1.70	1.19

Figure 26: (A) Log2 intensity plot displaying the normalised (mean of triplicate samples) gene expression of IKZF1 in each of the 4 cell lines pre (Con) and post 10 day Faslodex (FAS) treatment and (B) table displaying the fold change in gene expression exerted by 10 day Faslodex treatment in each cell line vs. control expression. Highlighted in red are Faslodex-promoted inductions in gene expression >1.5 fold.

5.3.1.1.2 GPR37

Although the log2 intensity plot showed basal expression level of GPR37 was quite variable across the 4 cell lines, it was induced by Faslodex in MCF-7 and BT474 cells (Figure 27A, B). A small increase in intensity was also observed in the MDA-MB-361 cell line, in contrast to its lack of induction in T47D cell line following Faslodex treatment. However, the majority of the samples, with the exception of the Faslodex-treated MCF-7, had very low log2 expression values (0 or below) indicative of extremely low/no expression of this gene in the cells examined, however all samples called present with the exception of BT474 control suggesting some expression could be reliably detected.

A

B

Gene Acronym	Fold change of expression following Faslodex treatment			
	BT474	MDA-MB-361	MCF-7	T47D
GPR37	4.46	1.44	3.91	1.05

Figure 27: (A) A log2 intensity plot displaying the normalised (mean of triplicate samples) gene expression of GPR37 in each of the 4 cell lines pre (Con) and post 10 day Faslodex (FAS) treatment and (B) table displaying the fold change in gene expression exerted by 10 day Faslodex treatment in each cell line vs. control expression. Highlighted in red are Faslodex-promoted inductions in gene expression >1.5 fold.

5.3.1.1.3 GABBR2

While the expression of GABBR2 was increased by Faslodex treatment across BT474, MDA361 and MCF-7 cells, the induction was most obvious in the latter (Figure 28A, B). In each instance, while the pre-treatment call for the gene was absent with log2 expression values below 0, the post-treatment expression call was present. Although some induction of GABBR2 was also recorded in T47D cells, the induced levels remained lower than in the other 3 cell lines and an absent call was recorded in both pre-treatment and on treatment samples for this model.
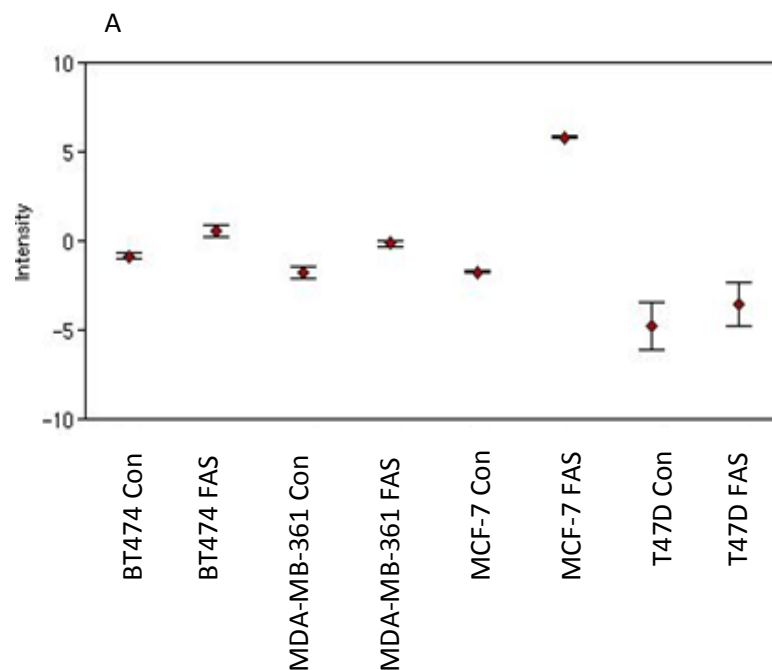
A

B

Gene Acronym	Fold change of expression following Faslodex treatment			
	BT474	MDA-MB-361	MCF-7	T47D
GABBR2	2.59	3.11	187.37	2.40

Figure 28: (A) Log2 intensity plot displaying the normalised (mean of triplicate samples) gene expression of GABBR2 in each of the 3 cell lines pre (Con) and post 10 day Faslodex (FAS) treatment (B) table displaying the fold change in gene expression exerted by 10 day Faslodex treatment in each cell line vs. untreated control. Highlighted in red are Faslodex-promoted inductions in gene expression >1.5 fold.

5.3.1.1.4 CXCR4

The log2 intensity plot for CXCR4 showed some induction of expression of this gene in the HER2+ and MCF-7 cell lines (Figure 29A). All detection calls were present in the 3 models and the error bars associated with the data were small, indicating reproducible detection of gene expression in all samples. The greatest induction promoted by Faslodex was seen in the BT474 and MCF-7 cell lines (Figure 29B). The MDA-MB-361 cell line, however, demonstrated the greatest basal expression level of CXCR4 which may explain the reduced level of induction detected in this cell model (fold change 1.37). An induction of CXCR4 gene expression by Faslodex was also observed in the T47D cell line (Figure 29B) but log2 expression values failed to reach 0 and expression calls were absent, suggesting extremely low/no CXCR4 expression.

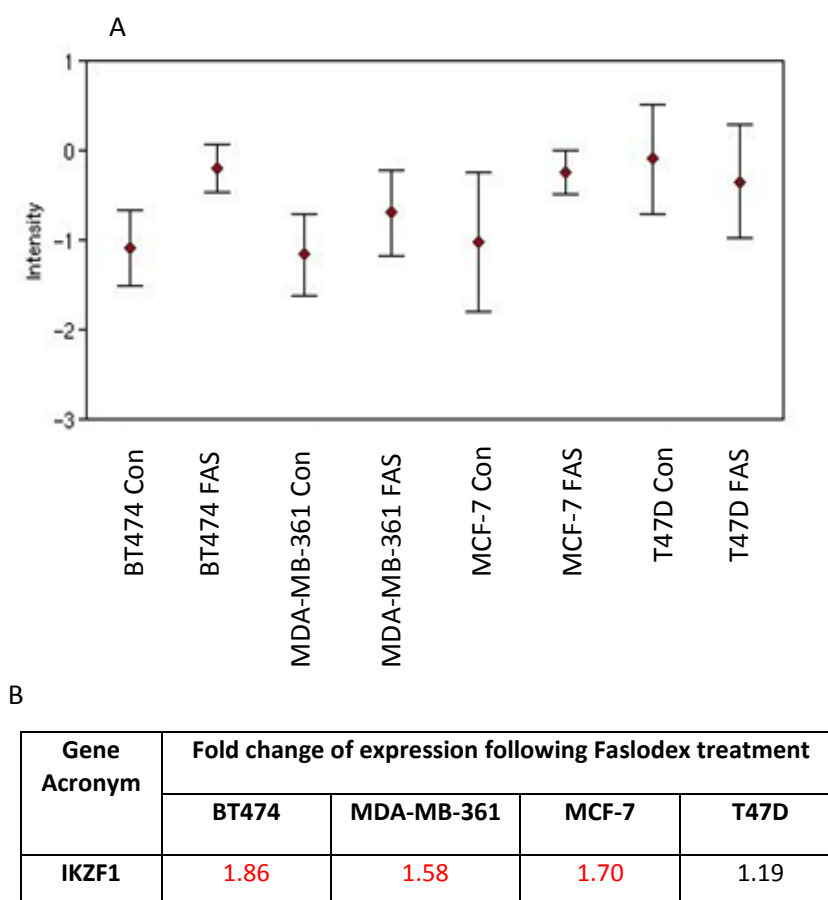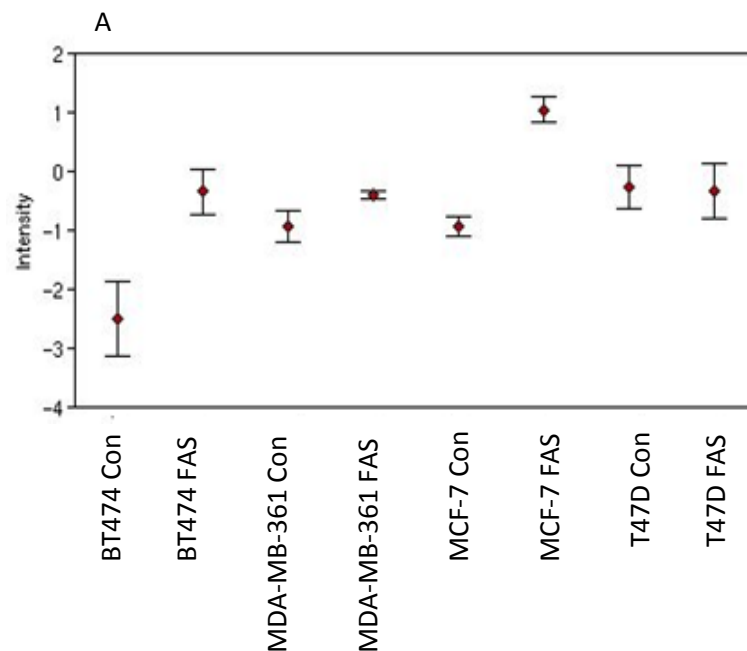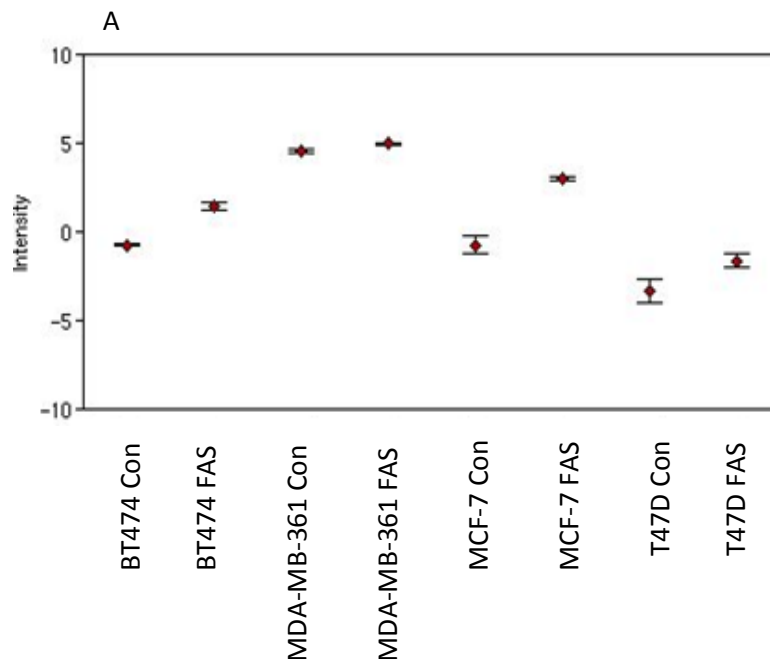| Gene Acronym	Fold change of expression following Faslodex treatment			
	BT474	MDA-MB-361	MCF-7	T47D
CXCR4	4.55	1.37	13.12	3.27

Figure 29: (A) Log2 intensity plot displaying the normalised (mean of triplicate samples) gene expression of CXCR4 in each of the 4 cell lines pre (con) and post 10 day Faslodex (FAS) treatment (B) table displaying the fold change in gene expression exerted by 10 day Faslodex treatment in each cell line vs. control expression. Highlighted in red are Faslodex-promoted inductions in gene expression >1.5 fold.

5.3.1.1.5 VEGFC

The log2 intensity plot showed basal expression level of VEGFC was similar in the HER2+ and MCF-7 cell lines, while reduced in the T47D cell line (Figure 30A). Following 10 day Faslodex treatment period, although VEGFC expression appeared up-regulated in all of the cell lines, the effect was greatest in MCF-7 and BT474 cells (Figure 30B). A small induction in VEGFC expression by Faslodex was observed in the T47D cell line, but the induction was <1.5 fold and failed to reach a log2 expression value of 0, suggestive of extremely low/no expression of this gene in T47D cells irrespective of treatment, contrasting the further models. However, the detection calls were found to be present indicative of some expression.
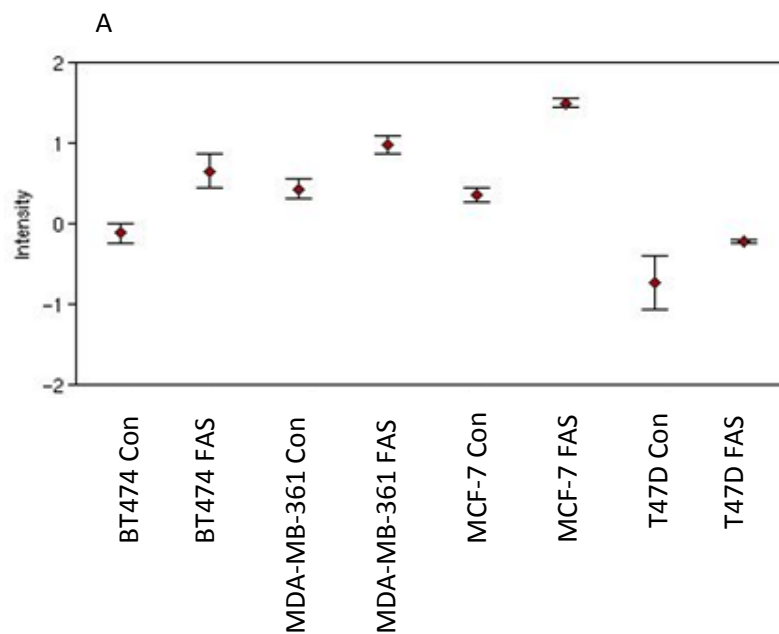
Gene Acronym	Fold change of expression following Faslodex treatment			
	BT474	MDA-MB-361	MCF-7	T47D
VEGFC	1.71	1.56	2.20	1.43

Figure 30: (A) Log2 intensity plot displaying the normalised (mean of triplicate samples) gene expression of VEGFC in each of the 4 cell lines pre and post 10 day Faslodex treatment (B) table displaying the fold change in gene expression exerted by 10 day Faslodex treatment in each cell line vs. control expression. Highlighted in red are Faslodex-promoted inductions in gene expression >1.5 fold.

5.3.1.1.6 KITLG

The log2 intensity plot (Figure 31A) revealed that although basal KITLG gene expression level was relatively low in all cell lines before Faslodex treatment, MCF-7, MDA-MB-361 and BT474 cells showed up-regulation of the expression of this gene (>1.5 fold induction) during therapy where a present call was recorded. The inductive effect was most obvious in MDA-MB-361 cells which showed almost a 4 fold induction of this gene (Figure 31B). While the T47D cells displayed an elevated basal expression level of KITLG compared to the 3 other models, KITLG was suppressed by Faslodex treatment in this cell line (Figure 31A, B).
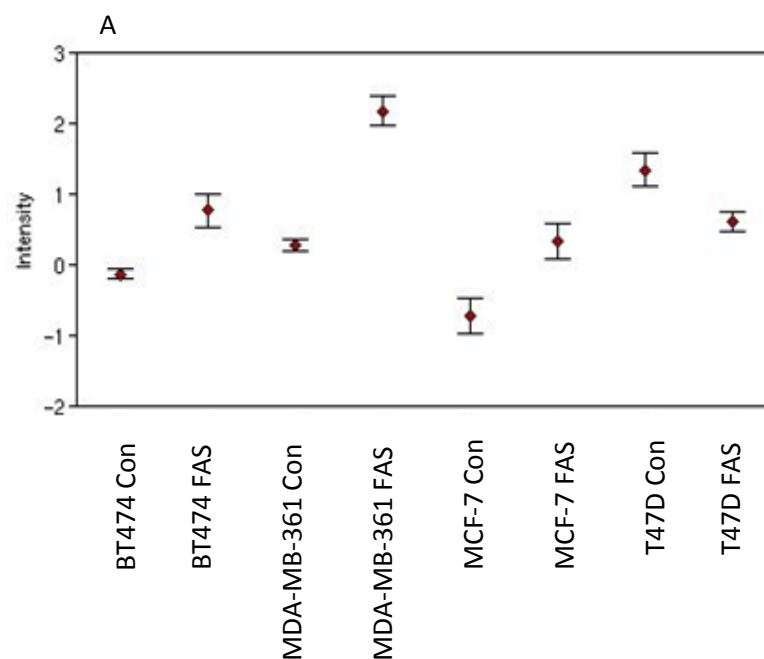
Gene Acronym	Fold change of expression following Faslodex treatment			
	BT474	MDA-MB-361	MCF-7	T47D
KITLG	1.87	3.74	2.08	1.67

Figure 31: (A) Log2 intensity plot displaying the normalised (mean of triplicate samples) gene expression of KITLG in each of the 4 cell lines pre (Con) and post 10 day Faslodex (FAS) treatment (B) table displaying the fold change in gene expression exerted by 10 day Faslodex treatment in each cell line vs. control expression. Highlighted in red are Faslodex-promoted inductions in gene expression and in green suppression of expression >1.5 fold.

5.3.1.1.7 PRKACB

The log2 intensity plot and associated fold changes (Figure 32A, B) showed that both the basal expression level of PRKACB and its induction by Faslodex was greatest in the two HER2+ cell lines in comparison to the HER2- cell models. Although the induction of PRKACB was relatively modest in MCF-7 cells, as for the HER2+ lines both pre- and post-treatment samples showed a present call, and contrasted with the lack of induction of this gene in T47D cells.
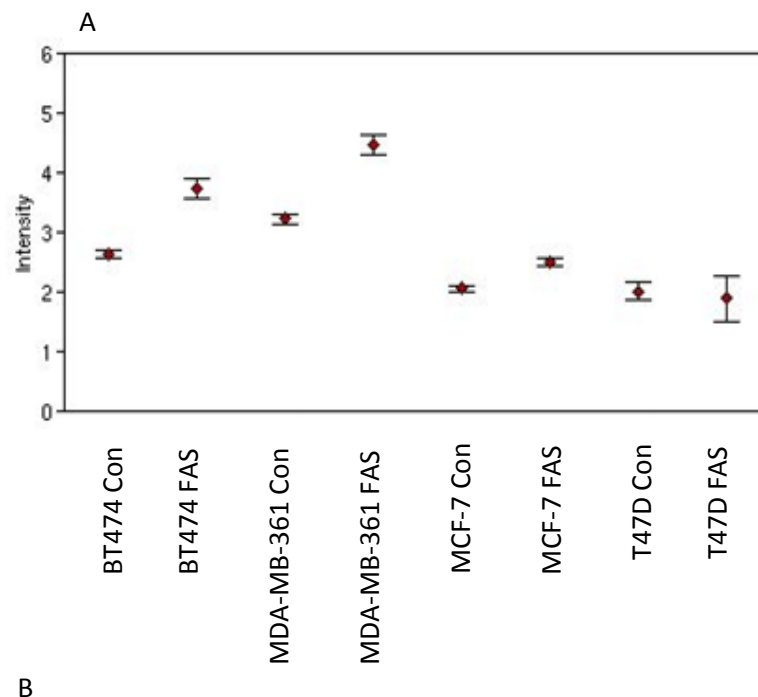
Gene Acronym	Fold change of expression following Faslodex treatment			
	BT474	MDA-MB-361	MCF-7	T47D
PRKACB	2.18	2.35	1.35	1.08

Figure 32: (A) Log2 intensity plot displaying the normalised (mean of triplicate samples) gene expression of PRKACB in each of the 4 cell lines pre (Con) and post 10 day Faslodex (FAS) treatment (B) table displaying the fold change in gene expression exerted by 10 day Faslodex treatment in each cell line vs. control expression. Highlighted in red are Faslodex-promoted inductions in gene expression >1.5 fold.

5.3.1.2 Genes suppressed by Faslodex in BT474, MDA-MB-361 and MCF-7 cells

5.3.1.2.1 ZNF343

The log2 intensity plot (Figure 34A) showed that although the basal expression level of ZNF343 was quite varied across all 4 cell lines, all values were below 0 and detection calls were found to be absent indicative of at best very low expression of this gene in these breast cancer cells. However, any ZNF343 appeared suppressed by Faslodex in the HER2+ and MCF-7 cell lines, as shown by the log2 intensity plot, with suppression greater than 2.5 fold being seen in each instance (Figure 34B). In contrast, the T47D cell line displayed an apparent up-regulation in the ZNF343 log2 intensity level by Faslodex.
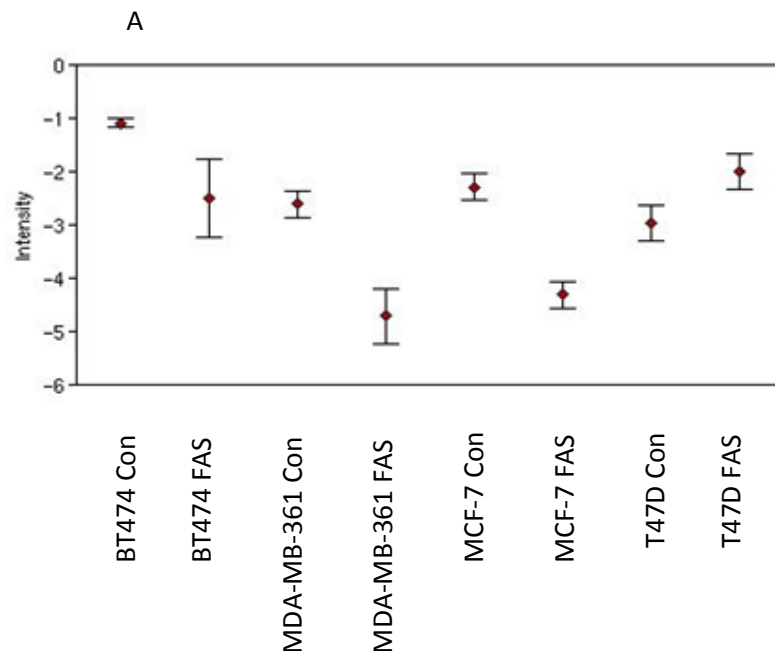
A

B

Gene Acronym	Fold change of expression following Faslodex treatment			
	BT474	MDA-MB-361	MCF-7	T47D
ZNF343	2.64	4.29	4.06	1.96

Figure 34: (A) Log2 intensity plot displaying the normalised (mean of triplicate samples) gene expression of ZNF343 in each of the 4 cell lines pre (Con) and post 10 day Faslodex (FAS) treatment (B) table displaying the fold change in gene expression exerted by 10 day Faslodex treatment in each cell line vs. control expression. Highlighted in red are Faslodex-promoted inductions in gene expression and in green suppression of expression >1.5 fold.

5.3.1.2.2 GFRA1

The log2 intensity plot and fold changes (Figure 35A and B) showed that GFRA1 was suppressed by Faslodex in the HER2+ and MCF-7 cell lines, despite variable basal expression levels of this gene. In contrast, no change was observed in GFRA1 levels during Faslodex treatment in T47D cells, where the log2 intensity levels of this gene were also extremely low both before and after treatment. Analysis of the detection calls found only the BT474 cell line to demonstrate a change from present to absent indicative of a robust down-regulation while the MDA-MB-361 and MCF-7 cell lines basally called present and remained present following treatment suggesting residual expression following treatment. Indicative of the very low expression observed in the T47D cell line by the log2 intensity plot, detection calls were found to be absent.
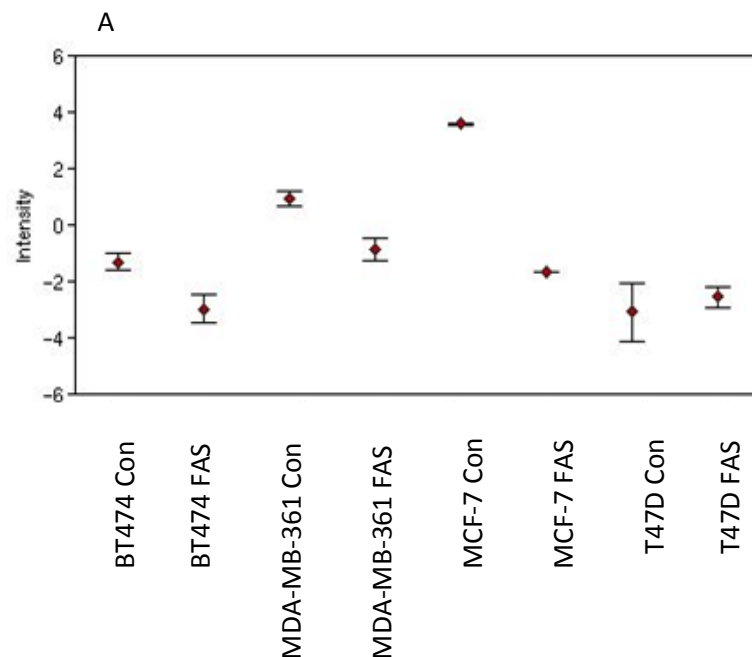
A

B

Gene Acronym	Fold change of expression following Faslodex treatment			
	BT474	MDA-MB-361	MCF-7	T47D
GFRA1	3.13	3.46	37.93	1.45

Figure 35: (A) Log2 intensity plot displaying the normalised (mean of triplicate samples) gene expression of GFRA1 in each of the 4 cell lines pre (Con) and post 10 day Faslodex (FAS) treatment (B) table displaying the fold change in gene expression exerted by 10 day Faslodex treatment in each cell line vs. control expression. Highlighted in green are Faslodex-promoted suppression in gene expression >1.5 fold.

To summarise the various array data for each gene, the jetset gene probe for IKZF1 was the only probe representing IKZF1 out of the 3 probes that exhibited a significant, greater than 1.5 fold change in expression following Faslodex treatment in the HER2+ and MCF7 models (Table 10, Figure 26). The remaining 2 probes for IKZF1 on the array underwent a suppression following treatment in at least one of the models questioning the reliability of the up-regulation of this gene across all 3 lines with the jetset probe. This unreliability was further confirmed by the large error bars and absent detection calls for this gene. Indeed, log2 expression values for IKZF1 jetset probe were also very low (Figure 26) suggesting PCR verification would be difficult so subsequently this gene was not taken forward for further investigation. Similarly, the very low log2 expression values (below 0) determined for GPR37 (Figure 27) particularly in the HER2+ cell lines and ZNF343 in all cell lines (Figure 34) pre and post Faslodex treatment again suggest PCR verification would be difficult for these genes and thus they were also not taken forward for further investigation.

5.3.2 Analysis of the HER2+ and MCF-7 shared potential resistance-promoting genes in an MCF-7-derived Faslodex-resistant gene expression array dataset

As the 6 remaining Faslodex de-regulated genes identified in this chapter are hypothesised to be involved in the onset and development of the Faslodex resistant phenotype in the HER2+ and MCF-7 cell lines, their expression profiles were subsequently analysed using Genesifter in a microarray dataset generated from an MCF-7-derived acquired Faslodex-resistant cell line (compared to oestrogen-treated control MCF-7 cells). The resultant heatmaps (Figure 36), log2 intensity plots and fold change data are shown for the Faslodex resistant model versus the control using the jetset probes for each gene. Of the 6 genes examined, 4 (GABBR2, PRKACB, CXCR4 and GFRA1; Figures 37, 38, 39 and 42 respectively) retained the expression profile identified during early Faslodex response into the acquired resistant state. On this further array set, PRKACB and CXCR4 (Figures 38, 39) showed the highest log2 intensity values in resistance for the induced genes, while the value for the suppressed gene GFRA1 fell below 0 in resistance (Figure 42). The

Faslodex induced gene VEGFC was lost in resistance (Figure 41), while KITLG showed no marked difference between oestradiol treated MCF-7 cells and those which had developed Faslodex resistance (Figure 40).
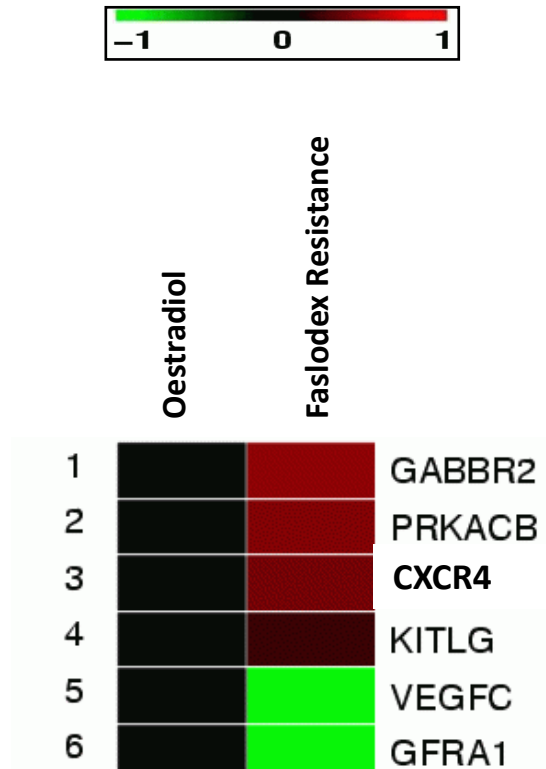
Figure 36: Heatmap displaying the 6 genes from the HER2+ and MCF-7 cell lines analysed in the MCF-7 Faslodex-resistant cell line compared to oestradiol (E2) treated MCF-7 cells. The heatmap has been generated using jetset affymetrix gene probe IDs (see Table 2).

5.3.2.1 Genes induced by 10 day Faslodex-treatment: GABBR2, PRKACB, CXCR4, KITLG and VEGFC

Gene Acronym	Fold change
GABBR2	1.47
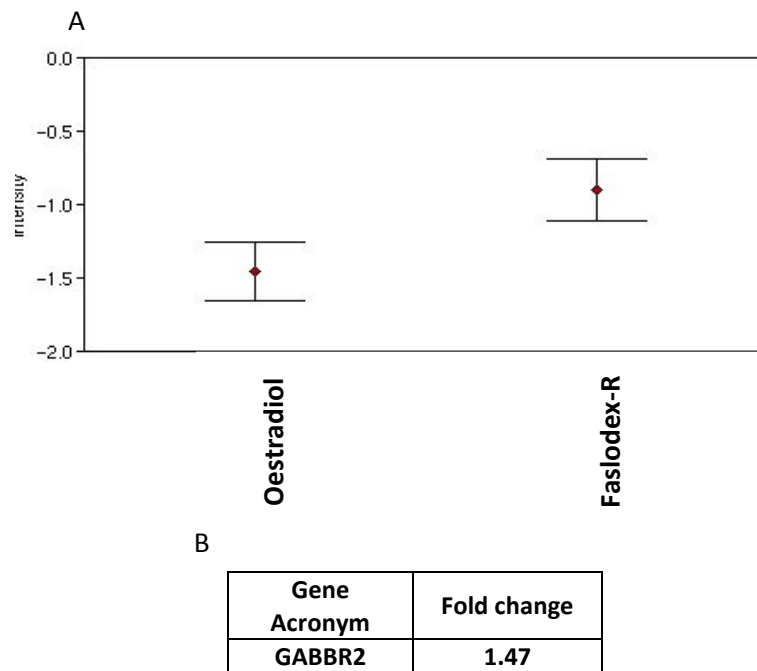
Figure 37: (A) Log2 intensity plot displaying the induction of GABBR2 gene expression in an MCF-7-derived, acquired Faslodex-resistant cell model in comparison to wild-type MCF-7 cells treated with oestradiol (10^{-9}M) using the jetset probe (B) Fold difference of GABBR2 expression in the resistant versus the oestradiol-treated control cells .
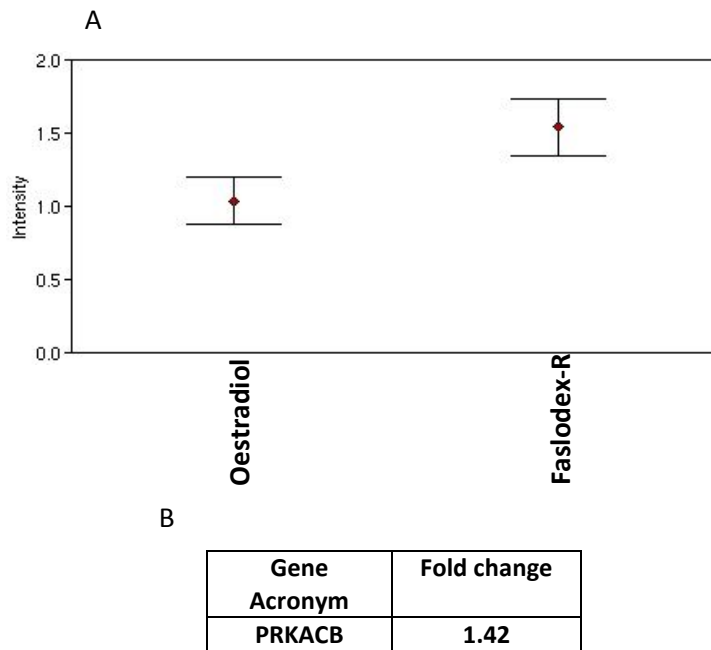
Figure 38: (A) Log2 intensity plot displaying the induction of PRKACB gene expression in an MCF-7-derived, Faslodex-resistant cell model in comparison to wild-type MCF-7 cells treated with oestradiol (10^{-9}M) using the jetset probe (B) Fold difference of PRKACB expression in the resistant versus the oestradiol-treated control cells.
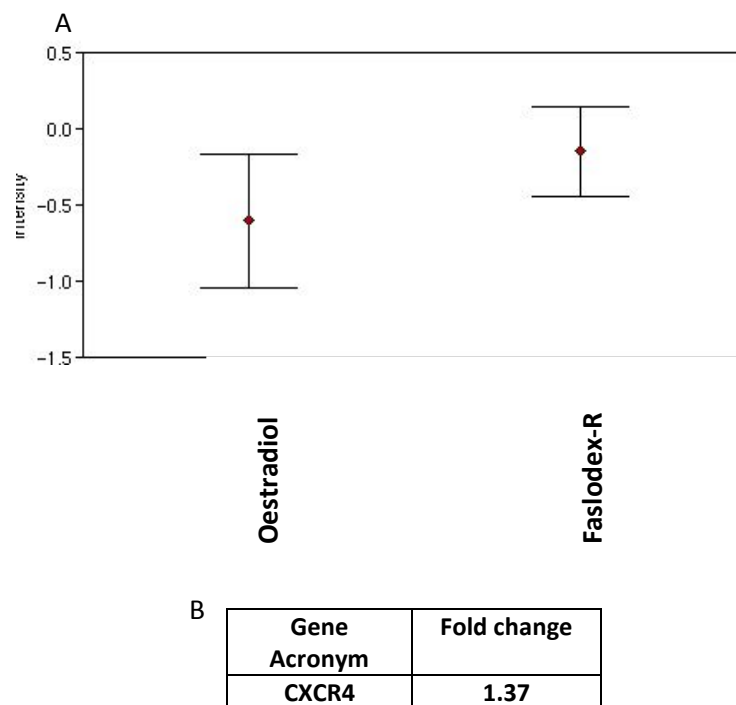
Figure 39: (A) Log2 intensity plot displaying the induction of CXCR4 gene expression in an MCF-7-derived, Faslodex-resistant cell model in comparison to wild-type MCF-7 cells treated with oestradiol (10^{-9}M) using the jetset probe (B) Fold difference of CXCR4 expression in the resistant versus the oestradiol-treated control cells.
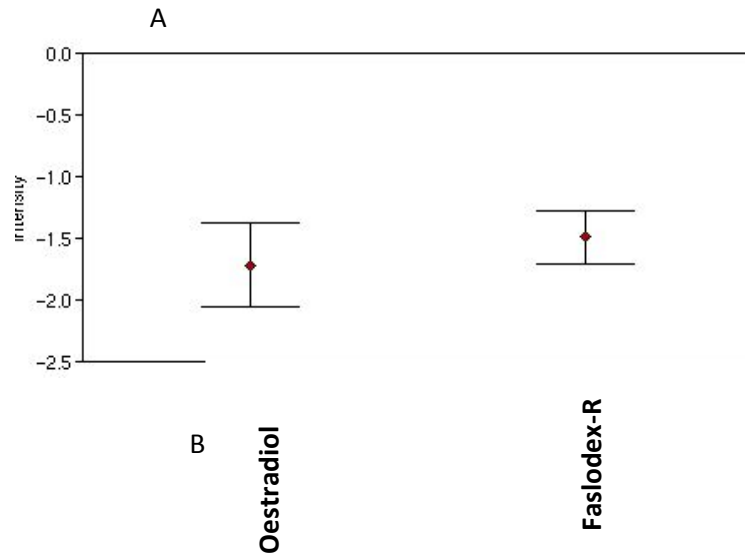
Figure 40: (A) Log2 intensity plot displaying the induction of KITLG gene expression in an MCF-7-derived, Faslodex-resistant cell model in comparison to wild-type MCF-7 cells treated with oestradiol (10^{-9}M) using the jetset probe (B) Fold difference of KITLG expression in the resistant versus the oestradiol-treated control cells.

Gene Acronym	Fold change
VEGFC	6.35
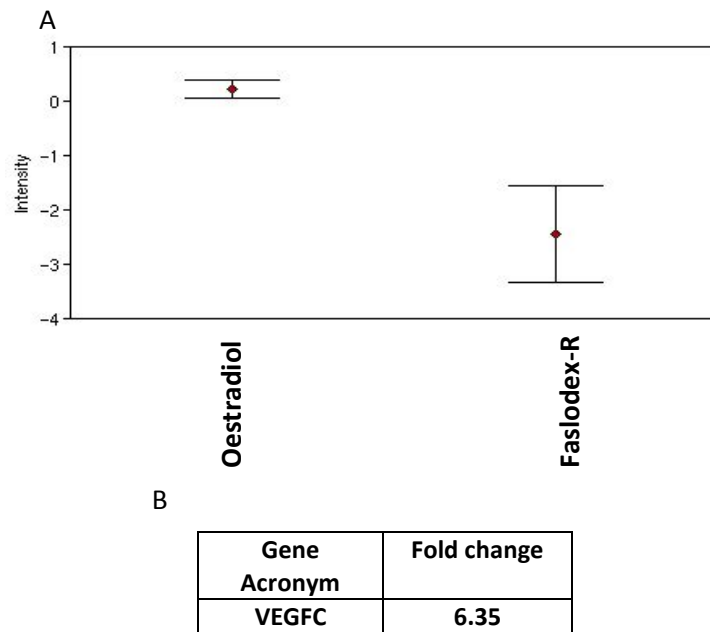
Figure 41: (A) Log2 intensity plot displaying the induction of VEGFC gene expression in an MCF-7-derived, Faslodex-resistant cell model in comparison to wild-type MCF-7 cells treated with oestradiol (10^{-9}M) using the jetset probe (B) Fold difference of VEGFC expression in the resistant versus the oestradiol-treated control cells.

5.3.2.2 Genes suppressed by 10 day Faslodex-treatment: GFRA1
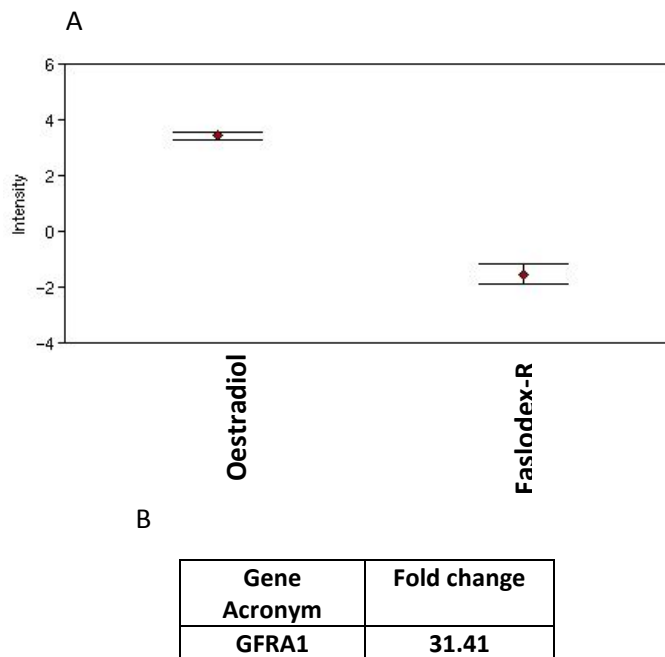
Figure 42: (A) Log2 intensity plot displaying the induction of GFRA1 gene expression in an MCF-7-derived, Faslodex-resistant cell model in comparison to wild-type MCF-7 cells treated with oestradiol (10^{-9}M) using the jetset probe (B) Fold difference of GFRA1 expression in the resistant versus the oestradiol-treated control cells.

5.3.3 Ontological investigation of potential resistance-promoting genes

An ontological investigation was also undertaken on the 6 genes to determine if they had been associated with:

- Breast cancer or any other cancer type;
- Known or potential adverse function (e.g. tumour growth or progression);
- Known or potential tumour suppressive function

The results of the ontological investigations are accumulated in Tables 12 to 17. Pubmed and Scopus were used throughout for these ontological studies using the gene name/acronym, together with selected keywords/phrases which included breast cancer, cancer, oncogene, proliferation, growth, metastasis, Faslodex, hormonal or endocrine therapy, survival, growth inhibition, tumour suppressor,

apoptosis. Gene acronyms highlighted in red were induced by Faslodex in T47D cells and those in green were suppressed.

Table 12: Summary of the function of GABBR2 including previous published reports regarding the role of GABBR2 and further aspects of GABA signalling in breast and other cancers.

Gene name/acronym	Gamma-aminobutyric acid (GABA) B receptor, 2: **GABBR2**
Function	Member of the G-protein coupled receptor 3 family and GABA-B receptor subfamily. The GABA-B receptors inhibit neuronal activity through G-proteins that inhibit adenylyl cyclase activity, stimulates phospholipase A2, activates potassium channels, inactivates voltage-dependent calcium-channels and modulates inositol phospholipids hydrolysis (reviewed by Bettler *et al.*, 2003).
Associations with breast cancer	Increased GABA content has been observed in a number of cancers including breast (Opolski *et al.*, 2000). GABAergic signalling is altered in cancer cells, particularly GABA levels and L-glutamate decarboxylase (GAD) activity (GABA is synthesised from glutamate using the GAD enzyme) which are increased in certain types of tumours, including ovarian and breast suggesting increased GABA production within such tumour cells. Baclophen, a GABA-B receptor agonist, has been shown to have a growth inhibitory effect on mammary cancer in mice. In both human and mice GABA levels and GAD activity were elevated in tumour tissue compared to normal tissue. Given the inhibitory effect of a GABA-B receptor agonist on mammary cancer growth, and the correlation between GABA level and the stage of breast pathology and/or hormonal activity, it is probable that the GABAergic system is involved in hormonal regulation and pathogenesis of breast cancer (Opolski *et al.*, 2000). In human breast cancer cells, migration was stimulated by the GABAA receptor agonist propofol (Garib *et al.*, 2002).

Associations with other cancers	In advanced prostate cancer patients, activation of GABA-B receptors induced MMP expression and stimulated the invasive capability of the cancer cells (Azuma *et al.*, 2003). GABBR2 mRNA expression has been found to be elevated in an aggressive lung cancer cell line, exhibiting enhanced spontaneous metastasis in nude mice in comparison to its parental cell line (de Lange *et al.*, 2003).

For GABBR2 to have a functional role in the onset and development of Faslodex resistance GABA must be produced by the cells. Endogenously GABA is synthesised from glutamate via the GAD enzyme thus increased GAD expression indirectly could suggest elevated GABA levels. Using the jetset gene probes for GAD1 and GAD2 (206669_at and 216651_s_at respectively), two forms of the GAD enzyme, the expression of these genes was thus analysed in the HER2+ and MCF-7 cell lines following Faslodex treatment (Figure 43). The heatmaps showed that Faslodex treatment also up-regulated the expression of these genes (Figure 43A) but subsequent analysis of the log2 expression intensity plots indicated at best very low expression in all cell models pre and post treatment (Figure 43B).
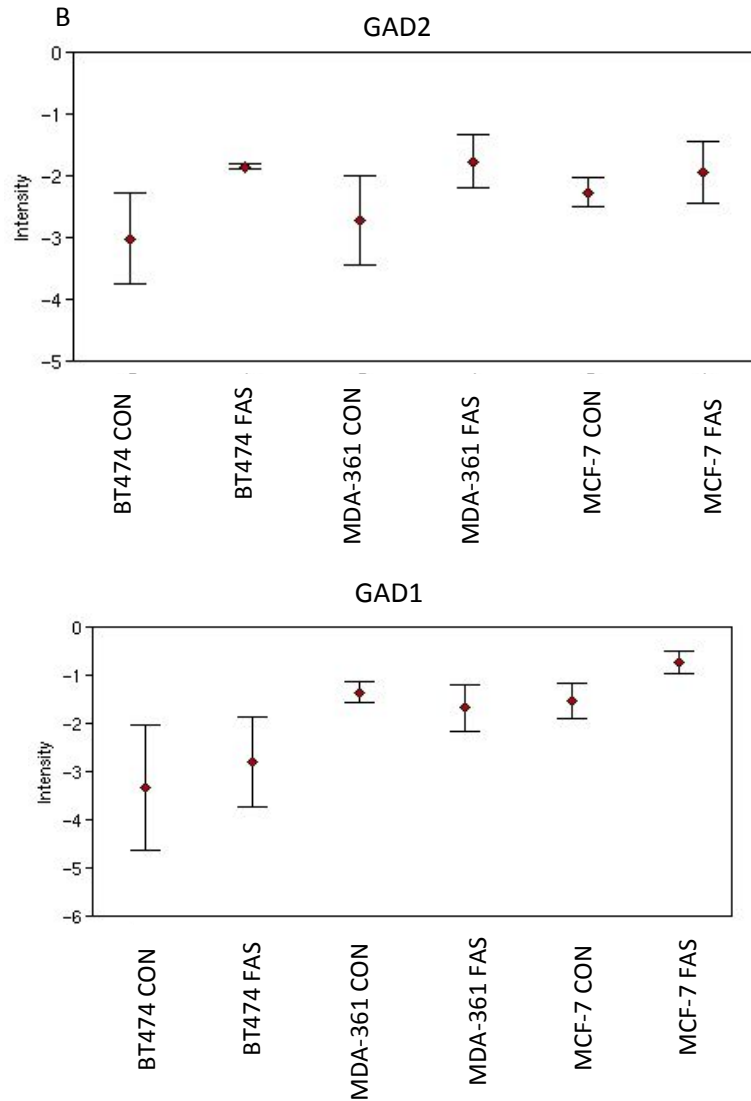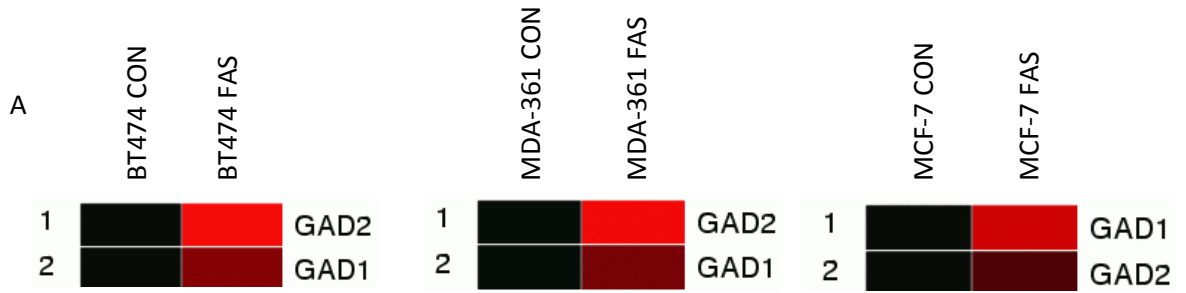
Figure 43: (A) Heatmaps generated by GeneSifter to assess the expression of the GAD enzyme, reported to be involved in the biosynthesis of GABA, in the HER2+ and MCF-7 cell lines and (B) Log2 normalised expression plots displaying expression in each cell line including T47D, pre and post 10 day Faslodex treatment. Jetset gene probes were used; GAD1-206669_at; GAD2-216651_s_at

Table 13: Summary of the function of CXCR4 including previous published reports surrounding the role of CXCR4 in breast and other cancers.

Gene name/acronym	Chemokine (C-X-C motif) receptor 4: **CXCR4**
Function	This gene encodes a CXC chemokine receptor specific for stromal cell-derived factor-1 (SDF-1). It is the receptor for CXCL12/SDF-1 (CXCL12) that transduces a signal by increasing intracellular calcium ion levels and enhancing MAPK1/MAPK3 activation (reviewed by Tiecher *et al.*, 2010).
Associations with breast cancer	CXCR4 has been shown to play a significant role in breast cancer as well as other cancers. In particular the CXCR4/SDF-1 signalling axis has been observed to have a primary role in metastasis, where organs secreting high amounts of SDF-1 tend to become the secondary tumour sites (Balkwill *et al.*, 2004). CXCR4 is expressed by cancer stem cells and thus increased secretions of SDF-1 result in the movement of cancer stem cells to those locations, usually metastatic sites (Kucia *et al.*, 2005).
	As well as the role for CXCR4 in tumour progression, more recently research has established a role for CXCR4 in breast cancer development (Yagi *et al.*, 2011).
	Rhodes *et al* reported a role for CXCR4 in the development of hormone-independence in ER+ breast cancer. The overexpression of CXCR4 in MCF-7 cells resulted in increased tumour growth in the presence of oestrogen, however, this increase in growth was also seen in the absence of oestrogen suggesting CXCR4 signalling contributes to hormone independence (Rhodes *et al.*, 2011). CXCR4 has the ability to activate ER in an oestrogen-independent manner (Sauve *et al.*, 2009), possibly increasing SDF-1 expression as a consequence and thus further promoting CXCR4 signalling.
	SDF-1 is an ER-regulated gene thus treatment with Faslodex has been shown to suppress SDF-1 expression. However, SDF-1

	expression in CXCR4-expressing cells has been shown to overcome Faslodex-induced growth inhibition (Rhodes *et al.*, 2011) and it has been hypothesised that there is a switch in cancer cells from oestrogen-dependent production of SDF-1 to SDF-1 produced by stromal cells (Sauve *et al.*, 2009). CXCR4 signalling has been found to be essential for the maintenance of the cancer stem cell population in a tamoxifen-resistant cell model derived from the MCF-7 cell line and thus a possible therapeutic target in the endocrine resistant clinical setting (Dubrovska *et al.*, 2012).
Associations with other cancers	CXCR4 has been shown to mediate many of same functions related to cancer development and progression in cancers in addition to breast. The CXCR4-SDF-1 signalling axis encourages metastasis in a variety of other cancers including prostate, small cell lung cancer, colorectal, melanoma and ovarian cancers (Sun *et al.*, 2003; Kijima *et al.*, 2002, Zeelenberg *et al.*, 2003; Scotton *et al.*, 2002).

As described in Table 13, the contribution of CXCR4 towards a limited Faslodex response is dependent on its activation by SDF-1 (CXCL12). SDF-1 is an ER-regulated gene and has been shown to be down-regulated by Faslodex treatment (Rhodes *et al.*, 2011). *In vivo*, CXCR4 has been speculated to continue to contribute to endocrine resistance via the alternative availability of SDF-1 from stromal cells. However, in the cell lines in this project, for CXCR4 to be functionally involved in Faslodex-resistance SDF-1 would have to be produced in an autocrine manner despite Faslodex treatment. From Figure 22 it can be seen that SDF-1 (CXCL12) gene expression was down-regulated by Faslodex treatment in both HER2+ and MCF-7 cell lines to log2 intensity values below 0 indicating extremely low/no expression after this antihormone but expression values were found to be present (with the exception of the MCF-7 Faslodex treated sample which called absent) indicative of some residual expression.

Figure 44: (A) Heatmaps generated by GeneSifter to assess the expression of CXCL12/SDF1, the reported ligand for CXCR4, in the HER2+ and MCF-7 cell lines and (B) Log2 normalised expression plots displaying expression in each cell line including T47D, pre and post 10 day Faslodex treatment. Jetset gene probe was used; CXCL12-209687_at

Table 14: Summary of the function of PRKACB including previous published reports surrounding the role of PRKACB in breast and other cancers.

Gene name/acronym	Protein kinase, cAMP-dependent, catalytic, beta: **PRKACB**
Function	The protein encoded by the gene PRKACB is a subunit of protein kinase A (PKA). It is a member of the Ser/Thr protein kinase family and is a catalytic subunit of cAMP-dependent protein kinase. PKA activation regulates a number of cellular processes such as cell proliferation, the cell cycle, differentiation as well as regulation of intracellular transport mechanisms and ion flux (Yu *et al.*, 2013)
Associations with breast cancer	PKA activation has been shown to induce tamoxifen-resistance in

	breast cancer. Overexpression of PKA as well as down regulation of the inhibitory subunit PKA-RIα has been observed in tamoxifen-resistant tumours (Michalides *et al.*, 2004). Further details of PKA contribution to tamoxifen resistance were uncovered by de Leeuw *et al* who showed that PKA can phosphorylate ER at Serine 305 resulting in conformation when exposed to tamoxifen that allows this antihormone to act as an ER agonist and thus exhibit tamoxifen resistance (de Leeuw *et al.*, 2012)
Associations with other cancers	PKA is overexpressed in many cancers and as a result it has been considered as a diagnostic marker as well as a therapeutic target (Caretta *et al.*, 2011). PKA has been identified as a critical mediator in prostate carcinogenesis via its crosstalk with the androgen receptor and activating other oncogenic signalling pathways including EGFR and RAS (Merkle *et al.,* 2011). In lung cancer, PKA has been shown to be involved in hypoxia-mediated EMT, migration and invasion (Shaikh *et al.,* 2012). Increased expression of PKA has been associated with resistance to MEK inhibitors in lung and colorectal cancer cells (Troiani *et al.,* 2012).

Table 15: Summary of the function of KITLG including previous published reports surrounding the role of KITLG in breast and other cancers.

Gene name/acronym	KIT ligand: KITLG/SCF
Function	KIT ligand is the ligand for tyrosine-kinase receptor c-kit. It plays an essential role in the regulation of cell survival and proliferation, hematopoiesis, stem cell maintenance, gametogenesis and mast cell development. KITLG/SCF binding can

	activate several signalling pathways (reviewed by Lennartsson *et al.*, 2012).
Associations with breast cancer	c-kit is infrequently expressed in breast cancer and expression in breast tumours is an indicator of a basal-like tumour (Nielsen *et al.*, 2004). It has also been found to be over-expressed in tumours with BRCA-1 mutation-associated breast cancer (Regan *et al.*, 2012).
	The KITLG-c-kit axis has been implicated in the metastasis of breast tumours in mouse models via HIF-1 mediated KITLG release (Kuonen *et al.*, 2012).
	KITLG has been reported to be produced by tumour cells (Hue *et al.*, 2005) and is widely distributed throughout the body, in particular stromal cells, and detectable at low levels in the blood (Ashman, 1999). In cancer the KITLG-c-kit axis is thought to function in both an autocrine and paracrine manner contributing to mammary malignancy (Hines *et al.*, 1995).
	c-Jun has been identified at the invasive front of breast cancer tumours (Vleugel *et al.*, 2006) and induction of this oncogene regulates the expression of a number of proteins involved in growth, proliferation and development (Shaulian *et al.*, 2002). Jiao *et al* have shown that c-Jun is involved in HER2-induced migration and invasion in mammary epithelial cells where c-Jun promoted the expression of KITLG and CCL5. KITLG and CCL5 encouraged the expansion of mammary cells with self-renewal activity and promoted invasiveness (Jiao *et al.*, 2010).
	Stimulation of c-kit activates a wide array of signalling pathways that are known to be involved in onogenic signalling such as PI3K, Src, Ras-Erk and JAK-STAT (reviewed in Kitamura *et al.*, 2004; Ronnstrand *et al.*, 2004).

	c-kit is also expressed on stem cells such as hematopoietic progenitors and has thus been used as a stem cell marker, and KITLG by binding to c-kit has been shown to contribute to the survival, self-renewal and maintenance of human stem cells. Stromal cells surrounding human stem cells can be a source of KITLG (Kent *et al.,* 2008).
Associations with other cancers	c-Kit acts as oncogene in several tumors, in particular gastrointestinal stromal tumors (GIST), mastocytosis, and melanoma (Pittoni *et al.,* 2011), through activating mutations in the extracellular or intracellular domain (Liu *et al.,* 2007) or through an autocrine KITLG/c-Kit loop (Stanulla *et al.*, 1995). A KIT inhibitor, Gleevec (Imatinib) has been generated and is approved for the use in GIST following therapy to prevent recurrence and for use in inoperable tumours. KITLG also activates tissue-resident mast cells to generate a tumor-promoting angiogenic microenvironment (Crivellato *et al.*, 2008). Hypoxia promotes the expression of HIFs which induce a number of factors that encourage angiogenesis, one being KITLG (Ceradini *et al.*, 2004).

KITLG is the ligand for c-kit and the activation of this RTK has been reported to be involved in a plethora of disease-progression events. Consequently, the expression of c-kit was also investigated in each of the 3 cell lines in this project that eventually develop Faslodex resistance. From the heatmaps in Figure 45A it can be seen that there was no consistent change in expression of c-kit in the 3 models and the log2 expression intensity plot revealed that c-kit is unlikely to be expressed either pre or post Faslodex treatment with all detection calls absent (Figure 45B).
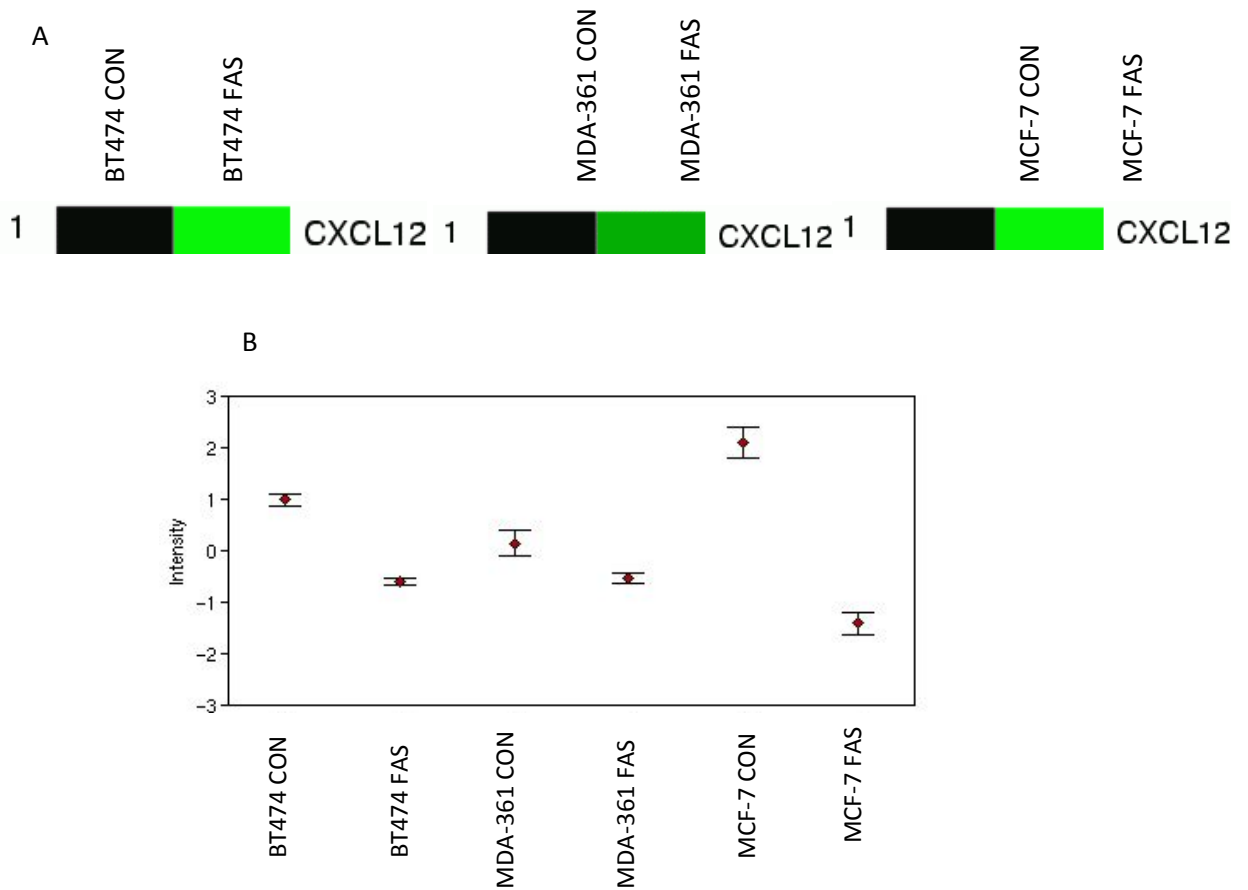
Figure 45: (A) Heatmaps generated by GeneSifter to assess the expression of c-kit, the reported receptor for KITLG, in the HER2+ and MCF-7 cell lines and (B) Log2 normalised expression plots displaying expression in each cell line including T47D, pre and post 10 day Faslodex treatment. Jetset gene probe was used; KIT-205051_s_at

Table 16: Summary of the function of VEGFC including previous published reports surrounding the role of VEGFC in breast and other cancers.

Gene name/acronym	Vascular endothelial growth factor C: **VEGFC**
Function	The protein encoded by this gene is a member of the vascular endothelial growth factor family. It is involved in angiogenesis and endothelial cell growth, stimulating their proliferation and migration while also affecting the permeability of blood vessels (Hirakawa *et al.,* 2007).
Associations with breast cancer	VEGFC has been identified to be particularly involved in intratumoral lymphangiogenesis resulting in enhanced metastasis to the lymph nodes and lungs and ultimately leading to a poorer prognosis (Skobe *et al.*, 2001).

	Expression of VEGFC also encourages metastasis of tumour cells thus contributing to a more aggressive behaviour (Burton *et al*., 2008). In agreement with this increased expression of VEGFC has been shown to correlate with lymph node metastasis in a number of tumour types (Rinderknecht *et al.,* 2009; He *et al.,* 2005). As well as its role in lymphangiogenesis VEGFC also promotes cell proliferation and invasion thus further promoting disease progression (Tobler *et al.,* 2006). All of the functions of VEGFC are mediated mainly through the VEGFR3 receptor and occasionally theVEGFR2 receptor (depending on the post-translational modifications that VEGFC has undergone) (Joukov *et al.,* 1994)
Associations with other cancers	VEGFC expression has been identified in several cancers where it has been associated with increased lymphatic metastases. These include colorectal cancer (Akagi *et al.*, 2000), cervical cancer (Hashimoto *et al.,* 2001), and gastric adenocarcinoma (Juttner *et al.,* 2006). Expression of VEGFC (and VEGFA) have been reported to predict a poorer prognosis in gastric cancer and combined suppression of both factors markedly suppresses cancer growth (Wang *et al.*, 2013).

As VEGFC is the ligand for the VEGFR3 (FLT4) receptor and has been shown to also signal through the VEGFR2 (KDR) receptor, the gene expression levels of these two receptors were also investigated from the microarray datasets for all 3 cell lines to determine if autocrine signalling was likely during Faslodex treatment (Figure 46). VEGFR3 (FLT4) appeared to be down-regulated in all cell lines by Faslodex and furthermore the log2 expression values were below 0 both pre and post Faslodex treatment with all detection calls being absent. VEGFR2 (KDR) gene expression was

suppressed by Faslodex in both HER2+ cell lines and again log2 expression values were below 0 and detection calls were absent. The MCF-7 cell line exhibited an up-regulation of VEGFR2 expression and although the detection call was shown to go from absent to present with Faslodex, it was notable that log2 expression values were below 0 indicating at best only low expression.
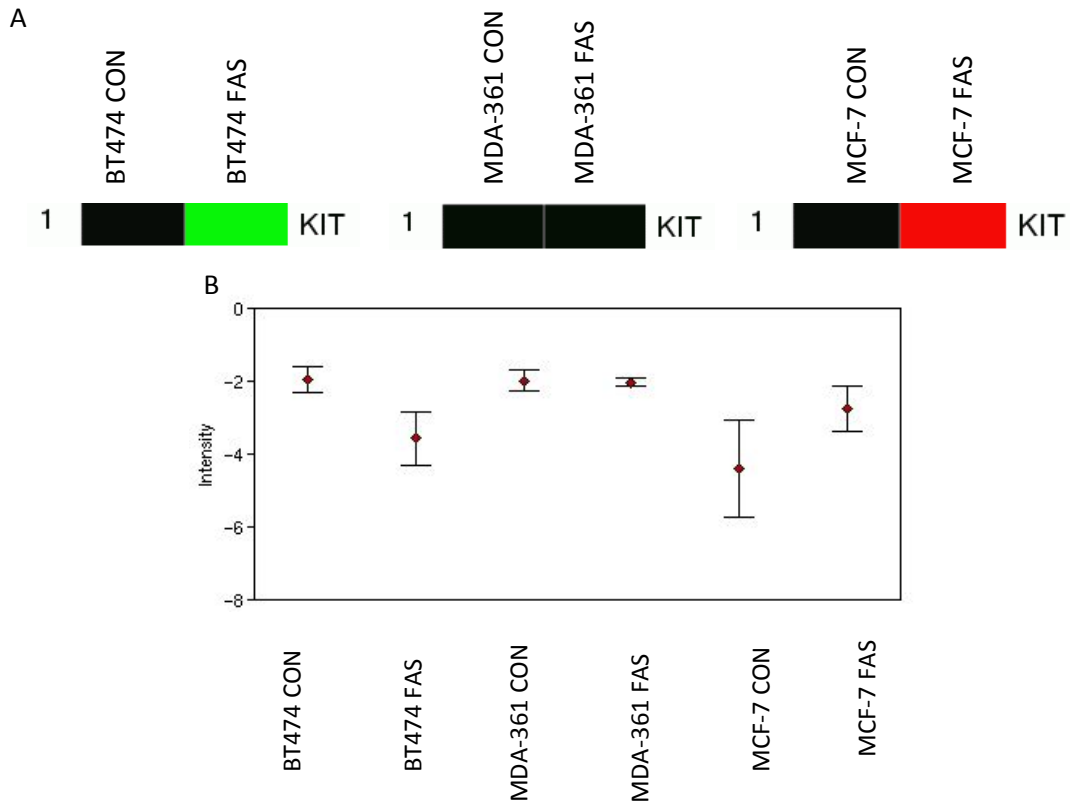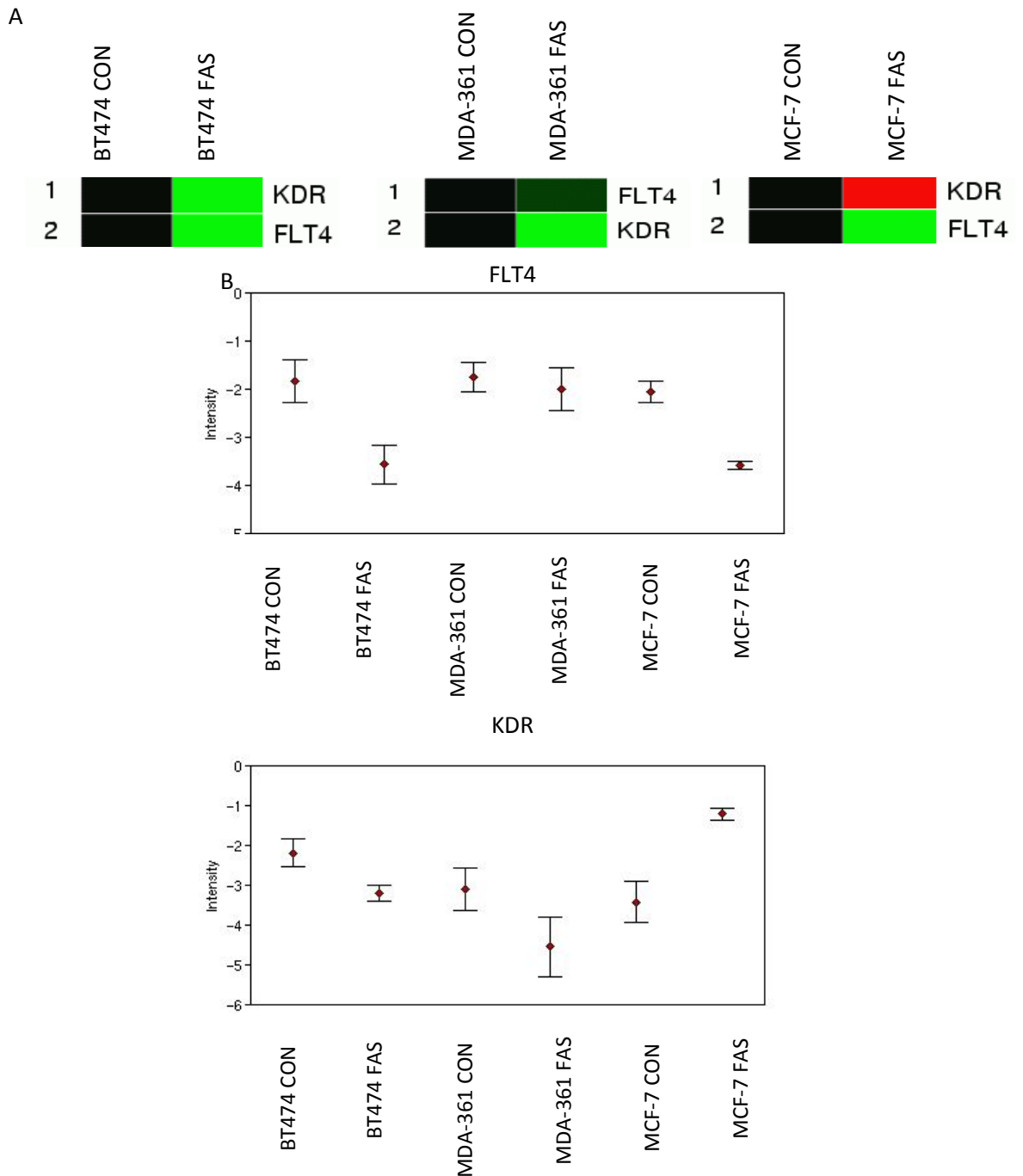
Figure 46: (A) Heatmaps generated by GeneSifter to assess the expression of VEGFR2 and VEGFR3, reported receptors for VEGFC, in the HER2+ and MCF-7 cell lines and (B) Log2 normalised expression plots displaying expression in each cell line including T47D, pre and post 10 day Faslodex treatment. Jetset gene probes were used; VEGFR2 (KDR)-203934_at; VEGFR3 (FLT4)-210316_at

Table 17: Summary of the function of GFRA1 including previous published reports surrounding the role of GFRA1 in breast and other cancers.

Gene name/acronym	GDNF family receptor alpha 1: **GFRA1**
Function	The protein encoded by this gene is a member of the GDNF receptor family. It is a glycosylphosphatidylinositol(GPI)-linked cell surface receptor primarily for GDNF, and mediates activation of the RET tyrosine kinase receptor (Takahashi *et al.*, 2001).
Associations with breast cancer	A subset of ER+ breast cancer patients have been shown to express elevated levels of RET and its co-receptor GFRA1 and that RET signalling in the ER+ setting can activate ERK1/2 and AKT signalling pathways (Esseghir *et al.*, 2007; Boulay *et al.,* 2008). These signalling pathways have been shown to be involved in limiting tamoxifen and aromatase inhibitor response and inhibition of RET in the resistant setting resensitised cells endocrine therapy (Plaza-Menacho *et al.*, 2010; Morandi *et al.,* 2013).
	GFRA1 has been found to be upregulated at the mRNA level in invasive breast cancer compared to normal breast tissue (Esseghir *et al.*, 2006).
	There is much evidence suggesting a link between cancer promotion and presence of chronic inflammation in the microenvironment. Most studies focus on the role of inflammatory chemokines and cytokines. However, it has now become clear that neurotrophic factors also play a role in the immune system homeostasis, inflammatory response and tumour progression (Albini *et al.*, 2007).
	The neurotrophic factor GDNF exerts its effects via binding to GFRα coreceptors (preferentially GFRα1), which recruit RET to form a signalling complex leading to RET autophosphorylation and activation of a signalling cascade (Manie *et al.,* 2001).

	GDNF has been shown to stimulate migration via activation of MAPK and PI3K pathways in a RET+/ GFRα1+ pancreatic cell line (Veit *et al.,* 2004) GFRα1 has also been found to be overexpressed in invasive breast cancer (Esseghir *et al.,* 2006). The data concludes that GDNF is induced by inflammatory signals and tumour fibroblasts in breast cancer cells activating RET and GFRα1 signalling cascades supporting both paracrine and autocrine stimulation of tumour cells in response to their microenvironment (Esseghir *et al.*, 2007).
Associations with other cancers	GDNF has been shown to stimulate migration via activation of MAPK and PI3K pathways in a RET+/ GFRα1+ pancreatic cell line (Veit *et al.,* 2004).

In order to further investigate the potential role of GFRA1 suppression by Faslodex treatment in the 3 models, other elements of the GFRA1 receptor complex were investigated using the gene microarrays to determine if all components of RET signalling were suppressed by this antihormone. From Figure 47 it can be seen that RET and GDNF were invariably suppressed by Faslodex treatment. For RET all basal log2 expression values were above 0 and called present indicative of expression in the 3 models prior to treatment. The greatest suppression was observed in the MCF-7 cell line leading to an absent detection call, while expression in the other models remained present after Faslodex. The log2 intensity plot showed GDNF was at best expressed at only extremely low levels pre and post Faslodex treatment with all detection calls absent.
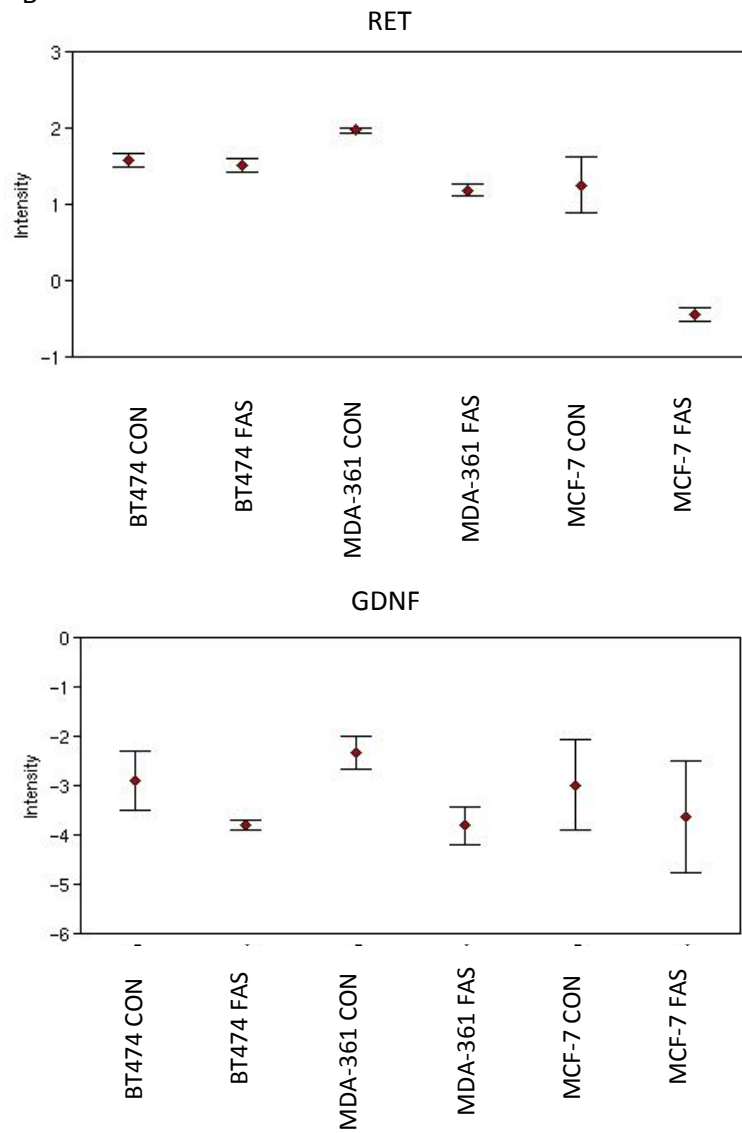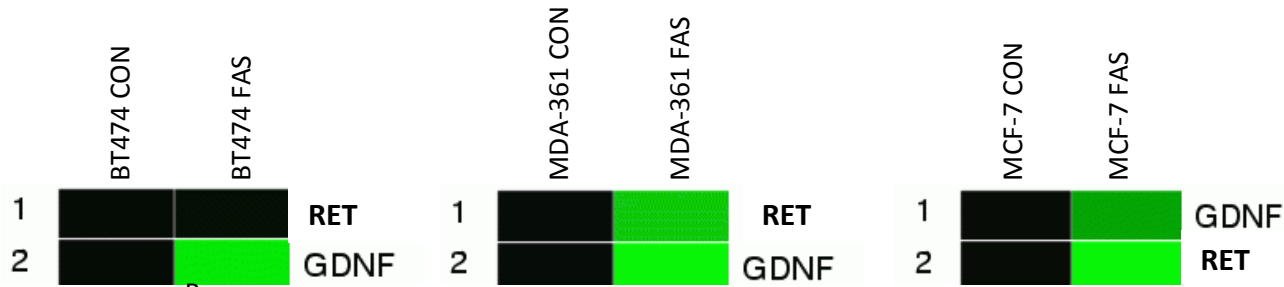
Figure 47: (A) Heatmaps generated by GeneSifter to assess the expression of RET and GDNF in the HER2+ and MCF-7 cell lines. GDNF is the reported ligand for GFRA1, which is a co-receptor for RET. (B) Log2 normalised expression plots displaying expression in each cell line including T47D, pre and post 10 day Faslodex treatment. Jetset probes were used; RET-211421_s_at; GDNF-221359_at

5.3.3.1 Summary of the microarray data and ontological information collated for the potential resistance genes

From the ontological studies, there was evidence that all of the genes identified could have a possible role in the limited Faslodex response and subsequent onset of Faslodex-resistance in the HER2+ and MCF-7 cell lines. Up-regulation of GABBR2, CXCR4, PRKACB, KITLG and VEGFC have all been reported to be involved in cell survival and growth signalling as well as disease progression (invasive and metastatic capability). GFRA1 (and associated RET signalling) has also been associated with disease progression in breast cancer. However, its suppression by short-term Faslodex and continued suppression in the MCF-7 FAS-R cells suggested it is unlikely to be involved in the promotion of resistance in the HER2+ and MCF-7 cell lines. GFRA1 is reported as being ER-regulated and thus its suppression may be an indicator of initial Faslodex response in these cell lines. The Faslodex-induced genes also showed evidence of induction in the MCF-7 Faslodex-resistant cell line versus hormone sensitive cells with the exception of VEGFC and KITLG. Initial induction by 10 day Faslodex treatment may suggest a potential role for these latter genes in early development of resistance but their continued induction may not be required for the subsequent maintenance of the resistant phenotype.

5.3.4 Establishing potential clinical relevance of the genes of interest in the context of endocrine resistance

All genes were further analysed in clinical breast cancer using the online tools KMPlotter and GOBO to determine their clinical prognostic and/or predictive value following anti-hormone treatment. These tools can use breast cancer gene microarray mRNA expression data collected from patients prior to tamoxifen treatment and also contain associated survival-related information. They generate survival curves that allow determination of whether an association exists between inherent expression level for genes of interest and clinical outcome, in this instance following tamoxifen treatment in ER+ breast cancer patients. Detailed information on these tools can be found in Section 2.6.1 of 'Materials and Methods'. There are no Faslodex-treated clinical microarray datasets as yet publically available for such analysis.

KMPlotter was initially used as this tool encompasses the largest dataset of relevant patients for analysis (n=657). All patients were ER positive and had undergone tamoxifen therapy. In order to analyse the association between a gene of interest and relapse free survival (RFS) in this project, the patient data was split into 2 groups using the best cut-off tool provided by KMPlotter and then compared by a Kaplan-Meier plot. The only genes to display a significant association (log rank P<0.05) with clinical outcome following tamoxifen treatment in ER+ breast cancer using KMPlotter were GABRR2 and VEGFC.

5.3.4.1 GABBR2

Figure 48 displays the significant association identified between inherent GABBR2 gene expression and subsequent duration of response to tamoxifen in ER+ clinical breast cancer. The red line depicts those patients with increased expression of GABBR2 which significantly associated with a reduced duration of response to tamoxifen in this analysis. A hazard ratio (HR) of 2 indicated twice as many patients underwent a relapse in the patient cohort with higher GABBR2 expression (HR= 2.46 95% CI 1.36-4.45), suggesting this gene may contribute to anti-hormone resistance and supportive of a potential role for Faslodex-induced GABBR2 in the eventual development of Faslodex resistance in HER2- and HER2+ ER+ cells *in vitro*.
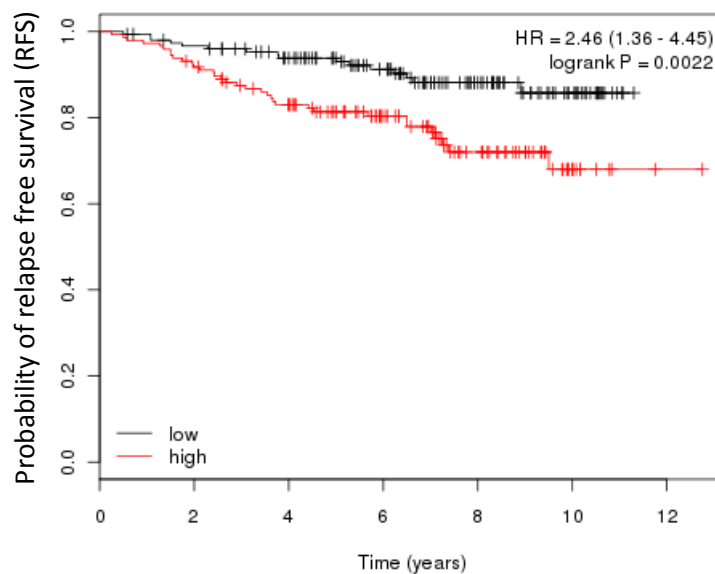
Figure 48: Kaplan-Meier survival curve generated using KMPlotter displaying probability of RFS according to high (red) or low (black) GABBR2 mRNA expression (red line)in tamoxifen-treated ER+ breast cancer patients (n=657).

GABBR2 was also analysed using the online tool GOBO, which not only enables the relationship between the expression of a given gene and patient prognosis to be determined, but also allows the patient expression data to be subdivided into more than 2 cohorts to determine if there is a graded relationship between level of gene expression and clinical outcome. Again, RFS was used as a measure of clinical outcome and patients selected (n=176) were ER+ and subsequently received tamoxifen treatment (Figure 49).
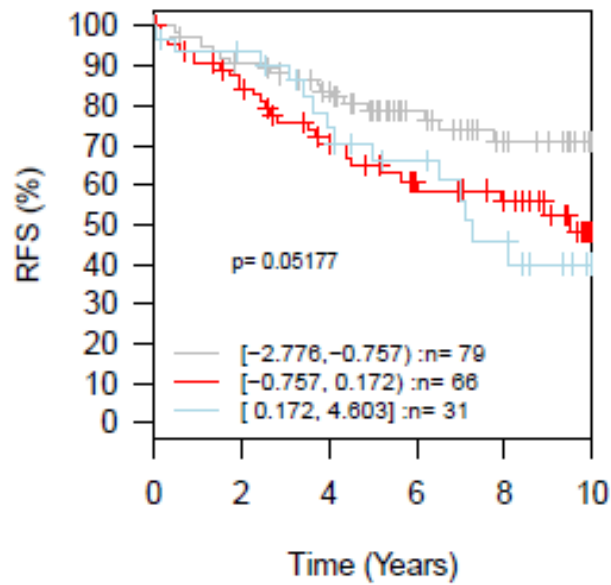
Figure 49: Kaplan Meier survival curve generated using GOBO displaying RFS according to high (blue), intermediate (red) or low (grey) GABBR2 gene expression data used was from ER+ tamoxifen treated breast cancer patients (n=176).

GABBR2 analysed in GOBO showed the same relationship as in the larger dataset within KMPlotter: increased levels of expression were associated with a reduced response to tamoxifen (p=0.05177) (Figure 49), although the data could not be discriminated further according to high or intermediate expression level.

5.3.4.2 VEGFC

Although there was no relationship in the smaller GOBO dataset, KMPlotter again revealed a significant association between increased expression of VEGFC and reduced RFS in tamoxifen treated ER+ breast cancer patients (Figure 50). The HR was greater than 1 in this group indicating patients with an increased VEGFC expression were associated with a poorer response (HR=1.46 95% CI 1.05-2.02).
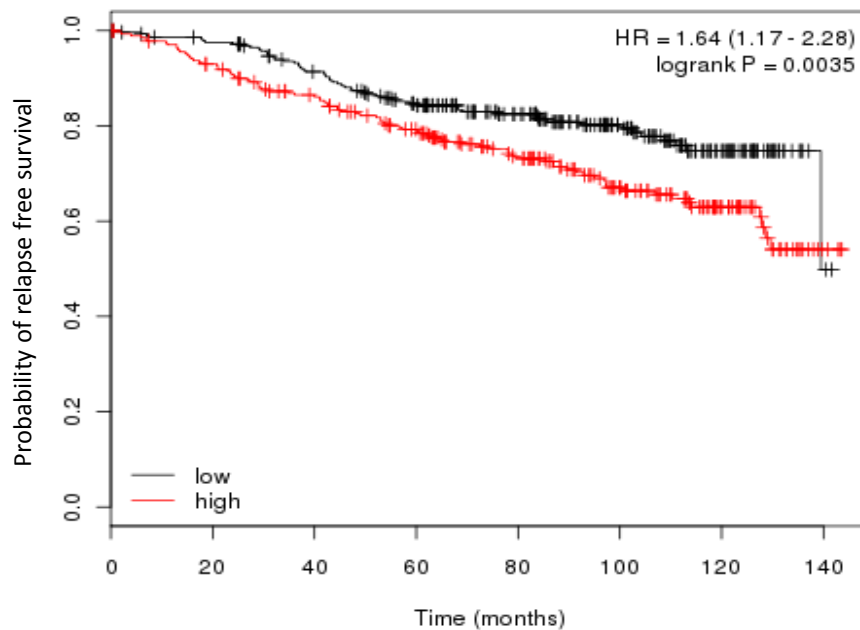
Figure 50: Kaplan-Meier survival curve generated using KMPlotter displaying probability of RFS according to high (red) or low (black) VEGFC mRNA expression (red line)in tamoxifen-treated ER+ breast cancer patients (n=657).

Both VEGFC and GABBR2 were also analysed in a cohort of ER+ breast cancer patients who had received no adjuvant therapy using KMPlotter. In this cohort, the same association between increased GABBR2 expression and reduced RFS was identified, suggesting that increased expression of GABBR2 could have prognostic value in ER+ breast cancer (Figure 51) (HR=1.57 (95%CI 1.2-2.04), p=0.00075). However, no association was seen for VEGFC, suggesting that it may be predictive in relation to antihormone (tamoxifen) treatment outcome.
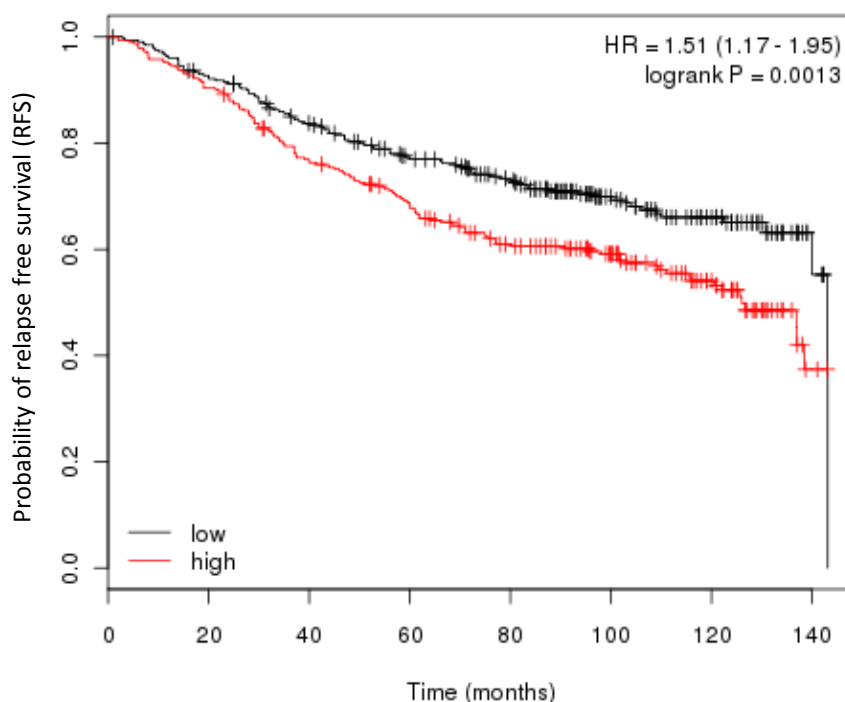
Figure 51: Kaplan-Meier survival curve generated using KMPlotter displaying probability of RFS according to high (red) or low (black) GABBR2 mRNA expression (red line)in ER+ breast cancer patients that were systemically untreated (n=785).

5.3.5 PCR verification of genes potentially involved in the development of resistance in the HER2+ and MCF-7 cell lines

Reverse-transcription (RT)-PCR was carried out using triplicate RNA from untreated and 10 day Faslodex treated cells (under the same conditions as those used to generate samples for the microarray gene expression profiling experiment) in an attempt to verify the Affymetrix expression profiles.

PCR verification was carried out for GABBR2, CXCR4, PRKACB, KITLG, VEGFC and GFRA1 (Figures 30-35).

5.3.5.1 GABBR2

GABBR2 gene expression was very low in the HER2+ and MCF-7 cell lines prior to Faslodex treatment and even lower in the T47D cell line, in agreement with the gene expression microarray data (Figure 28). GABBR2 was, however, significantly induced in the BT474 and MCF-7 cell lines by 10 day Faslodex treatment. In some samples GABBR2 was also up-regulated in the MDA-MB-361 cell line, but this was found not be significant across all replicates.

Gene Acronym	Fold change of expression following Faslodex treatment			
	BT474	MDA-MB-361	MCF-7	T47D
GABBR2	1.45	1.13	3.66	1.02

Figure 52: Representative PCR image (A) with the corresponding β-actin normalised densitometry graph (B), semi-quantitatively representing the data (CON-control; FAS-10 day Faslodex treatment). The results are expressed as means ± SEM of three separate experiments. *$P < 0.05$ versus control, ***$P < 0.001$ versus control. (C) Table displaying the fold changes of gene expression detected by PCR following Faslodex treatment

5.3.5.2 CXCR4

Basal expression of CXCR4 was found to be similar in the BT474 and MCF-7 cell lines, while elevated expression was observed in the MDA-MB-361 cell line (Figure 53), in agreement with the log2 normalised expression intensity plot generated from the microarray data (Figure 29). The greatest induction of CXCR4 gene expression was observed in the BT474 (1.44 fold) and MCF-7 (2.97 fold) cell lines, while a lack of induction was observed in the MDA-MB-361 cell line where its elevated basal expression remained unchanged. These profiles mimicked the microarray data for CXCR4, as shown in Figure 29.

Gene Acronym	Fold change of expression following Faslodex treatment			
	BT474	MDA-MB-361	MCF-7	T47D
CXCR4	1.44	1.0	2.97	1.01
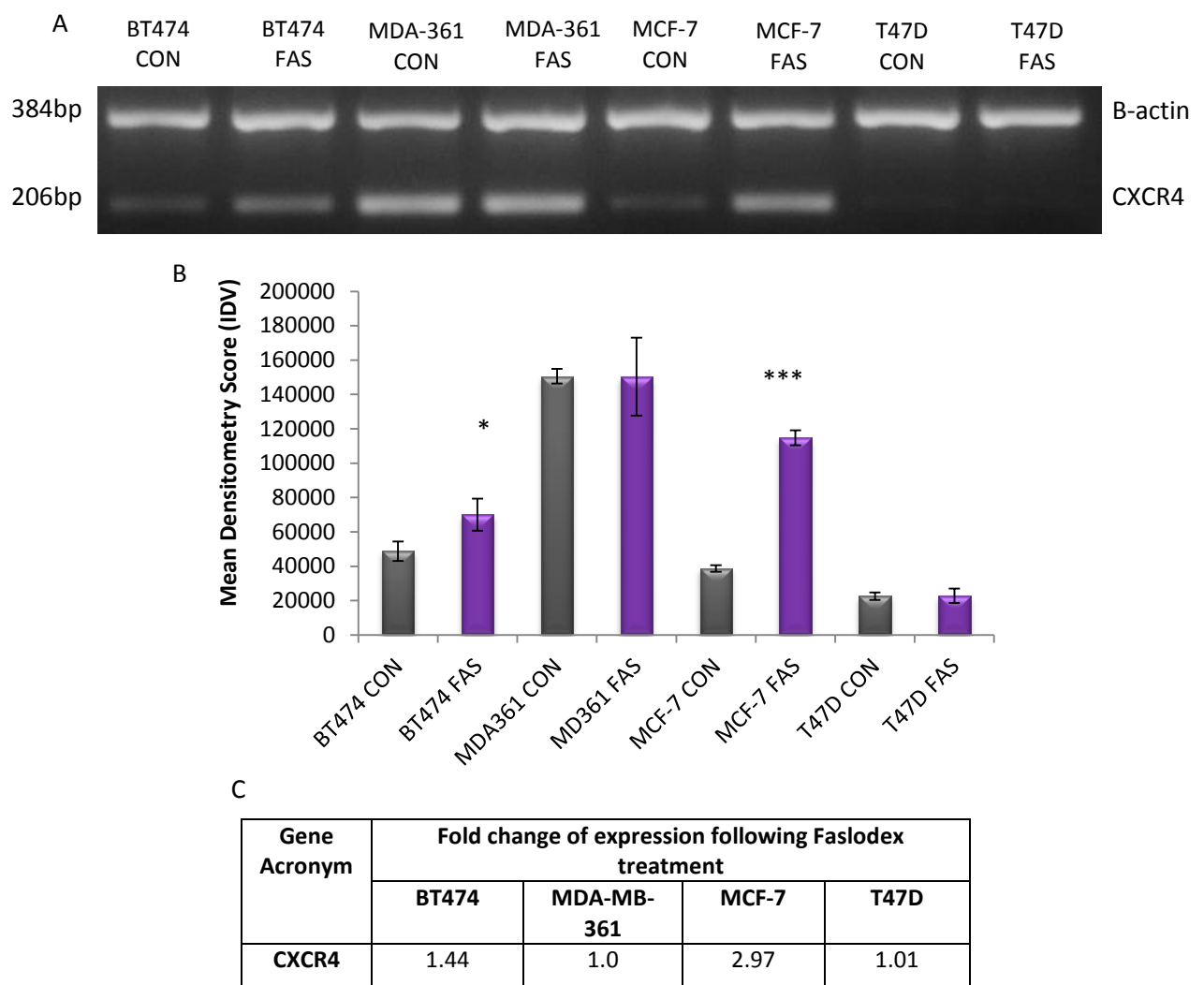
Figure 53: Representative PCR image (A) with the corresponding β-actin normalised densitometry graph (B), semi- quantitatively representing the data (CON-control; FAS-10 day Faslodex treatment). The results are expressed as means ± SEM of three separate experiments. *$P < 0.05$ versus control, ***$P < 0.001$ versus control. (C) Table displaying the fold changes of gene expression detected by PCR following Faslodex treatment.

5.3.5.3 PRKACB

Although previous gene expression data indicated that the basal levels of PRKACB were readily detected in all cell lines (log2 intensity value above 0), and that its expression was higher in the HER2+ models (Figure 32), the latter was not confirmed by PCR (Figure 54). Faslodex up-regulation of PRKACB was, greatest in the HER2+ cell lines (Figure 54) in parallel with the microarray data (Figure 32). There was little change in expression of PRKACB in the MCF-7 cell line during Faslodex treatment, and in T47D cells its level fell on exposure to the antihormone an observation not detected during the analysis of the microarray data (Figure 32).

Gene Acronym	Fold change of expression following Faslodex treatment			
	BT474	MDA-MB-361	MCF-7	T47D
PRKACB	1.84	1.39	1.06	1.97

Figure 54: Representative PCR image (A) with the corresponding β-actin normalised densitometry graph (B), semi-quantitatively representing the data (CON-control; FAS-10 day Faslodex treatment). The results are expressed as means ± SEM of three separate experiments. **$P < 0.01$ versus control, ***$P < 0.001$ versus control. (C) Table displaying the fold changes of gene expression detected by PCR following Faslodex treatment.

5.3.5.4 KITLG

As can be seen in Figure 55, the basal levels of KITLG expression detected by PCR were variable, with the lowest levels being seen in the BT474 cell line. This contrasted with the microarray gene expression data, where the lowest levels were recorded in MCF-7 cells (Figure 31). In all instances, KITLG was significantly up-regulated by Faslodex treatment, although this had not been observed on the arrays in the T47D cell line where a suppression of KITLG expression was observed (Figure 31).

Gene Acronym	Fold change of expression following Faslodex treatment			
	BT474	MDA-MB-361	MCF-7	T47D
KITLG	2.25	1.30	1.42	1.24

Figure 55: Representative PCR image (A) with the corresponding β-actin normalised densitometry graph (B), semi-quantitatively representing the data (CON-control; FAS-10 day Faslodex treatment). The results are expressed as means ± SEM of three separate experiments. *$P < 0.05$ versus control, **$P < 0.01$ versus control, ***$P < 0.001$ versus control. (C) Table displaying the fold changes of gene expression detected by PCR following Faslodex treatment.

154

5.3.5.5 VEGFC

PCR of VEGFC revealed similar basal gene expression profiles for this gene across the 4 cell lines (Figure 56), an observation in disagreement with the microarray data which suggested VEGFC expression was inherently lower in the T47D cell line (Figure 30). Importantly, 10 day Faslodex treatment significantly up-regulated VEGFC expression in all 3 cell lines that eventually develop resistance to Faslodex, while no change in expression was observed in the T47D cell line (Figure 56). The PCR data indicated that the MDA-MB-361 cell line underwent the greatest induction of expression in disagreement with the array data.

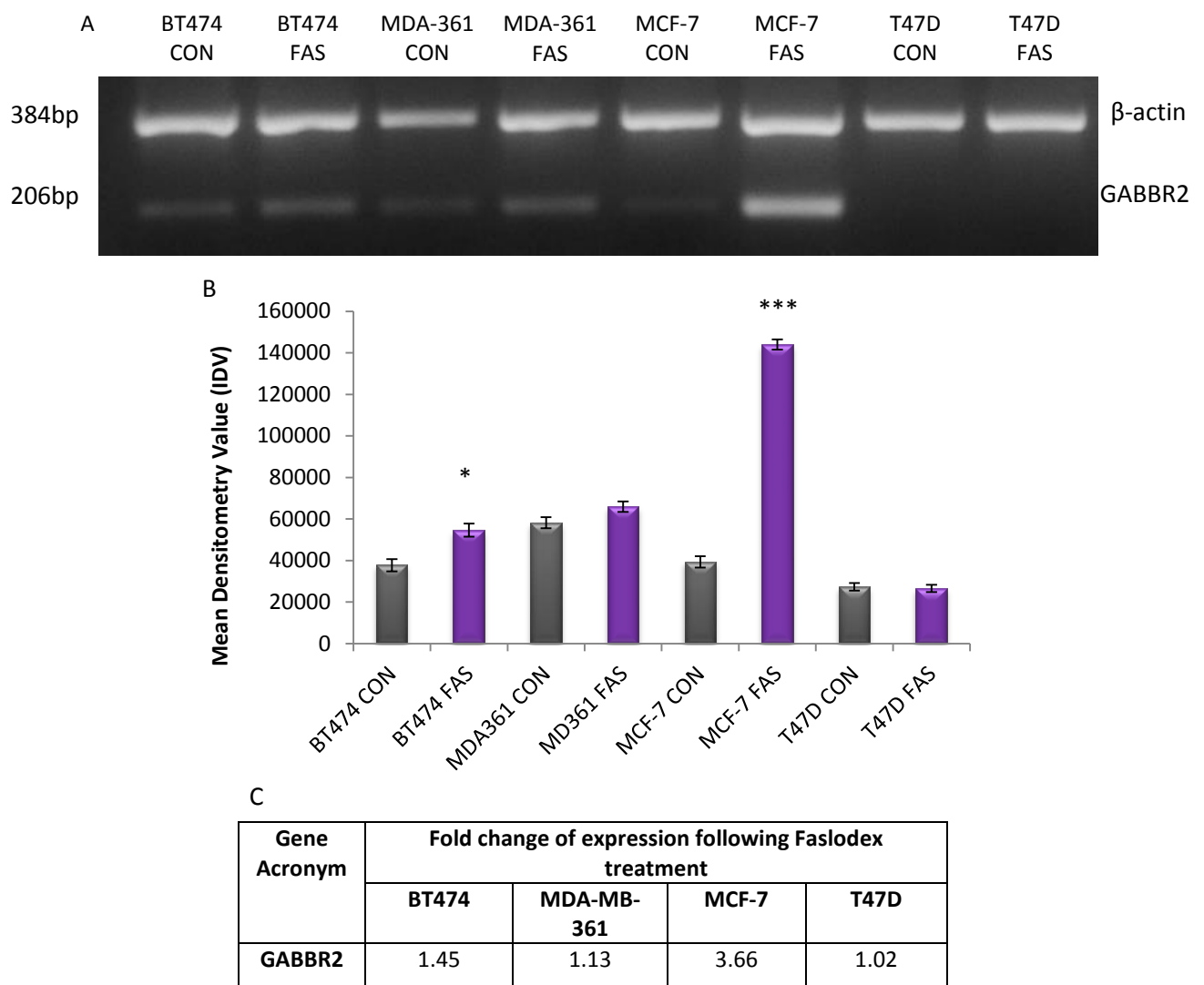| Gene Acronym	Fold change of expression following Faslodex treatment			
	BT474	**MDA-MB-361**	**MCF-7**	**T47D**
VEGFC	1.45	3.46	1.46	1.13
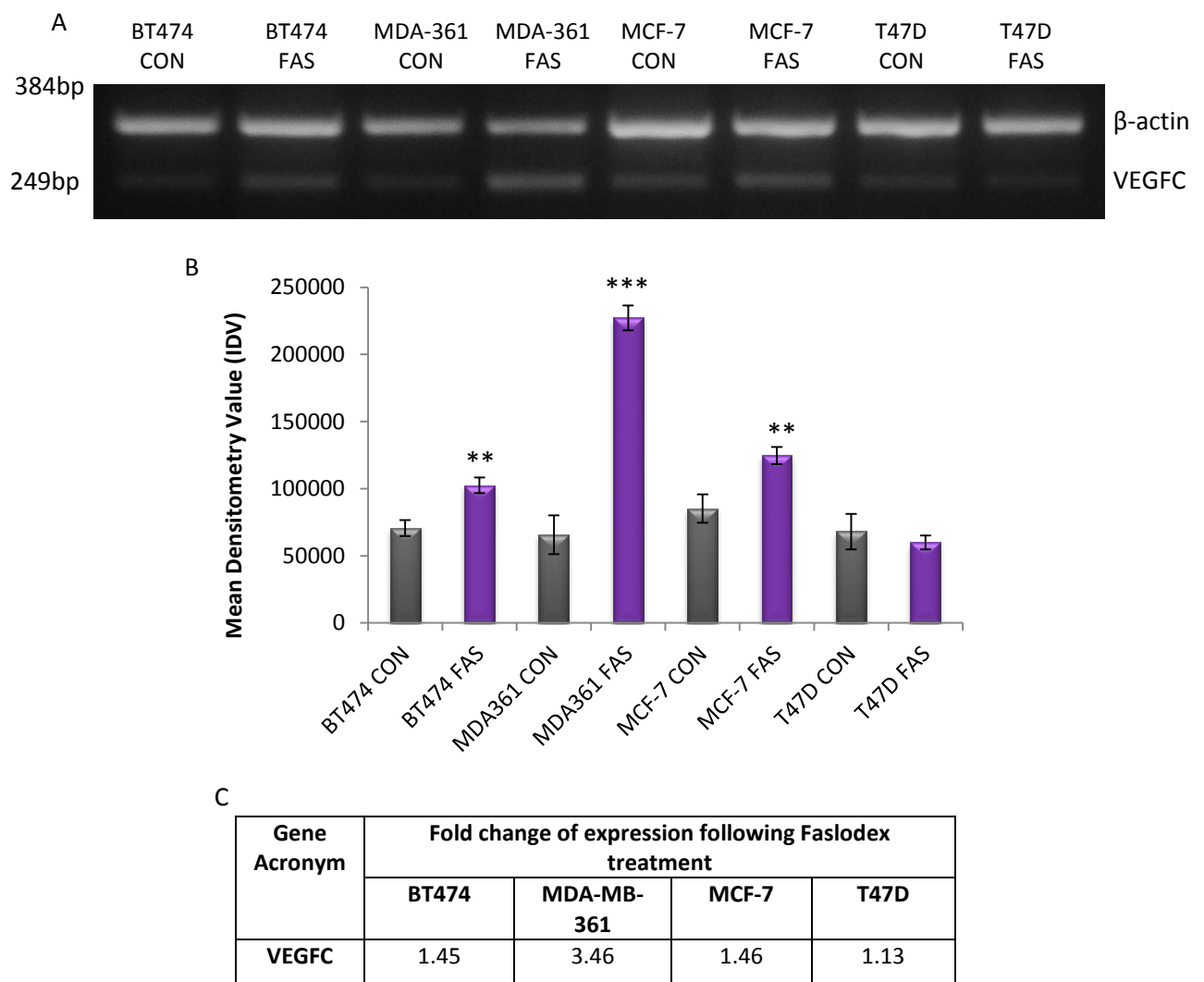
Figure 56: Representative PCR image (A) with the corresponding β-actin normalised densitometry graph (B), semi-quantitatively representing the data (CON-control; FAS-10 day Faslodex treatment). The results are expressed as means ± SEM of three separate experiments. **$P < 0.01$ versus control, ***$P < 0.001$ versus control. (C) Table displaying the fold change of gene expression detected by PCR following Faslodex treatment.

5.3.5.3 GFRA1

Although the basal expression of GFRA1 was variable, in agreement with the microarray data (Figure 35). As such, highest basal levels were detected in the MCF-7 cell line, with lowest levels being recorded in the T47D and BT474 cells. Again in parallel with the microarray data, the PCR data revealed that Faslodex treatment resulted in a significant suppression of GFRA1 expression in MCF-7 and MDA-MB-361 (Figure 35). GFRA1 could not be detected in BT474 or T47D cells; hence, any weak suppression with Faslodex after normalisation in these models was equivocal.

| Gene Acronym	Fold change of expression following Faslodex treatment			
	BT474	**MDA-MB-361**	**MCF-7**	**T47D**
GFRA1	1.24	1.60	7.28	1.57

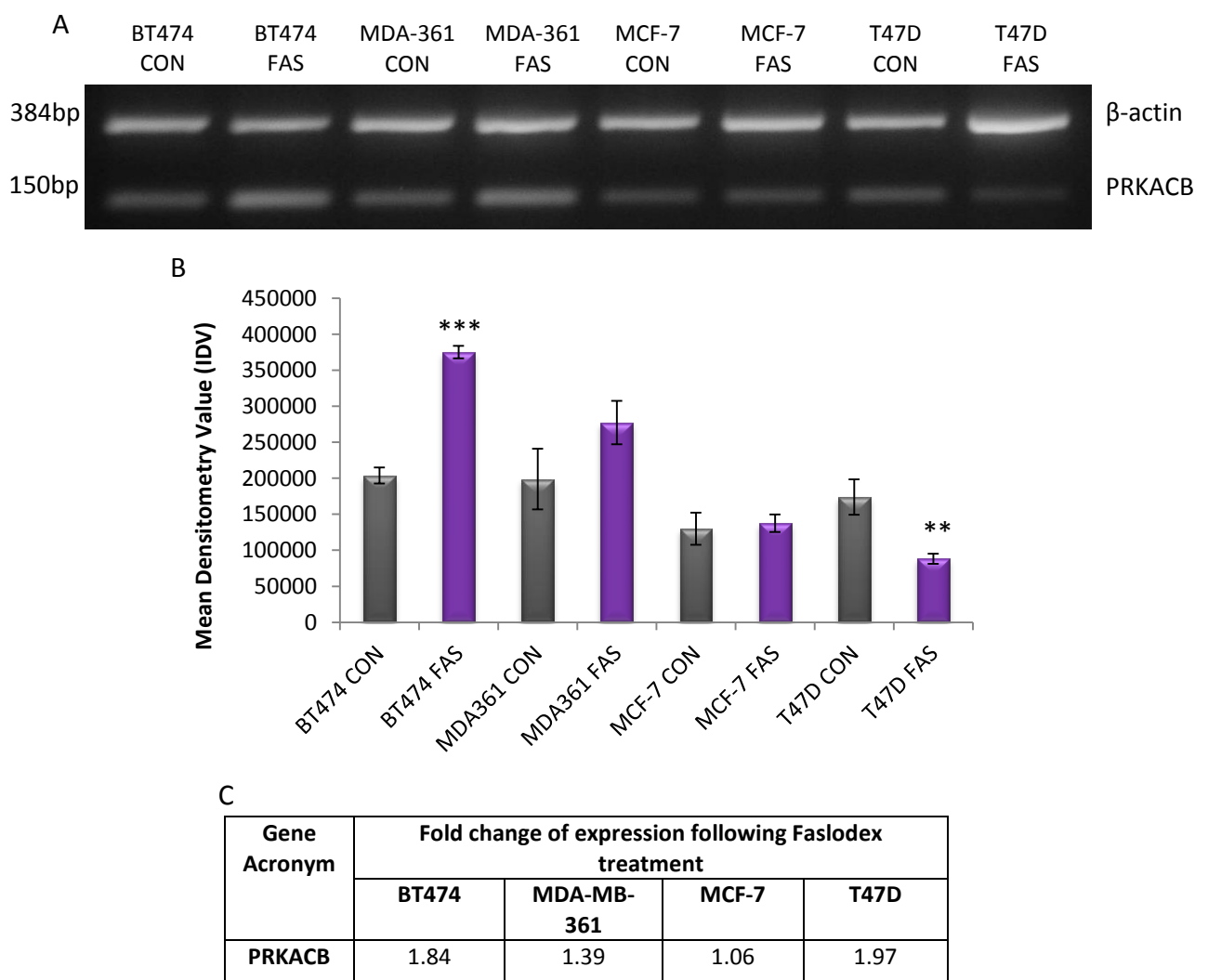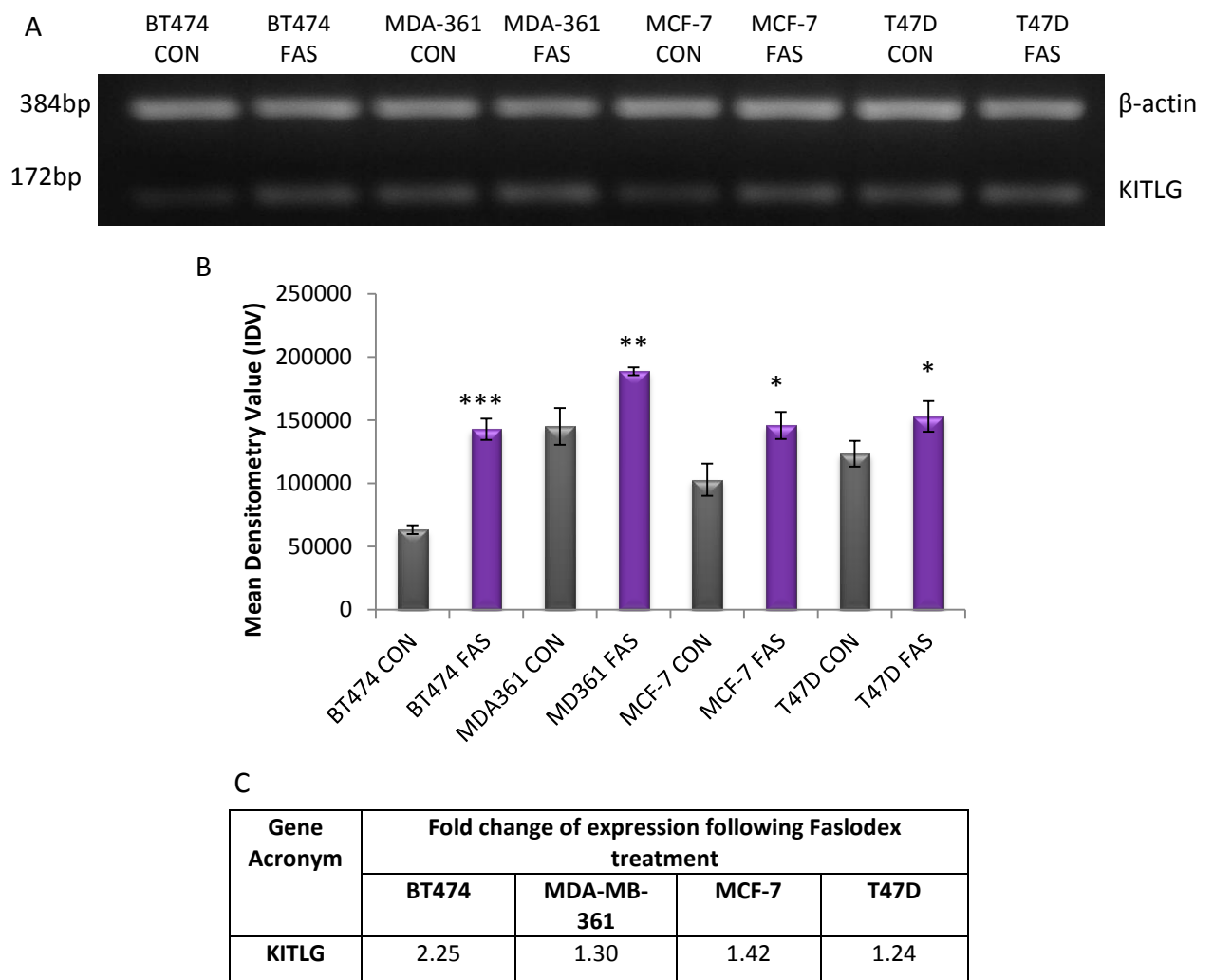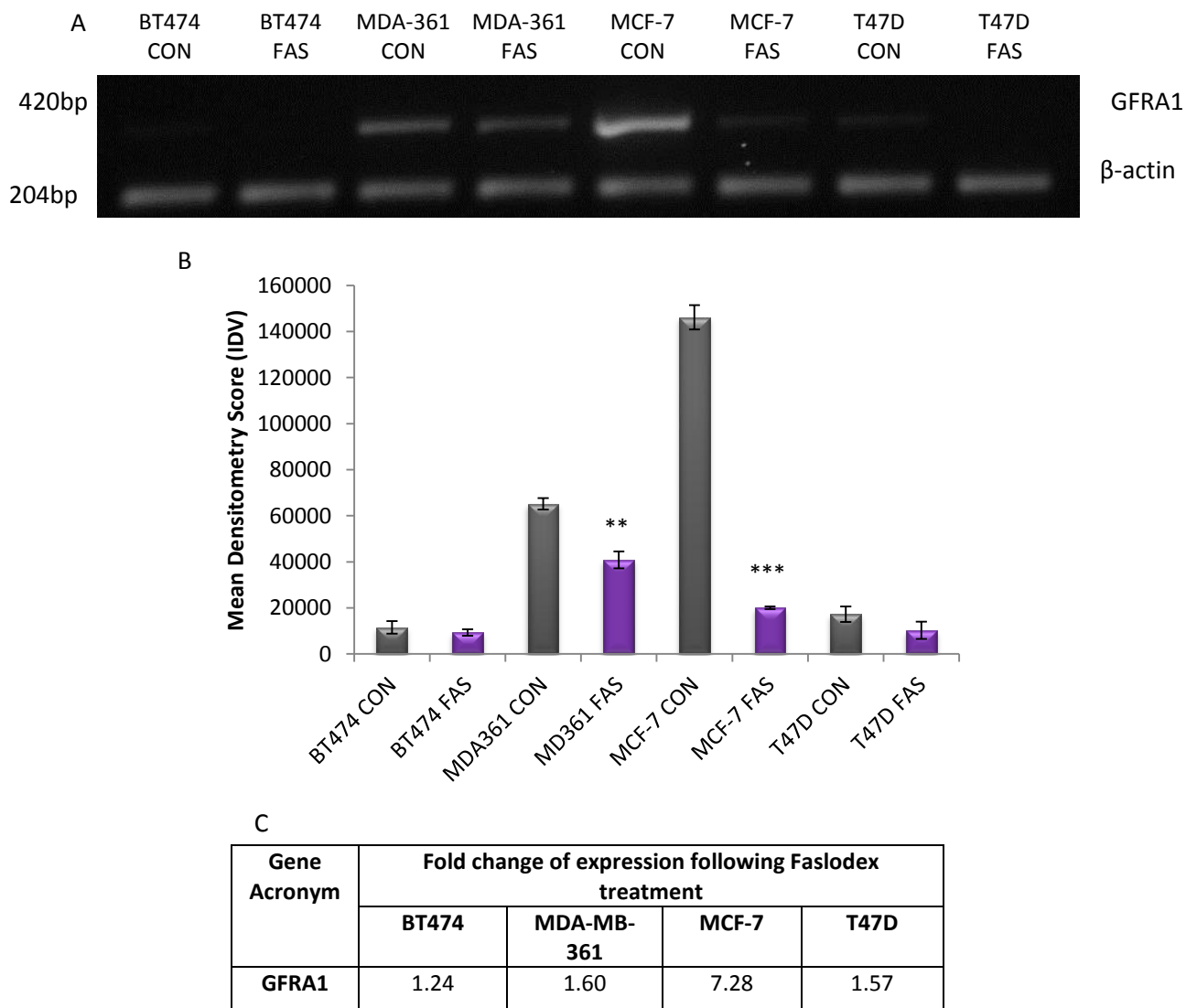Figure 57: Representative PCR image (A) with the corresponding β-actin normalised densitometry graph (B), semi-quantitatively representing the data (CON-control; FAS-10 day Faslodex treatment). The results are expressed as means ± SEM of three separate experiments. **$P < 0.01$ versus control, ***$P < 0.001$ versus control. (C) Table displaying the fold change of gene expression detected by PCR following Faslodex treatment.

Several of the genes induced on the arrays (e.g. VEGFC, KITLG, GABBR2) were PCR verified successfully with evidence for some induction by Faslodex in both HER2+ and MCF-7 cell lines, while CXCR4 and PRKACB showed induction in two models, in keeping with a role in the development of resistance. However, KITLG was also induced in the T47D cell line (albeit to a lesser extent) and so was dismissed from further investigation. GFRA1 was also selected for further investigation but in relation to the role of GFRA1 suppression and Faslodex response. This data is summarised in Table 18 which compares the results from the microarray data with the PCR results. There is generally a good concordance between the array and PCR results with the exception of KITLG.

Table 18: Comparison of Faslodex-deregulation of genes of interest from the microarray data and PCR results (I-Induced; S-Suppressed; ~ limited/no change)

Gene Name	Microarray (FAS de-regulation)				PCR (FAS de-regulation)			
	BT474	MDA-361	MCF-7	T47D	BT474	MDA-361	MCF-7	T47D
GABBR2	I	I	I	~	I	I	I	~
CXCR4	I	~	I	~	I	~	I	~
PRKACB	I	I	I	~	I	I	~	S
KITLG	I	I	I	S	I	I	I	I
VEGFC	I	I	I	~	I	I	I	S
GFRA1	S	S	S	~	~	S	S	~

5.4 Discussion

In this chapter a filtering process was undertaken to identify genes that were significantly altered by Faslodex treatment (by at least 1.5 fold) in those cell lines that eventually develop resistance to Faslodex (HER2+ and MCF-7 cell lines). 9 genes were initially identified as being de-regulated by Faslodex following analysis of the microarray gene expression data (Table 10). It was hypothesised that these may encompass genes that could be potential crucial signalling elements gained (i.e. growth promoters) or lost (i.e. tumour suppressive elements), independent of HER2 status, that if manipulated in combination with Faslodex may enhance the growth inhibition exerted by Faslodex, as well as providing earlier predictive elements for the Faslodex resistant state.

Of the 9 genes initially identified, three (IKZF1, GPR37 and ZNF343) were immediately dismissed from the investigation due to lack of significant expression (log2 intensity values below 0, absent expression calls) and unreliable changes in expression following Faslodex treatment (Figures 26, 27 and 34). Further filtering based on expression profile (including in a Faslodex resistant model), ontology and examination in virtual clinical datasets with endocrine outcome was undertaken to discriminate those remaining genes with the strongest potential association to resistance, before PCR verification was performed to confirm their Faslodex de-regulation in the cell models.

Induction of 5 of the remaining genes (CXCR4, GABBR2, PRKACB, VEGFC and KITLG) by Faslodex had potential importance in the eventual development of Faslodex-resistance. CXCR4 and GABBR2 were of much interest due to the lack of detectable gene expression in the T47D cell line pre and post Faslodex treatment (Figures 28, 29, 52 and 53). CXCR4 (which was induced in the HER2+ and MCF7 cells by Faslodex treatment and also elevated in the Faslodex resistant MCF7 cells) is particularly interesting because of the compelling literature surrounding the involvement of this gene in disease progression. The role of CXCR4 and its ligand SDF-1 in metastasis and cancer cell proliferation has been widely reported (Muller *et al.*, 2001., Smith *et al.,* 2004) but more recently CXCR4 has been implicated in the development of hormone-independence when over-expressed in ER+ breast cancer (Rhodes *et al.,* 2011). Rhodes *et al* have shown that CXCR4 has the ability to activate ER in an oestrogen-independent manner encouraging tumour growth where ER-regulated SDF-1 expression further promotes such growth. Faslodex treatment was reported to deplete ER expression and this inhibited CXCR4-mediated tumour growth via suppression of SDF-1 expression. Treatment with exogenous SDF-1, however, was able to overcome the anti-tumour effects of Faslodex in this model. Clinically, SDF-1 is likely to be provided by the tumour stroma to encourage resistance to Faslodex (Rhodes *et al.,* 2011). Assuming SDF-1 is not significantly present in the serum added to the cell growth medium, for CXCR4 to be functionally involved in the development of resistance in the *in vitro* models used in this project SDF-1 would have to be expressed by these cells. SDF-1 expression was investigated in the cell

lines by analysing the gene expression data and confirmed that the ER-regulated, SDF-1 gene was very much suppressed by 10 day Faslodex treatment in the 3 cell lines indicating CXCR4 signalling is unlikely to be functionally active in these cells following Faslodex treatment.

The literature supporting a role for GABBR2 in cancer progression is limited. There are two reports associating GABBR2 expression with a shift towards a more aggressive phenotype but neither is in relation to breast cancer. In prostate and lung cancer, GABBR2 activation and elevated GABBR2 levels were associated with an increase in invasive and metastatic potential (Azuma *et a*l., 2003; de Lange *et al.,* 2003). In contrast, there have also been reports stating that activation of GABBR2 is growth inhibitory (Opolski *et al.*, 2000). However, GABBR2 has never previously been associated with response or failure on anti-hormone treatment. Its expression increases in the HER2+ and MCF-7 models with Faslodex and its maintained induction into the MCF-7 Faslodex-resistant model setting (Figure 37) as well as its negative association with RFS duration in patients who received tamoxifen suggest that while the role of GABBR2 in ER+ breast cancer (Figure 48 and 49) has yet to be fully understood it may be adverse and contributory to endocrine resistance. Enzymes involved in the biosynthesis of GABA from glutamate were also investigated to determine if GABA may also be produced by the cells and thus GABA signalling was functionally active. L-glutamate decarboxylase (GAD) is the key enzyme involved in GABA biosynthesis and is represented by 2 genes, GAD1 and GAD2. Both genes were shown to up-regulated by Faslodex treatment in the 3 cell lines. Mean expression values failed to be above 0 indicative of very low expression, but none the less their Faslodex up-regulation may suggest some elevation of GABA signalling via GABBR2 receptor during treatment (Figure 43).

The remaining three induced genes, PRKACB, VEGFC and KITLG were all expressed by the T47D cell line pre and post treatment as well as in the other cell models, where they were predominantly induced by Faslodex (Figures 54-56). PRKACB was found to be significantly induced in the BT474 cell line by PCR with a modest, non-significant induction also observed in the MDA-MB-361 cell line (Figure 54). However, very little change in expression was observed in the MCF-7 cell line while

a significant suppression by Faslodex was seen in the T47D cell line (Figure 54) in keeping with a possible role for induction serving to limit Faslodex response. These data also suggest if PRKACB induction is involved in the subsequent development of resistance it may be particularly important in the ER+/HER2+ setting. The PRKACB gene encodes one of the catalytic subunits of the enzyme PKA. PKA has been reported to be involved in cancer progression (Michalides *et al.*, 2004; Merkle *et al.,* 2011) as well as the development of resistance to the anti-hormone treatment tamoxifen (Michalides *et al.*, 2004; de Leeuw *et al.*, 2012). While PKA signalling has not previously been associated with Faslodex failure, the induction of PRKACB by short-term Faslodex treatment and the maintained induction of PRKACB into resistance in the MCF-7-derived model suggest the PKA pathway could be a crucial survival signalling pathway utilised by ER+ breast cancer cells to overcome Faslodex challenge.

The T47D cell line also expressed VEGFC pre and post treatment, but Faslodex treatment had a minimal effect on expression (Figure 56). In contrast, significant induction of VEGFC was present in the 3 remaining models following Faslodex treatment in keeping with a possible role in the development of drug resistance. Published reports surrounding the role of VEGFC in disease progression were in agreement with our hypothesis of VEGFC possibly acting to limit Faslodex response (Table 16). In particular, VEGFC is thought to be involved in the process of lymphangiogenesis and thereby tumour spread via the lymphatic system via signalling through the VEGFR3 receptor and sometimes the VEGFR2 receptor (Skobe *et al.*, 2001). This process is believed to occur following the establishment of the primary tumour when metastasis to lymph nodes is subsequently ready to occur, but the timings for this event remains unclear (Wissmann *et al.,* 2006). The *in vitro* data presented here suggest that VEGFC may also have a functional role in disease progression prior to the process of lymphangiogenesis. Clinical data from KMPlotter revealed a negative association between VEGFC expression and RFS following tamoxifen treatment (Figure 50). Along with the induction of VEGFC by Faslodex treatment, this is in keeping with VEGFC being involved in onset of Faslodex resistance. However, the suppression of VEGFC expression in the MCF-7-

derived Faslodex resistant cell line was at odds with VEGFC being involved in maintenance of the resistant phenotype. In order to further explore if there was a potential role for induction of VEGFC in the HER2+ and MCF-7 cell lines, the expression of VEGFR2 and VEGFR3 in the 3 cell lines pre and post Faslodex treatment was analysed using the gene expression data (Figure 46). VEGFR3 was not expressed by any of the cell lines pre or post treatment, while VEGFR2 was also absent in the HER2+ cell lines and although induced in the MCF-7 cell line by Faslodex was still at a low expression level. In total, these findings suggest limited functional activity of VEGFC in the *in vitro* cell models following Faslodex treatment, questioning any contribution towards development of Faslodex resistance. Nevertheless, clinically it remains possible that cancer cells may express VEGFR2 or 3 in response to environmental factors allowing any Faslodex induction of VEGFC to promote disease progression and metastasis to the lymph nodes. Interestingly, it has been reported that high tumour VEGFC levels significantly correlated with lymph node metastasis in ER+ breast cancer patients (Morgillo *et al.*, 2013) while a recent phase II clinical study assessing the combination treatment of Faslodex and Cediranib (an inhibitor of all VEGF receptors) demonstrated non-significant improvements of clinical activity with respect to tumour size, progression free survival and objective response rate. It thus remains possible that inhibition of VEGF signalling may prevent or delay the onset of Faslodex resistance (Hyams *et al.,* 2013).

KITLG gene expression was induced by Faslodex in all the cell models, unfortunately including the T47D cell line (Figure 55) shedding doubt on its involvement with emergence of resistance. Furthermore, KITLG functions through its receptor c-kit and investigations of c-kit expression found the receptor not to be substantially expressed in either ER+/HER2+ cell lines or the MCF-7 model, with all log2 intensity values below 0 suggesting functional KITLG signalling was not active in the cell models post Faslodex treatment. Subsequently, therefore, no further work was carried out on KITLG.

It was interesting to note that Faslodex induction of the various genes in this project was observed following 10 days of treatment in the 3 models but resistance

did not emerge for a further number of weeks. This could be due to a threshold effect, where the initial induction observed following 10 days of treatment does not lead to sufficient expression of these genes to contribute to limiting drug response but the continued induction over time may lead to further increases in expression so that resistance can emerge. In this regard, GABBR2, PRKACB and CXCR4 could perhaps be most promising since they also showed some evidence of expression induction in the MCF7-derived acquired Faslodex resistant line. Also, it is clear that a number of the genes identified (e.g. CXCR4, GABBR2, VEGFC) require a ligand or receptor to be co-expressed for functional signalling to take place; it is feasible that more extended Faslodex treatment may lead to the eventual up-regulation of the receptors/ligands required for these genes to be actively involved in signal transduction and development of resistance. Even if this is not observed, such signalling elements may remain important for limiting Faslodex response *in vivo* where paracrine signalling initiated by the tumour microenvironment can lead to the activation of a number of signalling pathways within cancer cells failing to express a given ligand (Witz *et al.,* 2006).

GFRA1 expression was found to be suppressed significantly by Faslodex in both HER2+ and MCF7 models on the arrays. While ontological investigations found GFRA1 to be part of the RET signalling pathway and involved in cancer progression and tamoxifen or AI resistance (Plaza-Menacho *et al.*, 2010; Morandi *et al.*, 2013), its suppression by 10 day Faslodex (Figure 35) and continued suppression into the resistant setting (Figure 42) was in disagreement with an equivalent involvement for such signalling in Faslodex resistance. Indeed, the suppression of GFRA1 on the Faslodex-treated arrays could reflect ER regulation of this gene (Boulay *et al.,* 2008) and possibly even be an indicator of the initial Faslodex response that occurred to some degree in both the HER2+ and MCF-7 cell lines, all 3 cell lines. Analysis of the GFRA1 expression profile by PCR found GFRA1 to be suppressed by Faslodex in the MDA-MB-361 and MCF-7 cell lines, while expression was barely detectable basally in the BT474 and also the T47D cell line (Figure 57). These data suggest that if suppression of GFRA1 is a possible mediator of initial Faslodex response such changes are not required in all ER+ breast cancer cells. To examine this concept

further, investigations were carried out to determine the effects of Faslodex treatment on other elements of the RET signalling pathway utilising the microarray data (Figure 47); RET and the dominant GFRA1 ligand GDNF were assessed, where RET was suppressed in the MCF-7 and MDA-MB-361 cell lines while GDNF was suppressed in all models (although pre treatment log2 intensity values for GDNF were below 0 indicative of at best only very low basal expression). These data possibly provide further evidence that suppression of RET signalling may be an important mediator of initial Faslodex response *in vitro* in some ER+ breast cancer cells. However, it remains to be explored if this suppression is causative of response, or merely reflective of ER blockade with this agent.

To summarise, by carrying out whole genome analysis across the model panel, this project has successfully revealed several genes induced by short-term Faslodex treatment in the HER2+ and the MCF-7 cell lines of potential interest in relation to the development of Faslodex resistance (functionally or as biomarkers): VEGFC, PRKACB, GABBR2 and CXCR4. Also of interest is the suppression of GFRA1 in the cell models by Faslodex that, along with suppression of other elements of the RET pathway, comprises a possible mediator of initial Faslodex response.

Chapter 6

Identification of genes Faslodex-deregulated in the T47D cell line that are potentially involved in the complete-Faslodex-response

6.1 Introduction

The general consensus surrounding endocrine therapy of breast cancer is that even though these treatments have revolutionised treatment plans and survival statistics for ER+ breast cancer patients, they are unable to induce significant levels of cell death, rather their main action is to inhibit cancer cell proliferation (Gee *et al.*, 2003). Indeed, it has come to light that anti-hormone treatments are not entirely passive during their inhibition of breast cancer cell proliferation, but concurrently have the ability to rapidly induce alternative signal transduction pathways as a "compensatory" cell survival mechanism (Gee *et al.*, 2011). Critically, such induced signalling can limit the initial drug inhibitory effect and ultimately promote therapeutic resistance. In chapter 3 genes were identified that were de-regulated by Faslodex in the 3 ER+ cell models that develop anti-hormone resistance during continuous treatment. In this chapter the T47D cell line was used to identify early genes changes that could possibly be involved in the subsequent complete response to Faslodex that was observed following 8.5 weeks of culture with the drug. Certainly, early microarray gene expression analysis procedures in this project supported the concept of unique Faslodex-promoted gene changes in T47D cells, with the HCA diagrams showing the T47D model to cluster separately from the other ER+ cell lines after 10 days treatment. This potentially indicated the presence of Faslodex-altered gene changes that may influence intracellular signalling pathways in this model and may explain the complete response observed, for

example comprising Faslodex suppression of growth promoting genes and/or the induction of tumour suppressive genes.

As the first *in vitro* model reported to exhibit a complete-response with Faslodex, study of the T47D cell line provided a unique opportunity to investigate the underlying mechanisms of this response. Complete response to anti-hormone treatment is a rare phenomenon in the clinic, including for Faslodex, in the CONFIRM trial only 1.1% of patients exhibited a complete response (Di Leo *et al.*, 2010). Investigating this cell model could potentially reveal genes able to identify early those patients likely to display a superior response to Faslodex treatment, or determine mechanisms that if manipulated in combination with Faslodex could induce an enhanced anti-tumour response.

6.2 Results

6.2.1 Identification of genes uniquely Faslodex de-regulated in the T47D cell line

A similar 4 stage filtering process to that used in chapter 3 was carried out to (i) identify genes with a >1.5 fold change with Faslodex in the T47D cell line only, (ii) undertake an ontological investigation (iii) analyse their expression in Faslodex-resistance using an MCF-7 derived model, and (iv) determine their potential clinical relevance in relation to endocrine outcome using online tools and databases. As you can see from Figure 57, only 29 were significantly altered in the T47D cell line only and further only 11 were identified to exhibit at least 1.5 fold change in the T47D line with limited change in the 3 remaining cell models.
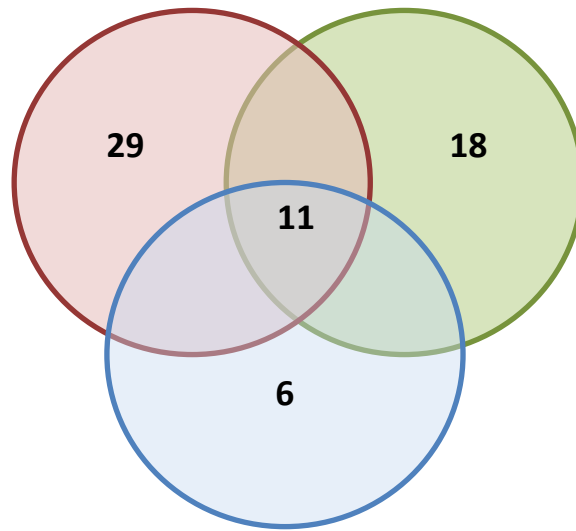
Figure 57: The Venn diagram illustrates the identification of the 11 genes taken forward as potential mediators/biomarkers of Faslodex complete-response observed in the T47D cell line. The red circle represents all those genes significantly altered in the T47D cell line. The green circle, shows the number of these genes that were not altered by at least 1.5 fold in this model and the blue circle are those that were found to be also altered to some extent in the BT474, MDA-MB-361 and MCF-7 cell lines. The 11 genes represented by the overlapping circles identify those genes that met the criteria to be taken forward for further investigation.

Table 18 lists those genes identified as having a >1.5 fold change in expression in the T47D cell line following 10 day Faslodex treatment. It can be seen that of the genes identified, a similar number were induced and suppressed. Importantly, for most of the genes identified, all of the multiple probes exhibited the same directional change in expression, the only exceptions being SEPT6 and ID4.

Table 18: Genes with a greater than 1.5 fold change in gene expression following 10 days Faslodex treatment in the T47D cell line. Also listed is the total number of probes representing each gene on the UI33Aplus2 genechip, together with the number of those probes which exhibited a robust change in expression with Faslodex.

Potential complete-response genes T47D unique genes	Gene Name	Gene expression change following Faslodex treatment (in T47D cell line)	Total number of probes per gene	Total number of probes exhibiting change in expression
CASP1	Caspase 1	Induced	5	5
DCN	Decorin	Induced	4	4
TXNIP	Thioredoxin interacting protein.	Induced	2	2
TGFB2	Transforming growth factor, beta 2	Induced	3	3
ADAM12	ADAM metallopeptidase domain 12	Induced	3	3
PTGER3	Prostaglandin E receptor 3 (subtype EP3)	Suppressed	8	8
SEPT6	Septin 6	Suppressed	5	3
IL6ST	Interleukin 6 signal transducer	Suppressed	5	5
SKAP2	src kinase associated phosphoprotein 2	Suppressed	3	3
DUSP4	Dual specificity protein phosphatase 4	Suppressed	2	2
ID4	Inhibitor of DNA binding 4	Suppressed	3	2

To further confirm the robust induction or suppression of the genes identified, the jetset gene probe was further analysed, this being the probe predicted to best represent a given gene (see Methods Section 2.3.6 for further information). The Affymetrix ID's for the jetset gene probes and jetset score are listed in Table 19.

TGFB2, PTGER3, IL6ST, SKAP2 and DUSP4 all had low jetset scores which indicated potentially poorer probe performance. The remaining genes all showed adequate jetset scores.

Table 19: Genes of interest in relation to the Faslodex promotion of a complete-response in the T47D cell line with their corresponding jetset gene probe Affymetrix ID's and jetset score (closer to 1 the better the predicted performance of the probe).

Gene Acronym	Jetset Affymetrix Probe ID	Jetset Score
CASP1	211368_s_at	0.38710235
DCN	209335_at	0.78909851
TXNIP	201010_s_at	0.476311939
TGFB2	209909_s_at	0.01054474
ADAM12	213790_at	0.2812175
PTGER3	210831_s_at	0.15459993
SEPT6	212414_s_at	0.41583468
IL6ST	212195_at	0.03510335
SKAP2	204362_at	0.03408559
DUSP4	204014_at	0.00307944
ID4	209291_at	0.41014426

Using the jetset Affymetrix gene probes ID for the induced and suppressed genes, the software program GeneSifter was used to determine the magnitude of de-regulation of these genes in the T47D cell line by Faslodex as well as their log2 expression profile across the remaining ER+ cell lines (Figures 58 to 69) also recording the gene detection calls from the arrays.
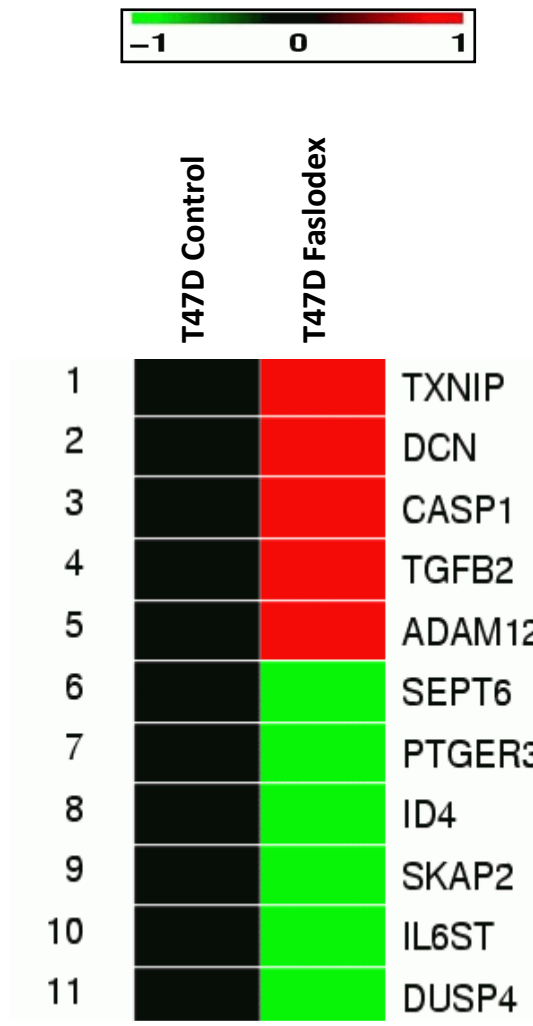
Figure 58: Heatmap displaying the significant induction or suppression of genes altered by 10 day Faslodex treatment in the T47D cell line generated by GeneSifter using the jetset probes.

6.2.1.1 Genes induced by Faslodex in T47D cells:

6.2.1.1.1 TXNIP

While the heatmap and log2 intensity plots for TXNIP confirmed its induction only in T47D cells (Figures 58 and 59 respectively), its basal expression in this cell line was lower than that observed in the HER2+ and MCF-7 cells where no Faslodex induction was seen (Figure 59). Log2 intensity values were above zero for each cell line pre- and post-Faslodex treatment, with the exception of the basal value for TXNIP in T47D cells which was found to call absent. As seen in Figure 59B, Faslodex induced the expression of TXNIP over 12 fold in the T47D cells.

B

Gene Acronym	Fold change of expression following Faslodex treatment			
	BT474	MDA-MB-361	MCF-7	T47D
TXNIP	3.18	1.01	1.57	12.69

Figure 59: (A) Log2 intensity plot displaying the normalised (mean of triplicate samples) gene expression of TXNIP in each of the 4 cell lines pre (Con) and post 10 day Faslodex (FAS) treatment (B) table displaying the fold change in gene expression promoted by 10 day Faslodex treatment in each cell line vs. untreated control. Highlighted in red are Faslodex-promoted inductions in gene expression and in green suppression of expression >1.5 fold.

6.2.1.1.2 DCN and CASP1

Basal log2 intensity values of DCN and CASP1 were similar across all 4 cell lines and found to below 0 with absent calls indicative of a lack of basal expression (Figure 60and 61). Following Faslodex treatment, log2 intensity values for both DCN and CASP1 were only induced in the T47D cell line, further confirmed by the substantial fold changes (approximately 5 fold) and a change in detection call to present. In the other cell models the detection calls remained absent after treatment.

Gene Acronym	Fold change of expression following Faslodex treatment			
	BT474	MDA-MB-361	MCF-7	T47D
DCN	1.20	1.23	1.22	4.93

Figure 60: (A) Log2 intensity plot displaying the normalised (mean of triplicate samples) gene expression of DCN in each of the 4 cell lines pre (Con) and post 10 day Faslodex (FAS) treatment (B) Table displaying the fold change in gene expression promoted by 10 day Faslodex treatment in each cell line vs. untreated control. Highlighted in red are Faslodex-promoted inductions in gene expression >1.5 fold.

A

B

Gene Acronym	Fold change of expression following Faslodex treatment			
	BT474	MDA-MB-361	MCF-7	T47D
CASP1	1.98	1.49	1.45	5.95

Figure 61: (A) Log2 intensity plot displaying the normalised (mean of triplicate samples) gene expression of CASP1 in each of the 4 cell lines pre (Con) and post 10 day Faslodex (FAS) treatment (B) Table displaying the fold change in gene expression promoted by 10 day Faslodex treatment in each cell line vs. untreated control. Highlighted in red are Faslodex-promoted inductions in gene expression and in green suppressions >1.5 fold.

6.2.1.1.3 TGFB2

The log2 intensity values for TGFB2 were very low in the HER2+ cell lines with no change in expression occurring following Faslodex treatment (Figure 62). The detection calls for this gene were also absent pre and post Faslodex treatment indicative of a lack of expression in these models. Although in MCF-7 cells, basal TGFB2 gene expression was elevated with a present call, Faslodex did not further induce its expression. In contrast to the other cell lines, a clear up-regulation of TGFB2 gene expression was observed in the T47D cell line following treatment (> 5 fold) where present detection calls were observed pre and post treatment. Although the jetset score for this gene probe was poor, all 3 gene probes demonstrated an induction in expression following treatment (Table 18), suggesting a robust up-regulation of TGFB2 in the T47D cell line.

A

B

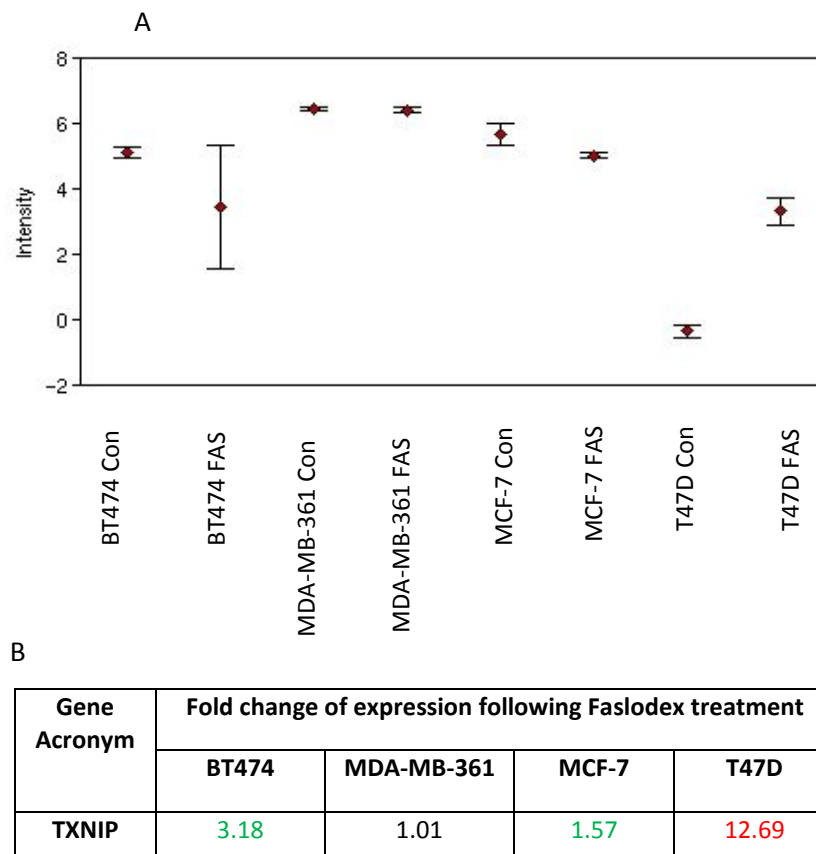| Gene Acronym	Fold change of expression following Faslodex treatment			
	BT474	MDA-MB-361	MCF-7	T47D
TGFB2	1.46	1.51	1.07	5.37

Figure 62: (A) Log2 intensity plot displaying the normalised (mean of triplicate samples) gene expression of TGFB2 in each of the 4 cell lines pre (Con) and post 10 day Faslodex (FAS) treatment (B) Table displaying the fold change in gene expression promoted by 10 day Faslodex treatment in each cell line vs. untreated control. Highlighted in red are Faslodex-promoted inductions in gene expression and in green suppression of expression >1.5 fold.

6.2.1.1.4 ADAM12

The log2 intensity values of ADAM12 were below 0 in all cell models and minimal changes were observed in the HER2+ and MCF-7 cell lines following treatment (Figure 63). This contrasted with the data derived for the T47D cell line where Faslodex promoted an induction its expression, although the log2 intensity value remained below 0. Significantly, analysis of the detection calls for the jetset probe found them to be absent for all of the cell lines pre and post treatment, indicative of a lack of expression, and an analysis of the remaining 2 gene probes showed them to also have unreliable profiles.

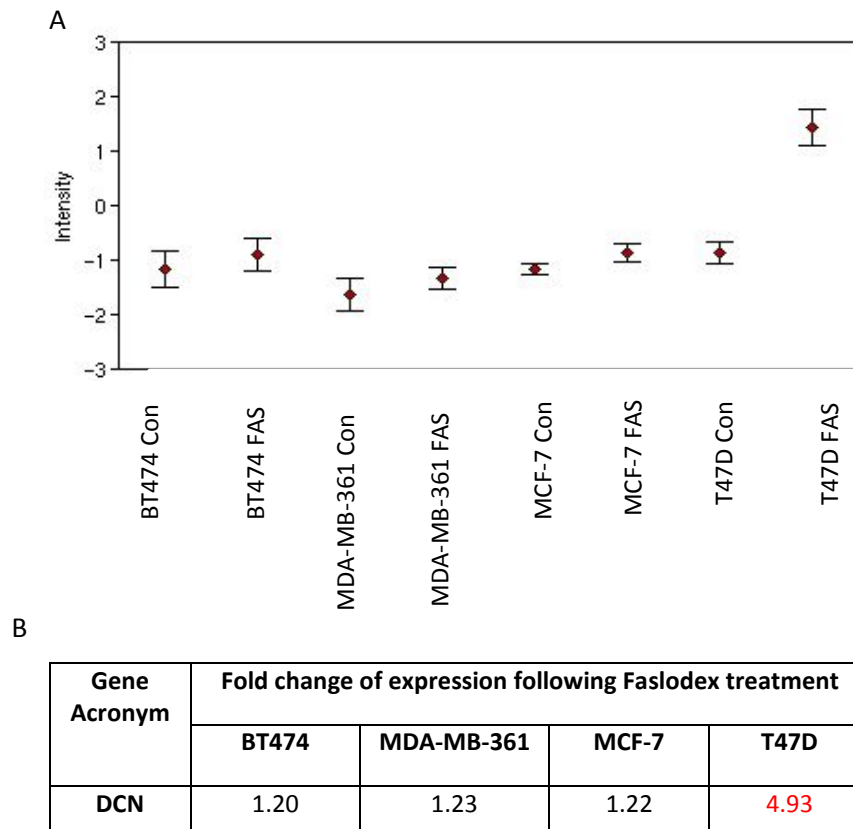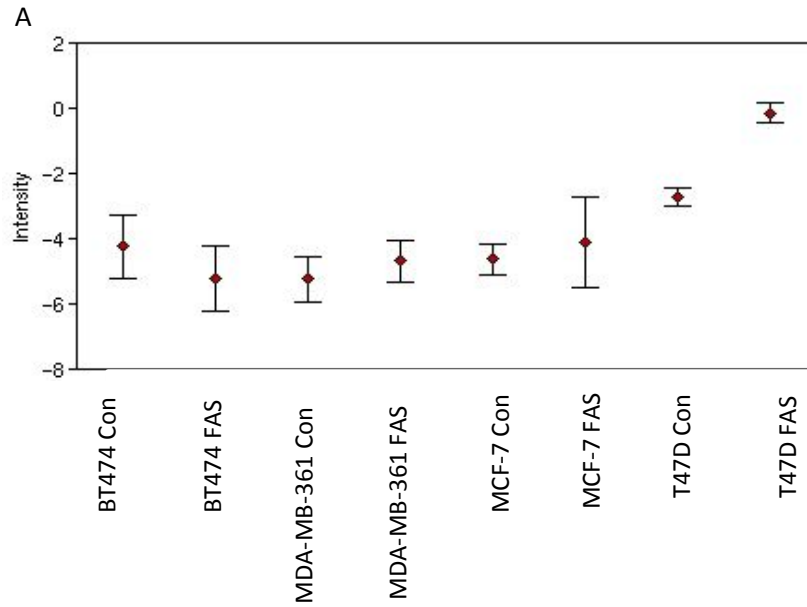| Gene Acronym	Fold change of expression following Faslodex treatment			
	BT474	MDA-MB-361	MCF-7	T47D
ADAM12	1.53	1.68	1.44	3.96

Figure 63: (A) Log2 intensity plot displaying the normalised (mean of triplicate samples) gene expression of ADAM12 in each of the 4 cell lines pre (Con) and post 10 day Faslodex (FAS) treatment (B) Table displaying the fold change in gene expression promoted by 10 day Faslodex treatment in each cell line vs. untreated control. Highlighted in red are Faslodex-promoted inductions in gene expression and in green suppressions >1.5 fold.

6.2.1.2 Genes suppressed by Faslodex in T47D cells:

6.2.1.2.1 SEPT6

Inherent log2 intensity values of SEPT6 were found to be equivalent in the HER2+ and T47D cell lines, but lower in the MCF-7 cell line (Figure 64). In each instance, however, values at or below 0 and called absent in the HER2+ and T47D cell lines, indicative of a lack of expression. Although the lower log2 intensity value observed in the MCF-7 cell line appeared further reduced by treatment, the detection calls also called absent pre and post treatment. Suppression in expression was also observed in the T47D cell line, but again absent detection calls were recorded post-treatment.

A

B

Gene Acronym	Fold change of expression following Faslodex treatment			
	BT474	MDA-MB-361	MCF-7	T47D
SEPT6	1.28	1.43	4.15	2.38

Figure 64: (A) Log2 intensity plot displaying the normalised (mean of triplicate samples) gene expression of SEPT6 in each of the 4 cell lines pre (Con) and post 10 day Faslodex (FAS) treatment (B) Table displaying the fold change in gene expression promoted by 10 day Faslodex treatment in each cell line vs. untreated control. Highlighted in green are Faslodex-promoted suppressions in gene expression >1.5 fold.

6.2.1.2.2 PTGER3

As seen in Figure 65, the inherent log2 intensity value of PTGER3 in the T47D cell line was elevated in comparison to the remaining cell models and a positive detection call was recorded. In contrast, the basal log2 intensity values in the HER2+ and MCF-7 cell lines were below 0 and called absent, indicative of a lack of expression. Following Faslodex treatment, minimal changes were observed in the HER2+ cell lines and detection calls remained absent indicating changes were equivocal. A small induction was observed in the MCF-7 cell line with a present detection call, indicative of up-regulation. In the T47D cell line, Faslodex treatment suppressed the PTGER3 log2 intensity value by ~5 fold, although the detection call remained present, indicative of some expression retained after treatment. Regardless of the poor jetset score of this gene probe, PTGER3 remained a gene of interest (Table 19).

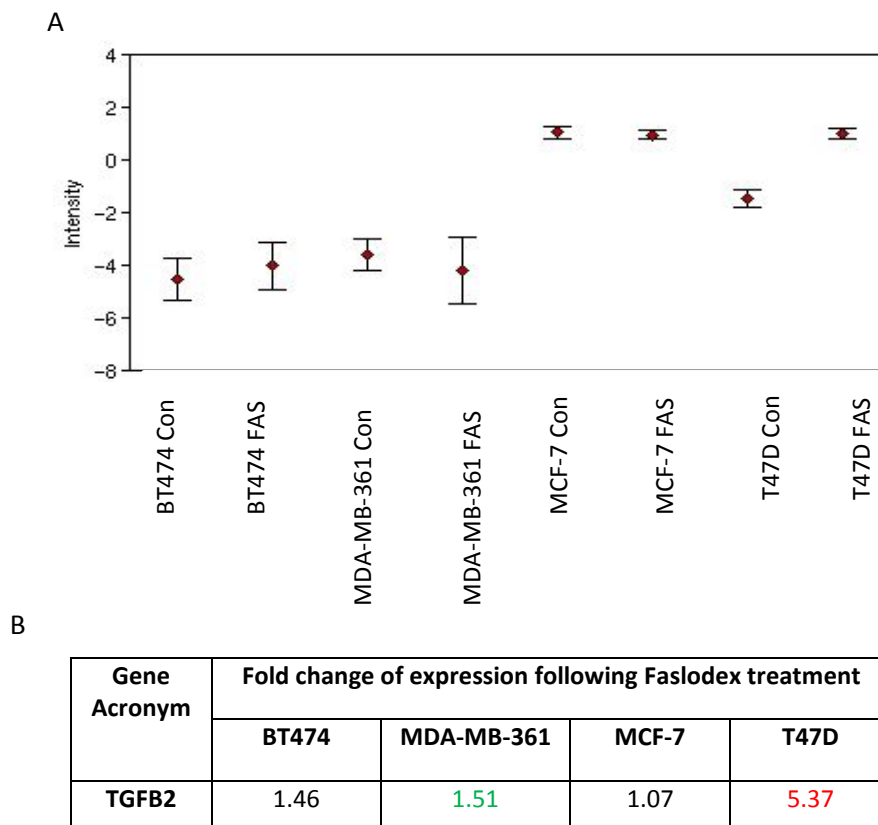| Gene Acronym	Fold change of expression following Faslodex treatment			
	BT474	MDA-MB-361	MCF-7	T47D
PTGER3	1.14	2.43	3.18	5.56
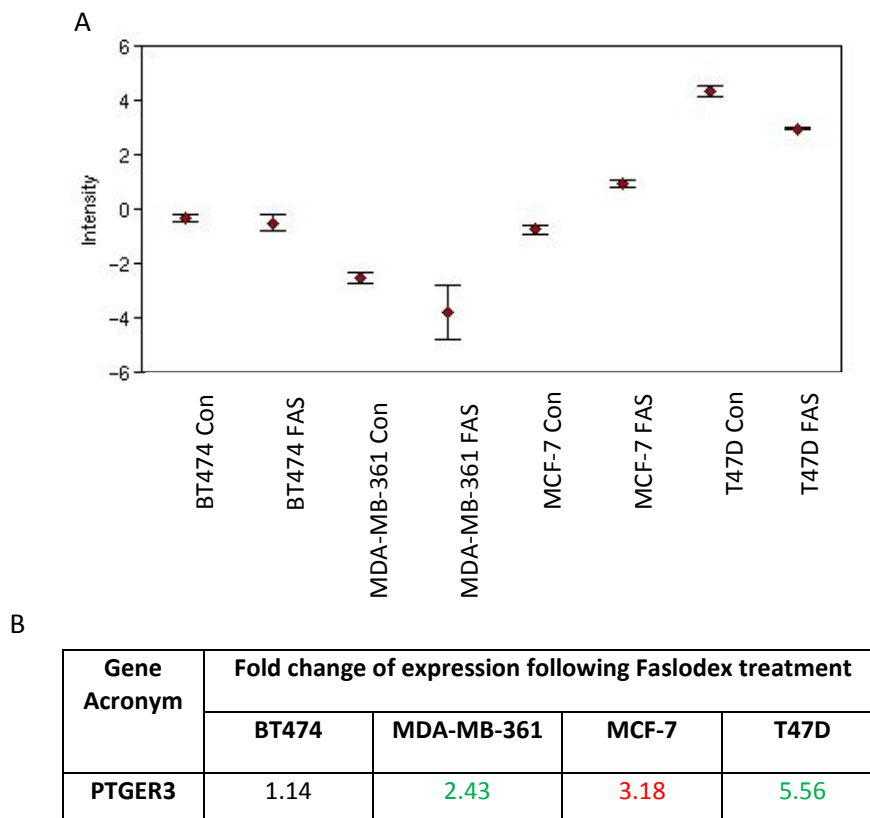
Figure 65: (A) Log2 intensity plot displaying the normalised (mean of triplicate samples) gene expression of PTGER3 in each of the 4 cell lines pre (Con) and post 10 day Faslodex (FAS) treatment (B) Table displaying the fold change in gene expression promoted by 10 day Faslodex treatment in each cell line vs. untreated control. Highlighted in green are Faslodex-promoted suppressions in gene expression and in red inductions >1.5 fold.

6.2.1.2.3 ID4

Although the inherent log2 intensity values of ID4 were variable across the 4 cell models (Figure 66), present detection calls were recorded. In contrast to the HER2+ and MCF-7 cells, Faslodex treatment of the T47D cell line suppressed ID4 log2 intensity values to a value below 0, although it retained a present detection call on the arrays.

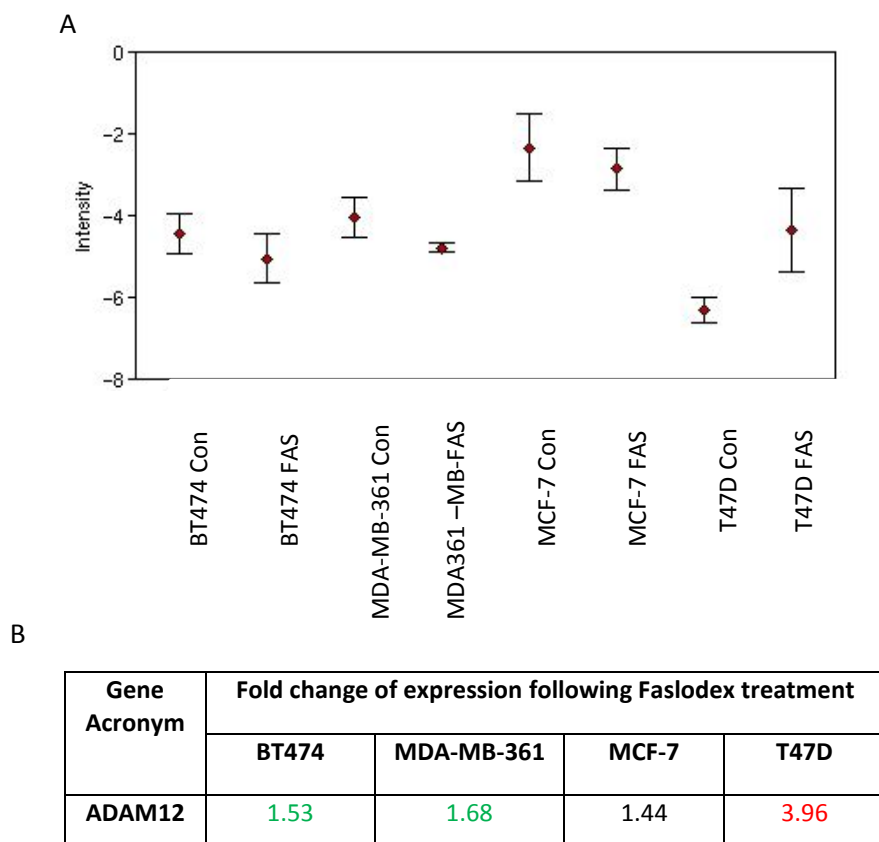| Gene Acronym	Fold change of expression following Faslodex treatment			
	BT474	MDA-MB-361	MCF-7	T47D
ID4	1.34	3.25	1.01	2.79

Figure 66: (A) Log2 intensity plot displaying the normalised (mean of triplicate samples) gene expression of ID4 in each of the 4 cell lines pre (Con) and post 10 day Faslodex (FAS) treatment (B) Table displaying the fold change in gene expression promoted by 10 day Faslodex treatment in each cell line vs. untreated control. Highlighted in green are Faslodex-promoted suppressions in gene expression and in red inductions >1.5 fold.

6.2.1.2.4 SKAP2

The basal log2 intensity values of SKAP2 were equivalent across the HER2+ and MCF-7 cell lines and positive detection calls were recorded (Figure 67). In these cell lines, Faslodex treatment resulted in very little change in the expression of SKAP2 and contrasted with a clear suppression of SKAP2 in the T47D cells. In T47D cells, detection calls were present pre and post treatment indicating some residual SKAP2 expression remained after treatment. Although the jetset score was poor for SKAP2, its other probes showed a similar suppression in expression in the T47D cell line (Table 18 and 19).

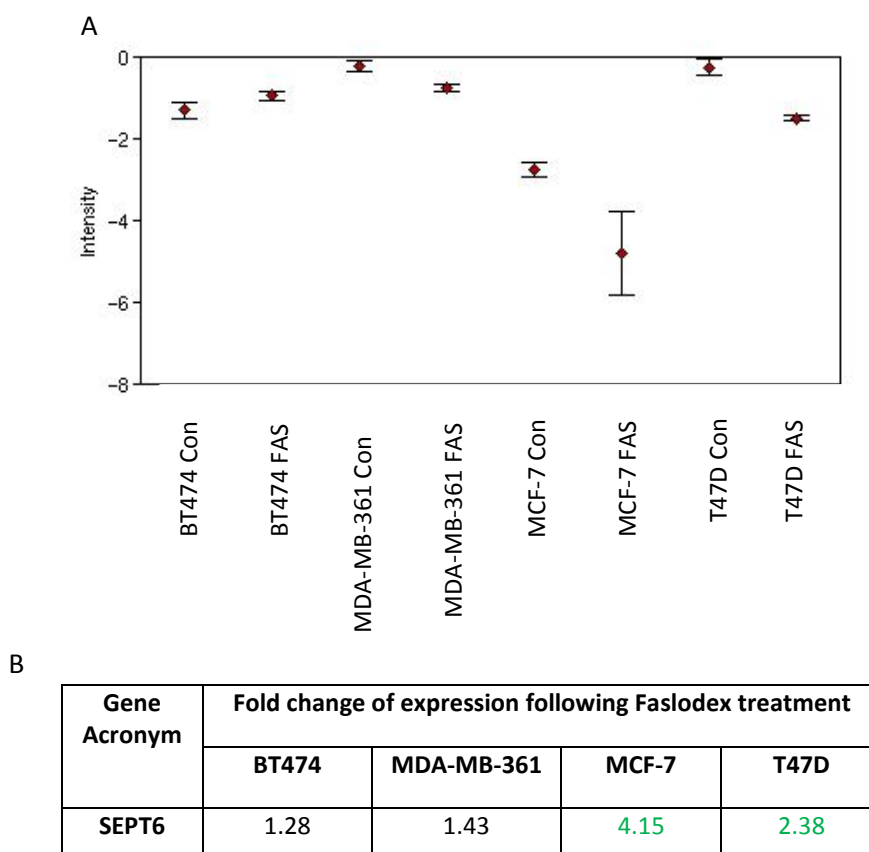| Gene Acronym	Fold change of expression following Faslodex treatment			
	BT474	MDA-MB-361	MCF-7	T47D
SKAP2	1.11	1.19	1.14	6.10
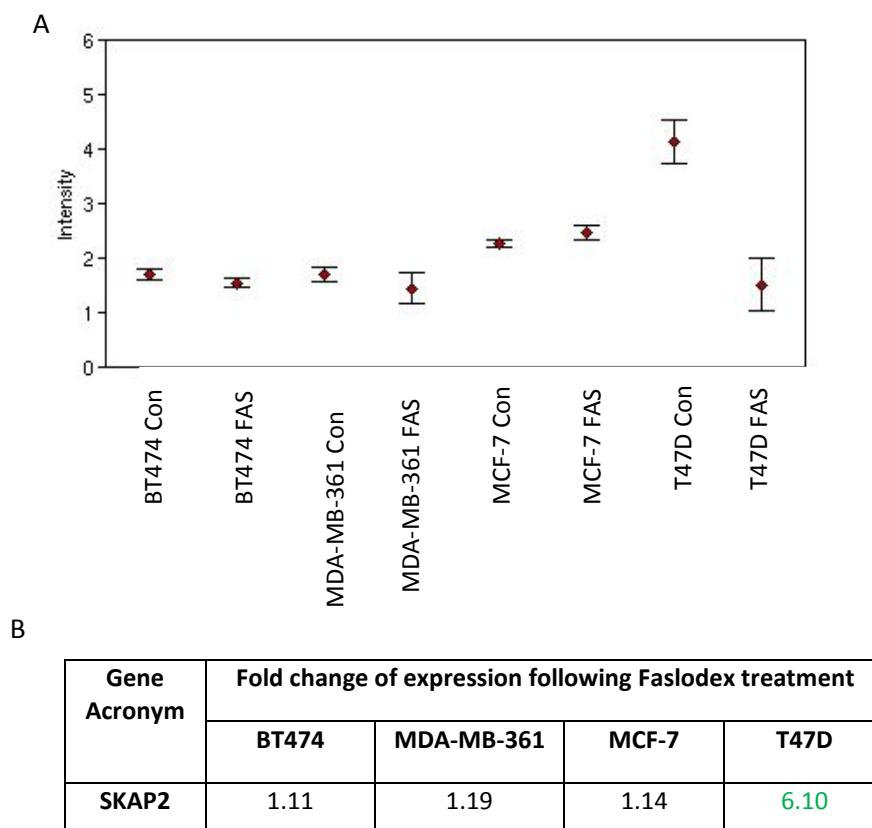
Figure 67: (A) Log2 intensity plot displaying the normalised (mean of triplicate samples) gene expression of SKAP2 in each of the 4 cell lines pre (Con) and post 10 day Faslodex (FAS) treatment (B) Table displaying the fold change in gene expression promoted by 10 day Faslodex treatment in each cell line vs. untreated control. Highlighted in green are Faslodex-promoted suppressions in gene expression >1.5 fold.

6.2.1.2.5 IL6ST

In contrast to the lack of effect of Faslodex treatment on IL6ST in the HER2+ and MCF-7 cell lines, the antihormone suppressed the expression of this gene in T47D cells (Figure 68). In all instances, positive detection calls were recorded pre and post Faslodex treatment. Although the jetset score for this gene probe was found to be particularly poor, all of the gene probes demonstrated a suppression increasing confidence of a robust down-regulation of the gene (Table 18).
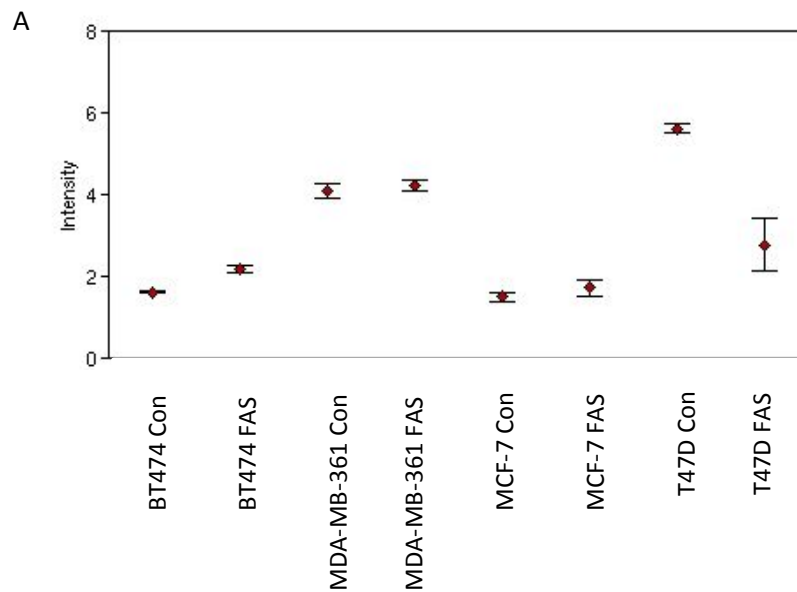
| Gene Acronym	Fold change of expression following Faslodex treatment			
	BT474	**MDA-MB-361**	**MCF-7**	**T47D**
IL6ST	1.46	1.10	1.17	7.20

Figure 68: (A) Log2 intensity plot displaying the normalised (mean of triplicate samples) gene expression of IL6ST in each of the 4 cell lines pre (Con) and post 10 day Faslodex (FAS) treatment (B) Table displaying the fold change in gene expression promoted by 10 day Faslodex treatment in each cell line vs. untreated control. Highlighted in green are Faslodex-promoted suppressions in gene expression >1.5 fold.

6.2.1.2.6 DUSP4

Basal log2 intensity values of DUSP4 were equivalent across the 4 cell models and present detection calls were recorded (Figure 69). In the HER2+ cells lines, Faslodex treatment did not alter the expression of DUSP4, while a small induction was observed in the MCF-7 cell line. In T47D cells, Faslodex treatment led to a clear suppression of the expression of DUSP4 further confirmed by a change in detection call from present to absent.

A

B

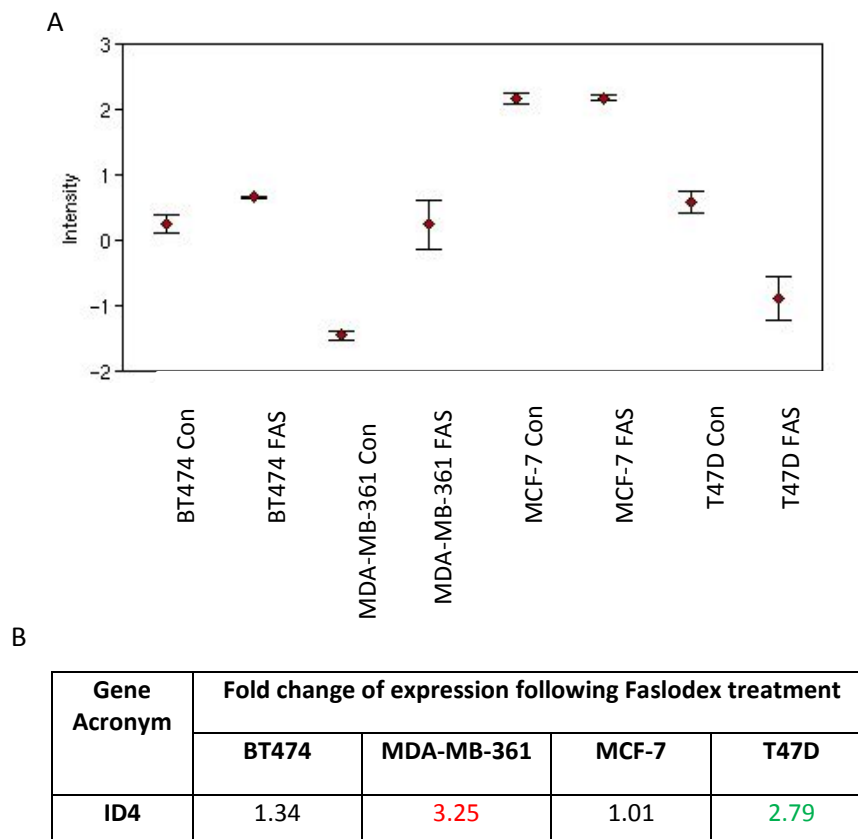| Gene Acronym	Fold change of expression following Faslodex treatment			
	BT474	MDA-MB-361	MCF-7	T47D
DUSP4	1.45	1.19	4.50	12.68
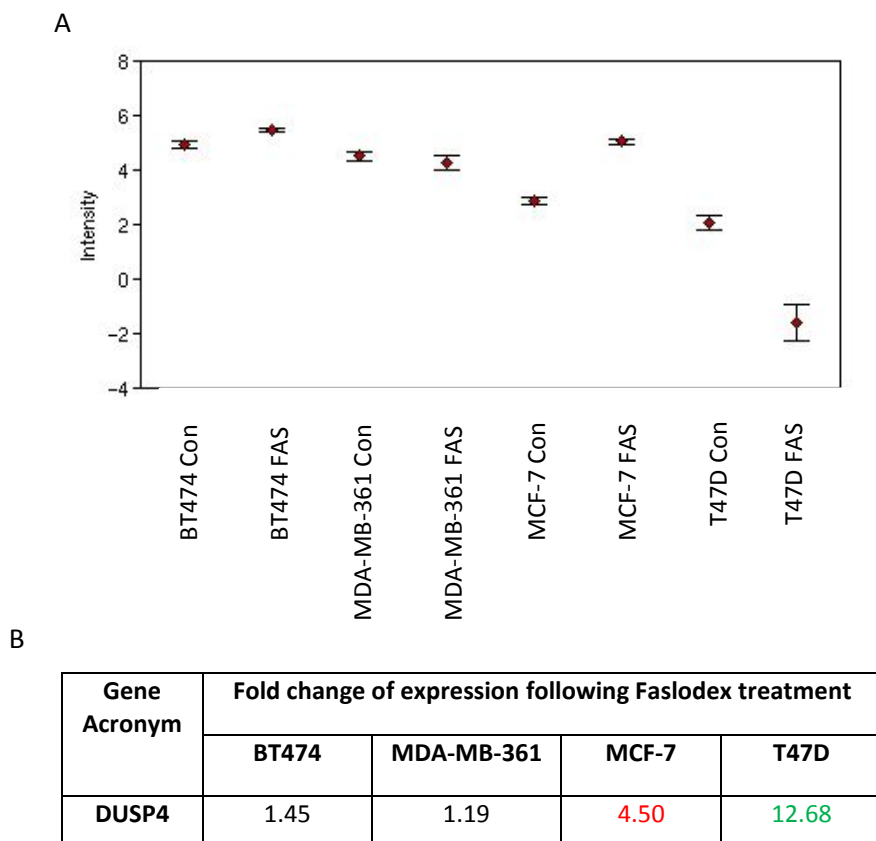
Figure 69: (A) Log2 intensity plot displaying the normalised (mean of triplicate samples) gene expression of DUSP4 in each of the 4 cell lines pre (Con) and post 10 day Faslodex (FAS) treatment (B) Table displaying the fold change in gene expression promoted by 10 day Faslodex treatment in each cell line vs. untreated control. Highlighted in green are Faslodex-promoted suppressions in gene expression >1.5 fold.

Following the analysis of the log2 intensity plots for these genes in the various ER+ cell lines ADAM12 and SEPT6 were immediately dismissed from further investigation due to the very low log2 intensity values and absent detection calls indicative of a lack of expression

6.2.3 Ontological investigation of the genes to determine their potential involvement in the anti-tumour -response mechanism

An ontological investigation was undertaken on the 9 remaining genes to determine if they had been associated with:

- Breast cancer or any other cancer type;
- Known or potential adverse function (e.g. tumour growth or progression);
- Known or potential tumour suppressive function

The results of the ontological investigations are accumulated in Tables 20 to 28. Pubmed and Scopus were used throughout using the gene name/acronym, together with selected keywords/phrases which included breast cancer, cancer, oncogene, proliferation, growth, metastasis, Faslodex, hormonal or endocrine therapy, survival, growth inhibition, tumour suppressor, apoptosis. Gene acronyms highlighted in red were induced by Faslodex in T47D cells and those in green were suppressed.

Table 20: Summary of published reports investigating the role of DCN in breast cancer disease as well as other cancers.

Gene name/acronym	Decorin: **DCN**
Function	The protein encoded by this gene is a small cellular or pericellular matrix proteoglycan that is closely related in structure to biglycan protein. This protein is a component of connective tissue, binds to type I collagen fibrils, and plays a role in matrix assembly. It contains one attached glycosaminoglycan chain. This protein is capable of suppressing the growth of various tumour cell lines (reviewed in Bi *et al.*, 2013).
Associations with breast cancer	While it can be expressed by tumour and stromal cells (Oda *et al.*, 2012; Soria-Valles *et al.*, 2013), decorin is primarily found in the ECM. It has been shown to bind and inhibit a number of growth factors such as TGFβ1 and a number of RTKs found on tumour cells known to be involved oncogenic signalling such as EGFR, IGF1R and MET (reviewed in Iozzo *et al.*, 2011), leading to

suppression of tumour growth, migration and angiogenesis (Goldoni *et al.*, 2008a). More recently, decorin has been shown to influence inflammatory responses in the tumour stroma via interaction with Toll-like receptors, again functioning to prevent tumour progression (Merline *et al.*, 2011).

Reduced decorin levels in the tumour stroma have been described as a poor prognostic indicator for invasive breast cancer (Troup *et al.*, 2003). Adenovirus gene transfer of decorin has been shown to prevent the growth of tumour xenografts from a number of malignancies including breast (Reed *et al.*, 2005). Goldoni *et al.*, have also demonstrated that exogenous decorin treatment in the MTLn3 (a rat mammary adenocarcinoma cell lines) was able to growth inhibit the cells, prevent anchorage-independent growth and reduce cell motility thus hindering their invasive capacity and importantly inducing significant apoptosis. They also assessed the effects of decorin treatment in a murine model of orthotopic breast carcinoma where it was able to prevent metastasis to the lungs possibly through the inhibition of EGFR, ERBB2 and Met (Goldoni *et al.*, 2008b).

DCN has been reported to be up-regulated in patients treated with neoadjuvant letrozole and included in a gene signature that predicted letrozole response (Makay *et al.*, 2007; Miller *et al.*, 2009) suggesting a possible role in the mechanism of AI response.

Reduced expression of decorin in the stroma surrounding invasive breast cancers or ductal carcinoma in situ was associated with more aggressive disease, thus decorin expression levels could relate to prognosis and malignant potential of a tumour (Oda *et al.*, 2012).

	Decorin has also been linked to the suppression of angiogenesis in a malignant setting. Treatment of MDA-MB-231 cells with decorin led to the suppression of HIF-1α and VEGFA, thought to be mediated by the ability of decorin to antagonise Met and thus downstream β-catenin signalling. Also, decorin treatment up-regulated an anti-angiogenic factors TIMP-3 and down-regulated two pro-angiogenic factors MMP-9 and MMP-2 (Neill *et al.*, 2012).
	However, there is one study where proteomic analysis established an association between increased decorin expression and disease progression; lymph node metastasis, increased number of positive lymph nodes and worse overall survival (Cawthorn *et al.*, 2012).
Associations with other cancers	Decorin levels are significantly reduced in colorectal cancer in keeping with a tumour suppressive function (Bi *et al.*, 2012). Forced expression of decorin results in suppression of growth and progression (Santra *et al.*, 1995). Loss of E-cadherin has been shown to promote disease progression via encouraging EMT (Schmalhofer *et al.*, 2009) and Bi *et al.*, have shown that decorin interacts with E-cadherin, stabilising the protein to attenuate colorectal tumour growth and migration *in vitro* and *in vivo* (Bi *et al.*, 2012).
	Decorin can inhibit the growth of ovarian cancer cells via upregulation of the cyclin-dependent kinase inhibitor p21. Decorin promoted a synergistic anti-tumour effect in these cells when treated in combination with carboplatin (Nash *et al.*, 1999).
	The ability of decorin to inhibit TGFβ1 was found to enhance the *in vivo* immune response (increased T-cells) to glioma cells with tumour formation suppressed *in vivo* (Stander *et al.*, 1998).
	Tralhao *et al.,* investigated the potential of decorin as a anti-

cancer therapy using adenovirus-mediated decorin gene transfer in nude mice. They found that decorin significantly reduced tumour volume and also that decorin could function in an autocrine and paracrine manner to prevent inhibit tumour growth at secondary sites. Importantly, they observed that the effects of decorin were selective to cancer cells and that evidence of apoptosis or growth inhibition was not observed in normal cells such as hepatocytes or endothelial cells (Tralhao *et al.*, 2003).

In hepatocarcinogenesis, decorin was found to bind to PDGF preventing its binding to PDGFRα. The PDGF receptors are known to have crucial roles in the development and maintenance of liver tumours and receptor levels can be used as prognostic markers. Thus inhibition of PDGF signalling has been reported to be tumour suppressive in liver cancer (Baghy *et al.*, 2013).

Table 21: Summary of published reports investigating the role of TXNIP in breast cancer disease as well as other cancers.

Gene name/acronym	Thioredoxin-interacting protein: **TXNIP**
Function	TXNIP (thioredoxin interacting protein, also known as Vitamin D3 up-regulated protein 1, VDUP-1; thioredoxin binding protein 2, TBP-2), is a key modulator of the redox system. It binds to the active cysteine residue of thioredoxin (TRX) and inhibits its antioxidative function (Cheng *et al.*, 2004). It can also function independently of TRX-binding and function to inhibit cell growth via arrestin domain-mediated suppression of glucose uptake and metabolic reprogramming (Elgort *et al.*, 2010)
Associations with breast cancer	Increased expression of TXNIP in breast cancer patients with lymph-node negative disease was associated with an increased metastasis-free interval (Zhou *et al.*, 2012).

	Butler *et al.*, demonstrated that expression of TXNIP in MCF-7 cells with metastatic capability could force the cells into senescence with parallel increased production of reactive oxygen species and oxidative stress. In agreement with suggestions of TXNIP being a potential tumour suppressor gene in breast cancer, in a small study of 9 patients, TXNIP expression was reduced in cancer tissue compared to normal matched controls (Butler *et al.*, 2002). Endocrine therapy has been shown to be capable of producing ROS exerting ROS-stress in cancer cells which can lead to the disruption of redox signalling. In this pro-oxidant state, there is an increase in the oxidised form of thioredoxin and high levels of oxidised thioredoxin has been speculated to be associated with anti-hormone resistance (Penney *et al.*, 2013). As TXNIP inhibits thioredoxin, it is essentially preventing one mechanism by which drug resistance could be developed.
Associations with other cancers	Goldberg *et al* identified an inverse correlation between TXNIP expression and metastatic potential in melanoma cancer cell lines (Goldberg *et al.*, 2003). In prostate and bladder cancer cell lines, TXNIP expression was further reduced in cancer cells compared to normal, potentially indicative of TXNIP being a tumour suppressor (Butler *et al.*, 2002). *In vivo*, overexpression of TXNIP has been shown to halt disease progression; reduced tumour growth and prevention of metastasis while TXNIP knockout increased the incidence of hepatocellular carcinoma (Sheth *et al.*, 2006).

Table 22: Summary of published reports investigating the role of TGFB2 in breast cancer disease as well as other cancers.

Gene name/acronym	Transforming growth factor beta-2: **TGFB2**
Function	This gene encodes a member of the transforming growth factor beta (TGFB) family of cytokines, which are multifunctional peptides that regulate proliferation, differentiation, adhesion, migration, and other functions in many cell types by transducing their signal through combinations of transmembrane type I and type II receptors (TGFBR1 and TGFBR2) and their downstream effectors, the SMAD proteins (Vilar *et al.*, 2006)
Associations with breast cancer	TGFβ signalling is somewhat of a paradox in breast cancer. In early-stage disease, TGFβ signalling is thought to be growth inhibitory, while in established disease it has been shown to promote progression (Muraoka-Cook *et al.*, 2005). Several studies in late-stage disease have correlated TGFβ signalling with breast cancer invasiveness, progression and metastasis (Walker *et al.*, 1992; Ivanovic *et al.*, 2003; Walker *et al.*, 1994). Inhibition of TGFβ signalling in this setting can successfully prevent metastasis (Muraoka *et al.*, 2002). Beisner *et al* have shown that an insertion polymorphism into the TGFβ2 promoter enhances the transcription of TGFβ2 and is potentially linked to metastasis of the primary tumour to the lymph nodes (Beisner *et al.*, 2006). Tamoxifen and Faslodex therapy induces TGFβ2 secretion. This induction of TGFB2 expression has been shown to be predictive of the antioestrogen activity of tamoxifen (Buck *et al.*, 2008; Gomes *et al*., 2011).
Associations with other cancers	A vaccine targeting TGFβ2 has shown to have significant activity in lung cancer by enhancing the immune system (Dasanu *et al.*, 2012).

	Due to the role of TGFβ2 in cancer progression and metastasis, a number of clinical trials are looking at the activity of TGFβ2 vaccines in a number of cancer settings, including advanced pancreatic cancer, metastatic melanoma and metastatic colon cancer (Jaschinski *et al.*, 2011)

Table 23: Summary of published reports investigating the role of CASP1 in breast cancer disease as well as other cancers.

Gene name/acronym	Caspase 1: **CASP1**
Function	This gene encodes a protein which is a member of the caspase family. Caspase-1 is an initiator caspase that cleaves inactive prointerleukin 1β to generate the active proinflammatory cytokine interleukin 1β and has been associated with inducing apoptosis (Thornberry *et al.*, 2001).
Associations with breast cancer	The transcription factor IRF-1 is a potential tumour suppressor gene which is lost in several cancers including breast (Willman *et al.*, 1996; Nozawa *et al.*, 1996; Doherty *et al.*, 2001). Its tumour suppressive functions are due to its ability to regulate apoptosis (Tanaka *et al.*, 1994) via activation of caspase-1 (Tamura *et al.*, 1995), caspase-7 (Sanceau *et al.*, 2000), caspase-8 (Suk *et al.*, 2001) and FAS ligand (Chow *et al.*, 2000). Expression of IRF-1 in breast cancer cells has been shown to be growth inhibitory *in vitro* and *in vivo* and these functions are mediated by caspase activation (Bouker *et al.*, 2005). This observation was taken further by Ning *et al* who reported that expression of IRF-1 increased responsiveness to antioestrogens and in the Faslodex-resistant setting low dose of IFNγ, a cytokine that induces the expression of IRF-1 is sufficient to overcome Faslodex-resistance and enhances anti-Oestrogen induced apoptosis (Ning *et al.*, 2010). IRF-1 has been shown to signal to apoptosis through a number of components including caspase 1 (Tamura *et al.*, 1995).

Associations with other cancers	The NLRP3 inflammasome is a protein complex that actiates caspase-1 leading to the secretion of pro-inflammatory cytokines such as IL-1β, IL-18 and IL-33. It has been shown by Aymeric *et al.*, that the NLRP3 inflammasome is critical for the immunogenicity of cell death triggered by anthracyclines, oxaloplatin, or radiotherapy (Aymeric *et al.*, 2010).
	Functional TGFβ1 signalling in human prostate cancer cells resulted in the activation of the apoptosis pathways leading to growth suppression. It was observed that the TGFβ1 pathway was inducing apoptosis via a caspase- 1 mediated pathway, involving induction of caspase-1 with a parallel down-regulation of bcl-2 and up-regulation of bax proteins (Guo *et al.*, 1999).

Table 24: Summary of published reports investigating the role of PTGER3 in breast cancer disease as well as other cancers.

Gene name/acronym	Prostaglandin E receptor 3: **PTGER3**
Function	The protein encoded by this gene is a member of the G-protein coupled receptor family. This protein is one of four receptors identified for prostaglandin E2 (PGE2). This receptor may have many biological functions, which involve digestion, nervous system, kidney reabsorption, and uterine contraction activities (Hatae *et al.*, 2002).
Associations with breast cancer	No direct associations with breast cancer but PTGER3 has been shown to be involved in stages of tumour progression (see below).
Associations with other cancers	PGE2-stimulated PTGER3/4 signalling has a prominent role in tumour stromal formation and tumour growth. Such signalling at stromal fibroblasts has been observed to induce CXCL12 in the fibroblasts enhancing CXCR4-CXCL12 signalling and thus encouraging the stroma formation. Targeting of PTGER3/4 or CXCR4 have been suggested to possibly prevent tumour development (Katoh *et al.*, 2010).

	PTGER3 expression in bone-marrow derived stromal cells has been linked to tumour-associated angiogenesis. Knockdown of PTGER3 within these cells led to the inhibition of such angiogenesis via reduction of VEGF in the tumour stroma and a reduction in the recruitment VEGFR1 and VEGFR2 positive cells for the bone marrow which aid tumour angiogenesis (Ogawa *et al.*, 2009). PTGER3 signalling has also been observed to initiate tumour invasion and metastasis in Lewis lung carcinoma cells via the upregulation of MMP-9 (Amano *et al.*, 2009). Increased amounts of IL-8 are produced by airway epithelial cancer cells initiating a pro-tumour response. Activation of EGFR by TGF-α has been shown to promote this IL-8 production. Kim *et al.*, have demonstrated a positive feedback loop between COX2/PGE2/PTGER3 receptor-dependent EGFR activation leading to the aberrant IL8 production observed in these cancer cells (Kim *et al.*, 2011)

Table 25: Summary of published reports investigating the role of IL6ST in breast cancer disease as well as other cancers.

Gene name/acronym	Interleukin 6 signal transducer (gp130, oncostatin M receptor): **IL6ST**/**GP130**
Function	Signal-transducing molecule. The receptor systems for IL6, LIF, OSM, CNTF, IL11, CTF1 and BSF3 can utilize IL6ST for initiating signal transmission. Binds to IL6/IL6R (alpha chain) complex, resulting in the formation of high-affinity IL6 binding sites, and transduces the signal (Waetzig *et al.*, 2012).
Associations with breast cancer	Following ligand binding, IL6ST supports the activation of the RTKs JAK1, JAK2 and Tyk2 for initiation of signalling (Taga *et al.*, 1997). JAK activation initiates a number of downstream growth-

	related signalling pathways including PI3K and MAPK.
	STAT3 is also a target of IL6ST; STAT3 becomes phosphorylated, dimerises and translocates to the nucleus, inducing transcription of a number of genes involved in growth, differentiation and cell cycle (Hirano *et al.*, 2000). STAT3 is an oncogene, found to be constitutively active in many tumours including breast where it is a key mediator of malignancy (Bromberg, 2002). IL6ST is expressed in most breast cancer cell lines and most primary tumours (Douglas *et al.*, 1997; Karczewska *et al.*, 2000). Inhibition of IL6ST in breast cancer cells *in vitro* and *in vivo* led to growth inhibition suggesting IL6ST could be a potential novel target for breast cancer (Selander *et al.*, 2004)
Associations with other cancers	Inhibition of IL6ST has also been seen to be growth inhibitory in colorectal cancer (Waldner *et al.*, 2012). Chronic STAT3 activation is observed in most gastric cancers and inhibtion of STAT3 signalling via IL6ST and/or EGFR inhibition could be potentially therapeutic (Giraud *et al.*, 2012)

Table 26: Summary of published reports investigating the role of SKAP2 in breast cancer disease as well as other cancers.

Gene name/acronym	Src kinase associated phosphoprotein 2: **SKAP2**
Function	The protein encoded by this gene is closely affiliated with the src family kinases (SFKs) and is an adaptor protein that may be involved in such signalling. Src family kinases (including Fyn and Lyn) have been found to have a high homology to src kinase , but no direct interaction with src kinase signalling has been reported (Wheeler *et al.*, 2009a).
Associations with breast cancer	No associations with breast cancer. However, a number of the SFKs have been associated with

	cancer progression and the src inhibitor dasatanib also inhibits this family (due to the high homology with src) so potentially the clinical activity of dasatanib may be due to SFK signalling inhibition (Wheeler *et al.*, 2009b)
Associations with other cancers	SKAP2 has been observed to be over expressed in pancreatic intraepithelial neoplasia (Buchholz *et al.*, 2005). Further work also displayed over-expression in pancreatic ductal carcinoma via a genetic gain of the gene. The authors predict that this genetic gain leading to deregulation of SKAP2 is likely to be involved in the development of this cancer (Harada *et al.,* 2008). SKAP2 has a an SH3 domain allowing the binding of focal adhesion protein RAFTK suggesting that its likely to modulate the motility and invasiveness of pancreatic ductal carcinoma cells (McLean *et al.*, 2005). SKAP2 was found to inhibit actin polymerisation and by modulating actin assembly reduced migration and proliferation of a glioblastoma cell line (Shimamura *et al.*, 2012).

Table 27: Summary of published reports investigating the role of DUSP4 in breast cancer disease as well as other cancers.

Gene name/acronym	Dual specificity phosphatase 4: **DUSP4**
Function	DUSP4 is a member of the dual specificity protein phosphatase subfamily. These phosphatases inactivate their target kinases by dephosphorylating phosphotyrosine residues. They negatively regulate members the MAPK superfamily which are associated with cellular proliferation and differentiation. DUSP4 inactivates ERK1, ERK2 and JNK, is expressed in a variety of tissues, and is localized in the nucleus (Kevse *et al.*, 2008).
Associations with breast cancer	Reduced expression of DUSP4 has recently been identified as a mediator of resistance to chemotherapy and a possible tumour suppressor in basal- like breast cancers. Reduced DUSP4

	expression was associated with activation of the Ras-ERK pathway that mediated resistance to neoadjuvant chemotherapy (Balko *et al.*, 2012).
	DUSP4 has been reported to be lost in early-onset and high-grade disease mimicking the behaviour of a tumour suppressor gene (Armes *et al.*, 2004).
Associations with other cancers	The DUSP4 promoter has been found hypermethylated astrocytic gliomas and glioma cell lines and forced expression of DUSP4 inhibited the growth of glioma cells suggesting tumour suppressive functions (Waha *et al.*, 2010). However, DUSP4 has been observed to be upregulated in pancreatic cell lines (Yip-Schneider *et al.*, 2001), rectal adenocarcinomas (Gaedcke *et al.*, 2010) and melanoma cell lines (Teutschbein *et al.*, 2010) suggesting that DUSP4 does not behave as a tumour suppressor in all instances. DUSP4 overexpression has also been shown to encourage cell proliferation in colorectal cancer cell line where it is an important regulator of cell growth (Gröschl *et al.*, 2013).

Table 28: Summary of published reports investigating the role of ID4 in breast cancer disease as well as other cancers.

Gene name/acronym	Inhibitor of DNA binding 4: **ID4**
Function	Id proteins are dominant negative inhibitors of DNA binding. They contain functional HLH dimerisation motifs, but lack the DNA-binding basic region found in the basic HLH (bHLH) proteins, thereby inhibiting DNA binding of bHLH transcription factors thus regulating transcription of bHLH-regulated genes (Benzera *et al.*, 1990).
Associations with breast cancer	ID4 has been found to be highly expressed in triple-negative breast cancers. It blocks BRCA1 gene transcription in triple-negative cell lines and down-regulates BRCA1 *in vivo*, thus

	inhibiting BRCA-1 mediated signalling (Wen *et al.*, 2012).
	ID4 has been found to be expressed in normal mammary tissue but suppressed in ER+ breast cancer. Further investigations have found ID4 to be tumour suppressor gene hypermethylated in breast cancer and thus silenced during disease progression and its methylation status has been suggested as prognostic marker (Noetzel *et al.*, 2008)
Associations with other cancers	In high grade ovarian cancer ID4 has been reported to be a contributory oncogene and knockdown of the protein in mouse models suppressed tumour growth and improved survival (Ren *et a*l., 2012).
	In prostate cancer ID4 has been described as a tumour suppressor; expressed in normal healthy tissue but silence by hypermethylation following onset of carcinogensis (Sharma *et al.*, 2012).
	ID4 has also been reported to promote the malignant transformation of astrocytes leading to the formation of glioblastomas via de-regulation of the cell cycle pathway (Jeon *et al.*, 2008)

Based on the above ontology, DUSP4 and ID4 were not taken forward for further analysis since both showed tumour suppressive actions and so their down-regulation by 10 day Faslodex treatment in the T47D cell line was counterintuitive in relation to its improved response.

DCN, TXNIP, TGFB2, and CASP1, whilst similarly having some tumour suppressive actions, are induced by Faslodex treatment and could thus be part of the complete response mechanism to Faslodex in this cell line. These genes were thus taken forward for further analysis.

SKAP2, PTGER3 and IL6ST were similarly taken forward for further analysis since their ontology suggests a role in disease progression and signalling. As such, their suppression by Faslodex may contribute to the complete response exerted by this drug in the T47D cell line.

6.2.4 Expression of the genes potentially involved in the T47D complete response in a Faslodex-resistant MCF-7 model.

To further clarify any involvement of changes in DCN, TXNIP, TGFB2, CASP1, SKAP2, PTGER3 and IL6ST in the initial Faslodex response, the expression of these genes were analysed using a microarray dataset generated from the MCF-7-derived Faslodex-resistant cell line versus its hormone responsive control (Figures 70-77). The rational was that if the Faslodex-promoted gene changes observed in the T47D cell line were also observed in the MCF-7 acquired Faslodex-resistance setting, then this might undermine any potential involvement in the T47D response mechanism.
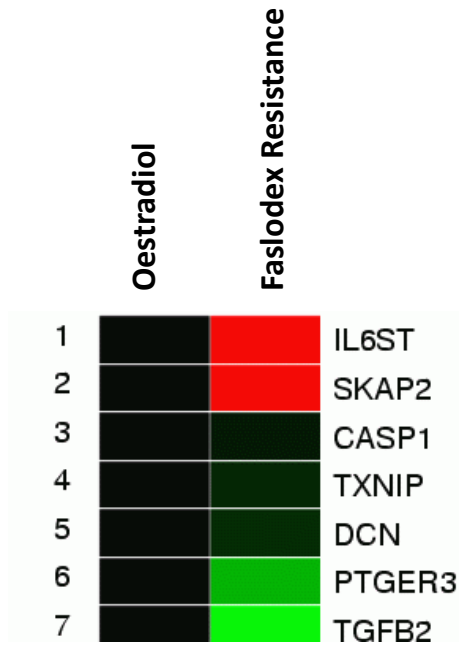
Figure 70: Heatmap generated by GeneSifter displaying the change in expression of these potential modulators of Faslodex response in MCF-7 Faslodex-resistance versus oestradiol-treated control using the jetset gene probes.6.2.4.1 Genes induced by 10 day Faslodex-treatment in the T47D cell line

A

B

Gene Acronym	Fold change
TXNIP	1.11
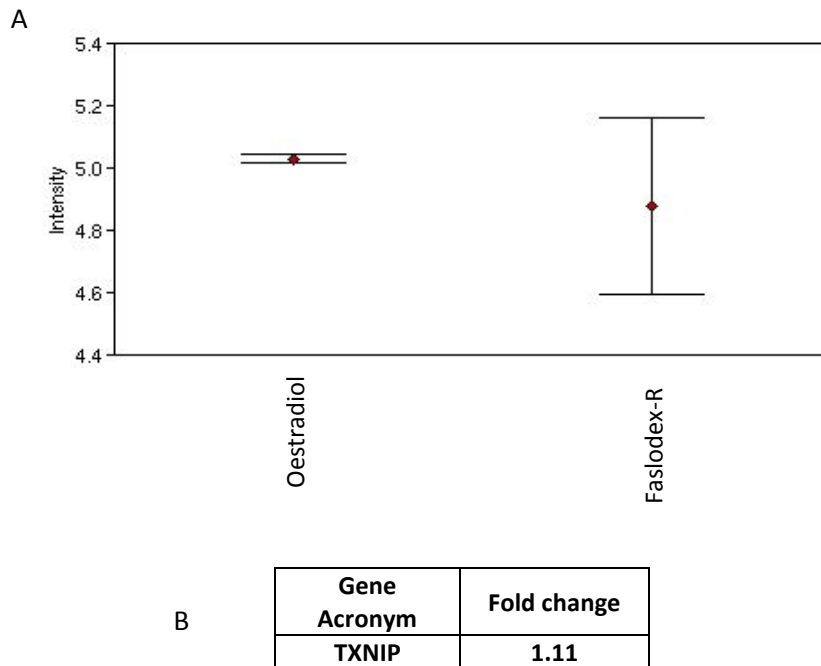
Figure 71: (A) Log2 expression intensity plot displaying the normalised (mean of triplicate samples) gene expression of TXNIP in an MCF-7 derived Faslodex-resistant cell line (Faslodex-R) versus oestradiol-treated control and (B) table displaying the fold change in gene expression

A

B

Gene Acronym	Fold change
DCN	1.01
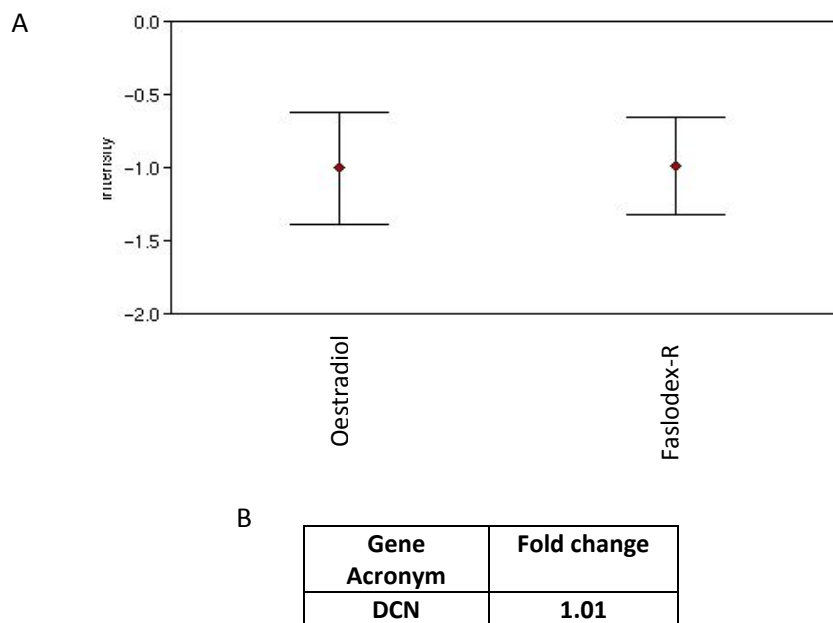
Figure 72: (A) Log2 expression intensity plot displaying the normalised (mean of triplicate samples) gene expression of DCN in an MCF-7 derived Faslodex-resistant cell line (Faslodex-R) versus oestradiol-treated control and (B) table displaying the fold change in gene expression.
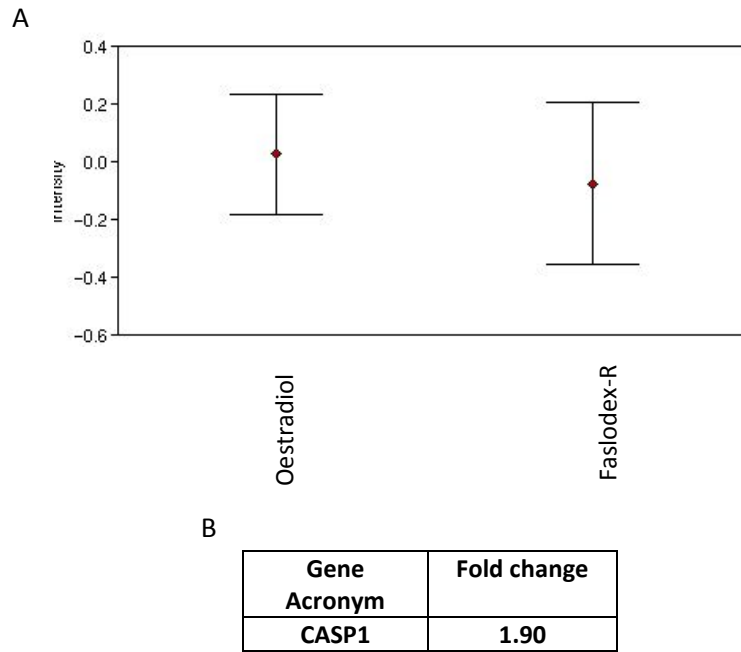
Figure 73: (A) Log2 expression intensity plot displaying the normalised (mean of triplicate samples) gene expression of CASP1 in an MCF-7 derived Faslodex-resistant cell line (Faslodex-R) versus oestradiol-treated control and (B) table displaying the fold change in gene expression.
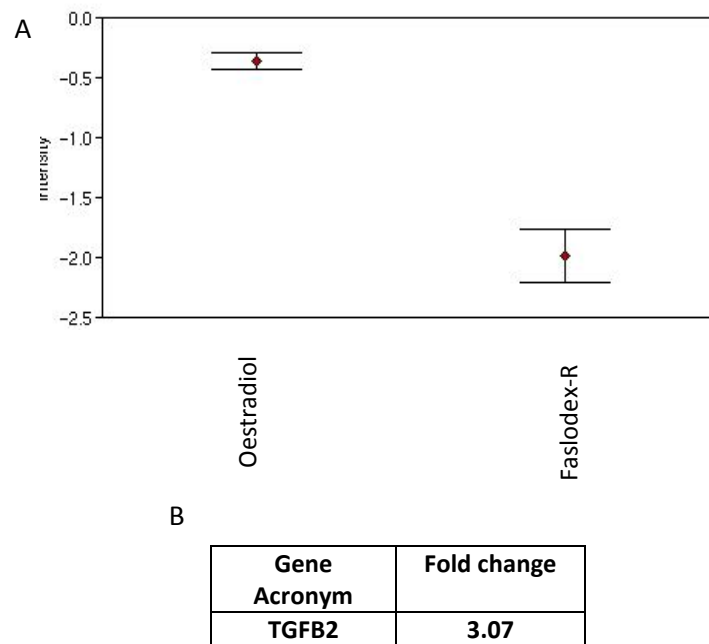
Figure 74: (A) Log2 expression intensity plot displaying the normalised (mean of triplicate samples) gene expression of TGFB2 in an MCF-7 derived Faslodex-resistant cell line (Faslodex-R) versus oestradiol-treated control and (B) table displaying the fold change in gene expression.

6.2.4.2 Genes suppressed by 10 day Faslodex-treatment in the T47D cell line
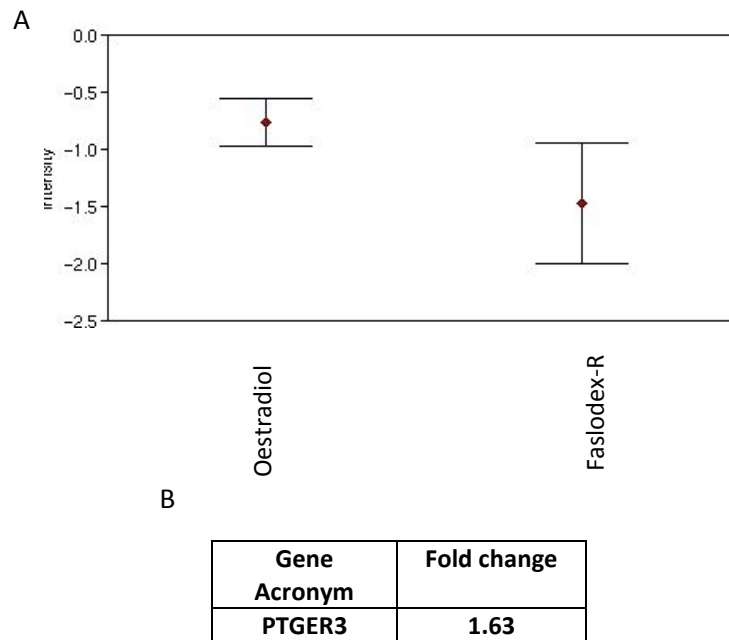
Figure 75: (A) Log2 expression intensity plot displaying the normalised (mean of triplicate samples) gene expression of PTGER3 in an MCF-7 derived Faslodex-resistant cell line(Faslodex-R) versus oestradiol-treated control and (B) table displaying the fold change in gene expression.
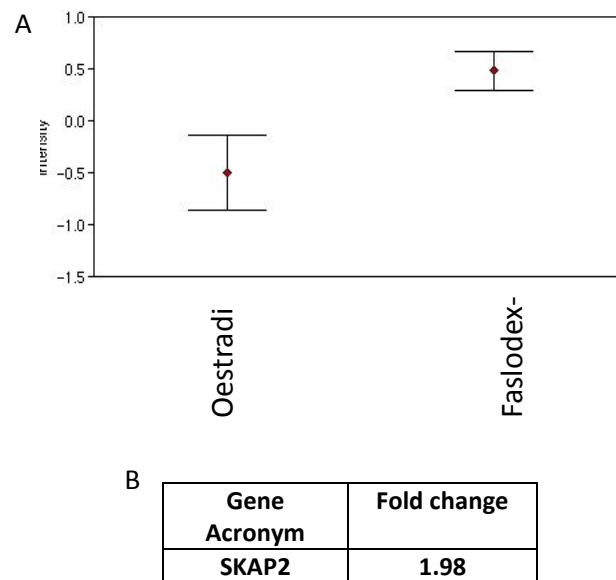
Figure 76: (A) Log2 expression intensity plot displaying the normalised (mean of triplicate samples) gene expression of SKAP2 in an MCF-7 derived Faslodex-resistant cell line (Faslodex-R) versus oestradiol-treated control and (B) table displaying the fold change in gene expression.

A

B

Gene Acronym	Fold change
IL6ST	2.37
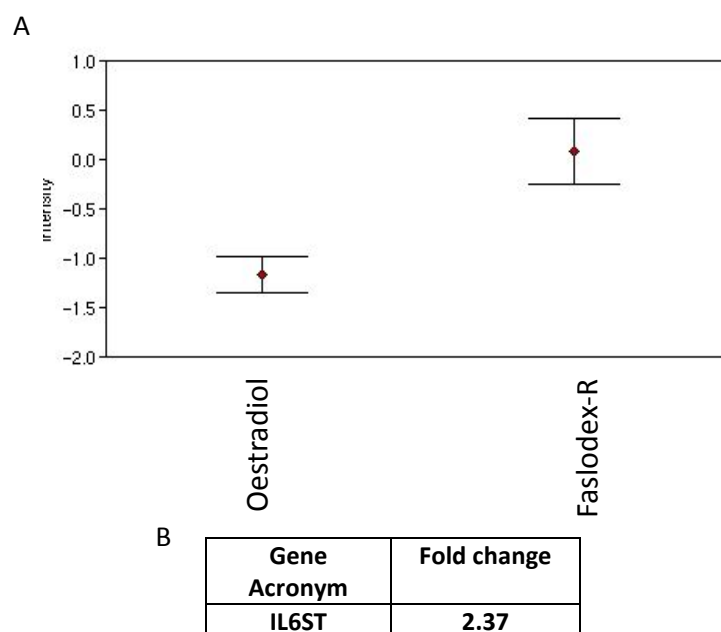
Figure 77: (A) Log2 expression intensity plot displaying the normalised (mean of triplicate samples) gene expression of IL6ST in an MCF-7 derived Faslodex-resistant cell line (Faslodex-R) versus oestradiol-treated control and (B) table displaying the fold change in gene expression.

DCN, CASP1, TXNIP, TGFB2 were thus all induced by short term Faslodex treatment in the T47D cell line and in contrast either remained at basal level or were suppressed in MCF-7 cells that acquired Faslodex-resistance (Figures 71-74), further suggesting a potential role for these genes in the complete response mechanism following their Faslodex induction. SKAP2 and IL6ST were suppressed in the T47D cell line by treatment but up-regulated in the resistant setting (Figures 76 and 77), suggesting their suppression by Faslodex in the T47D cell line may contribute to the anti-tumour response. PTGER3 was suppressed in the T47D cell line by Faslodex but there was also some evidence for its decline/absence of expression in resistance (Figure 75), suggesting suppression of this gene is unlikely to contribute to the complete response observed in the T47D cell line.

6.2.5 Establishing potential clinical relevance of the genes of interest in the context of endocrine outcome

Using the online tools KMPlotter (and for promising genes GOBO), the relationship was explored between inherent tumour gene expression levels of DCN, TXNIP,

TGFB2, CASP1, SKAP2, IL6ST, PTGER3 and duration of RFS to tamoxifen in ER+ breast cancer patients.

6.2.5.1 KMPLotter analysis of DCN, TXNIP, TGFB2 and CASP1 in tamoxifen treated breast cancer

Use of KMPlotter (Figures 78 and 79) revealed that ER+ breast cancer patients expressing higher levels of DCN and TXNIP had a significantly improved duration of RFS following tamoxifen treatment (HR=0.66; 95% CI 0.47-0.91 p=0.011, Figure 78 and HR=0.66 95% CI 0.48-0.92 p=0.013, Figure 79 respectively). TGFB2 and CASP1 failed to display significant associations with relapse free survival in this cohort of tamoxifen-treated patients.
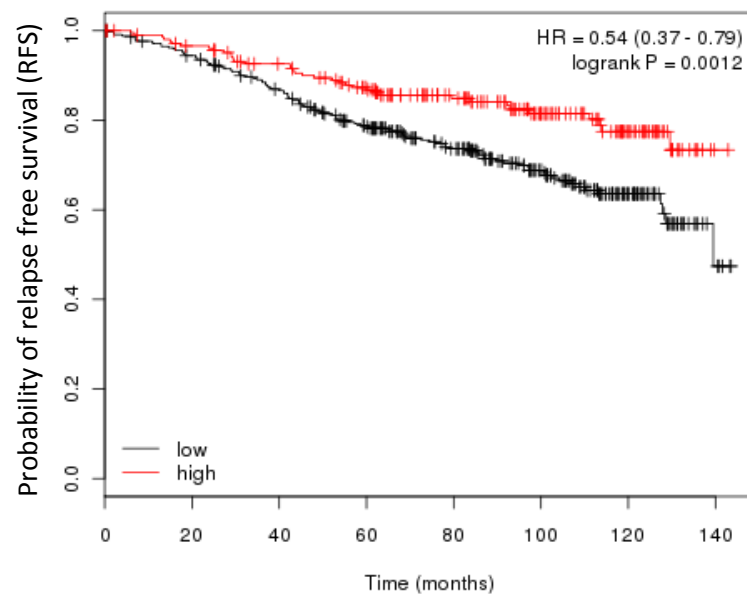
Figure 78: Kaplan Meier survival curve generated by KMPlotter displaying the association between DCN gene expression and relapse free survival (RFS) in ER+ tamoxifen treated patients. This survival curve was generated using the jetset affymetrix gene probe for DCN and grouping patients by best fit cutpoint (as calculated by KMPlotter) (n=657).

Figure 79: Kaplan Meier survival curve generated by KMPlotter displaying the association between TXNIP gene expression and relapse free survival (RFS) in ER+ tamoxifen treated patients. This survival curve was generated using the jetset affymetrix gene probe for TXNIP grouping patients by best fit (as calculated by KMPlotter) (n=657).

6.2.5.2 KMPlotter analysis of PTGER3, SKAP2 and IL6ST in tamoxifen treated breast cancer

The survival curves from KMPlotter in Figures 80-82 revealed significant associations between higher PTGER3, SKAP2 and IL6ST gene expression and increased duration of RFS following tamoxifen treatment. These data were not consistent with the concept derived from the Faslodex treated T47D cells that their suppression by Faslodex in this model related to its superior response, or with their reported adverse gene ontology.

Figure 80: Kaplan Meier survival curve generated by KMPlotter displaying the association between PTGER3 gene expression andrelapse free survival (RFS) In ER+ tamoxifen treated patients. This survival curve was generated using the jetset affymetrix gene probe for PTGER3 grouping patients by best fit (as calculated by KMPlotter) (n=657).
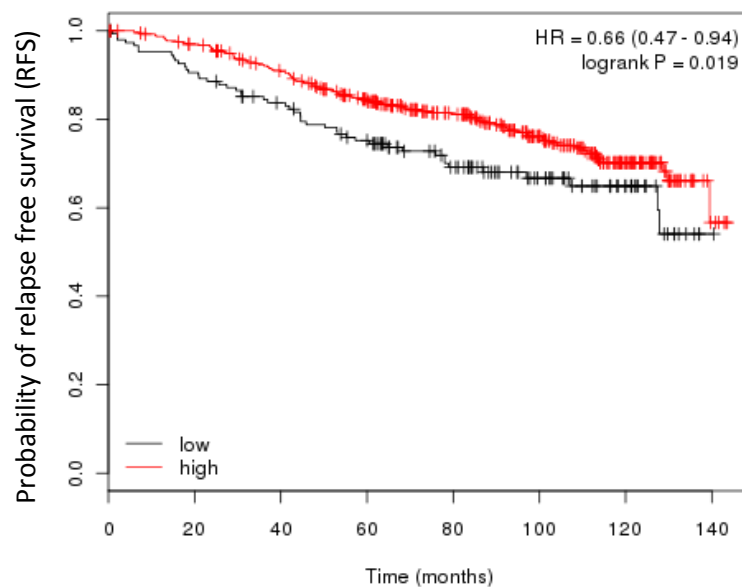
Figure 81: Kaplan Meier survival curve generated by KMPlotter displaying the association between SKAP2 gene expression and relapse free survival (RFS) in ER+ breast cancer patients. This survival curve was generated using the jetset affymetrix gene probe for SKAP2 grouping patients by best fit (as calculated by KMPlotter) (n=657).
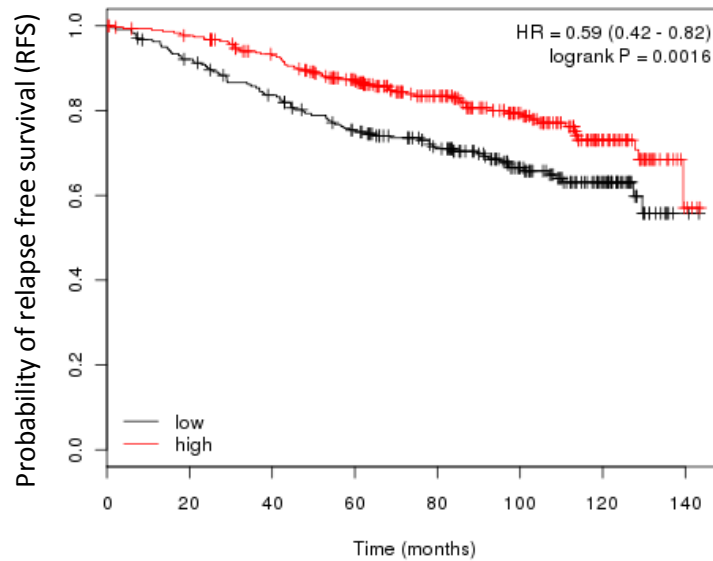
Figure 82: Kaplan Meier survival curve generated by KMPlotter displaying the association between IL6ST gene expression and relapse free survival (RFS) in ER+ tamoxifen treated patients. This survival curve was generated using the jetset affymetrix gene probe for IL6ST grouping patients by best fit (as calculated by KMPlotter) (n=657).

6.2.5.3 GOBO analysis of DCN and TXNIP in tamoxifen treated patients

Although GOBO used a smaller patient dataset than KMPlotter (n=176), it could be used to further determine how the degree of expression of genes of interest associated with RFS following tamoxifen treatment. Firstly, the gene expression levels can be grouped into more than 2 groups so it can be determined if there is a graded relationship between gene expression and survival. Further, expression levels can be linked to molecular subtype and tumour grade. As seen in Figure 83, the significant association between elevated DCN gene expression and improved response was retained, and this relationship was weakly graded (i.e. the more DCN expression, the better the RFS).
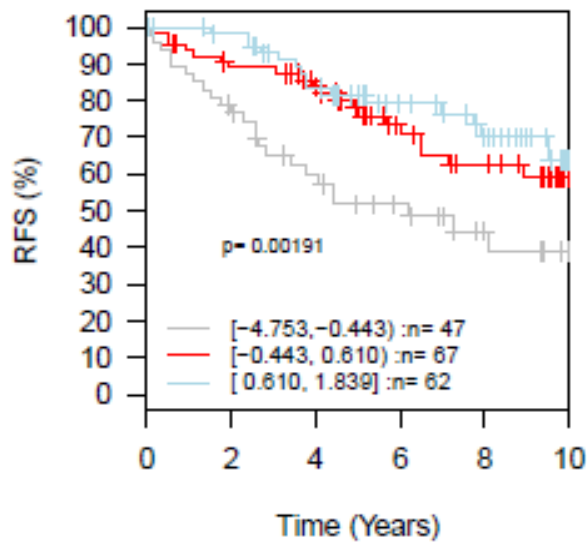
Figure 83: Kaplan Meier survival curve generated by GOBO displaying RFS according to high (blue), intermediate (red) or low (grey) DCN gene expression data used was from ER+ tamoxifen treated breast cancer patients (n=176).

In contrast to DCN, TXNIP failed to retain a significant relationship with RFS in the smaller GOBO dataset (not illustrated). However, higher DCN and TXNIP expression levels were significantly associated with normal-like and luminal A tumour molecular subtypes across the breast cancer database, subtypes reported to have improved prognosis, while the log2 expression level was found to be lower in luminal B subtype tumours which are reported to be a more aggressive ER+ subtype (Figure 84).
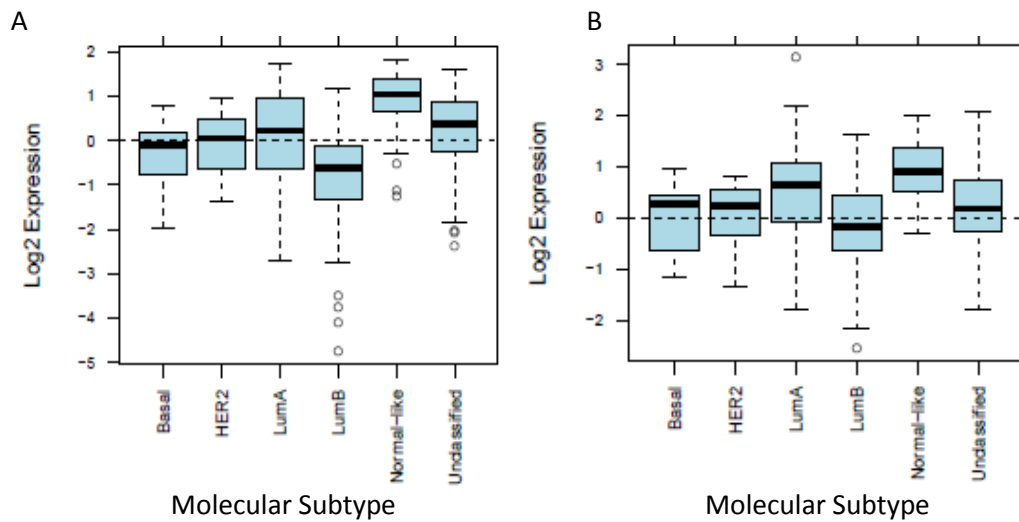
Figure 84: Association between expression of DCN (A) (p=<0.0001) and TXNIP (B) (p=<0.0001) with breast cancer molecular subtype.

A significant association was also revealed between elevated expression of DCN and TXNIP and lower histological grade of tumours in ER+ tamoxifen treated patients (Figure 85).
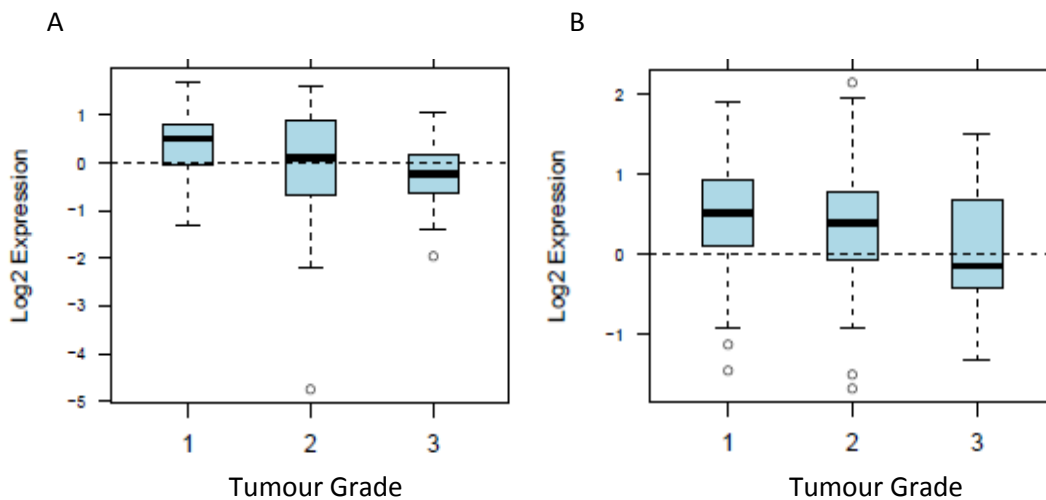
Figure 85: Association between expression of DCN (A) (P=0.01) and TXNIP (B) (P=0.04) and grade in tumours from ER+ breast cancer patients who received tamoxifen treatment

Finally, DCN and TXNIP were analysed using KMPlotter in a large cohort of untreated ER+ breast cancer patients versus RFS, where in both instances their increased expression significantly associated with improved patient outcome (Figure 86).
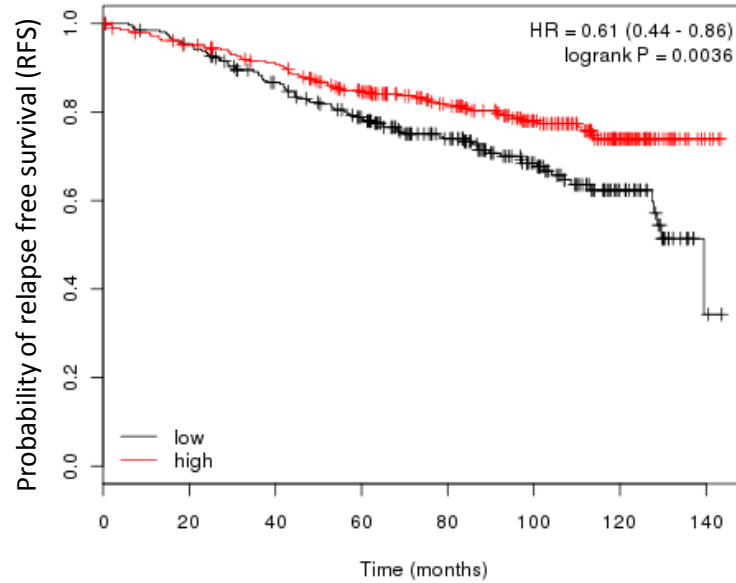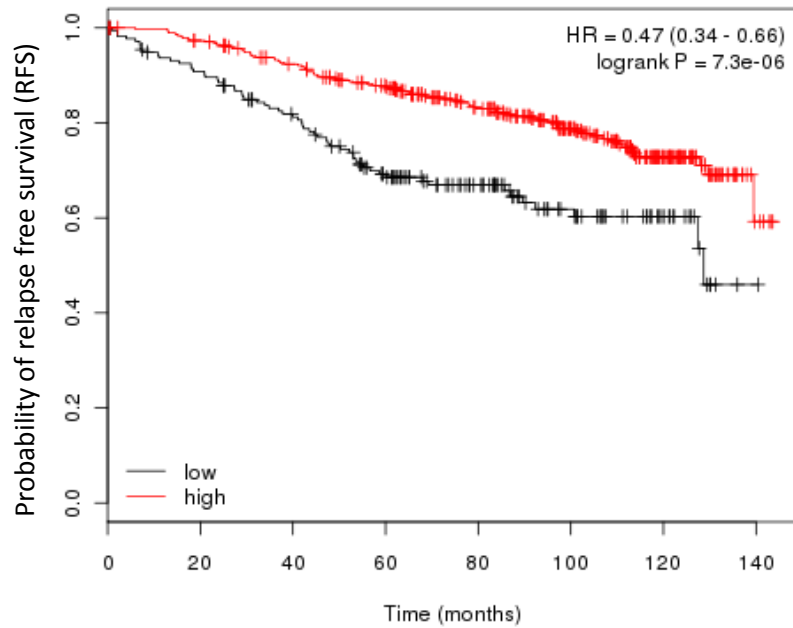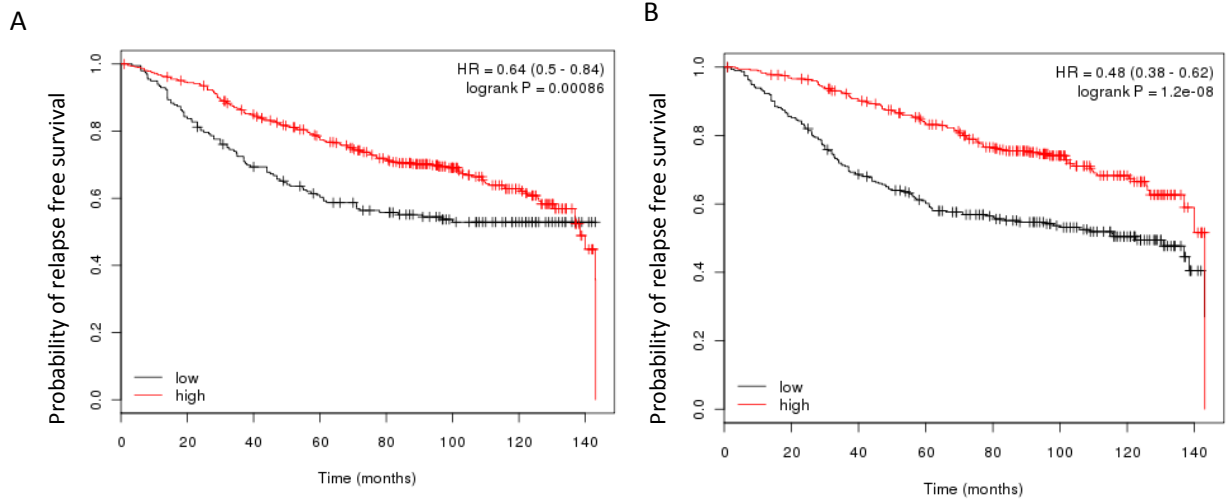
Figure 86: Kaplan Meier survival curves generated by KMPlotter displaying the association between (A) DCN (B) TXNIP gene expression and relapse free survival (RFS) In ER+ systemically untreated patients. The survival curves were generated using the jetset affymetrix gene probes for DCN and TXNIP grouping patients by best fit (as calculated by KMPlotter) (n=785).

6.2.6 PCR verification of genes hypothesised to be involved in the complete response mechanism exerted by Faslodex in the T47D cell line

Considering the various results of the profile interrogation in the 4 models and in the faslodex resistant MCF7 cells, ontological examination, and clinical examination using KMPlotter, the most promising genes (all Faslodex induced in T47D cells on the arrays), DCN, TXNIP, TGFB2 and CASP1, were taken forward for PCR verification.

6.2.6.1 DCN

PCR confirmed that DCN was significantly up-regulated only in the T47D cell line on exposure to Faslodex, with minimal expression observed in the remaining three cell models pre and post Faslodex treatment (Figure 87). As such the expression profile mirrored the log2 intensity plot generated from the microarray data (Figure 60).

Gene Acronym	Fold change of expression following Faslodex treatment			
	BT474	MDA-MB-361	MCF-7	T47D
DCN	1.01	1.17	1.1	4.8
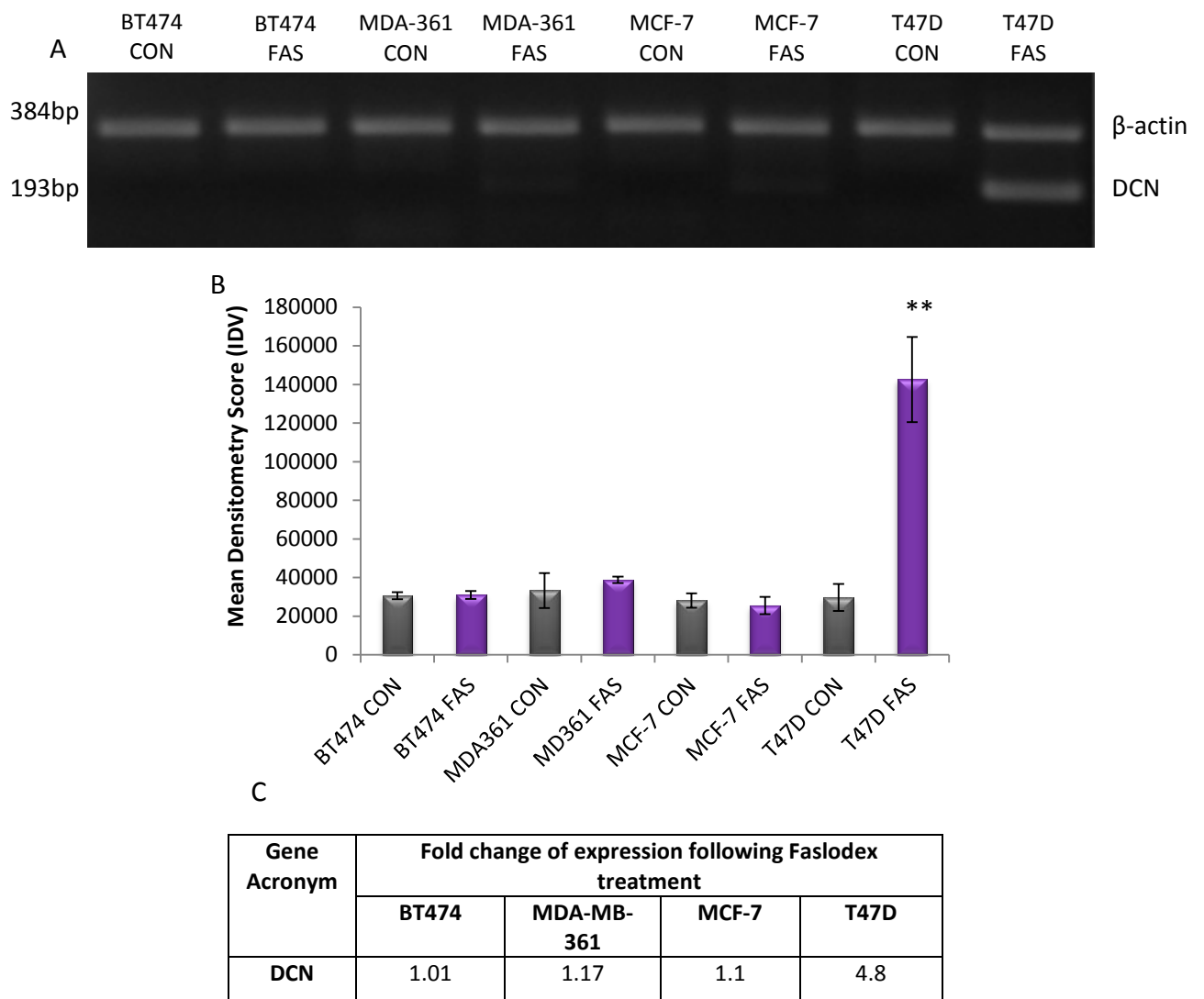
Figure 87: Representative PCR image (A) with the corresponding densitometry graph (B), semi-quantitatively representing the data (CON-Control; FAS-Faslodex). The results are expressed as means ± SEM of three separate experiments. **$P < 0.01$ versus control (C) Table displaying the fold change of gene expression following Faslodex treatment; highlighted in red are Faslodex induced changes

6.2.6.2 TXNIP

As seen in Figure 88, the basal expression of TXNIP was elevated in the MDA-MB-361 and MCF-7 cell lines compared to the T47D cell line (Figure 88). Following 10 day Faslodex treatment, the expression of TXNIP was significantly induced in both the BT474 and T47D cell lines. This PCR profile mirrored the TXNIP log2 intensity plot generated from the microarray data for T47D cells, but was discordant for the BT474 cell line (Figure 59).
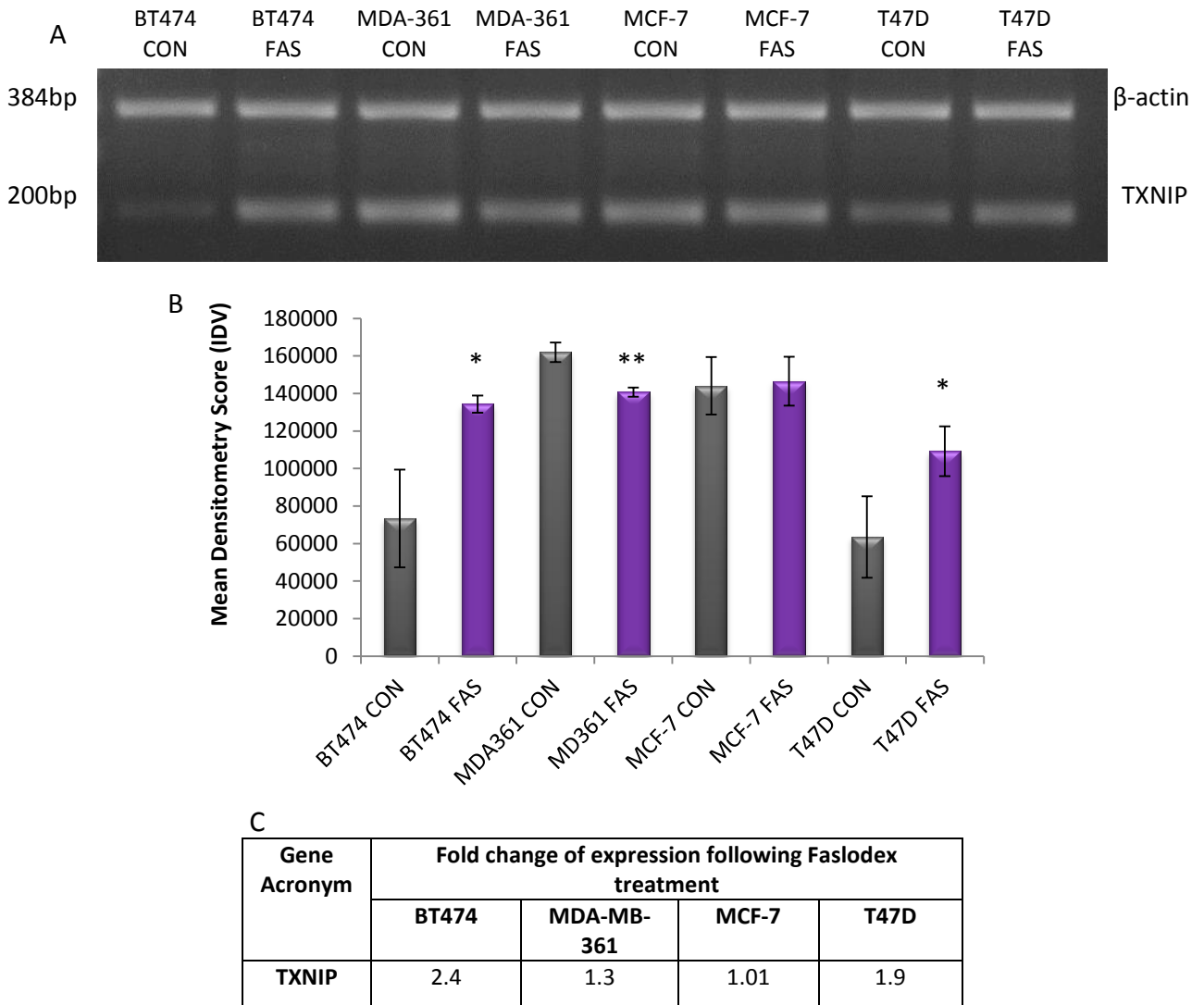
Figure 88: Representative PCR image (A) with the corresponding densitometry graph (B), quantitatively representing the data (CON-Control; FAS-Faslodex). The results are expressed as means ± SEM of three separate experiments. *$P < 0.05$ versus control, **$P < 0.01$ versus control (C) Table displaying the fold change of gene expression following Faslodex treatment

6.2.6.3 TGFB2

Basal expression of TGFB2 was very low in the HER2+ cell lines versus the HER2-cells (Figure 89). Faslodex treatment led to a substantial increase in TGFB2 expression in the T47D cells that was not seen in the HER2+ and MCF-7 cells. This profile mirrored the TGFB2 log2 intensity plot generated from the microarray data (Figure 62).

Gene Acronym	Fold change of expression following Faslodex treatment			
	BT474	MDA-MB-361	MCF-7	T47D
TGFB2	1.01	1.15	1.4	2.3
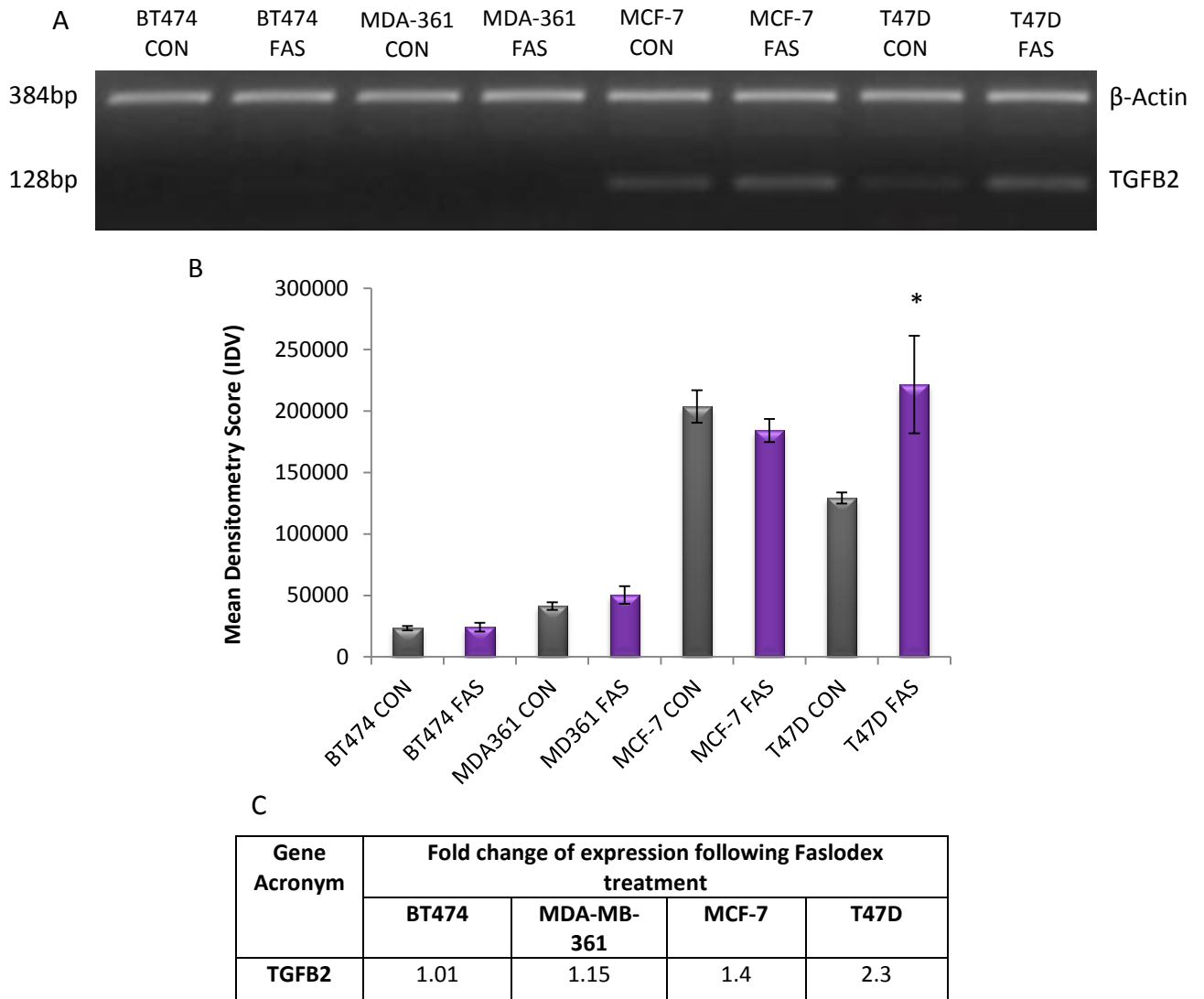
Figure 89: Representative PCR image (A) with the corresponding densitometry graph (B), quantitatively representing the data (CON-Control; FAS-Faslodex). The results are expressed as means ± SEM of three separate experiments. *$P < 0.05$ versus control (C) Table displaying the fold change of gene expression following Faslodex treatment.

6.2.6.4 CASP1

CASP1 was significantly up-regulated by Faslodex in both HER2- cell lines (Figure 90) although the induction was greatest in the T47D cell line. These data largely mirrored the CASP1 log2 intensity plots for the microarrays (Figure 61).

Gene Acronym	Fold change of expression following Faslodex treatment			
	BT474	MDA-MB-361	MCF-7	T47D
CASP1	1.1	1.1	1.8	2.3
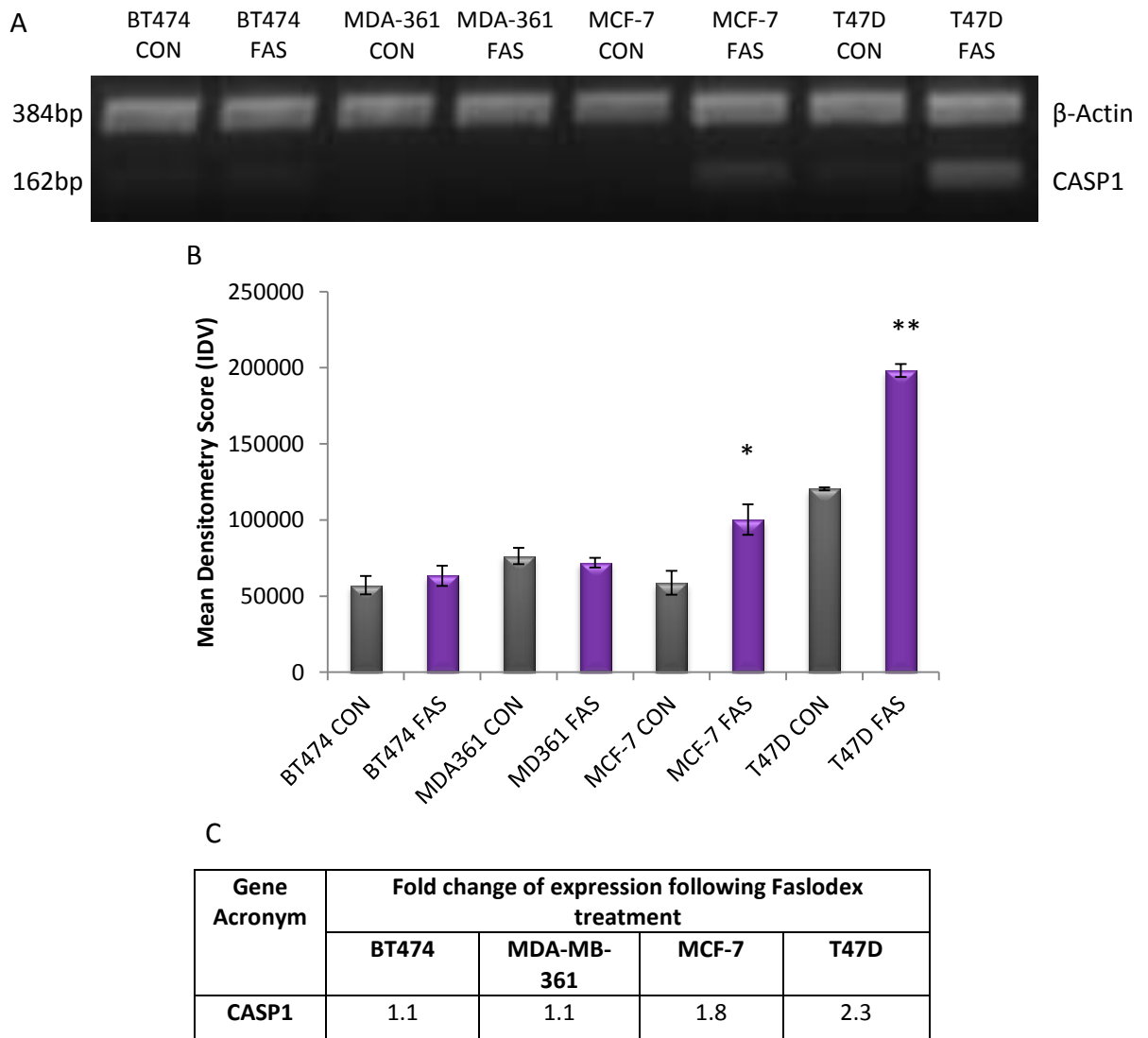
Figure 90: Representative PCR image (A) with the corresponding densitometry graph (B), quantitatively representing the data (CON-Control; FAS-Faslodex). The results are expressed as means ± SEM of three separate experiments. *$P < 0.05$ versus control, **$P < 0.01$ versus control (C) Table displaying the fold change of gene expression following Faslodex treatment

PCR verification thus confirmed Faslodex-promoted induction of all 4 genes in T47D cells. While DCN and TGFB2 were induced in the T47D cell line only, TXNIP and CASP1 were found to also be significantly induced in one of the other ER+ cell lines

following treatment. Table 29 compares the results of the microarray data with the results from the PCR validation.

Table 29: Comparison of Faslodex-deregulation of genes of interest from the microarray data and PCR results (I-Induced; S-Suppressed; ~ limited/no change)

Gene Name	Microarray (FAS de-regulation)				PCR (FAS de-regulation)			
	BT474	MDA-361	MCF-7	T47D	BT474	MDA-361	MCF-7	T47D
DCN	~	~	~	I	~	~	~	I
TXNIP	~	~	~	I	I	S	~	I
TGFB2	~	~	~	I	~	~	~	I
CASP1	~	~	~	I	~	~	I	I

6.3 Discussion

In the current study, the T47D cell line was found through continuous culture studies to be a model of Faslodex complete response. HCA diagrams of genes de-regulated by Faslodex in the 4 ER+ cell lines also revealed that the T47D cell line failed to cluster with its ER+/HER2- counterpart the MCF-7 cell line (or with the ER+ HER2+ lines) suggestive of unique gene changes that may impact on intracellular signalling pathways to ultimately prevent emergence of resistant growth in the presence of Faslodex. By carrying out a filtering process using the microarray data generated from the 4 ER+ cell lines treated for 10 days with Faslodex, particular genes were identified that were uniquely de-regulated by this antihormone in the T47D cell line and thus possibly contributory towards its eventual complete response. 11 genes were initially identified on the microarrays as being de-regulated by Faslodex by at least 1.5 fold in the T47D cell line only and the changes in these genes were hypothesised to include induction of tumour suppressive elements and down-regulation of growth-promoting genes. A further filtering procedure was then undertaken to identify genes with the strongest profiles, logical ontology in relation to the superior Faslodex response in T47D cells, and in some instances association with available clinical endocrine outcome using publically-available tamoxifen treated breast cancer datasets before PCR verification. 4 genes were thus identified as possible contributors towards the Faslodex-promoted T47D

complete response; DCN, TGFB2, TXNIP and CASP1.

Currently, the only biological indicators of Faslodex impact in the clinic are the down-regulation of ER, ER-regulated genes such as PgR, and Ki67 and thus these are the key endpoints measured in antihormone clinical trials (Kuter *et al.*, 2012; Robertson *et al.*, 2013). The suppression of ER and PgR is indicative of the Faslodex mechanism of action targeting ER. Ki67 is a marker of proliferation, and its superior inhibition has been demonstrated in neoadjuvant studies with 500mg Faslodex (Kuter *et al.*, 2012) that also improved patient clinical response in the CONFIRM study (Di Leo *et al.*, 2010). Research by the Dowsett laboratory has further shown that measurement of Ki67 following short-term endocrine treatment is predictive of RFS versus pre-treatment levels (Dowsett *et al.*, 2007). However, the suppression of these factors reveals very little information regarding the key signalling elements determining anti-tumour responses, and it is important these are determined if the value of Faslodex is to be maximised in the clinic. Faslodex led to complete cell loss in the T47D model preventing development of resistance; this is of much interest not only because such an effect is desirable clinically, but also because it is widely known that anti-oestrogens, in general, fail to induce substantial cell death (Wilson *et al.*, 1995). Their actions predominantly exert growth inhibition with only modest cell kill so that cells persist to support acquired resistance (Wilson *et al.*, 1995). As such, mechanistic deciphering of how Faslodex induces such a superior effect in T47D cells could potentially be informative in developing treatments to improve Faslodex impact in the clinic and could provide Faslodex-deregulated biomarkers to help identify early an ER+ patient cohort who would subsequently gain substantial benefit from Faslodex therapy. In this regard, successful identification, filtering and prioritisation of genes uniquely deregulated in T47D cells through the project has considerable potential to yield potentially-interesting elements.

Of the 11 genes initially identified as Faslodex deregulated, 5 were induced by the antihormone and 6 suppressed (Table 18). The log2 intensity plots for each of the genes were analysed using the jetset probes, as well as ensuring the multiple probes (Table 18) for each gene also showed the same change in expression and analysing the detection calls to determine if the change in expression was robust

and reliable. Following this stringent analysis ADAM12 and SEPT6 were dismissed from the investigation.

Ontological investigations of the remaining 9 genes confirmed tumour suppressive functions for DCN, TGFB2, TXNIP and CASP1, (Tables 20-23) which were all induced by 10 day Faslodex treatment in the T47D cell line. In contrast, PTGER3, SKAP2 and IL6ST had all been previously associated with disease progression (Tables 24-25) and thus their suppression in the T47D cell line by Faslodex may also contribute to the anti-tumour response observed. ID4 and DUSP4 were dismissed from the investigation following ontological investigation as although both genes were reported to be tumour suppressor genes (Tables 27 and 28), they were depleted in the T47D cell line by Faslodex and are thus unlikely to contribute to the complete growth inhibitory response. It is interesting that although the T47D cell line exhibits sensitivity to Faslodex not achieved in the further ER+ breast cancer cell lines with respect to this cell line exhibiting a complete response to long-term Faslodex treatment while the remaining 3 line eventually acquired resistance, this antihormone can also suppress certain tumour suppressor genes, an event which may feasibly act to delay the onset of complete-response. The remaining 7 genes were subsequently analysed using online tools to determine if their intrinsic expression in ER+ breast cancers was associated with RFS following tamoxifen treatment. While clinical associations were counterintuitive for PTGER3, IL6ST and SKAP2 (Figures 80-82), increased inherent expression of DCN and TXNIP associated with an improved RFS (Figures 78 and 79) in keeping with the concept that their induction by Faslodex in T47D cells may serve to promote superior response and subvert development of resistance. DCN and TXNIP were also associated with normal/luminal A molecular phenotype and reduced tumour grade in ER+ disease (Figures 84 and 85), again in keeping with higher levels of these genes relating to improved prognosis. Although CASP1 and TGFB2 failed to demonstrate a significant association with RFS, their ontology and lack of (or decreased) expression in the acquired Faslodex resistant MCF-7 cells warranted their further pursuit alongside DCN and TXNIP where PCR verification confirmed induction of all 4 genes by 10 day Faslodex treatment in the T47D model (Figures 87-90).

It is feasible that Faslodex induction of CASP1, a member of the caspase family could potentially be involved in the anti-tumour response in T47D cells by aiding cells to commit to cell death following such antihormone treatment. Importantly, a similar mechanism has already been demonstrated with respect to caspase 1 involvement in any tamoxifen-induced cell death (Bowie *et al.*, 2004). In this latter study, CASP1 gene expression was found to be suppressed by E2 and thus tamoxifen treatment increased CASP1 expression and promoted apoptosis. However, it must be noted here that in the study by Bowie *et al* a high tamoxifen concentration was used of 1μM to in order to induce cell death. In the cell models used in the present study, CASP1 was induced by Faslodex in the T47D cell line, with more modest up-regulation in the MCF-7 model (Figure 90) and loss of expression in Faslodex resistant MCF-7 model (Figure 73). It is possible that this up-regulation of CASP1 in the MCF-7 cell line during treatment contributes to the superior initial response observed in this cell line, while the larger induction in T47D cells ultimately contributes towards its better inhibitory effects (perhaps further increasing with more extended Faslodex exposure) and subverting resistance. While it remains unknown how caspase 1 increases in the T47D line to promote cell loss, it is possible that this may involve EGFR signalling in such cells. EGF is known to have the ability to aid cell survival and inhibit apoptosis in some cell types while inducing apoptosis in others (Armstrong *et al.,* 1994; Brabyn *et al.*, 1995). The latter is thought to be mediated by the activation of the STAT proteins by EGFR (Chin *et al.*, 1996), which can trigger apoptosis via activation of caspase 1 (Chin *et al.*, 1997). It is possible that Faslodex treatment may result in the changes in EGFR signalling (which can be oestrogen-repressed and antihormone-induced; Yarden *et al.*, 2001; McClelland *et al.*, 2001; Gee *et al.*, 2003) which in turn regulates CASP1 in the T47D cells to promote cell death. Further regulatory factors for CASP1 activity may comprise TGFB signalling (Guo *et al.*, 1999), and also the tumour suppressor IRF1 which interestingly has been reported to restore responsiveness to Faslodex resistant MCF7 cells (Ning *et al.*, 2010).

There is also rationale for the further 3 Faslodex-induced genes to be involved in the enhanced Faslodex response in T47D cells. TXNIP has been reported to be a

pro-apoptotic protein in cancer cells (Chen *et al.,* 2008) and thus the subsequent complete-response observed in Faslodex-treated T47D cells may in some way be due to the induction of this protein. Further support for a function of TXNIP in the T47D complete response mechanism is its association with superior RFS and lower grade disease in ER+ patients who underwent tamoxifen-treatment (Figures 79, 84B, 85B). In keeping with this, data from Cadenas *et al.,* have shown that increased TXNIP expression is associated with an improved prognosis in breast cancer patients (Cadenas *et al.,* 2010). TXNIP function may exert a complete response via its inhibitory action on thioredoxin. Anti-hormone treatment can lead to a pro-oxidant state within cancer cells which is associated with increased levels of oxidised thioredoxin. This form of thioredoxin has been hypothesised to be involved in the onset of drug-resistance (Penney *et al.*, 2013), thus the inhibition of thioredoxin by TXNIP could act to prevent a key survival signalling pathway. Although TXNIP was PCR verified as being induced in the T47D cell line by Faslodex, a significant induction was also observed in the BT474 cell line which was able to develop resistance (Figure 88). Further studies would be required to clarify this induction given the PCR discordance with the array data for BT474. However, it is possible that while induction of TXNIP promotes growth inhibition in the T47D cell line, such an effect is ultimately overridden in the BT474 cell line either by Faslodex induction of survival factors in this model or by its amplified HER2. Interestingly, Cadenas *et al.,* has reported that transfection of the MCF-7 cell line with HER2 can lead to a downregulation of TXNIP (Cadenas *et al.*, 2010).

TGFB2, which was another gene induced only in the T47D cell line by Faslodex, has been previously associated with tamoxifen response, where the extent of induction of this protein by this antioestrogen has been shown to positively correlate with response (MacCallum *et al.*, 1996). The data presented in the current study suggest TGFB2 induction by Faslodex in T47D cells could similarly equate with superior response to this further antihormone. PCR verification confirmed the significant induction of TGFB2 only in the T47D cell line by Faslodex, with inherent high levels observed in the MCF-7 cell line that were unchanged by treatment (Figure 89). This suggests that the significant degree of induction of TGFB2 could be an important

contributor to the complete response in the T47D cell line, while the inherently high levels in the MCF-7 cell line pre and post treatment may feasibly contribute to the substantial magnitude of initial response and its extended duration following long-term antihormone treatment (with evidence from the Faslodex resistant MCF-7 cell line for TGFB2 decrease once resistance is established, Figure 74).

The published findings with regards to DCN ontology (Table 20) and the successful PCR verification of its induction by Faslodex only in the T47D cell line (Figure 87) as well as its absence of expression in the MCF-7 Faslodex resistant (Figure 72) line fully support a role for decorin in the Faslodex complete response mechanism in T47D cells, and it is encouraging that it is also being explored as a potential anti-cancer therapy (Tralhao *et al.*, 2003). The survival curves in Figures 78 and 83 also highlight that any inherent increased expression of DCN in ER+ patients is associated with an improved RFS in patients who received tamoxifen therapy while Figures 84A and 85A show expression of DCN is elevated in molecular tumour subtypes with improved prognosis and also in ER+ patients with lower grade disease. Studies with more patients would allow multivariate analysis to determine the impact of molecular subtype/grade etc revealing the magnitude of decorin prognostic impact. However, the findings in total are supportive of the concept that decorin may have growth suppressive functions in breast cancer and could be integral in preventing emergence of Faslodex resistance in the complete responding T47D cells. Previous research into the signalling mechanisms underlying the onset and development of antihormonal resistance, primarily employing MCF-7-derived resistant cells, has invariably revealed the potential importance of the erbB family of growth factor receptor proteins (Gee *et al.*, 2003; Knowlden *et al.,* 2003). Interestingly, Santra *et al.,* (2000) have shown that decorin not only binds to EGFR instigating a number of events that ultimately lead to growth suppression but that the proteoglycan can also reduce total HER2 levels as well as nearly abolishing levels of tyrosyl phosphorylation of HER2, erbB3 and erbB4. Decorin is thus essentially an endogenous pan-erbB inhibitor, where its ability to decrease levels of erbB2 reduces potent oncogenic intracellular signalling (as all erbB receptors preferentially heterodimerise with HER2) leading to an induction of the cyclin-

dependent kinase inhibitor p21 and subsequent growth inhibition (Santra *et al.*, 2000). Any basal or antihormone-up-regulated erbB signalling would thus be inhibited following up-regulation of DCN by Faslodex in the T47D cell line. Moreover, it has also been reported that decorin can inhibit a number of further RTKs including IGF1R (Iozzo *et al.*, 2011), MET (Goldoni *et al.*, 2009) and PDGFRα (Baghy *et al.*, 2013), all of which have been associated with proliferation, cell survival and breast cancer progression. Decorin has also been reported to bind to key growth factors ligands of RTK's (Border *et al.*, 1992; Hildebrand *et al.*, 1994). This interaction between decorin and growth factors in the ECM has been reported to result in formation of a growth factor reservoir where any degradation/cleavage of DCN results in an increase in growth factor bioavailability (Imai *et al.*, 1997). An increase in the expression of DCN produced by the T47D cell line during Faslodex treatment may thus also feasibly prevent the action/availability of a number of growth factors (either secreted by the cells or present in the serum added to the culture medium), further limiting the activation of any potentially-compensatory signalling pathways and consequently leading to an enhanced growth inhibition and eventual cell kill. Since the potential mechanisms of decorin-induced growth inhibition/tumour suppressive functions are varied and may span multiple growth factor receptor pathways, its ontology is particularly compelling when considering a potential contribution to growth inhibition promoted by Faslodex.

Based on the above, the project has successfully obtained evidence to implicate Faslodex-induction of DCN, TXNIP, TGFB2 and CASP1 as potential contributors in the complete response mechanism seen in T47D cells following such antihormone treatment. However, it remains important to try to address in clinical breast cancers whether Faslodex similarly alters expression of these genes and if these changes are paralleled by growth inhibitory effects. Moreover, induction at the mRNA was examined after 10 day treatment, while the complete-response in T47D was not observed until 8.5 weeks of Faslodex treatment and so it is possible that further alterations in one or more of these elements may occur over time and be necessary for the complete response, requiring longer-term profiling. Ultimately, therefore further work must be carried out in this project in order to further

understand their involvement in the Faslodex response mechanism in order to clarify any potential either to provide new treatment approaches or as predictive biomarkers to maximise Faslodex response in breast cancer.

Chapter 7

Identification of Faslodex-de-regulated genes potentially involved in the extended Faslodex response observed in both the MCF-7 and T47D HER2- cell lines.

7.1 Introduction

As previously discussed ER tumour positivity is a key biomarker in selecting systemic endocrine therapy for patients with both early and metastatic disease and its presence predicts response to anti-hormone therapy (Goldhirsch *et al.*, 2006; Buzdar, 2001). The majority of ER+ tumours, approximately 86%, are HER2- (Osborne *et al.*, 2011) and in comparison to HER2+ tumours are associated with an improved response to endocrine therapy (reviewed by De Laurentiis *et al.*, 2005). However, despite an improved response to endocrine therapies a significant number of ER+/HER2- breast cancer patients' acquire resistance to antihormones. Preclinical research has been carried out in an attempt to identify modulators of resistance in this disease setting due to the lack of appropriate treatments for this patient cohort following relapse after initial responses. There are many reports investigating the mechanisms of resistance to anti-hormone treatments (particularly for tamoxifen and oestrogen deprivation and primarily using acquired resistant MCF-7-derived cells) and consequently developing inhibitors to such signalling pathways in order to examine if these counteract the emergence of resistance or regain sensitivity to anti-hormone treatments (Moulder *et al.*, 2001; Leary *et al.*, 2010; DeGraffenried *et al.*, 2004). However, even though promising *in vitro* data has been obtained, the impact of such approaches (e.g. erbB blockade) has been extremely limited in the clinic in ER+/HER2- disease (reviewed Johnston *et al.*, 2008). Interestingly, very little work has been carried out investigating the underlying mechanisms promoting Faslodex response. It is feasible that modulating

the signalling pathways potentially involved in this response could provide an alternative means whereby the timeframe of anti-hormone-induced growth inhibition could be further extended and subsequently delay the emergence of antihormone resistance. Moreover, determination of such elements could provide future biomarkers for patients most likely to benefit from Faslodex treatment.

The degree of down-regulation of ER and ER-regulated genes in the 4 cell lines in this project failed to predict the duration of response to Faslodex. Thus, following short-term 7 day Faslodex treatment the same degree of ER protein down-regulation was observed in all 4 cell lines (Chapter 3), as was the expression of PGR and GREB1 (ER-regulated genes, Chapter 4), and furthermore all of the cell lines showed initial growth inhibition the magnitude of which did not obviously relate to subsequent long-term outcome. Taken together, these data suggest that unknown factors are contributing to extended response in the ER+/HER2- cell lines and these are likely to be promoted during Faslodex treatment. In this regard, there was a unique opportunity to identify Faslodex de-regulated genes in both the T47D and MCF-7 cells that may potentially underlie the superior responses in HER2- breast cancer cells by examining their microarray expression profiles. It is hypothesised that potential genes of interest de-regulated by Faslodex in the T47D and MCF-7 cell line will primarily be anti-apoptotic or anti-proliferative. To further increase the likelihood of such genes being involved in improved response, expression profiles were also analysed in the HER2+ cell lines to ensure expression changes induced by Faslodex were not shared by these models. An examination of the literature indicates that there are no other published reports that have used multiple cell models to identify genes deregulated following early endocrine therapy that may subsequently contribute towards long-term treatment effect.

7.2 Results

7.2.1 Identification of genes de-regulated by Faslodex in the MCF-7 and T47D cell lines

Genes that displayed a significant change in gene expression (t-test <0.05; SAM FDR <0.05) following 10 day Faslodex treatment in both the HER2- cell lines of at least

1.5 fold were identified. 16 genes were detected which are listed in Table 29, along with the associated direction of change in expression (10 induced, 6 suppressed by Faslodex), the number of gene probes for each gene, and how many of these probes displayed the expected change in expression.

As you can see from Figure 90, of the 10517 gene probes that were found to be deregulated by Faslodex in one or more of the cell lines, only 44 were significantly altered in the ER+/HER2- cell lines and further only 16 were identified to exhibit at least 1.5 fold change in both models.
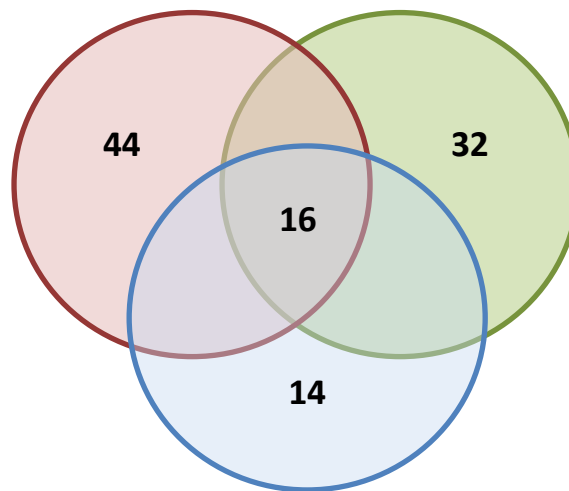
Figure 90: The Venn diagram illustrates the identification of the 16 genes taken forward as potential mediators/biomarkers of Faslodex improved response observed in the MCF-7 and T47D cell lines. The red circle represents all those genes significantly altered in the MCF-7 and T47D cell lines. The green circle, shows the number of these genes that were not altered by at least 1.5 fold in these two models and the blue circle are those that were found to be also altered to some extent in the BT474 and MDA-MB-361 cell lines. The 16 genes represented by the overlapping circles identify those genes that met the criteria to be taken forward for further investigation.

Table 29: List of genes whose expression was significantly altered in both HER2- cell lines (MCF-7 and T47D) following 10 day Faslodex treatment and the associated change in expression (induced or suppressed). Also listed is the number of gene probes representing a given gene on the UI33Aplus2 genechip and the number of probes also exhibiting the same change in expression in each HER2- cell line.

Potential response genes (genes shared by both MCF-7 & T47D)	Gene Name	Gene expression change following Faslodex treatment	Total n.o. gene probes	Total number of probes exhibiting expected change in expression	
				MCF-7	T47D
PTPRJ	Protein tyrosine phosphatase, receptor type, J	Induced	1	1	1
ITIH1	Inter-alpha-trypsin inhibitor heavy chain 1	Induced	1	1	1
KRT4	Keratin 4	Induced	1	1	1
VGLL1	Vestigial like 1	Induced	2	2	2
UPK3B	Uroplakin 3B	Induced	1	1	1
ANK1	Ankyrin 1	Induced	6	4	4
ALOX5	Arachidonate 5-lipoxygenase	Induced	3	3	3
PCDH7	Protocadherin 7	Induced	4	4	3
NR2F1	Nuclear receptor subfamily 2, group F, member 1	Induced	1	1	1
SH3TC2	SH3 domain and tetratricopeptide repeats 2	Induced	1	1	1
ARTN	Artemin	Suppressed	3	3	3
MYRIP	Myosin VIIA and Rab interacting protein	Suppressed	1	1	1
NPY5R	Neuropeptide Y receptor Y5	Suppressed	1	1	1
PYY	Peptide YY	Suppressed	2	2	2
SULF1	Sulfatase 1	Suppressed	3	3	3
ELOVL2	ELOVL fatty acid elongase 2	Suppressed	2	2	2

From Table 29 it can be seen that the majority of probes for each gene displayed the same directional change in expression following Faslodex treatment.

Low jetset scores (Table 30) were subsequently recorded for PTPRJ, SH3TC2 and PCDH7, suggesting that the changes in gene expression following Faslodex treatment may be unreliable. PCDH7, however, was also represented by a further 3 gene probes on the Affymetrix genechip and the majority of these probes exhibited a Faslodex-induction in both cell lines, increasing confidence that PCDH7 was reliably induced in HER2- cells.

Table 30: Genes identified as being Faslodex de-regulated in both HER2- cell lines and their associated jetset Affymetrix gene probe ID and jetset score (the closer to 1 the better the predicted performance).

HER2- shared genes	Jetset Affy Probe ID	Jetset Score
PTPRJ	210173_at	0.00085872
ITIH1	210888_s_at	0.34793661
KRT4	213240_s_at	0.73693584
VGLL1	215729_s_at	0.53307751
UPK3B	206658_at	0.50480997
ANK1	205390_s_at	0.50851937
ALOX5	204446_s_at	0.79570734
PCDH7	205534_at	0.10924584
NR2F1	209506_s_at	0.45285561
SH3TC2	219710_at	5.87E-17
ARTN	210237_at	0.24336664
MYRIP	214156_at	0.59824101
NPY5R	207400_at	0.32761039
PYY	207080_s_at	0.26026271
SULF1	212353_at	0.51716857
ELOVL2	213712_at	0.64165584
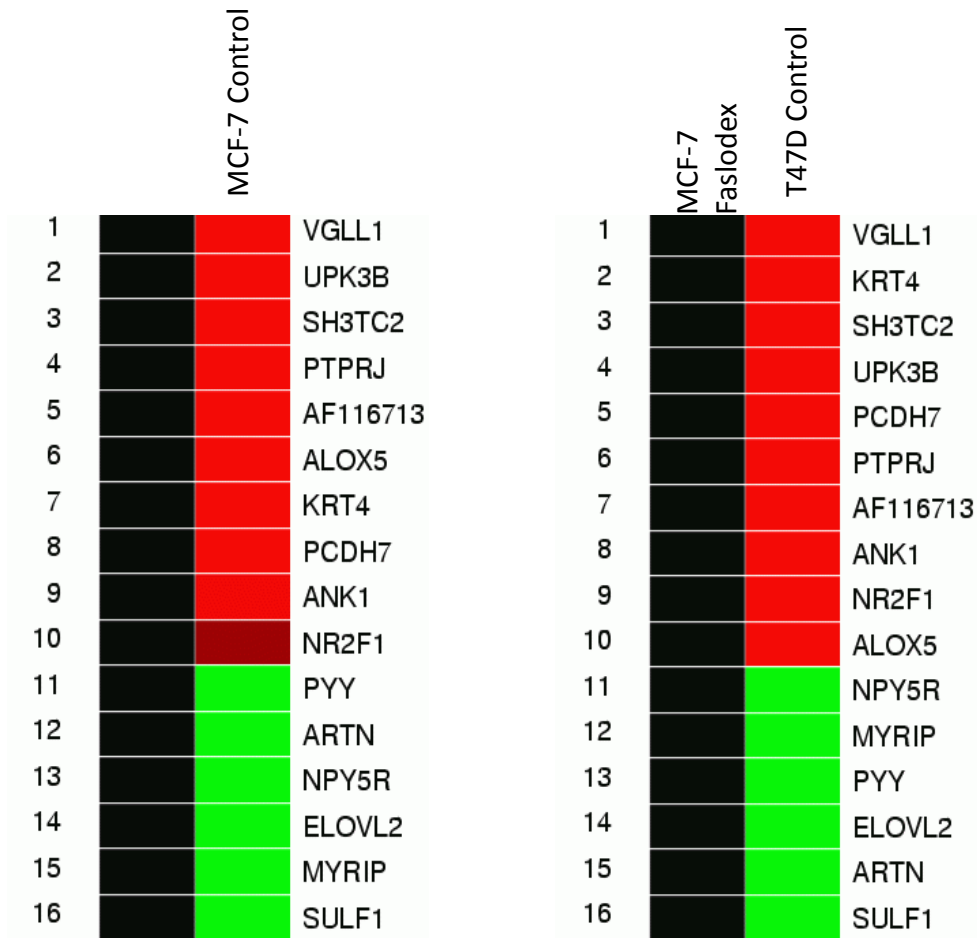
Figure 91: Heatmaps generated by GeneSifter displaying the induction or suppression of genes altered by 10 day Faslodex treatment in both HER2- cell lines using jetset gene probes.

7.2.1.1 Genes induced by Faslodex in MCF-7 and T47D (ER+/HER2-) cells:

7.2.1.1.1 PTPRJ

The log2 intensity plot for PTPRJ (Figure 92) showed the gene was highly up-regulated by Faslodex treatment in the HER2- cell lines, showing a >5 fold change in both of the models. In contrast, the HER2+ cell lines demonstrated either no effect of Faslodex or a modest decrease in PTPRJ. All log2 intensity values were below 0 basally, and it was noted that even following Faslodex induction in the HER2- lines log2 intensity values failed to be above 0 and detection calls for all samples were also absent indicative of probable lack of expression.

A

B

Gene Acronym	Fold change of expression following Faslodex treatment			
	BT474	**MDA-MB-361**	**MCF-7**	**T47D**
PTPRJ	1.96	1.25	5.80	5.92

Figure 92: (A) Log2 intensity plot displaying the normalised (mean of triplicate samples) gene expression of PTPRJ in each of the 4 cell lines pre (Con) and post 10 day Faslodex (FAS) treatment using the jetset probe for PTPRJ and (B) table displaying the fold change in gene expression promoted by 10 day Faslodex treatment in each cell line vs. control expression

(highlighted in red are those displaying a >1.5 fold induction in expression and in green a >1.5 fold suppression).

7.2.1.1.2 ITIH1

As seen in Figure 93, the basal log2 intensity of ITIH1 showed no obvious pattern across the 4 cell lines (Figure 93). Although Faslodex increases in expression were observed in both MCF-7 and T47D cells in line with the heatmap displayed in Figure 1, a more modest increase in expression was also noted in MDA-MB-361 cells following Faslodex treatment. All log2 values across the 4 cell lines, with the exception of the T47D cells post-Faslodex treatment where the log2 intensity value approached 0, had absent calls.

Gene Acronym	Fold change of expression following Faslodex treatment			
	BT474	MDA-MB-361	MCF-7	T47D
ITIH1	1.07	1.50	5.26	4.66

Figure 93: (A) Log2 intensity plot displaying the normalised (mean of triplicate samples) gene expression of ITIH1 in each of the 4 cell lines pre (Con) and post 10 day Faslodex (FAS) treatment using the jetset probe for ITIH1 (B) Table displaying the fold change in gene expression promoted by 10 day Faslodex treatment in each cell line vs. control expression (highlighted in red are those displaying a >1.5 fold induction in expression).

7.2.1.1.3 KRT4

The basal log2 intensity of KRT4 appeared (Figure 94) generally similar across the 4 cell lines and this gene was Faslodex induced not only in the HER2- models, but also in MDA-MB-361 cells. Again the majority of log2 values were recorded as below 0 with absent calls, with only the post-Faslodex T47D sample calling present.
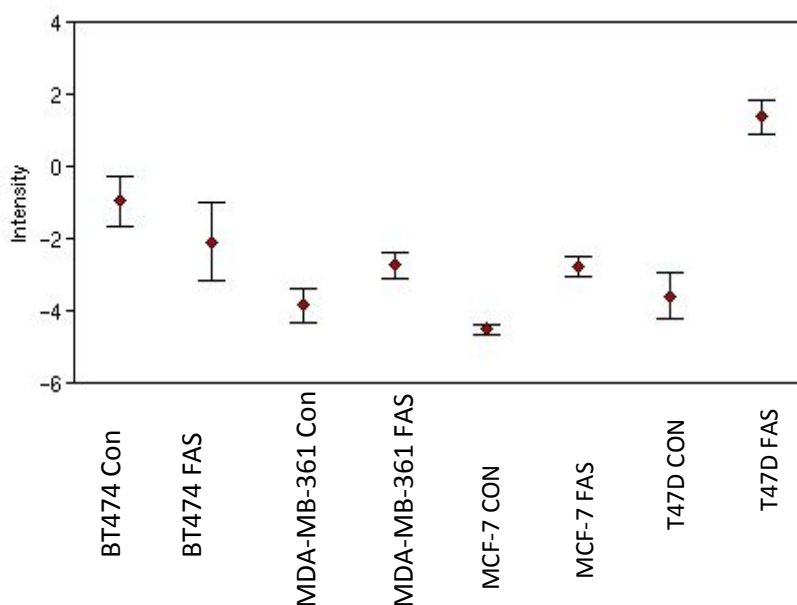
Gene Acronym	Fold change of expression following Faslodex treatment			
	BT474	MDA-MB-361	MCF-7	T47D
KRT4	2.19	2.13	3.39	31.21

Figure 94: (A) Log2 intensity plot displaying the normalised (mean of triplicate samples) gene expression of KRT4 in each of the 4 cell lines pre (Con) and post 10 day Faslodex (FAS) treatment using the jetset score for KRT4 (B) Table displaying the fold change in gene expression promoted by 10 day Faslodex treatment in each cell line vs. control expression (highlighted in red are those displaying a >1.5 fold induction in expression and in green a >1.5 fold suppression).

7.2.1.1.4 VGLL1

Figure 95 shows the low basal log2 intensity of VGLL1 recorded across the 4 cell lines. Although following Faslodex treatment some increase in its expression was evident in MDA-MB-361 cells (>2.5 fold), the level of expression of this gene was very substantially increased in MCF-7 and T47D cells (>100 and >60 fold respectively), with post-treatment values in these models attaining positive log2 scores and present expression calls.

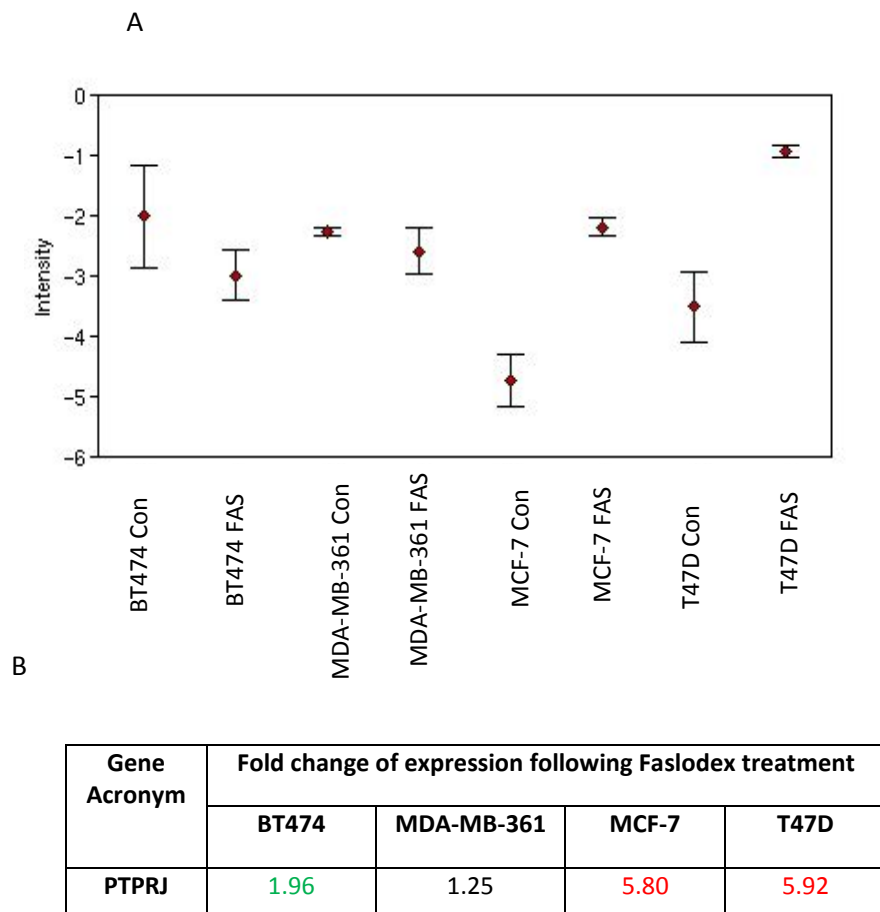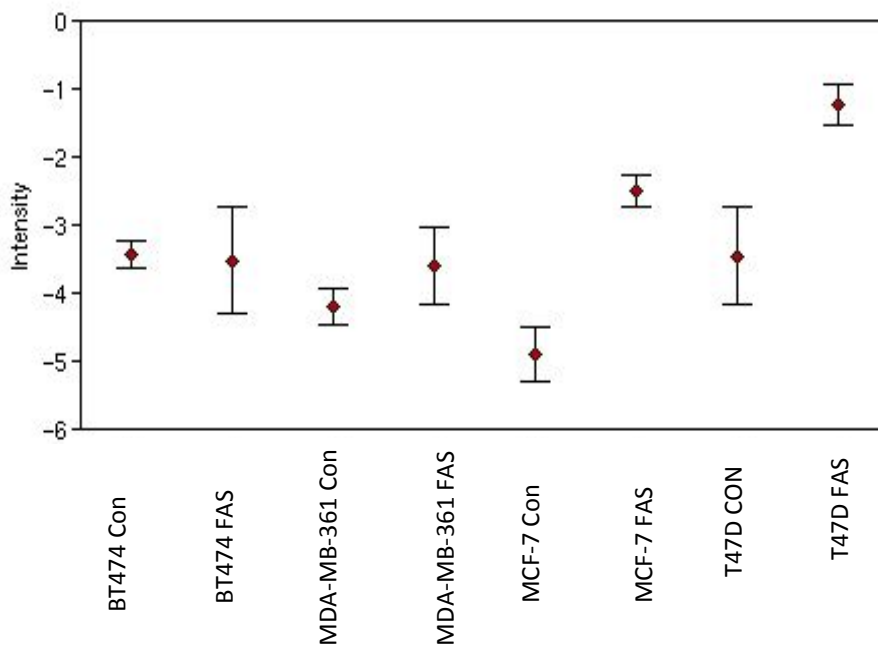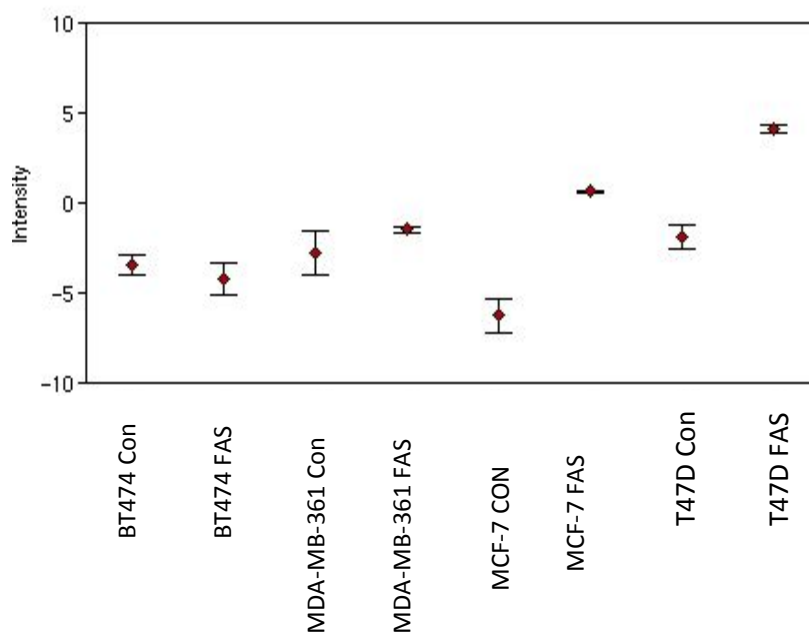| Gene Acronym	Fold change of expression following Faslodex treatment			
	BT474	MDA-MB-361	MCF-7	T47D
VGLL1	1.66	2.57	117.21	64.60

Figure 95: (A) Log2 intensity plot displaying the normalised (mean of triplicate samples) gene expression of VGLL1 in each of the 4 cell lines pre (Con) and post 10 day Faslodex (FAS) treatment using jetset gene probe (B) Table displaying the fold change in gene expression promoted by 10 day Faslodex treatment in each cell line vs. control expression (highlighted in red are those displaying a >1.5 fold induction in expression and in green a >1.5 fold suppression).

7.2.1.1.5 UPK3B

As seen in Figure 96, the HER2+ cell lines expressed a reduced basal level of UPK3B (log2 values below 0 and absent calls) in comparison to the present call in HER2- cell lines. Significantly, however, Faslodex treatment acted predominantly on the MCF-7 and T47D cells causing an up-regulation of UPK3B by >7 and 11 fold respectively.
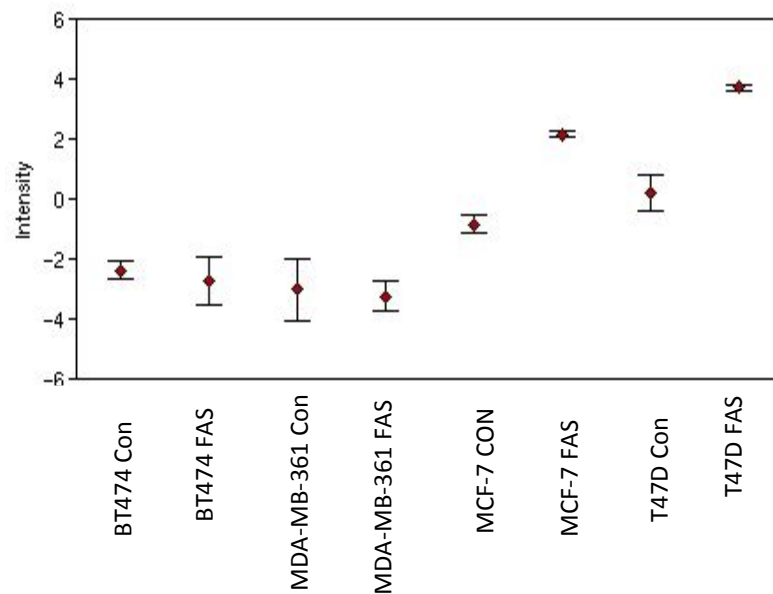
Gene Acronym	Fold change of expression following Faslodex treatment			
	BT474	MDA-MB-361	MCF-7	T47D
UPK3B	1.29	1.17	7.96	11.40

Figure 96: (A) Log2 intensity plot displaying the normalised (mean of triplicate samples) gene expression of UPK3B in each of the 4 cell lines pre (Con) and post 10 day Faslodex (FAS) treatment using jetset gene probe (B) Table displaying the fold change in gene expression promoted by 10 day Faslodex treatment in each cell line vs. control expression (highlighted in red are those displaying a >1.5 fold induction in expression).

7.2.1.1.6 ANK1

The expression of ANK1 across the 4 cell lines was below 0 with absent calls in all experimental arms indicating expression was unlikely, and there was also no obvious Faslodex induction in the T47D cells but an apparent induction in MDAMB361 cells (Figure 97).
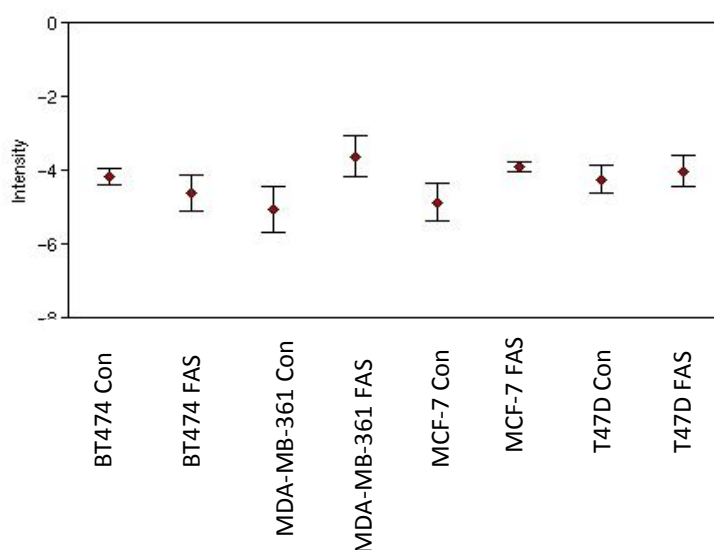
Gene Acronym	Fold change of expression following Faslodex treatment			
	BT474	MDA-MB-361	MCF-7	T47D
ANK1	1.35	2.71	1.94	1.17

Figure 97: (A) Log2 intensity plot displaying the normalised (mean of triplicate samples) gene expression of ANK1 in each of the 4 cell lines pre (Con) and post 10 day Faslodex (FAS) treatment using the jetset gene probe (B) Table displaying the fold change in gene expression promoted by 10 day Faslodex treatment in each cell line vs. control expression (highlighted in red are those displaying a >1.5 fold induction in expression).

7.2.1.1.7 ALOX5

Some apparent increases in ALOX5 were recorded in all the Faslodex treated HER2-models and HER2+ models. However, the log2 intensity values were, in all instances, low (Figure 98) with absent calls indicating expression was unlikely.
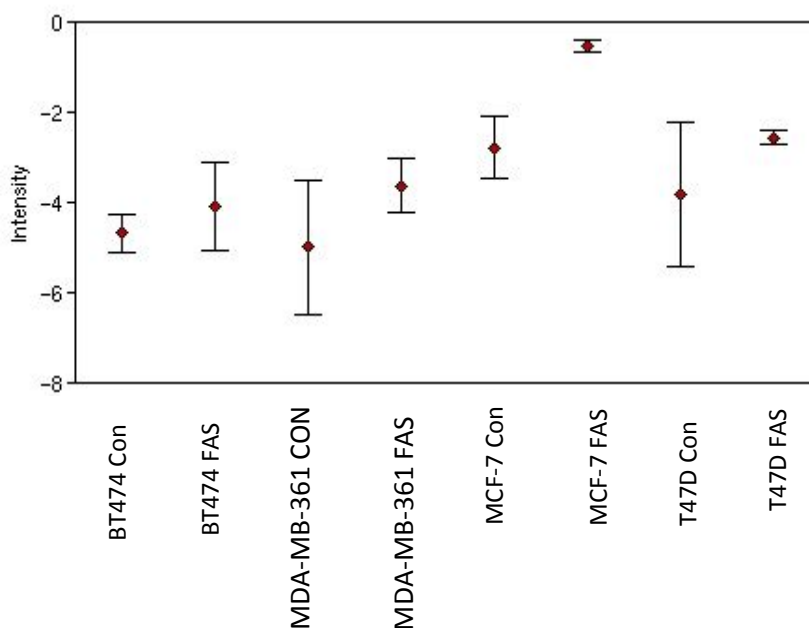
Gene Acronym	Fold change of expression following Faslodex treatment			
	BT474	MDA-MB-361	MCF-7	T47D
ALOX5	1.50	2.58	4.74	2.37

Figure 98: (A) Log2 intensity plot displaying the normalised (mean of triplicate samples) gene expression of ALOX5 in each of the 4 cell lines pre (Con) and post 10 day Faslodex (FAS) treatment using jetset gene probe (B) Table displaying the fold change in gene expression promoted by 10 day Faslodex treatment in each cell line vs. control expression (highlighted in red are those displaying a >1.5 fold induction in expression).

7.2.1.1.8 PCDH7

The basal log2 intensity values of PCDH7 were relatively similar and low across the 4 cell models (Figure 99), with Faslodex treatment increasing the expression of this gene only in the HER2- cells. In all but the post-treatment T47D cells, log2 values remained below 0 with absent calls.
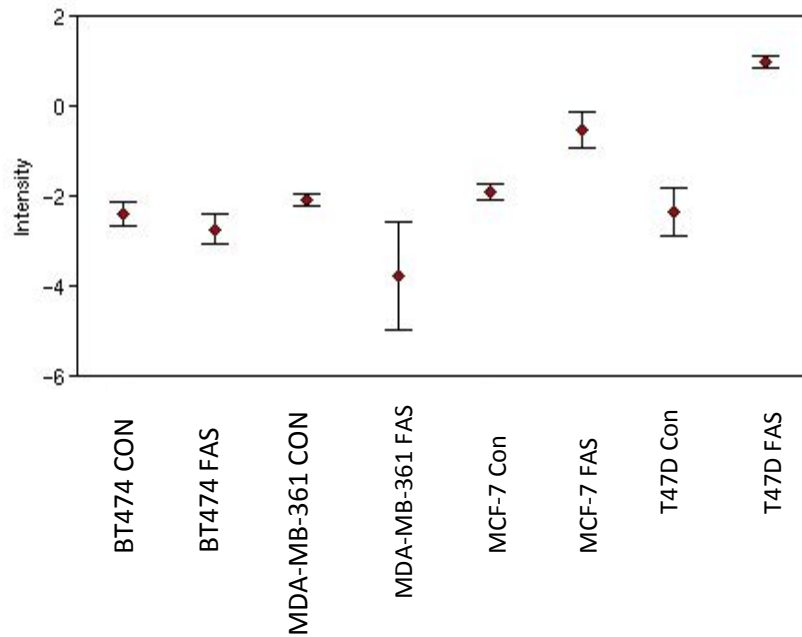
Gene Acronym	Fold change of expression following Faslodex treatment			
	BT474	MDA-MB-361	MCF-7	T47D
PCDH7	1.26	3.24	2.60	10.13

Figure 99: (A) Log2 intensity plot displaying the normalised (mean of triplicate samples) gene expression of PCDH7 in each of the 4 cell lines pre (Con) and post 10 day Faslodex (FAS) treatment using the jetset gene probe (b) Table displaying the fold change in gene expression promoted by 10 day Faslodex treatment in each cell line vs. control expression (highlighted in red are those displaying a >1.5 fold induction in expression and in green a >1.5 fold suppression).

7.2.1.1.9 NR2F1

Largely equivalent basal log2 intensity values of NR2F1 were observed in the HER2-and MDA-MB-361 cell lines, while a reduced value was observed in the BT474 cell line which remained unchanged following Faslodex treatment (Figure 100). A >1.5 fold Faslodex-promoted induction of NR2F1 was observed in both the HER2- cell lines with the greatest induction seen in T47D cells and a present call detected. In most instances, however, the log2 intensity values were below 0 with absent detection calls.
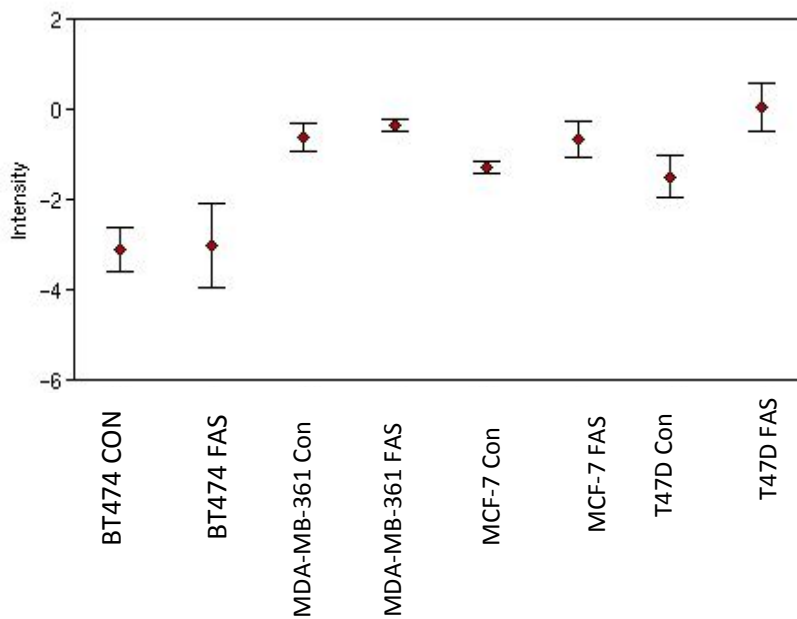
Gene Acronym	Fold change of expression following Faslodex treatment			
	BT474	MDA-MB-361	MCF-7	T47D
NR2F1	1.05	1.21	1.54	2.89

Figure 100: (A) Log2 intensity plot displaying the normalised (mean of triplicate samples) gene expression of NR2F1 in each of the 4 cell lines pre (Con) and post 10 day Faslodex (FAS) treatment using the jetset gene probe (B) Table displaying the fold change in gene expression promoted by 10 day Faslodex treatment in each cell line vs. control expression (highlighted in red are those displaying a >1.5 fold induction in expression).

7.2.1.1.10 SH3TC2

Although Faslodex increased the log2intensity value of SH3TC2 in the HER2-models, all log2 values remained below 0 with absent detection calls (Figure 101).
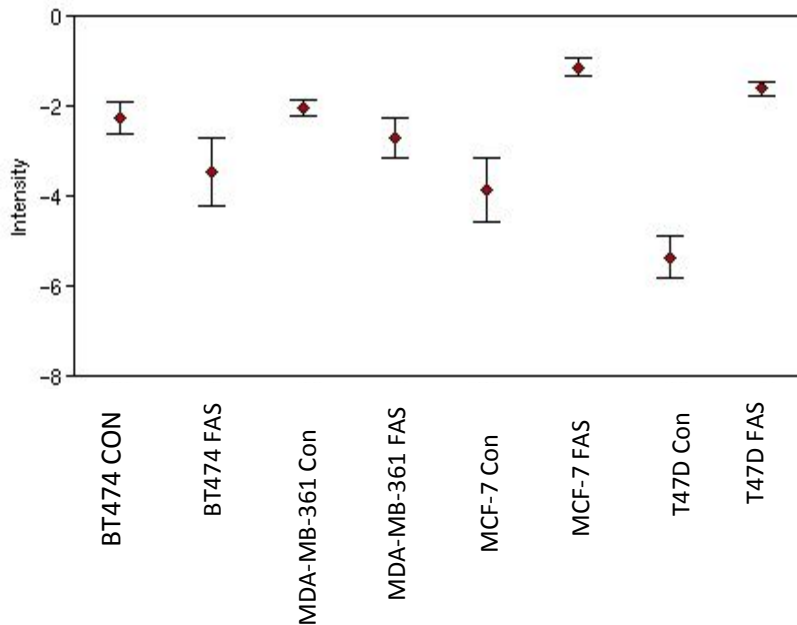
Gene Acronym	Fold change of expression following Faslodex treatment			
	BT474	MDA-MB-361	MCF-7	T47D
SH3TC2	2.32	1.59	6.68	13.39

Figure 101: (A) Log2 intensity plot displaying the normalised (mean of triplicate samples) gene expression of SH3TC2 in each of the 4 cell lines pre (Con) and post 10 day Faslodex (FAS) treatment using the jetset gene probe (B) Table displaying the fold change in gene expression promoted by 10 day Faslodex treatment in each cell line vs. control expression (highlighted in red are those displaying a >1.5 fold induction in expression and in green a >1.5 fold suppression).

7.2.1.2 Genes suppressed by Faslodex in MCF-7 and T47D (ER+/HER2-) cells:

7.2.1.2.1 ARTN

Of the 4 cell lines, the T47D cells displayed elevated ARTN basal log2 intensity values, whilst the BT474 cell line displayed reduced levels below 0 (Figure 102). Following Faslodex treatment ARTN was suppressed in the two HER2- cell lines only; the greatest suppression occurred in the T47D cell line. The detection calls for both the HER2+ and MCF-7 cell lines pre and post treatment were absent, while the T47D cell line demonstrated a change in call from present to absent indicative of a robust fall in gene expression in this model.
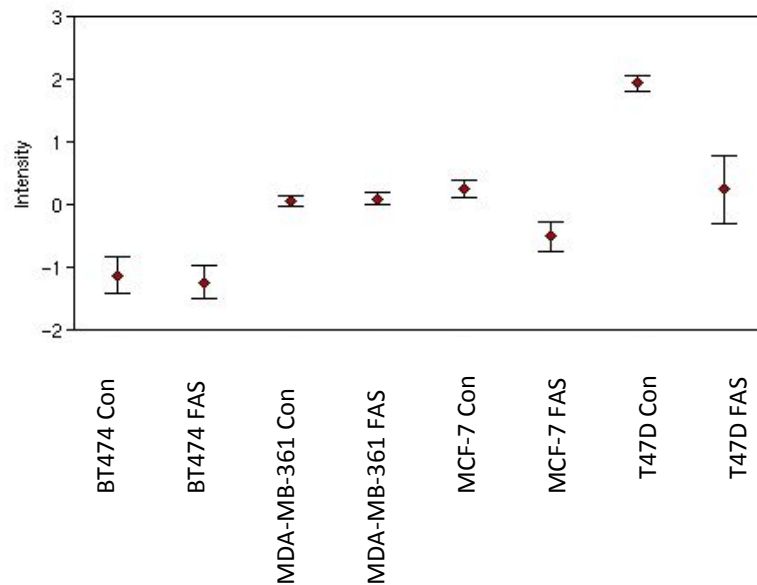
A

Gene Acronym	Fold change of expression following Faslodex treatment			
	BT474	MDA-MB-361	MCF-7	T47D
ARTN	1.08	1.03	1.69	3.24

Figure 102: (A) Log2 intensity plot displaying the normalised (mean of triplicate samples) gene expression of ARTN in each of the 4 cell lines pre (Con) and post 10 day Faslodex (FAS) treatment using the jetset gene probe (B) Table displaying the fold change in gene expression promoted by 10 day Faslodex treatment in each cell line vs. control expression (highlighted in green are those displaying a >1.5 fold suppression in expression).

7.2.1.2.2 MYRIP

Basal expression of MYRIP was uniform across the cell models (Figure 103) and was above 0 and called present. Faslodex treatment suppressed MYRIP expression only in the HER2- cell lines (Figure 103). For both MCF-7 and T47D cells, Faslodex treatment reduced the positive log2 intensity values to below 0 with an absent gene call in MCF-7 cells further indicating a robust suppression of this gene.
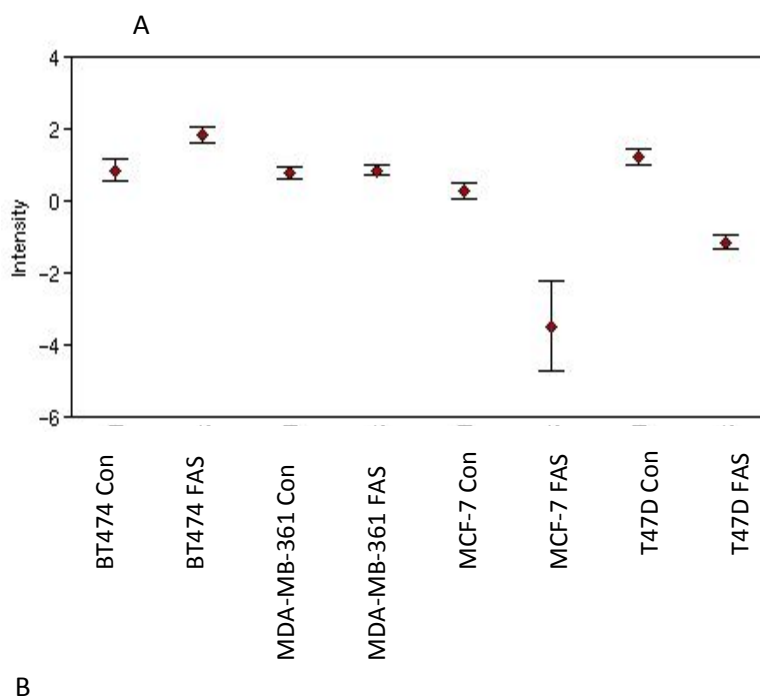
A

B

Gene Acronym	Fold change of expression following Faslodex treatment			
	BT474	MDA-MB-361	MCF-7	T47D
MYRIP	1.99	1.06	13.54	5.19

Figure 103: (A) Log2 intensity plot displaying the normalised (mean of triplicate samples) gene expression of MYRIP in each of the 4 cell lines pre (Con) and post 10 day Faslodex (FAS) treatment using the jetset gene probe (B) Table displaying the fold change in gene expression promoted by 10 day Faslodex treatment in each cell line vs. control expression (highlighted in red are those displaying a >1.5 fold induction in expression and in green a >1.5 fold suppression).

7.2.1.2.3 NPY5R

Basal NPY5R log2 intensity values were higher in the MCF-7 cell line compared to the other models. Faslodex treatment suppressed NPY5R gene expression in both HER2- cell lines to levels equivalent to those recorded in the HER2+ models pre and post drug treatment. However, the log2 intensity values were low for this gene (Figure 104) with absent calls throughout so that profiles were unreliable.
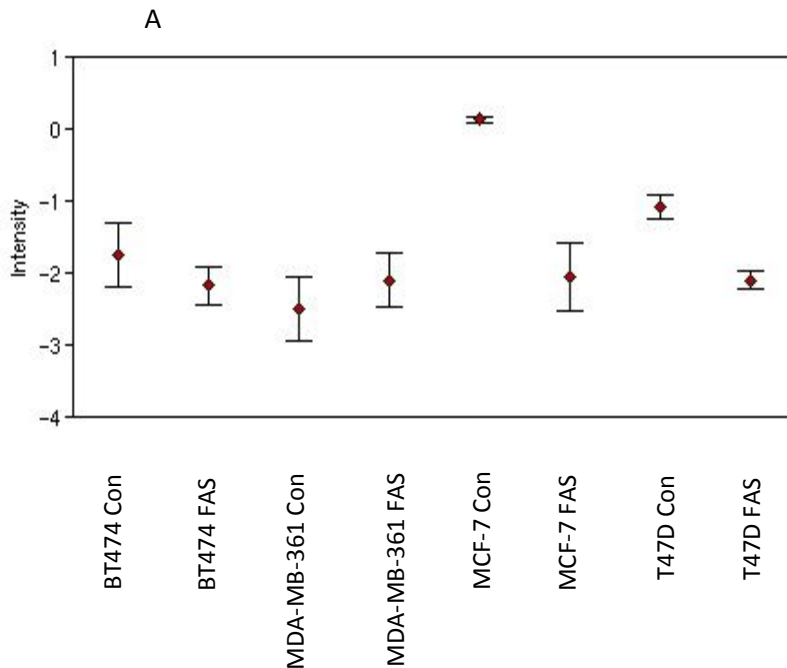
A

B

Gene Acronym	Fold change of expression following Faslodex treatment			
	BT474	MDA-MB-361	MCF-7	T47D
NPY5R	1.34	1.32	4.57	2.02

Figure 104: (A) Log2 intensity plot displaying the normalised (mean of triplicate samples) gene expression of NPY5R in each of the 4 cell lines pre (Con) and post 10 day Faslodex (FAS) treatment using the jetset gene probe (B) Table displaying the fold change in gene expression promoted by 10 day Faslodex treatment in each cell line vs. control expression (highlighted in green are those displaying a >1.5 fold suppression in expression).

7.2.1.2.4 PYY

Although some suppression of PYY expression was seen in the HER2- cells, the log2 intensity values were very low both pre- and post-Faslodex treatment with absent calls throughout, so profiles were unreliable (Figure 105).
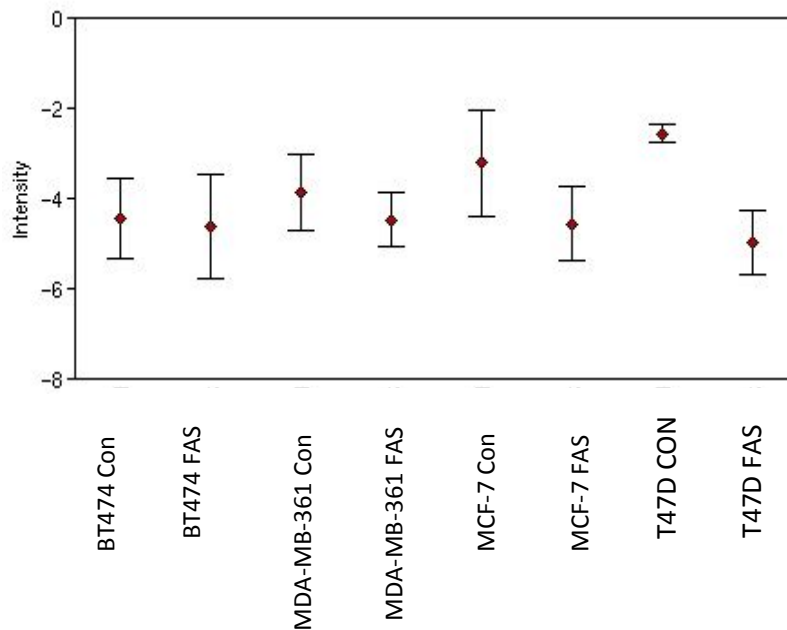
Gene Acronym	Fold change of expression following Faslodex treatment			
	BT474	MDA-MB-361	MCF-7	T47D
PYY	1.13	1.52	2.56	5.33

Figure 105: (A) Log2 intensity plot displaying the normalised (mean of triplicate samples) gene expression of PYY in each of the 4 cell lines pre (Con) and post 10 day Faslodex (FAS) treatment using the jetset gene probe (B) Table displaying the fold change in gene expression promoted by 10 day Faslodex treatment in each cell line vs. control expression (highlighted in green are those displaying a >1.5 fold suppression in expression).

7.2.1.2.5 SULF1

Basal log2 intensity values of SULF1 were elevated in both the HER2- cell lines compared to the HER2+ cell lines and showed Faslodex suppression (Figure 106). Indeed, in these HER2- cells a change in detection call from present to absent was observed on Faslodex treatment. Absent calls were seen throughout for the HER2+ lines and so the small fall detected in BT474 was unreliable.
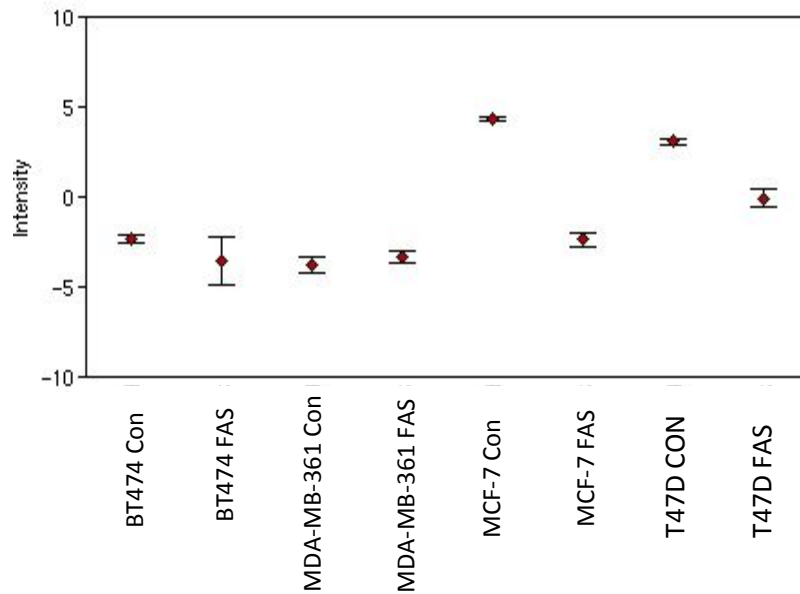
Gene Acronym	Fold change of expression following Faslodex treatment			
	BT474	MDA-MB-361	MCF-7	T47D
SULF1	2.27	1.38	103.49	9.03

Figure 106: (A) Log2 intensity plot displaying the normalised (mean of triplicate samples) gene expression of SULF1 in each of the 4 cell lines pre (Con) and post 10 day Faslodex (FAS) treatment using the jetset gene probe (B) Table displaying the fold change in gene expression promoted by 10 day Faslodex treatment in each cell line vs. control expression (highlighted in green are those displaying a >1.5 fold suppression in expression).

7.2.1.2.6 ELOVL2

Basal ELOVL2 log2 intensity values were lowest in the BT474 cell line compared to the 3 other cell models. Faslodex treatment led to >4 fold suppression of ELOVL2 expression in both HER2- cell lines, with minimal change being observed in the HER2+ models (Figure 107). Indeed, the HER2- cell models exhibited a change in detection call from present to absent following treatment, indicating a robust suppression of expression of this gene.
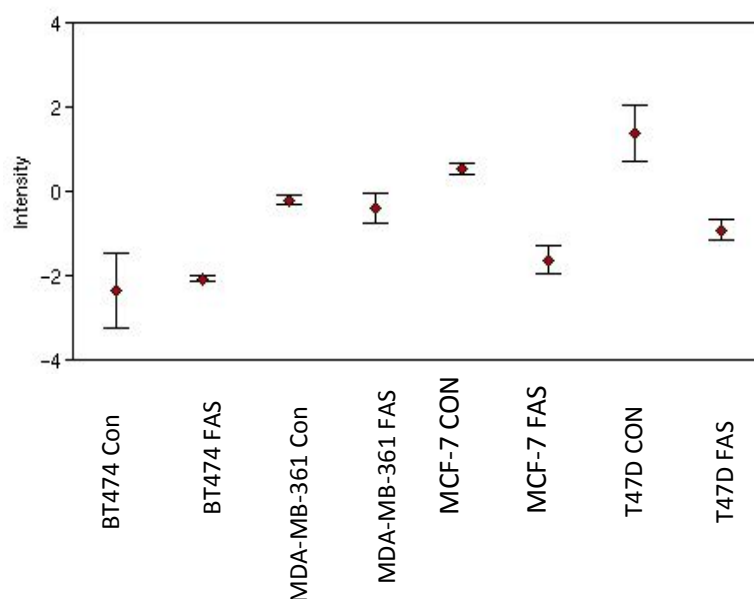
Gene Acronym	Fold change of expression following Faslodex treatment			
	BT474	MDA-MB-361	MCF-7	T47D
ELOVL2	1.21	1.16	4.46	4.90

Figure 107: (A) Log2 intensity plot displaying the normalised (mean of triplicate samples) gene expression of ELOVL2 in each of the 4 cell lines pre (Con) and post 10 day Faslodex (FAS) treatment using the jetset gene probe (B) Table displaying the fold change in gene expression promoted by 10 day Faslodex treatment in each cell line vs. control expression (highlighted in green are those displaying a >1.5 fold suppression in expression).

In summary, following the analysis of the gene log2 intensity plots, PTPRJ, ITIH1, ANK1, ALOX5, SH3TC2, KRT4, NPY5R and PYY were dismissed from further

investigation due to one or more of the following reasons; (i) low log2 intensity values (intensity below 0), (ii) absent detection calls, and (iii) Faslodex-de-regulation of expression was not unique to the HER2- cell lines. For PTPRJ and SH3TC2 there was also very poor jetset performance.

Investigations were, however, continued for the Faslodex-induced genes VGLL1, UPK3B, PCDH7, NR2F1 and suppressed genes ARTN, MYRIP, SULF1 and ELOVL2 as potential Faslodex response genes in the HER2- cell lines.

7.2.2 Analysis of potential superior response genes in an MCF-7-derived Faslodex-resistant gene expression array dataset

The above genes, identified as being Faslodex de-regulated in the HER2- cell lines, are hypothesised to be involved in the extended growth inhibitory response of the drug. They were thus subsequently analysed in an MCF-7-derived Faslodex-resistant cell line to determine any directional changes in their expression.

Figure 108 displays the heatmap showing the change in expression of the 8 genes of interest that occurred in the Faslodex resistant-phenotype compared to oestradiol-treated MCF-7 control cells. Figures 109-116 display the gene expression log2 expression intensity plots and fold change for each of the genes using their jetset gene probes, where these data confirmed the profiles of changes.

VGLL1 and UPK3B continued to be induced once the cells developed Faslodex resistance, with the highest log2 intensity and fold changes in the resistant cells achieved for these genes. ARTN, SULF1 and ELOVL2 continued to be suppressed once the cells developed Faslodex resistance, with log2 intensity levels below 0 in the resistant cells. PCDH7 gene expression was induced by 10 day Faslodex treatment but down-regulated in Faslodex resistance, the opposite was observed for MYRIP which was a gene suppressed by Faslodex treatment. NR2F1 (that was initially induced by Faslodex treatment) returned to the basal level expression seen in the oestradiol-treated control (Figure 108).
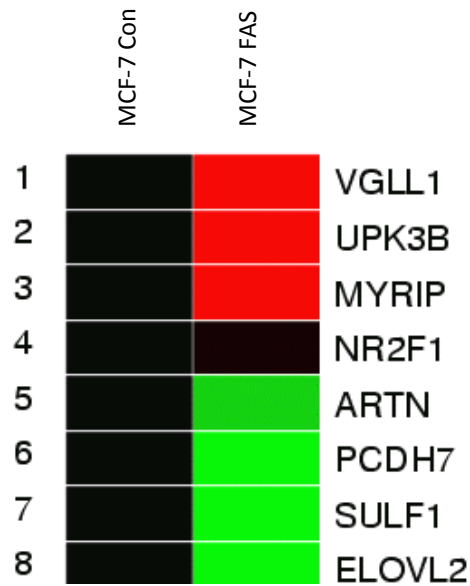
Figure 108: Heatmap displaying Faslodex de-regulated genes in the HER2- cell lines reanalysed in the MCF-7 Faslodex-resistant cell line compared to oestradiol (E2) treatment. The heatmap was generated using jetset affymetrix gene probe ID's.

7.2.2.1 Genes induced by 10 day Faslodex-treatment: VGLL1, UPK3B, PCDH7 and NR2F1
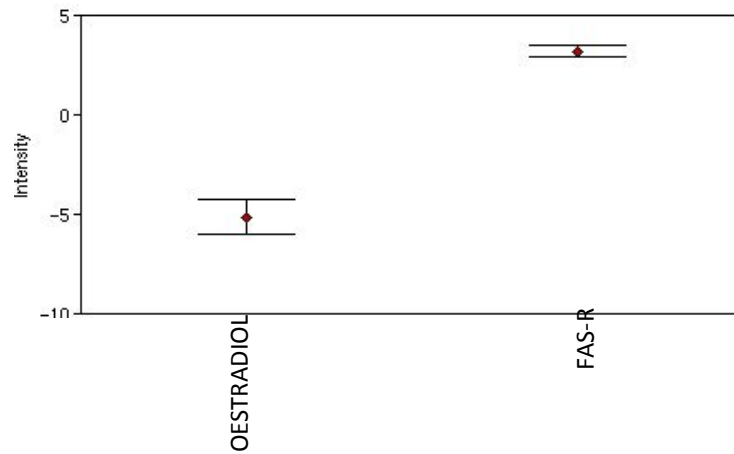
Gene Acronym	Fold change
VGLL1	322.63

Figure 109: (A) Log2 expression intensity plot displaying the substantial induction of VGLL1 expression level using the jetset gene probe in an MCF-7-derived, Faslodex-resistant cell model in comparison to wild-type MCF-7 cells treated with oestradiol (10^{-9}M) (B) table displaying the fold change in expression.
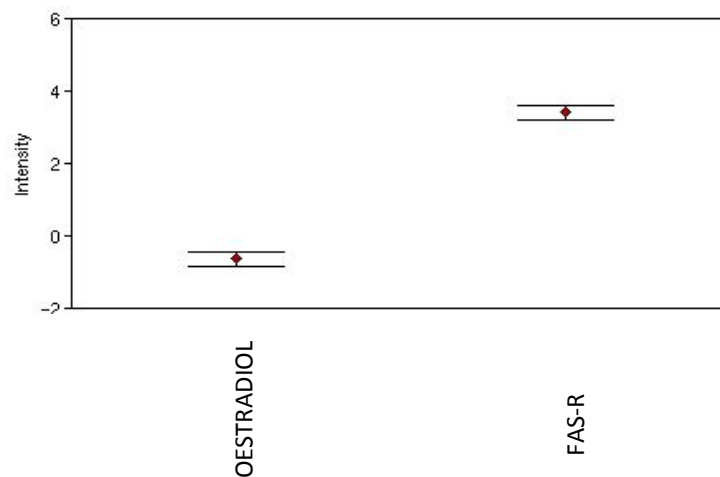
Gene Acronym	Fold change
UPK3B	16.35

Figure 110: (A) Log2 intensity plot displaying the induction of UPK3B expression level using the jetset gene probe in an MCF-7-derived, Faslodex-resistant cell model in comparison to

wild-type MCF-7 cells treated with oestradiol (10^{-9}M) (B) table displaying the fold change in expression.
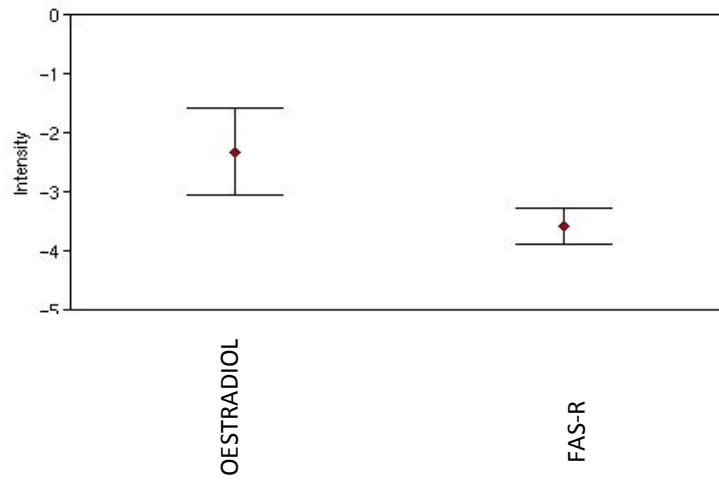
Gene Acronym	Fold change
PCDH7	2.39

Figure 111: (A) Log2 intensity plot displaying an apparent suppression of PCDH7 gene expression level using the jetset gene probe in an MCF-7-derived, Faslodex-resistant cell model in comparison to wild-type MCF-7 cells treated with oestradiol (10^{-9}M) (B) table displaying the fold change in expression.
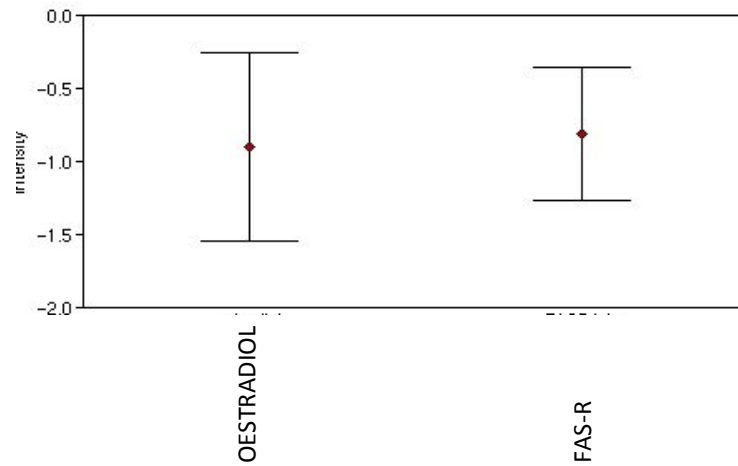
Gene Acronym	Fold change
NR2F1	1.06

Figure 112: Log2 intensity plot displaying the gene expression level of NR2F1 using the jetset gene probe in an MCF-7-derived, Faslodex-resistant cell model in comparison to wild-type MCF-7 cells treated with oestradiol (10^{-9}M) (B) table displaying the fold change in expression.

7.2.2.2 Genes suppressed by 10 day Faslodex-treatment: ARTN, MYRIP, ELOVL2 and SULF1
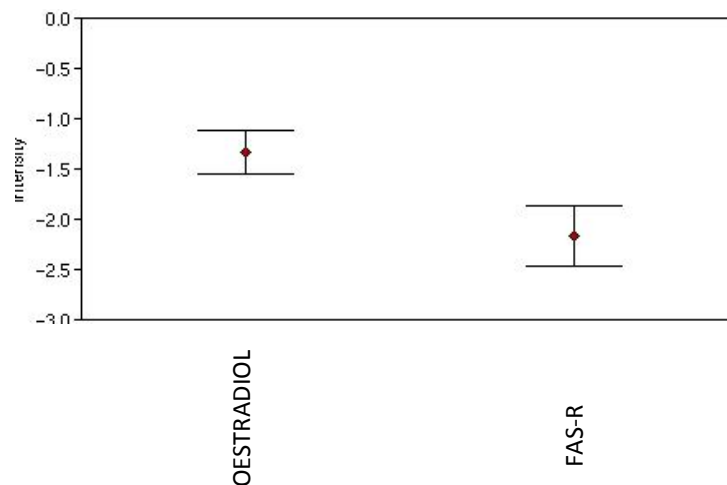
Gene Acronym	Fold change
ARTN	1.77

Figure 113: (A) Log2 intensity plot displaying an apparent suppression of ARTN gene expression level using the jetset gene probe in an MCF-7-derived, Faslodex-resistant cell

model in comparison to wild-type MCF-7 cells treated with oestradiol (10^{-9}M) (B) table displaying the fold change in expression.
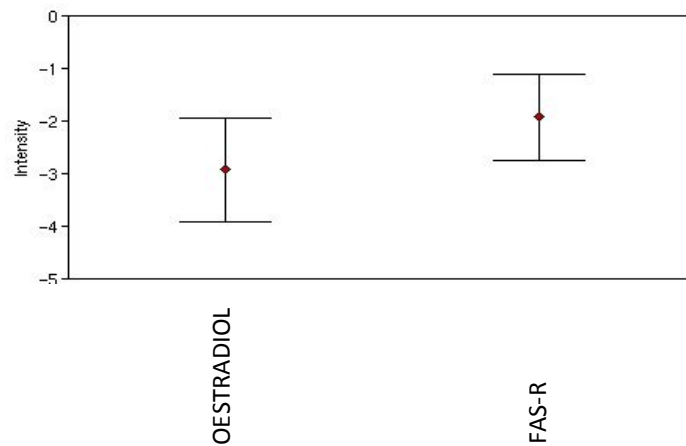
Gene Acronym	Fold change
MYRIP	1.99

Figure 114: (A) Log2 intensity plot displaying an apparent induction of MYRIP gene expression level using the jetset gene probe in an MCF-7-derived, Faslodex-resistant cell model in comparison to wild-type MCF-7 cells treated with oestradiol (10^{-9}M) (B) table displaying the fold change in expression.
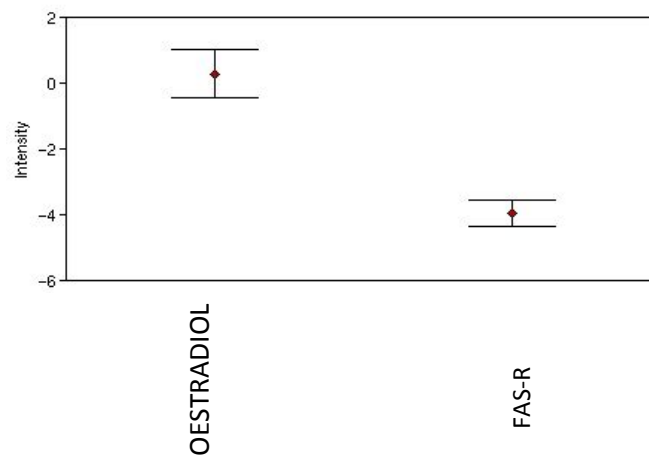
Gene Acronym	Fold change
ELOVL2	18.89

Figure 115: (A) Log2 intensity plot displaying the suppression of ELOVL2 expression level using the jetset gene probe in an MCF-7-derived, Faslodex-resistant cell model in

comparison to wild-type MCF-7 cells treated with oestradiol (10^{-9}M) (B) table displaying the fold change in expression.

Gene Acronym	Fold change
SULF1	18.25
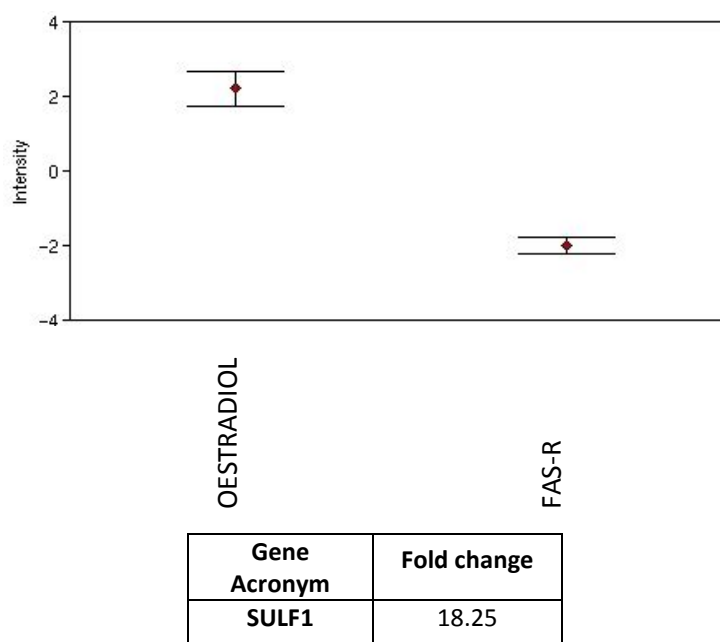
Figure 116: (A) Log2 intensity plot displaying the suppression of SULF1 gene expression level using the jetset gene probe in an MCF-7-derived, Faslodex-resistant cell model in comparison to wild-type MCF-7 cells treated with oestradiol (10^{-9}M) (B) table displaying the fold change in expression.

7.2.3 Ontological investigation of genes potentially involved in the extended Faslodex response in the HER2- cell lines

To help further determine if they might relate to Faslodex response, an ontological investigation was also undertaken on the 8 genes to determine if they had been associated with:

- Breast cancer or any other cancer type;
- Known or potential adverse function (e.g. tumour growth or progression);
- Known or potential tumour suppressive function

The results of the ontological investigations are accumulated in Tables 3 to 10. Pubmed and Scopus were used throughout for these ontological studies using the gene name/acronym, together with selected keywords/phrases which included breast cancer, cancer, oncogene, proliferation, growth, metastasis, Faslodex,

hormonal or endocrine therapy, survival, growth inhibition, tumour suppressor, apoptosis.

If the gene name is highlighted in red, expression was induced by 10 day Faslodex treatment and if green, the gene was suppressed by treatment.

Table 31: Summary of the function of VGLL1 including previous published reports surrounding the role of VGLL1 in breast and other cancers.

Gene Name/Acronym	Vestigial like 1: **VGLL1**
Function	VGLL1 binds proteins of the TEA (transcription enahancer activator) domain family of transcription factors through the Vg (vestigial) homology region found in its N-terminus. Subsequently it may function as a specific coactivator for this family of transcription factors (Pobbati *et al.*, 2012).
Associations with breast cancer	No direct associations with breast cancer but has been discussed as a potential mediator of disease progression. Pobbati *et al.,* have shown that VGLL1 interacts with TEAD (TEA domain) in a similar way to oncogenic transcription coactivators YAP and TAZ. The VGLL1-TEAD complex induces the expression of IGFBP-5, a known promoter of proliferation and encourages anchorage-independent cell proliferation (Pobbati *et al.*, 2012). The YAP/TAZ-TEAD complex has been shown to upregulate a number of other genes involved in the proliferation and anchorage-independent growth, thus given the similarities between these transcription factors and VGLL1, one may suspect that VGLL1 has potential to be involved cancer progression (Avruch *et al.*, 2012).
Associations with other cancers	No direct associations with cancer.

Table 32: Summary of the function of UPK3B including previous published reports surrounding the role of UPK3B in breast and other cancers.

Gene Name/Acronym	Uroplakin 3B: **UPK3B**
Function	UPK3B is a minor component of the apical plaques of mammalian urothelium that binds and dimerizes with uroplakin-1b (UPK1B), one of the major conserved urothelium membrane proteins. May play an important role in asymmetric unit membrane (AUM)-cytoskeleton interaction in terminally differentiated urothelial cells (Wu *et al.*, 2009).
Associations with breast cancer	No associations with breast cancer
Associations with other cancers	In bladder cancer, the loss of expression of FOXA1 is associated with advanced tumour stage and high histologic grade as well as a parallel upregulation of the uroplakin family including UPK3B. It has been suggested that FOXA1 regulates UPK expression but when FOXA1 is lost a compensatory mechanism is activated resulting in further increases in UPK expression. The regulation of the UPK proteins by FOXA1 is complex but further investigations may elucidate the mechanisms responsible for normal bladder development and urothelial differentiation. The effects of the UPK family directly on cancer growth are still unknown (DeGraff *et al.*, 2012).

Table 33: Summary of the function of PCDH7 including previous published reports surrounding the role of PCDH7 in breast and other cancers.

Gene Name/Acronym	Protocadherin 7: **PCDH7**
Function	This gene belongs to the protocadherin gene family, a subfamily of the cadherin superfamily. The gene encodes a protein with an extracellular domain containing 7 cadherin repeats. PCDH7 (NFPC) has four isoforms (7a, 7b, 7c and 7c1). The gene product is an integral membrane protein that is thought to function in cell-cell recognition and adhesion. PCDH7 interacts with TAF1 regulating the strong adhesive properties of PCDH7 (Heggem *et al.*, 2003).
Associations with	No direct associations with breast cancer.

breast cancer	
Associations with other cancers	The hypermethylation of PCDH7 has been suggested to be involved in the development of bladder cancer (Beukers *et al.*, 2013). Analysis of 60 bladder cancer tumours also found PCDH7 to be under expressed (Djyrskot *et al.*, 2004) indicative of tumour suppressor functions. Small polymorphisms within the PCDH7 gene have been shown to be associated with poor survival in early-stage NSCLC (Huang *et al.*, 2009).

Table 34: Summary of the function of NR2F1 including previous published reports surrounding the role of NR2F1 in breast and other cancers.

Gene Name/Acronym	Nuclear receptor subfamily 2, group F, member 1: **NR2F1**/COUP-TF1
Function	Coup (chicken ovalbumin upstream promoter) transcription factors binds to the ovalbumin promoter and, in conjunction with the protein S300-II stimulate the initiation of transcription. COUP-TFI is one of the two major homologues of the COUP-TF family. These factors belong to the nuclear receptor (NR) super family. There is much evidence suggesting that these transcription factors are involved in a number of biological processes including cell proliferation, survival, angiogenesis and migration. They have also been shown to modulate a number of other transcription factors known to be involved in carcinogenesis (Boudot *et al.*, 2011).
Associations with breast cancer	COUP-TFI has been shown to interact with ER leading to the recruitments of ERKs (in an E2-independent manner) resulting in the enhancement of ER transcriptional activity (Métivier *et al.*, 2002). Expression of COUP-TFI has been shown to be higher in more dedifferentiated breast cancer cell lines (MDA-MB-231) and tumour cells compared to the well-differentiated MCF-7 cell line and normal breast cells. Overexpression of COUP-TFI in MCF-7 cells resulted in enhanced motility and invasiveness as well as promoting cell

	proliferation (Le Dily *et al.*, 2008).
	Promoters I.3 and II have been identified as the key promoters in regulating aromatase expression in breast cancer (Zhou *et al.*, 1996). A negative regulatory element has been identified between these two promoters, S1, which downregulates the activity of these two promoters (Zhou *et al.*, 1998). COUP-TFI has been shown to interact with the S1 region (Yang *et al.*, 1998) in a negative regulatory manner (Yang *et al.*, 2002). In normal breast tissue the activity of promoters I.3 and II are suppressed by the binding of COUP-TF1 (as well as EAR-2 and RARγ). However, in breast cancer tissue these factors are decreased and thus activity of promoters I.3 and II is elevated leading to an induction of aromatase expression (Chen *et al.*, 2005).
	COUP-TFI and COUP-TFII (the other major homologue) has been shown to activate VEGF-C expression in the MCF-7 cell line suggesting an involvement in neo-angiogenesis and lymphangiogenesis (Nagasaki *et al.*, 2009).
	COUP-TFI and II overexpression has also been shown to induce tamoxifen-resistance (Le Dily *et al.*, 2008) but other research groups have suggested that increased expression of COUP-TFII may increase sensitivity to anti-estrogens (Riggs *et al.*, 2006). More work is required to determine the involvement of the COUP-TFs in anti-oestrogen sensitivity.
Associations with other cancers	Depending on the type of cancer the COUP-TFs have been suggested to act in a positive or negative manner (Boudot *et al.*, 2012). As seen in the breast cancer MCF-7 cell line, the COUP-TFs have been shown to induce the expression of VEGF-C in the MKN-45 gastric cancer cell line suggesting a role in lymphangiogenesis (Schafer *et al.*, 2008).
	COUP-TFI is negatively regulated by the androgen receptor; downregulated when androgen is bound to the androgen receptor

and upregulated when an androgen receptor antagonist is bound. COUP-TFI protein expression was found to be elevated in nucleoli of malignant prostate epithelium compared to normal epithelium (Perets *et al.*, 2012).

COUP-TFI expression seems to be lower in ovarian (De Sousa Damiao *et al.*, 2007) and bladder (Ham *et al.*, 2008) malignant tissue than in benign and normal tissue suggesting that loss of COUP-TF expression in these cancers is associated with such malignancy.

Table 35: Summary of the function of ARTN including previous published reports surrounding the role of ARTN in breast and other cancers.

Gene Name/Acronym	Artemin: **ARTN**
Function	ARTN is a member of the GDNF family of ligands which belong to the TGF-beta superfamily of signalling molecules. ARTN is a ligand for the GFR-alpha-3-RET receptor complex but can also activate the GFR-alpha-1-RET receptor complex (Baloh *et al.*, 1998).
Associations with breast cancer	Kang *et al.*, identified ARTN expression in 65% of mammary cancers and expression correlated with a reduced overall survival (Kang *et al.*, 2009). Transfection of breast cancer cells with ARTN resulted in anchorage-independent growth and enhanced migration and invasion and increased tumour growth *in vivo*. GFRA1 and RET (members of the ARTN receptor complex) and ARTN have been observed as E2 regulated (induced expression following E2 treatment) (Boulay *et al.*, 2008; Kang *et al.*, 2010). Kang *et al.*, have also showed that expression of ARTN can confer antiestrogen-resistance by reducing the efficacy of antiestrogens in breast cancer cell lines. They have suggested that this effect may be mediated by enhanced ERα transcriptional activity and increased expression of BCL-2. Combination therapy of an antiestrogen and an anti-ARTN antibody enhanced the activity of tamoxifen in sensitive and resistant cells (Kang *et al.*, 2010).

	As artemin is a ligand for RET forming a receptor complex along with a member of the GFRα family, it is of note to discuss the role of RET signalling in breast cancer. In summary RET expression has been found elevated in a subset of ER+ breast cancers (Esseghir *et al.*, 2007). *In vitro* activation of the RET signalling pathway in ER+ cells led to an E2-independent increase in ER phosphorylation and transcriptional activity (Plaza-Menacho *et al.*, 2010). The Isacke laboratory have reported that RET signalling is a key signalling pathway associated with aromatase inhibitor response and resistance in ER+ breast cancers clinically (Morandi *et al.*, 2013).
Associations with other cancers	Artemin and its further receptor GFRA3 have been linked to increased motility and invasion in pancreatic cancer, subsequently leading to a more aggressive phenotype (Meng *et al.*, 2012). ARTN expression was found to be significantly higher in esophageal carcinoma than in adjacent noninvasive tissues, and ARTN was shown to promote migration and invasion of esophageal carcinoma cells (Li *et al.*, 2011b). Artemin was also shown to be involved in the disease progression of non-small cell lung carcinoma and endometrial cancer by encouraging cell proliferation, migration and invasion (Tang *et al.*, 2010; Pandev *et al.*, 2010).

Ontology for ARTN indicates an adverse role related to cancer progression thus its suppression by Faslodex treatment is in keeping with a superior drug response in the HER2- cell lines. ARTN is the ligand for RET which form a receptor complex with GFRA1 or GFRA3 and so the gene expression of these additional factors were examined in the cell models pre and post Faslodex treatment.

GFRA1 in chapter 5 was identified as being significantly down-regulated by Faslodex in the cell lines that develop drug resistance (Figure 35 and 57). From the log2 intensity plot for GFRA1 the receptor was down-regulated in the 3 cell lines by Faslodex and very low log2 intensity values were observed in the T47D cell line pre and post treatment with detection calls absent indicative of lack of expression (Figure 35). GFRA3 was expressed at very similar, low levels in all models basally (Figure 117). Marginal inductions of GFRA3 were observed in the HER2- cell lines but all detection calls were found to be absent indicative of lack of expression. Log2 intensity values of RET were fairly uniform basally in the HER2+ and MCF-7 cell lines but reduced in the T47D cell line (Figure 117). Faslodex treatment led to a >1.5 fold suppression of RET in the HER2- cell lines (MCF-7-1.82 fold suppression; T47D-1.96 fold suppression) while no change was observed in the HER2+ cell lines. Detection calls were found to be present for all samples with the exception of the T47D samples pre and post treatment.
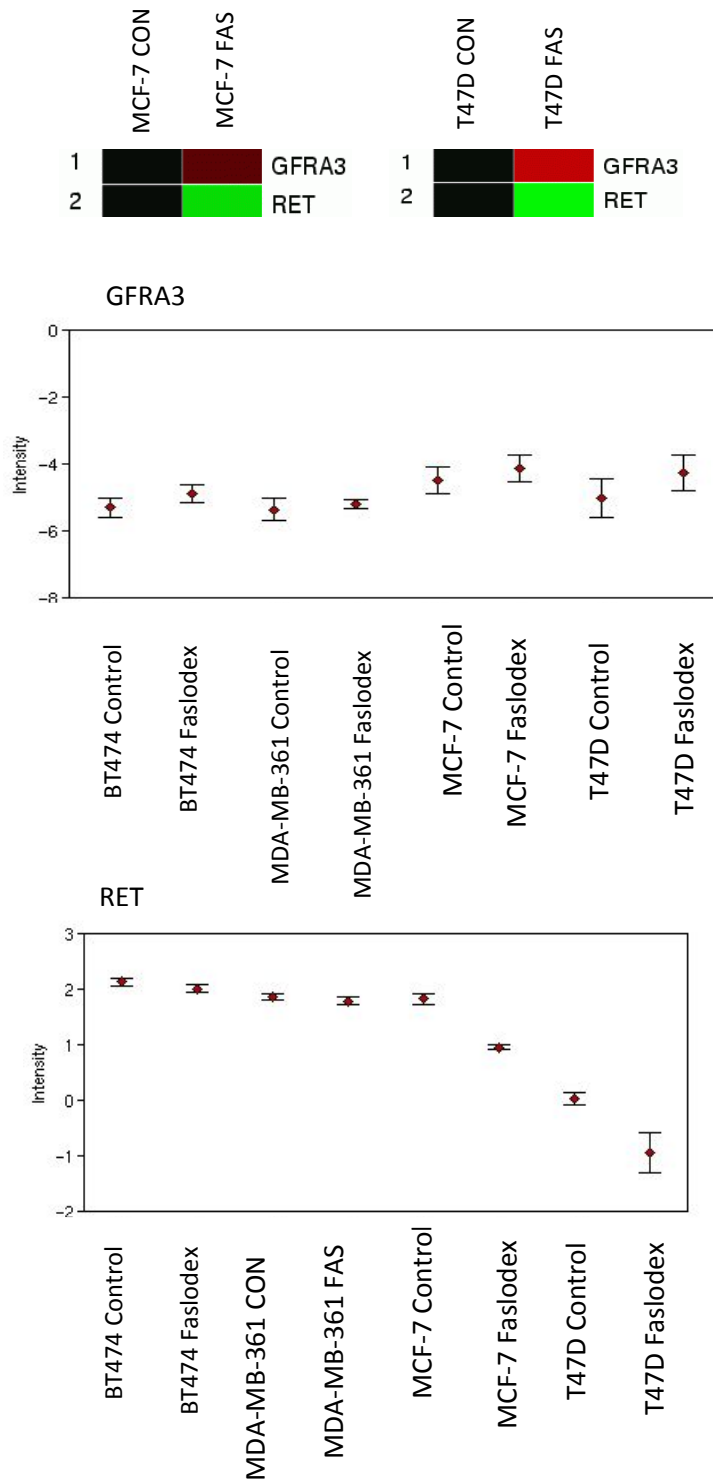
Figure 117: (A) Heatmaps and (B) log2 intensity plots generated by GeneSifter displaying

the change in expression of GFRA3 and RET promoted by 10 day Faslodex treatment in the

MCF-7 and T47D cell lines versus untreated control using the jetset gene probes (GFRA3-214479_at, RET-205879_x_at).

Table 36: Summary of the function of MYRIP including previous published reports surrounding the role of MYRIP in breast and other cancers.

Gene Name/Acronym	Myosin VIIA and Rab interacting protein: **MYRIP**
Function	MYRIP is a Rab effector protein involved in melanosome transport. Serves as link between melanosome-bound RAB27A and the motor proteins MYO5A and MYO7A. It can also function as a protein kinase A-anchoring protein (AKAP) (El-Amraoui *et al.*, 2002)
Associations with breast cancer	No associations with breast cancer
Associations with other cancers	MYRIP has been reported as a potential tumour suppressor gene in hepatocarcinogenesis due its methylation status (Yang *et al.*, 2011)

Table 37: Summary of the function of SULF1 including previous published reports surrounding the role of SULF1 in breast and other cancers

Gene Name/Acronym	Sulfatase 1: **SULF1**
Function	Heparan sulfate proteoglycans (HSPGs) act as coreceptors for numerous heparin-binding growth factors and cytokines and are involved in cell signalling (Forsten-Williams *et al.*, 2008). Heparan sulfate 6-O-endosulfatases, such as SULF1, selectively remove 6-O-sulfate groups from heparan sulfate. This activity modulates the activity of heparan sulfate by altering binding sites for signalling molecules (Ai *et al.*, 2006).
Associations with breast cancer	SULF1 has been found to be down-regulated in metastatic breast cancer (Narita *et al.*, 2007) and its expression is lost in many breast cancer cell lines in particular those deemed metastatic e.g. MDA-468 AND MDA-231 (Khurana *et al.*, 2011). Overexpression of SULF1 is able to suppress growth and

	angiogenesis (by suppressing VEGF signalling) *in vivo* suggesting that SULF1 is a tumour suppressor gene (Narita *et al.*, 2006). However, there is a paradox to SULFs in that they can promote Wnt signalling and thus tumorigenesis (Lai *et al.*, 2010).
Associations with other cancers	SULF1 overexpression in hepatocellular carcinoma cells suppressed KDR/VEGF and FGF2 signalling thus promoting sensitivity to a number of chemotherapy agents such as doxorubicin as well as the histone deacetylase inhibitor aphicidin (Lai *et al.*, 2008). Downregulation of SULF1 has been described in a number of tumours in keeping with a tumour suppressor function; including ovarian (Staub *et al.*, 2007), hepatocellular (Lai *et al.*, 2008), gastric (Gopal *et al.*, 2012) and kidney (Lai *et al.*, 2008) cancer. However overexpression of SULF1 has also been identified in adrenal carcinoma, brain cancer, breast cancer, colon adenocarcinoma as well as others (Rosen *et al.*, 2010) challenging the concept that SULF1 is simply a tumour suppressor.

Table 38: Summary of the function of ELOVL2 including previous published reports surrounding the role of ELOVL2 in breast and other cancers.

Gene Name/Acronym	ELOVL fatty acid elongase 2: **ELOVL2**
Function	Condensing enzyme that catalyzes the synthesis of polyunsaturated very long chain fatty acid (C20- and C22-PUFA) (Moon *et al.*, 2001; Leonard *et al.*, 2002)
Associations with breast cancer	No associations with breast cancer
Associations with other cancers	ELOVL2 gene expression has been found to be up-regulated in hepatocellular carcinoma (Zekri *et al.*, 2012)

7.2.3.1 Summary of the ontological data for the potential response-promoting genes

A number of the genes de-regulated by Faslodex in both HER2- cell lines have not previously been associated with breast cancer including UPK3B, PCDH7, MYRIP and ELOVL2 and so their further clarification may yield interesting data in relation to HER2- response. UPK3B has not been directly associated with growth regulation in any cancer. PCDH7 and MYRIP have both been suggested to be associated with growth inhibition but, there is very little published work on ELOVL2 in any cancer.

VGLL1 and NR2F1 have both been associated with disease progression suggesting that induction of these genes in the HER2- cell lines may not contribute to the superior Faslodex response. Induction of VGLL1 was furthermore maintained in Faslodex-resistance (Figure 109). ARTN was also involved in disease progression, so its suppression by Faslodex may enhance the growth inhibitory response, particularly as its co-receptors were also suppressed (Figure 117). Expression of SULF1 can growth inhibit breast cancer cells, thus its suppression by Faslodex seems unlikely to contribute to the growth inhibitory mechanism.

5 genes were selected for further investigation as a consequence:

- PCDH7
- UPK3B
- ARTN
- MYRIP
- ELOVL2

7.2.4 Establishing potential clinical relevance of the genes of interest in the context of endocrine outcome

Equivalent analyses, as performed in chapters 5 and 6 using KMPlotter and GOBO, were used to determine the potential clinical relevance of the 5 genes identified in HER2 – cells in relation to tamoxifen treated ER+ breast cancer.

In KMPlotter only UPK3B and PCDH7 were found to demonstrate an association with tamoxifen outcome. Increased expression of UPK3B and PCDH7 were significantly associated with an improved duration of response (Figure 118 and 119), in keeping with their induction in the ER+/HER2- cell lines. Hazard ratios of less than 1 confirmed improved RFS in those patients with increased expression of these genes (UPK3B: HR=0.66 (95% CI 0.47-0.92), p=0.014; PCDH7: HR=0.69 (95% CI 0.48-0.98), p=0.038).
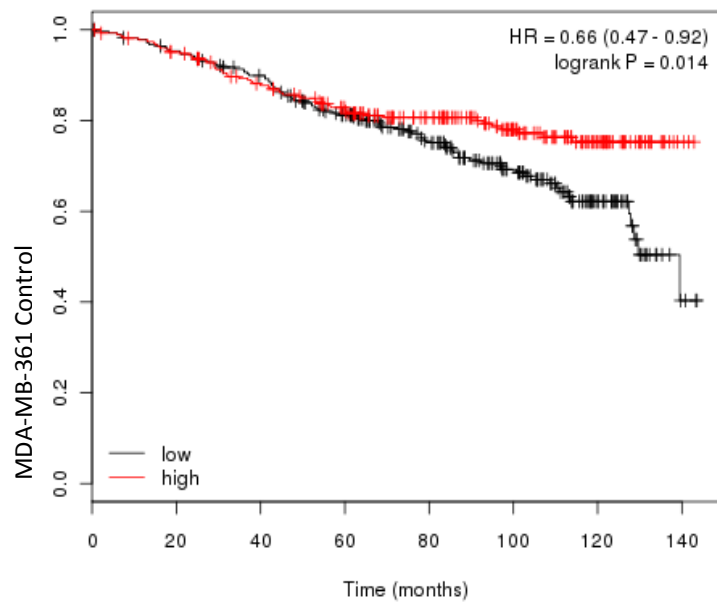
Figure 118: Kaplan-Meier survival curve generated using KMPlotter displaying probability of RFS according to high (red) or low (black) UPK3B mRNA expression in tamoxifen-treated ER+ breast cancer patients (n=553).
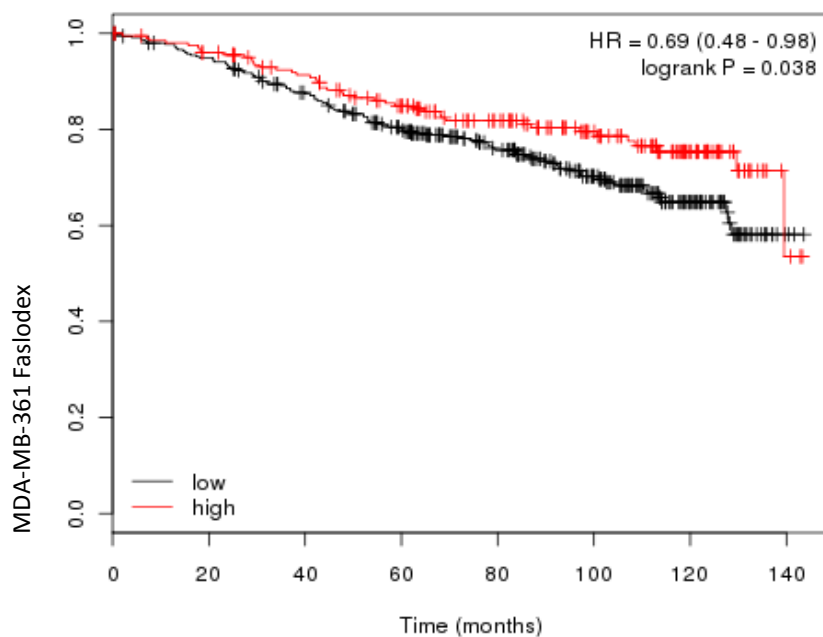
Figure 119: Kaplan-Meier survival curve generated using KMPlotter displaying probability of RFS according to high (red) or low (black) PCDH7 mRNA expression in tamoxifen-treated ER+ breast cancer patients (n=553).

UPK3B and PCDH7 were subsequently analysed using GOBO (splitting the ER+ tamoxifen treated patient cohort (n=176) into 3 groups), to further determine if RFS in tamoxifen treated patients was dependent on magnitude of gene expression.
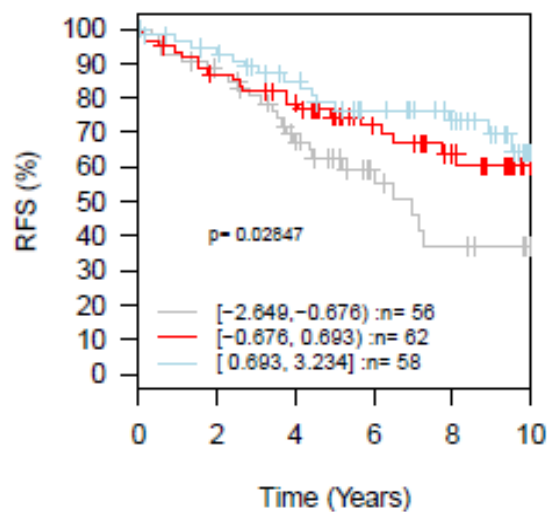
Figure 120: Kaplan Meier survival curve generated using GOBO displaying RFS according to high (blue), intermediate (red) or low (grey) UPK3B gene expression. Expression data used was from ER+ tamoxifen treated breast cancer patients.

The significant association between increased UPK3B expression and RFS following tamoxifen treatment was maintained in the GOBO dataset in ER+ patients treated with tamoxifen (Figure 120) and this relationship was also weakly graded, where greater gene expression of UPK3B appeared to relate to further improved RFS in tamoxifen-treated patients (Figure 120). No significant association was identified with respect to PCDH7 in this smaller patient dataset

UPK3B and PCDH7 were also analysed using KMPlotter in systemically untreated ER+ patients. UPK3B failed to demonstrate a significant association in this untreated group. PCDH7 retained a significant association, where increased expression was associated with an improved clinical outcome (Figure 121). The

hazard ratio was less than 1 indicating a superior RFS in patients with increased PCDH7 expression (HR=0.64 (95%CI 0.47-0.88), p=0.005).
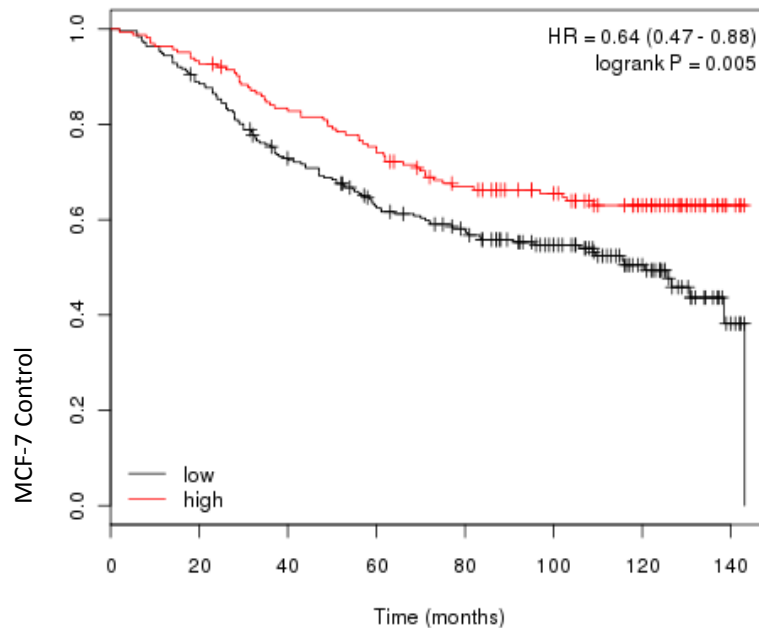
Figure 121: Kaplan-Meier survival curve generated using KMPlotter displaying probability of RFS according to high (red) or low (black) PCDH7 mRNA expression (red line)in ER+ breast cancer patients that were systemically untreated (n=785).

7.2.5 PCR verification of genes potentially involved in extended Faslodex response in the HER2- cell lines

After considering the profile, ontological and clinical expression findings, UPK3B, PCDH7 and additionally ARTN were chosen for PCR verification as genes potentially being involved in the extended Faslodex response in the HER2- cell lines. ELOVL2 and MYRIP were not taken forward as they both failed to demonstrate clinical relevance with respect to tamoxifen using KMPlotter and GOBO and also had very little ontological information available to help relate these gene changes to improved response. Triplicate RNA from untreated and 10 day Faslodex treated cells were used for PCR in an attempt to verify the Affymetrix expression profiles.

7.2.5.1 UPK3B

The microarray data indicated that basal UPK3B expression was elevated in the HER2- cell lines in comparison to the HER2+ models and this was confirmed by PCR (Figure 122). While UPK3B was also increased in the BT474 cell line (Figure 122A and B) which was not seen in the arrays (Figure 96). Indeed, the biggest fold induction was observed in the BT474 cell line by PCR, possibly because of its low basal expression. However, Faslodex treatment in the HER2- cell lines led to a higher UPK3B expression (Figure 122) as seen in the array data. It is possible that the induction observed in the BT474 cell line may be due to sample variation.

Gene Acronym	Fold change of expression following Faslodex treatment			
	BT474	MDA-MB-361	MCF-7	T47D
UPK3B	2.64	0.88	1.50	1.66
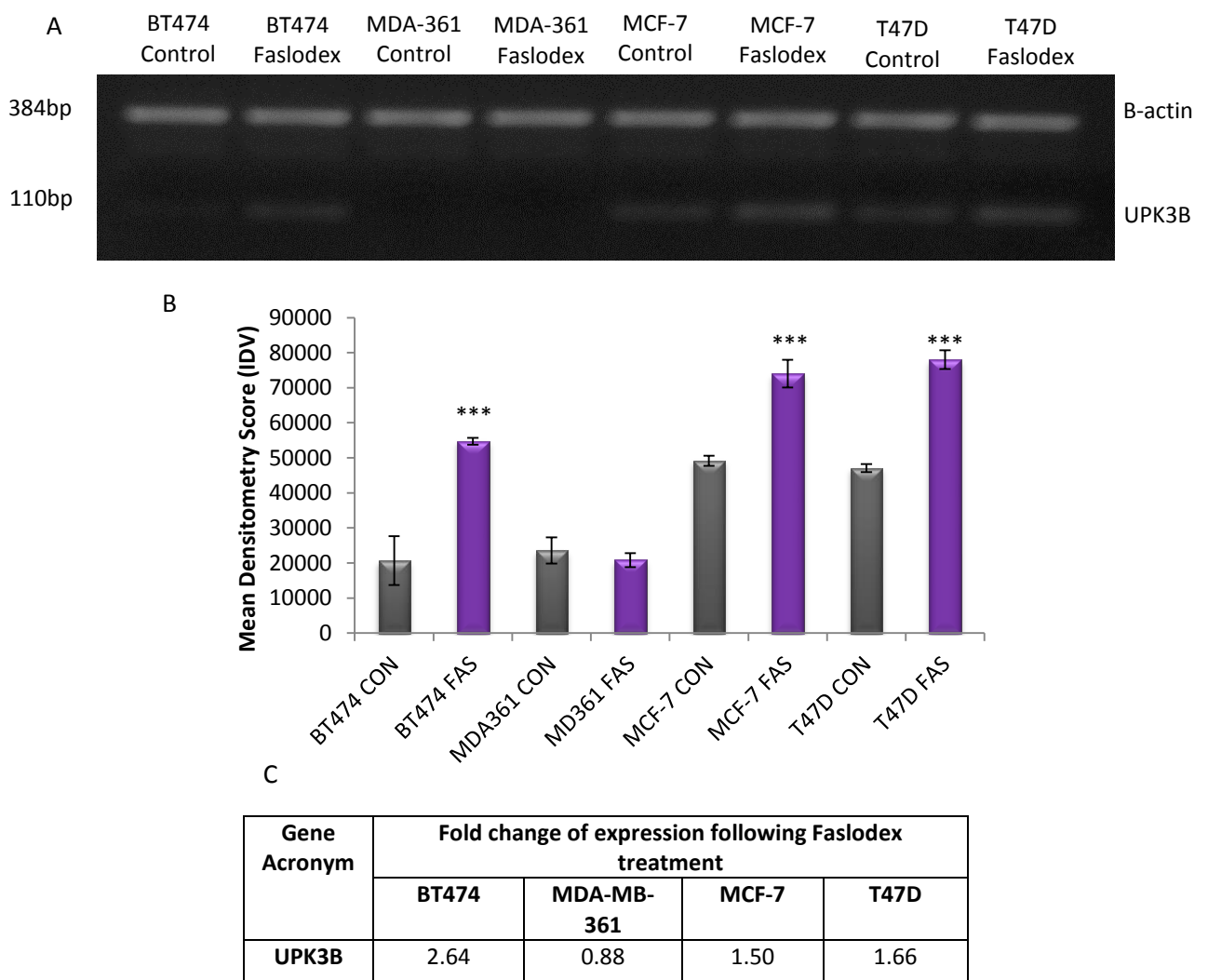
Figure 122: (A) Representative PCR image and (B) the corresponding β-actin-normalised densitometry graph (CON-Control; FAS-10 days Faslodex) for UPK3B. The results are expressed as means ± SEM of three separate experiments. ***$P < 0.001$ versus control. (C) Table displaying the fold change of gene expression following Faslodex treatment.

7.2.5.2 PCDH7

As for the microarray data, basal expression of PCDH7 was largely equivalent across the 4 cell lines, with significant induction of expression by Faslodex only in the HER2- cells (Figure 123). Fold Induction of expression was prominent in both cell lines (Figure 123C) and, in agreement with the array data, the biggest induction was observed in the T47D cell line (Figure 99).
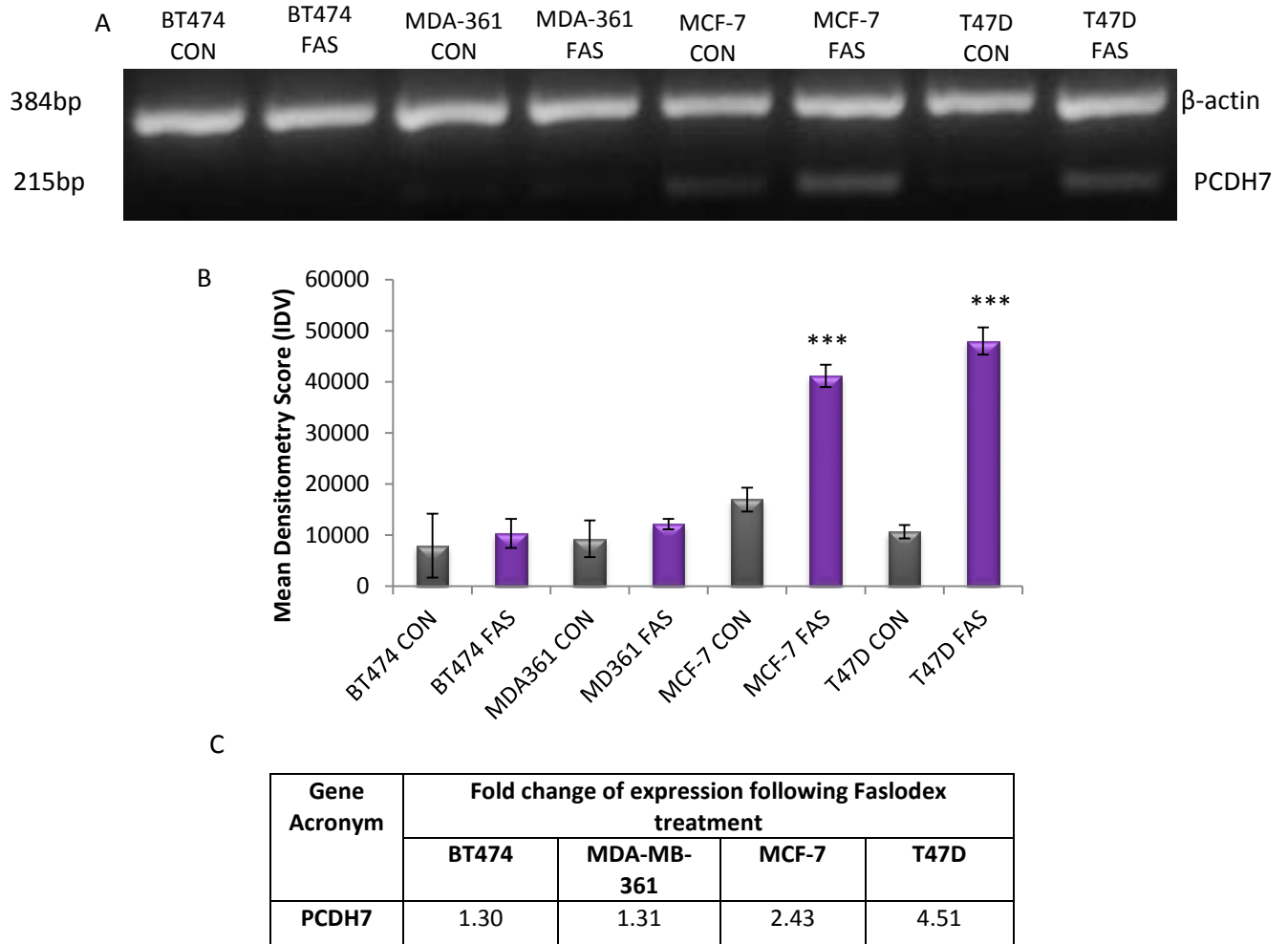
Figure 123: (A) Representative PCR image and (B) the corresponding β-actin-normalised densitometry graph (B (CON-Control; FAS-10 day Faslodex) for PCDH7. The results are expressed as means ± SEM of three separate experiments. ***$P < 0.001$ versus control. (C) Table displaying the fold change of gene expression detected by PCR following Faslodex treatment.

7.2.5.3 ARTN

Using PCR, ARTN was significantly suppressed by 10 day Faslodex treatment in the HER2- cell lines, particularly T47D, (>1.5 fold) in agreement with the microarray data (Figure 102). These findings contrasted the significantly induced of this gene in the HER2+ cell lines which was not seen on the arrays (Figure 124), disparity which may be due to a somewhat sub-optimal performance of the jetset gene probe in the HER2+ cells on the arrays (since the jetset score was 0.2; Table 30).

Gene Acronym	Fold change of expression following Faslodex treatment			
	BT474	MDA-MB-361	MCF-7	T47D
ARTN	3.43	1.40	2.11	2.89
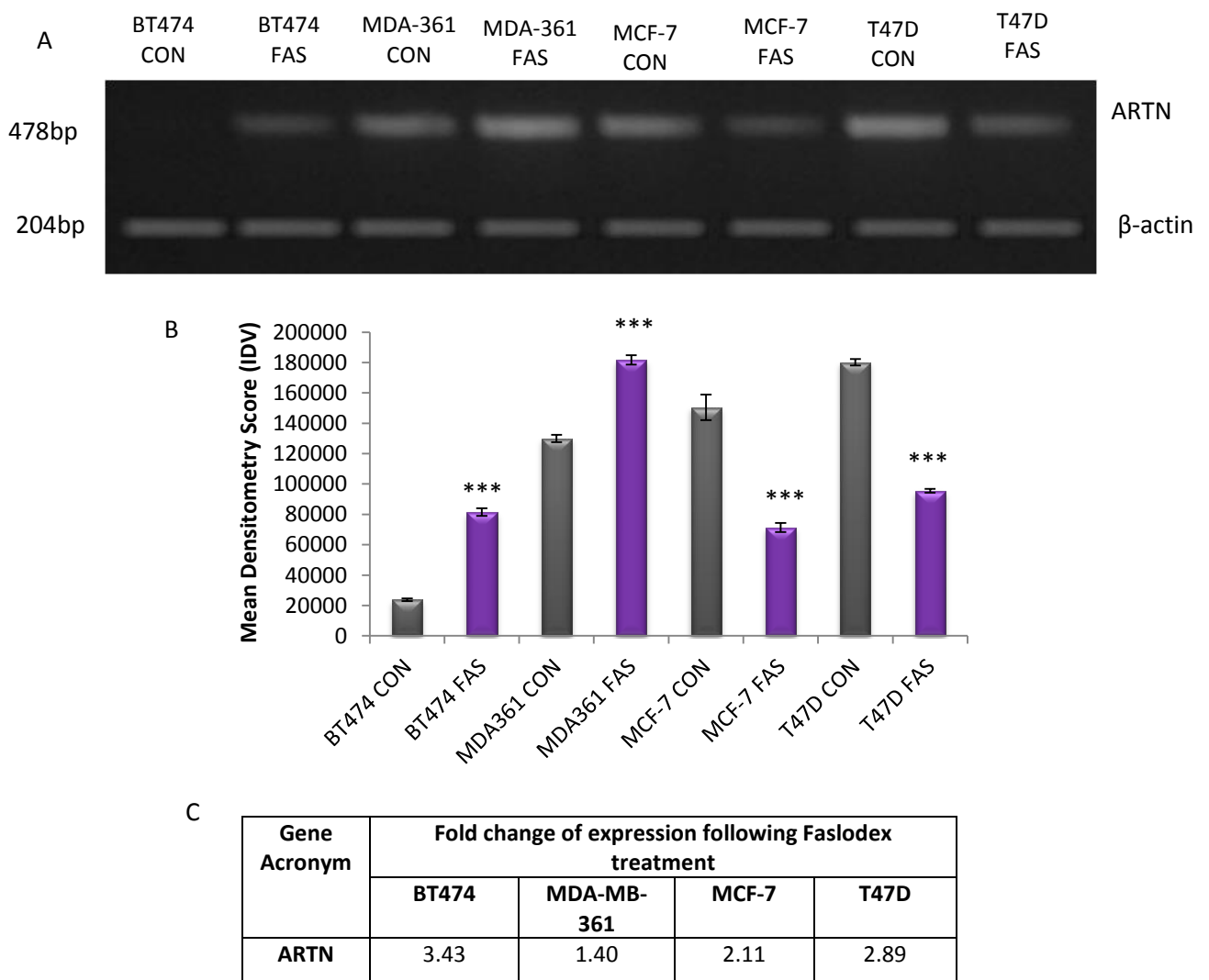
Figure 124: (A) Representative PCR image and (B) the corresponding β-actin-normalised densitometry graph (CON-Control; FAS-10 day Faslodex) for ARTN. The results are expressed as means ± SEM of three separate experiments. ***$P < 0.001$ versus control. (C) Table displaying the fold change of gene expression detected by PCR following Faslodex treatment.

In summary, PCDH7 and UPK3B were thus confirmed to be significantly up-regulated in the HER2- cell lines by 10 day Faslodex treatment, while ARTN was significantly suppressed, in agreement with the array data for these two models.

This data is summarised in Table 39 which compares the results from the microarray data with the PCR results. There is generally a good concordance between the array and PCR results with the exception of the induction of UPK3B in the BT474 cell line as validated by PCR and the unexpected induction of ARTN in the ER+/HER2- (BT474 and MDA-MB-361) cell models.

Table 39: Comparison of Faslodex-deregulation of genes of interest from the microarray data and PCR results (I-Induced; S-Suppressed; ~ limited/no change)

Gene Name	Microarray (FAS de-regulation)				PCR (FAS de-regulation)			
	BT474	MDA-361	MCF-7	T47D	BT474	MDA-361	MCF-7	T47D
UPK3B	~	~	I	I	I	~	I	I
PCDH7	~	~	I	I	~	~	I	I
ARTN	~	~	S	S	I	I	S	S

7.3 Discussion

HER2- MCF-7 and T47D cells underwent a superior Faslodex anti-tumour response during long term *in vitro* culture compared with their HER2+ counterparts. In Chapter 3 it was shown that Faslodex promoted a similar down-regulation of ER and ER-regulated genes in all of the models and thus this phenomenon fails to explain the varying anti-tumour responses observed between HER2+ and HER2- cells. However, it is feasible that there may be Faslodex de-regulated genes shared by both the MCF-7 and T47D cell lines whose discovery may be more informative regarding the mechanism of Faslodex response in HER2- breast cancer.

In light of this, in this chapter following initial SAM analysis and t-test filtering 16 genes were successfully identified as being significantly Faslodex de-regulated in both these HER2- cell lines by at least 1.5 fold. 10 were found to be induced by Faslodex treatment in both cell lines and 6 were suppressed (Table 29). These genes then underwent further filtering, by using their Jetset probes to interrogate

expression using intensity plots and also ensuring any additional gene probes for the individual genes showed the same change in expression. No genes were rejected on the basis of multiple probe profile but half were dismissed following analysis of the intensity plots (i.e. PTPRJ, ITIH1, ANK1, ALOX5, SH3TC2, KRT4, NPY5R and PYY) because Faslodex induction was also noted in HER2+ cells or because of low log2 intensity values/absent detection calls indicating unreliable expression. This filtering strategy was successful in prioritising 8 genes for further investigation. VGLL1, UPK3B, PCDH7 and NR2F1 were all induced by Faslodex treatment in the HER2- cells on the arrays while ARTN, MYRIP, SULF1 and ELOVL2 were suppressed. One of the rejected genes, KRT4 (CK4), highlights a potential limitation of the stringent filtering process that was essential in the thesis to achieve prioritisation. The KRT4 log2 intensity plot (Figure 94) showed a present call for expression after Faslodex induction in T47D but not MCF7 cells, so this gene could still potentially contribute to response in the former model. Indeed, further cytokeratins have been associated with breast cancer patient outcome (Alshareeda *et al.*, 2013) while their down-regulation can encourage epithelial-mesenchymal transition (Thiery *et al.*, 2006).

The 8 prioritised genes were subsequently assessed in MCF-7 derived acquired Faslodex-resistant cells (Hiscox *et al.*, 2006) in an attempt to confirm or refute the hypothesis that changes in their expression may be involved in response (Figures 108-116). 5 of the genes exhibited the same direction of expression change in the Faslodex-resistant cells as seen following 10 day treatment (i.e. induction of VGLL1 and UPK3B, suppression of ARTN, SULF1 and ELOVL2), which may mean these particular genes do not contribute to response in the HER2- cells. Alternative explanations could be that these gene changes contribute to early "compensatory" survival signalling, limiting initial antitumour effect and permitting resistance development in MCF7 cells. However, it is also feasible that the 5 genes do contribute to response, but their beneficial effects are bypassed by alternative signalling pathways in the resistant MCF7 cells or perhaps that they have a change in function, contributing to growth inhibition in the Faslodex sensitive phase while positively involved in resistant growth. Indeed, dual function has been reported for

TGF-β which can act as a tumour suppressor in early stage breast cancer but contribute to progression later in the course of this disease (Tian *et al.*, 2009). The remaining genes PCDH7, NR2F1 and MYRIP exhibited different changes in expression when analysed in the resistant model setting compared with 10 day Faslodex treatment (Figure 18). While these profiles were weaker for NR2F1 and MYRIP, PCDH7 was clearly induced by early treatment but was not expressed in resistance. Based on expression profiles, it was thus also feasible that PCDH7 could be involved in HER2- responses to Faslodex.

However, ontological interrogation was required to further determine if any of the priortised genes, notably PCDH7, VGLL1, UPK3B, ARTN, SULF1 and ELOVL2, were likely candidates in relation to anti-tumour response of the HER2- models. The Faslodex upregulated gene VGLL1 had been previously associated with disease progression (Pobbati *et al.*, 2012; Avruch *et al.*, 2012), and coupled with its induction in both HER2- cell lines and maintained induction in the Faslodex resistant MCF-7 cells, this did not support a contribution for VGLL1 in drug responses so this gene was rejected from further analysis. The Faslodex suppressed gene SULF1 was also eliminated because of its reported role as a tumour suppressor (Narita *et al.*, 2006, 2007). Interestingly, however, analysis of published literature showed that the further Faslodex-suppressed gene ARTN had been associated with cancer progression (Kang *et al.*, 2010) including in breast cancer. ARTN is a ligand for GFRA1 or GFRA3 which are RET co-receptors, and increases in such signalling have also been associated with tamoxifen or oestrogen deprivation resistance (Morandi *et al.*, 2013). Using microarrays, GFRA1 and RET were Faslodex-suppressed and GFRA3 expression was absent in the HER2- cells (Figures 35 and 117). GFRA1, ARTN and RET are reported to be induced by oestrogen (Kang *et al.*, 2011) in accordance with the Faslodex suppression observed, and so in total it is feasible that suppression of ARTN/RET signalling is an important mediator of superior Faslodex response in HER2- cells. As ARTN was not recovered in the Faslodex-resistant MCF-7 line (Figure 113) ARTN-independent signalling seems likely to promote emergence of resistance with this particular antihormone.

The further genes UPK3B, PCDH7 and ELOVL2 had no or very limited useful ontological information (Tables 32, 33 and 38) so this approach precluded assumptions on their possible involvement in the HER2- growth inhibitory response with Faslodex. Consequently, KMPlotter and GOBO proved invaluable as these tools were able to show that inherent elevated UPK3B and PCDH7 expression associated with an improved duration of response to tamoxifen, in keeping with tumour suppressive functions and supportive of a role in contributing to superior Faslodex response in the HER2- cells (Figures 118-120). PCDH7 also displayed predictive biomarker potential for tamoxifen since the relationship was absent in untreated patients (Figure 121).

PCR was thus performed on ARTN, UPK3B and PCDH7 since these comprised the strongest candidates for relationship to Faslodex response in the HER2- cells following the ontological or clinical interrogation. PCR was able to successfully verify that Faslodex repression of ARTN and induction of PCDH7 occurred in the HER2- cells only (Figures 122 and 123), further confirming that these changes may contribute to the extended Faslodex response in HER2- cells. Interestingly, PCR also suggested that ARTN could be up-regulated by Faslodex in the HER2+ cell lines (Figure 124). This may indicate that induction of ARTN (along with RET co-expression (Figure 117)) could be involved in the onset of resistance and in limiting Faslodex impact in the HER2+ cells, in keeping with the literature associating such signalling with disease progression and resistance (Kang *et al.*, 2010; Plaza-Menacho *et al.*, 2010; Morandi *et al.*, 2013). It was perhaps surprising that ARTN, reported to be oestrogen regulated, is induced in these models despite Faslodex treatment. However, ARTN has been associated with TWIST1 and VEGFA signalling in ER- breast cancer (Banerjee *et al.*, 2012), and so it is feasible that alternative signalling is similarly promoted when Faslodex suppresses ER in HER2+ cells, driving ARTN expression. Also, ARTN has been shown to be regulated by miR-223 in oesophogeal cancer (Li *et al.*, 2011b) and so it's up-regulation in the HER2+ lines may reflect impact of Faslodex on micro-RNA profile in these cells. The PCR studies in this project were also able to confirm that UPK3B was significantly induced by Faslodex in the HER2- cell lines. However, the significant induction of UPK3B also

detected in the HER2+ BT474 cell line questioned any involvement for this gene in the superior responses to Faslodex in the HER2- cells (Figure 122).

Thus, genes of prime importance for further study emerging in this chapter are PCDH7 and ARTN. Cumulatively, the data presented suggest that PCDH7 could be a Faslodex-induced tumour suppressive gene while ARTN could be a Faslodex-suppressed growth-promoting gene in the HER2- cells. As shown in chapter 3, HER2 positivity is a likely factor contributing to the inferior Faslodex anti-tumour responses in BT474 and MDA-MB-361 cells, but further study of PCDH7 and ARTN could help understand the mechanism of superior drug response in the HER2- lines and in turn the varying drug responses that occur within ER+/HER2- patients to anti-hormones including Faslodex (Di Leo *et al*,. 2010). Their continued study could potentially reveal new therapeutic approaches or biomarkers to maximise Faslodex response in breast cancer.

Chapter 8

Identification of Faslodex-de-regulated genes potentially involved in shortened Faslodex responses observed in both the BT474 and MDA-MB-361 HER2+ cell lines

8.1 Introduction

Although HER2 over-expression has been correlated with an inferior response to tamoxifen and AIs (Rasmussen *et al.*, 2008), its clinical relationship to Faslodex response does not seem so clear cut, with Faslodex responses having been reported in ER+/HER2+ disease in more than one trial (Robertson *et al.*, 2009; Mello *et al.*, 2011). Nevertheless, many ER+ breast cancer patients treated with Faslodex ultimately develop resistance during treatment and this project has also shown ER+/HER2+ cells have potential to develop such resistance more rapidly.

In the ER+ MCF-7 breast cancer line, it has been reported that short-term anti-hormone treatments, including Faslodex, can promote the up-regulation of erbB/HER family members and that such elements are maintained into emerging resistant lines and can be targeted alongside anti-hormone to control resistant growth (Gee *et al.*, 2011). Co-treatment of ER+/HER2+ cell lines with erbB inhibitors (including trastuzumab or lapatanib) and endocrine agents has also been reported to have a superior inhibitory effect versus monotherapy with respect to delaying the onset of resistance, suggesting that for improved drug response inhibition of ER and erbB signalling pathways may be required (Kunisue *et al.*, 2000). However, despite these promising results *in vitro* and some improved response in ER+/HER2+ patients during anti-hormone and trastuzumab/lapatanib co-treatment, a common outcome for these patients is relapse. This suggests that there are likely to be other compensatory mechanisms utilised to overcome endocrine therapy and establish a resistant phenotype in ER+/HER2+ disease. Such mechanisms could be due to

inherent genetic background (not just HER2 status) or be due to unknown anti-hormone induced events.

In this chapter gene expression data from BT474 and MDA-MB-361 HER2+ cell lines has been used to attempt to identify Faslodex-induced genomic changes not apparent in the HER2- lines, where it is hypothesised that such changes could potentially be involved in ER+/HER2+ cell acquisition of resistance to Faslodex. By identifying further induced genes, novel mechanisms of Faslodex resistance may be identified that could encompass potential therapeutic targets to maximise Faslodex response in the ER+/HER2+ disease cohort or biomarkers of reduced Faslodex response.

8.2 Results

8.2.1 Identification of genes uniquely Faslodex de-regulated in the HER2+ cell lines

A similar filtering process to that used in previous chapters was employed to identify potential resistance-promoting genes altered by Faslodex only in the HER2+ cell lines. Genes significantly altered (SAM FDR <0.05; t-test p <0.05) were further analysed to identify those genes exhibiting a change in expression greater than 1.5 fold following 10 day Faslodex treatment in both the BT474 and MDA-MB-361 cell lines and these are listed in Table 39.

As you can see from Figure 124 only 24 were significantly altered in the ER+/HER2+ cell lines and further only 10 were identified to exhibit at least 1.5 fold change in both models.
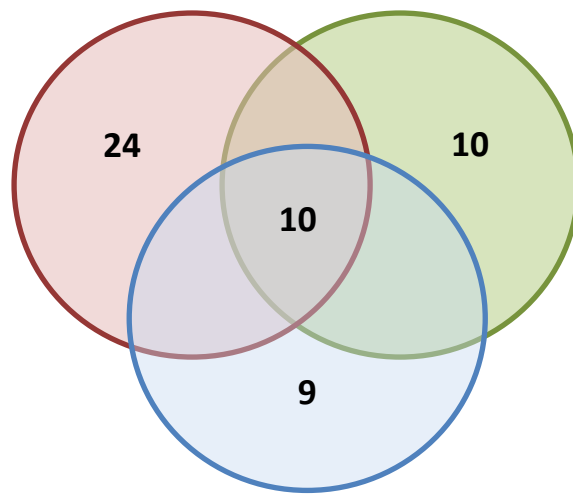
Figure 124: The Venn diagram illustrates the identification of the 10 genes taken forward as potential mediators/biomarkers of reduced Faslodex response as observed in the BT474 and MDA-MB-361 cell lines. The red circle represents all those genes significantly altered in the BT474 and MDA-MB-361 cell lines. The green circle, shows the number of these genes that were not altered by at least 1.5 fold in these two models and the blue circle are those that were found to be also altered to some extent in the T47D and/or MCF-7 cell lines. The 10 genes represented by the overlapping circles identify those genes that met the criteria to be taken forward for further investigation.

273

Table 39: Genes whose expression was significantly altered in both HER2+ cell lines (BT474 and MDA-MB-361) following 10 day Faslodex treatment and the associated change in expression (induced or suppressed). Also listed is the number of gene probes that represent a given gene on the Affymetrix UI33A genechip and the number of probes exhibiting the same change in expression.

Potential resistance promoting-genes in BT474 & MDA-MB-361	Gene Name	Gene expression change following Faslodex treatment	Total n.o. gene probes	Total number of probes exhibiting expected change in expression	
				BT474	MDA-MB-361
SERPINI1	Serpin peptidase inhibitor, clade I (neuroserpin), member 1.	Induced	1	1	1
CDH2	Cadherin 2	Induced	2	2	2
FAM155A	Family with sequence similarity 155, member A.	Induced	1	1	1
CYP2B6	Cytochrome P450 2B6	Suppressed	1	1	1
CYP2B7P1	Cytochrome P450, family 2, subfamily B, polypeptide 7 pseudogene 1.	Suppressed	1	1	1
DDX3Y	DEAD box polypeptide 3, Y-linked.	Suppressed	2	2	2
SLC6A14	Solute carrier family 6 (amino acid transporter), member 14.	Suppressed	1	1	1
GOLM1	Golgi membrane protein 1	Suppressed	1	1	1
HSPG2	Heparan sulfate proteoglycan 2.	Suppressed	2	2	1
HFE	Human hemochromatosis protein	Suppressed	13	7	1

From Table 39 it can be seen that 7 of the 10 gene probes were suppressed by Faslodex treatment in the HER2+ cell lines, and that for most of the genes identified the multiple probes showed the same directional change in expression in both HER2+ cell lines. The exceptions were HSPG2 where only 1 of the 2 gene probes

was suppressed in the MDA-MB-361 cell line, and HFE which was represented by 13 gene probes, where only 7 were suppressed in the BT474 cell line and only 1 in the MDA-MB-361 cell line. Analysis of the HFE jetset probe (211330_s_at) in the HER2+ cell lines was not consistent with suppression in both models and as a consequence no further work was undertaken for HFE.

All further analyses investigating the potential of the remaining gene changes to be involved in the poorer Faslodex response in HER2+ cells was carried using the jetset Affymetrix gene probes for these genes. Table 40 lists the gene names along with their associated jetset Affymetrix probe ID and jetset score. Even though the gene probe ID's had been selected as the best probe for a given gene based on specificity, coverage and degradation resistance (as predicted by jetset), some of the jetset scores were low (e.g. FAM155A, CYP2B6) suggesting caution was needed when considering the expression profiles of such genes in the HER2+ cells.

Table 40: Genes identified as being Faslodex de-regulated in both HER2+ cell lines and their associated jetset Affymetrix gene probe ID and jetset score (closer to 1 the better the predicted performance).

HER2+ shared genes	Jetset Affy Probe ID	Jetset score
SERPINI1	205352_at	0.52263382
CDH2	203440_at	0.60799729
FAM155A	214825_at	0.04316956
CYP2B6	206754_s_at	0.17823764
CYP2B7P1	210272_at	0.20452182
DDX3Y	205000_at	0.24612241
SLC6A14	219795_at	0.52499114
GOLM1	217771_at	0.32647773
HSPG2	201655_s_at	0.54826069

Using the jetset Affymetrix gene probes, the genes were further analysed using the software program GeneSifter. Figure 125 display the direction of expression change for those genes identified as being de-regulated by Faslodex in the HER2+ cell lines using heatmaps, confirming that 6 were suppressed and 3 were induced in both models. Further investigation of gene expression changes were carried out by analysis of the intensity plots generated using the log2 transformed normalised data (Figures 126-134). Analysis of these plots allowed an investigation of the magnitude of induction or suppression of the gene in all 4 cell lines. By investigating the log2 transformed intensity values, as well as the detection call, it was possible to determine whether gene expression was robust and thus could be potentially PCR verified
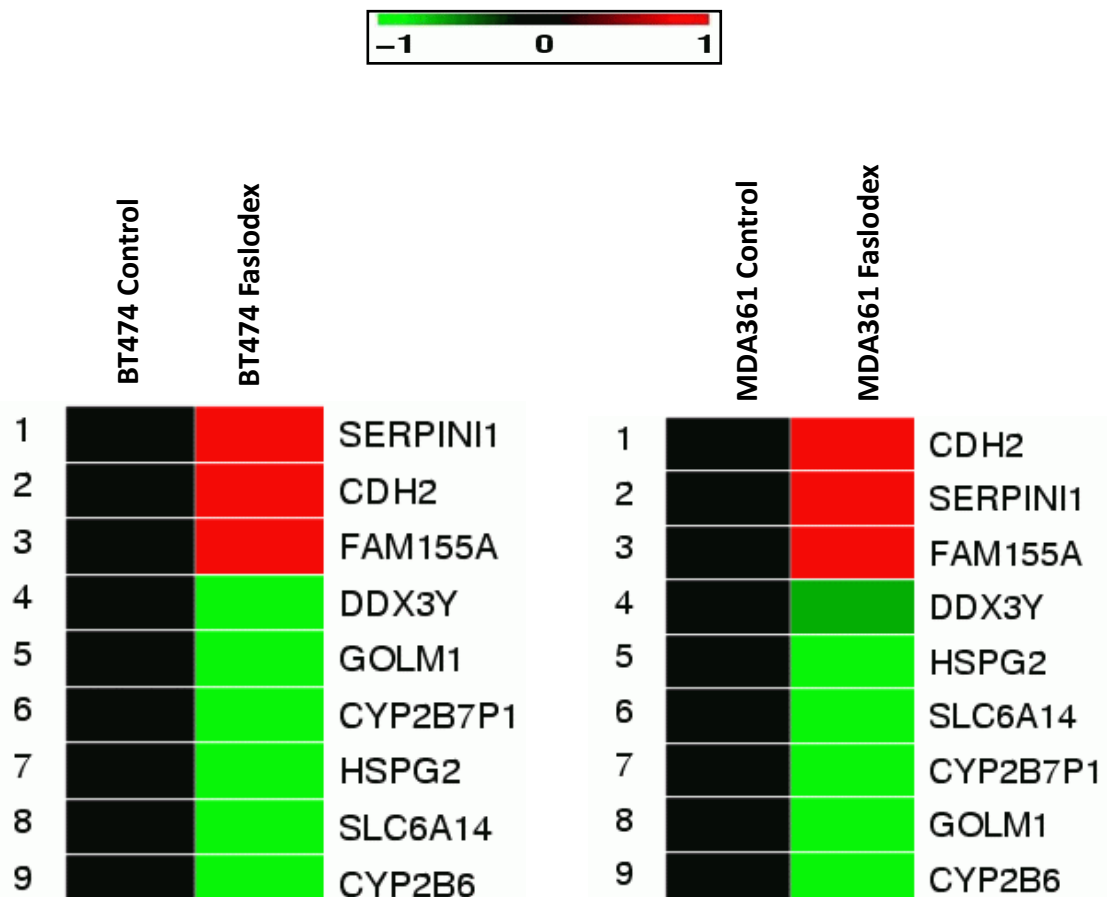
Figure 125: Heatmaps displaying the induction or suppression of genes altered by 10 day Faslodex treatment in both HER2+ cell lines generated by GeneSifter using jetset probes.

8.2.1.1 Genes induced by Faslodex in the ER+/HER2+ cell lines

8.2.1.1.1 SERPINI1

SERPINI1 was substantially induced by 10 day Faslodex treatment in both HER2+ cell lines (Figure 126). All detection calls were present in the HER2+ cell lines pre and post treatment with positive log2 intensity values after Faslodex, indicative of robust induction which was further confirmed by the good jetset score of the SERPINI1 gene probe (Table 40). In the MCF-7 cell lines basal expression was very low and Faslodex exerted no expression change. In contrast, in the T47D cell line, basal expression was relatively high and SERPINI1 was suppressed 8 fold following Faslodex treatment.
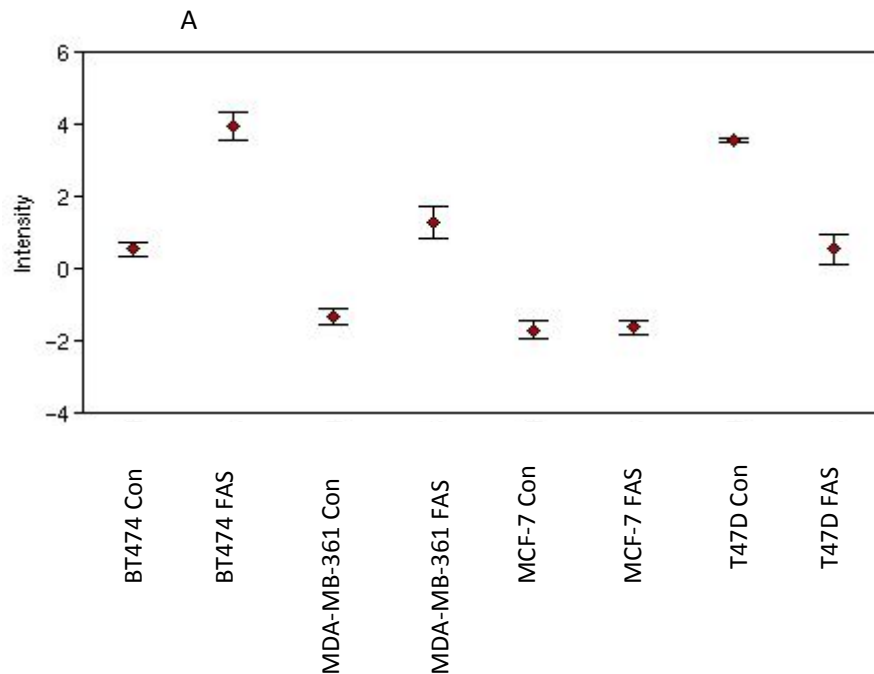
Gene Acronym	Fold change of expression following Faslodex treatment			
	BT474	MDA-MB-361	MCF-7	T47D
SERPINI1	10.64	6.16	1.05	8.12

Figure 126: (A) Log2 intensity plot displaying the normalised (mean of triplicate samples) gene expression of SERPINI1 in each of the 4 cell lines pre (Con) and post 10 day Faslodex (FAS) treatment (B) Table displaying the fold change in gene expression promoted by 10 day Faslodex treatment in each cell line vs. untreated control. Highlighted in red are inductions in gene expression and in green suppression of expression >1.5 fold.

8.2.1.1.2 CDH2

Basal gene expression of CDH2 was elevated in the HER2+ cell models compared to the HER2- cell lines, where Faslodex treatment further induced CDH2 expression (8 fold) in the HER2+ cells (Figure 127). Pre and post treatment, CDH2 detection calls were present in the HER2+ cell lines, while absent calls were recorded in the HER2- cell lines where all log2 intensity values were below 0, indicative of a lack of expression and so unreliable profile in the HER2- cells. As may be seen in Table 40, the jetset probe performance was predicted to be relatively high, providing further confidence in the gene expression profiles generated.
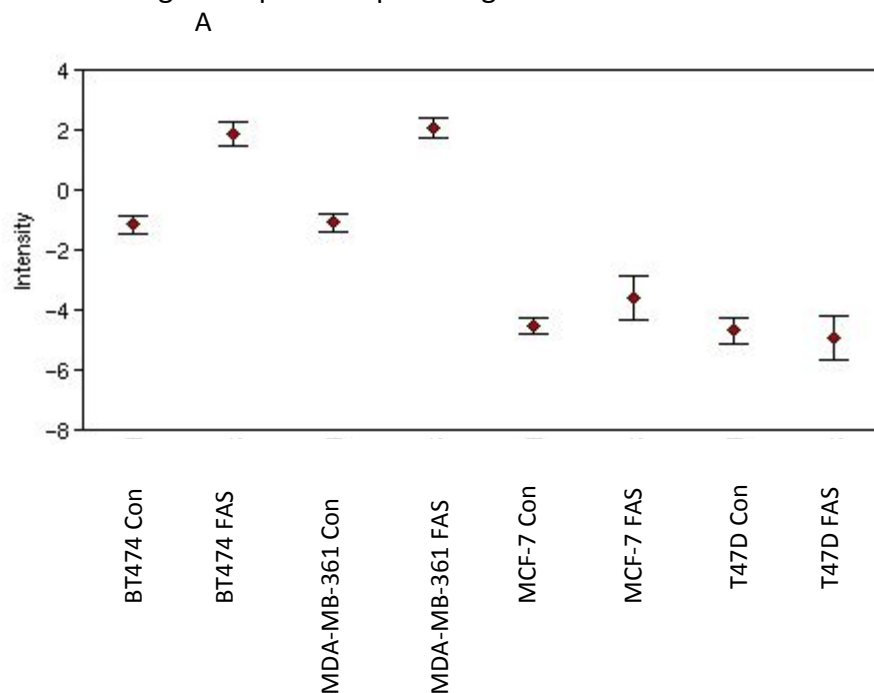
A

B

Gene Acronym	Fold change of expression following Faslodex treatment			
	BT474	MDA-MB-361	MCF-7	T47D
CDH2	8.24	8.83	1.88	1.18

Figure 127: (A) Log2 intensity plot displaying the normalised (mean of triplicate samples) gene expression of CDH2 in each of the 4 cell lines pre (Con) and post 10 day Faslodex (FAS) treatment (B) Table displaying the fold change in gene expression promoted by 10 day Faslodex treatment in each cell line vs. untreated control. Highlighted in red are inductions in gene expression >1.5 fold.

8.2.1.1.3 FAM155A

Although FAM155A level was induced in both HER2+ cell lines, the increase was greatest in the MDA-MB-361 cell line (Figure 128). Log2 transformed intensity levels, however, were low pre and post treatment (below 0) in all cell lines and the detection calls were absent so that any changes were unreliable. The poor jetset score for FAM155A (Table 40) may contribute to its weak expression profile.
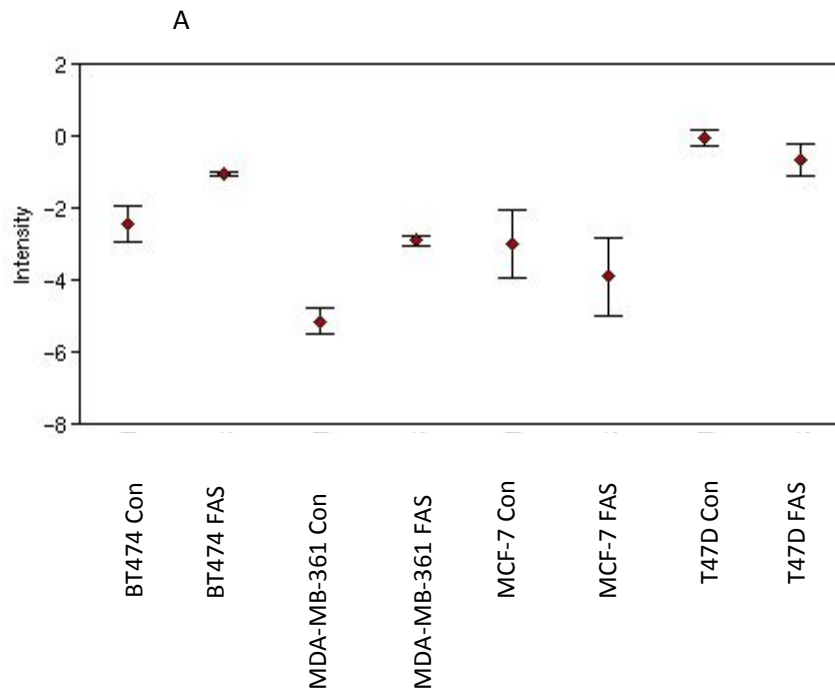
A

B

Gene Acronym	Fold change of expression following Faslodex treatment			
	BT474	MDA-MB-361	MCF-7	T47D
FAM155A	2.62	4.75	1.88	1.51

Figure 128: (A) Log2 intensity plot displaying the normalised (mean of triplicate samples) gene expression of FAM155A in each of the 4 cell lines pre (Con) and post 10 day Faslodex (FAS) treatment (B) Table displaying the fold change in gene expression exerted by 10 day Faslodex treatment in each cell line vs. untreated control. Highlighted in red are the inductions in gene expression and green the suppression in expression >1.5 fold.

8.2.1.1.4 CYP2B6

The basal log2 intensity values of CYP2B6 in the HER2+ cell lines were higher than those recorded in the HER2- cells, where positive calls were detected in the HER2+ lines only. While following Faslodex treatment, the log2 intensity values of CYP2B6 were minimally changed in the HER2- cell lines with detection calls remaining absent, the HER2+ cell lines showed a substantial suppression in CYP2B6 expression. The BT474 cell line showed a change in detection call from present to absent following Faslodex, indicative of a particularly large suppression, while both detection calls for the MDA-MB-361 cell line remained present, indicative of some residual expression. In total, CYP2B6 appeared substantially suppressed in HER2+ cells following Faslodex, although some caution should be observed due to the poorer jetset score for this gene (Table 40).
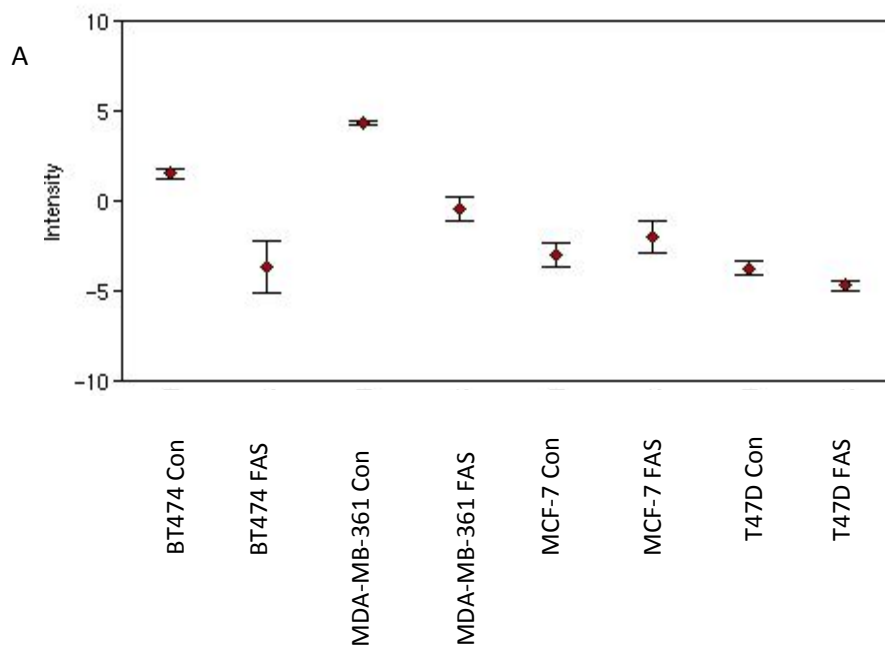
Gene Acronym	Fold change of expression following Faslodex treatment			
	BT474	MDA-MB-361	MCF-7	T47D
CYP2B6	36.04	27	1.96	1.89

Figure 129: (A) Log2 intensity plot displaying the normalised (mean of triplicate samples) gene expression of CYP2B6 in each of the 4 cell lines pre (Con) and post 10 day Faslodex (FAS) treatment (B) Table displaying the fold change in gene expression exerted by 10 day Faslodex treatment in each cell line vs. untreated control. Highlighted in red are the inductions in gene expression and in green the suppressions >1.5 fold.

8.2.1.1.5 CYP2B7P1

From the log2 intensity plot presented in Figure 130, it can be seen that CYP2B7P1 basal expression was elevated (with positive log2 intensity values) in the HER2+ versus the HER2- cell lines and that Faslodex treatment suppressed its expression in both HER2+ models. In each instance in the HER2+ models, detection calls altered from present to absent on Faslodex treatment, indicative of a robust suppression of gene expression. Log2 intensity levels were below 0 in the HER2- cell lines both before and after Faslodex and detection calls were absent.
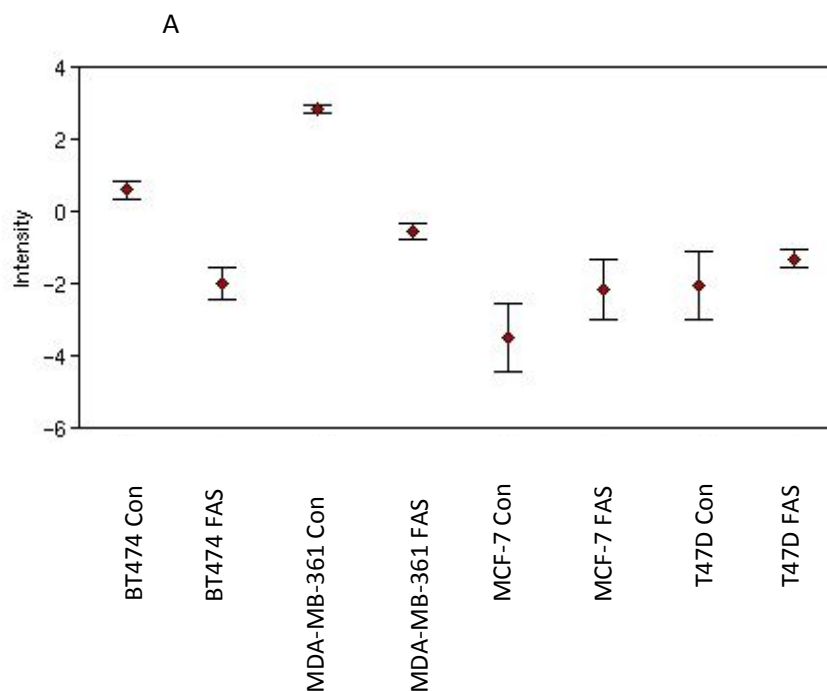
A

B

Gene Acronym	Fold change of expression following Faslodex treatment			
	BT474	MDA-MB-361	MCF-7	T47D
CYP2B7P1	5.96	10.53	2.52	1.65

Figure 130: (A) Log2 intensity plot displaying the normalised (mean of triplicate samples) gene expression of CYP2B7P1 in each of the 4 cell lines pre (Con) and post 10 day Faslodex (FAS) treatment (B) Table displaying the fold change in gene expression exerted by 10 day Faslodex treatment in each cell line vs. untreated control. Highlighted in red are the inductions and in green suppressions in gene expression >1.5 fold

8.2.1.1.6 DDX3Y

From the log2 intensity values in Figure 143 it can be seen that levels of DDX3Y were very low in all cell models both pre and post Faslodex (all below 0) and that some suppression of its expression appeared to be detected in all models post-Faslodex treatment. All detection calls were, however, absent and together with a poor jetset probe score (Table 40) this suggested an unreliable profile.
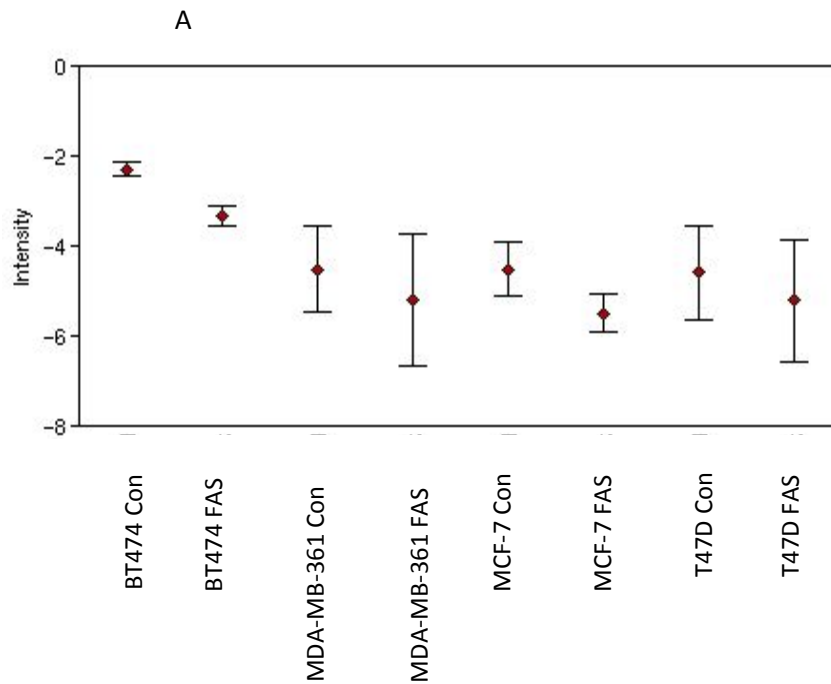
A

B

Gene Acronym	Fold change of expression following Faslodex treatment			
	BT474	MDA-MB-361	MCF-7	T47D
DDX3Y	2.05	1.61	1.98	1.55

Figure 131: (A) Log2 intensity plot displaying the normalised (mean of triplicate samples) gene expression of DDX3Y in each of the 4 cell lines pre (Con) and post 10 day Faslodex (FAS) treatment (B)A table displaying the fold change in gene expression exerted by 10 day Faslodex treatment in each cell line vs. untreated control. Highlighted in green are the suppressions in gene expression >1.5 fold.

8.2.1.1.7 SLC6A14

The log2 intensity data suggested that basal expression of SLC6A14 was elevated in the HER2+ cell models in comparison to the HER2- cell lines, and in both HER2+ models Faslodex treatment suppressed its expression level (Figure 132). In the BT474 cell line, the detection call changed from present to absent after Faslodex treatment, while in the MDA-MB-361 cell line the detection call remained present. Although there was an apparent >1.5 fold suppression of SLC6A14 expression in MCF-7 cells, the detection calls were absent pre and post treatment, indicative of an unreliable profile in this model. Very little change in expression was observed in the T47D cell and very low log2 intensity values were noted pre and post treatment. The jetset score for the SLC6A14 probe was adequate (Table 40), suggestive of a good performing gene probe.

Gene Acronym	Fold change of expression following Faslodex treatment			
	BT474	MDA-MB-361	MCF-7	T47D
SLC6A14	33.14	7.68	1.55	1.41
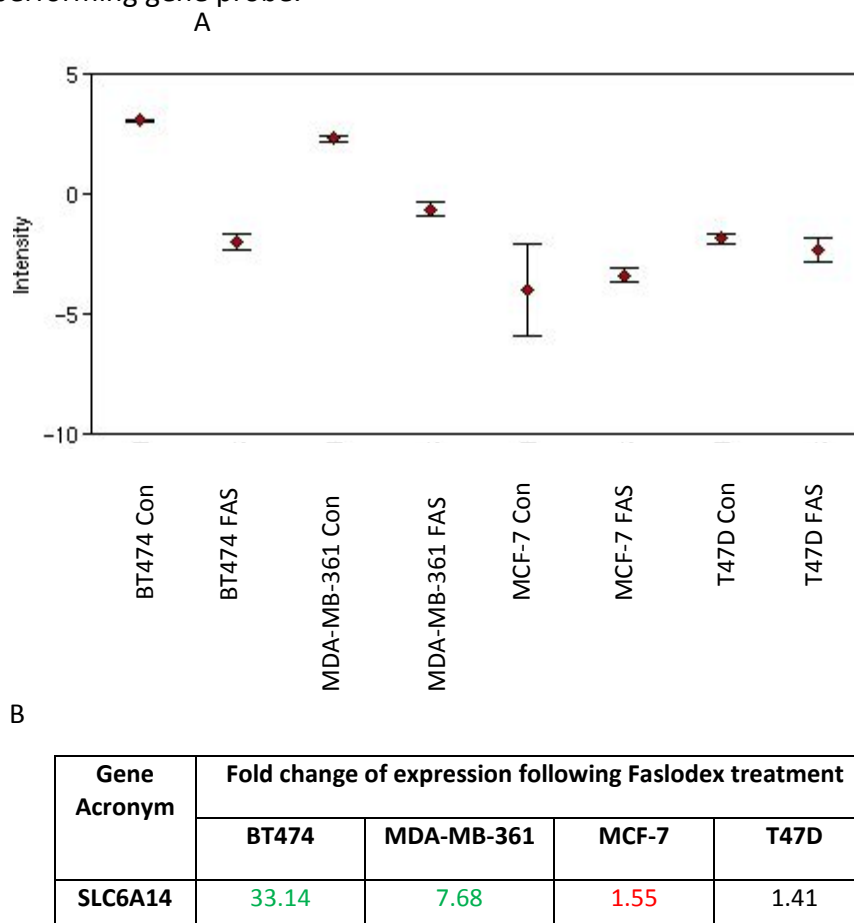
Figure 132: (A) Log2 intensity plot displaying the normalised (mean of triplicate samples) gene expression of SLC6A14 in each of the 4 cell lines pre (Con) and post 10 day Faslodex (FAS) treatment (B) Table displaying the fold change in gene expression exerted by 10 day Faslodex treatment in each cell line vs. untreated control. Highlighted in green are the suppressions in gene expression and red induction of expression >1.5 fold.

8.2.1.1.8 GOLM1

Log2 intensity control values of GOLM1 were similar across the HER2+ and MCF-7 cell lines (although slightly elevated in the T47D cell line) (Figure 133) and suppression of GOLM1 by 10 day Faslodex treatment was found to occur not only in the HER2+ cell lines but also in the T47D model. Each HER2+ cell line showed a change in detection call from present to absent, indicative of a robust suppression. In contrast, the T47D cell line call remained present after Faslodex treatment. Regardless of the adequate predicted jetset performance (Table 40), the robust suppression of GOLM1 in the T47D cell line as well as in the HER2+ cell lines suggested GOLM1 changes were not unique to HER2+ cells; no further work was carried out on this gene.
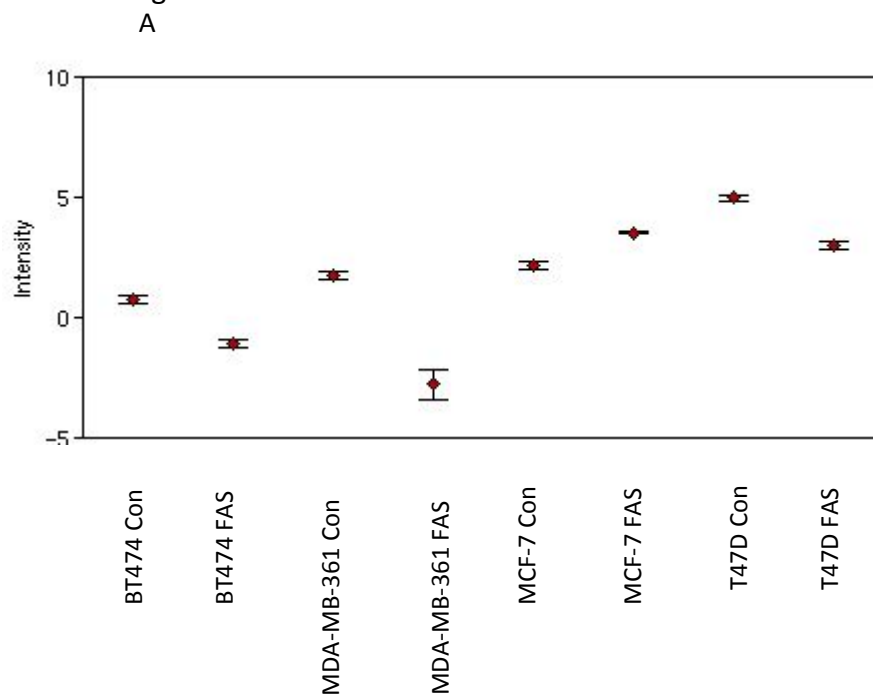
A

B

Gene Acronym	Fold change of expression following Faslodex treatment			
	BT474	MDA-MB-361	MCF-7	T47D
GOLM1	3.50	22.48	2.55	3.97

Figure 133: (A) Log2 intensity plot displaying the normalised (mean of triplicate samples) gene expression of GOLM1in each of the 4 cell lines pre (Con) and post 10 day Faslodex (FAS) treatment (B) Table displaying the fold change in gene expression exerted by 10 day Faslodex treatment in each cell line vs. untreated control. Highlighted in green are the suppressions in gene expression and red inductions of expression >1.5 fold.

8.2.1.1.9 HSPG2

Log2 intensity control values of HSPG2 were similar in the HER2- and BT474 cell lines, while very much suppressed in MDA-MB-361 cells (Figure 134). Faslodex treatment suppressed HSPG2 expression in both the HER2+ cell lines and to an extent in the T47D cell line. However, despite the good predicted performance of this gene probe (Table 40), HSPG2 log2 intensity values in all models pre and post treatment were low and all detection calls were found to be absent, indicative of a lack of expression and so unreliable profile. As HSPG2 was represented by 2 gene probes on the Affymetrix gene chip the second gene probe was also analysed, but found to exhibit an even poorer profile than the jetset gene probe.
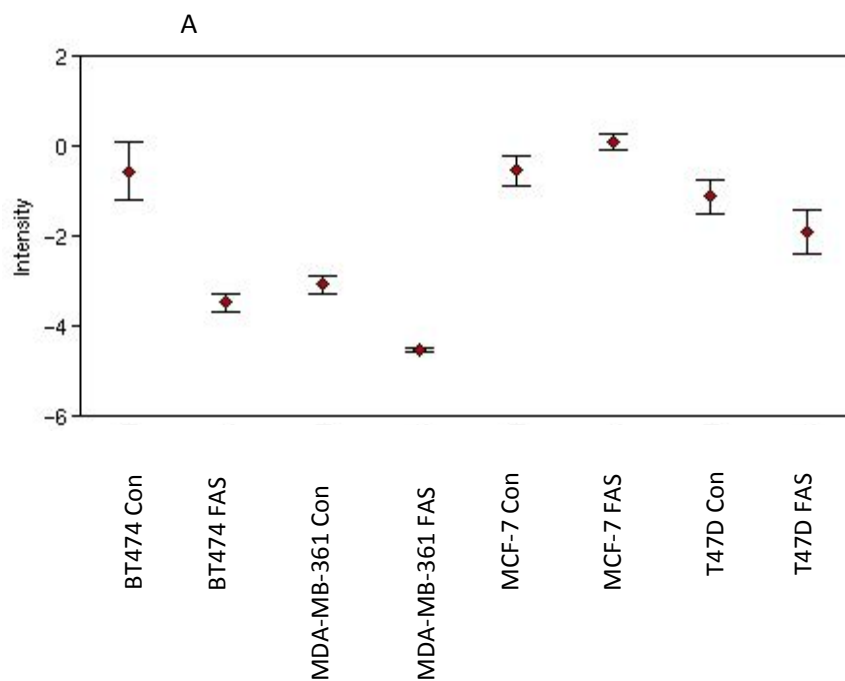
A

B

Gene Acronym	Fold change of expression following Faslodex treatment			
	BT474	MDA-MB-361	MCF-7	T47D
HSPG2	7.54	2.78	1.56	1.73

Figure 134: (A) Log2 intensity plot displaying the normalised (mean of triplicate samples) gene expression of HSPG2 in each of the 4 cell lines pre (Con) and post 10 day Faslodex (FAS) treatment (B) Table displaying the fold change in gene expression exerted by 10 day Faslodex treatment in each cell line vs. untreated control. Highlighted in green are the suppressions in gene expression and red inductions of expression >1.5 fold.

In summary, following analysis of the log2 intensity plots and expression calls, the following genes were dismissed from the investigation; FAM155A, DDX3Y, GOLM1 and HSPG2 due either to a lack of expression and/or not being uniquely de-regulated by Faslodex in the HER2+ cell models.

Further investigations were carried out on the following genes:

- SERPINI1
- CDH2
- CYP2B6
- CYP2B7P1
- SLC6A14

8.2.2 Ontological investigation on those genes potentially involved in limiting Faslodex response in the HER2+ setting.

Ontological investigations were carried out on each of the 5 short-listed genes to determine if they had been previously associated with:

- Breast cancer or any other cancer type;
- Known or potential adverse function (e.g. tumour growth or progression);
- Known or potential tumour suppressive function

The results of the ontological investigations are accumulated in Tables 41 to 45. Pubmed and Scopus were used throughout using the gene name/acronym, together with selected keywords/phrases which included breast cancer, cancer, oncogene, proliferation, growth, metastasis, Faslodex, hormonal or endocrine therapy, survival, growth inhibition, tumour suppressor, apoptosis. Gene acronyms highlighted in red were induced by Faslodex in T47D cells and those in green were suppressed.

Table 41: Summary of published reports investigating the function of SERPINI1 including any reports in breast and other cancers.

Gene Name/Acronym	Serpin peptidase inhibitor, clade 1: **SERPINI1**
Function	SERPINI1 is a serine protease inhibitor that inhibits

	plasminogen activators and plasmin. It may also be involved in the formation or reorganization of synaptic connections as well as synaptic plasticity in the nervous system (Lee *et al.*, 2008)
Associations with breast cancer	No associations with breast cancer
Associations with other cancers	miR21 is overexpressed in gastric carcinoma (Volinia *et al.*, 2006) and has been shown to downregulate SERPINI1 releasing cells from the G1-S transition checkpoint, ultimately leading to an increase in tumour growth. Thus expression of SERPINI1 in gastric cancer has tumour suppressive functions (Yamanaka *et al.*, 2012). The PDCD10 (programmed cell death gene 10) gene is adjacent to the SERPINI1 gene. It has been shown by Chen *et al.*, that transcription of these genes is promoted by the c-myc oncogene and potentially involved in central nervous system (CNS) diseases such as brain cancer (Chen *et al*., 2009). However, SERPINI1 is down-regulated in brain cancer tissues and in cell lines derived from brain cancer suggesting that its expression in brain cancer is tumour suppressive (Chang *et al.*, 2000).

Table 42: Summary of published reports investigating the function of CDH2 including any reports in breast and other cancers.

Gene Name/Acronym	Cadherin 2, N-cadherin: **CDH2/NCAD**
Function	CDH2 is a classical member of the cadherin superfamily. Cadherins play an important role in cell recognition, adhesion, and signalling, and have a significant effect on the progression of tumours (reviewed by Maitre *et al.*, 2008)
Associations with breast cancer	It has been recently noted, that the loss of E-cadherin is associated with an upregulation in N-cadherin in invasive tumour cell lines, including those derived from breast cancer (Hazan *et al.*, 1997). Forced expression of N-CAD in the

	MCF-7 and BT-20 breast cancer cell lines leads to increased motility and a pro-invasive phenotype (Neiman *et al.*, 1999) and metastatic behaviour in nude mice (Hazan *et al.*, 2000). The invasive phenotype encouraged by N-CAD expression is due to its interaction with FGFR1 at the cell membrane (Suyama *et al.*, 2002; Kim *et al.*, 2000). Binding of N-CAD to FGFR1 causes receptor stabilisation and continuous MAPK/ERK activation resulting in enhanced transcription of MMP-9 that leads to the pro-invasive phenotype (Suyama *et al.*, 2002). N-CAD can also encourage metastasis independent of its interaction with FGFR1; namely by homophilic interaction between N-CAD expressing tumour cells and tissues such as the stroma (Hazaan *et al.*, 1997) and endothelium (Hazan *et al.*, 2000) assisting the movement of tumour cells to secondary sites. N-CAD has also been shown to correlate with HER2+ status as well as a HER2+ enriched triple negative molecular subtype in breast cancer patients who underwent surgery for invasive ductal carcinoma (Lee *et al.*, 2012) N-CAD has also been shown to interact with a further cadherin VE-CAD (vascular endothelial cadherin), the main component of endothelial cell adherens junction with prominent roles in angiogenesis and vascular permeability (Dejana *et al.*, 2009). VE-CAD and N-CAD have been shown to be co-expressed in aggressive mouse breast cancer cells, where N-CAD controls the expression of VE-CAD. N-CAD maintains the mesenchymal phenotype thus promoting disease progression, while VE-CAD regulates the intracellular localisation of N-CAD by displacing it from the cell membrane (Rezaei *et al.*, 2012).
Associations with other cancers	Increased levels of circulating N-CAD have been identified as a prognostic marker for high-risk multiple myeloma patients (Vandyke *et al.*, 2013).

	Deregulation of N-CAD expression is associated with the promotion of cell migration in prostate cancer (Cui *et al.*, 2013). In osteosarcoma, the downregulation of N-CAD prevents cell migration and metastasis (Kashima *et al.*, 2003).
	In contrast, in neuroblastoma, reduced N-CAD expression was associated with metastasis. However, inhibition of N-CAD using an N-CAD antagonist had antitumour activity suggesting it could still be a valid target in this disease setting (Lammens *et al.*, 2011)

Table 43: Summary of published reports investigating the function of CYP2B6 including any reports in breast and other cancers.

Gene Name/Acronym	Cytochrome P450, family 2, subfamily B, polypeptide 6: **CYP2B6**
Function	CYP2B6 encodes a member of the cytochrome P450 superfamily of enzymes. The cytochrome P450 proteins are monooxygenases which catalyze many reactions involved in drug metabolism and synthesis of cholesterol, steroids and other lipids (reviewed by Danielson, 2002).
Associations with breast cancer	Tamoxifen is a prodrug that is converted to endoxifen and 4-hydroxy-tamoxifen (metabolites have 33 times greater affinity for ER than tamoxifen) by several CYP-P450's, including CYP2B6, CYP2C9, CYP2C19 and CYP2D6). The CYP-P450 enzymes are polymorphic and based on SNPs they can have increased or decreased activity. While a patient's genotype for CYP2D6 has been shown to affect tamoxifen metabolism and thus the plasma concentration of endoxifen (Goetz *et al.*, 2005), CYP2B6 is less active in this respect (Boocock *et al.*, 2002). CYP2B6 has been identified as an ER-regulated gene through an ERE site located on the CYP2B6 promoter in the T47D breast cancer cell line. In this context, E2 leads to the up-regulation of CYP2B6, an effect not observed in the MCF-7 cell line, suggestive

	of cell-type specific transcriptional regulation of CYP2B6 by ER (Lo *et al.*, 2010).
Associations with other cancers	No associations with other cancers.

Table 44: Summary of published reports investigating the function of CYP2B7P1 including any reports in breast and other cancers.

Gene Name/Acronym	cytochrome P450, family 2, subfamily B, polypeptide 7 pseudogene 1. **CYP2B7P1**
Function	Pseudogenes are relatives of genes that have lost their protein-coding ability. By definition, pseudogenes lack a function (Poliseno *et al.*, 2010)
Associations with breast cancer	No associations to breast cancer
Associations with other cancers	No associations to cancer

Table 45: Summary of published reports investigating the function of SLC6A14 including any reports in breast and other cancers.

Gene Name/Acronym	Solute carrier family 6 (amino acid transporter), member 14: **SLC6A14**
Function	SLC6A14 is a member of the solute carrier family 6; sodium and chloride dependent neurotransmitter transporters. The encoded protein transports both neutral and cationic amino acids (Ganapathy *et al.*, 2003).
Associations with breast cancer	SLC6A14 transports all essential amino acids as well as glutamate (an important precursor for nucleotide synthesis) and arginine (which is essential for tumour growth) but the transporter is only expressed at low levels in normal cells. Due to the increased need by tumour cells for amino acids it has been hypothesised that SLC6A14 maybe upregulated in cancer cells (Karunakaren *et al.*, 2011).

	SLC6A14 has been found to be upregulated by E2 in HER2+/ER+ breast cancer cell lines (BT474 and ZR-75 cell lines) and inhibition of the transporter in these cell lines prevented the uptake of many essential amino acids leading to growth inhibition and apoptosis (Karunakaran *et al.*, 2008)
Associations with other cancers	SLC6A14 has been shown to up-regulated in colon and cervical cancer in order to cope with the increased demand for nutrients (Gupta *et al.*, 2005; Gupta *et al.*, 2006).

The only gene whose expression profile and ontology were in keeping with a likely in involvement in the reduced Faslodex response observed in the HER2+ cell lines was CDH2 (Table 42). CDH2 (N-cadherin) has been associated with cancer progression in breast and other cancers and thus its up-regulation by short-term Faslodex treatment in the HER2+ cell lines may contribute to swifter development of drug resistance. Subsequently, all further investigations were carried out solely on CDH2.

8.2.3 Establishing potential clinical relevance of CDH2 in the context of endocrine outcome

Equivalent analysis, as performed in previous chapters using KMPlotter and GOBO, were used to determine if there was a potential clinical relevance of CDH2 in relation to tamoxifen-treated ER+ breast cancer. Although no significance was observed in the smaller GOBO dataset, in KMPlotter (n=657) a significant association was identified (Figure 135), where increased inherent CDH2 expression (red line) was associated with a reduced RFS in tamoxifen treated patients. The hazard ratio was found to be greater than 1, indicated patients with an increased CDH2 expression (red line) were at an increased risk of earlier relapse following tamoxifen therapy (HR=1.39, 95% CI 1.04-1.85). No significant associations were identified when using KMPlotter to investigate CDH2 gene expression in ER+ systemically untreated ER+ patients.
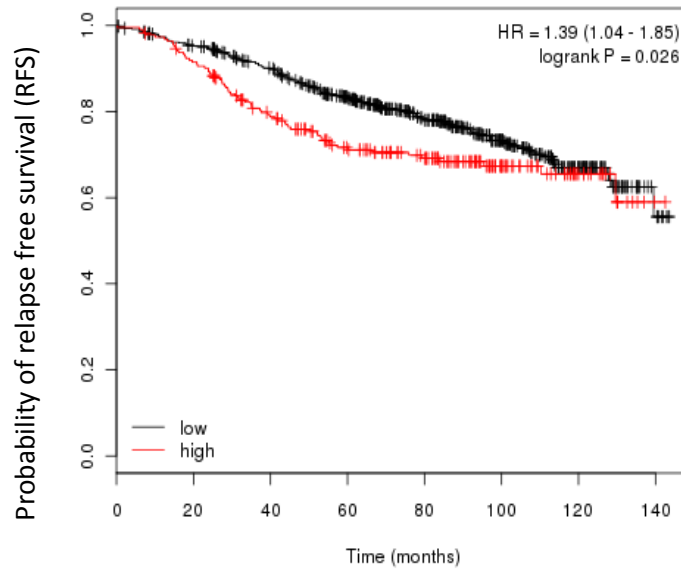
Figure 135: Kaplan-Meier survival curve generated using KMPlotter displaying probability of RFS according to high (red) or low (black) CDH2 mRNA expression in tamoxifen-treated ER+ breast cancer patients (n=657). This survival curve was generated using the jetset affymetrix gene probe for CDH2 grouping patients by best fit cut-point (calculated by KMPlotter).

8.2.4 PCR verification of CDH2 potentially involved in reduced Faslodex response duration in the HER2+ cell lines

Based on a promising Faslodex induced profile in the HER2+ cell lines, adverse ontology and clinical relationship to poor tamoxifen outcome, CDH2 was deemed a good candidate to be subsequently PCR verified. Triplicate RNA from untreated and 10 day Faslodex treated cells were used for PCR (Figure 136) in an attempt to verify the Affymetrix expression profile. CDH2 expression was elevated basally in the HER2+ compared to the HER2- cell lines, as observed in the microarray data (Figure 127). However, following 10 day Faslodex treatment only very minimal further inductions were detected by PCR in the HER2+ cell lines, contrasting the microarray findings. In agreement with the microarray data CDH2 expression was extremely low in the MCF-7 cell line despite a small Faslodex induction. While there was little change in the modest CDH2 expression in the T47D cell line.
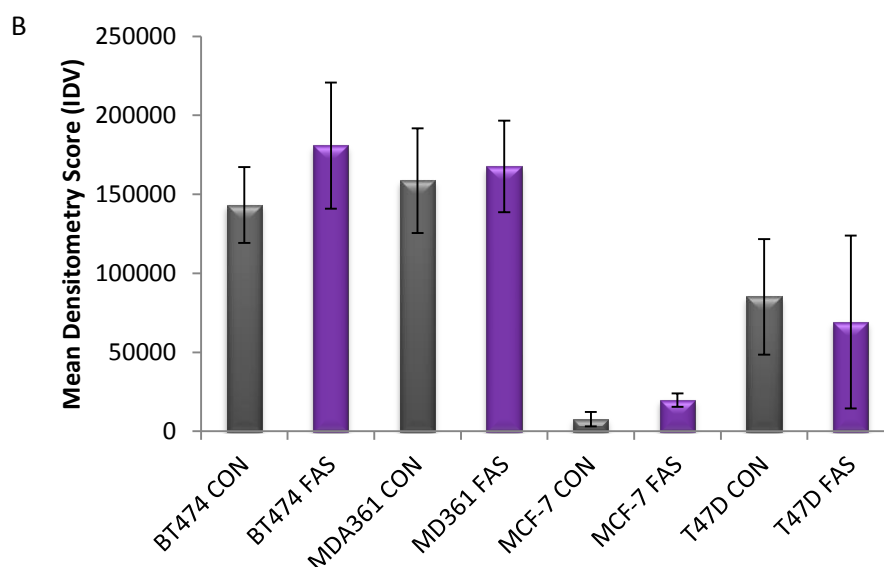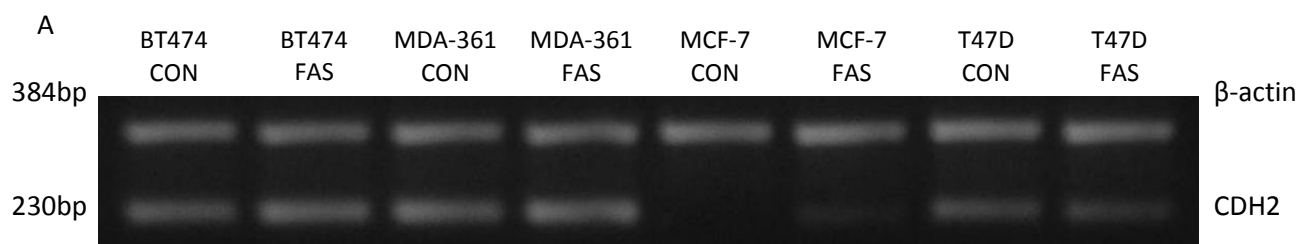
Figure 136: Representative PCR image (A) with the corresponding β-actin normalised densitometry graph (B) quantitatively representing the data (CON-control; FAS-10 day Faslodex treatment) for CDH2. The results are expressed as means ± SEM of three separate experiments. (C) Table displaying the fold change of gene expression following Faslodex treatment.

8.3 Discussion

HER2+ BT474 and MDA-MB-361 cells had a reduced response duration to Faslodex during long-term *in vitro* culture compared with their HER2+ counterparts. It is feasible that along with their intrinsic amplified HER2, Faslodex-deregulated genes (i.e. induced proliferative/cell survival genes, or alternatively decreased tumour suppressive elements) also contribute towards this earlier development of resistance in these models. In this light, following SAM analysis and t-test filtering 10 genes were initially identified as being uniquely Faslodex de-regulated (by at least 1.5 fold) in the HER2+ cell lines. Of those, 3 were induced by 10 day Faslodex

treatment and 7 were suppressed. Half of these were lost following further filtering by analysis of the log2 intensity plots (which eliminated genes because Faslodex changes were also noted in HER2- cells or because of low log2 intensity values/absent calls indicating unreliable expression), and by ensuring that the change in expression observed using the jetset probe was shared by the majority of any further probes for a given gene.

This filtering strategy was successful in prioritising 5 genes for subsequent ontological investigation, comprising SERPINI1 and CDH2 which were Faslodex induced and CYP2B6, CYP2B7P1 and SLC6A14 which were Faslodex suppressed on the arrays in HER2+ cells. Ontological studies led to the dismissal of 4 of these genes, leaving CDH2 as the highest priority gene potentially-contributory towards the earlier development of Faslodex resistance in the ER+/HER2+ cell lines. CDH2 has been widely associated with disease progression, increased motility, invasive capacity, metastasis and angiogenesis in breast cancer as well as other cancers (Hazan *et al.*, 2000; Suyama *et al.*, 2002; Hazaan *et al.*, 1997, Rezaei *et al.*, 2012), while an N-CAD antagonist exhibited anti-tumour activity in neuroblastoma (Lammens *et al.*, 2011). It has also been associated with HER2 positivity in breast cancer (Lee *et al.*, 2012), and in agreement its basal expression in this project was found to be higher in HER2+ compared with HER2- cells on the arrays. CDH2 has not been previously associated with anti-hormone failure in breast cancer.

Unfortunately, however, although the basal expression profile was verified in the HER2+ versus HER2- cells, PCR was unable to detect significant further induction of the gene in either of the HER2+ cell lines with Faslodex. No non-specific binding was identified suggesting the PCR primers were specific for CDH2. However, from the PCR densitometry graph (Figure 136) the error margins were relatively large suggesting expression was variable in the different samples analysed which may have masked any significant Faslodex change. Alternatively, it may be that because expression of CDH2 was elevated basally in the HER2+ cells, observing further significant increases was not feasible by end-point PCR.

Although further approaches are therefore needed to definitively confirm or refute Faslodex impact on CDH2 expression in the HER2+ cells, it is certainly interesting that there were inherently high levels of CDH2 gene expression in the HER2+ cell lines. Based on its adverse ontology, it is feasible that this intrinsic CDH2 may contribute to limiting the duration of Faslodex response in this model. This concept is in part supported by the relationship between increased intrinsic CDH2 level and poorer RFS in tamoxifen treated ER+ patients observed using KMPlotter (Figure 135) (although it was not possible with this tool to explore the association within an ER+/HER2+ cohort). Indeed, the lack of relationship in systemically untreated patients further suggested that CDH2 expression level related specifically to anti-hormone outcome within ER+ disease. Although data from Lee *et al* suggest that expression of CDH2 may be dependent on elevated HER2 levels (Lee *et al.*, 2012) and the transcription factor AP2 gamma has been implicated in regulation of both genes (Ailan *et al.*, 2009), no relationships have previously been reported linking CDH2 and HER2 signal transduction in cancer or in the context of endocrine resistance. However, the data in this project gives reason to believe that elevated basal CDH2 could contribute to limiting Faslodex response in the HER2+ setting, and so future work is certainly warranted in this regard since this may yield new therapeutic strategies to improve endocrine outcome or potentially a novel resistance biomarker.

Chapter 9

Analysis of genes of interest in the NEWEST (Neoadjuvant Endocrine Therapy for Women with Estrogen-Sensitive Tumours) trial to determine clinical impact of Faslodex and relation to anti-tumour impact.

9.1 Introduction

In the previous chapters, this project has begun to determine potential clinical relevance of genes of interest in relation to antihormone outcome using publically available breast cancer datasets within KMPlotter and GOBO. While these datasets allow determination of the relationship between inherent gene expression and duration of response in tamoxifen treated ER+ breast cancer patients, they fail to determine the effect of endocrine treatment on the expression level of the gene. Furthermore, the prioritised genes of interest in this project have been identified as being potentially involved in the varying Faslodex responses shown by ER+ breast cancer cell lines *in vitro* by determining their expression de-regulation by Faslodex in one or more of the cell models. Critically, however, the endocrine-treated datasets used by KMPlotter and GOBO are generated from tamoxifen-treated patients and do not address Faslodex promoted events and gene expression data from patients treated with Faslodex is not as yet publically available.

Fortunately, however, for this project access to gene microarray and parallel immunohistochemical (IHC) data from the NEWEST (Neoadjuvant Endocrine therapy for Women with Estrogen-Sensitive Tumours) trial carried out by AstraZeneca was granted. NEWEST comprises a recently-completed randomised Phase II trial in newly diagnosed ER+ postmenopausal with locally advanced breast cancer who had received no prior treatment (Kuter *et al.*, 2012). It was the first trial

to assess the biological and clinical activity of 500mg/month (plus 500mg on day 14 of month 1) versus 250mg/month Faslodex in the neoadjuvant breast cancer setting for 16 weeks prior to surgery. Neoadjuvant treatment is a systemic cancer therapy given to patients for a number of weeks prior to surgery for the primary tumour in an attempt to reduce tumour size (Liu *et al.*, 2010; Mathew *et al.*, 2009). Such treatments, if they cause anti-tumour effects, can result in patients being appropriate for breast conserving surgery and can make inoperable tumours operable (Makris *et al.*, 1998). Most neoadjuvant approaches to date relate to the use of chemotherapy but following the success of adjuvant endocrine treatments more studies are assessing the benefit of anti-hormones in the neoadjuvant setting (Coombes *et al.*, 2007; Coates *et al.*, 2007). Importantly, studies in this pre-operative setting also allow new treatments to be investigated, providing a "window-of-opportunity" to collect matched tumour samples prior and subsequent to treatment for biological studies (Krainick-Strobel *et al.*, 2008; Baselga *et al.*, 2009).

In the NEWEST trial, gene expression and various IHC data from core biopsies were accrued at week 0 (baseline) and at week 4 during Faslodex treatment. Unfortunately, sufficient data relating to the HER2 status of patients was not collected as well as clinical response data. The primary endpoint of the trial was IHC-detected Ki67 (proliferation marker) expression from baseline to week 4, and secondary endpoints were ER and ER-regulated PGR protein expression, and tolerability (Kuter *et al.*, 2012). The trial was instigated as a consequence of previous observations that ER down-regulation appeared to be dose-dependent, thus it was hypothesised for the NEWEST trial that by increasing the dose of Faslodex to 500mg further ER antagonism may occur improving anti-tumour response (Robertson *et al.*, 2001). NEWEST went on to show that 500mg Faslodex was indeed superior to 250mg in terms of significantly greater down-regulation of KI67 (-78.8% vs. -47.4% ; $p < 0.0001$), as well as ER (-50.3 vs. -13.7%; $p < 0.0001$) and also PGR (-80.5 vs. -46.3%; $p = 0.0018$) protein expression, although the underlying mechanisms of the anti-proliferative impact remain unknown.

Since gene expression data were available, therefore, the NEWEST trial provided a unique opportunity in this project to determine the initial effects of Faslodex treatment on the expression of the 12 *in vitro*-derived, prioritised genes of interest (Table 46) from Chapters 3-6 to address; (1) if they were commonly altered in ER+ breast cancer patients treated with Faslodex in the neoadjuvant setting and (2) if they were related to changes in Ki67 and thus potentially linked to mechanistic regulation of proliferation by Faslodex. By carrying out these investigations, potential clinical relevance of the genes of interest could be determined for the first time in relation to Faslodex treatment in ER+ breast cancer (although unfortunately it was not possible to further stratify patients by HER2 status).

Table 46: Key genes prioritised from the 4 ER+ breast cancer cell lines treated with Faslodex (FAS) for 10 days. Genes highlighted in green comprise those suppressed by at least 1.5 fold Faslodex treatment while those in red were Faslodex-induced by at least 1.5 fold.

HER2+ and MCF-7 FAS de-regulated genes (n=5) (potentially resistance-promoting)	T47D FAS de-regulated genes (n=4) (potentially involved in Faslodex complete response)	HER2- FAS de-regulated genes (n=2) (potentially involved in extended HER2-Faslodex response)	HER2+ FAS de-regulated genes (n=1) (potentially involved in HER2+early onset of resistance)
PRKACB	DCN	PCDH7	CDH2
VEGFC	TXNIP	ARTN	
CXCR4	TGFB2		
GABBR2	CASP1		
GFRA1			

FDA approval has been granted for the increased dose of Faslodex at 500mg and this dose has been shown to be superior in down-regulating ER, consistent with an improved tumour delivery of the drug in comparison to the sub-optimal 250mg dose (Di Leo *et al.*, 2010; Kuter *et al.*, 2012). Hence all initial analyses to identify associations between the expression of the genes of interest, Faslodex treatment impact and anti-proliferative effect were carried out using matched sample data

collected from patients in the 500mg treatment arm of the trial, only examining resultant significant genes for any emerging trends using the matched 250mg data.

9.2 Results

The NEWEST gene expression data and IHC data (Ki67, and for more limited analysis ER) were uploaded into SPSS to carry out statistical tests to determine if any of the 12 prioritised Faslodex-influenced genes (Table 46) were significantly altered following 4 weeks neoadjuvant Faslodex treatment versus baseline (using paired t-test analysis on matched patient sample) and if the direction of any Faslodex-induced change in gene expression associated with the degree of Ki67 suppression (using Mann Whitney analysis). Kuter *et al*., reported that core biopsies were taken from 60 patients in the 500mg Faslodex trial arm, but only a subset were processed for microarrays. For the patients chosen for microarray analysis, magnitude of Ki67 fall (and also ER down-regulation) was calculated and is displayed in Tables 2 and 3 along with the changes reported by Kuter *et al.,* (Kuter *et al.*, 2012) for the full patient study.

Absolute Ki67 change was not substantially different between the patient cohort chosen for microarray analysis and the whole trial cohort (Table 47).

Table 47: Absolute reduction in Ki67 positivity from baseline in the NEWEST trial for all patients from the 500mg Faslodex trial arm and for those with samples processed for microarray analysis

Patient cohort	Absolute Ki67 reduction from baseline
N=60 500mg trial arm	17.5
N=24 500mg trial arm used for microarray	24.4

9.2.1 Analysis of the 5 genes de-regulated by Faslodex in the MCF-7 and HER2+ models within the NEWEST clinical trial microarray dataset.

9.2.1.1 Determining if the genes were de-regulated by Faslodex in the clinic

A paired t-test was performed to determine if any of the genes potentially contributory towards acquired Faslodex resistance in both the ER+/HER2+ and ER+/HER2- setting were also significantly altered in expression in patient samples during Faslodex treatment (Table 48) using normalised gene array data and comparing their expression after 4 weeks 500mg Faslodex treatment versus baseline.

Table 48: Paired t-test results from NEWEST data for genes de-regulated by Faslodex in the HER2+ and MCF-7 cell lines, and number of patients showing an induction or suppression in gene expression following 4 weeks 500mg Faslodex treatment versus baseline (n=24).

Gene Symbol	P-value	Number of patients showing gene change	
		Induction	Suppression
PRKACB	0.167	12	12
VEGFC	0.276	13	11
CXCR4	0.675	17	7
GABBR2	0.592	11	13
GFRA1	<0.0001	1	23

The only gene to meet significance was GFRA1 (Table 48). GFRA1 was identified as a Faslodex-suppressed gene in the HER2+ and MCF-7 cell lines, and similarly the NEWEST dataset revealed that of the 24 patients analysed from the 500mg trial arm, 23 demonstrated suppression in GFRA1 after 4 weeks 500mg Faslodex treatment (Table 48, Figure 137). Varying degrees of suppression in the patient samples were reflected by the broad range of fold change after Faslodex treatment (1.04-8.3 fold suppression; mean = 1.97, very similar to the inductions observed in the PCR validation of the ER+/HER2+ cell lines (~1.7) while the MCF-7 cell line

exhibited a much greater induction at the top end of the scale observed in NEWEST (7.28).
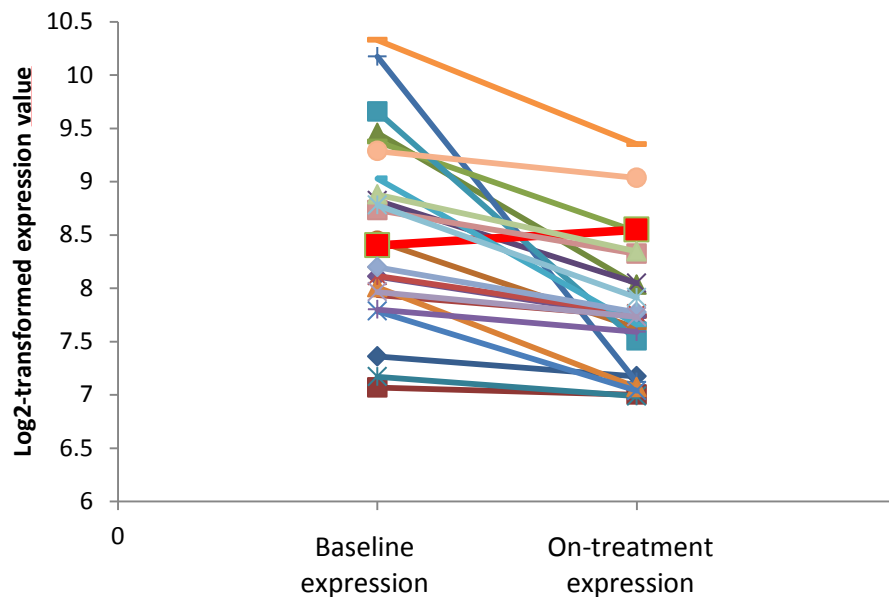
Figure 137: Microarray log2 baseline expression and on-treatment mRNA expression of GFRA1 following 4 week neoadjuvant 500mg Faslodex, p=<0.0001 (n=24).

Examining the 250mg trial arm versus baseline, a significant association was also identified for GFRA1 (p=<0.001), with the majority of patients again demonstrating a suppression by 4 weeks Faslodex at this dosage. Of the 17 patients analysed, 16 showed decreased GFRA1 expression following treatment, while the remaining patient exhibited an induction (Figure 138). The baseline log2 expression range of GFRA1 from patients in the 250mg trial arm (7-9.5) was comparable with the 500mg arm (7-10) (Figures 137 and 138) and again varying degrees of suppression were observed following Faslodex treatment (Figure 138), although a somewhat smaller range of GFRA1 fold change was observed with 250mg Faslodex (1.02-2.8 fold suppression, mean= 1.5) with no large fold changes.
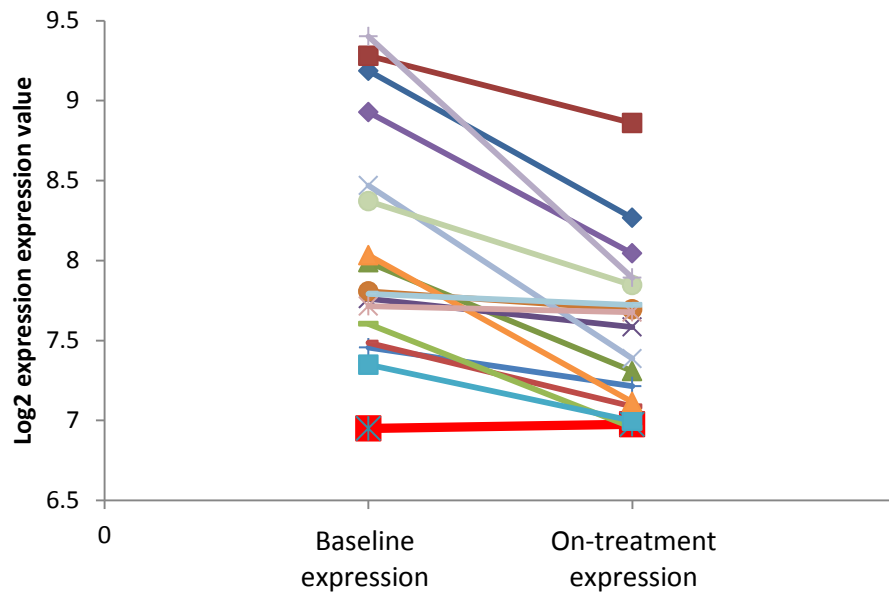
Figure 138: Microarray log2 baseline expression and on-treatment mRNA expression of GFRA1 following 4 week neoadjuvant 250mg Faslodex, p=<0.0001 (n=17).

Although significance was not met for the 48 remaining genes induced by Faslodex in the HER2+ and MCF-7 cell lines, the clinical sample data were interrogated further to determine the number of patients showing an induction or suppression for each gene following 4 week 500mg Faslodex treatment (Table 48) to see if any of these genes could potentially be important in limiting drug response in a patient sub-population. For PRKACB, VEGFC and GABBR2, approximately half of patients showed an induction while others showed suppression of gene expression (Table 48). In contrast, the majority of patients showed induction of CXCR4 expression following treatment (n=17), as displayed in Figure 139A, with few patients showing suppressed CXCR4 expression in 139B. Even though in the majority of patients Faslodex induced CXCR4, the magnitude of induction was relatively low (fold induction range 1.02-1.68, average= 1.2 fold, similar to the induction observed in the PCR validation of the cell lines; in both ER+/HER2+ cell lines induction was 1 fold while the MCF-7 cell line exhibited an of approximately 3 fold. The baseline CXCR4 log2 expression level was comparable between both patient cohorts (range ~7-9, Figure 139).

Figure 139: Microarray Log2 baseline expression and the on-treatment mRNA expression of CXCR4 in (A) patients that showed Faslodex-induction of expression (n=17), and (B) patients that exhibited suppression (n=7) following 4 week neoadjuvant 500mg Faslodex treatment.

9.2.1.2 Determining if Faslodex change in expression of the 5 genes related to Ki67 change

Further analyses were carried out for the 5 genes to determine if magnitude of suppression of Ki67 (baseline % – 4 week treatment %) related to direction of change of gene expression following Faslodex treatment using a Mann-Whitney U test. No p-value was reported for GFRA1 as only one patient showed an induction of GFRA1 expression following treatment (Table 49). It was hypothesised from the

cell models that induction of PRKACB, VEGFC, CXCR4 or GABBR2 and GFRA1 suppression would be associated with a reduced magnitude of Ki67 suppression.

Table 49: Relationship between direction of gene change and the magnitude of change in Ki67 (using Mann-Whitney U test) following 4 weeks of 500mg Faslodex (n=24).

Gene Name	P-value	Number of patients with gene suppression	Median suppression of Ki67 (%)	Number of patients with gene induction	Median suppression of Ki67 (%)
PRKACB	0.905	9	14	15	12
VEGFC	0.296	11	11	13	13.88
CXCR4	0.445	7	31	17	12
GABBR2	0.817	12	14.5	12	12
GFRA1	N/A	23	14	1	11

For these remaining genes there was unfortunately no significant difference in magnitude of suppression of Ki67 between the induced or suppressed gene expression cohorts (Table 49). However, the majority of patients from the 500mg Faslodex trial arm showed an induction in CXCR4 expression following treatment and there was a reduced median suppression of Ki67 in this group.

9.2.2 Analysis of the 4 genes de-regulated by Faslodex in the T47D cell line within the NEWEST clinical trial microarray dataset.

9.2.2.1 Determining if the genes were de-regulated by Faslodex in the clinic

A paired t-test was performed to determine if any of those genes hypothesised to contribute to the complete response in the T47D cell line were also significantly altered in expression in patient samples during Faslodex treatment in the NEWEST trial.

Table 50: Pared t-test results from NEWEST data for genes de-regulated by Faslodex in the T47D cell line only, and number of patients showing an induction or suppression of gene expression following 4 weeks 500mg Faslodex treatment versus baseline (n=24).

Gene Symbol	P-value	Number of patients showing gene change	
		Induction	Suppression
DCN	0.070	17	7
TXNIP	0.714	12	12
TGFβ2	0.137	12	12
CASP1	0.815	14	10

After such analysis, DCN was the only gene nearing significance (Table 50). DCN was a Faslodex induced gene in the T47D line, and the majority of patients showed induction of DCN following 4 weeks of Faslodex treatment (n=17) (Figure 140A), while only 7 patients displayed down-regulation of expression (Figure 140B). Patients that exhibited induction of DCN expression with Faslodex (Figure 140A) showed a broad range of fold change (1.1-4.5 fold induction; mean= 2.3 which is lower than that observed in the PCR validation of DCN induction in the T47D cell line which was calculated as 4.8 fold).

A

B
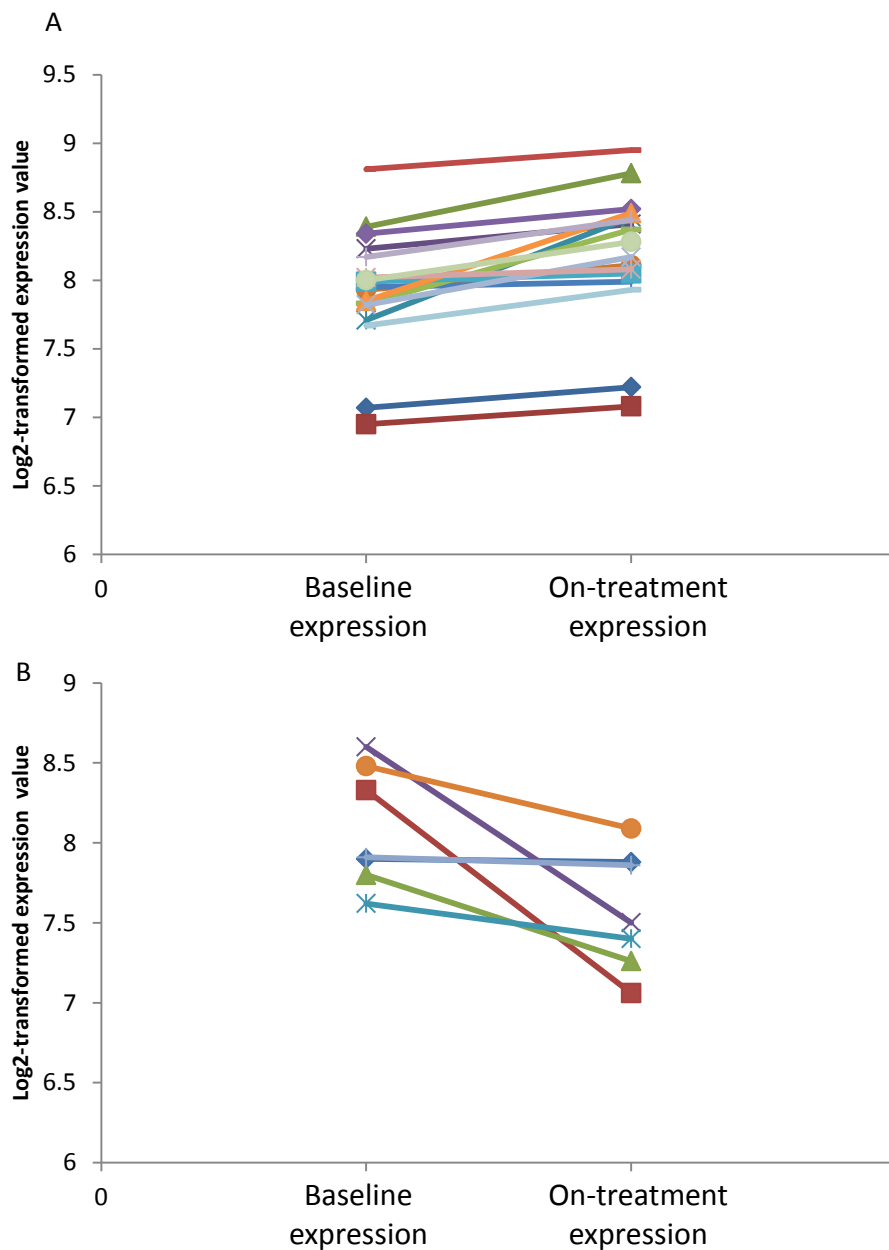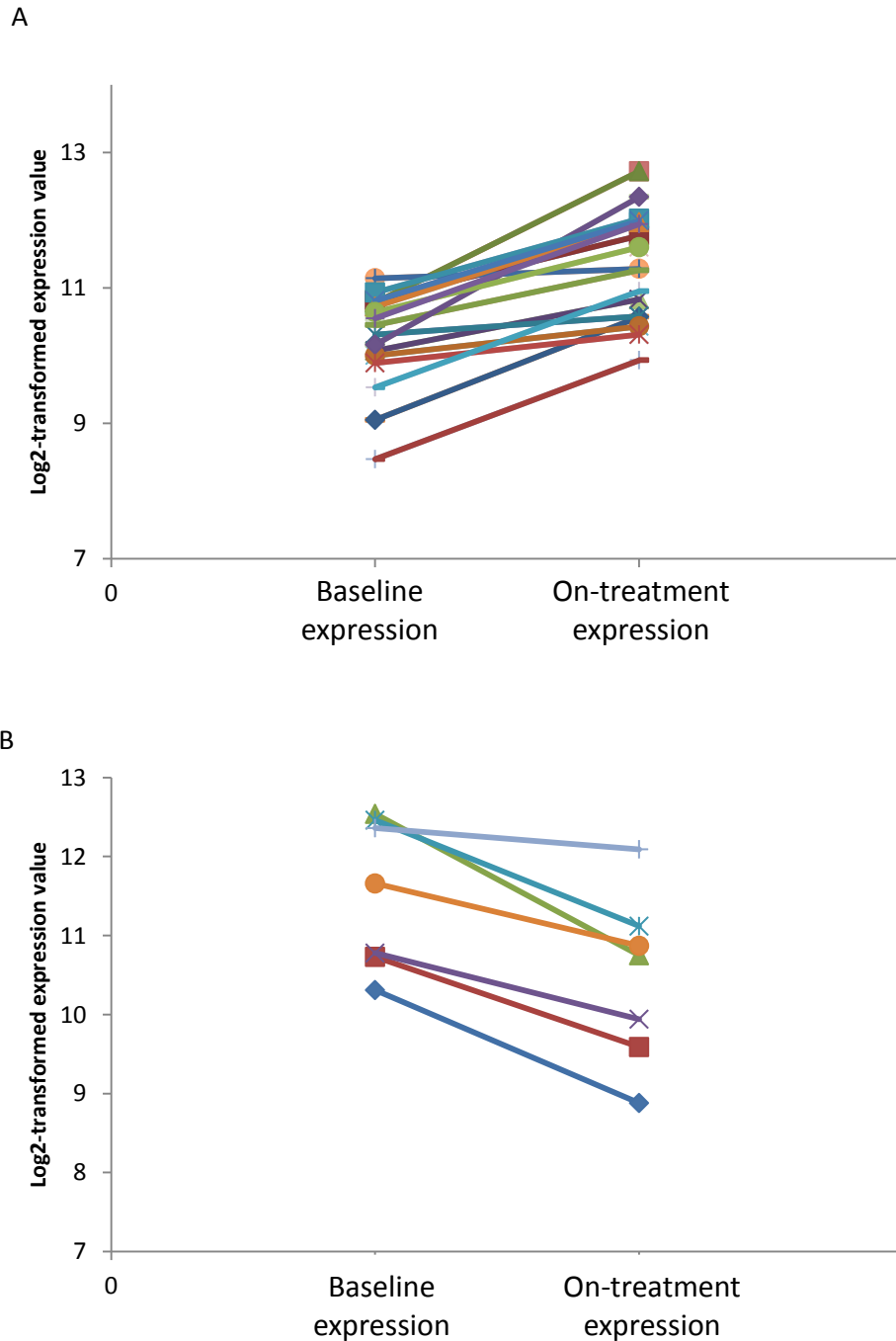

Figure 140: Microarray log2 baseline expression and on-treatment mRNA expression of DCN in (A) patients that showed a Faslodex-induction of expression (n=17), and (B) patients that exhibited suppression (n=7) following 4 week neoadjuvant 500mg Faslodex treatment.

There also seemed to be some difference in the intrinsic DCN gene expression in relation to whether a patient subsequently showed Faslodex induction or suppression of this gene. Thus, the baseline log2 expression range for those patients where Faslodex subsequently induced DCN expression was 8-11 while for those where Faslodex suppressed expression the baseline log2 intensity was

generally higher (range=10-12.5). An independent t-test determined this difference was significant (p=0.003).

While there was evidence that 500mg Faslodex induced DCN expression, with 250mg treatment no prevalent pattern of change was observed (p=0.776), where 9 patients displayed induction and 8 suppression in DCN gene expression (Figure 5). Fold induction also appeared lower (range=1.06-3.1) compared with 500mg Faslodex (Figure 141).
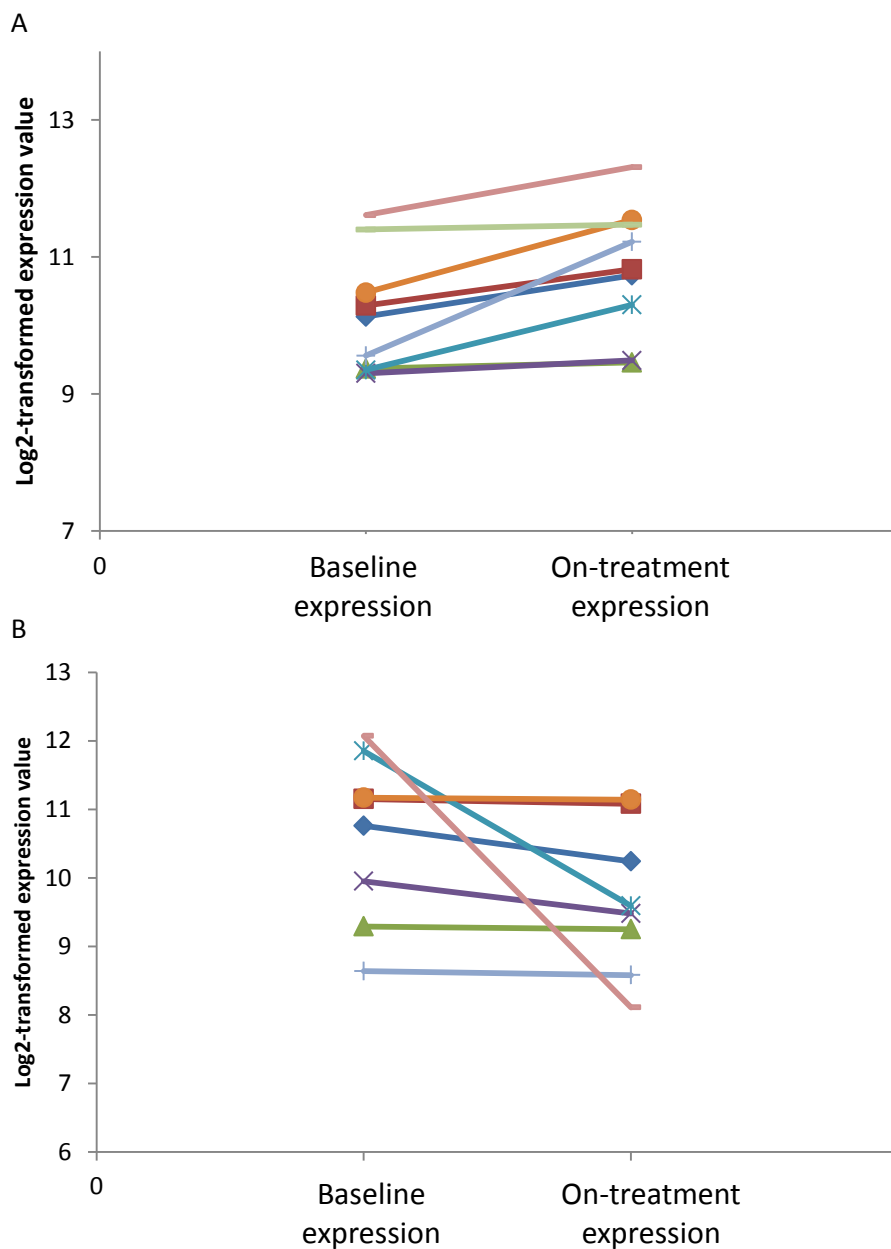
Figure 141: Microarray log2 baseline expression and on-treatment mRNA expression of DCN in (A) patients that showed a Faslodex-induction of expression (n=9), and (B) patients that exhibited suppression (n=8) following 4 week neoadjuvant 250mg Faslodex treatment.

TXNIP, CASP1 and TGFB2 were also identified as Faslodex-induced genes in the T47D cell line. Although none of these genes neared significance (Table 50), the 500mg data were again further analysed to determine the magnitude of any patient cohort demonstrating induction. Approximately half of the patients displayed an induction of gene expression following 4 weeks Faslodex treatment (Table 50).

9.2.2.2 Determining if Faslodex change in expression of the 4 genes related to Ki67 change

In order to further determine if induction of the genes of interest was associated with an improved anti-proliferative response to Faslodex in the clinic, a Mann-Whitney U test was performed to determine if magnitude of Ki67 fall (baseline % - 4 weeks 500mg Faslodex %) was greater in those patients exhibiting Faslodex-induced gene expression. Both DCN and TXNIP neared significance (Table 51). Graphical display of these data revealed increases in expression of either DCN or TXNIP were associated with a greater median fall in Ki67 protein expression following Faslodex treatment (Figure 142 and 143) compared to patients displaying suppression of expression.

Table 51: Relationship between direction of gene change and magnitude of change in Ki67 (using Mann-Whitney U test) following 4 weeks of 500mg Faslodex (n=24).

Gene Symbol	P-value
DCN	0.075
TXNIP	0.089
TGFB2	0.147
CASP1	0.240
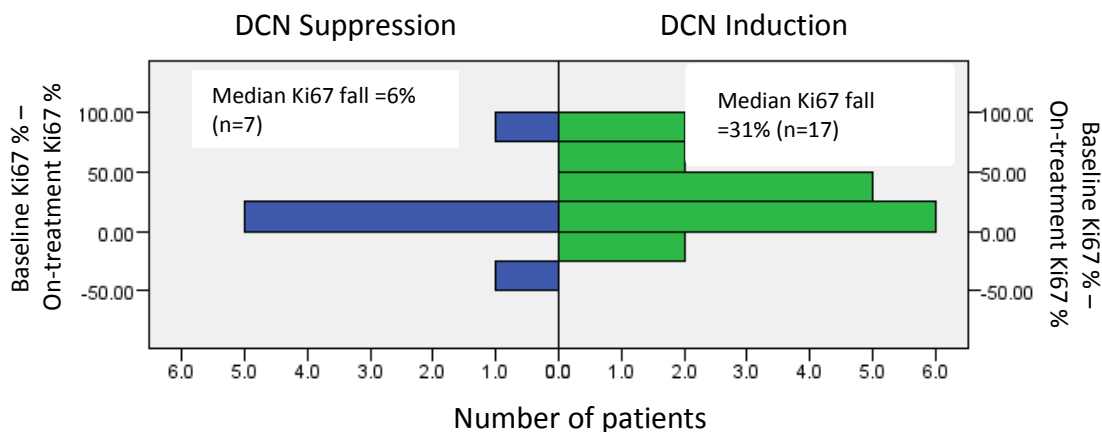
Figure 142: Change in Ki67 in patients exhibiting induction of DCN following 4 weeks 500mg Faslodex treatment compared to those with suppression.
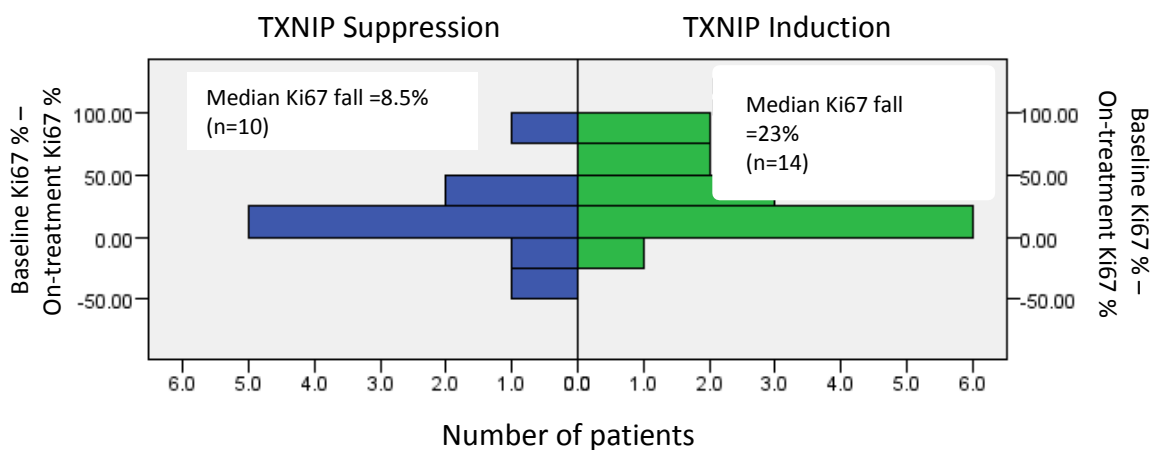
Figure 143: Change in Ki67 in patients exhibiting induction of TXNIP following 4 weeks 500mg Faslodex treatment compared to those with suppression.

While induction of TGFB2 or CASP1 was not statistically associated with an improved fall in Ki67 protein expression (Table 51), induction of expression of these genes by Faslodex was associated with a modestly improved median Ki67 suppression (Table 52).

Table 52: Relationship between direction of gene change for TGFB2 and CASP1 and the magnitude of change in Ki67 following 4 weeks of 500mg Faslodex (n=24).

Gene Name	Number of patients with gene suppression	Median suppression of Ki67	Number of patients with gene induction	Median suppression of Ki67
TGFB2	12	11.5	12	23
CASP1	12	13	12	21.5

Of the 24 patients analysed from the 500mg trial arm, 3 displayed an up-regulation in Ki67 expression during Faslodex treatment and it is possible that such increases in Ki67 during treatment could be an indication of a distinct patient cohort "intrinsically resistant" to therapy (although this is yet to be confirmed in relation to endocrine therapy). To examine whether induction of the most promising genes DCN and TXNIP was also informative in relation to patients showing some initial anti-tumour "responsiveness", Mann-Whitney U analysis was repeated for these genes using the 21 patients showing any suppression in Ki67 during treatment. The relationship between changes in Ki67 and DCN was found to reach significance (p=0.047) (Figure 144): the 15 patients who showed an increase in DCN with Faslodex also showed a significantly greater fall in Ki67 (Figure 144). While not significant (Table 53), induction of TXNIP by 500mg Faslodex was also associated with a somewhat improved fall in Ki67.
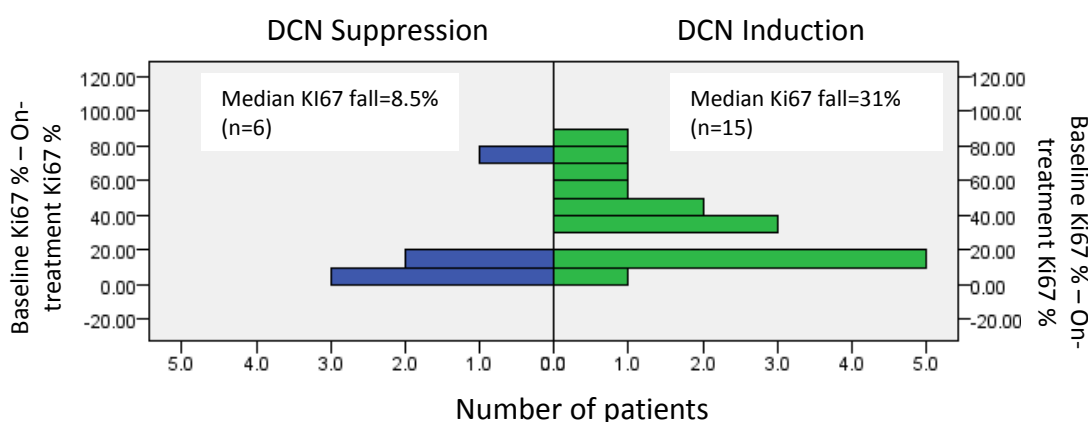
Figure 144: Change in Ki67 in patients exhibiting induction of DCN following 4 weeks 500mg Faslodex treatment compared to those with suppression after excluding 3 potentially resistant patients.

Table 53: Relationship between direction of gene change for TXNIP and the magnitude of change of Ki67, excluding 3 potentially resistant patients following 4 weeks of 500mg Faslodex (Mann-Whitney test).

Gene Name	P-value	Number of patients with gene suppression	Median suppression of Ki67	Number of patients with gene induction	Median suppression of Ki67
TXNIP	0.147	8	11	13	31

Following the analysis of DCN, TXNIP, CASP and TGFB2 in the NEWEST trial dataset, induction of all 4 genes was associated with improved Ki67 fall (even though some were not statistically significant). However, following this observation, the 4 genes were analysed as a metagene. This was carried out in 2 ways, firstly by determining the average log2 expression change of all 4 genes (on-treatment expression-pre-treatment expression) and how this associated with magnitude of Ki67 change (Figure 145) and secondly by identifying all those patients that exhibited an induction in all 4 genes (only 6 patients identified) and how this associated with magnitude of Ki67 change (Figure 146).
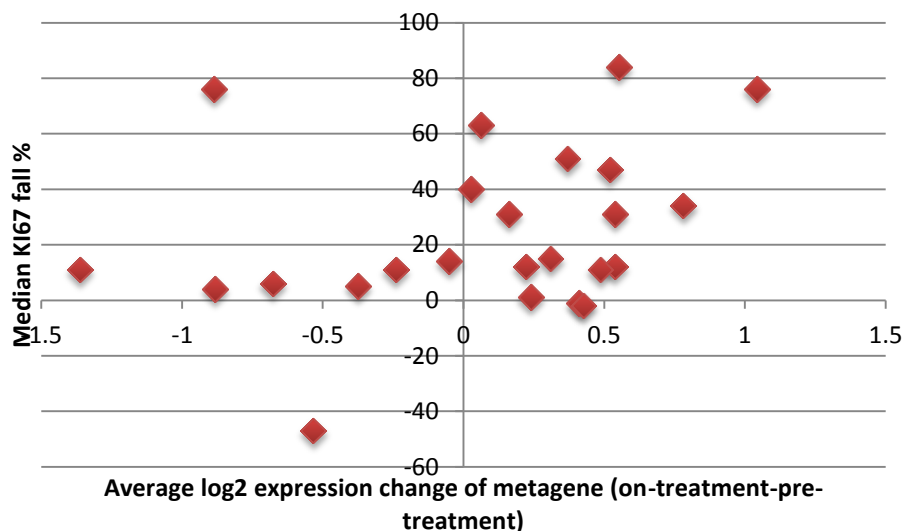
Figure 145: The association between the change in expression of the metagene by 4 weeks Faslodex treatment and magnitude of Ki67 fall.

From Figure 145 it can be seen that with the exception of 1 outlier the majority of patients with a low average expression change of the metagene (left-hand side of graph) show a very small reduction in Ki67 following Faslodex treatment while those that show a positive induction of expression of all 4 genes show a range of reductions in expression. However, it is of worth to note that again with the exception of the outlier, all patients that exhibit a fall of at least 50% in Ki67 expression show a positive induction of expression of the metagene.

In Figure 146, a Mann Whitney U analysis was carried out to determine if the magnitude of Ki67 fall was significantly greater in those 6 patients that exhibited an induction of all 4 genes part of the metagene. The analysis determined that the 6 patients who did exhibit an induction in all genes part of the metagene did indeed demonstrate an improved fall in Ki67 expression and this was found to be significant (p=0.039) suggesting that the induction of all four genes may co-operatively contribute to an improved Faslodex response. However, as only 6 patients exhibited an increase in all 4 genes a bigger sample size must be used to confirm this result.
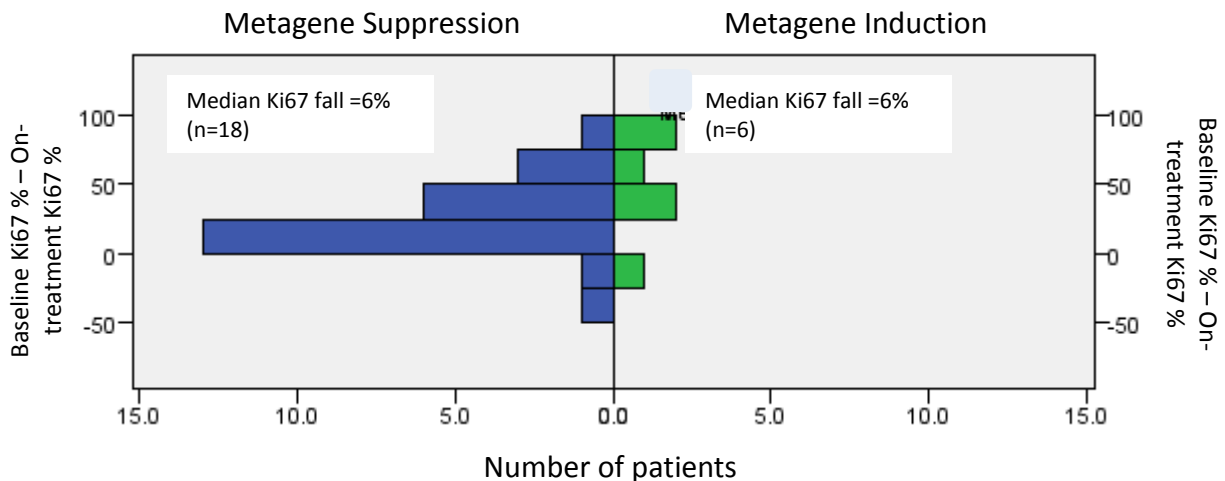
Figure 146: Change in Ki67 in patients exhibiting induction of all 4 genes part of the metagene following 4 weeks 500mg Faslodex treatment compared to those with suppression.

9.2.3 Analysis of the 2 genes de-regulated by Faslodex in both HER2-MCF-7 and T47D models within the NEWEST clinical trial microarray dataset.

9.2.3.1 Determining if the genes were de-regulated by Faslodex in the clinic

A paired t-test analysis examining those genes hypothesised to be contributory to the superior HER2- drug response observed in the MCF7 and T47D lines found the Faslodex suppressed gene ARTN was also significantly suppressed by 500mg Faslodex in the NEWEST trial (Table 54). ARTN suppression was seen in the majority of patients (21) (Figure 145A), while only 3 displayed very minimal induction in expression (Figure 145B). In the 21 patients, there was varied suppression of ARTN following treatment (range of fold change= 1.01-2.01), and the average fall was relatively-modest (1.2 fold).

Table 54: Paired t test results from NEWEST data for gene de-regulated by Faslodex in both the MCF-7 and T47D cell lines, and the number of patients showing an induction or suppression in gene expression following 4 weeks 500mg Faslodex treatment versus baseline (n=24).

Gene Symbol	P-value	Number of patients showing gene change	
		Induction	Suppression
PCDH7	0.581	15	9
ARTN	0.001	21	3

Figure 145: Microarray log2 baseline expression and on-treatment mRNA expression of ARTN in (A) patients with Faslodex-suppressed expression (n=21) and (B) patients that showed induction (n=3) following 4 week neoadjuvant 500mg Faslodex treatment.

ARTN changes were subsequently investigated in patients who received 250mg Faslodex. A paired t-test test confirmed that ARTN was also significantly altered by Faslodex treatment, with the majority of patients again displaying some suppression of ARTN (p=0.003). 14 showed suppression of expression while 3 showed induction (Figure 146). In the 14 patients, there was varied suppression of ARTN following treatment (fold range=1.01-1.39) and again the average fall was

quite modest (1.1 fold), lower than that observed in the cell lines where the in both ER+/HER2- cell lines suppression was approximately 2 fold. There were no patients who displayed greater than 1.5 fold suppression in contrast to the 500mg arm.

Figure 146: Microarray log2 baseline expression and on-treatment mRNA expression of ARTN in (A) patients with Faslodex-suppressed expression (n=14) and (B) patients that showed induction (n=3) following 4 week neoadjuvant 250mg Faslodex treatment.

While an overall dominant pattern of change was absent PCDH7 (Table 54), in keeping with its Faslodex-induced expression *in vitro* over half of the patients displayed up-regulation of PCDH7 with 500mg Faslodex (Table 54, Figure 147). However, the degree of induction was minimal in all these patients (fold range 1-

1.29, average fold induction=1.1 (much lower than that observed in ER+/HER2- cell lines where the average fold induction was calculated as approximately 3 fold in the ER+/HER2- cell lines).
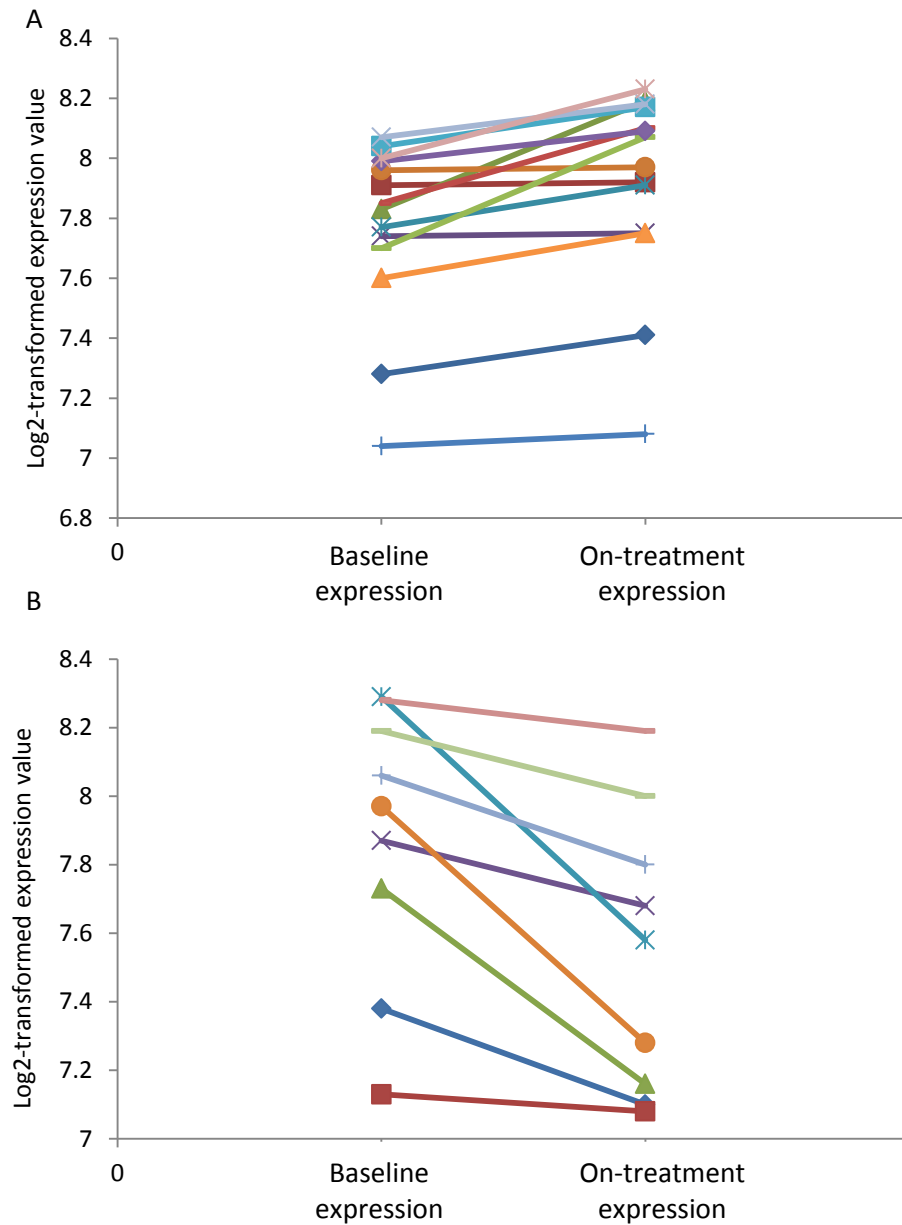
Figure 147: Microarray log2 baseline expression and on-treatment mRNA expression of PCDH7 in (A) patients with Faslodex-induced expression (n=15), and (B) patients that exhibit suppression (n=9) following 4 week neoadjuvant 500mg Faslodex treatment.

9.2.3.2 Determining if Faslodex change in expression of the 2 genes related to Ki67 change

A Mann-Whitney U test was used to determine if any induction of PCDH7 or suppression of ARTN was associated with a greater fall in Ki67 and thus in keeping

with the hypothesis derived from HER2- cells that such changes may contribute to improved Faslodex response. ARTN was found to meet significance in the NEWEST dataset (Table 55). Graphical display of these data revealed the median fall in Ki67 expression was greater in those patients who displayed suppression in ARTN during Faslodex treatment (Figure 148). However, it was noted that there was only a very small patient cohort inducing ARTN during treatment within this analysis.

Table 55: Relationship between direction of gene change and magnitude of Ki67 change (using Mann Whitney U test) following 4 weeks 500mg Faslodex treatment (n=24).

Gene Symbol	P-value
PCDH7	0.403
ARTN	0.040
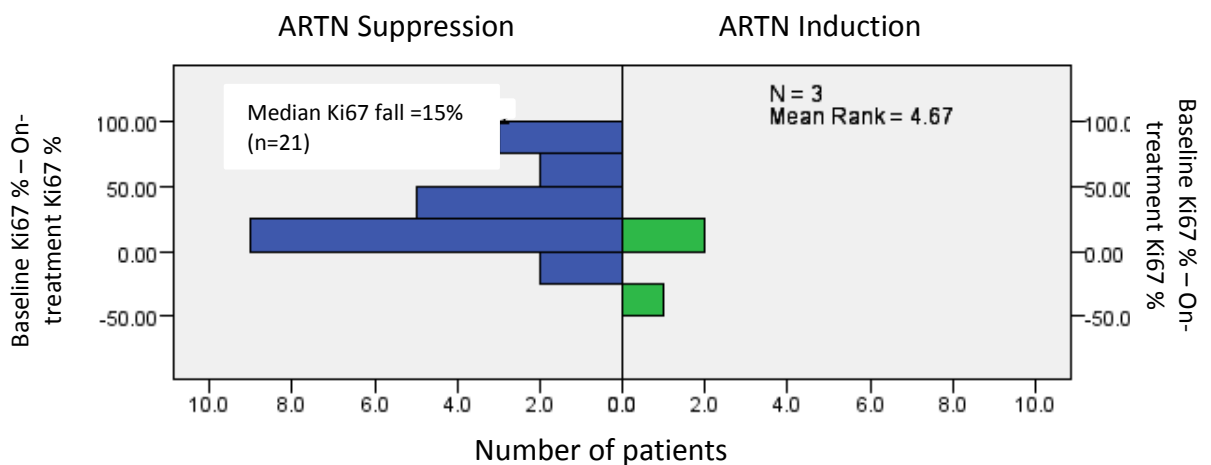
Figure 148: Change in Ki67 in patients exhibiting suppression of ARTN following 4 weeks 500mg Faslodex treatment compared to those with ARTN induction.

Although significance was not met, induction of PCDH7 was also associated with a somewhat improved median suppression of Ki67 (Table 56).

Table 56: Relationship between direction of gene change for PCDH7 and the magnitude of change of Ki67 following 4 weeks of 500mg Faslodex (n=24).

Gene Name	Number of patients with gene suppression	Median suppression of Ki67	Number of patients with gene induction	Median suppression of Ki67
PCDH7	9	11	15	31

9.2.3.3 Determining if RET expression was also de-regulated by 500mg Faslodex treatment within the NEWEST clinical trial microarray dataset.

The major ligand for RET, ARTN, was suppressed by Faslodex in both HER2- cell lines while the RET co-receptor GFRA1 was also suppressed or at a very low expression in these models. RET was also suppressed in both HER2- cell lines by Faslodex. The NEWEST data also showed that both ARTN and GFRA1 expression were suppressed to some degree by Faslodex treatment in many patients in the clinic, with a possible relationship between ARTN and Ki67 suppression, and so RET gene expression was also analysed to further determine any relationship between RET signalling and Faslodex treatment.

A paired t-test revealed that RET was significantly suppressed by 500mg Faslodex treatment (Figure 149) (p=0.010). 16 of the 24 patients analysed demonstrated suppression, which varied in magnitude between patients (fold range 1.02-3.4, average fold suppression=1.48). All 4 patients who had the highest baseline log2-expression value (>8.5) demonstrated a suppression of RET (Figure 149A).
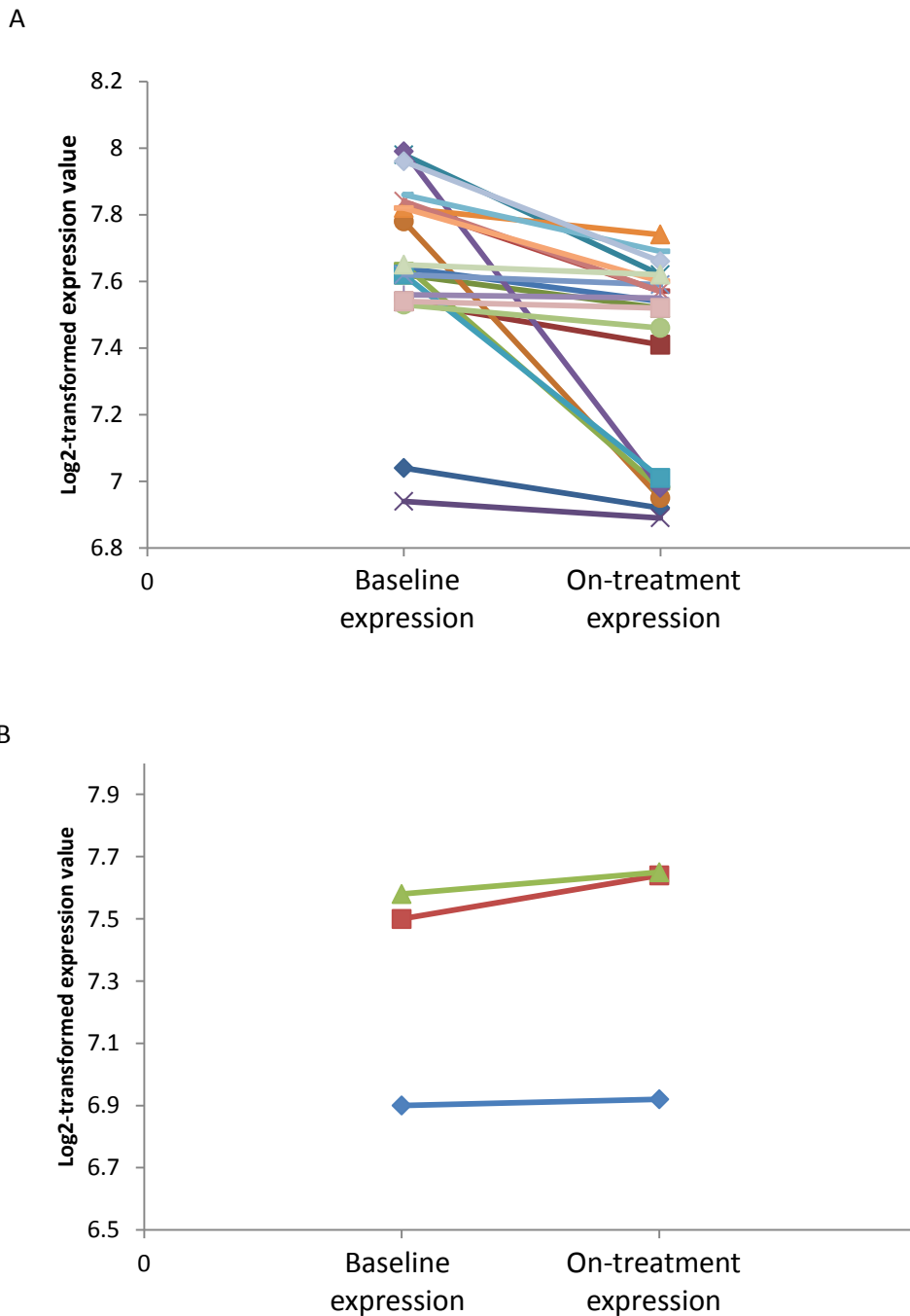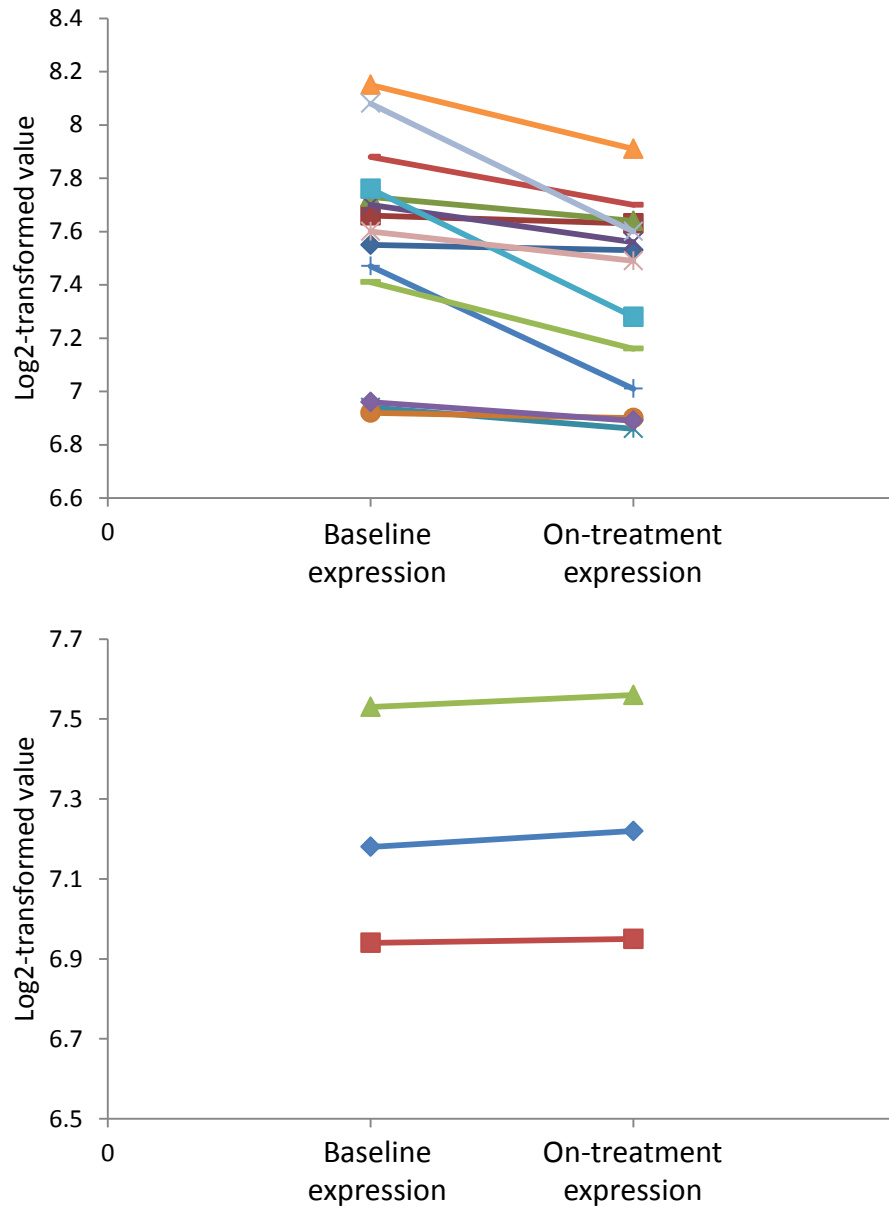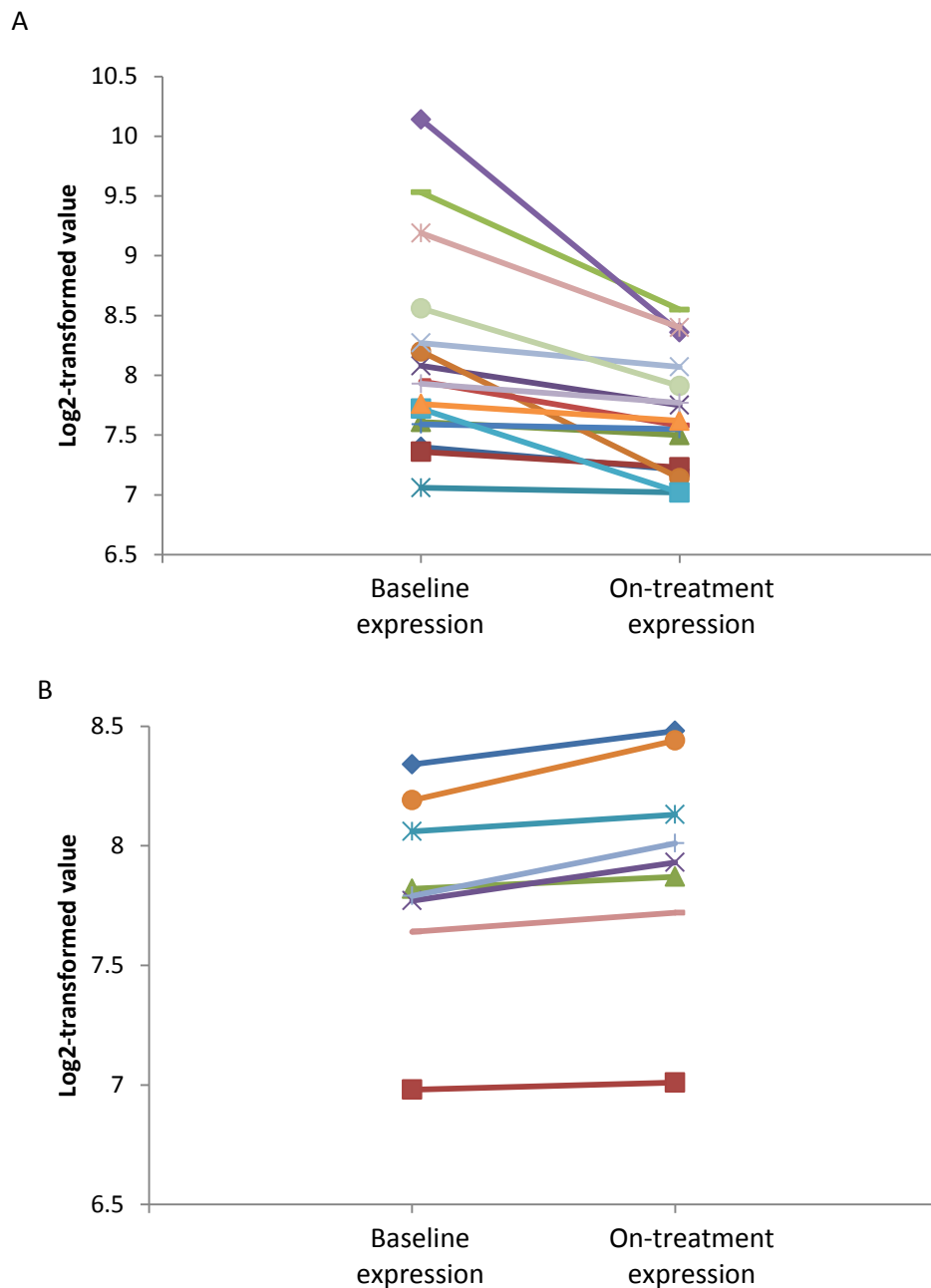
Figure 149: Microarray log2 baseline expression and on-treatment mRNA expression of RET in (A) patients that exhibited Faslodex-suppression (n=16) and, (B) patients that exhibited induction (n=8) following 4 week neoadjuvant 500mg Faslodex treatment.

Subsequent analysis of RET in the Faslodex 250mg trial arm failed to demonstrate a significant pattern of change (p=0.188), although of the 17 patients analysed 10 exhibited suppression (fold range 1-3.3). Average fold suppression of RET was similar in both the 500mg and 250mg patient cohorts (1.48 and 1.49 respectively).

Since the majority of patients exhibited a fall in GFRA1 and ARTN, statistical analysis to assess relationship with Ki67 change was problematic. Such analysis was possible

for RET. The relationship was not significant, although there was a somewhat poorer fall in Ki67 for patients that showed RET suppression (Table 57).

Table 57: Relationship between direction of gene change for RET and the magnitude of change of Ki67 following 4 weeks of 500mg Faslodex (n=24, Mann Whitney U test).

Gene Name	P-value	Number of patients with gene suppression	Median suppression of Ki67	Number of patients with gene induction	Median suppression of Ki67
RET	0.232	16	11.5	8	37

9.2.4 Analysis of CDH2, a gene de-regulated by Faslodex in both ER+/HER2+ cell lines, within the NEWEST clinical trial microarray dataset.

Based on microarray findings, expression and modest induction of CDH2 in the HER2+ cell lines was hypothesised to contribute to limited Faslodex response in HER2+ breast cancer. PCR had been unable to verify a Faslodex-induced profile although it had confirmed that higher basal CDH2 levels were a feature of the poorer-responding HER2+ cells (Chapter 8). Unfortunately, it was not possible in NEWEST to exclusively analyse Faslodex-promoted changes of CDH2, or indeed examine inherent CDH2 expression level, in ER+/HER2+ patients as HER2 data was not available and HER2+ patient numbers are likely to be low. A paired t-test analysis of CDH2 in the 500mg trial arm of the NEWEST trial also found that CDH2 was not consistently de-regulated by Faslodex in these unstratified ER+ patients (Table 58). A similar number of patients displayed induction or suppression of CDH2 following treatment. Analysis of the relationship between Faslodex change in CDH2 and magnitude of Ki67 suppression was also non-significant (Table 59).

Table 58: Paired t test results from NEWEST data for CDH2, and the number of patients showing and induction or suppression of CDH2 following 4 weeks 500mg Faslodex treatment versus baseline (n=24).

Gene Symbol	P-value	Number of patients showing gene change	
		Induction	Suppression
CDH2	0.617	11	13

Table 59: Relationship between direction of gene change for CDH2 and the magnitude of change of Ki67 following 4 weeks of 500mg Faslodex (n=24, Mann-Whitney test).

Gene Name	P-value	Number of patients with gene suppression	Median suppression of Ki67	Number of patients with gene induction	Median suppression of Ki67
CDH2	0.362	13	15	11	12

9.2.5 Further analysis of genes of interest to assess any relationship between change in gene expression and ER-down-regulation following 4 weeks Faslodex treatment.

Genes that showed some evidence of a Faslodex-altered profile in NEWEST (CXCR4, DCN, TXNIP, RET, PCDH7) were further investigated to determine if any relationship existed between their direction of change and degree of ER protein down-regulation by 500mg Faslodex (matched data was available for 23 patients). While of additional interest, due to the very low patients numbers exhibiting an increase in ARTN and GFRA1 following Faslodex treatment these genes were not examined. The absolute change of ER H-score was calculated following 4 weeks 500mg Faslodex treatment (absolute change range=10-125), where all patients in the 500mg trial arm suppressed ER protein expression to a greater or lesser extent. From Table 60 it can be seen that none of the examined genes met significance and thus magnitude of ER down-regulation was not related to their gene change.

Table 60: Relationship between direction of gene changes and the magnitude of change of ER following 4 weeks of 500mg Faslodex (n=23, Mann-Whitney U test).

Gene Name	P-value	Number of patients with gene suppression	Median suppression of ER	Number of patients with gene induction	Median suppression of ER
CXCR4	0.452	7	40	16	56.3
DCN	0.286	6	40	17	52.5
TXNIP	0.235	9	40	14	48.8
PCDH7	0.781	9	40	14	48.8
RET	0.875	15	45	8	50

9.3 Discussion

The neoadjuvant setting confers a number of advantages for investigating the biological characteristics of response and resistance. The primary tumour remains in situ while treatment ensues, and biopsy samples can be taken prior to and during treatment before surgery to remove tumour bulk. IHC analysis of key biomarkers and gene expression profiling can thus be used to assess changes in expression in the sequential samples as treatment proceeds. In this project, a number of genes whose expression is altered by Faslodex in the model panel have been identified and prioritised using microarray and PCR mRNA profiles, ontological studies and KMplotter, with changes in the genes hypothesised to be involved in the varying anti-tumour responses achieved with Faslodex in the cells (summarised in Table 46). Subsequent analysis of these genes in NEWEST clinical trial samples, which had previously been used to evaluate impact of 500mg versus 250mg Faslodex in the neoadjuvant setting on proliferation (Ki67) and ER (Kuter *et al.*, 2012), has provided a unique opportunity to determine if any of these genes were commonly altered by Faslodex and associated with magnitude of Ki67 suppression, thus determining if their de-regulation by Faslodex is potentially relevant to mechanisms of response or may act to limit anti-tumour impact of the drug in the clinic. The majority of the statistical tests to analyse gene expression were carried out using samples from the 500mg Faslodex trial arm: this dose has recently obtained FDA approval following the CONFIRM trial findings showing its clinical anti-tumour superiority versus 250mg antihormone (Di Leo *et al.*, 2010) and the NEWEST trial showing 500mg Faslodex promotes a greater ER and Ki67 down-regulation versus 250mg indicative of superior biological activity (Kuter *et al.*, 2012).

In chapter 3, 5 genes were verified as being Faslodex de-regulated in the HER2+ and MCF-7 cell lines and changes in these genes were hypothesised to be involved in the emergence of Faslodex-resistance regardless of HER2 status. These comprised Faslodex-induced genes PRKACB, VEGFC, CKCR4 and GABBR2, and also one Faslodex suppressed gene GFRA1. Unfortunately, the 4 induced genes hypothesised to be involved in acquisition of Faslodex resistance *in vitro* failed to

meet significance in the NEWEST trial for a dominant pattern of Faslodex impact on their expression using a paired t test (Table 48). Furthermore, where inductions were observed these were generally only modest (e.g. 1.2 fold for CXCR4). While this lack of significant change suggests that Faslodex induction of these genes is not robust *in vivo* and therefore unlikely to underlie subsequent emergence of Faslodex resistance which ultimately occurs in many patients, the lack of significant induction could simply be due to the limitations of the clinical trial studied. The NEWEST trial samples can only allow identification of changes in gene expression, and their relationship with proliferation, over a 4 week treatment timeframe. Although inductive events were rapid *in vitro* (apparent in the models at 10 days along with complete ER down-regulation), more prolonged treatment may be required to observe maximal ER blockade by Faslodex and in turn the necessary magnitude of up-regulation of these genes of interest to ultimately promote emergence of acquired resistance.

Despite the lack of significant pattern with Faslodex, further profile interrogation was performed and revealed that for PRKACB, VEGFC and GABBR2 approximately half of the patients showed increases in expression during treatment, while 17 of the 24 patients showed some up-regulation of CXCR4 with 500mg Faslodex at 4 weeks (Table 48). Future studies would be required to determine if there were further expression increases with more extended Faslodex exposure and also to determine if those patients showing CXCR4 increases, or indeed increases in PRKACB, VEGFC or GABBR2, ultimately acquired resistance following continued treatment to confirm or refute their hypothesised role in emergence of this state. Although no association with proliferation was seen for PRKACB, VEGFC or GABBR2, further data supportive of such a hypothesis were derived here for CXCR4, since patients who did show increases in this gene following 500mg Faslodex treatment had a somewhat inferior decline in Ki67 compared to patients where CXCR4 was suppressed during treatment (Table 49).

Thus, of the genes identified as potentially relating to emergence of acquired resistance in the MCF7 and HER2+ models, CXCR4 perhaps has the most promise as a Faslodex-induced gene that may act to limit anti-proliferative response in some

patients. CXCR4 has previously been reported to be induced by oestrogen in MCF-7 and ZR-75 ER+ breast cancer cell lines and suppressed by Faslodex (Boudot *et al.*, 2011). However, our HER2+ and MCF7 model data with Faslodex, and the NEWEST array data showing that Faslodex treatment induces expression in many patients, are at odds with this observation. The mechanism of CXCR4 induction by this antihormone remains unclear. *In vivo*, activation of CXCR4 by its stromal ligand SDF-1 can induce CXCR4 expression (Rhodes *et al.*, 2011). However, this mechanism seems unlikely to contribute since it is dependent on interplay with ER, which is significantly reduced after 500mg Faslodex treatment in many NEWEST trial patients. Furthermore, such a mechanism does not explain the parallel *in vitro* observation of CXCR4 induction where ER loss was almost complete with Faslodex and also SDF-1 expression was also suppressed by Faslodex *in vitro*. It seems more likely that up-regulation of CXCR4 is via an oestrogen-repressed mechanism that is reversed following ER depletion with Faslodex in some breast cancers. In mouse models, the importance of the CXCR4-MAPK pathway has been established for hormone-independent tumour growth and thus an induction of MAPK signalling elements by Faslodex treatment may be important for the induction of CXCR4 (Rhodes *et al.*, 2011; Hutcheson *et al.*, 2003). This event appears to be context-dependent, as Faslodex suppression of CXCR4 in 7 patients in NEWEST also indicated some capacity for positive CXCR4 regulation by oestrogen (as observed experimentally by Boudot *et al.,* 2011) in a minority of patients.

In accordance with its Faslodex suppression in both the HER2+ and MCF-7 cells, interrogating the NEWEST sample gene microarray data revealed that the further prioritised gene GFRA1 was also significantly decreased by 4 weeks 500mg Faslodex treatment in clinical breast cancers (Table 48 and Figure 137), as well as by 250mg Faslodex (Figure 139). While suppression was generally comparable with the two doses (mean suppression: 500mg-1.97 fold; 250mg-1.5fold), it was notable that the largest changes (up to 8.3 fold) were seen in the 500mg treatment arm. These data in total suggest that GFRA1 is a classical ER-regulated gene in some breast cancers given the decreases in expression with Faslodex. In keeping with this, GFRA1 has been reported to be a luminal A gene and is induced by oestradiol stimulation of

the ER+ ZR-75-1 cell line (Dorssers *et al.*, 2005), while in turn it was Faslodex-suppressed in both the HER2+ and MCF-7 cell lines (PCR revealed very low expression in the BT474 cell line) in this project (Figure 57). Unfortunately, GFRA1 suppression could not be formally associated with magnitude of Ki67 suppression in NEWEST since only 1 patient showed induction of GFRA1 following 500mg treatment (Table 48). However, based on ontology it seems unlikely that the loss of GFRA1 that is common to the 3 models that developed resistance and in most clinical breast cancers during early Faslodex treatment acts to limit response. GFRA1 is a co-receptor for the tyrosine kinase RET, and it is gain in GFRA/RET signalling that has been linked to downstream proliferation and cell survival kinase activity as well as tamoxifen and also aromatase inhibitor resistance (Morandi *et al.*, 2013). Where ER is retained, such endocrine resistance can involve productive GFRA/RET cross talk with this receptor (Plaza-Menacho *et al.*, 2010). It seems more likely, therefore, that depletion of GFRA/RET signalling during early treatment of the models and in clinical disease is a component of the initial Faslodex anti-tumour response mechanism, but further studies are required to confirm or refute this and to address whether such signalling ultimately recovers to drive acquisition of resistance to Faslodex.

Interestingly, a further RET pathway gene ARTN (a GFRA ligand that can interplay with GFRA1 (Airaksinen *et al.*, 2002)) was Faslodex depleted in both HER2- lines MCF-7 and T47D which exhibited superior anti-tumour response. Decreases in ARTN were thus hypothesised to be involved in an improved Faslodex response in the ER+/HER2- setting. Although HER2 status was not available for the NEWEST trial, it is assumed that the majority of patients were also HER2- since only 10% of ER+ tumours are HER2+ (Dowsett *et al.*, 2008). In keeping with the HER2- cell model observations, ARTN was significantly decreased by both 500mg and 250mg Faslodex in the majority of the trial patients (Table 54 and Figure 145, 146). The average fold suppression was quite modest and comparable for both treatment arms (1.1 and 1.2 fold respectively) indicating some suppression of ARTN during early treatment can be achieved without maximal ER blockade. However, all patients with >1.5 fold changes had undergone 500mg treatment and in total this gene appears to be ER

regulated in some breast cancers. Further analysis determined that suppression of ARTN was significantly associated with a greater fall in Ki67 (Table 55 and Figure 148) but as so few patients demonstrated an increase in ARTN expression (n=3) this requires future verification. Nevertheless, the observations of Faslodex depletion of ARTN *in vivo* and *in vitro*, as for GFRA1, and the adverse ontology previously reported for ARTN (Kang *et al.*, 2010) again imply that depletion of ARTN/GFRA/RET signalling may be contributory to Faslodex response. In keeping with this, in chapter 5 it was also shown that RET was Faslodex suppressed in the HER2- cell lines (Figure 47) and similarly analyses of NEWEST revealed that RET was significantly decreased by 500mg treatment and was also depleted in a proportion of the 250mg cohort (Figure 149). These data suggest that like ARTN and GFRA1, RET can be ER-regulated *in vivo*, and RET expression has also been previously reported to be prominent in a subset of ER+ disease (Morandi *et al.*, 2011) and oestrogen regulated *in vitro* (Stine *et al.*, 2011; Dorssers *et al.*, 2005). However, this Faslodex suppression of RET was not associated with an improved Ki67 fall (Table 57). It is feasible that measuring phosphorylation of RET, which is promoted by ARTN binding to co-receptors including GFRA1, would provide a better correlate for proliferation. However, it remains possible that Faslodex-depleted GFRA1, ARTN and RET merely comprise indicators of ER blockade rather than being substantially-contributory towards the Faslodex response mechanism, and so further studies are required to confirm such a relationship in ER+ breast cancer, including after HER2 subdivision. Interestingly, 8 of the patients showed induction of RET during short term treatment. As up-regulation of RET has been associated with anti-oestrogen resistance (Morandi *et al.*, 2013), it is possible that these patients may have had a more limited drug response, but NEWEST follow-up data would be required to confirm this.

A gene shown to be Faslodex induced in both the HER2- lines was PCDH7, and so potentially its induction could also be linked to their superior anti-tumour response. In NEWEST, there was no significant dominant change in PCDH7 expression with Faslodex and relationship with Ki67 change was also non-significant for this gene (Tables 55 and 56). However, 15 patients did show some induction and this appeared to be associated with a somewhat greater fall in Ki67 (Table 56). This is in

keeping with the hypothesis that induction of PCDH7 by Faslodex can associate with an improved anti-tumour response, but it seems this may only be applicable to a subpopulation of ER+ patients, again requiring further consolidation in ER+ patients of known HER2 status. Currently, there are no clinical trials involving Faslodex where ER+ patients are subdivided based on HER2 positivity or negativity.

However, there are some trials on-going that are exclusively recruiting ER+/HER2+ patients to assess Faslodex impact with and without lapatanib (ClinTrial.gov: NCT00390455). Such trials will be valuable to further investigate CDH2, the only gene whose intrinsic level, possibly further augmented by Faslodex treatment, this project has determined may contribute to earlier emergence of Faslodex resistance in both ER+/HER2+ cell models. Analysis of CDH2 in the NEWEST clinical trial determined that a similar number of ER+ patients demonstrated an induction or suppression following 500mg Faslodex treatment (Table 58) and that there was very little relationship to median fall of Ki67 (Table 59). This lack of association is perhaps to be expected since it was not possible to confine analysis to ER+/HER2+ patients in NEWEST or to explore impact of intrinsic CDH2 expression in such a cohort. Moreover, given this is a neoadjuvant trial with sample analysis after only 4 weeks treatment, any Faslodex-induced changes in CDH2 that relate to subsequent development of resistance in ER+/HER2+ breast cancer may not be observed. Some reports have also linked CDH2 expression with increased invasion and motility (Hazan *et al.*, 1997), and so CDH2 may only contribute to disease progression during extended treatment.

Of particular interest in this project were 4 genes, DCN, TXNIP, TGFB2 AND CASP1, identified as being induced by Faslodex in the T47D cell line only and so hypothesised to be involved in the complete-response mechanism observed exclusively in this model and potentially to improved anti-tumour response clinically. TXNIP, TGFB2 and CASP1 unfortunately did not show a dominant pattern of induction by 500mg Faslodex in the clinic (Table 50) but it remains feasible that induction within some ER+ patients is associated with an improved anti-tumour response. Of some interest in this regard was TXNIP, where there was a trend for an association between Faslodex-induced expression and an improved fall in Ki67 (Table

51/Figure 143). TXNIP has been described as a potential tumour suppressor gene and increased expression of TXNIP has been associated with improved prognosis (Zhou *et al.*, 2012). Increase in the oxidation of thioredoxin has been associated with endocrine resistance (Penney *et al.*, 2013), and so the ability of TXNIP to inhibit thioredoxin could contribute to an improved Faslodex response. In addition, there was a somewhat greater median fall in Ki67 expression in patients who induced TGFB2 or CASP1 (Table 52) and the available ontological literature (Buck *et al.*, 2008; Gomes *et al.*, 2011; Tamura *et al.*, 1995; Bouker *et al.*, 2005) is also supportive that these genes may relate to an improved Faslodex response in a sub-group of ER+ breast cancers.

However, of the 4 genes induced by Faslodex in T47D cells, DCN was the most promising in the clinical samples. DCN was found to be consistently de-regulated by 500mg Faslodex (Table 50). DCN changes were close to significance and further profile analysis confirmed that the majority of patients showed Faslodex-induced DCN expression following 4 week neoadjuvant treatment (average induction of 2.3 fold), in keeping with the induction observed in the T47D cell line with this antihormone. Analysis of the effect of 250mg Faslodex on DCN gene expression found no such trend suggesting that induction of DCN for the majority of patients only occurs with the higher dosage where there is more efficient tumour delivery of drug and thus ER blockade (Kuter *et al.*, 2012). However, analysis of DCN change in relation to degree of ER suppression was found to be non-significant (Table 60) and so the mechanisms underlying its significant induction by 500mg Faslodex remain enigmatic. The observation that the gene was suppressed in 7 patients also implies context-dependent ER regulation of DCN expression: however, decorin has not been described as oestrogen regulated and subsequent analysis of promoter sites on the DCN gene using the UCSC genome browser (http://genome.ucsc.edu/) in this project did not identify an ERE site. Interestingly, those patients that suppressed DCN had a significantly higher log2 expression value than those that induce expression suggesting baseline DCN expression may be a contributory factor in determining the direction of change in expression observed with antihromone (Figure 140). Another factor to consider is that decorin is also expressed by cells of

328

the tumour stroma (Oda *et al.*, 2012). Differences in stromal decorin between tumours and its regulation may also contribute to baseline DCN level and whether induction or suppression of expression is subsequently recorded during Faslodex treatment *in vivo*. Future clarification will be required via IHC using Faslodex-treated clinical trial material to verify DCN localisation in relation to epithelial and stromal cells within breast cancers.

Critically, further analysis of the 500mg trial data identified that patients who had induced DCN with Faslodex also demonstrated an improved fall in Ki67 proliferative capacity (Table 51, Figure 142), in keeping with a role for DCN induction driving improved Faslodex anti-tumour response both *in vitro* and *in vivo*. Of the 24 patients analysed, 3 displayed an up-regulation of Ki67 during Faslodex treatment. These proliferation increases could be an indication of intrinsic Faslodex resistance. In the IMPACT clinical trial, mean % change of Ki67 was greater in responders versus non-responders (determined by objective clinical response) in the combination arm of anastrozole and tamoxifen following 2 or 12 weeks of treatment but this was not significant. However, when the individual treatment arms were assessed responders exhibited a significantly greater fall in Ki67 versus non-responders following 2 weeks tamoxifen therapy (Dowsett *et al.*, 2005). As DCN was hypothesised to contribute to the Faslodex promoted complete-response in the T47D cell line and thus superior Faslodex response *in vivo*, DCN was thus reanalysed using only patients who showed a Ki67 fall and so potentially responding to treatment. This analysis was significant, with 500mg Faslodex induction of DCN associating with a greater median fall in Ki67 (Figure 144).

DCN has been widely reported to have anti-tumour capabilities via its ability to inhibit a number of RTK's known to be involved in oncogenic signalling including EGFR, HER2, c-MET and IGF1R (reviewed in Iozzo *et al.*, 2011). In conjunction with this decorin has been reported to sequester a number of RTK ligands further preventing tumour growth (Iozzo *et al.*, 2011; Goldoni *et al.*, 2008a). Cumulatively, therefore, the expression and ontological data suggest that up-regulation of DCN in the T47D cell line is likely to contribute to its complete response to Faslodex and importantly, in a number of patients Faslodex also induces tumour decorin which

may improve reduction of Ki67 during treatment. It is feasible in turn this may relate to improved clinical response *in vivo* and possibly for some patients a complete response. Follow-up data are required for patient outcome with Faslodex to confirm this observation. Complete response is not a common phenomenon (CONFIRM trial 1.1% of patients receiving 500mg Faslodex exhibited a complete response (Di Leo *et al.*, 2010), so the data here suggest that up-regulation of DCN by Faslodex *in vivo* is not solely responsible for complete response clinically. Induction of other factors may be required such as the further Faslodex induced gene TXNIP or potentially there may be absence of Faslodex-induced genes involved in adverse growth (e.g. CXCR4). However, tracking of DCN expression is also required over a more prolonged Faslodex treatment period to determine of DCN expression is further altered only in the proportion of patients who go on to elicit a complete response.

In summary, therefore, NEWEST has proved extremely valuable in accumulating clinical evidence that several of the genes prioritised in previous chapters are influenced by Faslodex treatment as in the cell models, and in some instances also relate to proliferation changes during treatment in clinical disease, successfully re-enforcing hypotheses in relation to Faslodex response or failure. Of note, the majority of the most promising genes were those hypothesised to be involved in an improved Faslodex response, although success for such genes may in part be due to the limitations of such a neoadjuvant trial. While changes in some of the prioritised genes may potentially contribute in sub-populations of ER+ disease, the genes most promising in the context of determining Faslodex impact were a:

- Faslodex-decreased RET pathway elements (i.e. ARTN and RET which were also Faslodex- depleted in both HER2- lines; GFRA1 which was also Faslodex depleted in HER2+ and MCF7 cells) in relation to improved Faslodex response
- Faslodex-induced DCN and TXNIP (which were also induced in T47D cells only) in relation to improved Faslodex response.
- Faslodex-increased CXCR4 (which was also Faslodex induced in HER2+ and MCF-7 cells) in relation to limiting response.

Of these, DCN was deemed of most interest, where the data in this Chapter are highly suggestive that induction of DCN by 500mg Faslodex could be very important in determining superior Faslodex growth-inhibitory responses. Based on the NEWEST findings, its profile with Faslodex in the complete responding T47D cells and PCR verification and ontology, DCN was chosen to go forward for mechanistic studies to further determine if it has an important causal involvement with superior Faslodex response using the T47D cell line.

Chapter 10

Further investigation of decorin function in relation to the complete-response exerted by Faslodex in T47D cells

10.1 Introduction

Following long-term treatment with Faslodex *in vitro*, T47D cells underwent a complete response. The microarray work in chapter 6 aimed to identify Faslodex-altered gene expression in this model (e.g. drug-promoted genes with a potential tumour inhibitory function) that may subsequently contribute towards the mechanism of this Faslodex-promoted complete response. Further study of strong candidates could be useful in determining novel therapeutic strategies to encourage improved response to Faslodex clinically and *in vitro*, as well as biomarkers that may relate to drug outcome.

In this regard, the microarray data indicated that mRNA expression of the gene decorin (DCN) was up-regulated by 10 day Faslodex treatment in T47D cells, contrasting the additional ER+ models. Further investigations in chapter 6 verified the unique induction of decorin in this cell line and identified published reports that had also described decorin as anti-tumorigenic (summarised in Table 20 of Chapter 6) as well as providing supportive KMplotter observations in relation to tamoxifen outcome. Subsequent analysis of DCN mRNA expression in the NEWEST clinical breast cancer trial revealed that DCN was consistently up-regulated in the majority of patients who received 500mg Faslodex treatment and that this associated with an improved fall in Ki67 proliferative activity. These data in total suggested that decorin was a strong candidate for involvement in the Faslodex-promoted T47D complete-response and (although it was not possible to ascertain from the NEWEST

series involvement with clinical outcome) also possibly involved in the growth inhibitory mechanism seen with this antihormone in ER+ breast cancer patients.

In this chapter, several experimental approaches have thus been taken to further determine if induction of decorin contributed to the superior response mechanism in T47D cells with Faslodex. Firstly, DCN immunocytochemistry was optimised and used to confirm if Faslodex induction at the mRNA level in T47D cells was also mirrored at the protein level. It was also important to perform *in vitro* experiments to more fully monitor the expression profile of decorin induction with continuous Faslodex treatment of T47D cells, since the Faslodex-induced complete response in this model did not occur until post week 5 of treatment despite significant induction of DCN expression by day 10. While its localisation remains controversial and no studies have been performed with Faslodex treatment, reports indicate decorin is a proteoglycan that can be synthesised by cancer epithelial and stromal cells and secreted into the microenvironment to subsequently regulate tumour signalling pathways in an autocrine and/or paracrine manner by binding to RTKs at the tumour cell membranes (Csordas *et al.*, 2000). A purified peptide is commercially available that can be used for DCN growth challenge experiments *in vitro*, and so growth experiments were conducted to determine any growth inhibitory impact of exogenous decorin in the presence and absence of Faslodex on the T47D cells, as well as in further ER+ lines to determine if any effect was exclusive to this model. Furthermore, studies with DCN shRNA were carried out in the T47D cells to see if prevention of Faslodex-induction of the gene could be achieved and if such DCN knockdown was able to hinder Faslodex growth inhibitory effect.

Finally, the project investigated if there was any evidence for a broader contribution for DCN in determining endocrine response by exploring evidence for its regulation by ER (using online bioinformatic resources) and examining whether DCN induction also occurs during treatment with further antihormonal agents tamoxifen or oestrogen-deprivation. The latter was achieved (i) PCR studies monitoring DCN expression during antihormone treatment in T47D, and (ii) examining DCN changes in a further clinical dataset from Trial 223 (Smith *et al.*,

2007). This is a neoadjuvant study sponsored by AstraZeneca to investigate if combination of gefitinib and the AI anastrozole effectively led to a greater response in breast cancer. In this project, the initial 2 week data from the trial were analysed since these patients had only received anastrozole and microarray and IHC data was available for a cohort of these patients where DCN expression could be profiled prior and subsequent to treatment. Using the Trial 223 data it was also possible to address if any DCN induction by AI related to anti-proliferative effect and so may contribute to anti-tumour response.

10.2 Results

10.2.1 DCN Immunocytochemistry

Immunocytochemistry was successfully optimised for DCN in the models Ssubsequent HScore analysis revealed only very low levels of cytoplasmic DCN protein prior to treatment in all models (Figure 150). Following 10 day Faslodex treatment, the T47D cell line was the only model to substantially up-regulate expression of DCN protein, as observed at the mRNA level (Figure 150), with high levels of cytoplasmic and also plasma membrane staining in some cells after treatment. There was only very modest Faslodex up-regulation in the MCF-7 and MDA-MB-361 cell lines and no plasma membrane-localised protein detected.

	Control	Faslodex 10^{-7}M
T47D ER+/HER2-	Hscore: 45	Hscore: 180
MCF-7 ER+/HER2-	Hscore: 20	Hscore: 40
BT474 ER+/HER2+	Hscore: 10	Hscore: 10
MDA-MB-361 ER+/HER2+	Hscore: 65	Hscore: 80
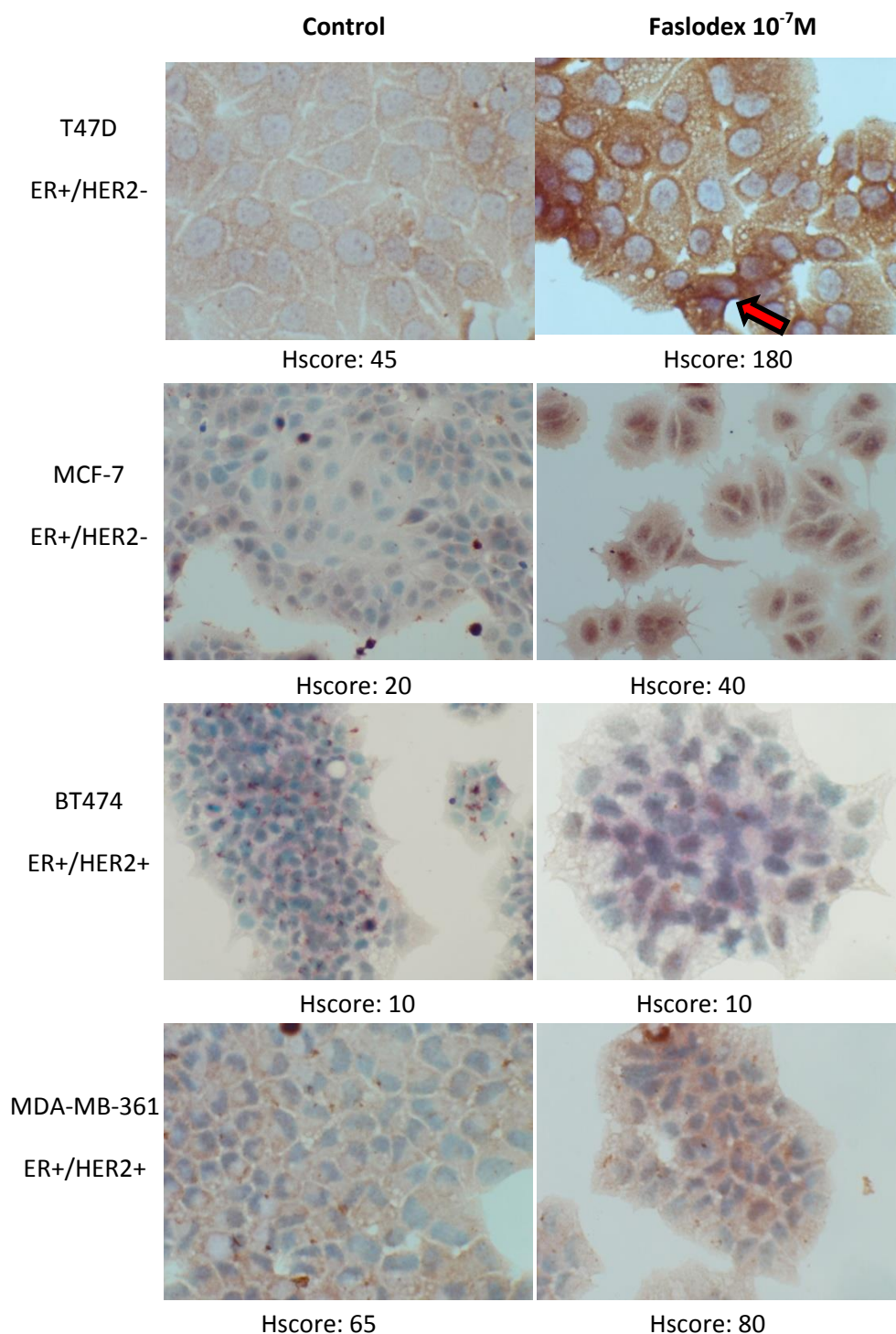
Figure 150: Immunocytochemical analysis of DCN expression in the 4 ER+ breast cancer cell lines pre and post 10 day Faslodex treatment (10^{-7}M) with associated staining Hscores. Along with prominent cytoplasmic staining, Faslodex-induced plasma membrane staining (red arrow) is shown in the T47D cells (Original magnifications x40).

10.2.2 Temporal relationship between DCN expression and duration of Faslodex treatment

 To monitor if there were further increases in DCN with increasing duration of antihormone exposure, PCR was used to monitor the expression profile of DCN following extended culture of T47D cells with/without Faslodex. DCN level appeared to be temporally related to Faslodex treatment. Its expression was up-regulated in the T47D cell line over 10-28 days Faslodex treatment versus time-matched untreated control cells. This resulted in 6 fold increase in DCN expression by 28 days with Faslodex that was significantly increased versus earlier treatment timepoints (Figure 151).
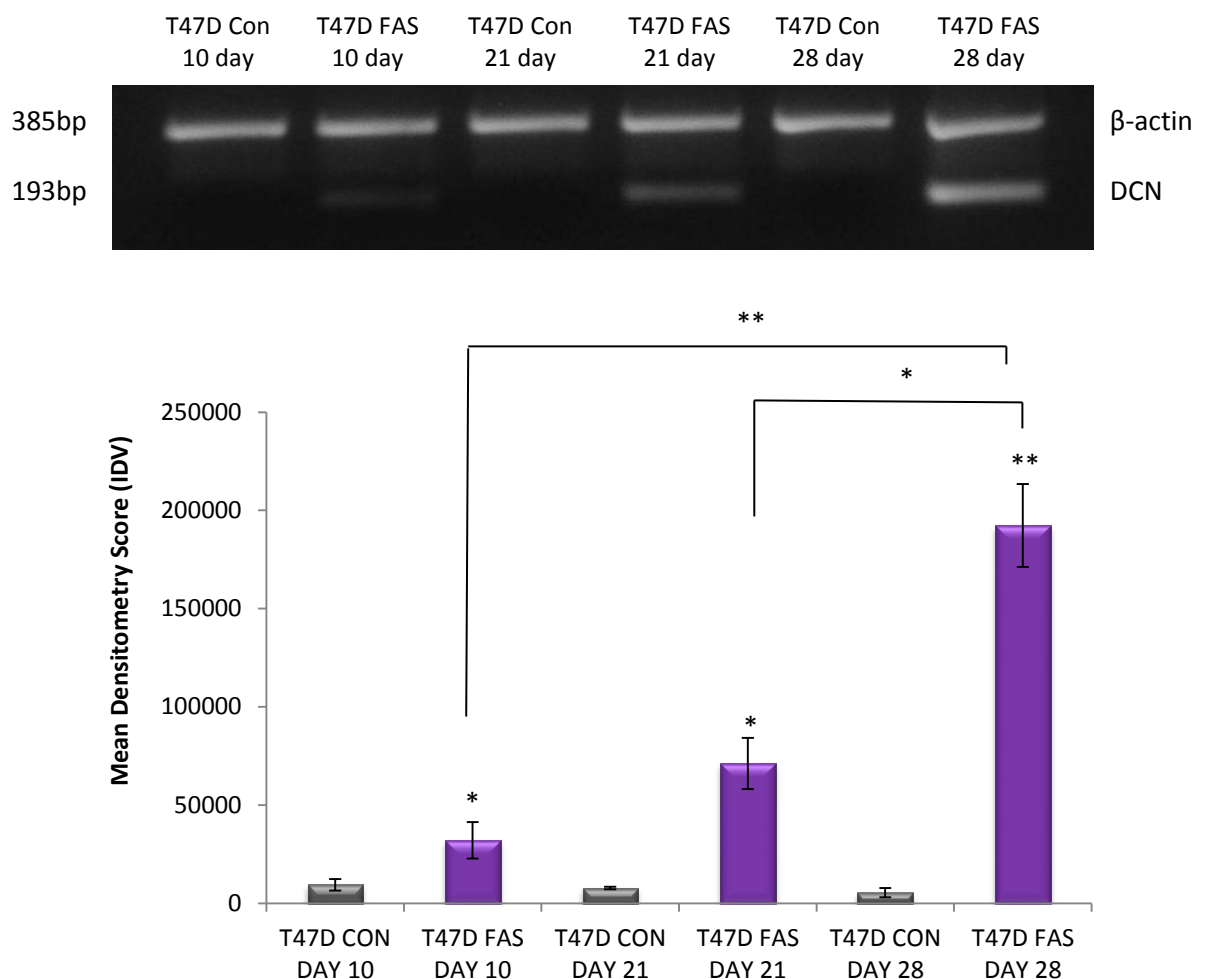
Figure 151: Effect of increasing duration of Faslodex treatment (10-28 days) on DCN gene expression in T47D cells: (A) Representative PCR image (Con-Control; FAS-Faslodex) (B) with the corresponding actin-normalised densitometry graph .The results are expressed as

means ± SEM of three separate experiments. *P < 0.05, **P < 0.01 for treatment versus its respective time point control. Additional statistical comparison has been made between Day 28 and the further treatment timepoints (*P <0.05, ** P<0.01)

10.2.3 Effect of exogenous decorin on growth of ER+ breast cancer cell lines

10.2.3.1 ER+/HER2- T47D cells:

To determine if decorin was capable of inhibiting T47D cells, these cells were treated with exogenous decorin and growth and morphology analysed after 10 days treatment by phase contrast microscopy and Coulter counting studies (Figures 152 and 153). Comparison was also made with the anti-tumour impact of Faslodex and with Faslodex plus decorin combination treatment. Decorin and also all further treatment strategies significantly inhibited growth (by 60-70%) of the T47D cell line in comparison to untreated control (p<0.001) (Figures 152 and 153). Exogenous decorin treatment also further significantly growth inhibited the T47D cells compared with Faslodex alone (p=0.007) alone. Combining decorin with Faslodex also gave some further growth inhibition but this failed to reach significance versus Faslodex alone. However, the phase contrast images (Figure 152) tentatively suggested that exogenous decorin treatment either alone or in combination with Faslodex not only reduced culture growth but (in contrast to Faslodex alone) also induced significant changes in morphology and occasional small bright, disrupted cells, possibly evidencing instigation of some cell death.

Figure 152: Phase contrast microscope images of T47D cells following 10 days of culture with decorin (100µM), Faslodex (10^{-7}M), a combination of these treatments or untreated control (original magnification= x10).

Figure 153: Effect of 10 day treatment with decorin (100µM dose), Faslodex (10^{-7}M dose) or their combination on growth of the T47D cell line. The results are expressed as means ± SEM of three separate experiments and presented as % of untreated control. *** $P < 0.001$, versus untreated control; ** $P < 0.01$ versus Faslodex treatment.

10.2.3.2 ER+/HER2- MCF-7 cells:

The *in vitro* growth experiments with exogenous decorin were also repeated using MCF7 cells to determine if its growth inhibitory and associated morphological effects were limited to the T47D cell line or if such effects could also be observed in another ER+/HER2- breast cancer cell line (Figures 154 and 155). Decorin induced a partial growth inhibitory effect in the MCF-7 cell line versus untreated control cells (~30%; $p<0.05$). Growth inhibition was also significant for Faslodex treatment in this model (~60%; $p<0.001$). The decorin impact appeared inferior in MCF-7 cells to that in T47D cells ($p<0.05$), and Faslodex also appeared to be a superior inhibitor versus decorin in MCF-7 contrasting T47D observations (Figure 155). The combination of decorin and Faslodex was growth inhibitory ($p<0.01$) but in Coulter counting studies failed to growth inhibit the cells further than Faslodex treatment alone (Figure 155). Nevertheless, phase contrast images possibly suggested a slightly greater inhibitory effect when decorin and Faslodex were in combination (Figure 154).

Control | Decorin

Faslodex | Decorin+Faslodex
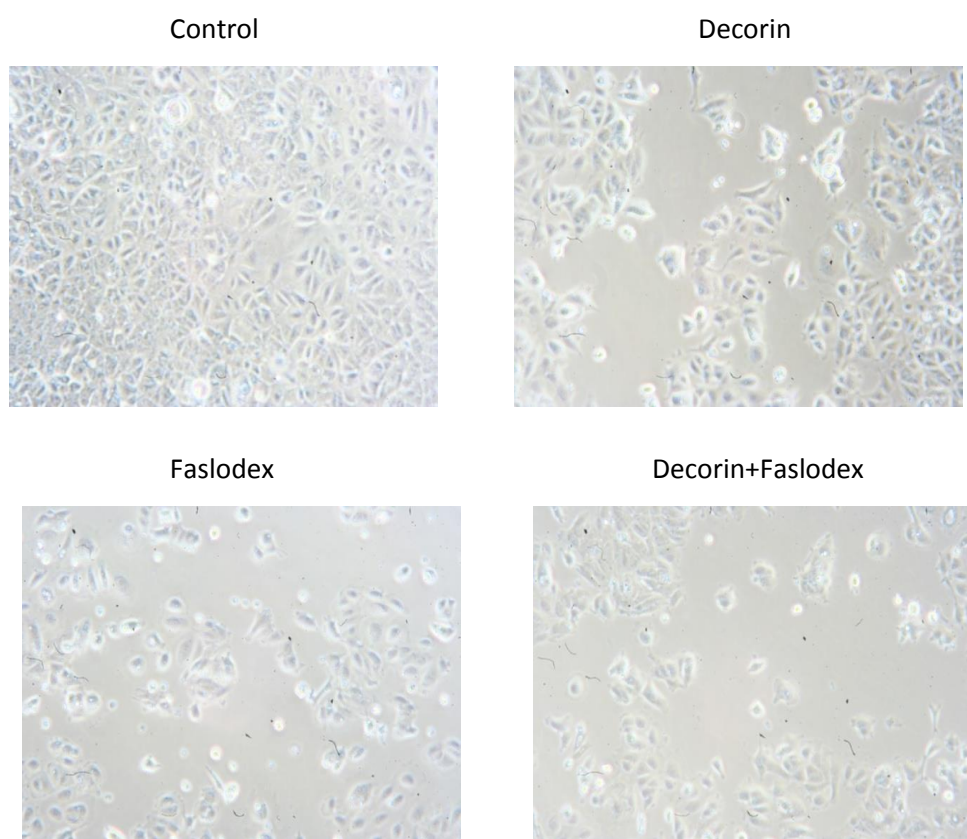
Figure 154: Phase contrast images of MCF-7 cells following 10 days of culture with decorin (100µM), Faslodex (10^{-7}M), a combination of these treatments or untreated control (original magnification= x10).
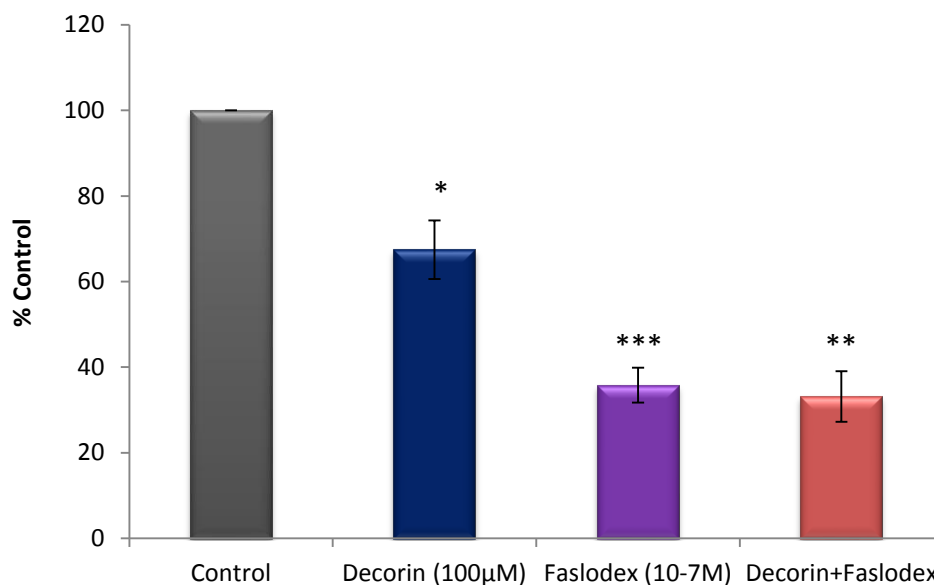
Figure 155: Effect of 10 day treatment with decorin (100μM dose), Faslodex (10^{-7}M dose) or their combination on growth of the MCF-7 cell line. The results are expressed as means ± SEM of three separate experiments and presented as % of untreated control. *** P < 0.001, **p<0.001, *P<0.05, versus untreated control.

10.2.3.3 ER+/HER2+ BT474 cells:

The growth inhibitory effects of exogenous decorin were also investigated in an ER+/HER2+ line BT474 (Figures 156 and 157). As in MCF7 cells, in BT474 cells exogenous decorin induced a modest significant growth inhibitory effect versus untreated control cells (~30%; p=0.03). Growth inhibition was also significant for Faslodex treatment in this model (~50%; p=0.002) (Figures 156 and 157). Of note, as in MCF7 cells, the decorin impact was inferior in BT474 cells to that in T47D cells and there was also a trend for Faslodex to be a superior inhibitor versus decorin (p=0.061), again contrasting T47D observations. As seen with the single agents, combination of decorin and Faslodex was significantly growth inhibitory (p<0.05) but failed to promote any further growth inhibitory activity compared to Faslodex alone (Figure 157). Phase contrast images confirmed the growth inhibitory impact of decorin, Faslodex or combination treatment (Figure 156), and that there was no apparent further impact of the combination treatment versus Faslodex alone.
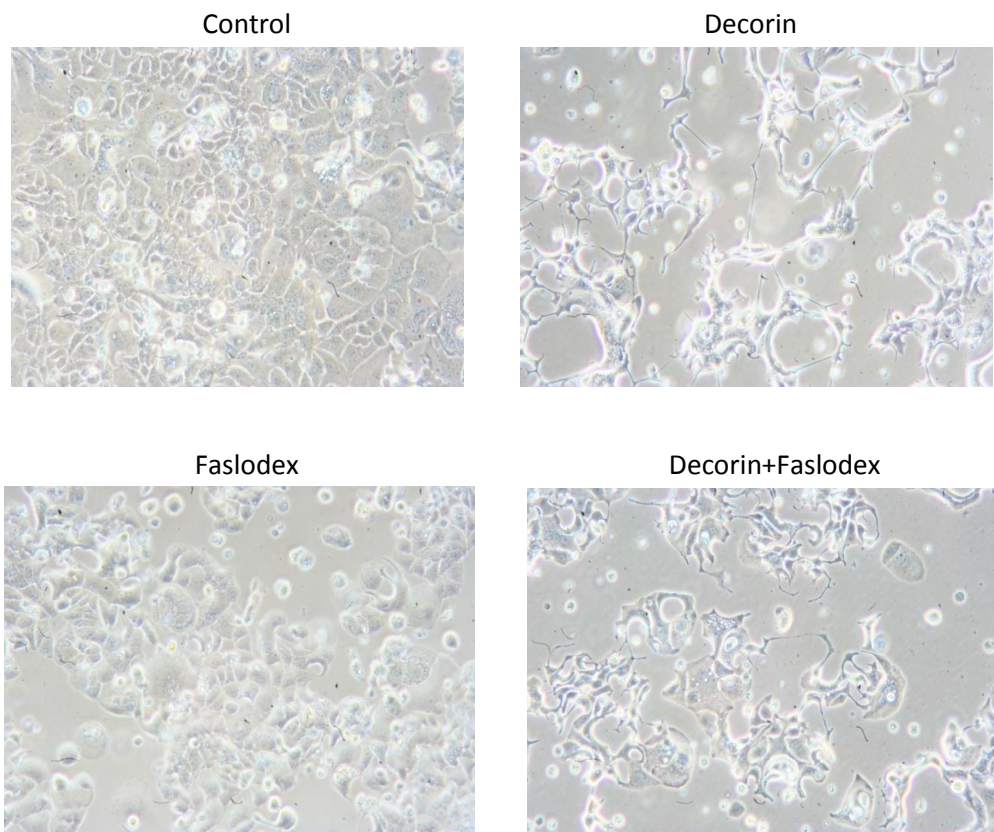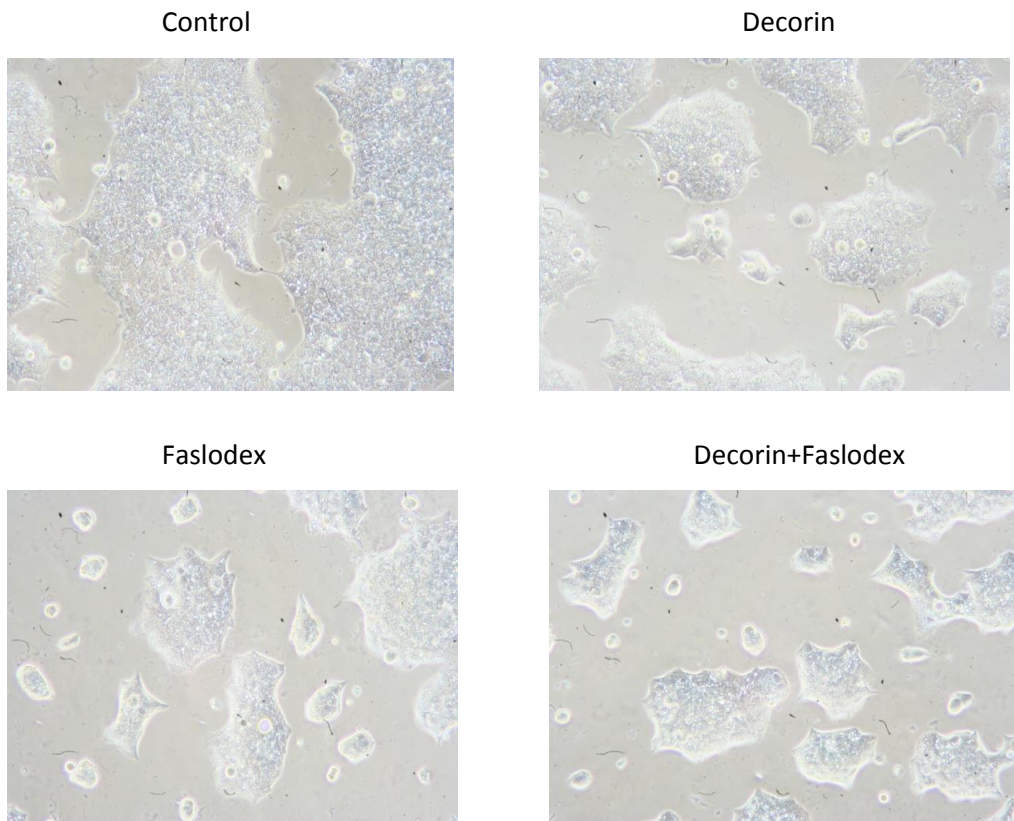
Figure 156: Phase contrast images of BT474 cells following 10 days of culture with decorin (100µM), Faslodex (10^{-7}M), a combination of these treatments, or untreated control (original magnification= x10).
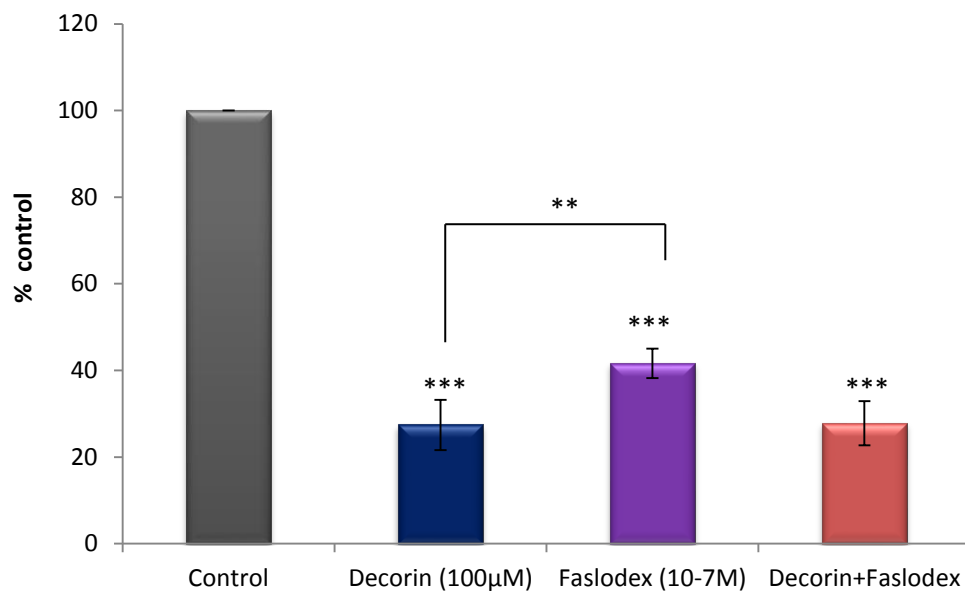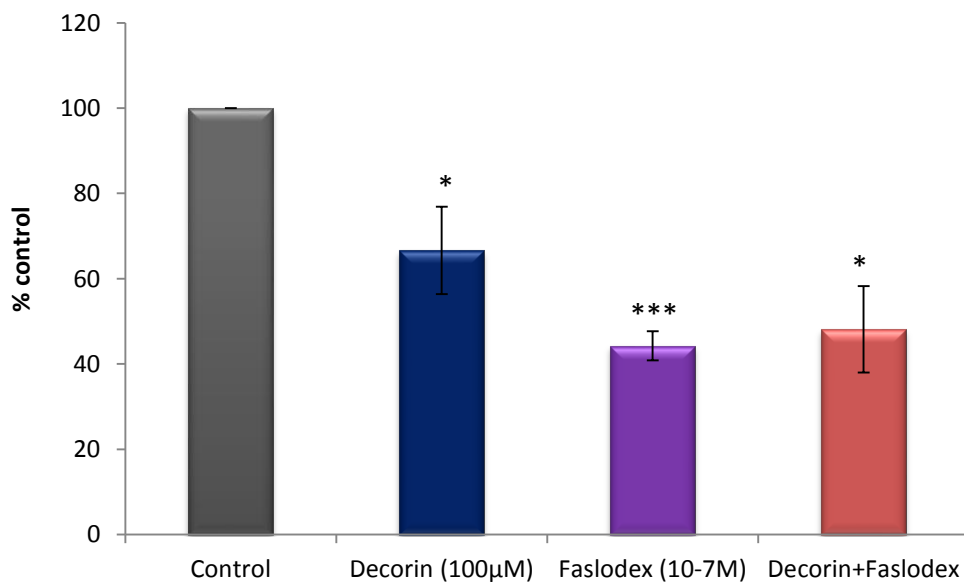

Figure 157: Effect of 10 day treatment with decorin (100µM), Faslodex (10^{-7}M) or their combination on growth of the BT474 cell line. The results are expressed as means ± SEM of three separate experiments and presented as % untreated control. ***P<0.001, *P<0.05, versus untreated control.

These experiments in the BT474 cell line revealed that decorin was unable to promote a growth inhibitory effect as great as Faslodex, and was also inferior versus the decorin impact in T47D cells. As the BT474 cells are HER2+ it was possible that HER2 signalling may limit decorin impact in this model, and so further experiments were carried out to examine if Herceptin co-treatment could improve its effect. While decorin again promoted modest inhibition versus untreated BT474 (p=0.01), Herceptin (10nM) promoted a more substantial growth inhibition versus untreated cells (p=0.004) which was significantly greater than decorin alone (p=<0.001). Herceptin was also able to add to decorin anti-tumour effect in this model (p=0.005) (Figure 158).
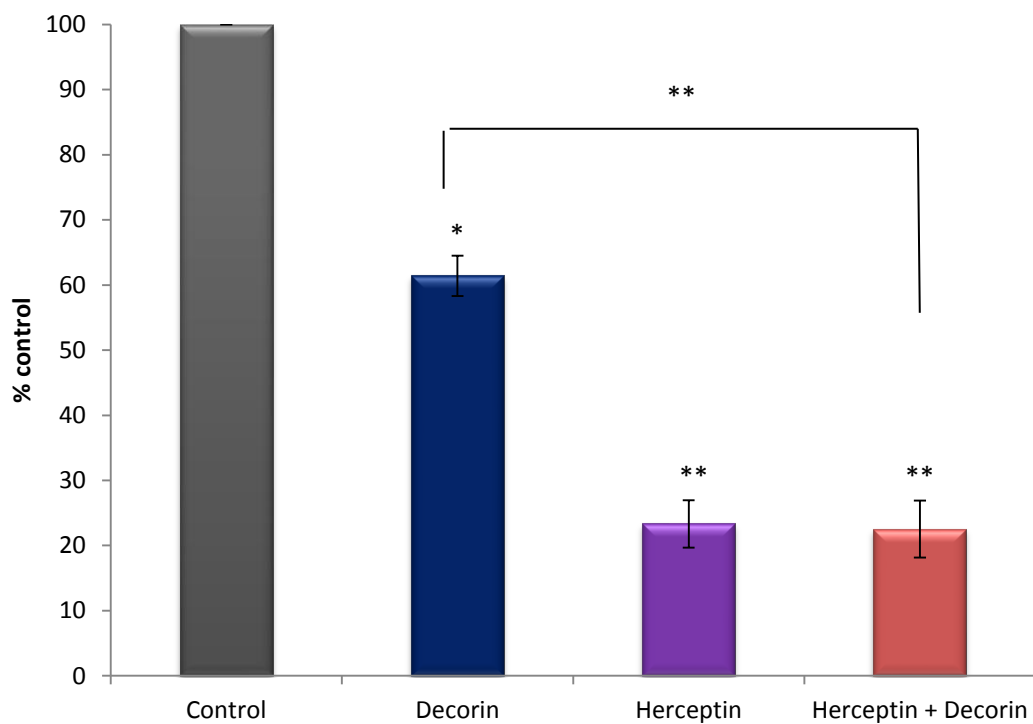
Figure 158: Effect of 10 day treatment with decorin (100µM), Herceptin (10nM) or their combination on growth of the BT474 cell line. The results are expressed as means ± SEM of three separate experiments and presented as % untreated control. **P<0.001, *P<0.05 versus untreated control **P<0.001 for decorin vs Herceptin treatment

10.2.4 Impact of DCN knockdown in the T47D cell line

10.2.4.1 Verification of DCN expression knockdown by shRNA

In order to further determine the role of DCN in the Faslodex-induced complete response in the T47D cell line, short-hairpin (sh) RNA studies were carried out in the T47D cell line to permanently suppress DCN expression. The shRNA constructs also contained a GFP gene and a puromycin resistant gene, which allowed the degree of transfection to be monitored and to select for cells that had been successfully transfected with the constructs. 2 DCN-targeting constructs (sh1, sh2) were evaluated in an attempt to permanently knockdown DCN gene expression in T47D cells, comparing with a non-targeting (NT) control construct. Figure 159 shows fluorescence microscope images following transfection and puromycin selection.

NT-control   **Sh-construct 1 (sh1)**

Sh-construct 2 (sh2)
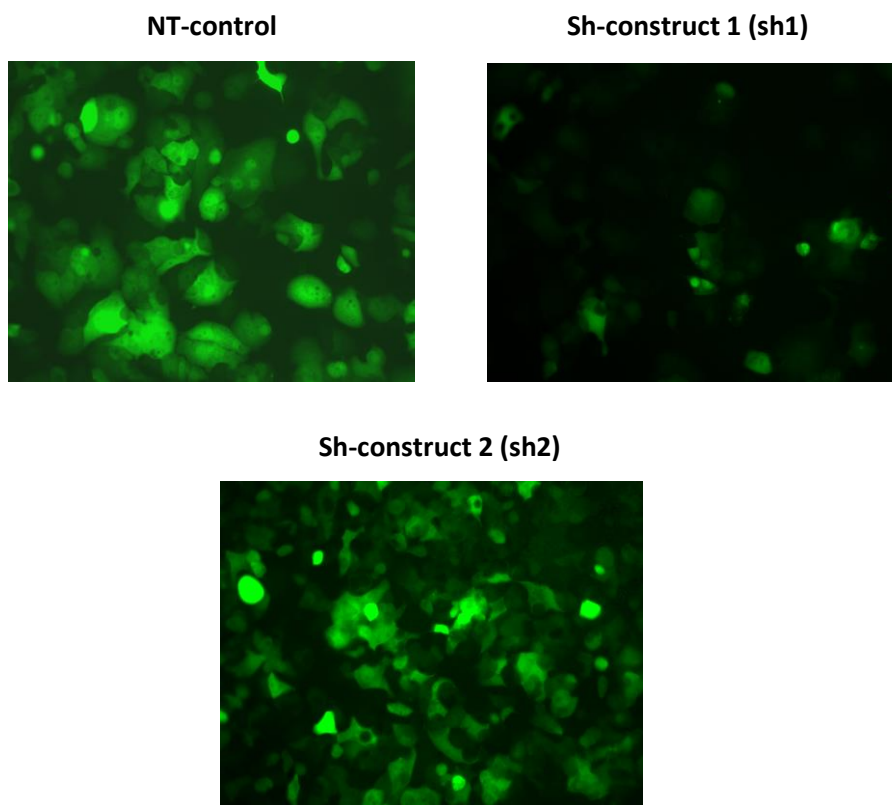
Figure 159: Fluorescent microscope images of T47D cells expressing GFP following shRNA transfection with 2 DCN-targeting constructs and a non-targeting control to assess degree of shRNA transfection. (Original magnification=x10)

Following transfection and puromycin selection, initially end-point-PCR gels (Figure 160A) and subsequently real-time-PCR studies (Figure 160B) were carried out

following 10 days Faslodex treatment versus untreated control for the NT, sh1 and sh2 construct cells. This was performed to determine if DCN gene expression knockdown had been achieved with the DCN shRNA constructs preventing Faslodex induction in T47D cells. T47D wild-type cells express very little DCN basally, and in keeping with this basal DCN expression was virtually undetectable (also reflected in large error bars as DCN was too low to be accurately quantified; Figure 160B) in all the transfected models. DCN expression was significantly up-regulated by 10 day Faslodex treatment in the NT-control transfected T47D cells and also unfortunately in those transfected with sh1 (Figure 160). In contrast, the sh2 construct successfully prevented up-regulation of DCN expression with Faslodex. Indeed, 92% knockdown of DCN expression was achieved with sh2 when compared to 10 day Faslodex treated NT-control cells. Subsequently, therefore, the DCN knockdown sh2-transfected cells were used for all further experiments versus the NT control cells.
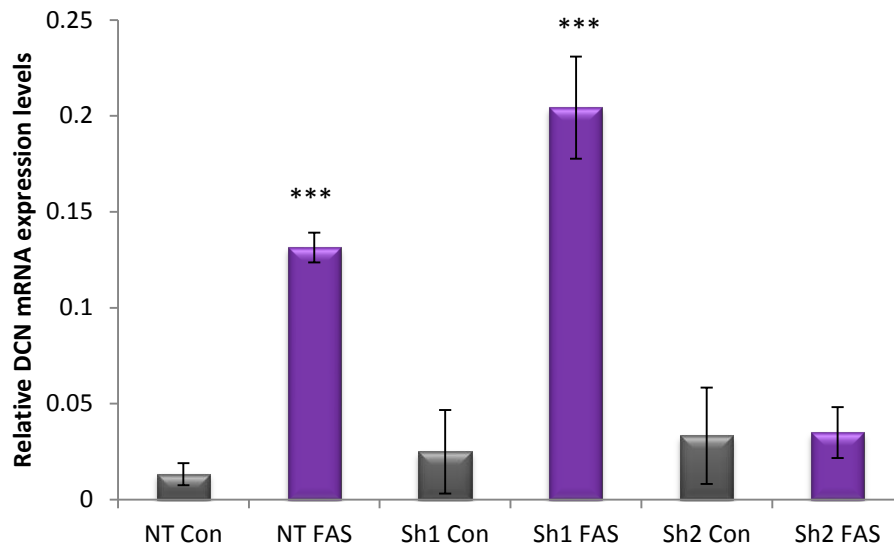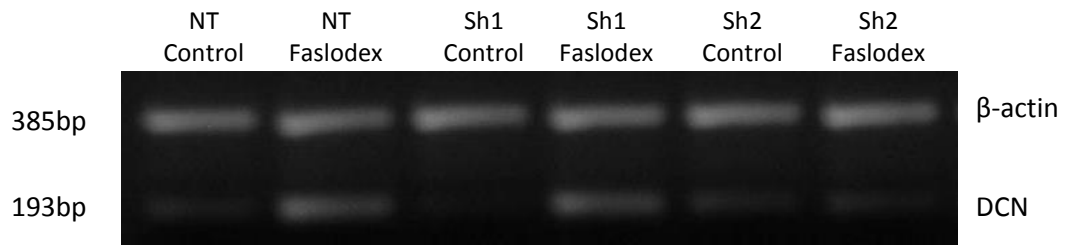
Figure 160: (A) Representative end-point PCR gel image of DCN gene expression following shRNA transfection of the T47D cell line with NT-control, sh1-construct and sh2-construct comparing 10 day Faslodex versus untreated control (B) Real-time PCR results for equivalent experiments, with relative DCN mRNA expression levels expressed as means ± SEM of three separate experiments ***P<0.001 versus matched cell line control.

10.2.4.2 Decorin protein evaluation by ICC in NT control and DCN knockdown (sh2) stably-transfected T47D cells

To determine if the DCN-targeting shRNA sh2 also prevented the up-regulation of decorin by Faslodex at a protein level, decorin ICC was carried out. While NT-control cells continued to show a substantial induction of decorin protein following 10 days Faslodex treatment, no induction (either for cytoplasmic or plasma membrane staining) was observed in the DCN-knockout (sh2) cells (Figure 161).

Non-targeting Control	Non-targeting Faslodex
Hscore=65	Hscore=160
DCN-knockout Control	DCN-knockout Faslodex
Hscore=40	Hscore=45
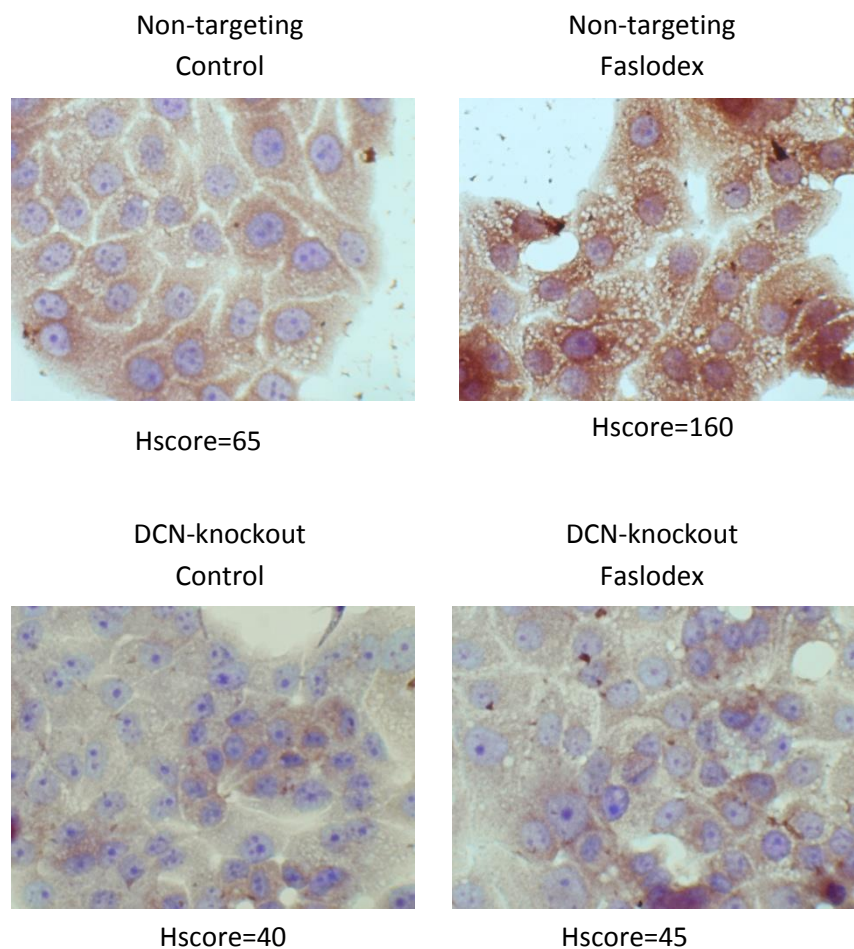
Figure 161: ICC analysis of decorin expression in T47D cells transfected with non-targeting (NT) shRNA or DCN-targeting shRNA sh1, comparing 10 days Faslodex (10^{-7}M) treatment versus control. Associated Hscores are given. (Original magnifications x40).

10.2.4.3 Effect of DCN knockdown on Faslodex-induced growth inhibition

Subsequently growth experiments were carried out using the NT-control and sh2 constructs in the presence and absence of Faslodex over 10 days to determine if the suppression of DCN expression in sh2 also limited Faslodex growth inhibitory impact in the transfected T47D cells. Faslodex treatment of the NT -control cells led to 70% suppression of growth in comparison to their untreated control (p=<0.001). Faslodex treatment of the sh2-transfected cells resulted in 50% growth suppression (p=<0.001) (Figure 162A). Faslodex-promoted inhibition in the NT-transfected cells was superior to that in the sh2-transfected cells (p=0.004). Phase contrast

microscopy confirmed the reduced growth inhibitory impact of Faslodex in the sh2 versus NT control cell lines (Figure 162B).
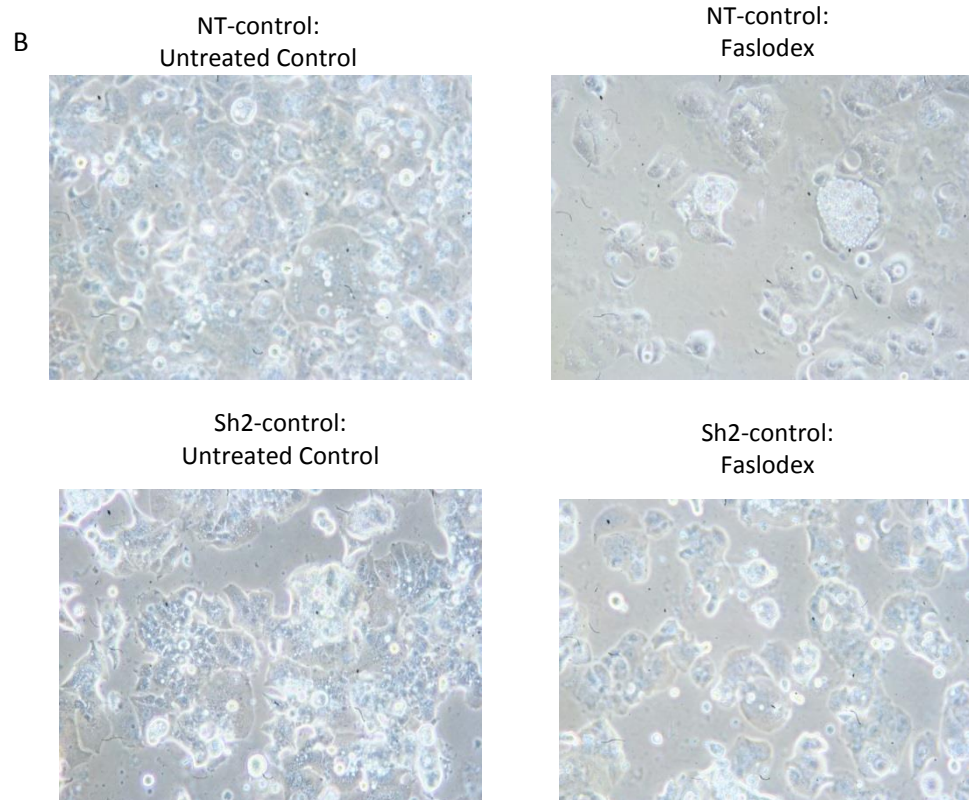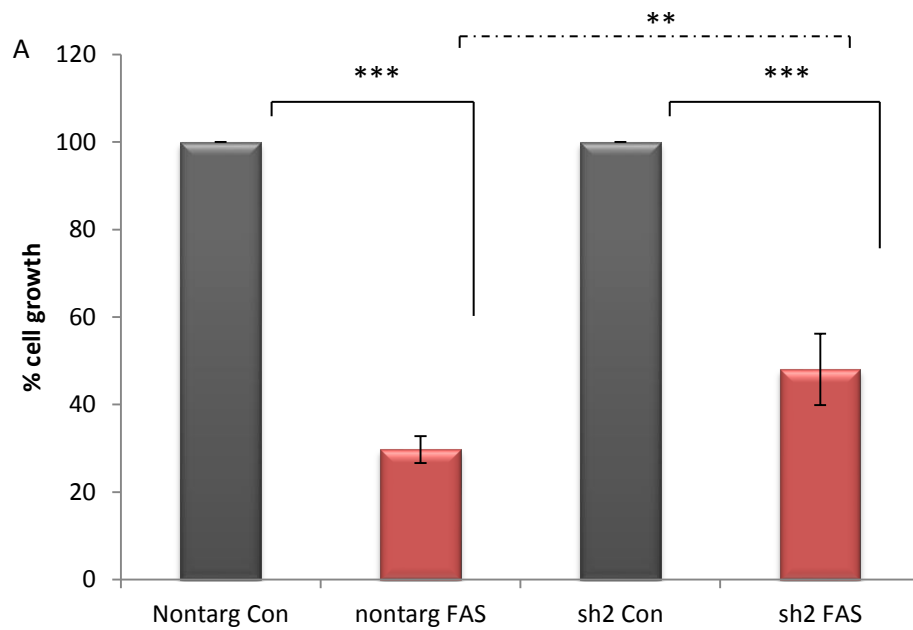
Figure 162: (A) Graph displaying the degree of growth inhibition promoted by 10 day Faslodex (10^{-7}M) treatment in NT non-targeting control and sh2 DCN shRNA T47D cells. The results are expressed as means ± SEM of three separate experiments and presented as % untreated respective control. ***P<0.001; **P < 0.01 versus NT control cells with Faslodex; (B) Phase contrast microscope images taken at day 10 of the experiment (original magnification= x10).

10.2.4.4 Effect of DCN knockdown on Ki67 (proliferation) suppression by Faslodex

Ki67 ICC was used to compare impact of 10 day Faslodex on proliferative activity in the NT control cells and sh2-DCN shRNA transfected T47D cells. There was a substantial decrease in proliferation (% nuclear Ki67 staining) with Faslodex treatment in the NT-control cells. In the sh2 cells where induction of DCN expression by Faslodex was prevented there was a smaller decrease in proliferation after Faslodex treatment (Figure 163)

NT
Control

NT
Faslodex

85% positivity

20% positivity

Sh2
Control

Sh2
Faslodex

75% positivity
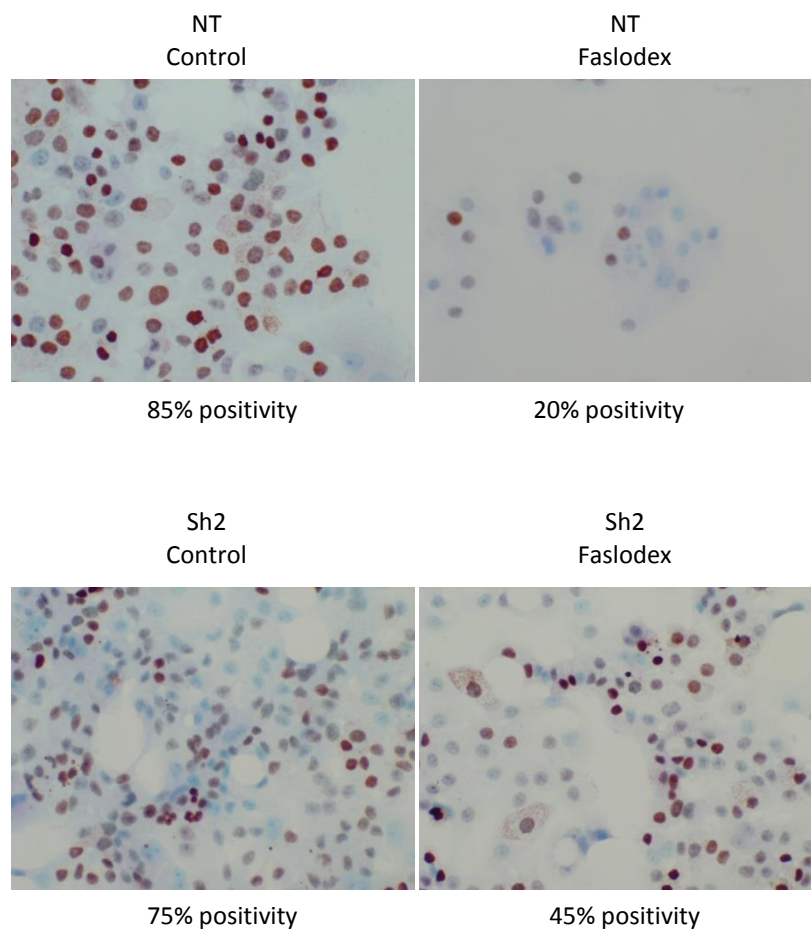
45% positivity

Figure 163: Nuclear Ki67 positivity (%) in T47D cells transfected with NT-control or sh2 DCN shRNA pre and post 10 day Faslodex treatment. Original magnification= x20

10.2.4.5 Long term culture of DCN knockout cells with Faslodex

It is hypothesised that the Faslodex-induced complete response that ultimately occurs in T47D cells is promoted by the progressive up-regulation of decorin by this drug. Using the sh2 DCN knockdown T47D cell line versus the NT-control cells, long term growth experiments were conducted to determine if sh2 preventing DCN promotion by Faslodex (which initially partially-reduced the anti-tumour impact of

this agent) would ultimately allow the cell line to acquire Faslodex resistance. Non-targeting (NT)-transfected cells and DCN knockdown sh2-transfected cells were cultured in the presence and absence of Faslodex in continuous culture for up to ~7 weeks and growth was monitored by documenting any cell passaging required over this time (Figure 164). In the absence of Faslodex, both cell lines were cultured routinely (passaging on average every 10 days), growing approximately at the rate observed for wild-type T47D cells. In the presence of Faslodex, the NT-transfected cells did not require passaging and remained growth inhibited over the 46 days examined in culture (Figure 164). In contrast, in the presence of Faslodex, DCN-knockout sh2 cells (DCN-KO) after a period of growth inhibition (25 days) reinstated some growth, indicated by passaging being carried out, although at 46 days the growth rate of such cells had not reached that of the untreated control cells (Figure 164). Phase contrast microscopy (Figure 165) performed at 30 days in culture confirmed that the NT-transfected control cells were growth inhibited by Faslodex while the DCN-KO cells had reinstated some growth.
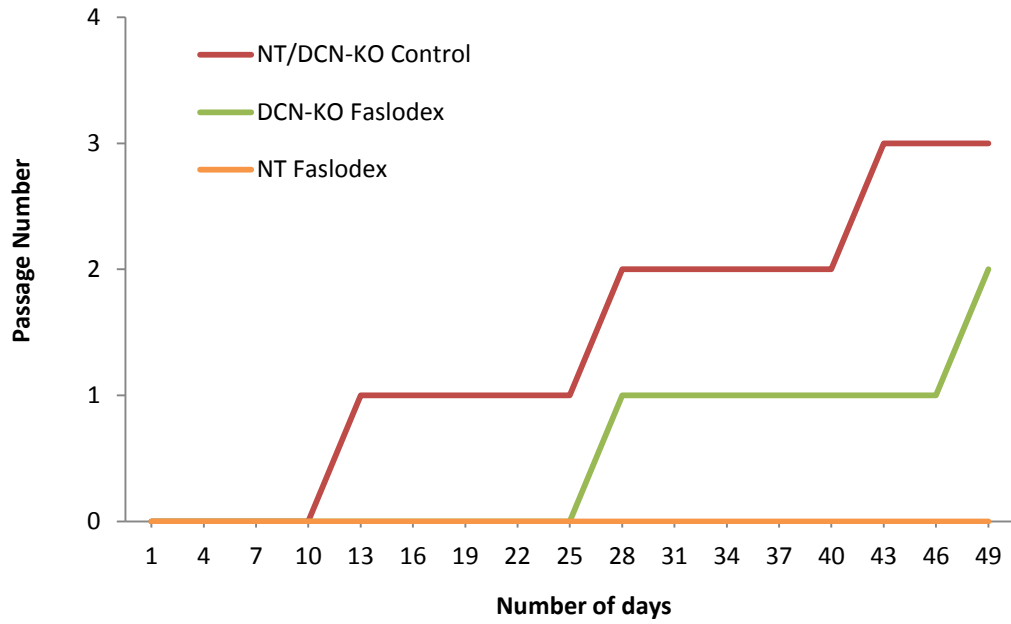
Figure 164: Impact of continuous Faslodex (10^{-7}M) on T47D cell lines stably-transfected with a non-targeting (NT) control shRNA (in orange) or a DCN-targeting shRNA sh2 (in green) *in vitro* versus their respective untreated controls (in red). The graph displays the number of passages each experimental arm underwent over 46 days in continuous culture.

| Non-targeting NT control | DCN-KO sh2 control |
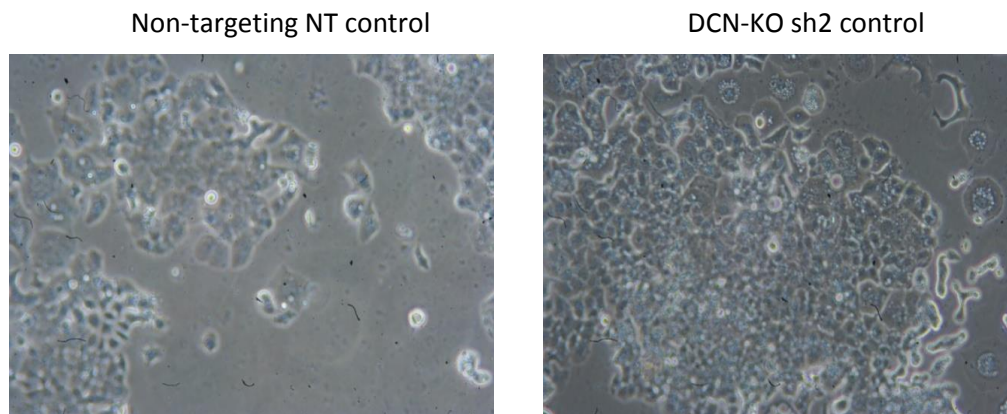
Figure 165: Phase contrast images of T47D cell lines transfected with non-targeting (NT) control shRNA or DCN-targeting sh2 shRNA *in vitro* at day 34 of culture in the continuous presence of Faslodex (10^{-7}M). Original magnification= x10

10.2.5 Evidence for induction of DCN potentially determining response to further endocrine agents

10.2.5.1 Bioinformatic evaluation of ER-regulation of DCN

Since DCN was Faslodex-induced in T47D cells and also in breast cancers *in vivo*, it was possible that DCN was an oestrogen-suppressed gene and so potentially inducible by further endocrine agents. The DCN gene is found on chromosome12q21.33 and analysis of the DCN promoter sequence using the UCSC genome browser (http://genome.ucsc.edu/) in this project revealed that no ERE-site was present on the DCN gene. However, the project did obtain evidence of DCN being oestrogen-suppressed. 'Transcriptomine' is an online database (http://www.nursa.org/nursaGrails/transcriptomine/) that allows mining for tissue-specific or cell-line specific nuclear receptor transcriptomes based on annotated, publically-available microarray gene expression experiments (Ochsner *et al.*, 2012). DCN was searched for in this transcriptome database, specifically interrogating any studies in the T47D cell line treated with 17β-oestradiol versus untreated control, where one microarray dataset was available generated by the Lippman laboratory (Rae *et al.*, 2005). These array data indicated that 24 hour 10nM 17β-oestradiol treatment led to a 0.781 fold suppression of DCN expression (p=0.0004).

10.2.5.2 Impact of further endocrine treatments (oestrogen deprivation, tamoxifen) on the expression of DCN in the T47D cell line

To determine if decorin expression was induced by endocrine agents in addition to Faslodex, the wild-type T47D cell line was treated with Faslodex, tamoxifen or oestrogen-deprivation (using medium containing heat inactivated, charcoal stripped serum, in an attempt to mimic AI treatment) for 10 days and DCN expression analysed using PCR. From Figure 166 it can be seen that like Faslodex, oestrogen-deprivation led to a significant increase in DCN expression versus untreated T47D cells. Tamoxifen had no inductive effect on DCN expression. No significant difference was determined between the magnitude of DCN induction oestrogen deprivation compared with Faslodex.
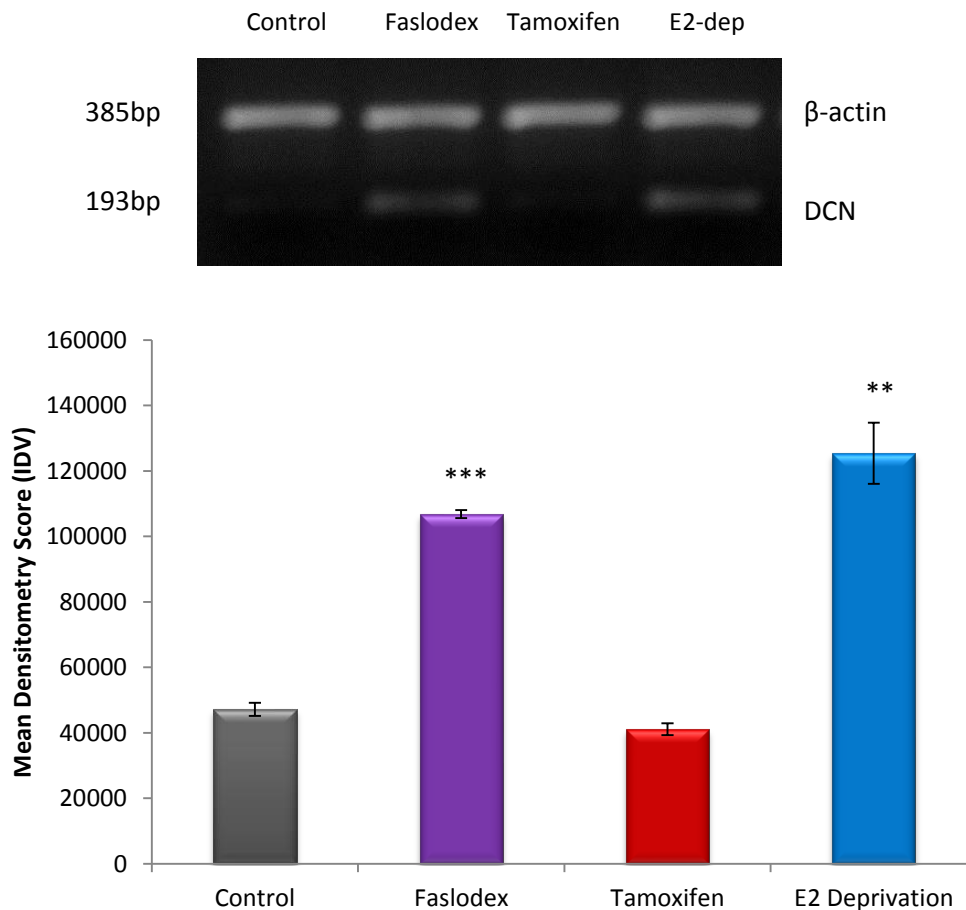
Figure 166: mRNA expression of DCN in T47D cells following 10 days treatment with Faslodex (10^{-7}M), tamoxifen (10^{-7}M) or oestrogen (E2)-deprivation versus untreated control (A) Representative PCR image and (B) corresponding actin-normalised densitometry graph. The results are expressed as means ± SEM of three separate experiments. ***P<0.001, **P < 0.01 versus untreated control.

10.2.5.3 Impact of Oestrogen deprivation on DCN expression in clinical breast cancers treated with the aromatase inhibitor anastrazole (Trial 223) and relation to anti-tumour activity

DCN expression was also significantly up-regulated in the T47D cells following oestrogen deprivation. Therefore, its expression was also analysed using microarray data from Trial 223 to address if aromatase inhibition (anastrozole) induced DCN in clinical breast cancer and if this event related to anti-proliferative effect and so may contribute to anti-tumour response. Trial 223 was a phase II neoadjuvant clinical trial assessing clinical activity of anastrozole treatment alone and in combination with the EGFR inhibitor gefitinib. The trial was designed following the preclinical

observation that resistance to tamoxifen or oestrogen deprivation could involve ligand-independent activation of ER by growth factor receptors such as EGFR (Johnston *et al.*, 2003), where dual blockade of ER and EGFR could enhance endocrine response. Data from previous clinical trials with anastrozole revealed that some patients had a persistently poor anti-proliferative response ("intrinsic resistance") or demonstrated an initial response before tumour growth resumed (acquired resistance) (Dowsett *et al.*, 2005; Baum *et al.*, 2002). It was thus hypothesised that tumours that were less sensitive to anastrozole may benefit from the addition of gefitinib. In trial 223, all ER+ breast cancer patients received anastrozole (1mg/day) for a 16-week treatment period. Patients were randomly assigned to receive gefitinib 250mg/day for 16 weeks (arm A); placebo 1 tablet/day for 2 weeks, followed by gefitinib 250 mg/day for 14 weeks (arm B); or placebo 1 tablet/day for 16 weeks (arm C). Matched core biopsies were taken at week 0, week 2 and week 16 for Ki67 IHC analysis. RNA samples were also taken for microarray analysis from matched core biopsies from patients in arm A and B.

To specifically address impact of oestrogen deprivation on DCN expression in the present project, profile interrogation was carried out only on the microarray data available from week 0 and week 2 for Arm A and B so that all patients included (n=92) had only received anastrozole treatment. Microarray data normalisation and subsequent DCN profile analysis (in SPSS) using the matched pre and post treatment samples was performed as in Chapter 9 for the NEWEST trial. Interrogation of the available Ki67 IHC data revealed the mean % fall in Ki67 at this time point for these Trial 223 patients from baseline was 62% (range -47 to 98%) and the mean absolute Ki67 fall was 11.3% (range -10 to 33.4%).

A paired t-test revealed that DCN gene expression was induced in the majority of patients examined by neoadjuvant anastrozole treatment ($p<0.001$) (Figure 167). 59 patients showed a variable induction in DCN expression (fold change range: 1.01-3.6; mean: 1.65 fold). 33 patients showed some suppression of expression (fold range: 1.0-2.2; mean: 1.29 fold) after treatment.
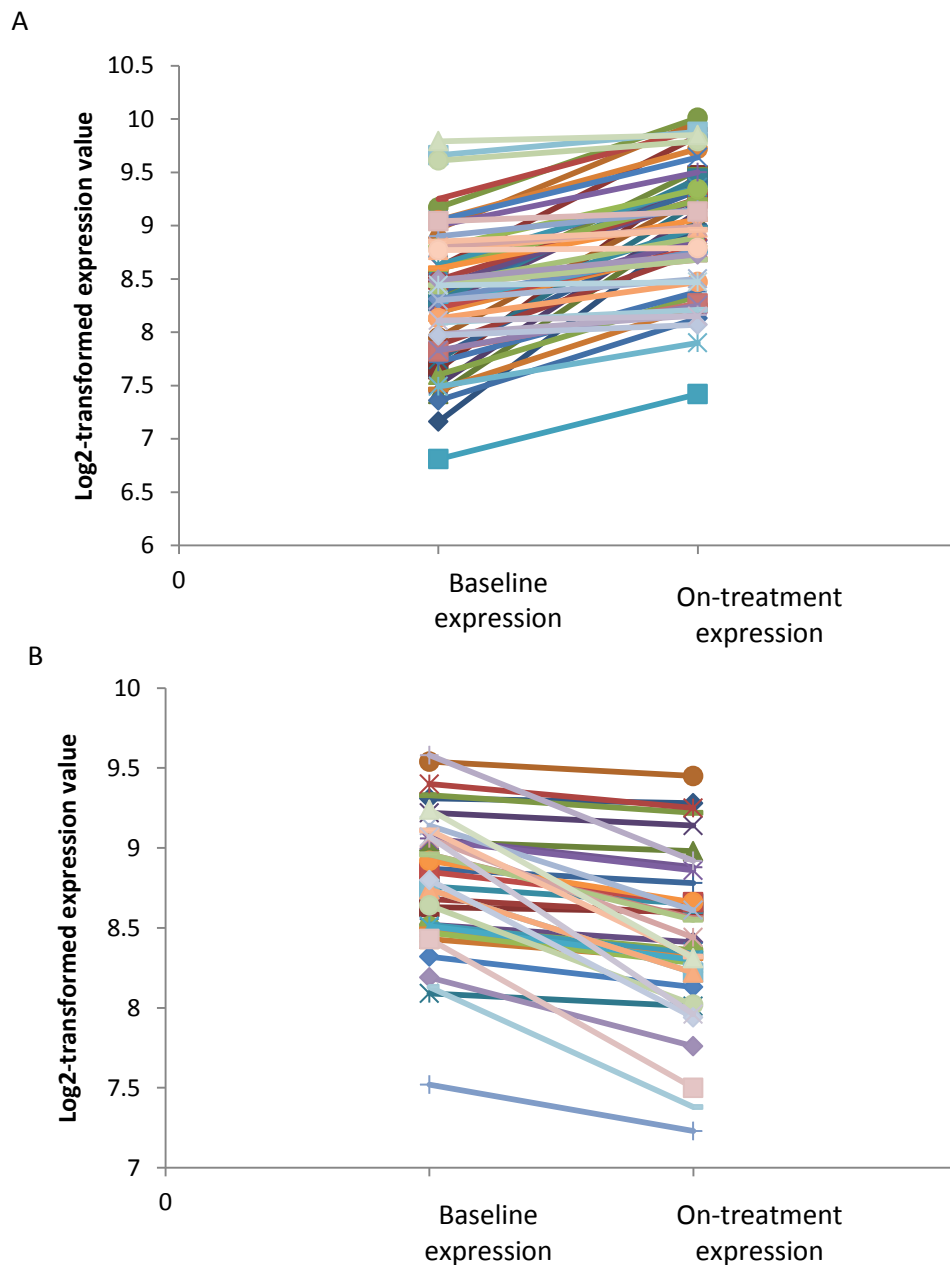
Figure 167: Microarray log2 baseline and on-treatment mRNA expression of DCN before and after 2 week neoadjuvant (1mg/day) anastrozole treatment in ER+ breast cancer patients (n=92); (A): treatment-induced expression, (B): treatment suppressed expression).

A Mann-Whitney U test was also performed to determine if the induction in DCN expression promoted by anastrozole treatment in many patients was associated with a decline in Ki67 expression and thus potentially related to anti-tumour impact of the antihormone. Of the 92 patients investigated with matched array and Ki67 IHC data, 85 demonstrated a fall in Ki67 positivity, while 7 demonstrated an increase or no change in Ki67 during treatment. There was no significant association between magnitude of Ki67 change and either induction or suppression

of DCN (Figure 168). This analysis was repeated removing 7 "intrinsically resistant" patients who showed an increase/no change in Ki67 expression. Again significance was not met (Figure 169)
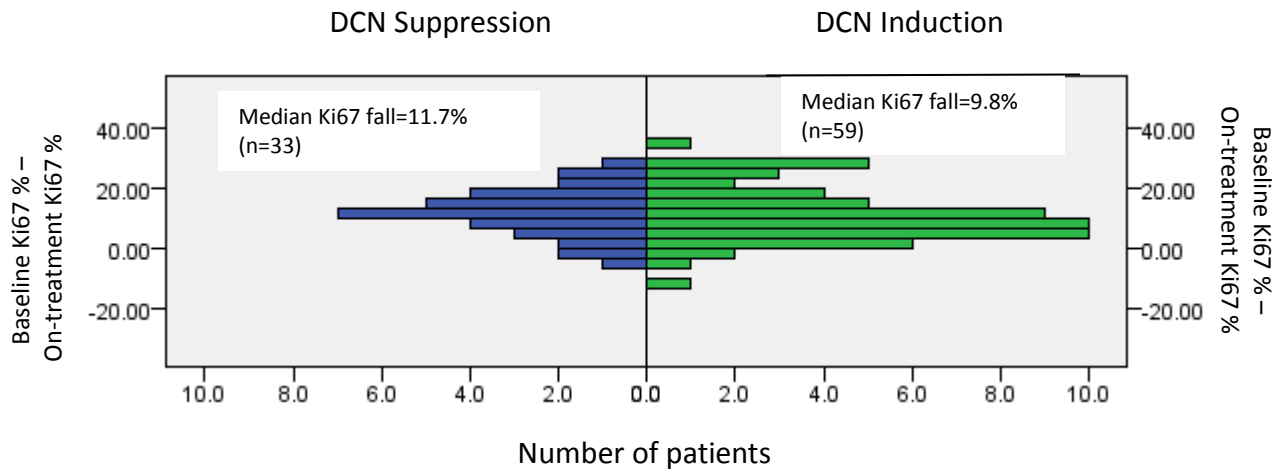
Figure 168: Change in Ki67 % positivity in patients with induction of DCN expression following 2 weeks aromatase inhibitor treatment compared to those with DCN suppression (Mann-Whitney analysis, p=0.580).
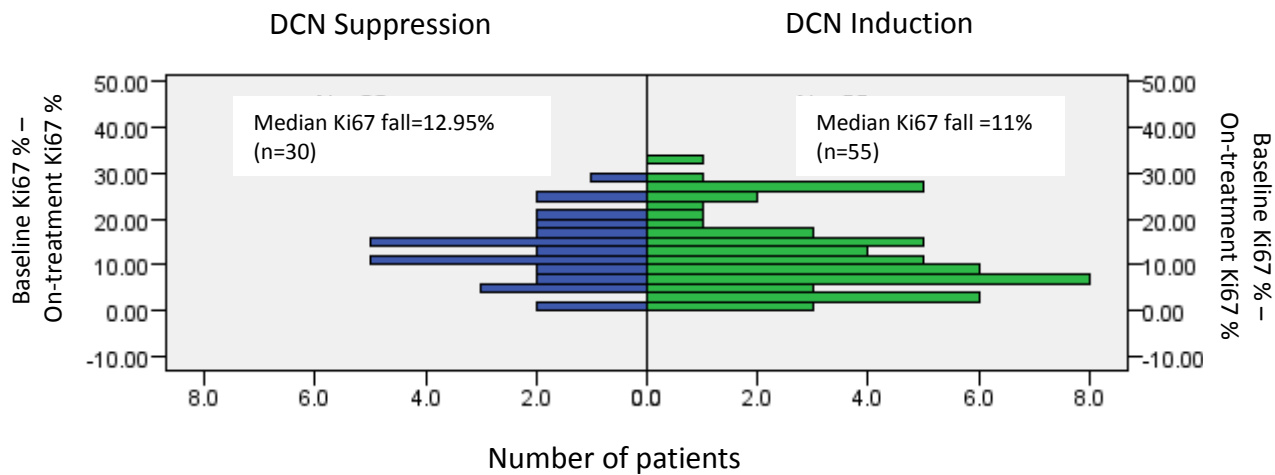
Figure 169: Change in Ki67 % positivity in patients with induction of DCN expression following 2 weeks anastrozole treatment compared to those with DCN suppression, excluding those who demonstrated an increase/ no change in Ki67 (Mann-Whitney analysis, p=0.413).

10.3 Discussion

The data associated with this chapter have further confirmed a role for decorin in the Faslodex-induced complete-response mechanism in the T47D cell line. DCN expression was not only up-regulated at the mRNA level by 10 day Faslodex treatment but it was also increased at the protein level in the T47D line, as shown by ICC. Prolonged Faslodex treatment led to a temporal increase in DCN mRNA expression in keeping with the complete response not being observed until post 8 weeks of Faslodex treatment. Treatment of the T47D cell line with exogenous decorin led to a substantial growth inhibition, greater than that observed in the BT474 or MCF-7 cell lines, suggesting the T47D cell line has particular sensitivity to decorin-induced growth inhibition. Permanent knockdown of DCN expression by use of an shRNA (sh2) further clarified the importance of DCN induction in Faslodex response in the T47D cell line; knockdown led to a reduced suppression of Ki67 by Faslodex and also a growth advantage in the presence of Faslodex with the T47D cell line now able to develop Faslodex resistance. Critically, however, despite the growth advantage observed in the DCN-knockout T47D cell line there was still some suppression of Ki67 by Faslodex and long-term Faslodex treatment suppressed growth for approximately 25 days before resistance. These data indicate that suppression of DCN failed to render T47D cells completely Faslodex insensitive. Further experimental data indicated that DCN mRNA expression was up-regulated by oestrogen-deprivation in the T47D cell line, suggesting AI treatment may also induce DCN expression. This was further confirmed via analysis of clinical breast cancer Trial 223 where the majority of patients who received 2 weeks neoadjuvant anastrozole treatment also exhibited an up-regulation of DCN expression, although this failed to associate with improved Ki67 suppression.

ICC analysis of T47D cells treated with Faslodex for 10 days confirmed that the induction of DCN observed at the mRNA level was mirrored by substantial increases at the protein level (Figure 1), providing further confidence that decorin was functionally involved in the superior Faslodex response observed in this cell line. Due to the mechanism of action of decorin in cells, where it binds to RTKs and encourages their degradation via endocytosis (Zhu *et al.*, 2005), immuno-staining

for this protein was expected at the cell plasma membrane and cytoplasm and this was observed (Figure 150). Despite the induction of decorin protein being in the T47D cell line following 10 days Faslodex treatment, a complete response was not observed until post week 8 of Faslodex treatment. This suggests that either the de-regulation of other elements may be involved in the complete response or the induction of decorin expression at day 10 has not reached a sufficient concentration to promote a complete response. An experiment investigating the mRNA expression of DCN during continuous Faslodex treatment showed that DCN was further induced by more extended Faslodex treatment (Figure 151). Significantly, previous reports associated with the inhibitory actions of decorin have used single concentrations of exogenous decorin and have not, therefore, considered any dose-related aspects (Buraschi *et al.*, 2013; Neill *et al.*, 2013). In this study we have only used a single dose of exogenous decorin but the dose-related effects between DCN mRNA expression and duration of Faslodex treatment suggests that the complete-response exhibited in the T47D cell line may be dose-dependent.

The presence of decorin with tumour cells has also not been extensively reported, with most studies recording that decorin expression is limited to the tumour stroma, thus acting in a paracrine manner (Nash *et al.*, 2002; Oda *et al.*, 2012; Buraschi *et al.*, 2012). The present ICC study shows, however, that the anti-cancer drug Faslodex is able to induce DCN expression directly in a cancer epithelial cell line, potentially contributing to therapeutic response in an autocrine manner. Little work has been carried out previously on antihormone-de-regulated genes and their contribution to clinical response; however, previous experimental studies have shown that EGFR is suppressed by oestrogen and induced by antihormone treatment where it contributes to the development of an antihormone resistant phenotype (Yarden *et al.*, 2001). Although DCN has not been reported to be ER-regulated and in the present study no EREs were found in the DCN promoter using the UCSC genome browser, further investigations using the online tool 'Transcriptomine' (a database of publically available microarray datasets for mining nuclear receptor transcriptomes) revealed that in one dataset the low basal DCN level was further suppressed 0.7 fold by 24 hour oestradiol treatment (Rae *et al.*,

2005). The absence of an ERE in the decorin promoter does not in itself negate its oestrogen regulation since it may be indirectly ER-regulated through other ER regulated transcription factors such as AP-1, Sp-1 or NF-κB.

Although there have been many reports regarding the tumour suppressive actions of decorin in cancer cells *in vitro* and *in vivo*, its actions in T47D cells have not been previously investigated and it was thus significant to observe that exogenous decorin was an effective inhibitory agent in these cells, with responses to decorin exceeding those recorded with Faslodex (Figures 152 and 153). Importantly, not only did the growth inhibition recorded with decorin exceed the responses seen in either MCF-7 or BT474 cells (Figures 154 to 157), but preliminary evidence was seen that decorin was able to induce cell death in T47D (Figure 152). Disappointingly, combination therapy of decorin and Faslodex in T47D cells failed to produce a synergistic effect (Figure 153), but it is likely that the substantial 100μM dose of decorin used for these studies had achieved the maximal growth inhibition response in these cells. Interestingly the addition of decorin to Faslodex in the BT474 or MCF-7 cell lines failed to further improve the further growth inhibitory effect of Faslodex alone. While the reason for the lack of sensitivity of these cells to decorin is not known, HER2 amplification in BT474 cells could contribute to this phenomenon. Thus although decorin is able to inhibit normal HER2 signalling (Goldoni *et al.*, 2008b) in cancer cells, the HER2 over expression apparent in BT474 cells may overwhelm decorin responses. To further explore this possibility, the combined actions of Herceptin and decorin were investigated in BT474 cells. Once again, however, no synergistic effects were observed, in this instance due to the considerable effectiveness of Herceptin alone (Figure 158). Further experiments should be carried out investigating the combination of decorin with a sub-maximal concentration of Herceptin to delineate the potential of the combination of such treatments. Additional contributory factors limiting decorin impact in both MCF-7 and BT474 in the presence of Faslodex may be antihormone up-regulation of potential protective factors such CXCR4 or VEGFC as demonstrated in this project.

Additional evidence implicating decorin in the superior growth inhibitory effects of Faslodex in T47D cells was gained from one of the shRNA DCN-targeting constructs

(sh2) where its ability to reduce the Faslodex promotion of decorin mRNA and protein expression associated with a partial loss of Faslodex inhibition of growth (Figure 162) and Ki67 immunostaining (Figure 163). Although these effects were not as dramatic as was expected given the magnitude (>90%) of gene knockdown, the long-term decorin knock-down data showing that decorin shRNA negates the complete response to Faslodex and leads to the development of resistance point to an important role for Faslodex induced decorin expression in the sensitivity of T47D cells to the anti-hormonal drug. Critically, in the shRNA studies the Faslodex promoted complete response was not converted into immediate de novo insensitivity to Faslodex on decorin knock-down, suggesting that even in the absence of decorin, Faslodex retains growth inhibitory properties in T47D cells. This may be due to Faslodex induction of CASP1, TXNIP or TGFB2, as indentified in this project, or via its reported suppression of known oestrogen-induced growth-promoting elements such as c-src, IGF1R or PAK1 (Migliacci *et al.*, 2002; Kahlert *et al.*, 2000; Gururaj *et al.*, 2006). Indeed, its non-decorin mediated growth inhibitory effects in MCF-7, MDA-MD-361 and BT474 cells are testimony to additional growth-suppressive properties.

Although this project primarily focused upon the antihormone Faslodex and the identification of elements involved in mediating varying responses to the drug, PCR investigations revealed that decorin was also up-regulated by oestrogen-deprivation (Figure 166). To some degree, this is not an unexpected observation since both Faslodex and oestrogen deprivation effectively starves tumour cells of ER signalling (Dos Santos *et al.*, 2002). In contrast, tamoxifen did not promote decorin expression in T47D cells, possibly due to its reported lack of suppressive impact on AF-1 activity in breast cancer cells (Metzger *et al.*, 1992). Excitingly, therefore, differences in the capacity of varying classes of anti-hormone to induce decorin expression may contribute towards their anti-tumour capacity as reflected, for example, in the ATAC trial where the aromatase inhibitor anastrozole was shown to be superior to tamoxifen in improving survival in primary breast cancer patients (Howell *et al.*, 2005). In order to begin to address its relation with oestrogen deprivation in the clinic, decorin expression was analysed in AstraZeneca-sponsored

Trial 223. This is a phase II study that investigated combination of anastrozole with gefitinib to determine if the addition of gefitinib led to an increase in patients demonstrating an initial response, since it was hypothesised that the expression of inherent EGFR or EGFR induced by anastrozole treatment might limit antihormone response. Microarray experiments were carried out within the trial on a cohort of patients and IHC data for Ki67 was also provided. The present study, focussing on trial arms encompassing aromotase inhibitor alone, determined that 2 weeks treatment with anastrozole significantly induced decorin expression in the majority of patients but that this induction was not necessarily associated with an improved Ki67 fall (Figures 167-169). Such a lack of association does not in itself rule out a contributory role for decorin in the tumour growth inhibition in some patients, and in keeping with this hypothesis, the laboratories of Miller and Dowsett have each reported DCN to also be up-regulated following neoadjuvant letrozole treatment (Mackay *et al.*, 2007; Miller *et al.*, 2009; Dunbier et al., 2013). Miller *et al* showed that decorin was part of a 205 gene signature predictive of response to letrozole (measured by tumour volume; Miller *et al.*, 2009), and hence while decorin on an individual gene basis did not associate with clinical outcome, it clearly remained important alongside   other signalling elements as determinants of response.

Chapter 11

Concluding remarks and future studies

While antihormone treatments are a mainstay for early and advanced ER+ breast cancer, responses to treatment are variable and resistance is eventually acquired by many patients. In this regard, the work presented in this thesis has focused on an examination of the pure-antioestrogen Faslodex and its capacity to (i) influence the growth of 4 ER+ cell lines and (ii) alter gene expression profiles in the cells based on an Affymetrix microarray gene expression analysis. Importantly, the cell lines used in this project aimed to represent 2 clinical phenotypes, ER+/HER2+ and ER+/HER2- tumours, which are known to differ in their response to further anti-hormonal drugs. Through a comparison of the data derived from (i) and (ii) several key observations have been made which largely fulfilled the aims of the project outlined at the end of chapter 1 (section 1.7). These were:

1. That the 4 ER+ cell lines used in this study showed varying initial responses to Faslodex and short-term responses to Faslodex did not predict for the period of time to acquisition of drug resistance. Furthermore the time taken to develop an acquired resistant phenotype differed, with HER2- cells (MCF-7 and T47D) being more responsive than the HER2+ cells (BT474 and MDA-MB-361). Importantly, T47D cells were fully growth inhibited by Faslodex and therefore represent a novel model for complete response to an anti-hormonal drug.

2. That hierarchical clustering of microarray data can be used to determine Faslodex-induced transcriptome alterations that may explain these varying drug responses. Indeed, the clustering patterns based on both induced and suppressed genes identified gene cohorts which relate to (i) complete response to Faslodex versus incomplete response (i.e. T47D versus MCF-7,

MDA-MB-361 and BT474 cells respectively), where the 3 latter cell lines acquire Faslodex resistance and (ii) increased duration of response in HER2- versus HER2+ following long-term Faslodex treatment (i.e. MCF-7 and T47D versus MDA-MB-361 and BT474 cells respectively).

Specifically, genes of interest that were identified following various prioritisation steps in the thesis were:

VEGFC, PRKACB, GABBR2 and CXCR4, which were Faslodex-induced in those breast cancer cell lines that subsequently developed resistance and may be contributory to this process. In contrast, GFRA1, an element within the RET pathway, was Faslodex suppressed in those cell lines which subsequently developed resistance and its ontology suggested such an expression change may contribute towards their initial responsiveness (Chapter 5).

DCN, TXNIP, TGFB2 and CASP1, which were Faslodex induced in the T47D cell line and may contribute to the complete response seen in this model (Chapter 6).

PCDH7 was Faslodex induced in the ER+/HER2- cell lines and ARTN suppressed in this setting and these expression changes may associate with their superior response to Faslodex versus the HER2+ cell lines (Chapter 7).

CDH2, which was elevated intrinsically and modestly Faslodex induced in HER2+ cells, and may relate to their capacity to rapidly develop Faslodex resistance.

The most promising genes were subsequently analysed in the NEWEST Faslodex clinical trial dataset where a number (CXCR4, GFRA1, RET, ARTN, and DCN) showed expression changes similar to those detected in the in vitro studies. Of these, DCN (which promisingly associated with anti-proliferative impact of the antihormone in NEWEST) was taken forward for an in depth experimental analysis involving (i) its knockdown in T47D cells using a shRNA which, in part, blocked the ability of Faslodex to induce a complete response and (ii) the exposure of T47D cells to exogenous decorin which promoted growth inhibition of the cells. These data reinforce the concept of a major role for DCN in the induction of a favourable anti-

tumour response in experimental and clinical ER+ breast cancer scenarios following Faslodex treatment.

Although considerable progress has obviously been made within the current project to identify genes involved in cellular response to Faslodex, as well as those involved in the development of resistance, several broader issues have become evident which will be discussed further below:

11.1 Can this type of analysis fully explain the varying responses observed *in vitro* and *in vivo*?

Despite the research successes here in identifying a number of genes associated with the various Faslodex responses demonstrating the importance of analysing genes and pathways de-regulated by Faslodex treatment, it is clear that the de-regulation of single genes by Faslodex fails to fully explain a given response. Thus, while the induction of DCN has been shown to be involved in the Faslodex response mechanism and looks promising both in the context of determining new therapeutic strategies and as a novel biomarker of response, its induction by Faslodex fails to fully explain either the complete response to the drug in the T47D cell line or the subsequent clinical variability of response to Faslodex seen in patients. Identification of these additional mechanisms contributing to response (possibly involving induction of CASP1, TGFB2 or TXNIP, and perhaps inhibition of RET signalling, together with their subsequent integration into more complex signalling models should allow us, in the future, to devise regimes to simultaneously target multiple pathways to maximise therapeutic response to Faslodex.

Significantly, such signalling models should also take into account paracrine pathways, since the ontology of a number of the genes identified in this project indicated a potentially-greater functional role in the in vivo setting e.g. CXCR4, VEGFC and DCN. Thus, while the ligand for CXCR4 and the receptors for VEGFC were not expressed *in vitro,* and DCN is reported (albeit in the absence of antihormone) to be primarily produced by the tumour stroma rather than the tumour epithelial cells, it is feasible *in vivo* that such signalling elements may gain a greater

significance as determinants of therapeutic response/resistance. Examination of these elements in ER+ breast cancer *in vivo* models or in 3D tumour/stromal cell co-culture following Faslodex treatment may help to resolve these issues.

11.2 The use of a wider array of experimental material

Although the present study is one of a small number that have attempted to use multiple cell lines to examine response/resistance mechanisms, breast cancer is a highly heterogeneous disease and equivalent investigations in other cell lines reflective of this heterogeneity is necessary. Within this context, the tumour suppressor genes p53 and PTEN are often lost or mutated in clinical breast cancer (Hollstein et al., 1991; Li et al., 1997), yet they were not adequately represented in the limited number of models presently used. Equally, an increasing number of molecular sub-types are being discovered in breast cancer (Cutis et al., 2012) and hence such studies are also likely to benefit in the future by extending to primary breast cancer cells. Importantly, within the context of the present study and its approach, the issue of heterogeneity may be partially addressed through the development of isotypic cell lines where the expression of genes of interest are genetically modified, as with DCN. Finally, the experimental context within any expanded array of tumour models could also be usefully broadened to incorporate additional anti-hormonal measures.

11.3 The need for on-therapy clinical samples

As previously stated in this project, to further verify genes of interest as biomarkers of response or to implicate them in a given response in clinical breast cancer, additional on-therapy samples are required which are more fully reflective of current treatment practices. Unfortunately, obtaining such material remains intrinsically difficult and even when obtained may be limited by the clinical context of the samples. Thus for example, while the NEWEST trial reported in this study clearly provided some useful information concerning the capacity of Faslodex to alter the expression of genes, such as DCN, it is a neoadjuvant study which cannot address issues of long-term response to a drug. Such difficulties should not, however, be insurmountable in the future as the techniques relating to tissue

sampling become less invasive and we are able to profile more on ever diminishing amounts of material (Heitzer *et al.,* 2013).

References

Ai, X., Do, A. T., Kusche-Gullberg, M., Lindahl, U., Lu, K., Emerson, C. P. Jr. Substrate specificity and domain functions of extracellular heparan sulfate 6-O-endosulfatases, QSulf1 and QSulf2. Journal of Biological Chemistry 2006: 281: 4969-4976

Ailan, H., Xiangwen, X., Daolong, R., Lu, G., Xiaofeng, D., Xi, Q., Xingwang, H., Rushi, L., Jian, Z., Shuanglin, X. Identification of target genes of transcription factor activator protein 2 gamma in breast cancer cells. BMC Cancer 2009: 279: [Epub]

Airaksinen, M. S., Saarma, M. The GDNF family: signalling, biological functions and therapeutic value. Nature Reviews Neuroscience 2002: 3: 383–394

Akagi, K., Ikeda, Y., Miyazaki, M., Abe, T., Kinoshita, J., Maehara, Y., Sugimachi, K. Vascular endothelial growth factor-C (VEGF-C) expression in human colorectal cancer tissues. British Journal of Cancer 2000: 83: 887–891

Albini, A., Sporn, M. B. The tumour microenvironment as a target for chemoprevention. Nature Reviews Cancer 2007: 7: 139–147.

Alshareeda, A. T., Soria, D., Garibaldi, J. M., Rakha, E., Nolan, C., Ellis, I. O., Green, A. R. Characteristics of basal cytokeratin expression in breast cancer. Breast Cancer Research and Treatment 2013: 139: 23-37

Amano. H., ito, Y., Suzuki, T., Kato, S., Matsui, Y., Ogawa, F., Murata, T., Sugimoto, Y., Senoir, R., Kitasato, H., Hayashi, I., Satoh, Y., Narumiya, S., Majima, M. Roles of a prostaglandin E-type receptor, EP3, in upregulation of matrix metalloproteinase-9 and vascular endothelial growth factor during enhancement of tumor metastasis. Cancer Science 2009: 100: 2318-2324

Armes, J. E., Hammet, F., de Silva, M., Ciciulla, J., ramus, S. J., Soo, W. K., Mahoney, A., Yarovava, N., Henderson, M. A., Hutchins, A. M., Price, G. R., Venter, D. J. Candidate tumor-suppressor genes on chromosome arm 8p in early-onset and high-grade breast cancers. Oncogene 2004: 23: 5697-5702

Armstrong, D. K., Kaufmann, S. H., Ottaviano, Y. L., Furuya, Y., Buckley, J. A., Isaacs, J. T., Davidson, N. E. Epidermal growth factor-mediated apoptosis of MDA-MB-468 human breast cancer cells. Cancer Research 1994, 54; 5280-5283.

Arnold, S. F., Obourn, J. D., Jaffe, H., Notides, A. C. Serine 167 is the major estradiol-induced phosphorylation site on the human estrogen receptor. Molecular Endocrinology 1994: 8: 1204-1214

Ashman, L. K. The biology of stem cell factor and its receptor C-KIT. International Journal of Biochemistry and Cell Biology 1999: 31: 1037-1051

Avruch, J., Zhou, D., Bardeesy, N. YAP oncogene overexpression supercharges colon cancer proliferation. Cell Cycle 2012: 11: 1090-1096

Aymeric, L., Apetoh, L., Ghiringhelli, F., Tesneiere, A., Martins, I., Kroemer, G., Smyth, M. J., Zitvogel, L. Tumor Cell Death and ATP Release Prime Dendritic Cells and Efficient Anticancer Immunity. Cancer Research 2010:70: 855-858

Azuma, H., Inamoto, T., Sakamoto, T., Kiyama, S., Ubai, T., Shinohara, Y., Maemura, K., Tsuji, M., Segawa, N., Masuda, H., Takahara, K., Katsuoka, Y., Watanabe, M. Gamma-aminobutyric acid as a promoting factor of cancer metastasis; induction of matrix metalloproteinase production is potentially its underlying mechanism. Cancer Research 2003: 63: 8090-8096

Baehner, F. L., Achacoso, N., Maddala, T., Shak, S., Quesenberry, C. P., Goldstein, L. C., Gown, A. M., Habel, L. A. Human epidermal growth factor receptor 2 assessment in a case-control study: comparison of fluorescence in situ hybridization and quantitative reverse transcription polymerase chain reaction performed by central laboratories. Journal of Clinical Oncology 2010: 28: 4300–4306.

Baghy, K., Horvath, Z., Regos, E., kiss, K., Schaff, Z., Iozzo, R. V., Kovalszky, I. Decorin interferes with platelet-derived growth factor receptor signaling in experimental hepatocarcinogenesis. FEBS Journal 2013: 280: 2150-2164

Baloh, R. H., Tansey, M. G., Lampe, P. A., Fahmer, T. J., Enomoto, H., Simburger, K. S., Leitner, M. L., Araki, T., Johnson, E. M Jr., Milbrandt, J. Artemin, a novel member of the GDNF ligand family, supports peripheral and central neurons and signals through the GFRalpha3-RET receptor complex. Neuron 1998: 21: 1291-1302

Balko, J. M., Cook, R. S., Vaught, D. B., Kuba, M. G., Miller, T. W., Bhola, N. E., Sanders, M. E., Granja-Ingram, N. M., Smith, J. J., Meszoely, I. M., Salter, J., Dowsett, M., Stemke-Hales, K., Gonzalez-Angulo, A. M., Mills, G. B., Pinto, J. A., Gomez, H. L., Arteaga, C. L. Profiling of residual breast cancers after neoadjuvant chemotherapy identifies DUSP4 deficiency as a mechanism of drug resistance. Nature Medicine 2012: 18: 1052-1059

Balkwill, F. The significance of cancer cell expression of the chemokine receptor CXCR4. Seminars in Cancer Biology 2004: 14:171-179

Banerjee, A., Wu, Z. S., Qian, P. X., Kang, J., Liu, D. X., Zhu, T., Lobie, P. E. ARTEMIN promotes de novo angiogenesis in ER negative mammary carcinoma through activation of TWIST1-VEGF-A signalling. PLoS One 2012: 7: [Epub]

Baselga, J., Semiglazov, V., van Dam, P., Manikhas, A., Bellet, M., Mayordomo, J., Campone, M., Kubista, E., Greil, R., Bianchi, G., Steinseifer, J., Molloy, B., Tokaji, E., Gardner, H., Phillips, P., Stumm, M., Lane, H. A., Dixon, J. M., Jonat, W., Rugo, H. S. Phase II randomized study of neoadjuvant everolimus plus letrozole compared with placebo plus letrozole in patients with estrogen receptor-positive breast cancer. Journal of Clinical Oncology 2009: 27: 2630-2637

Baum, M., Budzar, A. U., Cuzick, J., Forbes, J., Houghton, J. H., Klijn, J. G., Sahmoud, T; ATAC Trialists' Group. Anastrozole alone or in combination with tamoxifen versus tamoxifen alone for adjuvant treatment of postmenopausal women with early breast cancer: first results of the ATAC randomised trial. Lancet 2002: 359: 2131-2139

Beatson, G.T. On the treatment of inoperable cases of carcinoma of the mamma: suggestions for a new method of treatment with illustrative cases. Lancet 1896: 2: 104-107

Beisner, J., Buck, M. B., Fritz, P., Dippon, J., Schwab, M., Brauch, H., Zugmaier, G., Pfizenmaier, K., Knabbe, C. A novel functional polymorphism in the transforming growth factor-beta2 gene promoter and tumor progression in breast cancer. Cancer Research 2006: 66: 7554-7561

Benezra, R., Davis, R., Lockshon, D., Turner, D., Weintraub, H. The protein Id: a negative regulator of helix-loop-helix DNA binding proteins. Cell 1990: 61: 49-59.

Bettler, B., Kaupmann, K., Mosbacher, J., Gassmann, M. Molecular Structure and Physiological Functions of GABA$_B$ Receptors. Physiological reviews 2004: 84: 835-867

Beukers, W., Hercegovac, A., Vermeij, M., Kandimalla, R., Blok, A. C., van der Aa, M. M., Zwarthoff, E. C., Zuiverloon, T. C. Hypermethylation of the Polycomb Group Target Gene PCDH7 in Bladder Tumors from Patients of all Ages. Journal of Urology 2013: 190: 311-316

Bi, X. L., Yang, W. Biological functions of decorin in cancer. Chinese Journal of Cancer 2013: 32: 266-269

Bjornstrom, L., Sjoberg, M. Estrogen receptor- dependent activation of AP-1 via non-genomic signalling. Nuclear Receptors 2004: 2: [Epub]

Bjornstrom, L., Sjoberg, M. Mechanisms of estrogen receptor signalling: convergence of genomic and nongenomic actions on target genes. Molecular Endocrinology 2005, 19; 833-842

Bock, C., Rack, B., Kuhn, C., Hofmann, S., Finkenzeller, C., Jager, B., Jeschke, U., Doisneau-Sixou, S. F. Heterogeneity of ERα and ErbB2 Status in Cell Lines and Circulating Tumor Cells of Metastatic Breast Cancer Patients. Translational Oncology 2012: 5: 475-485

Boocock, D. J., Brown, K., Gibbs, A. H., Sanchez, E., Turteltaub, K. W., White, I. N. Identification of human CYP forms involved in the activation of tamoxifen and irreversible binding to DNA. Carcinogenesis 2002: 23: 7891-7901

Boudot, A., Kerdivel, G., Habauzit, D., Eeckhoute, J., Le Dily, F., Flouriot, G., Samson, M., Pakdel, F. Differential estrogen-regulation of CXCL12 chemokine receptors, CXCR4 and CXCR7, contributes to the growth effect of estrogens in breast cancer cells. PloS One 2011: 6: [Epub]

Bouker, K. B., Skaar, T. C., Fernandez, D. R., O'Brien, K. A., Riggins, R. B., Cao, D., Clarke, R. Interferon regulatory factor-1 mediates the proapoptotic but not cell cycle arrest effects of the steroidal antiestrogen ICI 182,780 (Faslodex, Fulvestrant). Cancer Research 2004: 64: 4030-4039.

Boulay, A., Breuleux, M., Stephan, C., Fux, C., Brisken, C., Fiche, M., Wartmann, M., Stumm. M., Lane, H. A., Hynes, N. E. The ret receptor tyrosine kinase pathway functionally interacts with the ERalpha pathway in breast cancer. Cancer Research 2008: 68: 3743-3751

Border, W. A., Noble, N. A., Yamamoto, T., Harper, J. R., Yamaguchi, Y., Pierschbacher, M. D., Ruoslahti, E. Natural inhibitor of transforming growth factor-beta protects against scarring in experimental kidney disease. Nature 1992: 360: 361-364

Bowie, M. L., Dietze, E. C., Delrow, J., Bean, G. R., Troch, M. M., Marjoram, R. J., Seewaldt, V. L. Interferon-regulatory factor-1 is critical for tamoxifen-mediated apoptosis in human mammary epithelial cells. Oncogene 2004: 23: 8743-8755

Brabyn, C. J., Kleine, L. P. EGF causes hyperproliferation and apoptosis in T51B cells: involvement of high and low affinity EGFR binding sites. Cellular Signalling 1995, 7; 139-150

Britton, D. J., Hutcheson, I. R., Knowlden, J. M., Barrow, D., Giles, M., McClelland, R. A., Gee, J. M., Nicholson, R. I. Bidirectional cross talk between ERalpha and EGFR signalling pathways regulates tamoxifen-resistant growth. Breast Cancer Research and Treatment 2006: 96: 131-146

Britton, D., Scott, G., Schilling, B., Atsriku, C., Held, J., Gibson, B., Benz, C., Baldwin, M. A novel serine phosphorylation site detected in the N-terminal domain of estrogen receptor isolated from human breast cancer cells. Journal of the American Society for Mass Spectrometry 2008: 19: 729-740

Bromberg, J. Stat proteins and oncogenesis. Journal of Clinical Investigation 2002: 109: 1139-1142.
Buchholz, M., Braun, M., Heidenblut, A., Kestler, H. A., Kloppel, G., Schmiegel. W., Hahn, S. A., Luttges, J., Gress, T. M. Transcriptome analysis of microdissected pancreatic intraepithelial neoplastic lesions. Oncogene 2005: 24: 6626-6636.

Buck, M. B., Coller, J .K., Murdter, T. E., Eichelbaum, M., Knabble, C. TGFβ2 and TβRII are valid molecular biomarkers for the antiproliferative effects of tamoxifen and tamoxifen metabolites in breast cancer cells. Breast Cancer Research and Treatment 2008: 107: 15-24

Bulun, S. E., Price, T. M., Aitken, J., Mahendroo, M. S., Simpson, E. R. A link between breast cancer and local estrogen biosynthesis suggested by quantification of breast adipose tissue aromatase

cytochrome P450 transcripts using competitive polymerase chain reaction after reverse transcription. Journal of Clinical Endocrinology and Metabolism 1993: 77: 1622–1628.

Buraschi, S., Neill, T., Owens, R. T., Iniguez, L. A., Purkins, G., Vadigepalli, R., Evans, B., Schaefer, L., Peiper, S. C., Wang, Z. X., Iozzo, R.V. Decorin protein core affects the global gene expression profile of the tumor microenvironment in a triple-negative orthotopic breast carcinoma xenograft model. PLoS One: 2012: 7: [Epub]

Burton, J. B., Priceman, S. J., Sung, J. L., Brakenhielm, E., An, D. S., Pytowski, B. Alitalo, K., Wu, L. Suppression of prostate cancer nodal and systemic metastasis by blockade of the lymphangiogenic axis. Cancer Research 2008: 68: 7828-7837.

Butler, L. M., Zhou, X., Xu, W. S., Scher, H. I., Rifkind, R. A., Marks, P. A., Richon, V. M. The histone deacetylase inhibitor SAHA arrests cancer cell growth, up-regulates thioredoxin-binding protein-2, and down-regulates thioredoxin. Proceedings of the National Academy of Sciences USA 2002: 99: 11700-11705

Butt, A. J., McNeil, C. M., Musgrove, E. A., Sutherland, R. L. Downstream targets of growth factor and oestrogen signalling and endocrine resistance: the potential roles of c-Myc, cyclin Dl and cyclin E. Endocrine Related Cancer 2005: 12: 47-59

Buzdar, A., Howell, A. Advances in aromatase inhibition: clinical efficacy and tolerability in the treatment of breast cancer. Clinical Cancer Research 2001: 7: 2620-2635

Cadenas, C., Franckenstein, D., Schmidt, M., Gehrmann, M., Hermes, M., Geppert, B., Schormann, W., Maccoux, L. J., Schug, M., Schumann, A., Wilhelm, C., Freis, E., ickstadt, K., Rahnenfuhrer, J., Baumbacj, J. I., Sickmann, A., Hengstler, J. G. Role of thioredoxin reductase 1 and thioredoxin interacting protein in prognosis of breast cancer. Breast Cancer Research 2010, 12; R44 [Epub]

Caldon, C. E., Sutherland, R. L., Musgrove, E. Cell cycle proteins in epithelial cell differentiation: implications for breast cancer. Cell Cycle 2010: 9: 1918-1928

Campbell, R. A., Bhat-Nakshatri, P., Patel, N. M., Constantinidou, D., Nakshatri, H. Phosphatidylinositol 3-kinase/AKT-mediated activation of estrogen receptor alpha: a new model for anti-estrogen resistance. Journal of Biological Chemistry 2001: 276: 9817-9824

Cancer Genome Atlas Network. Comprehensive molecular portraits of human breast tumours. Nature 2012: 490: 61-70

Cancer Research UK, 2010. Breast Cancer Risk Factors [online]. Available at: http://info.cancerresearchuk.org/cancerstats/types/breast/riskfactors/ [Accessed August 2013]

Carey, L. A., Berry, D. A., Ollila, D., Harris, L., Krop, I. E., Weckstein, D., Henry, L. H., Anders, C. K., Cirrincione, C., Winer, E. P., Perou, C. M., Hudis, C. Clinical and translational results of CALGB 40601: a neoadjuvant phase III trial of weekly paclitaxel and trastuzumab with or without lapatinib for HER2-positive breast cancer. Journal of Clinical Oncology 2013: 31: abstract 500

Carlson, R. W., O'Neill, A., Vidaurre, T., Gomez, H. L., Badve, S. S., Sledge, G. W. A randomized trial of combination anastrozole plus gefitinib and of combination fulvestrant plus gefitinib in the treatment of postmenopausal women with hormone receptor positive metastatic breast cancer. Breast Cancer Research and Treatment 2012: 133: 1049-1056

Caretta, A., Mucignat-Caretta, C. Protein Kinase A in Cancer. Cancers 2011: 3: 913-926

Carroll. J. S., Liu, X. S., Brodsky, A. S., Li, W., Meyer, C. A., Szary, A. J., Eeckhoute, J., Shao, W., Hestermann, E. V., Geistlinger, T. R., Fox, E. A., Silver, P. A., Brown, M. Chromosome-wide mapping

of estrogen receptor binding reveals long-range regulation requiring the forkhead protein FoxA1. Cell 2005: 122: 33-43

Castro-Rivera, E., Samudio, I., Safe, S. Estrogen regulation of cyclin D1 gene expression in ZR-75 breast cancer cells involves multiple enhancer elements. Journal of Biological Chemistry 2001: 276: 30853-30861

Cerillo, G., Rees, A., Manchanda, N., Reilly, C., Brogan, I., White, A., Needham, M. The oestrogen receptor regulates NFkappaB and AP-1 activity in a cell-specific manner. Journal of Steroid Biochemistry and Molecular Biology 1998, 67; 79-88.

Cawthorn, T. R., Moreno, J. C., Dharsee, M., Tran-Thanh, D., Ackloo, S., Zhu, P. H., Sardana, G., Chen, J., Kupchak, P., Jacks, L. M., Miller, N. A., Youngson, B., Iakovlev, V., Guidos, C. J., Vallis, K. A., Evans, K. R., McCready, D., Leong, W. L., Done, S. L. Proteomic Analyses Reveal High Expression of Decorin and Endoplasmin (HSP90B1) Are Associated with Breast Cancer Metastasis and Decreased Survival. PLOS One 2012: 7: [Epub]

Ceradini, D. J., Kulkarni, A.R., Callaghan, M. J., Tepper, O. M., Bastidas, N., Kleinman, M. E., Capla, J. M., Galiano, R. D., Levine, J. P., Gurtner, G. C. Progenitor cell trafficking is regulated by hypoxic gradients through HIF-1 induction of SDF-1. *Nature Medicine* 2004: **10:** 858-864

Certa, U., de Saizieu, A., Mous, J, Methods in Molecular Biology, vol. 170: DNA Arrays: Methods and Protocols 2001: p141-156

Chan, C. M., Martin, L. A., Johnston, S. R., Ali, S., Dowsett, M. Molecular changes associated with the acquisition of oestrogen hypersensitivity in MCF-7 breast cancer cells on long-term oestrogen deprivation. Journal of Steroid Biochemistry 2002: 81: 333-341

Chang, W. S., Chang, N. T., Lin, S. C., Wu, C. W., Wu, F. Y. Tissue-specific cancer-related serpin gene cluster at human chromosome band 3q26. Genes, Chromosomes and Cancer 2000, 29: 240-255

Charpin, C., Martin, P. M., De Victor, B., Lavaut, M. N., Habib, M. C., Abdrac, L., Toga, M. Multiparametric study (SAMBA 200) of estrogen receptor immunocytochemical assay in 400 human breast carcinomas: Analysis of estrogen receptor distribution heterogeneity in tissues and correlations with dextran coated charcoal assays and morphological data. Cancer Research 1988: 48: 1578-1586

Chen, C. L., Lin, C. F., Chang, W. T., Huang, W. C., Teng, C. F., Lin, Y. S. Ceramide induces p38 MAPK and JNK activation through a mechanism involving a thioredoxin-interacting protein-mediated pathway. *Blood.* 2008, 111**;** 4365-4374.

Chen, M., Cui, Y. K., Huang, W. H., Man, K., Zhang, G. J. Phosphorylation of estrogen receptor α at serine 118 is correlated with breast cancer resistance to tamoxifen. Oncology Letters 2013: 6: 118-124

Chen, P. Y., Chang, W. S., Lai, Y. K., Wu, C. K. c-Myc regulates the coordinated transcription of brain disease-related PDCD10-SERPINI1 bidirectional gene pair. Molecular and Cellular Neuroscience 2009: 42: 23-32

Chen, S., Ye, J., Kijima, I., Kinoshita, Y., Zhou, D. Positive and negative transcriptional regulation of aromatase expression in human breast cancer tissue. Journal of Steroid Biochemistry and Molecular Biology 2005: 95: 17-23

Cheng, G. C., Schulze, P. C., Lee, R. T., Sylvan, J., Zetter. B. R., Huang, H. Oxidative stress and thioredoxin-interacting protein promote intravasation of melanoma cells. Experimental Cell Research 2004: 300: 297-307.

Chin, Y. E., Kitagawa, M., Kuida, K., Flavell, R. A., Fu, X. –Y. Activation of the STAT signalling pathway can cause expression of caspase 1 and apoptosis. Molecular and Cellular Biology 1997, 17; 5328-5337

Chin, Y. E., Kitagawa, M., Su, W.-C. S., You, Z.-H., Iwamoto, Y., Fu, X. –Y. Cell growth arrest and induction of cyclin-dependent kinase inhibitor p21WAF1/CIP1 mediated by STAT1. Science 1996, 272; 719-722

Chow, W. A., Fang, J. J., Yee, J. K. The IFN regulatory factor family participates in regulation of Fas ligand gene expression in T cells. Journal of Immunology 2000: 164: 3512–3518.

Chu, I. M., Hengst, L., Slingerland, J. M. The Cdk inhibitor p27 in human cancer: prognostic potential and relevance to anticancer therapy. Nature Reviews Cancer 2008: 8: 253-267

Clemons, M., Goss, P., Estrogen and the risk of breast cancer. New England Journal of Medicine 2001: 344: 276-285

Coates, A. S., Keshaviah, A., Thurlimann, B., Mouridsen, H., mairiac, L., Forbes, J. F., Paridaens, R., Castiglione-Gertsch, M., Gelber, R. D., Colleoni, M., Lang, I., Del Mastro, L., Smith, I., Chirgwin, J., Nogaret, J. M., Pienkowski, T., Wardley, A., Jakobsen, E. H., Price, K. N., Goldhirsch, A. Five years of letrozole compared with tamoxifen as initial adjuvant therapy for postmenopausal women with endocrine-responsive early breast cancer: update of study BIG 1-98. Journal of Clinical Oncology 2007: 25: 486-492

Cole, P. A., Robinson, C. H. Mechanism and inhibition of cytochrome P-450 aromatase. Journal of Medicinal Chemsitry 1990, 33; 2933-2942

Collaborative Group on Hormonal Factors in Breast Cancer: Breast cancer and hormone replacement therapy: collaborative reanalysis of data from 51 epidemiological studies of 52,705 women with breast cancer and 108,411 women without breast cancer. Lancet 1997: 350: 1047-1059.

Coombes, R. C., Kilburn, L. S., Snowdon, C. F., Paridaens, R., Coleman, R. E., Jones, S. E., Jassem, J., Van de Velde, C. J., Delozier, T., Alvarez, I. Del Mastro, L., Ortmann, O., Diedrich, K., Coates, A. S., bajetta, E., Holmberg, S. B., Dodwell, D., Mickiewicz, E., Anderson, J., Lonning, P. E., Cocconi, G., Forbes, J., Castiglione, M., Stuart, N., Stewart, A., Fallowfield, L. J., Bertelli, G., Hall, E., Bogle, R. G., Carpentieri, M., Colajori, E., Subar, M., Ireland, E., Bliss, J. M: Intergriup Exemstane Study. Survival and safety of exemestane versus tamoxifen after 2–3 years' tamoxifen treatment (Intergroup Exemestane Study): a randomized controlled trial. Lancet 2007: 369: 559-570

Crawford, A. C., Riggins, R. B., Shajahan, A. N., Zwart, A., Clarke, R. Co-inhibition of BCL-W and BCL2 restores antiestrogen sensitivity through BECN1 and promotes an autophagy-associated necrosis. PloS One 2010: 5: [Epub]

Cristofanilli, M., Valero, V., Mangalik, A., Royce, M., Rabinowitz, I., Arena, F. P., Kroener, J. F., Curcio, E., Watkins, C., Bacus, S., Cora, E. M., Anderson, E., Magill, P. J. Phase II, randomized trial to compare anastrozole combined with gefitinib or placebo in postmenopausal women with hormone receptor-positive metastatic breast cancer. Clinical Cancer Research 2010: 16: 1904-1914

Crivellato, E., Nico, B., Ribatti, D. Mast cells and tumour angiogenesis: new insight from experimental carcinogenesis. Cancer Letters 2008; 269: 1-6

Csordas, G., Santra, M., Reed, C. C., Eichstetter, I., McQuillan, D. J., Gross, D., Nugent, M. A., Hajnoczky, G., Iozzo, R. V. Sustained down-regulation of the epidermal growth factor receptor by decorin. A mechanism for controlling tumor growth in vivo. Journal of Biological Chemistry 2000: 275: 32879-32887

Cui, Y., Yamada, S. N-Cadherin Dependent Collective Cell Invasion of Prostate Cancer Cells Is Regulated by the N-Terminus of α-Catenin. Plos One 2013: 8: [Epub]

Curtis, C., Shah, S. P., Chin, S. F., Turashvili, G., Rueda, O. M., Dunning, M. J., Speed, D., Lynch, A. G., Samarajiwa, S., Yuan, Y., Gräf, S., Ha, G., Haffari, G., Bashashati, A., Russell, R., McKinney, S.; METABRIC Group., Langerød, A., Green, A., Provenzano, E., Wishart, G., Pinder, S., Watson, P., Markowetz, F., Murphy, L., Ellis, I., Purushotham, A., Børresen-Dale, A. L., Brenton, J. D., Tavaré, S., Caldas, C., Aparicio, S. The genomic and transcriptomic architecture of 2,000 breast tumours reveals novel subgroups. Nature 2012: 18: 46-52

Cuzick, J., Sestak, I., Bonanni, B., Costantino, J. P., Cummings, S., DeCensi, A., Dowsett, M., Forbes, J. F., Ford, L., LACroix, A. Z., Mershon, J., Mitlak, B. H., Powles, T., veronesi, U., Vogel, V., Wickerham, D. L.; SERM Chemoprevention of Breast Cancer Overview Group. Selective oestrogen receptor modulators in prevention of breast cancer: an updated meta-analysis of individual participant data. Lancet 2013: 381: 1827-1834

Danielson, P. B.The cytochrome P450 superfamily: biochemistry, evolution and drug metabolism in humans. Current Drug Metaolism 2002: 3: 561-97.

Dauvois, S., White, R., Parker, M. G. The antiestrogen ICI 182780 disrupts estrogen receptor nucleocytoplasmic shuttling. Journal of Cell Science 1993, 106; 1377-1388

Dasanu, C. A., Sethi, N., Ahmed, N. Immune alterations and emerging immunotherapeutic approaches in lung cancer. Expert Opinions in Biological Therapeutics 2012: 12: 923-937

Davies, C., Pan, H., Godwin, J., Gray, R., Arriagada, R., Raina, V., Abraham, M., Medeiros Alencar, V. H., Badran, A., Bonfill, X., Bradbury, J., Clarke, M., Collins, R., Davis, S. R., Delmestri, A., Forbes, J. F., Haddad, P., Hou, M. F., Inbar, M., Khaled, H., Kielanowska, J., Kwan, W. H., Mathew, B. S., Mittra, I., Müller, B., Nicolucci, A., Peralta, O., Pernas, F., Petruzelka, L., Pienkowski, T., Radhika, R., Rajan, B., Rubach, M. T., Tort, S., Urrútia, G., Valentini, M., Wang, Y., Peto, R.; Adjuvant Tamoxifen: Longer Against Shorter (ATLAS) Collaborative Group. Long-term effects of continuing adjuvant tamoxifen to 10 years versus stopping at 5 years after diagnosis of oestrogen receptor-positive breast cancer: ATLAS, a randomised trial. Lancet 2013: 381: 805-816

DeFriend, D. J., Howell, A., Nicholson, R. I., Anderson, E., Dowsett, M., Mansel, R. E., Blamey, R. W., Bundred, N. J., Robertson, J. F., Saunders C., Baum, M., Walton, P., Sutcliffe, S., Wakeling, A. E. Investigation of a new pure antiestrogen (ICI 182780) in women with primary breast cancer. Cancer Research 1994: 54: 408-414

DeGraff, D. J., Clark, P. E., Cates, J. M., Yamashita, H., Robinson, V. L., Xiuping, Y., Smolkin, M. E., Chang, S. S., Cookson, M. S., Herrick, M. K., Shariat, S. F., Steinberg, G. D., Frierson, H. F., Xue-Ru, W., Theodorescu, D., Matusik, R. J. Loss of the Urothelial Differentiation Marker FOXA1 Is Associated with High Grade, Late Stage Bladder Cancer and Increased Tumor Proliferation. PLoS ONE 2012: 7: [Epub]

deGraffenried, L. A., Friedrichs, W. E., Russell, D. H., Donzis, E. J., Middleton, A. K., Silva, J. M., Roth, R. A., Hidalgo, M. Inhibition of mTOR activity restores tamoxifen response in breast cancer cells with aberrant Akt Activity. Clinical Cancer Research 2004: 10: 8059-8067

Dejana, E., Tournier-Lasserve, E., Weinstein, B. M. The control of vascular integrity by endothelial cell junctions: molecular basis and pathological implications. Developmental Cell 2009: 16: 209-221.

de Lange, R., Dimoudis, N., Weidle, U. H. Identification of genes associated with enhanced metastasis of a large cell lung carcinoma cell line. Anticancer Research 2003: 23: 187-194

De Laurentiis, M., Cancello, G., Zinno, L., Montagna, E., Malorni, L., Esposito, A., Pennacchio, R., Silvestro, L., Giuliano, M., Giordano, A., Caputo, F., Accurso, A., De Placido, S. Targeting HER2 as a

therapeutic strategy for breast cancer: a paradigmatic shift of drug development in oncology. Annals of Oncology 2005: 16: Supplement 4

de Leeuw, R., Flach, K., Bentin Toaldo, C., Alexi, X., Canisius, S., Neefjes, J., Michalides, R., Zwart, W. PKA phosphorylation redirects ERα to promoters of a unique gene set to induce tamoxifen resistance. Oncogene 2013: 32: 3543-3551

De Sousa Damiao, R., Fujiyama Oshima, C. T., Stavale, J. N., Goncalves, W. J. Analysis of the expression of estrogen receptor, progesterone receptor and chicken ovalbumin upstream promoter-transcription factor I in ovarian epithelial cancers and normal ovaries. Oncology Reports 2007: 18: 25-32

Di Leo, A., Jerusalem, G., Petruzelka, L., Torres, R., Bondarenko, I. N., Khasanov, R., Verhoeven, D., Pedrini, J. L., Smirnova, I., Lichinitser, M. R., Pendergrass, K., Garnett, S., Lindemann, J. P., Sapunar, F., Martin, M. Results of the CONFIRM phase III trial comparing fulvestrant 250 mg with fulvestrant 500 mg in postmenopausal women with estrogen receptor-positive advanced breast cancer. Journal of Clinical Oncology 2010: 28: 4594-4600

Djyrskot, L., Kruhoffer, M., Thykjaer, T., Marcussen, N., Jensen, J. L., Moller, K., Omtoft, T. F. Gene expression in the urinary bladder: a common carcinoma in situ gene expression signature exists disregarding histopathological classification. Cancer Research 2004: 64: 4040-4048

Dobrzycka, K. M., Townson, S. M., Jiang, S., Oesterreich, S. Estrogen receptor corepressors – A role in human breast cancer? Endocrine-Related Cancer 2003, 10; 517-536

Doherty, G. M., Boucher, L., Sorenson, K., Lowney, J. Interferon regulatory factor expression in human breast cancer. Annals of Surgery 2001:233: 623-629.

Dorssers, L. C., van Agthoven, T., Brinkman, A., Veldscholte, J., Smid, M., Dechering, K. J. Breast cancer oestrogen independence mediated by BCAR1 or BCAR3 genes is transmitted through mechanisms distinct from the oestrogen receptor signalling pathway or the epidermal growth factor receptor signalling pathway. Breast Cancer Research 2005: 7: 82-92

Dos Santos, E. G., Dieudonne, M. N., Pecquery, R., Le Moal, V., Giudicelli, Y., Lacasa, D. Rapid non-genomic E2 effects on p42/p44 MAPk, activator-protein-1, and cAMP response element binding protein in rat white adipocytes. Endocrinology 2002, 143; 930-940

Douglas, A. M., Goss, G. A., Sutherland, R. L, Hilton, D. J., Berndt, M. C., Nicola, N. A., Begley, C. G. Expression and function of members of the cytokine receptor superfamily on breast cancer cells. Oncogene 1997; 14: 661-669

Dowsett, M., Allred, C., Knox, J., Quinn, E., Salter, J., Wale, C., Cuzick, J., Houghton, J., Williams, N., Mallon, E., Bishop, H., Ellis, I., Larsimont, D., Sasano, H., Carder, P., Cussac, A. L., Knox, F., Speirs, V., Forbes, J., Buzdar, A. Relationship between quantitative estrogen and progesterone receptor expression and human epidermal growth factor receptor 2 (HER-2) status with recurrence in the Arimidex, Tamoxifen, Alone or in Combination trial. Journal of Clinical Oncology 2008: 26: 1059-1065

Dowsett, M, Ebbs, S. R., Dixon, J. M., Skene, A., Griffith, C., Boeddinghaus, I., Salter, J., Detre, S., Hills, M., Ashley, S., Francis, S., Walsh, G., Smith, I. E. Biomarker changes during neoadjuvant anastrozole, tamoxifen, or the combination: influence of hormonal status and HER-2 in breast cancer--a study from the IMPACT trialists. Journal of Clinical Oncology 2005: 23: 2477-2492

Dowsett, M., Nicholson, R. I., Pietras, R. J. Biological characteristics of the pure antiestrogen fulvestrant: overcoming endocrine resistance. Breast Cancer Research and Treatment 2005: 93: 11-8

Dowsett, M., Smith, I. E., Ebbs, S. R., Dixon, J. M., Skene, A., A'Hern, R., Salter, J., Detre, S., Hills, M., Walsh, G: On behalf of the IMPACT Trialists Group. Prognostic value of Ki67 expression after short-

term presurgical endocrine therapy for primary breast cancer. Journal of National cancer Institute 2007: 99: 167-170

Dubik, S., Shiu, R. P. Mechanism of estrogen activation of c-myc oncogene expression. Oncogene 1992: 7: 1587-1594

Dubrovska, A., Hartung, A., Bouchez, L. C., Walker, J. R., Reddy, V. A., Cho, C. Y., Schultz, P. G. CXCR4 activation maintains a stem cell population in tamoxifen-resistant breast cancer cells through AhR signalling. British Journal of Cancer 2012: 107: 43-52

Dunbier, A. K., Ghazoui, Z., Anderson, H., Salter, J., Nerurkar, A., Osin, P., A'hern, R., Miller, W. R., Smith, I. E., Dowsett, M. Molecular profiling of aromatase inhibitor-treated postmenopausal breast tumors identifies immune-related correlates of resistance. Clinical Cancer Research 2013: 19: 2775-286

Driggers, P. H., Segars, J. H. Estrogen action and cytoplasmic signaling pathways. Part II: the role of growth factors and phosphorylation in estrogen signaling. Trends in endocrinology and metabolism 2002: 13: 422-427

Early Breast Cancer Trialists' Collaborative Group (EBCTCG). Relevance of breast cancer hormone receptors and other factors to the efficacy of adjuvant tamoxifen: patient-level meta-analysis of randomised trials. Lancet 2011: 378: 771-784

Eklund, A. C., Friis, P., Wernersson, R., Szallasi, Z. Optimization of the BLASTN substitution matrix for prediction of non-specific DNA microarray hybridization. Nucleic Acids Research 2010: 38: [Epub]
Eklund, A. C., Szallasi, Z. Correction of technical bias in clinical microarray data improves concordance with known biological information. Genome Biology 2008: 9: [Epub]

El-Amraoui, A., Schonn, J. S., Kussel-Andermann, P., Blanchard, S., Desnos, C., Henry, J. P., Wolfrum, U., Darchen, F., Petit, C. MyRIP, a novel Rab effector, enables myosin VIIa recruitment to retinal melanosomes. EMBO Reports 2002: 3: 463-47

Elgort, M. G., O'Shea, J. M., Jiang, Y., Ayer, D. E. Transcriptional and translational downregulation of thioredoxin interacting protein is required for metabolic reprogramming during G(1). Genes and Cancer 2010: 1: 893-907

Endogenous Hormones and Breast Cancer Collaborative Group: Endogenous sex hormones and breast cancer in postmenopausal women: reanalysis of nine prospective studies. Journal of the National Cancer Institute 2002: 94: 606-616

Esseghir, S., Reis-Filho, J. S., Kennedy, A., James, M., O'Hare, M. J., Jeffery, R., Poulsom, R., Isacke, C. M. Identification of transmembrane proteins as potential prognostic markers and therapeutic targets in breast cancer by a screen for signal sequence encoding transcripts. Journal of Pathology 2006: 210: 420–430

Esseghir, S., Todd, K. S., Hunt, T., Poulsom, R., Plaza-Menacho, I., Reis-Filho, J., Isacke, C. M. A Role for Glial Cell–Derived Neurotrophic Factor–Induced Expression by Inflammatory Cytokines and RET/GFRα1 Receptor Up-regulation in Breast Cancer. Cancer Research 2007: 67: 11732-11741

Fan, P., Wang, J., Santen, R. J., Yue, W. Long-term treatment with tamoxifen facilitates translocation of estrogen receptor alpha out of the nucleus and enhances its interaction with EGFR in MCF-7 breast cancer cells. Cancer Research 2007: 67: 1352-1360

Food and Drug Administration (FDA)/Center for Drug Evaluation and Research. Approval: Exemestane (Aromasin) 1999. Oct 21, Available at: http://www.accessdata.fda.gov/scripts/cder/drugsatfda/index.cfm?fuseaction=Search.DrugDetail; Accessed: August 2013.

Forsten-Williams, K., Chua, C. C., Nugent, M. A. The kinetics of FGF-2 binding to heparin sulfate proteoglycans and MAP kinase signaling. Journal of Theoretical Biology 2005: 233: 483-499

Frasor, J., Danes, J. M., Komm, B., Chang, K. C., Lyttle, C. R., Katzenellenbogen, B. S. Profiling of estrogen up- and down-regulated gene expression in human breast cancer cells: insights into gene networks and pathways underlying estrogenic control of proliferation and cell phenotype. Endocrinology 2003: 144: 4562-4574

Frasor, J., Stossi, F., Danes, J. M., Komm, B., Lyttle, R. C., Katzenellenbogen, S. Selective estrogen receptor modulators: Discrimination of agonistic versus antagonistic activities by gene expression profiling in breast cancer cells. *Cancer Research* 2004, 64; 1522-1533

Frogne, T., Benjaminsen, R. V., Sonne-Hansen, K., Sorensen, B. S., Nexo, E., Laenkholm, A. V., Rasmussen, L. M., Riese, D. J., de Cremoux, P., Stenvang, J., Lykkesfeldt, A. E. Activation of ErbB3, EGFR and Erk is essential for growth of human breast cancer cell lines with acquired resistance to fulvestrant. Breast Cancer Research and Treatment 2009: 114: 263-275

Gaedcke, J*.,* Grade, M*.,* Jung, K*.,* Camps, J*.,* Jo, P*.,* Emons, G*.,* Gehoff, A*.,* Sax, U*.,* Schirmer, M*.,* Becker, H*.,* Beissbarth, T*.,* Ried, T*.,* Ghadimi, B. M*.* Mutated KRAS results in overexpression of DUSP4, a MAP-kinase phosphatase, and SMYD3, a histone methyltransferase, in rectal carcinomas*.* Genes, Chromosomes and Cancer 2010: 49*:* 1024-*10*34*.*

Ganapathy, V., Ganapathy, M. E., Leibach, F. H. Protein digestion and assimilation. T. Yamada (Ed.), Textbook of Gastroenterology (4th ed.), Lippincott Williams and Wilkins, Philadelphia, United States 2003: 438-448

Garib, V., Lang, K., Niggemann, B., Zänker, K. S., Brandt, L., Dittmar, T. Propofol-induced calcium signalling and actin reorganization within breast carcinoma cells. European Journal of Anaesthesiology 2005: 22: 609-661

Garnett, M. J., Edelman, E. J., Heidorm, S. J., Greenman, C. D., Dastur, A., lau, K. W., Greninger, P., Thompson, I. R., Luo, X., Soares, J., Liu, Q., Iorio, F., Surdez, D., Chen, L., Milano, R. J., Bignell, G. R., Tam, A. T. et al. Systemic identification of genomic markers of drug sensitivity in cancer cells. Nature 2012: 483: 570-575

Gee, J. M., Harper, M. E., Hutcheson, I. R., Madden, T. A., Barrow, D., Knowlden, J. M., McClelland, R. A., Jordan, N., Wakeling, A. E., Nicholson, R. I. The antiepidermal growth factor receptor agent gefitinib (ZD1839/Iressa) improves antihormone response and prevents development of resistance in breast cancer in vitro. Endocrinology 2003: 144: 5105-5117

Gee, J. M., Hutcheson, I. R. Understanding endocrine resistance: the critical need for sequential samples from clinical breast cancer and novel in vitro models. Breast Cancer Research and Treatment 2005: 7: 187-189.

Gee, J. M. W., Nicholson, R. I., Barrow, D., Dutkowski, C. M., Goddard, L., Jordan, N. J., McClelland, R. A., Knowlden, J. M., Francies, H. E., hiscox, S. E., Hutcheson, I. R. Antihormone induced compensatory signalling in breast cancer: an adverse event in the development of resistance. Hormone Molecular Biology and Clinical Investigation 2011: 5: 67-77

Gee, J. M., Robertson, J. F., Gutteridge, E., Ellis, I. O., Pinder, S. E., Rubini, M., Nicholson, R. I. Epidermal growth factor receptor/HER2/insulin-like growth factor receptor signalling and oestrogen receptor activity in clinical breast cancer. Endocrine Related Cancer 2005: Supplement 1: S99-S111

Geisler, J., King, N., Dowsett, M., Ottestad, L., Lundgren, S., Walton, P., Kormeset, P. O., Lonning, P. E. Influence of anastrozole (Arimidex), a selective, non-steroidal aromatase inhibitor, on in vivo aromatisation and plasma oestrogen levels in postmenopausal women with breast cancer. British Journal of Cancer 1996: 74: 1286-1291

Giacinti, L., Claudio, P. P., Lopez, M., Giordano, A. Epigenetic information and estrogen receptor alpha expression in breast cancer. The Oncologist 2006: 11: 1-8

Gilles, C., Thompson, E. W. The Epithelial to Mesenchymal Transition and Metastatic Progression in Carcinoma. The Breast Journal 1996: 2: 83-96

Giordano, S. H., Perkins, G. H., Broglio, K., Garcia, S. G., Middleton, L. P., Buzdar, A. U., Hortobagyi, G. N. Adjuvant systemic therapy for male breast carcinoma. Cancer 2005: 104: 2359-2364.

Goetz, M. P., Rae, J. M., Suman, V. J., Safgren, S. L., Ames, M. M., Visscher, D. W., Reynolds, C., Couch, F. J., Lingle, W. L., Flockhart, D. A., Desta, Z., Perez, E. A., Ingle, J. N. Pharmacogenetics of tamoxifen biotransformation is associated with clinical outcomes of efficacy and hot flashes. Journal of Clinical Oncology 2005:23:9312-9318

Goldberg, S. F., Miele, M. E., Hatta, N., Takata, M., Paquette-Straub, C., Freedman, L. P., Welch, D. R. Melanoma Metastasis Suppression by Chromosome 6: Evidence for a Pathway Regulated by CRSP3 and TXNIP. Cancer Research 2003: 63: 432-440

Goldhirsch, A., Ingle, J. N., Gelber, R. D., Thuerliman, G., Senn, H. J. Thresholds for therapies: highlights of the St Gallen International Expert Consensus on the primary therapy of early breast cancer 2009. Annals of Oncology 2009: 20: 1319-1329

Goldoni, S., Humphries, A., Nystrom, A., Sattar, S., Owens, R. T., McQuillan, D. J., Ireton, K., Iozzo, R. V. Decorin is a novel antagonistic ligand of the Met receptor. Journal of Cell Biology 2009: 185: 743-754

Goldoni, S., Iozzo, R. V. Tumor microenvironment: modulation by decorin and related molecules harboring leucine-rich tandem motifs. International Journal of Cancer 2008a: 123: 2473-2479

Goldoni, S., Seidler, D. G., Heath, J., Fassan, M., baffa, R., Thakur, M. L., Owens, R. T., McQuillan, D. J., Iozzo, R. V. An antimetastatic role for decorin in breast cancer. American Journal of Pathology 2008b:173: 844-855

Gomes, G. R. O., Yasuhara, F., Siu, E . R., Fernandes, S. A. F., Avellar, M. C. W., Lazari, M. F. M. Porto, C. S. In Vivo Treatments with Fulvestrant and Anastrozole Differentially Affect Gene Expression in the Rat Efferent Ductules. Biology of Reproduction 2011: 84: 152-161

Gopal, G., Shirley, S., Raja, U. M., Rajkumar, T. Endo-sulfatase Sulf-1 protein expression is down-regulated in gastric cancer. Asian Pacific Journal of Cancer Prevention 2012: 13: 641-646

Gottlicher, M., Heck, S., Herrlich, P. Transcriptional cross-talk, the second mode of steroid hormone recptor action. Journal of Molecular Medicine 1998, 46; 480-48

Groschl, B., Bettstetter, M., Giedl, C., Woenckhaus, M., Edmonston, T., Hofstadter, F., Dietmaier, W. Expression of the MAP kinase phosphatase DUSP4 is associated with microsatellite instability in colorectal cancer (CRC) and causes increased cell proliferation.International Journal of Cancer 2013: 132: 1537-1546

Gu, Z., Lee, R. Y., Skaar, T. C., Bouker, K. B., Welch, J. N., Lu, J., Liu, A., Zhu, Y., Davis, N., Leonessa, F., Brünner, N., Wang, Y., Clarke, R. Association of interferon regulatory factor-1, nucleophosmin, nuclear factor-κB, and cyclic AMP response element binding with acquired resistance to faslodex (ICI 182,780). Cancer Research 2002: 62: 3428-3437.

Gupta, N., Miyauchi, S., Martindale, R. G., Herdman, A. V., Podolsky, R., Miyake, K., Mager, S., Prasad, P. D., Ganapathy, M. E., Ganapathy, V. Upregulation of the amino acid transporter ATB0,+ (SLC6A14) in colorectal cancer and metastasis in humans. Biochimica et Biophysica Acta 2005: 1741: 215-223

Gupta, N., Prasad, P. D., Ghamande, S., Moore-Martin, P., Herdman, A. V., Martindale, R. G., Podolsky, R., mager, S., Ganapathy, M. E., Ganapathy, V. Up-regulation of the amino acid transporter ATB(0,+) (SLC6A14) in carcinoma of the cervix. Gynecology Oncology 2006: 100: [Epub]

Guo, Y., Kyprianou, N. Restoration of Transforming Growth Factor β Signaling Pathway in Human Prostate Cancer Cells Suppresses Tumorigenicity via Induction of Caspase-1-mediated Apoptosis. Cancer Research 1999: 59: 1366-1371

Gururaj, A. E., Rayala, S. K., Vadlamudi, R. K., Kumar, R. Novel mechanisms of resistance to endocrine therapy: genomic and nongenomic considerations. Clinical Cancer Research 2006: 12: 1001s–1007s

Gutierrez, M. C., Detre, S., Johnston, S., Mohsin, S. K., Shou, J., Allred, D. C., Schiff, R., Osborne, C. K., Dowsett, M. Molecular changes in tamoxifen-resistant breast cancer: relationship between estrogen receptor, HER-2, and p38 mitogen-activated protein kinase. Journal of Clinical Oncology 2005: 23: 2469-2476

Györffy, B., Lanczky, A., Eklund, A. C., Denkert, C., Budczies, J., Li, Q., Szallasi, Z. An online survival analysis tool to rapidly assess the effect of 22,277 genes on breast cancer prognosis using microarray data of 1,809 patients. Breast Cancer Research and Treatment 2010: 123: 725-731

Ham, W. S., Lee, J. H., Yu, H. S., Choi, Y. D., Expression of chicken ovalbumin upstream promoter-transcription factor I (COUP-TFI) in bladder transitional cell carcinoma. Urology 2008: 72: 921-926

Hammond, M. E., Hayes, D. F., Wolff, A. C., Mangu, P. B., Temin, S. American society of clinical oncology/college of American pathologists guideline recommendations for immunohistochemical testing of estrogen and progesterone receptors in breast cancer. Journal of Oncology Practice 2010: 6: 195-197

Harada, T., Chelala, C., Bhakta, V., Chaplin, T., Caulee, K., Baril, P., Young, P. D., Lemoine, N. R. Genome-wide DNA copy number analysis in pancreatic cancer using high-density single nucleotide polymorphism arrays. Oncogene 2008: 27: 1951-1960

Harvey, J. M., Clark, G. M., Osborne, C. K., Allred, D. C. Estrogen receptor status by immunohistochemistry is superior to the ligand-binding assay for predicting response to adjuvant endocrine therapy in breast cancer. Journal of Clinical Oncology 1999: 17: 1474-1481

Hashimoto, I., Kodama, J., Seki, N., Hongo, A., Yoshinouchi, M., Okuda, H., Kudo, T. Vascular endothelial growth factor-C expression and its relationship to pelvic lymph node status in invasive cervical cancer. British Journal of Cancer 2001: 85: 93–97

Hatae, N., Sugimoto, Y., Ichikawa, A. Prostaglandin receptors: advances in the study of EP3 receptor signaling. Journal of Biochemistry 2002: 131: 781-784

Hazan, R. B., Kang, L., Whooley, B. P., Borgen, P. I. N-cadherin promotes adhesion between invasive breast cancer cells and the stroma.Cell Adhesion and Commununication 1997: 4: 399-411.

Hazan, R. B., Phillips, G. R., Qiao, R. F., Norton, L., Aaronson, S. A. Exogenous expression of N-cadherin in breast cancer cells induces cell migration, invasion, and metastasis. Journal of Cell Biology 2000: 148: 779-790

He, Y., Rajantie, I., Pajusola, K., Jeltsch, M., Holopainen, T., Yla-Herttuala, S., Harding, T., Jooss, K., Takahashi, T., Alitalo, K.Vascular endothelial cell growth factor receptor 3-mediated activation of lymphatic endothelium is crucial for tumor cell entry and spread via lymphatic vessels. Cancer Research 2005: 65: 4739-4746

Heggem, M. A., Bradley, R. S. The cytoplasmic domain of Xenopus NF-protocadherin interacts with TAF1/set. Developmental Cell 2003: 4: 419-429.

Heitzer, E., Auer, M., Ulz, P., Geigl, J. B., Speicher, M. R. Circulating tumor cells and DNA as liquid biopsies. Genome Medicine 2013: 5: [Epub ahead of print]

Higgins, M. J., Baselga, J. Targeted therapies for breast cancer. Journal of Clinical Investigation 2011: 121: 3797-3803.

Hildebrand, A., Romaris, M., Rasmussen, L. M., Heinegard, D., Twardzik, D. R., Border, W. A., Ruoslahti, E. Interaction of the small interstitial proteoglycans biglycan, decorin and fibromodulin with transforming growth factor beta. Biochemical Journal 1994: 302: 527-534

Hines, S. J., Organ, C., Kornstein, M. J., Krystal, G. W. Coexpression of the c-KIT and stem cell factor genes in breast carcinomas. Cell Growth and Differentiation 1995: 6: 769–779.

Hirakawa, S., Brown, L. F., Kodama, S., Paavonen, K., Alitalo, K., Detmar, M. VEGF-C-induced lymphangiogenesis in sentinel lymph nodes promotes tumor metastasis to distant sites. Blood 2007: 109: 1010-1017

Hirano, T., Ishihara, K., Hibi, M. Roles of STAT3 in mediating the cell growth, differentiation and survival signals relayed through the IL-6 family of cytokine receptors. Oncogene 2000*: 19: 2548-56.*

Hiscox, S., Jiang, W. G., Obermeier, K., Taylor, K., Morgan, L., Burmi, R., Barrow, D., Nicholson, R. I. Tamoxifen resistance in MCF7 cells promotes EMT-like behaviour and involves modulation of beta-catenin phosphorylation. International Journal of Cancer 2006: 118: 290-301

Hiscox, S., Jordan, N. J., Jiang, W., Harper, M., McClelland, R., Smith, C., Nicholson, R. I. Chronic exposure to fulvestrant promotes overexpression of the c-Met receptor in breast cancer cells: implications for tumour–stroma interactions. Endocrine Related Cancer 2006: 13: 1085-1099

Holliday, D. L., Speirs, V. Choosing the right cell line for breast cancer research. Breast Cancer Research 2011: 13: [Epub]

Hollstein, M., Sidransky, D., Vogelstein, B., Harris, C. C. p53 mutations in human cancers*. Science 1991: 253:* 49–53

Hong, D.S., Angelo, L.S., and Kurzrock, R. 2007. Interleukin-6 and its receptor in cancer: implications for translational therapeutics. Cancer 2007, 110; 1911-1928

Horwitz, K. B., Jackson, T. A., Bain, D. L., Richer, J. K., Takimoto, G. S., Tung, L. Nuclear receptor coactivators and corepressors. Molecular Endocrinology 1996, 10; 1167-1177

Howell, A., Cuzick, J., Baum, M., Buzdar, A., Dowsett, M., Forbes, J. F., Hoctin-Boes-G., Houghton, J., locker, G. Y., Tobias, J. S; ATAC Trialists' Group. Results of the ATAC (Arimidex, Tamoxifen, Alone or in Combination) trial after completion of 5 years' adjuvant treatment for breast cancer. Lancet 2005: 365: 60-62
Howell, A., DeFriend, D. J., Robertson, J. F., Blamey, R. W., Anderson, E., Sutcliffe, F. A., Walton, P. Pharmacokinetics, pharmacological and anti-tumour effects of the specific anti-oestrogen ICI 182780 in women with advanced breast cancer. British Journal of Cancer 1996: 74: 300-308

Howell, A., Robertson, J. F., Quaresma Albano, J., Aschermannova, A., Mauriac, L., Kleeberg, U. R., Vergote, I., Erikstein, B., Webster, A, Morris, C. Fulvestrant, formerly ICI 182,780, is as effective as anastrozole in postmenopausal women with advanced breast cancer progressing after prior endocrine treatment. Journal of Clinical Oncology 2002: 20: 3396-3403

Huang, Y. T., Heist, R. S., Chirieac, L. R., Lin, X., Skaug, V., Zienolddiny, S., Haugen, A., Wu, M. C., Wang, Z., Su, L., Asomaning, K., Christiani, D. C. Genome-wide analysis of survival in early-stage non-small-cell lung cancer. Journal of Clinical Oncology 2009: 27: 2660-2667

Hue, J., Kim, A., Song, H., Choi, I., Park, H., Kim, T., Lee, W. J., Kang, H., Cho, D. IL-18 enhances SCF production of melanoma cells by regulating ROI and p38 MAPK activity. Immunology Letters 2005: 96: 211-217

Hunter, D. J., Spiegelman, D., Adami, H. O., van den Brandt, P. A., Folsom, A. R., Goldbohm, R. A., Graham, S., Howe, G. R., Kushi, L. H., Marshall, J. R., Miller, A. B., Speizer, F. E., Willett, W., Wolk, A., Yaun, S. S. Non-dietary factors as risk factors for breast cancer, and as effect modifiers of the association of fat intake and risk of breast cancer. Cancer Causes Control 1997: 8: 49-56.

Hurtado, A., Holmes, K. A., Geistlinger, T. R., Hutcheson, I. R., Nicholson, R. I., Brown, M., Jiang, J., Howat, W. J., Ali, S., Carroll, J. S. Regulation of ERBB2 by oestrogen receptor-PAX2 determines response to tamoxifen. Nature 2008: 456: 663-666

Hurtado, A., Holmes, K. A., Ross-Innes, C. S., Schmidt, D., Carroll, J. S. FOXA1 is a key determinant of estrogen receptor function and endocrine response. Nature Genetics 2011: 43: 27-33

Hutcheson, I. R., Knowlden, J. M., Madden, T. A., Barrow, D., Gee, J. M., Wakeling, A. E., Nicholson, R. I. Oestrogen receptor-mediated modulation of the EGFR/MAPK pathway in tamoxifen-resistant MCF-7 cells. Breast Cancer Research and Treatment 2003: 81: 81-93

Hyams, D. M., Chan, A., deOliveira, C., Snyder, R., Vinholes, J., Audeh, M. W., Alencar, V. M., Lombard, J., Mookerjee, B., Xu, J., Brown, K., Klein, P. Cediranib in combination with fulvestrant in hormone-sensitive metastatic breast cancer: a randomized Phase II study. Investigation of New Drugs 2013: [Epub ahead of print]

Imai, K., Hiramatsu, A., Fukushima, D., Pierschbacher, M. D., Okada, Y. Degradation of decorin by matrix metalloproteinases: identification of the cleavage sites, kinetic analyses and transforming growth factor-beta1 release. Biochemical Journal 1997: 322: 809–814.

Ingle, J. N., Rowland, K. M., Suman, V. J., Mirchandani, D., Bernath, A. M., Camoriano, J. K., Perez, E. A. Evaluation of fulvestrant in women with advanced breast cancer and progression on prior aromatase inhibitor therapy: a phase II trial of the North Central Cancer Treatment Group. Breast Cancer Research and Treatment 2004: 88(Suppl 1): S38, (abstract 409)

Iozzo, R. V., Buraschi, S., Genua, M., Xu, S. Q., Solomides, C. C., Peiper, S. C., Gomella, L. G., Morrione, A. Decorin antagonizes IGF receptor I (IGF-IR) function by interfering with IGF-IR activity and attenuating downstream signaling. Jounral of Biological Chemistry 2011: 286: 34712-34721

Ithimakin, S., Day, K. C., Malik, F., Zen, Q., Dawsey, S. J., Bersano-Begey, T. F., Quraishi, A. A., Ignatoski, K. W., Daignault, S., Davis, A., Hall, C. L., Palaisamy, N., Heath, A. N., Tawakkol, N., Luther, T. K., Clouthier, S. G., Chadwick, W. A., Day, M. L., Kleer, C. G., Thomas, D. G., Hayes, D. F., Korkaya, H., Wicha, M. S. HER2 drives luminal breast cancer stem cells in the absence of HER2 amplification: implications for efficacy of adjuvant trastuzumab. Cancer Research 2013: 73: 1635-1646

Ivanovic, V., Todorovic-Rakovic, N., Demajo, M., Neskovic-Konstantinovic, Z., Subota, V., Ivanisevic-Milovanovic, O., Nikolic-Vukosavljevic, D. Elevated plasma levels of transforming growth factor-β_1 (TGF-β_1) in patients with advanced breast cancer: association with disease progression. European Journal of Cancer 2003: 39: 454–461.

Jaschinski, F., Rothhammer, T., Jachimczak, P., Seitz, C., Schneider, A., Schlingensiepen, K. H. The antisense oligonucleotide trabedersen (AP 12009) for the targeted inhibition of TGF-β2. Current Pharmaceutical Biotechnology 2011: 12: 2203-2213

Jepsen, K., Hermanson, O., Onami, T. M., Gleiberman, A. S., Lunyak, V., McEvilly, R. J., Liu, F., Seto, E., Hedrick, S.M., Mandel, G., Glass, R. J., Rose, D. W., Rosenfeld, M. G. Combinatorial roles of the nuclear receptor corepressor in transcription and development. Cell 2000, 102; 753-763

Jeon, H. M., Jin, X., Lee, J. S., Oh, S. Y., Sohn, Y. W., Park, H. J., Joo, K. M., Park, W. Y., Nam, D. H., DePinho, R. A., Chin, L., Kim, H. Inhibitor of differentiation 4 drives brain tumor-initiating cell genesis through cyclin E and notch signaling. Genes and Development 2008: 22: 2028-2033.

Jiao, X., Kativar, S., Willmarth, N. E., Liu, M., Ma, X., Flomenberg, N., Lisanti, M. P., Pestell, R. G. c-Jun induces mammary epithelial cellular invasion and breast cancer stem cell expansion. Journal of Biological Chemistry 2010: 12: 8218-8226

Joel, P., Smith, J., Sturgill, T., Fisher, T., Blenis, J., Lannigan, D. A. pp90rsk1 regulates estrogen receptor-mediated transcription through phosphorylation of Ser-167. Molecular and Cellular Biology 1998: 1978-1984

Joensuu, H., Ejlertsen, B., Lonning, P. E., Rutqvist, L. E. Aromatase inhibitors in the treatment of early and advanced breast cancer. Acta Oncology 2005: 44: 23-31

Johnston, S., Pippen, J Jr., Pivot, X., Lichinitser, M., Sadeghi, S., Dieras, V., Gomez, H. L., Romieu, G., Manikhas, A., Kennedy, M. J., Press, M. F., Maltzman, J., Florance, A., O'Rourke, L., Oliva, C., Stein, S., Pegram, M. Lapatinib combined with letrozole versus letrozole and placebo as first-line therapy for postmenopausal hormone-receptor-positive metastatic breast cancer. Journal of Clinical Oncology 2009: 27: 5538–5546

Johnston S. R. D., Anderson E., Dowsett M., Howell A. Hormonal resistance in breast cancer Oettel M. Schillinger E. eds. Handbook of Experimental Pharmacology: Estrogens and Antiestrogens II, 205-221, Springer-Verlag Berlin 1999.

Johnston, S. R., Head, J., Pancholi, S., Martin, L. A., Smith, I. E., Dowsett, M. Integration of signal transduction inhibitors with endocrine therapy: an approach to overcoming hormone resistance in breast cancer. Clinical Cancer Research 2003: 9: 524-532

Johnston, S. R., Saccani-Jotti, G., Smith, I. E., Salter, J., Newby, J., Coppen, M., Ebbs, S. R., Dowsett, M. Changes in estrogen receptor, progesterone receptor, and pS2 expression in tamoxifen-resistant human breast cancer. Cancer Research 1995: 55: 3331-3338

Jordan, N. J., Gee, J. M., Barrow, D., Wakeling, A. E., Nicholson, R. I. Increased constitutive activity of PKB/Akt in tamoxifen resistant breast cancer MCF-7 cells. Breast Cancer Research and Treatment 2004: 87: 167-180

Jordan, V. C., Obiorah, I., Fan, P., Kim, H. R., Ariazi, E., Cunliffe, H., Brauch, H. The St. Gallen Prize Lecture 2011: evolution of long-term adjuvant anti-hormone therapy: consequences and opportunities. Breast 2011: 20:S1-S11

Joukov, V., Pajusola, K., Kaipainen, A., Chilov, D., Lahtinen, I., Kukk, E., Saksela, O., Kalkkinen, O., Alitalo, K. A novel vascular endothelial growth factor, VEGF-C, is a ligand for the Flt4 (VEGFR-3) and KDR (VEGFR-2) receptor tyrosine kinases. EMBO Journal 1996: 15: 290-298

Joyce, J. A., Pollard, J. W. Microenvironmental regulation of metastasis. Nature Reviews Cancer 2009: 9: 239-252

Juttner, S., Wissmann, C., Jons, T., Vieth, M., Hertel, J., Gretschel, S., Schlag, P. M., Kemmner, W., Hocker, M. Vascular endothelial growth factor-D and its receptor VEGFR-3: two novel independent prognostic markers in gastric adenocarcinoma. Journal of Clinical Oncology 2004: 24: 228–240

Kalyuga, M., Gallego-Ortega, D., Lee, H. J., Roden, D. L., Cowley, M. J., Caldon, C. E., Stone, A., Allerdice, S. L., Valdes-Mora, F., Launchbury, R., Statham, A. L., Armstrong, N., Alles, M. C., Young, A., Egger, A., Au, W., Piggin, C. L., Evans, C. J., Ledger, A., Brummer, T., Oakes, S. R., Kaplan, W., Gee, J. M., Nicholson, R. I., Sutherland, R. L., Swarbrick, A., Naylor, M. J., Clark, S. J., Carroll, J. S., Ormandy,

C. J. ELF5 suppresses estrogen sensitivity and underpins the acquisition of antiestrogen resistance in luminal breast cancer. PLos Biology 2012: 10: [Epub]

Kang, J., Perry, J. K., Pandey, V., Fielder, G. C., Mei, B., Qian, P. X., Wu, Z. S., Zhu, T., Liu, D. X., Lobie, P. E. Artemin is oncogenic for human mammary carcinoma cells. Oncogene 2009: 28: 2034–2045

Kang, J., Qian, P. X., Pandey, V., Perry, J. K., Miller, L. D., Liu, E. T., Zhu, T., Liu, D. X., Lobie, P. E. Artemin is estrogen-regulated and mediates antiestrogen resistance in mammary carcinoma. Oncogene 2010: 29: 3228-3240

Karczewska, A., Nawrocki, S., Breborowicz, D., Filas, V., Mackiewicz, A. Expression of interleukin-6, interleukin-6 receptor, and glycoprotein 130 correlates with good prognoses for patients with breast carcinoma. Cancer (Phila) 2000: 88: 2061-2071.

Karunakaren, S., Umapathy, N. S., Thangaraju, M., hatnaka, T., Itagaki, S., Munn, D. H., Prasad, P. D., Ganapathy, V. Interaction of tryptophan derivatives with SLC6A14 (ATB0,+) reveals the potential of the transporter as a drug target for cancer chemotherapy. Biochemistry Journal 2008: 414: 343-355

Karunakaren, S., Ramachandran, S., Cookthankandaswamy, V., Elangivan, S., Babu, E., Perivasamy-Thandavan, S., Guray, A., Gnanprakasam, J. P., Singh, N., Schoenlein, P. V., Prasad, P. D., Thangaraju, M., Ganapathy, V. SLC6A14 (ATB0,+) protein, a highly concentrative and broad specific amino acid transporter, is a novel and effective drug target for treatment of estrogen receptor-positive breast cancer. Journal of Biological Chemistry 2011: 286: 31830-31838

Kashima, T., Nakamura, K., Kawaguchi, J., Takanashi, M., Ishida, T., Aburatani, H., Kudi, H., Fukayama, M., Grigoriadis, A. E. Overexpression of cadherins suppresses pulmonary metastasis of osteosarcoma in vivo. International Journal of Cancer 2003: 104: 147–154

Katoh, H., Hosono, K., Ito, Y., Suzuki, T., Ogawa, Y., Kubo, H., Kamata, H., Mishima, T., Tamaki, H., Sakagami, H., Sugimoto, Y., Narumiya, S., Watanabe, M., Majima, M. COX-2 and prostaglandin EP3/EP4 signaling regulate the tumor stromal proangiogenic microenvironment via CXCL12-CXCR4 chemokine systems. American Journal of Pathology 2010: 176: 1469-1483

Kato, S., Endoh, H., Masuhiro, Y., Kitamato, T., Uchiyama, S., Sasaki, H., Masushige, S., Gutoh, Y., Nishida, E., Kawashima, H., Metzger, D., Chambon, P. Activation of the estrogen receptor through phosphorylation by mitogen-activated protein kinase. Science 1995, 270; 1491-1494

Kahlert, S., Neudling, S., van Eickels, M., Vetter, H., Meyer, R., Grohe, C. Estrogen receptor alpha rapidly activates the IGF-1 receptor pathway. Journal of Biological Chemistry 2000: 275: 18447-18453

Kent, D., Copley, M., Benz, C., Dykstra, B., Bowie, M., Eaves, C. Regulation of hematopoietic stem cells by the steel factor/KIT signaling pathway. Clinical Cancer Research 2008: 14: 1926–30.
Kevse, S. M. Dual-specificity MAP kinase phosphatases (MKPs) and cancer. Cancer Metastasis Reviews 2008: 27: 253-261

Khurana, A., Liu, P., Mellone, P., Lorenzon, L., Vincenzi, B., Datta, K., Yang, B., Linhardt, R. J., Lingle, W., Chien, J., Baldi, A., Shridhar, V. HSulf-1 modulates FGF2- and hypoxia-mediated migration and invasion of breast cancer cells. Cancer Research 2011: 71: 2152-2161.

Kijima, T., Maulik, G., Ma, P. C., Tibaldi, E. V., Turner, R. E., Rollins, B., Sattler, M., Johnson, B. E., Salgia, R. Regulation of cellular proliferation, cytoskeletal function, and signal transduction through CXCR4 and c-Kit in small cell lung cancer cells. Cancer Research 2002: 62: 6304-6311

Kim, J.B., Islam, S., Kim, Y. J., Prudoff, R. S., Sass, K. M., Wheelock, M.J., Johnson, K. R. N-Cadherin extracellular repeat 4 mediates epithelial to mesenchymal transition and increased motility. Journal of Cell Biology 2000: 151: 1193–1206

Kim, S., Lewis, C., Nadel, J. A. Epidermal growth factor receptor reactivation induced by E-prostanoid-3 receptor- and tumor necrosis factor-alpha-converting enzyme-dependent feedback exaggerates interleukin-8 production in airway cancer (NCI-H292) cells. Experimental Cell Research 2011: 317: 2650-2660

Kitamura, Y., Hirotab, S. Kit as a human oncogenic tyrosine kinase. Cell and Molecular Life Sciences 2004: 61: 2924-2931.

Knowlden, J., Hutcheson, I., Jones, H., Madden, T., Gee, J., Harper, M., Barrow, D., Wakeling, A., Nicholson, R. Elevated levels of epidermal growth factor receptor/c-erbB2 heterodimers mediate an autocrine growth regulatory pathway in tamoxifen-resistant MCF-7 cells. Endocrinology 2003: 144: 1032-1044

Konecny, G. E., Pegram, M. D., Venkatesan, N., Finn, R., yang, G., Rahmeh, M., Untch, M., Rusnak, D.W., Spehar, G., Mullin, R. J., Keith, B. R., Gilmer, T. M., Berger, M., Podratz, K. C., Slamon, D. J. Activity of the dual kinase inhibitor lapatinib (GW572016) against HER-2-overexpressing and trastuzumab-treated breast cancer cells. Cancer Research 2006: 66: 1630-1639

Kousteni, S., Bellido, T., Plotkin, L. I., O'Brien, C. A., Bodenner, D. L., Han, L., Han, K., DiGregorio, G. B., Katzenellenbogen, J. A., Katzenellenbogen. B. S., Roberson, P. K., Weinstein, R. S., Jilka, R. L., Manolagas, S. C. Nongenotropic, sex-non-specific signalling through the estrogen or androgen receptors:dissociation from transcriptional activity. Cell 2001, 104; 719-730

Kousteni, S., Han, L., Chen, J. R., Almeida, M., Plotkin, L. I., Bellido, T., manoalgas, S. C. Kinase-mediated regulation of common transcription factors accounts for the bine-protective effects of sex steroids. Journal of Clinical Investigation 2003, 111; 1651-1664

Krainick-Strobel, U. E., Lichtenegger, W., Wallwiener, D., Tulusan, A. H., Jänicke, F., Bastert, G., Kiesel, L., Wackwitz, B., Paepke, S. Neoadjuvant letrozole in postmenopausal estrogen and/or progesterone receptor positive breast cancer: a phase IIb/III trial to investigate optimal duration of preoperative endocrine therapy. BMC Cancer 2008: 28: [Epub]

Kraus, M. H., Issing, W., Miki, T., Popescu, N. C., Aaronson, S. A. Isolation and characterisation of ERBB3, a third member of the ERBB/epidermal growth factor receptor family: evidence for overexpression in a subset of human mammary tumours. Proceedings of the National Academy of USA 1989, 86; 9193-9197

Kucia, M., Reca, R., Miekus, K., Wanzeck, J., Wojakowski, W., Janowska-Wieczorek, A., Ratajczak, J., Ratajczak, M. Z. Trafficking of normal stem cells and metastasis of cancer stem cells involve similar mechanisms: pivotal role of the SDF-1-CXCR4 axis. Stem Cells 2005: 23: 879-894.

Kumar, V., Green, S., Stack, G., Berry, M., Jin, J. R., Chambon, P. Functional domains of the human estrogen receptor. Cell 1987: 51: 941-951

Kumar, R., Mandal, M., Lipton, A., Harvey, H., Thompson, C. B. Overexpression of HER2 modulates bcl-2, bcl-XL, and tamoxifen-induced apoptosis in human MCF-7 breast cancer cells. Clinical Cancer Research 1996: 2: 1215-1219

Kunisue, H., Kurebavashi, J., Otsuki, T., tang, C. K., Kurosumi, M., Yamamoto, S., Tanaka, K., Doihara, H., Shimizu, N., Sonoo, H. Anti-HER2 antibody enhances the growth inhibitory effect of anti-oestrogen on breast cancer cells expressing both oestrogen receptors and HER2. British Journal of Cancer 2000: 82: 46-51

Kuonen, F., Laurent, J., Secondini, C., Lorusso, G., Stehle, J., Rausch, T., Hull, E., Bieler, G., Alghisi, G., Scwendener, R., Anddrejevic-Blant, S., Mirimanoff, R., Rüegg, C. Inhibition of the Kit Ligand/c-Kit Axis Attenuates Metastasis in a Mouse Model Mimicking Local Breast Cancer Relapse after Radiotherapy. Clinical Cancer Research 2012: 18: 4365-4374

Kushner, P.J., Agard, D.A., Greene, G.L., Scanlan, T.S., Shiau, A.K., Uht, R.M., Webb, P., 2000. Estrogen receptor pathways to AP-1. Journal of Steroid Biochemistry and Molecular Biology 2000, 74; 311–317.

Kuter, I., Gee. J. M., Hegg, R., Singer, C. F., Badwe, R. A., Lowe, E. S., Emeribe, U. A., Anderson, E., Sapunar, F., Finaly, P., Nicholson, R . I., Bines, J., Harbeck, N. Dose-dependent change in biomarkers during neoadjuvant endocrine therapy with fulvestrant: results from NEWEST, a randomized Phase II study. Breast Cancer Research and Treatment 2012: 133: 237-246

Lai, J. P., Oseini, A. M., Moser, C. D., Yu, C., Elsawa, S. F., Hu, C., Nakamura, I., Han, T., Aderca, I., Isomoto, H., Garrity-Park, M. M., Shire, A. M., Li, J., Sanderson, S. O., Adjei, A. A., Fernandez-Zapico, M. E., Roberts, L. R. The oncogenic effect of sulfatase 2 in human hepatocellular carcinoma is mediated in part by glypican 3-dependent Wnt activation. Hepatology 2010: 52: 1680–1689.

Lai, J. P., Thompson, J. R., Sandhu, D. S., Roberts, L. R. Heparin-degrading sulfatases in hepatocellular carcinoma: roles in pathogenesis and therapy targets. Future Oncology 2008: 4: 803–814

Lammens, T., Swerts, K., Dervcke, L., De Craemer, A., De Preter, K., Van Roy, N., Vandesompele, J., Speleman, F., Phillipe, J., benoit, Y., beiske, K., Bracke, M., Laureys, G. N-cadherin in neuroblastoma disease: expression and clinical significance. PLoS One 2012: 7: [Epub]

Lannigan, D. Estrogen receptor phosphorylation. Steroids 2003: 68: 1-9

Larsson, O., Wahlestedt, C., Timmons, J. A. Considerations when using the significance analysis of microarrays (SAM) algorithm. BMC Bioinformatics 2005: 6: 129

Lavinsky, R. M., Jepsen, K., Heinzel, T., Torchia, J., Mullen, T., Schiff, R., Del-Rio, A. L., Ricote, M., Ngo, S., Gemsch, J., Hilsenbeck, S. G., Osborne, C. K., Glass, C. K., Rosenfeld, M. G., Rose, D. W. Diverse signaling pathways modulate nuclear receptor recruitment of N-CoR and SMRT complexes. Proceedings of the National Academy of Science USA 1998, 6; 2920-2925

Lazennec, G., Thomas, J. A., Katzenellenbogen, B. S. Involvement of cyclic AMP response element binding protein (CREB) and estrogen resceptor phosphorylation in the synergistic activation of the estrogen receptor by estradiol and protein kinase activators. Journal of Steroid Biochemistry 2001, 77; 193-203

Leary, A. F., Drury, S., Detre, S., Pancholi, S., Lykkesfeldt, A. E., Martin, L. A., Dowsett, M., Johnston, S. R. Lapatinib restores hormone sensitivity with differential effects on estrogen receptor signaling in cell models of human epidermal growth factor receptor 2-negative breast cancer with acquired endocrine resistance. Clinical Cancer Research 2010: 16: 1486-1497

Le Dily, F., Metivier, R., Gueguen, M. M., Le Peron, C., Flouriot, G., Tas, P., Pakdel, F. COUP-TFI modulates estrogen signaling and influences proliferation, survival and migration of breast cancer cells. Breast Cancer Research and Treatment 2008: 110: 69-83

Lee, J., Yang, G., Paik, S. S., Chung, M. S. Does E-cadherin or N-cadherin or epithelial-mesenchymal transition have a probability of clinical implication of the prognostic marker in invasive ductal carcinoma? Cancer Research 2012: 72: Poster 2 10-39

Lee, T. W., Coates, L. C., Birch, N. P. Neuroserpin regulates N-cadherin-mediated cell adhesion independently of its activity as an inhibitor of tissue plasminogen activator. Journal of Neuroscience Research 2008: 86:1243-1253.

Lennartsson, J., Ronnstrand, L. Stem cell factor receptor/c-Kit: from basic science to clinical implications. Physiological Reviews 2012: 92: 1619-1649

Leonard, A. E., Kelder, B., Bobik, E. G., Chuang, L. T., Lewis, C. J., Kopchick, J. J., Mukerji, P., Huang, Y. S. Identification and expression of mammalian long-chain PUFA elongation enzymes. Lipids 2002: 37: 733-740

Levenson, A. S., Jordan, V. C. MCF-7: the first hormone-responsive breast cancer cell line. Cancer Research 1997: 57: 3071-3078

Li, S., Li, Z., Guo, F., Qin, X., Liu B., Lei, Z., Song, Z., Sun, L., Zhang, H-T., You, J., Zhou, Q. miR-223 regulates migration and invasion by targeting Artemin in human esophageal carcinoma. Journal of Biomedical Science 2011b: 18: [Epub]

Li, Q., Birkbak, N. J., Gyorffy, B., Szallasi, Z., Eklund, A. C. Jetset: selecting the optimal microarray probe set to represent a gene. BMC Bioinformatics 2011a: 12: [Epub]

Li, J., Yen, C., Liaw, D., Podsypanina, K., Bose, S., Wang, S. I., Puc, J., Miliaresis, C., Rodgers, L., McCombie, R., Bigner, S. H., Giovanella, B. C., Ittmann, M., Tycko, B., Hibshoosh, H., Wigler, M. H., Parsons, R. PTEN, a putative protein tyrosine phosphatase gene mutated in human brain, breast, and prostate cancer. *Science* 1997, 275: 1943-1947

Linstedt, A. D., West, N. B., Brenner, R. M. Analysis of monomeric-dimeric states of the estrogen receptor with monoclonal antiestrophilins. Journal of Steroid Biochemistry 1986, 24; 677–686

Liu, H., Wing, L., De Los Reyes, A., Jordan, V. C. Long-term fulvestrant treatment results in irreversible loss of estrogen receptor alpha expression in MCF-7 human breast cancer cells. Proceedings of the American Association of Cancer Research 2004: 45: Abstract 5600

Liu, H., Chen, X., Focia, P. J., He, X. Structural basis for stem cell factor-KIT signaling and activation of class III receptor tyrosine kinases. Embo Journal 2007: 26: 891–901.

Liu, S. V., Melstrom, L., Yao, K., Russell, C. A., Sener, S. F. Neoadjuvant therapy for breast cancer. Journal of Surgical Oncology 2010: 101: 283-291

Lobanova, Y. S., Scherbakov, A. M., Shatskaya, V. A., Krasil'nikov, M. A. Mechanism of estrogen-induced apoptosis in breast cancer cells: role of the NF-kappaB signaling pathway. Biochemistry (Mosc) 2007: 72: 320–327.

Lo, R., Burgoon, L., Macpherson, L., Ahmed, S., Matthews, J. Estrogen receptor-dependent regulation of CYP2B6 in human breast cancer cells. Biochimica et Biophysica Acta 2010: 1799: 469-479

Lupien, M., Meyer, C. A., Bailey, S. T., Eeckhoute, J., Cook, J., Westerling, T., Zhang, X., Carroll, J. S., Rhodes, D. R., Liu, X. S., Brown, M. Growth factor stimulation induces a distinct ER(alpha) cistrome underlying breast cancer endocrine resistance. Genes and Development 2010: 24: 2219-2227

Lynch, T. J., Bell, D. W., Sordella, R., Gurubhangavatula, S., Okimoto, R. A., Brannigan, B. W., Harris, P. L., Haserlet, S. M., Supko, J. G., Haluska, F. G., Louis, D. N., Christiani, D. C., Settleman, J., Haber, D. A. Activating mutations in the epidermal growth factor receptor underlying responsiveness of non-small-cell lung cancer to gefitinib. New England Journal of Medicine 2004: 350: 2129-2139

Ma, X. J., Wang, Z., Ryan, P. D., Isakoff, S. J., Barmettler, A., Fuller, A., Muir, B., Mohpatra, G., Salunga, R., Tuggle, J. T., Tran, Y., Tassin, A., Amon, P., Wang, W., Wang, W., Enright, E., Stecker, K., Estepa-Sabal, E., Smith, B., Younger, J., Balis, U., Michaelson, J., Bhan, A., Habin, K., Brugge, J., Haber, D. A., Erlander, M. G., Sgroi, D. C. A two-gene expression ratio predicts clinical outcome in breast cancer patients treated with tamoxifen. Cancer Cell 2004: 5: 607–616

MacCallum, J., Keen, J. C., Bartlett, J. M. S., Thompson, A. M., Dixon, J. M., Miller, W. R. Changes in expression of transforming growth factor beta mRNA isoforms in patients undergoing tamoxifen therapy. British Journal of Cancer 1996, 74; 474-478

MacGregor, J. I., Jordan, V.C. Basic guide to the mechanisms of antiestrogen action. *Pharmacology Reviews* 1998, 50; 151–196

Mackay, A., Urruticoechea, A., Dixon, J. M., Dexter, T., Fenwick, K., Ashworth, A., Drury, S., Larionov, A., Young, O., White, S., Miller, W. R., Evans, D. B., Dowsett, M. Molecular response to aromatase inhibitor treatment in primary breast cancer. Breast Cancer Research 2007: 9: [Epub]

MacMahon, B., Cole, P., Lin, T. M., Lowe, C. R., Mirra, A. P., Ravnihar, B., Salber, E. J., Valaoras, V. G., Yuasa, S. Age at first birth and breast cancer risk. Bulletins of the World Health Organisation 1970: 43: 209-221

Maitre, J. L., Heisenberg, C. P. Three functions of cadherins in cell adhesion. Current Biology 2013: 23: 626-633

Makris, A., Powles, T. J., Ashley, S. E., Chang, J., Hickish, T., tidy, V. A., Nash, A. G., Ford, H. T. A reduction in requirements for mastectomy in a randomised trial of neoadjuvant chemoendocrine therapy in breast cancer. Annals of Oncology 1998: 9: 1179-1184

Malek, D., Gust, R., Kleuser, B. 17-Beta-estradiol inhibits transforming-growth-factor-beta-induced MCF-7 cell migration by Smad3-repression*. European Journal of Pharmacology 2006, 534**; 39-*47.*

Manie, S., Santoro, M., Fusco, A., Billaud, M. The RET receptor: function in development and dysfunction in congenital malformation. Trends in Genetics 2001: 17: 580–589.

Martin, L. A., Dowsett, M. BCL-2: A new therapeutic target in estrogen receptor-positive breast cancer? Cancer Cell 2013: 24: 7-9

Masamura, S., Santner, S. J., Heitjan, D. F., Santen, R. J. Estrogen deprivation causes estradiol hypersensitivity in human breast cancer cells. Journal of Clinical Endocrinology and Metabolism 1995: 80: 2918-2925

Mathew, J., Asgeirsson, K. S., Jackson, L. R., Cheung, K. L., Robertson, J. F. Neoadjuvant endocrine treatment in primary breast cancer - review of literature. Breast 2009: 18: 339-344

McLean, G. W., Carragher, N. O., Avizienyte, E., Evans, J., Brunton, V. G., Frame, M. C. The role of focal-adhesion kinase in cancer—a new therapeutic opportunity. Nature Reviews Cancer 2005: 5: 505–515.

McClelland, R. A., Barrow, D., Madden, T. A., Dutkowski, C. M., Pamment, J., Knowlden, J. M., Gee, J. M., Nicholson, R. I. Enhanced epidermal growth factor receptor signaling in MCF7 breast cancer cells after long-term culture in the presence of the pure antiestrogen ICI 182,780 (Faslodex). Endocrinology 2001: 142: 2776-2788

McDermott, U., Settleman, J. Personalized cancer therapy with selective kinase inhibitors: an emerging paradigm in medical oncology. Journal of Clinical Oncology 2009: 27: 5650-5659

McKenna, N. J., Lanz, R. B., O'Malley, B. W. Nuclear receptor coregulators: cellular and molecular biology. Endocrinology Reviews 1999: 20: 321-344

Mehta, R. S., Barlow, W. E., Albain, K. S., Vandenberg, T. A., Dakhil, S. R., Tirumali, N. R., Lew, D. L., Hayes, D. F., Gralow, J. R., Livingston, R. B., Hortobagyi, G. N. Combination Anastrozole and Fulvestrant in Metastatic Breast Cancer. New England Journal of Medicine 2012: 367: 435-444

Mello, C. A., Chinen, L. T., da Silva, S. C., do Nascimento Matias, C., Benevides, C. F., Gimenes, D. L., Fanelli, M. F. Prolonged time to progression with fulvestrant for metastatic breast cancer. Medical Oncology 2011: 28: 416-419

Memminger, M., Keller, M., Lopuch, M., Pop, N., Bernhardt, G., von Angerer, E., Buschauer, A. The Neuropeptide Y Y_1 Receptor: A Diagnostic Marker? Expression in MCF-7 Breast Cancer Cells Is Down-Regulated by Antiestrogens *In Vitro* and in Xenografts. PLoS One 2012: 7

Meng, L. X., Chi, Y. H., Wang, X. X., Ding, Z. J., Fei, L. C., Zhang, H., Mou, L., Cui, W., Xue, Y. J. Neurotrophic artemin promotes motility and invasiveness of MIA PaCa-2 pancreatic cancer cells. Asian Pacific Journal of Cancer Prevention. 2012: 13: 1793-1797

Merkle, D., Hoffmann, R. Roles of cAMP and cAMP-dependent protein kinase in the progression of prostate cancer: Cross-talk with the androgen receptor. Cellular signalling 2011: 23: 507-515

Merline, R., Moreth, K., Beckmann, J., Nastase, M. V., Zeng-Brouwers, J., Tralhao, J. G., Lemarchand, P., Pfeilschifter, J., Schaefer, R. M., Iozzo, R. V., Chaefer, L. Signaling by the matrix proteoglycan decorin controls inflammation and cancer through PDCD4 and MicroRNA-21. Science Signalling 2011: 4: [Epub]

Metivier, R., Gay, F. A., Hübner, M. R., Flouriot, G., Salbert, G., Gannon, F., Kah, O., Pakdel, F. Formation of an hER alpha-COUP-TFI complex enhances hER alpha AF-1 through Ser118 phosphorylation by MAPK. EMBO Journal 2002: 21: 3443-3453

Metivier, R., Penot, G., Hubner, M. R., Reid, G., Brand, H., Kos, M., Gannon, E. Estrogen receptor-alpha directs ordered, cyclical, and combinatorial recruitment of cofactors on a natural target promoter. Cell 2003: 115: 751-763

Metzger, D., Losson, R., Bornert, J. M., Lemoine, Y., Chambon, P. Promoter specificity of the two transcriptional activation functions of the human oestrogen receptor in yeast. Nucleic Acids Research 1992: 20: 2813-2817

Michalides, R., Griekspoor, A., Balkenende, A., Verwoerd, D., Janssen, L., Jalink, K., Floore, A., Velds, A., van't Veer, L., Neefjes, J. Tamoxifen resistance by a conformational arrest of the estrogen receptor alpha after PKA activation in breast cancer. Cancer Cell 2004: 5: 597-605

Michaud, L. B., Jones, K. L., Buzdar, A. U. Combination endocrine therapy in the management of breast cancer. Oncologist 2001: 6: 538-546.

Migliaccio, A., Castoria, G., Di Domenico, M., De Falco, A., Bilancio, A., Auricchio, F. Src is an initial target of sex steroid hormone action. Annual New York Academy of Sciences 2002: 963: 185–190.

Miki, Y., Suzuki, T., Tazawa, C., Yamaguchi, Y., Kitada, K., Honma, S., Moriva, T., Hirakawa, H., Evans, D. B., Havashi, S., Ohuchi, N., Sasano, H. Aromatase localization in human breast cancer tissues: possible interactions between intratumoral stromal and parenchymal cells. Cancer Research 2007: 67: 3945-3954

Milla-Santos, A., Milla, L., Calvo, N., Portella, J., Rallo, L., Casanovas, J. M., Pons, M., Rodes, J. Anastrozole as neoadjuvant therapy for patients with hormone-dependent, locally-advanced breast cancer. Anticancer Research 2004: 24: 1315-1318

Miller, W. R., Larionov, A., Renshaw, L., Anderson, T. J., Walker, J. R., Krause, A., Sing, T., Evans, D. B., Dixon, J. M. Gene expression profiles differentiating between breast cancers clinically responsive or resistant to letrozole. Journal of Clinical Oncology 2009: 27: 1382-1387

Miller, W. R., Larionov, A., Renshaw, L., Anderson, T. J., White, S., Hampton, G., Walker, J. R., Ho, S., Krause, A., Evans, D. B., Dixon, J. M. Aromatase inhibitors--gene discovery. Journal of Steroid Biochemistry and Molecular Biology 2007: 106: 130-142

Moon, Y., Sahah, N. A., Mohapatra, S., Warrington, J. A., Horton, J. D. Identification of a mammalian long chain fatty acyl elongase regulated by sterol regulatory element-binding proteins. Journal of Biological Chemistry 2001: 276: 45358-45366

Morandi, A., Martin, L. A., Gao, Q., Pancholi, S., Mackay, A., Robertson, D., Zvelebil, M., Dowsett, M., Plaza-Menacho, I., Isacke, C. M. GDNF-RET Signaling in ER-Positive Breast Cancers Is a Key Determinant of Response and Resistance to Aromatase Inhibitors. Cancer Research 2013: 73: 3783-3795

Morgillo, D., De Vita, F., Antoniol, G., Orditura, M., Auriemma, P. P., Diadema, M. R., Lieto, E., Savastano, B., Festino, L., Laterza, M. M., Fabozzi, A., Ventriglia, J., Petrillo, A., Ciardiello, F., Barbarisi, A., Iovino, F. Serum insulin-like growth factor 1 correlates with the risk of nodal metastasis in endocrine-positive breast cancer. Current Oncology 2013: 20: 283-288

Moulder, S. L., Yakes, F. M., Muthuswamy, S. K., Bianco, R., Simpson, J. F., Arteaga, C. L. Epidermal growth factor receptor (HER1) tyrosine kinase inhibitor ZD1839 (Iressa) inhibits HER2/neu (erbB2)-overexpressing breast cancer cells in vitro and in vivo. Cancer Research 2001: 61: 8887-8895

Muller, A., Homey, B., Soto, H., Ge, N., Catron, D., Buchanan, M. E., McClanahan, T., Murphy, E., Yuan, W., Wagner, S. N., Barrera, J. L., Mohar, A., Verastegui, E., Zlotnik, A. Involvement of chemokine receptors in breast cancer metastasis. Nature 2001: 410: 50-56

Muraoka-Cook, R. S., Dumont, N., Arteaga, C. L. Dual role of transforming growth factor β in mammary tumorigenesis and metastatic progression. Clinical Cancer Research 2005: 11: 937–943

Muraoka, R. S., Dumont, N., Ritter, C. A., Dugger, T. C., Brantley, D. M., Chen, J., Easterley, E., Roebuck, L. R., Ryan, S., Gotwals, P. J., Koteliansky, V., Arteaga, C. L. Blockade of TGF-β inhibits mammary tumor cell viability, migration, and metastases. Journal of Clinical Investigation 2002: 109: 1551–1559.

Musgrove, E. A., Lee, C. S., Buckley, M. F., Sutherland, R. L. Cyclin D1 induction in breast cancer cells shortens G1 and is sufficient for cells arrested in G1 to complete the cell cycle. Proceedings of the National Academy of Science USA 1994: 91: 8022-8026

Musgrove, E. A., Sutherland, R. L. Biological determinants of endocrine resistance in breast cancer. Nature Reviews Medicine 2009: 9: 631-643

Nagasaki, S., Suzuki, T., Miki, Y., Akahira, J., Shibita, H., Ishida, T., Ohuchi, N., Sasano, H. Chicken ovalbumin upstream promoter transcription factor II in human breast carcinoma: possible regulator of lymphangiogenesis via vascular endothelial growth factor –C expression. Cancer Science 2009: 100: 639-345

Narita, K., Chien, J., Mullany, S. A., Staub, J., Qian, X., Lingle, W. L., Shridhar, V. Loss of HSulf-1 expression enhances autocrine signaling mediated by amphiregulin in breast cancer. Journal of Biological Chemistry 2007: 282: 14413-14420.

Narita, K., Staub, J., Chien, J., Meyer, K., Bauer, M., Friedl, A., Ramakrishnan, S., Shridhar, V. HSulf-1 inhibits angiogenesis and tumorigenesis in vivo. Cancer Research 2006: 66: 6025-6032.

Nash, M. A., Loercher, A. E., Freedman, R. S. In vitro growth inhibition of ovarian cancer cells by decorin: synergism of action between decorin and carboplatin. Cancer Research 1999: 59: 6192-6196

Nassar, A., Radhakrishnan, A., Carreor, I. A., Cotsonis, G. A., Cohen, C. Intratumoral heterogeneity of immunohistochemical marker expression in breast carcinoma: a tissue microarray-based study. Applied Immunohistochemistry 2010: 18: 433-441

Neill, T., Jones, H. R., Crane-Smith, Z., Owens, R. T., Schaefer, L., Iozzo, R. V. Decorin induces rapid secretion of thrombospondin-1 in basal breast carcinoma cells via inhibition of Ras homolog gene family, member A/Rho-associated coiled-coil containing protein kinase 1. FEBS Journal 2013: 280: 2353-2368

Neve, R. M., Chin, K., Fridlyand, J., Yeh, J., baehner, F. L., Fevr, T., Clark, L., Bayani, N., Coppe, J. P., Tong, F., Speed, T., Spellman, P. T., DeVries, S., Lapuk, A., Wang, N. J., Kuo, W. L., Stilwell, J. L., Pinkel, D., Albertson, D. G., Waldman, F. M., McCormick, F., Dickson, R. B., Johnson, M. D., Lippman, M., Ethier, S., gazdar, A., Gray, J. W. A collection of breast cancer cell lines for the study of functionally distinct cancer subtypes. Cancer Cell 2006: 10: 515-527

Nicholson, R. I., Gee, J. M., Manning, D. L., Wakeling, A. E., Montano, M. M. Katzenellenbogen, B. S. Responses to pure antiestrogens (ICI 164384, ICI 182780) in estrogen-sensitive and -resistant experimental and clinical breast cancer. Annals of the New York Academy of Sciences 1995: 761: 148-163

Nicholson, R. I., Gee, J. M., Francis, A. B., Manning, D. L., Wakeling, A. E., Katzenellenbogen, B. S. Observations arising from the use of pure antioestrogens on oestrogen-responsive (MCF-7) and oestrogen growth-independent (K3) human breast cancer cells. Endocrine Related Cancer 1995: 2: 115–121.

Nicholson, R. I., Hutcheson, I. R., Harper, M. E., Knowlden, J. M., Barrow, D., McClelland, R. A., Jones, H. E., Wakeling, A. E., Gee, J. M. Modulation of epidermal growth factor receptor in endocrine-resistant, oestrogen receptor-positive breast cancer. Endocrine Related Cancer 2001: 8: 175–182

Nicholson, R. I., Hutcheson, I. R., Hiscox, S. E., Knowlden, J. M., Giles, M., Barrow, D., Gee, J. M. Growth factor signalling and resistance to selective oestrogen receptor modulators and pure anti-oestrogens: the use of anti-growth factor therapies to treat or delay endocrine resistance in breast cancer. Endocrine Related Cancer 2005: 12: 29-36

Nicholson, R. I., Hutcheson, I. R., Jones, H. E., Hiscox, S. E., Giles, M., Taylor, K. M., Gee, J. M. Growth factor signalling in endocrine and anti-growth factor resistant breast cancer. Reviews in Endocrine and Metabolic Disorders 2007: 8: 241-253.

Nielsen, T, O., Hsu, F, D., Jensen, K., Cheang, M., Karaca, G., Hu, Z., Hernandez-Boussard, T., Livasy, C., Cowan, D., Dressler, L., Akslen, L. A., Ragaz, J., Gown, A. M., Gilks, C. B., van de Rijn, M., Perou, C. M. Immunohistochemical and clinical characterization of the basal-like subtype of invasive breast carcinoma. Clinical Cancer Research 2004:10:5367-5374

Nieman, M. T., Prudoff, R. S., Johnson, K. R., Wheelock, M. J. N-cadherin promotes motility in human breast cancer cells regardless of their E-cadherin expression. Journal of Cell Biology 1999: 147: 631-644

Ning, Y., Riggins, R. B., Mulia, J. E., Chung, H., Zwart, A., Clarke, R. IFNgamma restores breast cancer sensitivity to fulvestrant by regulating STAT1, IFN regulatory factor 1, NF-kappaB, BCL-2 family members, and signalling to caspase-dependent apoptosis. Molecular Cancer Therapeutics 2010: [Epub]

Noetzel, E., Veeck, J., Niederacher, D., Galm, O., Horn, F., Hartmann, A., Knuchel, R., Dahl, E. Promoter methylation-associated loss of ID4 expression is a marker of tumour recurrence in human breast cancer. BMC Cancer 2008: 8: [Epub]

Nomura, A. M. Y., colonel, L. N., Hirohata, T., Lee, J. The association of replacement estrogens with breast cancer. International Journal of Cancer 1986: 37: 49-53

Normanno, N., Di Maio, M., De Maio, E., De Luca, A., de Matteis, A., Giordano, A., Perrone, F; NCI-Naple Breast Cancer Group. Mechanisms of endocrine resistance and novel therapeutic strategies in breast cancer. Endocrine Related Cancer 2005: 12: 721-747

Nozawa, H., Oda, E., Ueda, S., Tamura, G., Maesawa, C., Muto, T., Taniguchi, T., Tanaka, N. Functionally inactivating point mutation in the tumor-suppressor IRF-1 gene identified in human gastric cancer. International Journal of Cancer 1998: 77: 522–527

Ochsner ,S. A., Watkins, C. M., McOwiti, A., Xu, X., Darlington, Y. F., Dehart, M. D., Cooney, A. J., Steffen, D. L., Becnel, L. B., McKenna, N. J. Transcriptomine, a web resource for nuclear receptor signaling transcriptomes. Physiology Genomics 2012: 44: 853-63

Oda, G., Sato, T., Ishikawa, T., Kawachi, H., Nakagawa, T., Kuwayama, T., Ishiguro, M., Iida, S., Uetake, H., Sugihara, K. Significance of stromal decorin expression during the progression of breast cancer. Oncology Reports 2012: 28: 2003-2008

Ogawa, Y., Suzuki, T., Oikawa, A., Hosono, K., Kubo, H., Amano, H., Ito, Y., Kitasato, H., Hayashi, I., Kato, T., Sugimoto, Y., Natumiya, S., Watanabe, M., Majima, M. Bone marrow-derived EP3-expressing stromal cells enhance tumor-associated angiogenesis and tumor growth. Biochemica et Biophysica Research Communications 2009: 382: 720-725

Oh, A. S., Lorant, L. A., Holloway, J. N., Miller, D. L., Kern, F. G., El-Ashry, D. Hyperactivation of MAPK induces loss of ERalpha expression in breast cancer cells. Molecular Endocrinology 2001: 15: 1344-1359

Okoniewski, M. J., Miller, C. J. Hybridization interactions between probesets in short oligo microarrays lead to spurious correlations. BMC Bioinformatics 2006: 7: [Epub]

O'Lone, R., Frith, M. C., Karlsson, E. K., Hansen, U. Genomic targets of nuclear estrogen receptors. Molecular Endocrinology 2004: 18: 1859-1875

Olson Jr, J. A., Budd, G. T., Carey, L. A., Harris, L. A., Esserman, L. J., Fleming, G. F., Marcom, P. K., Leight Jr, G. S., Giuntoli, T., Commean, P., Bae, K., Luo, J., Ellis, M. J. Improved surgical outcomes for breast cancer patients receiving neoadjuvant aromatase inhibitor therapy: results from a multicenter phase II trial. Journal of the American College of Surgeons 2009: 208: 906–914

Opolski, A., Mazurkiewicz, M., Wietrzyk, J., Kleinrok, Z., Radzikowski, C. The role of GABA-ergic system in human mammary gland pathology and in growth of transplantable murine mammary cancer. Journal of Experimental Clinical Cancer Research 2000: 19: 383-390

Osborne, C. K., Bardou, V., Hopp, T. A., Chamness, G. C., Hilsenbeck, S. G., Fuqua, S. A., Wong, J., Allred, D. C., Clark, G. M., Schiff, R. Role of the estrogen receptor coactivator AIB1 (SRC-3) and HER-2/neu in tamoxifen resistance in breast cancer. Journal of the National Cancer Institute 2003: 95: 353-361

Osborne, C. K., Pippen, J., Jones, S. E., Parker, L. M., Ellis, M., Come, S., Gertler, S. Z., May, J. T., Burton, G., Dimery, I., Webster, A., Morris, C., Elledge, R., Buzdar, A. Double-blind, randomized trial comparing the efficacy and tolerability of fulvestrant versus anastrozole in postmenopausal women with advanced breast cancer progressing on prior endocrine therapy: results of a North American trial. Journal of Clinical Oncology 2002: 20: 3386-3395

Osborne, C. K., Neven, P., Dirix, L. Y., Mackey, J. R., Robert, J., Underhill, C., Schiff, R., Gutierrez, C., Migliaccio, I., Anagnostou, V. K., Rimm, D. L., Magill, P., Sellers, M. Gefitinib or placebo in combination with tamoxifen in patients with hormone receptor-positive metastatic breast cancer: a randomized phase II study. Clinical Cancer Research 2011: 17: 1147-1159

Osborne, C. K., Wakeling, A., Nicholson, R. I. Fulvestrant: an oestrogen receptor antagonist with a novel mechanism of action. British Journal of Cancer 2004: 90: S2-S6

Pagani, O., Gelber, S., Simoncini, E., Vastiglione-Gertsch, M., Price, K. N., Gelber, R. D., Holmberg, S. B., Crivellari, D., Collins, J., Lindtner, J., Thurlimann, B., Fey, M. F., Murray, E., Forbes, J. F., Coates, A. S., Goldhirsch, A; International Breast Cancer Study Group. Is adjuvant chemotherapy of benefit for postmenopausal women who receive endocrine treatment for highly endocrine-responsive node-positive breast cancer? International breast cancer study group trials VII and 12-93. Breast Cancer Research and Treatment 2009: 116: 491-500

Paik, S., Shak, S., Tang, G., A., Kim, C., Baker, J., Cronin, M., Baehner, F. L., Walker, M. G., Watson, D., Park, T., Hiller, W., Fisher, E. R., Wickerham, D. L., Bryant, J., Wolmark, N. A multigene assay to predict recurrence of tamoxifen-treated, node-negative breast cancer. New England Journal of Medicine 2004: 351: 2817-2826

Pandev, V., Qian, P. X., Kang, J., Perry, J. K., Mitchell, M. D., Yin, Z., Wu, Z. S., Liu, D. X., Zhu, T., Lobie, P. E. Artemin stimulates oncogenicity and invasiveness of human endometrial carcinoma cells. Endocrinology 2010: 151: 909-920

Penney, R. B., Roy, D. Thioredoxin-mediated redox regulation of resistance to endocrine therapy in breast cancer. Biochimica et Biophysica Acta 2013: 1836: 60-79

Perets, R., Kaplan, T., Stein, I., Hidas, G., Tayeb, S., Avraham, E., Ben-Neriah, Y., Simon, I., Pikarsky, E. Genome-Wide Analysis of Androgen Receptor Targets Reveals COUP-TF1 as a Novel Player in Human Prostate Cancer. PLoS One. 2012: 7: [Epub]

Perey, L., Paridaens, R., Nole´, F., Bonnefoi, H., Aebi, S., Goldhirsch, A., Dietrich, D., Thurlimann, B., for the Swiss Group for Clinical Cancer Research (SAKK): Fulvestrant (Faslodex_) as hormonal treatment in postmenopausal patients with advanced breast cancer (ABC) progressing after treatment with tamoxifen and aromatase inhibitors: update of a phase II SAKK trial. Breast Cancer Research and Treatment 2004: 88(Suppl 1): S236, (abstract 6048)

Perez-Tenorio, G., Berglund, F., Esguerra Merca, A., Nordenskjold, B., Rutqvist, L. E., Skoog, L. Cytoplasmic p21WAFl/CIPl correlates with Akt activation and poor response to tamoxifen in breast cancer. International Journal of Cancer 2006: 28: 1031-1042

Perillo, B., Sasso, A., Abbondanza, C., Palumbo, G. 17β-Estradiol Inhibits Apoptosis in MCF-7 Cells, Inducing *bcl-2* Expression via Two Estrogen-Responsive Elements Present in the Coding Sequence. Molecular and Cell Biology 2000: 20: 2890-2901

Perou, C. M., Sørlie, T., Eisen, M. B., van de Rijn, M., Jeffrey, S. S., Rees, C. A., Pollack, J. R., Ross, D. T., Johnsen, H., Akslen, L. A., Fluge, O., Pergamenschikov, A., Williams, C., Zhu, S. X., Lønning, P. E., Børresen-Dale, A. L., Brown, P. O., Botstein, D. Molecular Portraits of human breast tumours. Nature 2000, 406; 747-752

Piccart-Gebhart, M. J., Procter, M., Leyland-Jones, B., Goldhirsch, A., Untch, M., Smith, I., Gianni, L., Baselga, J., Bell, R., Jackisch, C., Cameron, D., Dowsett, M., Barrios, C. H., Steger, G., Huang, C. S., Andersson, M., Inbar, M., Lichinitser, M., Láng, I., Nitz, U., Iwata, H., Thomssen, C., Lohrisch, C., Suter, T. M., Rüschoff, J., Suto, T., Greatorex, V., Ward, C., Straehle, C., McFadden, E., Dolci, M. S., Gelber, R. D; Herceptin Adjuvant (HERA) Trial Study Team. Trastuzumab after adjuvant chemotherapy in HER2-positive breast cancer. New England Journal of Medicine 2005: 353: 1659-1672

Pietras, R. J., Arboleda, J., Reese, D. M., Wongvipat, N., Pegram, M. D., Ramos, L., Gorman, C. M., Parker, M. G., Sliwkowski, M. X., Slamon, D. J. HER-2 tyrosine kinase pathway targets estrogen receptor and promotes hormone-independent growth in human breast cancer cells. Oncogene 1995: 10: 2435-2446

Pittoni, P., Piconese, S., Tripodo, C., Colombo, M, P. Tumor-intrinsic and -extrinsic roles of c-Kit: mast cells as the primary off-target of tyrosine kinase inhibitors. Oncogene 2011: 30: 757–769

Plaza-Menacho, I., Morandi, A., Robertson, D., Pancholi, S., Drury, S., Dowsett, M., Martin, L-A., Isacke, C. M. Targeting the receptor tyrosine kinase RET sensitizes breast cancer cells to tamoxifen treatment and reveals a role for RET in endocrine resistance. Oncogene 2010: 29: 4648-4657

Pobbati, A. V., Hong, W. Emerging roles of TEAD transcription factors and its coactivators in cancers. Cancer Biology and Therapeutics 2013: 14: 390-398

Poliseno, L., Salmena, L., Zhang, J., Carver, B., Haveman, W. J., Pandolfi, P. P. A coding-independent function of gene and pseudogene mRNAs regulates tumour biology. Nature 2010: 465: 1033-1038

Press, M. F., Bernstein, L., Thomas, P. A., Meisner, L. F., Zhou, J. Y., Ma, Y., Hung, G., Robinson, R. A., Harris, C., El-Naggar, A., Slamon, D. J., Phillips, R, N., Ross, J. S., Wolman, S. R., Flom, K. J. HER-2/neu gene amplification characterized by fluorescence in situ hybridization: poor prognosis in node-negative breast carcinomas. Journal of Clinical Oncology 1997: 15: 2894-2904.

Rae, J. M., Johnson, M. D., Scheys, J. O., Cordero, K. E., Larios, J. M., Lippman, M. E. GREB 1 is a critical regulator of hormone dependent breast cancer growth. Breast Cancer Research and Treatment 2005: 92: 141-149.

Rasmussen, B. B., Andersson, M., Christensen, I. J., Møller, S. Evaluation of and quality assurance in HER2 analysis in breast carcinomas from patients registered in Danish Breast Cancer Group (DBCG) in the period of 2002-2006. A nationwide study including correlation between HER-2 status and other prognostic variables. Acta Oncology 2008: 47: 784-788

Rao, R. D., Cobleigh, M. A. Adjuvant endocrine therapy for breast cancer. Oncology (Williston Park) 2012: 26: 541-547

Ray, P., Ghosh, S.K., Zhang, D.H., Ray, A. Repression of interleukin-6 gene expression by 17 beta-estradiol: inhibition of the DNA-binding activity of the transcription factors NF-IL6 and NF-kappa B by the estrogen receptor. FEBS Letters 1997, 409; 79–85.

Reed, C. C., Waterhouse, A., Kirby, S., Kay, P., Owens, R. T., McQuillan, D. J., Iozzo, R. V. Decorin prevents metastatic spreading of breast cancer. Oncogene 2005: 24: 1104-1110

Reis-Filho, J. S., Weigelt, B., Fumagalli, D., Sotiriou, C. Molecular profiling: moving away from tumor philately. Science Translational Medicine 2010: 2: 47

Regan, J. L., Kendrick, H., Magnay, F. A., Vafaizadeh, V., Groner, B., Smalley, M. J. c-Kit is required for growth and survival of the cells of origin of Brca1-mutation-associated breast cancer. Oncogene 2012: 31: 869-883

Ren, Y., Cheung, H. W., von Maltzhan, G., Agrawal, A., Cowley, G. S., Weir, B. A., Boehm, J. S., Tamayo, P., Karst, A. M., Liu, J. F., Hirsch, M. S., Mesiroy, J. P., Drapkin, R., Root, D. E., Lo, J., Fogal, V., Ruoslahti, E., Hahn, W. C., Bhatia, S. N. Targeted tumor-penetrating siRNA nanocomplexes for credentialing the ovarian cancer oncogene ID4. Science Translational Medicine 2012: 4: [Epub]

Rezaei, M., Friedrich, K., Wielockxz, B., Kuzmanov, A., Kettelhake, A., Labelle, M., Schnittler, H., Baretton, G., Breier, G. Interplay between neural-cadherin and vascular endothelial-cadherin in breast cancer progression. Breast Cancer Research 2012: 14: [Epub]

Riggins, R. B., Zwart, A., Nehra, R., Clarke, R. The nuclear factor kappa B inhibitor parthenolide restores ICI 182,780 (Faslodex; fulvestrant)-induced apoptosis in antiestrogen-resistant breast cancer cells. Molecular Cancer Therapeutics 2005: 4: 33-41

Riggs, K. A, Wickramasinghe, N. S., Cochrum, R. K., Watts, M. B., Klinge, C. M. Decreased chicken ovalbumin upstream promoter transcription factor II expression in tamoxifen-resistant breast cancer cells. Cancer Research 2006: 66: 10188-10198

Rinderknecht, M., Detmar, M. Molecular mechanisms of lymph node metastasisi. In: Stacker SA, Achen MG (eds). Lymphangiogenesis in Cancer Metastasis. Springer Science+Business Media BV, 2009.

Rhodes, L. V., Short, S. P., Neel, N. F., Salvo, V. A., Zhu, Y., Elliott, S., Wei, Y., Yu, D., Sun, M., Muir, S. E., Fonseca, J. P., Bratton, M. R., Segar, C., Tilghman, S. L., Sobolik-Delmaire, T., Horton, L. W., Zaja-Milatovic, S., Collins-Burow, B. M., Wadsworth, S., Beckman, B. S., Wood, C. E., Fuqua, S. A., Nephew, K. P., Dent, P., Worthylake, R. A., Curiel, T. J., Hung, M., Richmond, A., Burow, M. E. Cytokine receptor CXCR4 mediates estrogen-independent tumorigenesis, metastasis and resistance to endocrine therapy in human breast cancer. Cancer Research 2011, 71; 603-610

Robertson, J. F. Faslodex (ICI 182, 780), a novel estrogen receptor downregulator--future possibilities in breast cancer. Journal of Steroid Biochemistry and Molecular Biology 2001: 79: 209-212

Robertson, J. F., Llombart-Cussac, A., Rolski, J., Feltl, D., Dewar, J., Macpherson, E., Lindemann, J., Ellis, M. J. Activity of fulvestrant 500 mg versus anastrozole 1 mg as first-line treatment for advanced breast cancer: results from the FIRST study. Journal of Clinical Oncology 2009: 27: 4530-4535

Robertson, J. F., Nicholson, R. I., Bundred, N. J., Anderson, E., Ravter, Z., Dowsett, M., Fox, J. N., Gee, J. M., Wakeling, A. E., Morris, C., Dixon, M. Comparison of the short-term biological effects of 7alpha-[9-(4,4,5,5,5-pentafluoropentylsulfinyl)-nonyl]estra-1,3,5,(10)-triene-3,17beta-diol (Faslodex) versus tamoxifen in postmenopausal women with primary breast cancer. Cancer Research 2001: 61: 6739-6746

Robertson, J. F., Osborne, C. K., Howell, A., Jones, S. E., Mauriac, L., Ellis, M., Kleeberg, U. R., Come, S. E., Vergote, I., Gertler, S., Buzdar, A., Webster, A., Morris, C. Fulvestrant versus anastrozole for the treatment of advanced breast carcinoma in postmenopausal women: a prospective combined analysis of two multicenter trials. Cancer 2003: 98: 229-238

Robertson, J. F., Steger, G. G., Neven, P., Barni, S., Gieseking, F., Nolè, F., Pritchard, K. I., O'Malley, F. P., Simon, S. D., Kaufman, B., Petruzelka, L. Activity of fulvestrant in HER2-overexpressing advanced breast cancer. Annals of Oncology 2010: 21: 1246-1253

Rönnstrand, L. Signal transduction via the stem cell factor receptor/c-Kit. Cell and Molecular Life Sciences 2004: 61: 2535-2548.

Rosen, S. D., Lemjabbar-Alaoui, H. Sulf-2: an extracellular modulator of cell signaling and a cancer target candidate. Expert Opinions on Therapeutic Targets 2010: 14: 935–949.

Ross-Innes, C. S., Stark, R., Teschendorff, A. E., Holmes, K. A., Ali, H. R., Dunning, M. J., Brown, G. D., Gojis, O., Ellis, I. O., Green, A. R., Ali, S., Chin, S. F., Palmieri, C., Caldas, C., Carroll, J. S. Differential oestrogen receptor binding is associated with clinical outcome in breast cancer. Nature 2012: 481: 389-393

Rozen, S., Skaletsky, H. J. Primer3 on the WWW for General Users and for Biologist Programmers. In: Misener, S. & S.A. Krawetz (Eds.). Bioinformatics Methods and Protocols: Methods in Molecular Biology. Humana Press Inc., Totowa (NJ) 2000: pp 365-386.

Russell, K. S., Hung, M. C. Transcriptional repression of the neu protooncogene by estrogen stimulated estrogen receptor. Cancer Research 1992: 52: 6624–6629.

Sabnis, G., Schayowitz, A., Goloubeva, O., Macedo, L., Brodie, A. Trastuzumab reverses letrozole resistance and amplifies the sensitivity of breast cancer cells to estrogen. Cancer Research 2009: 69: 1416-1428

Salvatori, L., Caporuscio, F., Coroniti, G., Starace, G., Frati, L., Russo, M. A., Petrangeli, E. Down-regulation of epidermal growth factor receptor induced by estrogens and phytoestrogens promotes the differentiation of U2OS human osteosarcoma cells. Journal of Cell Physiology 2009: 220: 35-44

Sanceau, J., Hiscott, J., Delattre, O., Wietzerbin, J. IFN-beta induces serine phosphorylation of Stat-1 in Ewing's sarcoma cells and mediates apoptosis via induction of IRF-1 and activation of caspase-7. Oncogene 2000 19: 3372–3383.

Santra, M., Eichstetter, I., Iozzo, R. V. An anti-oncogenic role for decorin: down-regulation of ErbB2 leads to growth suppression and cytodifferentiation of mammary carcinoma. Journal of Biological Chemistry 2000, 275; 35153-35161

Santra, M., Skorski, T., Calabretta, B., Lattime, E. C., Iozzo, R. V. De novo decorin gene expression suppresses the malignant phenotype in human colon cancer cells. Proceedings of the National Academy of Science USA 1995: 92: 7016-7020

Sauve, K., Lepage, J., Sanchez, M., Heveker, N., Tremblay, A. Positive feedback activation of estrogen receptors by the CXCL12-CXCR4 pathway. Cancer Research 2009, 69; 5793-5800

Schafer, G., Wissmann, C., Hertel, J., Lunyak, V., Hocker, M. Regulation of vascular endothelial growth factor D by orphan receptors hepatocyte nuclear factor- 4 alpha and chicken ovalbumin upstream promoter transcription factor s 1 and 2. Cancer Research 2008: 68: 457-466

Schiff, R., Massarweh, S., Shou, J., Osborne, C. K. Breast cancer endocrine resistance: how growth factor signalling and estrogen receptor coregulators modeulate response. Clinical Cancer Research 2003, 9; 447-454

Schiff, R., Osborne, C. K. Endocrinology and hormone therapy in breast cancer: new insight into estrogen receptor-alpha function and its implication for endocrine therapy resistance in breast cancer. Breast Cancer Research 2005: 7: 205-211

Schiff, R., Reddy, P., Ahotupa, M., Coronado-Heinsohn, E., Grim, M., Hilsenbeck, S. G., Lawrence, R., Deneke, S., Herrera, R., Chamness, G. C., Fuqua, S. A., Brown, P. H., Osborne, C. K. Oxidative stress and AP-1 activity in tamoxifen-resistant breast tumors in vivo. Journal of the National Cancer Institute 2000: 92: 1926-1934

Schmalhofer, O., Brabletz, S., Brabletz, T. E-cadherin, beta-catenin, and ZEB1 in malignant progression of cancer. Cancer Metastasis Reviews 2009: 28: 151-166

Scotton, C. J., Wilson, J. L., Scott, K., Stamp, G., Wilbanks, G. D., Fricker, S., Bridger, G., Balkwill, F. R. Multiple actions of the chemokine CXCL12 on epithelial tumor cells in human ovarian cancer. Cancer Research 2002: 62: 5930-5938

Selander, K. S., Li, L., Watson, L., Merrell, M., Dahmen, H., Heinrich, P. C., Muller-Newen, G., Harris, K. W. Inhibition of gp130 signaling in breast cancer blocks constitutive activation of Stat3 and inhibits in vivo malignancy. Cancer Research 2001: 64: 6924-6933

Shaikh, D., Zhou, Q., Chen, T., Ibe, J. C., Raj, J. U., Zhou, G. cAMP-dependent protein kinase is essential for hypoxia-mediated epithelial-mesenchymal transition, migration, and invasion in lung cancer cells. Cell Signalling 2012: 12: 2396-2406

Sharma, P., Chinaranagari, S., Patel, D., Carey, J., Chaudhary, J. Epigenetic inactivation of inhibitor of differentiation 4 (Id4) correlates with prostate cancer. Cancer Medicine 2012: 1: 176-186

Shaulian, E., Karin, M. AP-1 as a regulator of cell life and death. Nature Cell Biology 2002: 4: 131-136

Shaw, V. E., Gee, J. M.W.,.McClelland. R. A.,.Morgan, H., Rushmere, N., Nicholson, R. I. Identification of anti-hormone induced genes as potential therapeutic targets in breast cancer. Proceedings of the American Association for Cancer Research 2005: 46: (Abstract 3706).

She, Q-B., Chandarlapaty, S., Ye, Q., Lobo, J., Haskell, K. M., Leander, K. R., DeFeo-Jones, D., Huber, H. E., Rosen, N. Breast cancer cells with PI3K mutation or HER2 amplification are selectively addicted to Akt signalling. PLos ONE 2008: 3: [Epub]

Sheth, S. S., Bodnar, J. S., Ghazalpour, A., Thipphavong, C. K., Tsutsumi, S., tward, A. D., Demant, P., Kodama, T., Aburatani, H., Lusis, A. J. Hepatocellular carcinoma in Txnip-deficient mice. Oncogene. 2006: 25: 3528–353

Shimamura, S., Sasaki, K., Tanaka, M. The Src substrate SKAP2 regulates actin assembly by interacting with WAVE2 and cortactin proteins. Journal of Biological Chemistry 2013: 288: 1171-1183

Shim, W. S., Conaway, M., Masamura, S., Yue, W., Wang, J. P., Kmar, R., Santen. R. J. Estradiol hypersensitivity and mitogen-activated protein kinase expression in long-term estrogen deprived human breast cancer cells in vivo. Endocrinology 2000: 141: 396–405.

Shou, J., Massarweh, S., Osborne, C. K., Wakeling, A. E., Ali, S., Weiss, H., Schiff, R. Mechanisms of tamoxifen resistance: increased estrogen receptor-HER2/neu cross-talk in ER/HER2-positive breast cancer. Journal of the National Cancer Institute 2004: 96: 926-935

Simoncini, T., Maffei, S., Basta, G., Barsacchi, G., Genazzani, A.R., Liao, J.K., De Caterina, R. Estrogens and glucocorticoids inhibit endothelial vascular cell adhesion molecule-1 expression by different transcriptional mechanisms. *Circulation Research* 2000, 87; 19–25.

Siskind, V., Schofield, F., Rice, D., Bain, C. Breast cancer and breast feeding: results from an Australian case-control study. American Journal of Epidemiology 1989: 130: 229-236

Slamon, D. J., Clark, G. M., Wong, S. G., Levin, W. J., Ullrich, A., McGuire, W. L. Human breast cancer: correlation of relapse and survival with amplification of the HER-2/neu oncogene. Science 1987: 235: 177-182

Skobe, M., hawighorst, T., Jackson, D. G., Prevo, R., Janes, L., Velasco, P., Riccardi, L., Alitalo, K., Claffey, K., Detmar, M. Induction of tumor lymphangiogenesis by VEGF-C promotes breast cancer metastasis. Nature Medicine 2001: 7: 192-198

Smith, C. L., Nawaz, Z., O'Malley, B. W. Coactivator and corepressor regulation of the agonist/antagonist activity of the mixed antiestrogen, 4-hydroxytamoxifen. Molecular Endocrinology 1997, 11; 657-666

Smith, M. C., Luker, K. E., Garbow, J. R., Prior, J. L., Jackson, E., Piwnica-Worms, D., Luker, G. D. CXCR4 regulates growth of both primary and metastatic breast cancer. Cancer Research 2004: 64: 8604-8612

Smith, I. E., Walsh, G., Skene, A., Llombart, A., Mayordomo, J. I., Detre, S., Salter, J., Clark, E., Magill, P., Dowsett, M. A phase II placebo-controlled trial of neoadjuvant anastrozole alone or with gefitinib in early breast cancer. Journal of Clinical Oncology 2007: 25: 3816-3822

Spector, N. L., Blackwell, K. L. Review Understanding the mechanisms behind trastuzumab therapy for human epidermal growth factor receptor 2-positive breast cancer. Journal of Clinical Oncology 2009: 27: 5838-5847

Sonne-Hansen, K., Norrie, I. C., Emdal, K. B., Benjaminsen, R. V., Frogne, T., Christiansen, I. J., Kirkegaard, T., Lykkesfeldt, A. E. Breast cancer cells can switch between estrogen receptor alpha and ErbB signaling and combined treatment against both signaling pathways postpones development of resistance. Breast Cancer Research and Treatment 2010: 121: 601-613.

Soria-Valles, C., Gutiérrez-Fernández, A., Guiu, M., Mari, B., Fueyo, A., Gomis, R. R., López-Otín, C. The anti-metastatic activity of collagenase-2 in breast cancer cells is mediated by a signaling pathway involving decorin and miR-21. Oncogene 2013: [Epub ahead of print]

Sorlie, T., Perou, C., Tibshirani, R., Aas, T., Geisler, S., Johnsen, H., Hastie, T., Eisen, M., van de Rijn, M., Jeffrey, S., Thorsen, T., Quist, H., Matese, J., Brown, P., Botstein, D., Lønning, P. E., Børresen-Dale, A. Gene expression patterns of breast carcinomas distinguish tumor subclasses with clinical implications. Proceedings of the National Academy of the USA 2001: 98: 10869-10874

Sotiriou, C., Pusztai, L. Gene-expression signatures in breast cancer. New England Journal of Medicine 2009: 360: 790-800

Stander, M., Naumann, U., Dumitrescu, L., Heneka, M., Loschmann, P., Gulbins, E., Dichgans, J., Weller, M. Decorin gene transfer-mediated suppression of TGF-beta synthesis abrogates experimental malignant glioma growth in vivo. Gene Therapy 1998: 5: 1187-1194

Stanulla, M., Welte, K., Hadam, M. R., Pietsch, T. Coexpression of stem cell factor and its receptor c-Kit in human malignant glioma cell lines. Acta Neuropathologica 1995: 89:158–165

Staub, J., Chien, J., Pan, Y., Qian, X., Narita, K., Aletti, G., Scheerer, M., Roberts, L. R., Molina, J., Shridhar, V. Epigenetic silencing of HSulf-1 in ovarian cancer: implications in chemoresistance. Oncogene. 2007: 26: 4969–4978.

Stine, Z. E., McGaughev, D. M., Bessling, S. L., Li, S., McCallion, A. S. Steroid hormone modulation of RET through two estrogen responsive enhancers in breast cancer. Human Molecular Genetics 2011: 20: 3746-3756

Stoica, G. E., Franke, T. F., Wellstein, A., Morgan, E., Czubayko, F., List, H. J., Reiter, R., Martin, M. B., Stoica, A. Heregulin-β1 regulates the estrogen receptor-alpha gene expression and activity via the ErbB2/PI 3-K/Akt pathway. Oncogene 2003**:** 10: 2073-2087

Suk, K., Chang, I., Kim, Y. H., Kim, S., Kim, J. Y., Kim, H., Lee, M. S. Interferon gamma (IFNgamma) and tumor necrosis factor alpha synergism in ME-180 cervical cancer cell apoptosis and necrosis. IFNgamma inhibits cytoprotective NF-kappa B through STAT1/IRF-1 pathways. Journal of Biological Chemistry *2001:* 276: 13153–13159.

Sun, Y. X., Wang, J., Shelburne, C. E., Lopatin, D, E., Chinnaivan, A. M., Rubin, M. A., Pienta, K. J., Taichman, R. S. Expression of CXCR4 and CXCL12 (SDF-1) in human prostate cancers (PCa) in vivo. Journal of Cellular Biochemistry 2003: 89: 462–473

Suyama, *K.*, Shapiro, I., Guttman, M., Hazan, R. B. A signaling pathway leading to metastasis is controlled by N-cadherin and the FGF receptor. Cancer Cell 2002*: 2:* 301–314*.*

Taga, T., Kishimoto, T. Gp130 and the interleukin-6 family of cytokines. Annual Reviews of Immunology 1997: 15: 797-819.

Takahashi, M. The GDNF/RET signaling pathway and human diseases. Cytokine and Growth Factor Reviews 2001: 12: 361-373

Tamura, T., Ishihara, M., Lamphier, M. S., Tanaka, N., Oishi, I., Alzawa, S., Matsuyama, T., Mak, T. W., Taki, S.,Taniguchi, T. An IRF-1-dependent pathway of DNA damage-induced apoptosis in mitogen-activated T lymphocytes. Nature 1995 376*:* 596–599.

Tanaka, N., Ishihara, M., Kitagawa, M., Harada, H., Kimura, T., Matsuyama, T., Lamphier, M. S., Aizawa, S., Mak, T. W., Taniguchi,T. Cellular commitment to oncogene-induced transformation or apoptosis is dependent on the transcription factor IRF-1. Cell 1994: 77: 829–839.

Tang, J. Z., Kong, X. J., Kang, J., Fielder, G. C., Steiner, M., Perry, J. K., Wu, Z. S., Yin, Z., Zhu, T., Liu, D. X., Lobie, P. E. Artemin-stimulated progression of human non-small cell lung carcinoma is mediated by BCL2. Molecular Cancer Therapeutics 2010: 9: 1697-1708

Teicher, B. A., Fricker, S. P. CXCL12 (SDF-1)/CXCR4 Pathway in Cancer. Clinical Cancer Research 2010: 16: 2927-2931

Teixeira, C., Reed, J. C., Pratt, M. A. Estrogen promotes chemotherapeutic drug resistance by a mechanism involving Bcl-2 proto-oncogene expression in human breast cancer cells. Cancer Research 1995: 55: 3902-3907

Teyssier, C., Belguise, K., Galtier, F., Chalbos, D. Characterization of the physical interaction between estrogen receptor alpha and JUN proteins. Journal of Biological Chemistry 2001, 276; 36361–36369

Teutschbein, J., Haydn, J. M., Samans, B., Krause, M., Eilers, M., Schartl, M., Meierjohann, S. Gene expression analysis after receptor tyrosine kinase activation reveals new potential melanoma proteins. BMC Cancer 2010: 10: [Epub]

Thiery, J. P., Sleeman, J. P. Complex networks orchestrate epithelial-mesenchymal transitions. Nature Reviews Molecular Cell Biology 2006: 7: 131–142.

Thornberry, N., Bull, H., Calaycay, J., Chapman, K., Howard, A., Kostura, M., Miller, D., Molineaux, S., Weidner, J., Aunins, J., Elliston, K., Ayala, J., Casano, F., Chin, J., Ding, G., Egger, L., Gaffney, E., Limjuco, G., Palyha, O., Raju, S., Rolando, A., Salley, J., Yamin, T., Lee, T., Shively, J., MacCross, M., Mumford, R., Schmidt, J., Tocci, M. A novel heterodimeric cysteine protease is required for interleukin-1 β processing in monocytes. Nature 1992: 356: 768-774

Tian, M., Schiemann, W. P. The TGF-beta paradox in human cancer: an update. Future Oncology 2009: 5:259-271

Thrane, S., Lykkesfeldt, A. E., Larson, M. S., Sorenson, M. S., Yde, C. W. Estrogen receptor α is the major driving factor for growth in tamoxifen-resistant breast cancer and supported by HER/ERK signaling. Breast Cancer Research and Treatment 2013: 139: 71-80

Tobler, N. E., Detmar, M. Tumor and lymph node lymphangiogenesis—impact on cancer metastasis. Journal of Leukocyte Biology 2006: 80:691-696

Tralhao, J. G., Schaefer, L., Micegiva, M., Evaristo, C., Schonherr, E., Kaval, S., Veiga-Fernandes, H., Danel, C., Iozzo, R. V., Kresse, H., Lemarchand, P. In vivo selective and distant killing of cancer cells using adenovirus-mediated decorin gene transfer. FASEB Journal 2003: 17: 464-466

Troiani, T., Vecchione, L., Martinelli, E., Capasso, A., Constantion, A., Ciuffreda, L. P., Morgillo, F., Vitagliano, D., D'Aiuto, E., De Palma, R., Tejpar, S., Van Cutsem, E., De Lorenzi, M., Caraglia, M., Berriono, L., Ciardiello, F. Intrinsic resistance to selumetinib, a selective inhibitor of MEK1/2, by cAMP-dependent protein kinase A activation in human lung and colorectal cancer cells. British Journal of Cancer 2012: 106: 1648-1659

Troup, S., Njue, C., Kliewer, E. V., Parisien, M., Roskelley, C., Chakravarti, S., Roughley, P. J., Murphy, L. C., Watson, P. H. Reduced expression of the small leucine-rich proteoglycans, lumican, and decorin is associated with poor outcome in node-negative invasive breast cancer. Clinical Cancer Research 2003: 9: 207-214

Tsai, M-J., O'Malley, B. W. Molecular mechanisms of action of steroid/thyroid receptor superfamily members. Annula Reviews of Biochemistry 1994: 63: 451-486

Tzukerman, M. T., Esty, A., Santisomere, D., Danielian, P., Parker, M. G., Stein, R. B., Pike, J. W., McDonnell, D. P. Human estrogen receptor transactivational capacity is determined by both cellular and promoter context and mediated by two functionally distinct intramolecular regions. Molecular Endocrinology 1994, 8; 21-30

Vandyke, K., Chow, A. W., Williams, S. A., To, L. B., Zannettino, A. C. Circulating N-cadherin levels are a negative prognostic indicator in patients with multiple myeloma. British Journal of Haematology 2013: 8: [Epub ahead of print]

Veit, C., Genze, F., Menke, A., Hoeffert, S., Gress, T. M., Gierschik, P., Giehl, K. Activation of phosphatidylinositol 3-kinase and extracellular signalregulated kinase is required for glial cell line-derived neurotrophic factor-induced migration and invasion of pancreatic carcinoma cells. Cancer Research 2004: 64: 5291–5300

Vergote, I., Robertson, J. F., Kleeberg, U., Burton, G., Osborne, C. K., Mauriac, L.; Trial 0020 Investigators; Trial 0021 Investigators. Postmenopausal women who progress on fulvestrant ('Faslodex') remain sensitive to further endocrine therapy. Breast Cancer Research and Treatment 2003: 79: 207-211

Vilar, J. M. G., Jansen, R., Sander, C. Signal Processing in the TGF-β Superfamily Ligand-Receptor Network. PLoS Computational Biology 2006: 2: [Epub]

Vleugel, M. M., greijer, A. E., Bos, R., van der Wall, E., van Diest, P. J. c-Jun activation is associated with proliferation and angiogenesis in invasive breast cancer. Human Pathology 2006: 37: 668-674

Vogel. C. L., Cobleigh, M. A., Tripathy, D., Gutheil, J. C., Harris, L. N., Fehrenbacher, L., Slamon, D. J., Murphy, M., Novotny, W. F., Burchmore, M., Shak, S., Stewart, S. J., Press, M. Efficacy and safety of trastuzumab as a single agent in first-line treatment of HER2-overexpressing metastatic breast cancer. Journal of Clinical Oncology 2002: 20: 719-726

Volinia, S., Calin, G. A., Liu, C. G., Ambs, S., Cimmino, A., Petrocca, F., Visone. R., Iorio, M., Roldo, C., Ferracin, M., Prueitt, R. L., Yanaihara, N., Lanza, G., Scarpa, A., Vecchione, A., Negrini, M., Harris, C. C., Croce, C. M. A microRNA expression signature of human solid tumours defines cancer gene targets. Proceeding of the National Academy of Sciences USA 2006: 103: 2257-2261

Waetzig, G. H., Rose-John, S. Hitting a complex target: an update on interleukin-6 trans-signalling. Expert Opinions on Therapeutic Targets 2012: 16: 225-236

Waha, A., Felsberg, J., Hartmann, W., dem Knesebeck, A., von Mikeska, T., Joos, S., Wolter, M., Koch, A., Yan, P. S., Endl, E., Wiestler, O. D., Reifenberger, G., Pietsch, T., Waha, A. Epigenetic downregulation of mitogen-activated protein kinase phosphatase MKP-2 relieves its growth suppressive activity in glioma cells. Cancer Research 2010: 70: 1689–1699.

Wakeling, A. E., Bowler, J. ICI 182,780, a new antioestrogen with clinical potential. Journal of Steroid Biochemistry and Molecular Biology 1992: 43: 173-177

Wakeling, A. E. Similarities and distinctions in the mode of action of different classes of antioestrogens. Endocrine Related Cancer 2000: 7: 17-28

Walker, R. A., Dearing, S. J. Transforming growth factor β_1 in ductal carcinoma in situ and invasive carcinomas of the breast. European Journal of Cancer 1992: 28: 641–644.

Walker, R. A., Dearing, S. J., Gallacher, B. Relationship of transforming growth factor β_1 to extracellular matrix and stromal infiltrates in invasive breast carcinoma. British Journal of Cancer 1994: 69*: 1160–*1165*

Wang, X., Chen, X., Fang, J., Yang, C. Overexpression of both VEGF-A and VEGF-C in gastric cancer correlates with prognosis, and silencing of both is effective to inhibit cancer growth. International Journal of Clinical and Experimental Pathology 2013: 6: 586-597

Wardley, A. M., Howell, A. Does HER2 overexpression affect response to endocrine therapy in advanced cancer? Nature Clinical and Practical Oncology 2006: 3: 78-79

Webb, P., Nguyen, P., Kushner, P.J. Differential SERM effects on corepressor binding dictate ERalpha activity in vivo. Journal of Biological Chemistry 2003, 278; 6912–6920.

Wei, M., Xu, J., Dignam, J., Nanda, R., Sveen, L., Fackenthal, J., Grushko, T. A., Olopade, O. I. Estrogen receptor alpha, BRCA1, and FANCF promoter methylation occur in distinct subsets of sporadic breast cancers. Breast Cancer Research and Treatment 2008: 111: 113-120

Weigel, M. T., Ghazoui, Z., Dunbier, A., Pancholi, S., Dowsett, M., Martin, L. A. Preclinical and clinical studies of estrogen deprivation support the PDGF/Abl pathway as a novel therapeutic target for overcoming endocrine resistance in breast cancer. Breast Cancer Research 2012: 14: [Epub]

Weigelt, B., Baehner, F. L., Reis-Filho, J., S. The contribution of gene expression profiling to breast cancer classification, prognostication and prediction: a retrospective of the last decade. Journal of Pathology 2010: 220: 263-280

Weigelt, B., Reis-Filho, J. S. Molecular profiling currently offers no more than tumour morphology and basic immunohistochemistry. Breast Cancer Research and Treatment 2010: 12: Supplement 4: S5

Wen, Y. H., Ho, A., Patil, S., Akram, M., Catalano, J., Eaton, A., Norton, L., Benezra, R., Brogi, E. Id4 protein is highly expressed in triple-negative breast carcinomas: possible implications for BRCA1 downregulation. Breast Cancer Research and Treatment 2012: 135: 93-102

Wheeler, D.L., Iida, M., Dunn, E. F. The role of Src in solid tumors. Oncologist 2009a: 14: 667-678

Wheeler, D. L., Iida, M., Kruser, T. J., Nechreback, M. M., Dunn, E. F., Armstrong, E. A., Huang, S., Harari, P. M. Epidermal growth factor receptor cooperates with Src family kinases in acquired resistance to cetuximab. Cancer Biology and Therapy 2009b: 8: 696-703

Willman, C. L., Sever, C. E., Pallavicini, M. G., Harada, H., Tanaka, N., Slovak, M. L., Yamamoto, H., Harada, K., Meeker, T. C., List, A. F., Taniguchi, T. Deletion of IRF-1, mapping to chromosome 5q31.1, in human leukemia and preleukemic myelodysplasia. Science 1993*: 259: 965–971.*

Wilson, J. W., Wakeling, A. E., Morris, I. D., Hickman, J. A., Dive, C. MCF-7 human mammary adenocarcinoma cell death in vitro in response to hormone-withdrawal and DNA damage. International Journal of Cancer 1995: 61: 502-508

Wissmann, C., Detmar, M. Review Pathways targeting tumor lymphangiogenesis. Clinical Cancer Research 2006: 12: 6865-6868

Witz, I. P. Tumor-microenvironment interactions: the selectin-selectin ligand axis in tumor-endothelium cross talk. Cancer Treatment and Research 2006: 130: 125-140

Wolff, A. C., Hammond, M. E., Schwartz, J. N., Hagerty, K. L., Allred, D. C., Cote, R. J., Dowsett, M., Fitzgibbons, P. L., Hanna, W. M., Langer, A., McShane, L. M., Paik, S., Pegram, M. D., Perez, E. A., Press, M. F., Rhodes, A., Sturgeon, C., Taube, S. E., Tubbs, R., Vance, G. H., van de Vijver, M.,

Wheeler, T. M., Hayes, D. F.; American Society of Clinical Oncology; College of American Pathologists. American Society of Clinical Oncology/College of American Pathologists guideline recommendations for human epidermal growth factor receptor 2 testing in breast cancer. Journal of Clinical Oncology 2007: 25: 118-145

Wong, C. W., McNally, C., Nickbarg, E., Komm, B. S., Cheskis, B. J. Estrogen receptor-interacting protein that modulates its nongenomic activity-crosstalk with Src/Erk phosphorylation cascade. Proceedings of the National Academy of Science USA 2002, 99; 14783-14788

Wu, X. R., Kong, X. P., Pellicer, A., Krebich, G., Sun, T. T. Uroplakins in urothelial biology, function, and disease. Kidney International 2009: 75: 1153-1165

Yagi, H., Tan, W., Dillenburg-Pilla, P., Armando, S., Amornphimoltham, P., Simaan, M., Weigert, R., Molinolo, A. A., Bouvier, M., Gutkind, J. S. A synthetic biology approach reveals a CXCR4-G13-Rho signaling axis driving transendothelial migration of metastatic breast cancer cells. Science Signalling 2011: 4: [Epub]

Yamanaka, S., Olaru, A. V., An, F., Luvsaniav, D., Jin, Z., Agarwal, R., Tomuleasa, C., Popescu, I., Alexandrescu, S., Dima, S., Chivu-Economescu, M., Montgomery, E. A., Torbenson, M., Meltzer, S. J., Selaru, F. M. MicroRNA-21 inhibits Serpini1, a gene with novel tumour suppressive effects in gastric cancer. Digestive Liver Disease 2012: 44: 589-596

Yang, C., Yu, B., Zhou, D., Chen, S. Regulation of aromatase promoter activity in human breast tissue by nuclear receptors EAR-2, COUP-TF1 (EAR-3), and RARγ. Oncogene 2002: 21: 2854-2863

Yang, C., Zhou, D., Chen, S. Modulation of aromatase expression in the breast tissue by ERRα-1 orphan receptor. Cancer Research 1998: 58: 5695-5700

Yang, J. D., Seol, S. Y., Leem, S. H., Kim, Y. H., Sun, Z., Thorgeirsson, S. S., Chu, I. S., Roberts, L. R., Kang, K. J. Genes associated with recurrence of hepatocellular carcinoma: integrated analysis by gene expression and methylation profiling. Journal of Korean Medical Sciences 2011: 26: 1428-1438

Yarden, R. I., Wilson, M. A., Chrysogelos, S. A. Estrogen suppression of EGFR expression in breast cancer cells: a possible mechanism to modulate growth. Journal of Cellular Biochemistry Supplements 2001: Supplement 36: 232-246

Yip-Schneider ,M. T., Lin, A., Marshall, M. S. Pancreatic tumor cells with mutant K-ras suppress ERK activity by MEK-dependent induction of MAP kinase phosphatase-2. Biochemical and Biophysical Research Communications. 2001: 280: 992–997

Yu, F. X., Zhang, Y., Park, H. W., Jewell, J. L., Chen, Q., Deng, Y., Pan, D., Taylor, S. S., Lai, Z. C., Guan, K. L. Protein kinase A activates the Hippo pathway to modulate cell proliferation and differentiation. Genes and Development 2013: 27: 1223-1232

Zeelenberg, I. S., Ruuls-Van Stalle, L., Roos, E. The chemokine receptor CXCR4 is required for outgrowth of colon carcinoma micrometastases. Cancer Research 2003: 63: 3833-3839

Zekri, A. R., Hassan, Z. K., Bahnassy, A. A., Sherif, G. M., Eldahshan, D., Abouelhoda, M., Ali, A., Hafez, M. M. Molecular prognostic profile of Egyptian HCC cases infected with hepatitis C virus. Asian Pacific Journal of Cancer Prevention 2012: 13: 2433-5438

Zhang, X., Diaz, M. R., Yee, D. Fulvestrant regulates epidermal growth factor (EGF) family ligands to activate EGF receptor (EGFR) signaling in breast cancer cells. Breast Cancer Research and Treatment 2013: 139: 351-360

Zhou, C., Zhou, D., Esteban, J., Murai, J., Siiteri, P. K., Wilczynski, S., Chen, S. Aromatase gene expression and its exon I usage in human breast tumors. Detection of aromatase messenger RNA by

reverse transcription-polymerase chain reaction (RT-PCR). Journal of Steroid Biochemistry and Molecular Biology 1996: 59: 163-171

Zhou, D., Chen, S. Characterization of a silencer element in the human aromatase gene. Archives of Biochemistry and Biophysics 1998: 353: 213-220

Zhou, J., Cheng, W. J. Roles of thioredoxin binding protein (TXNIP) in oxidative stress, apoptosis and cancer. Mitochondrion 2012: [Epub]

Zhou, Y., Yau, C., Gray, J. W., Chew, K., Dairkee, S. H., Moore, D. H., Eppenberger, U., Eppenburger-Castori, S., Benz, C. C. Enhanced NF kappa B and AP-1 transcriptional activity associated with antiestrogen resistant breast cancer. BMC Cancer 2007: 7: [Epub]

Zhu, J. X., Goldoni, S., Bix, G., Owens, R. T., McQuillan, D. J., Reed, C. C., Iozzo, R. V. Decorin evokes protracted internalization and degradation of the epidermal growth factor receptor via caveolar endocytosis. Journal of Biological Chemistry 2005: 280: 32468-32479

Appendices

Appendix A: Charcoal stripping procedure for 100ml FCS

Charcoal-stripped FCS was used in order for the culture media to mimic oestrogen deprivation via the removal of as many steroids as possible (Morandi et al, 2013).

A charcoal solution (2g activated charcoal, 0.01g dextran T70 in 18ml dH20) was stirred for at least one hour. FCS was adjusted to pH=4.2 using HCl (5M) and left to equilibriate for 30minutes at 4oC. 5ml of charcoal solution was added to 100ml FCS and the solution and stirred gently for 16 hours at 4oC. Charcoal was then removed by centrifugation (12000rpm for 40 minutes) and the supernatant coarse-filtered through Whatman filter paper NO. 4 to ensure complete removal of charcoal. The solution was re-adjusted to pH=7.2 using NaOH (5M) and filter sterilised using a 2μM Super Vacucap membranes (Gellman Laboratory Pall, Ann Arbor, USA). Characoal stripped FCS was aliquotted into sterile universal containers and stored at 120oC

Appendix B: ICC protocols

Appendix B.1 3-aminopropyltriethoxysilane-coating of coverslips

Coverslips were cleaned by immersing in 100% ethanol before being left to air dry.

Once dry, coverslips were firstly immersed in 2% 3-aminopropyltriethoxysilane (A3648, Signal-Aldrich UK) in acetone for 5 seconds before being placed in 100% acetone for 2 minutes and distilled water 2 x 1 minute. Coated-coverslips were then left to air-dry before being sterilised.

Appendix B.2 Formal saline solution

3.7% Formal saline solution: 0.9g sodium chloride, 10ml 37% formaldehyde solution, 90ml distilled water

Appendix B.3 Sucrose storage medium

42.8g sucrose + 0.33g magnesium chloride dissolved in 250ml PBS then add 250 ml of glycerol. Stored in -20°C freezer prior to use.

Appendix B.4 PBS (0.01M)

8.5g sodium chloride, 1.43g di-potassium hydrogen orthophosphate anhydrous, 0.25g potassium dihydrogen orthophosphate and 1 litre distilled water.

## Appendix B.5 0.02% PBS/Tween

100µl of Tween 20 to 500ml PBS.

<u>Appendix C: Jetset gene probes</u>

The Affymetrix microarray platform contains multiple gene probe sets for a given gene which can deliver inconsistent or even contradictory measurements subsequently determining an estimate of gene expression can be difficult. Li et al developed a method to score each of the probe sets in order to determine their suitability as a probe set (Li et al, 2011). Three factors were considered; first the probe set should respond to the target gene only (probes partially matching other untended targets may deliver misleading results (Eklund et al, 2010; Okiniewski et al, 2006)). Secondly, the probe should detect as many splice isoforms as possible of the target gene in order to estimate overall gene expression and finally, the gene probe set should target the gene at a position near the 3' end of the corresponding transcript as it has been determined that probes too far from the 3' end of the target are likely to have a reduced signal and are susceptible to false signal changes due to variations in RNA integrity (Eklund et al, 2008). In summary, the scoring

methods assess each probe for specificity, coverage and degradation resistance. The probe with the highest score for a given gene was deemed the most optimal probe. All scores range from 0-1 and the higher the score the better the predicted performance of the given gene probe.

Appendix D: Faslodex dose-response graph using the MCF-7 cell line
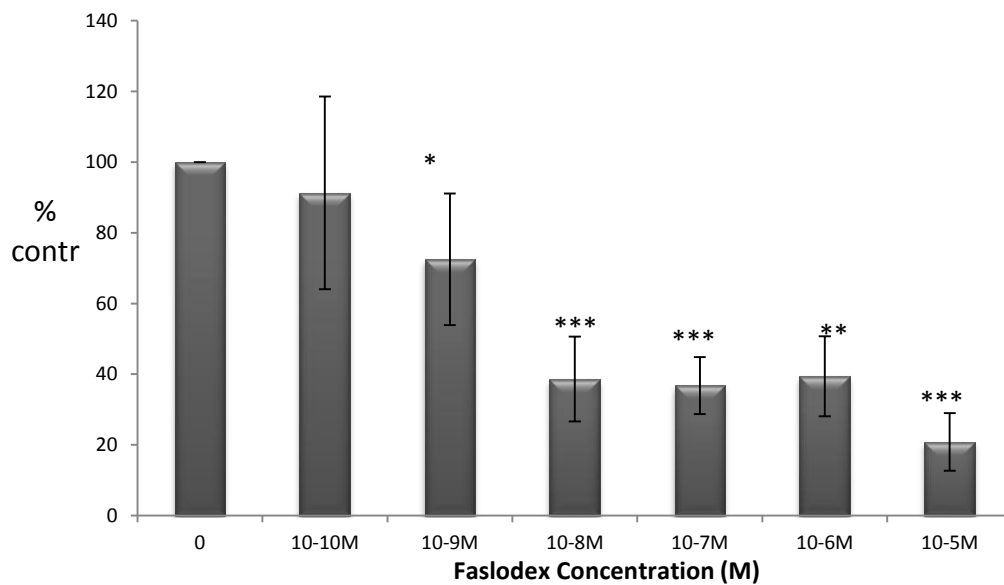
The effect of increasing concentrations of Faslodex on the basal growth of MCF-7 cells on day 7 after initial treatment. The results are expressed as means ± SEM of triplicate wells and are representative of three separate experiments. *$P < 0.05$ versus control, **$P < 0.01$ versus control, ***$P < 0.001$ versus control. No significant difference between 10^{-7}M Faslodex and 10^{-5}M

Appendix E: Pathway Analysis.

Genes identified as being significantly de-regulated (SAM: FDR <0.05) and used for pathway analysis.

- Resistance (BT474, MDA-MB-361 and MCF-7) genes- 42 genes identified
- T47D-unique genes-29 genes identified
- HER2- (MCF-7 and T47D) genes-44 genes identified
- HER2+ (BT474+MDA-MB-361) genes-24 genes identified

RESISTANCE GENES (HER2+ AND MCF7)	T47D UNIQUE	HER2- ONLY	HER2+ ONLY
ABCA1	SEPT6	A2BP1	CD8B
ADAM22	ADAM12	ABP1	CDH2
ATP11A	AFF3	ALDH4A1	CYP2A6
BCL2	ANGPT1	ALOX5	CYP2B6
BST1	ANK1	ANK1	CYP2B7
C18orf1	APBB2	ANK2	CYP2B7P1
CXCR4	AZGP1	ARTN	CYP2C9
DAB2	CA12	C14orf139	DDX3Y
DAB2	CASP1	CEACAM1	DICER1
EPHA3	CDC25A	CEACAM6	DMD
FLT4	DCN	CLGN	FAM155A
FRMD4B	DUSP4	CT62	GFRA2
FRZB	EPB41L3	CXCL12	GOLM1
GABBR2	ID4	DSCAM	HSPG2
GFRA1	IL6ST	EFNB2	ID3
GPR37	KCNAB1	ELOVL2	IGF2BP3
GRN	KCNMA1	F5	LTF
HLA-DQB1	LRRN3	IL6R	MPPED2
HS3ST1	MCM5	ITIH1	PVALB
IGFBP3	NRIP1	KLF12	SERPINI1
IKZF1	OLFM1	KRT4	SLC6A14
IL1R1	PEG10	MAP1B	SLC6A2
IVD	PTGER3	MLLT4	THBS1
KITLG	SKAP2	MYB	TRIP6
MAOA	STC1	MYRIP	
NLRP3	TGFB2	NCAM1	
NOV	TOX3	NPY5R	
NR4A3	TRIM29	NR2F1	
PDE4B	TXNIP	PCDH11X	
PDE4DIP		PCDH7	
PIK3R1		PMAIP1	
PKIA		PSCA	
PPP3CA		PTPRJ	

PRKACB		PYY	
RGS12		RUNX1T1	
RPS6KA3		SERHL2	
STS		SH3TC2	
TLE4		SLC39A9	
VCAN		SLC7A1	
VEGFC		SSX4	
ZEB1		SULF1	
ZNF343		SYNJ2	
		UPK3B	
		VGLL1	

Pathway analysis was carried out using Ingenuity Pathway Analyser. The genes of interest were input along regulators and ligands of the subsequent proteins.
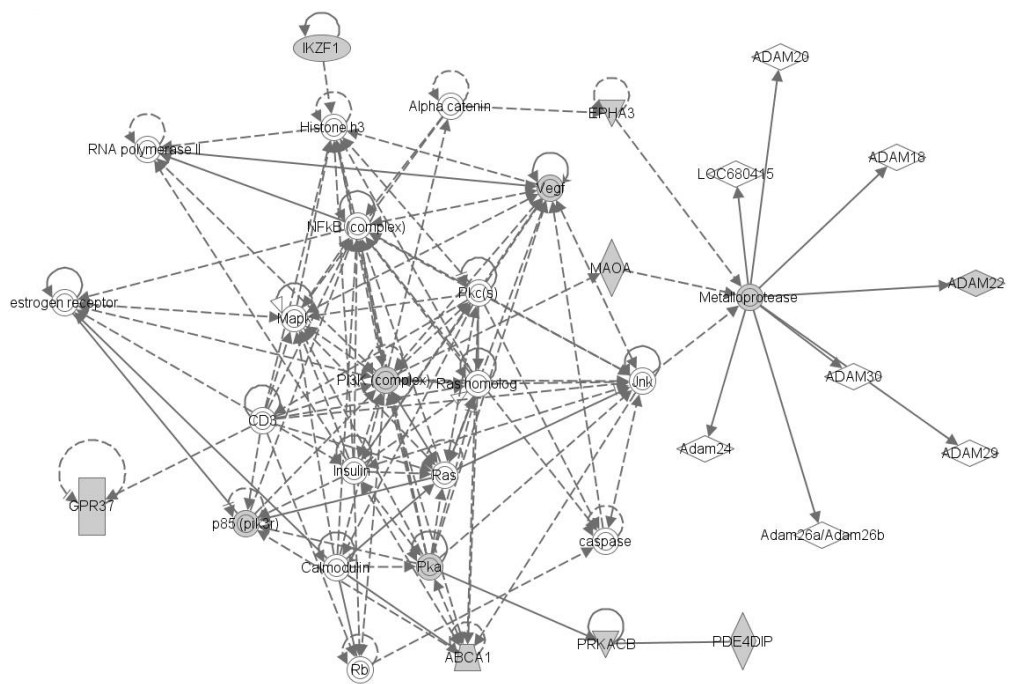
Resistance/MCF-7, BT474 and MDA-MB-361 shared genes

For those genes identified as possible resistance genes 4 pathways were identified as shown below (those shaded indicate the genes that are present in the gene list).
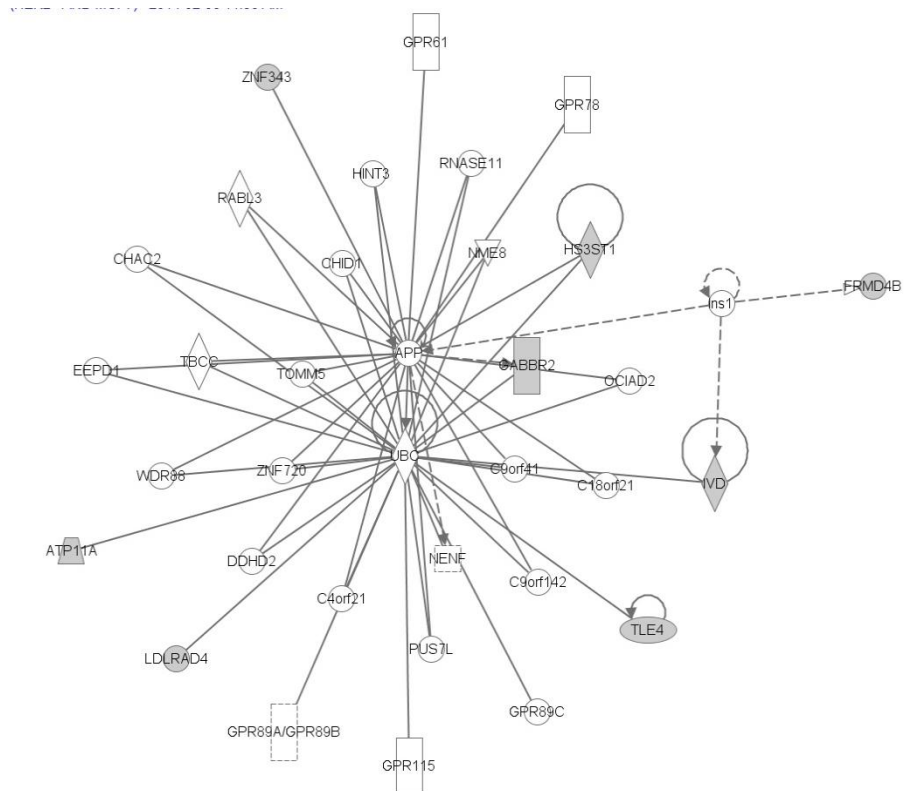
A: Cancer, Cellular Development, Cellular Growth and Proliferation
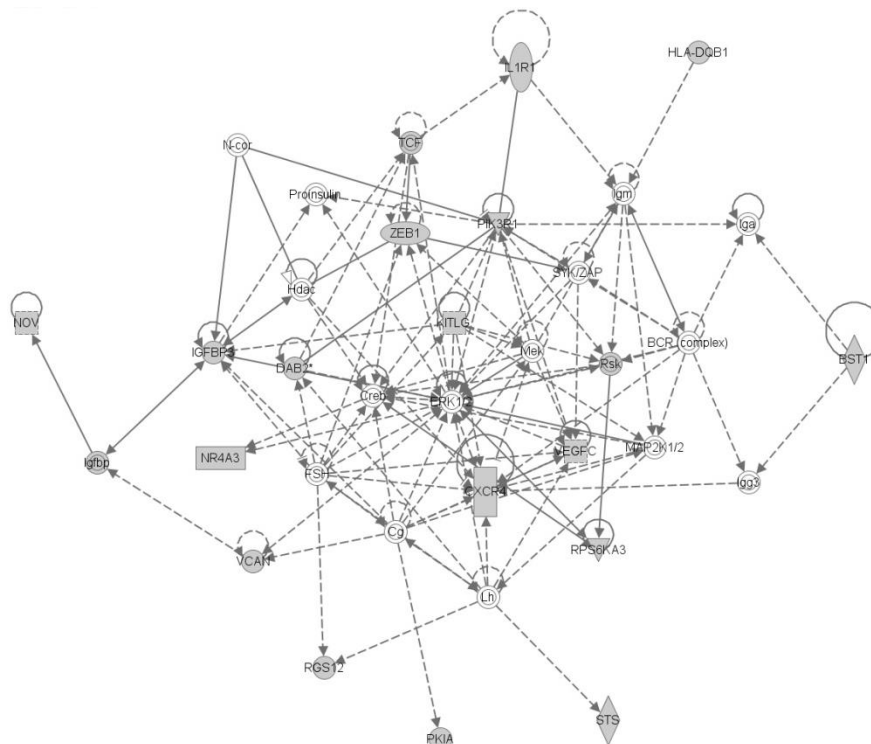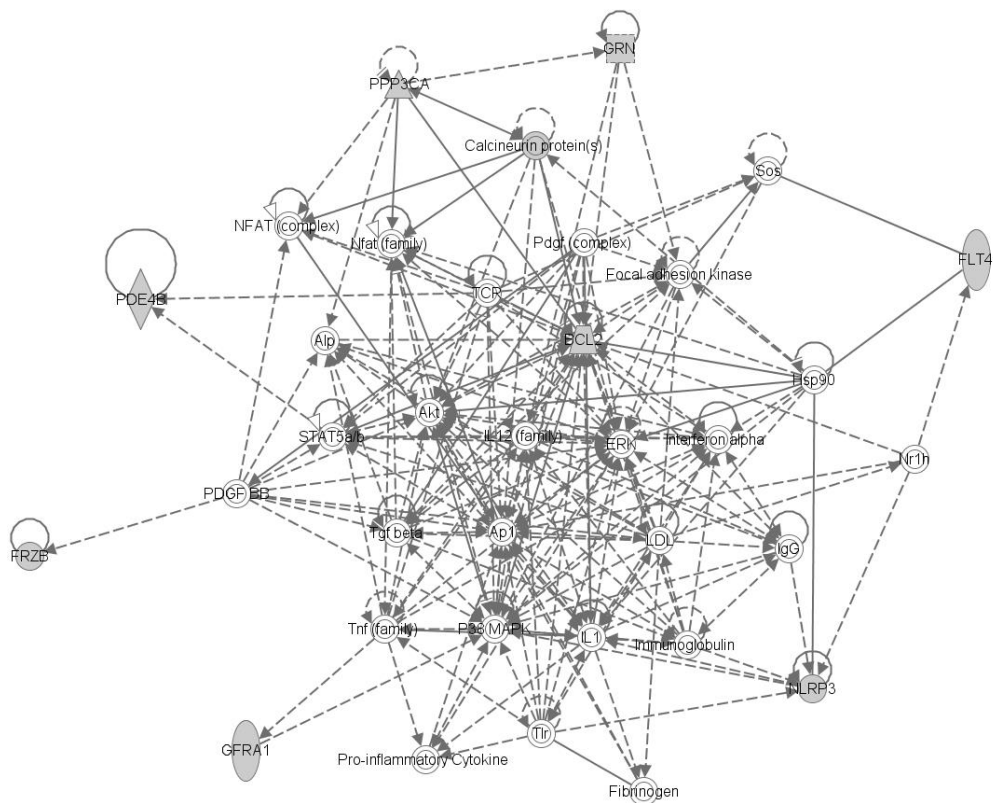
B: Cellular Assembly and Organization, Cellular Movement, Cardiovascular Disease

C: Molecular Transport, Small Molecule Biochemistry, Carbohydrate Metabolism

D: Cell Death and Survival, Gastrointestinal Disease, Inflammatory Disease

Of particular interest was pathways A and D due to their potential roles in cell survival and thus possible acquisition of resistance to Faslodex. However, very few of the central nodes of the pathways included genes identified as being de-regulated and listed in the Table of Appendix E with the exception of CXCR4 in pathway A and BCL2 in pathway D.

**Complete response/T47D unique genes**

For those genes identified as possible T47D unique/complete response genes, 2 pathways were identified as shown below. Those shaded indicate the genes that are present in the gene list.

With regards to a complete response both pathways identified are of interest, however pathway A includes more genes that are directly from the genes of interest list and with a few being present in the same pathway. Chapter 6 looks at many of these genes in further detail and analyses those that are more strictly de-regulated in the T47D line only and by a given a fold change.

A: Cell Death and Survival, Cell-To-Cell Signaling and Interaction, Connective Tissue Development and Function

B: Cellular Compromise, Organismal Injury and Abnormalities, Cell Cycle

Extended response/HER2- only genes

2 pathways were identified from the analysis of gene identified as being Faslodex de-regulated in the ER+/HER2- cell lines (MCF-7 and T47D). Neither of the identified pathways are suggested to be involved in mechanisms that could be associated with an extended duration of Faslodex response suggesting that the de-regulation of these pathways is not the cause of the increased response.

A: Cellular Movement, Digestive System Development and Function, Hematological System Development and Function
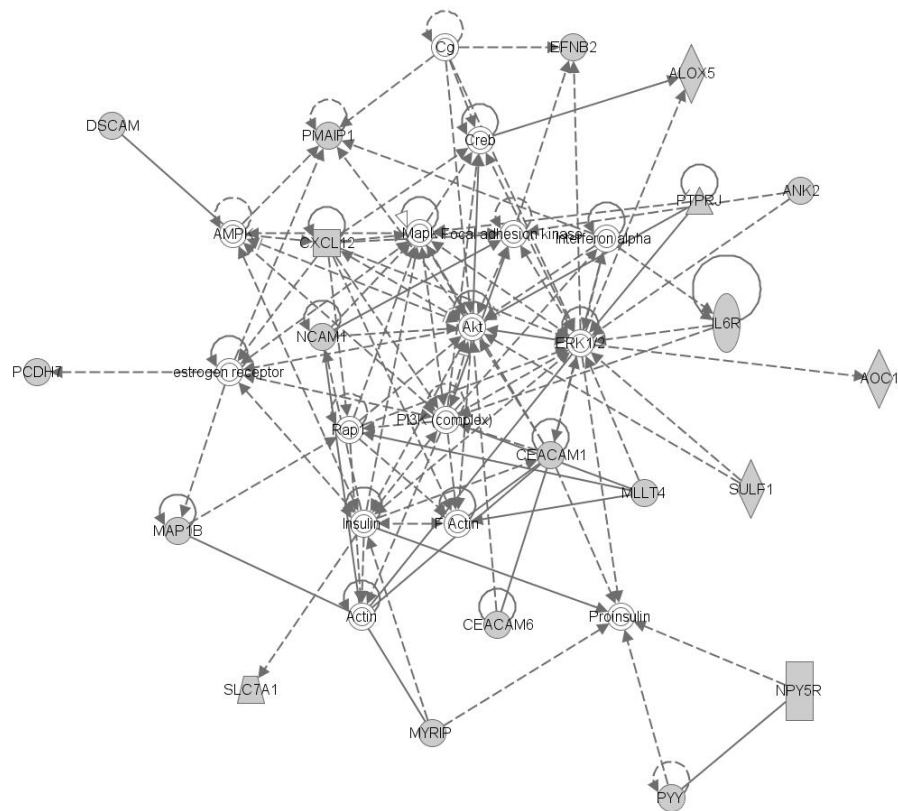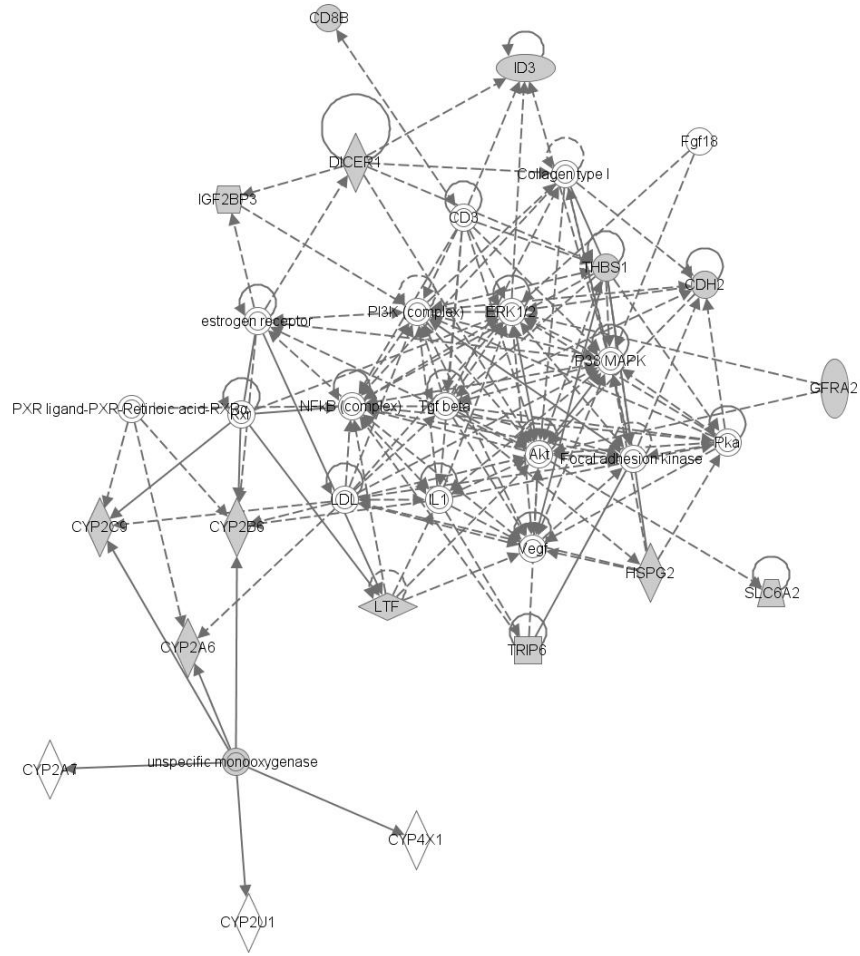

B: Digestive System Development and Function, Organ Morphology, Cancer
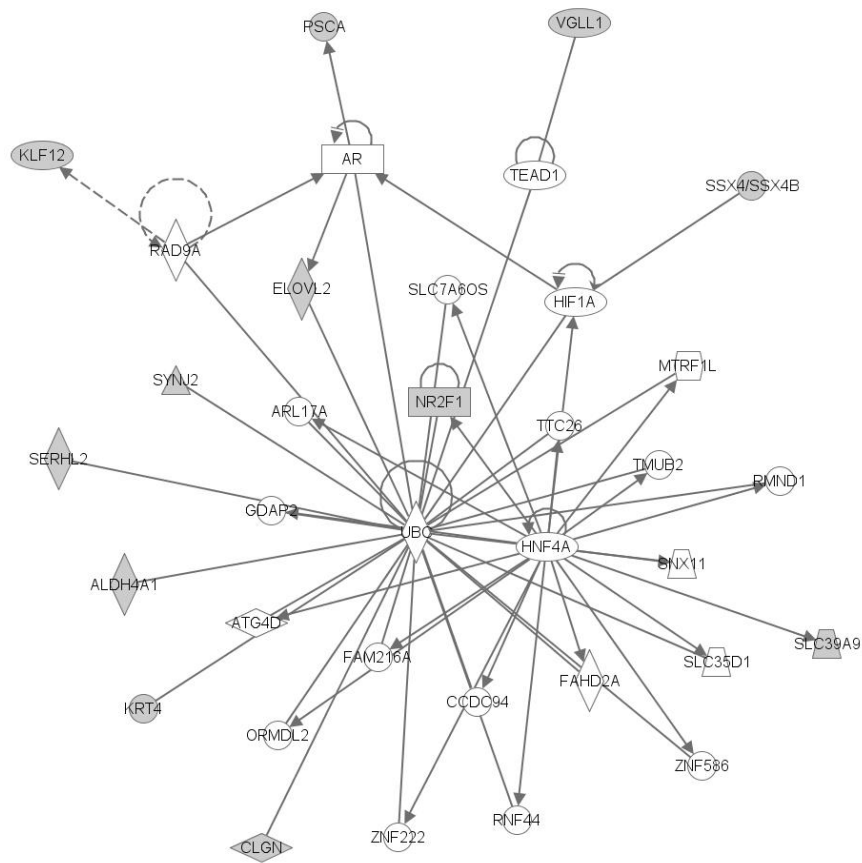
Reduced response/HER2+ (BT474 and MDA-MB-361) shared genes

Again only 2 pathways were identified following the analysis of genes de-regulated by both ER+/HER2+ cell lines. Pathway B could be of interest due its possible involvement in survival but none of the genes found to de-regulated in the both HER2+ lines (shaded genes) form central components of this pathway suggesting a minimal effect on cell survival.

A: Drug Metabolism, Small Molecule Biochemistry, Lipid Metabolism

B: Cell Death and Survival, Nervous System Development and Function, Cardiovascular Disease